

CE-QUAL-W2: A Two-Dimensional, Laterally Averaged, Hydrodynamic and Water Quality Model, Version 3.2

User Manual

by Thomas M. Cole
Environmental Laboratory
U.S. Army Corps of Engineers
Waterways Experiment Station
Vicksburg, MS 39180-6199

and

Scott A. Wells
Department of Civil and Environmental Engineering
Portland State University
Portland, OR 97207-0751

Draft Report
Not approved for public release
(Supersedes Instruction Report E-95-1)

DRAFT

Prepared for U.S. Army Corps of Engineers
Washington, DC 20314-1000

Contents

Contents	ii
Preface	xi
List of Figures	xii
List of Tables	xvii
Model Package	xix
Programs	xix
Input Files	xix
Output Files	xx
1 Introduction	1
Model Overview	1
Model Background	1
Manual	3
2 Capabilities and Limitations	4
Capabilities	4
Limitations	6
Theoretical	6
Numerical	7
Input Data	7
3 Model Application	8
Overview	8
Data Preparation	8
Geometric Data	8
Initial Conditions	13
Boundary Conditions	13
Hydraulic Parameters (required)	15
Kinetic Parameters (optional)	16
Calibration Data (required)	16
Simulations	20
Model Preparation	20
Calibration	20
Lake/Reservoir	24
Water budget	24
Hydrodynamics and Temperature	26
Water Quality	37
Estuary	58
Boundary conditions	58
Water surface elevations and flows	58
Time of Travel	61
Temperature and Salinity	61

CONTENTS

Water Quality.....	64
River	65
Channel Slope.....	65
Hydrodynamics and Temperature.....	71
Water Quality.....	76
Summary.....	84
References	85
CE-QUAL-W2 Publications.....	106
Peer Reviewed Publications.....	106
Presentations at Scientific Meetings	108
Reports and Miscellaneous Articles	114
Appendix A Hydrodynamics and Transport	A-1
Coordinate System.....	A-1
Turbulent Time-Averaged Equations	A-2
Continuity.....	A-3
x-Momentum Equation	A-3
y-Momentum Equation	A-4
z-Momentum Equation	A-5
Coriolis Effect.....	A-6
Adjusting the Coordinate System	A-7
Governing Equations for General Coordinate System	A-9
Continuity.....	A-9
x-Momentum Equation	A-9
y-Momentum Equation	A-9
z-Momentum Equation	A-10
Simplification of z-Momentum Equation	A-10
Lateral Averaging	A-10
Continuity Equation.....	A-11
x-Momentum Equation	A-13
Shear stresses.....	A-15
Summary of Laterally Averaged Equations.....	A-15
Continuity Equation.....	A-15
x-Momentum Equation	A-15
z-Momentum Equation	A-15
Simplification of Pressure Term	A-16
Free Water Surface.....	A-17
Equation of State.....	A-20
Summary of Governing Equations.....	A-20
Branch Linkage with Internal Head Boundary Conditions	A-21
Linkage of Mainstem Branches.....	A-21
Linkage of Tributary Branches	A-23
Longitudinal Momentum	A-24
Cross-shear of Tributary Inflow	A-25
River Basin Theory.....	A-26
Free-Water Surface Numerical Solution	A-26
Horizontal Momentum Numerical Solution	A-32
Explicit Solution	A-32
Implicit Solution.....	A-34

CONTENTS

Turbulent Advection-Diffusion Equation	A-35
Water Quality Transport	A-38
Numerical Solution	A-40
Non-Uniform Grid QUICKEST Formulation	A-43
ULTIMATE/QUICKEST Numerical Transport Solution Scheme	A-45
Vertical Implicit Transport	A-53
Auxiliary Functions	A-54
Surface Shear Stress	A-54
Bottom Shear Stress	A-57
Vertical Shear Stress	A-58
Formulation	A-61
RNG Turbulent Eddy Viscosity Formulation	A-63
Nikuradse Formulation	A-65
Parabolic Formulation	A-66
W2N Formulation	A-67
TKE Formulation	A-67
Effect of Vertical Layer Numbers on Vertical Turbulence	A-68
Longitudinal Shear Stress	A-72
Hydraulic Structures	A-72
Internal Weirs	A-76
Water Level Control	A-76
Outlet Structures	A-76
Spillways/Weirs	A-79
Gates	A-84
Branch Momentum Exchange	A-86
Lateral Inflows	A-88
Heat Exchange	A-88
Surface Heat Exchange	A-88
Evaporation	A-90
Equilibrium Temperature	A-93
Sediment Heat Exchange	A-93
Dynamic Shading	A-94
Solar Altitude and Azimuth	A-94
Topographic Shading	A-96
Vegetative Shading	A-96
Data Requirements	A-99
Ice Cover	A-99
Initial Ice Formation	A-101
Air-Ice Flux Boundary Condition and Ice Surface Temperature Approximation	A-101
Absorbed Solar Radiation by Water Under Ice	A-102
Ice Melt at Air-Ice Interface	A-102
Ice-Water Flux Boundary Condition Formulation	A-103
Density	A-104
Selective Withdrawal	A-105
Sediment Resuspension	106
Appendix B Water Quality	B-1
Overview of Kinetic Source/Sink Term	B-1

CONTENTS

Generic Constituent	B-3
Conservative Tracer.....	B-3
Coliform Bacteria.....	B-4
Water Age or Residence time.....	B-4
Inorganic Suspended Solids.....	B-5
Total Dissolved Solids or Salinity.....	B-6
Labile DOM	B-6
Refractory DOM.....	B-7
Labile Particulate Organic Matter	B-8
Refractory Particulate Organic Matter.....	B-9
Carbonaceous Biochemical Oxygen Demand (CBOD).....	B-10
Algae	B-11
Epiphyton.....	B-15
Phosphorus	B-19
Ammonium	B-22
Nitrate-Nitrite	B-24
Dissolved Silica.....	B-25
Particulate Biogenic Silica.....	B-27
Total Iron.....	28
Dissolved Oxygen	B-29
River Reaeration Equations.....	B-31
Lake Reaeration Equations	B-33
Estuarine Equations.....	B-37
Reaeration Temperature Dependence	B-38
Dam Reaeration.....	B-39
Small Dams or Weirs	B-39
Large Dam Spillways/Gates	B-39
DO Impacts of Spillways	B-40
Dissolved Oxygen Saturation Computations.....	B-41
Sediments.....	B-42
Total Inorganic Carbon.....	B-44
Alkalinity.....	B-46
pH and Carbonate Species.....	B-47
Temperature Rate Multipliers	B-50
Appendix C Input/Output Data Description	C-1
Input Files	C-1
Control File	C-1
Title (TITLE C).....	C-2
Grid Dimensions (GRID)	C-3
Inflow/Outflow Dimensions (IN/OUTFLOW).....	C-4
Constituent Dimensions (CONSTITUENTS).....	C-5
Miscellaneous Dimensions (MISCELL).....	C-6
Time Control (TIME CON).....	C-7
Timestep Control (DLT CON)	C-8
Timestep Date (DLT DATE).....	C-9
Maximum Timestep (DLT MAX).....	C-10
Timestep Fraction (DLT FRN)	C-11
Timestep Limitations (DLT LIMIT).....	C-12

CONTENTS

Branch Geometry (BRANCH G).....	C-13
Waterbody Definition (LOCATION).....	C-15
Initial Conditions (INIT CND).....	C-17
Calculations (CALCULAT).....	C-18
Dead Sea (DEAD SEA).....	C-20
Interpolation (INTERPOL).....	C-21
Heat Exchange (HEAT EXCH).....	C-23
Ice Cover (ICE COVER).....	C-25
Transport Scheme (TRANSPORT).....	C-27
Hydraulic Coefficients (HYD COEF).....	C-28
Vertical Eddy Viscosity (EDDY VISC).....	C-29
Number of Structures (N STRUC).....	C-31
Structure Interpolation (STR INT).....	C-32
Structure Top Selective Withdrawal Limit (STR TOP).....	C-33
Structure Bottom Selective Withdrawal Limit (STR BOT).....	C-34
Sink Type (SINK TYPE).....	C-35
Structure Elevation (E STRUC).....	C-36
Structure Width (W STRUC).....	C-37
Pipes (PIPES).....	C-38
Upstream Pipe (PIPE UP).....	C-43
Downstream Pipe (PIPE DOWN).....	C-44
Spillways (SPILLWAYS).....	C-45
Upstream Spillways (SPILL UP).....	C-49
Downstream Spillways (SPILL DOWN).....	C-50
Spillway Dissolved Gas (SPILL GAS).....	C-51
Gates (GATES).....	C-54
Gate Weir (GATE WEIR).....	C-59
Upstream Gate (GATE UP).....	C-60
Downstream Gate (GATE DOWN).....	C-61
Gate Dissolved Gas (GATE GAS).....	C-62
Pumps 1 (PUMPS 1).....	C-65
Pumps 2 (PUMPS 2).....	C-69
Internal Weir Segment Location (WEIR SEG).....	C-70
Internal Weir Top Layer (WEIR TOP).....	C-73
Internal Weir Bottom Layer (WEIR BOT).....	C-74
Withdrawal Interpolation (WD INT).....	C-75
Withdrawal Segment (WD SEG).....	C-76
Withdrawal Elevation (WD ELEV).....	C-77
Withdrawal Top Layer (WD TOP).....	C-78
Withdrawal Bottom Layer (WD BOT).....	C-79
Tributary Inflow Placement (TRIB PLACE).....	C-80
Tributary Interpolation (TRIB INT).....	C-81
Tributary Segment (TRIB SEG).....	C-82
Tributary Inflow Top Elevation (TRIB TOP).....	C-83
Tributary Inflow Bottom Elevation (ELEV BOT).....	C-84
Distributed Tributaries (DST TRIB).....	C-85
Pump Storage Operations (PUMPBACK).....	C-86
Printer Control (PRINTER).....	C-87

CONTENTS

Hydrodynamic Output Control (HYD PRINT).....	C-88
Snapshot Print (SNP PRINT)	C-89
Snapshot Dates (SNP DATE).....	C-90
Snapshot Frequency (SNP FREQ).....	C-91
Snapshot Segments (SNP SEG).....	C-92
Screen Print (SCR PRNT).....	C-93
Screen Dates (SCR DATE).....	C-94
Screen Frequency (SCR FREQ).....	C-95
Profile Plot (PRF PLOT).....	C-96
Profile Date (PRF DATE)	C-97
Profile Frequency (PRF FREQ)	C-98
Profile Segment (PRF SEG).....	C-99
Spreadsheet Plot (SPR PLOT).....	C-100
Spreadsheet Date (SPR DATE).....	C-101
Spreadsheet Frequency (SPR FREQ).....	C-102
Spreadsheet Segment (SPR SEG).....	C-103
Vector Plot (VPL PLOT).....	C-104
Vector Plot Date (VPL DATE).....	C-105
Vector Plot Frequency (VPL FREQ).....	C-106
Contour Plot (CPL PLOT)	C-107
Contour Plot Dates (CPL DATE).....	C-108
Contour Plot Frequency (CPL FREQ).....	C-109
Kinetic Flux Output (FLUXES).....	C-110
Kinetic Flux Date (KFL DATE).....	C-111
Kinetic Flux Frequency (FLX FREQ).....	C-112
Time Series Plot (TSR PLOT).....	C-113
Time Series Date (TSR DATE)	C-114
Time Series Frequency (TSR FREQ).....	C-115
Time Series Segment (TSR SEG).....	C-116
Time Series Elevation (TSR ELEV).....	C-117
Withdrawal Output (WITH OUT)	C-118
Withdrawal Output Date (WDO DATE).....	C-119
Withdrawal Output Frequency (WDO FREQ).....	C-120
Withdrawal Output Segment (WITH SEG).....	C-121
Restart (RESTART).....	C-122
Restart Date (RSO DATE).....	C-123
Restart Frequency (RSO FREQ).....	C-124
Constituent Computations (CST COMP).....	C-125
Active Constituents (CST ACTIVE).....	C-126
Derived Constituents (CST DERIVE).....	C-128
Constituent Fluxes (CST FLUX).....	C-129
Constituent Initial Concentration (CST ICON).....	C-131
Constituent Output (CST PRINT).....	C-132
Inflow Active Constituent Control (CIN CON).....	C-133
Tributary Active Constituent Control (CTR CON).....	C-134
Distributed Trib Active Constituent (CDT CON).....	C-135
Precipitation Active Constituent Control (CPR CON).....	C-136
Extinction Coefficient (EX COEF).....	C-137

CONTENTS

Algal Extinction (ALG EX)	C-139
Generic Constituent (GENERIC).....	C-140
Suspended Solids (S SOLIDS)	C-141
Algal Rates (ALGAL RATE).....	C-142
Algal Temperature Rate Coefficients (ALG TEMP).....	C-149
Algal Stoichiometry (ALG STOICH).....	C-150
Epiphyte Control (EPIPHYTE).....	C-152
Epiphyte Print (EPI PRINT).....	C-153
Epiphyte Initial Density (EPI INI).....	C-154
Epiphyte Rate (EPI RATE).....	C-155
Epiphyte Half-Saturation (EPI HALF)	C-156
Epiphyte Temperature Rate Coefficients (EPI TEMP)	C-158
Epiphyte Stoichiometry (EPI STOICH).....	C-159
Dissolved Organic Matter (DOM).....	C-160
Particulate Organic Matter (POM).....	C-161
Organic Matter Stoichiometry (OM STOICH).....	C-163
Organic Matter Temperature Rate Multipliers (OM RATE).....	C-164
Carbonaceous Biochemical Oxygen Demand (CBOD).....	C-165
CBOD Stoichiometry (CBOD STOICH).....	C-166
Inorganic Phosphorus (PHOSPHOR)	C-167
Ammonium (AMMONIUM).....	C-168
Ammonium Temperature Rate Multipliers (NH4 RATE).....	C-169
Nitrate (NITRATE).....	C-170
Nitrate Temperature Rate Multipliers (NO3 RATE).....	C-171
Silica (SILICA).....	C-172
Iron (IRON).....	C-173
Sediment Carbon Dioxide Release (SED CO2)	C-174
Oxygen Stoichiometry 1 (STOICH 1)	C-175
Oxygen Stoichiometry 2 (STOICH 2)	C-176
Oxygen Stoichiometry 3 (STOICH 3)	C-177
Oxygen Limit (O2 LIMIT).....	C-178
Sediment Compartment (SEDIMENT)	C-179
SOD Temperature Rate Multipliers (SOD RATE)	C-180
Zero-Order Sediment Oxygen Demand (S DEMAND)	C-181
Reaeration (REAERAT).....	C-182
Restart Input Filename (RSI FILE)	C-186
Withdrawal Filename (QWD FILE)	C-187
Gate Outflow Filename (QGT FILE)	C-188
Wind Sheltering Filename (WSC FILE)	C-189
Dynamic Shading Filename (SHD FILE)	C-190
Bathymetry Filename (BTH FILE).....	C-191
Meteorology Filename (MET FILE).....	C-192
Light Extinction Filename (EXT FILE).....	C-193
Vertical Profile Filename (VPR FILE).....	C-194
Longitudinal Profile Filename (LPR FILE).....	C-195
Branch Inflow Filename (QIN FILE).....	C-196
Branch Inflow Temperature Filename (TIN FILE)	C-197
Branch Inflow Constituent Filename (CIN FILE).....	C-198

CONTENTS

Branch Outflow Filename (QOT FILE)	C-199
Tributary Inflow Filename (QTR FILE)	C-200
Tributary Inflow Temperature Filename (TTR FILE)	C-201
Tributary Inflow Concentration Filename (CTR FILE)	C-202
Distributed Tributary Inflow Filename (QDT FILE)	C-203
Distributed Tributary Inflow Temperature Filename (TDT FILE)	C-204
Distributed Tributary Inflow Concentration Filename (CDT FILE)	C-205
Precipitation Filename (PRE FILE)	C-206
Precipitation Temperature Filename (TPR FILE)	C-207
Precipitation Concentration Filename (CPR FILE)	C-208
External Upstream Head Filename (EUH FILE)	C-209
External Upstream Head Temperature Filename (TUH FILE)	C-210
External Upstream Head Concentration Filename (CUH FILE)	C-211
External Downstream Head Filename (EDH FILE)	C-212
External Downstream Head Temperature Filename (TDH FILE)	C-213
External Downstream Head Concentration Filename (CDH FILE)	C-214
Snapshot Filename (SNP FILE)	C-215
Profile Plot Filename (PRF FILE)	C-216
Vector Plot Filename (VPL FILE)	C-217
Contour Plot Filename (CPL FILE)	C-218
Spreadsheet Plot Filename (SPR FILE)	C-219
Flux Filename (FLX FILE)	C-220
Time Series Plot Filename (TSR FILE)	C-221
Withdrawal Output Filename (WDO FILE)	C-222
Sample Control Input File	C-223
Bathymetry File	C-248
Meteorology File	C-253
Gate File	C-254
Light Extinction File	C-256
Wind Sheltering Coefficient File	C-257
Shade Input File	C-258
Branch Inflow File	C-264
Branch Inflow Temperature File	C-265
Branch Inflow Constituent Concentration File	C-266
Branch Outflow File	C-268
Withdrawal File	C-269
Tributary Inflow File	C-270
Tributary Inflow Temperature File	C-271
Tributary Inflow Concentration File	C-272
Branch Distributed Tributary Inflow File	C-273
Branch Distributed Tributary Inflow Temperature File	C-274
Branch Distributed Tributary Inflow Concentration File	C-275
Branch Precipitation File	C-276
Branch Precipitation Temperature File	C-277
Branch Precipitation Concentration File	C-278
Branch External Upstream Head Elevation File	C-279
Branch External Upstream Head Temperature File	C-280
Branch External Upstream Head Constituent Concentration File	C-281

CONTENTS

Branch External Downstream Head Elevation File	C-282
Branch External Downstream Head Temperature File.....	C-283
Branch External Downstream Head Concentration File.....	C-284
Vertical Profile File	C-285
Longitudinal Profile File	C-286
Graph Input File	C-289
Output Files	C-292
Snapshot.....	C-292
Title Cards	C-292
Time Parameters	C-292
Meteorological Parameters	C-293
Inflow/Outflow Parameters.....	C-293
Balances	C-295
Geometry	C-297
Water Surface	C-298
Temperature/Water Quality.....	C-298
Time Series	C-300
Preprocessor.....	C-302
Output (pre.opt).....	C-302
Warning Messages (pre.wrn).....	C-317
Error Messages (pre.err).....	C-318
Spreadsheet Plot.....	C-319
Profile Plot	C-320
Vector Plot.....	C-324
Contour Plot	C-325
Kinetic Fluxes.....	C-326
Withdrawal Outflow	C-328
Run-time Warnings	C-330
Run-time Errors	C-332

Preface

This manual documents the two-dimensional, laterally averaged, hydrodynamic and water quality model CE-QUAL-W2. This manual was prepared in the Environmental Laboratory (EL), US Army Engineer Waterways Experiment Station (WES), Vicksburg, MS. Bonita Niel and Dr. William Roper, CERD-C provided funding for Version 3.1 of the manual under the Numerical Model Maintenance Program.

The principal investigator for Version 3.2 of CE-QUAL-W2 and the User Manual was Mr. Thomas M. Cole of the Water Quality and Contaminant Modeling Branch (WQCMB), Environmental Processes and Effects Division (EPED), EL.

This report was prepared by Mr. Cole under the direct supervision of Dr. Mark Dortch, Chief, WQCMB, and under the general supervision of Dr. Richard Price, Chief, EPED, and Dr. Ed Theriot, Director, EL. Technical reviews by Dr. Dortch, Dr. Billy Johnson, and Ms. Toni Toney are gratefully acknowledged.

At the time of publication of this manual, Dr. James R. Houston was Director of WES. COL James S. Weller, EN, was Commander.

This report should be cited as follows:

Cole, T.M., and S. A. Wells (2003). "CE-QUAL-W2: A two-dimensional, laterally averaged, Hydrodynamic and Water Quality Model, Version 3.2," Instruction Report EL-03-1, US Army Engineering and Research Development Center, Vicksburg, MS.

LIST OF FIGURES

List of Figures

Figure 1. Sample computational grid in the x-z plane showing active and inactive cells.	10
Figure 2. Sample computational grid in the x-y plane showing cell numbering and branch and water body connections.	12
Figure 3. Allatoona Reservoir computed (lines) vs. observed (symbols) water surface elevations for 1992, 1993, 1996, and 1997.....	25
Figure 4. 1989 Pineflat Reservoir computed versus observed temperatures.	30
Figure 5. 1993 Pineflat Reservoir computed versus observed temperatures.	30
Figure 6. 1981 Bluestone Reservoir computed versus observed temperatures.	31
Figure 7. 1983 Bluestone Reservoir computed versus observed temperatures.	31
Figure 8. 1988 Richard B. Russell computed versus observed temperatures.	32
Figure 9. 1994 Richard B. Russell computed versus observed temperatures.	33
Figure 10. 1996 Richard B. Russell computed versus observed temperatures.	33
Figure 11. Paintsville Reservoir computed versus observed temperatures.	34
Figure 12. 1992 Brownlee Reservoir computed versus observed temperatures.....	35
Figure 13. 1995 Brownlee Reservoir computed versus observed temperatures.....	35
Figure 14. C.J. Strike Reservoir computed versus observed temperatures.	36
Figure 15. Allatoona Reservoir computed vs. observed DO.	39
Figure 16. Brownlee Reservoir computed vs. observed DO.	39
Figure 17. C.J. Strike Reservoir computed vs. observed DO.	40
Figure 18. DeGray Reservoir computed vs. observed DO.	40
Figure 19. Richard B. Russell Reservoir computed vs. observed DO, March through June, 1988.....	41
Figure 20. Richard B. Russell Reservoir computed vs. observed DO, June through October, 1988.....	41
Figure 21. 1996 Richard B. Russell computed vs. observed DO.	42
Figure 22. Neely Henry Reservoir computed vs. observed DO.....	42
Figure 23. J. Strom Thurmond Reservoir computed vs. observed DO.	43
Figure 24. Monroe Reservoir computed vs. observed DO.	43
Figure 25. Rimov Reservoir computed vs. observed DO.	44
Figure 26. Shepaug Reservoir computed vs. observed DO.....	44
Figure 27. Shepaug Reservoir computed vs. observed DO.....	45
Figure 28. Weiss Reservoir computed vs. observed DO.....	45
Figure 29. West Point Reservoir computed vs. observed DO.	46
Figure 30. Walter F. George Reservoir computed vs. observed DO.....	46
Figure 31. Rimov Reservoir computed vs. observed phytoplankton biomass.....	48
Figure 32. Rimov Reservoir computed vs. observed phytoplankton biomass.....	48
Figure 33. Rimov Reservoir computed vs. observed phytoplankton biomass.....	49
Figure 34. Rimov Reservoir computed vs. observed phytoplankton biomass.....	49

LIST OF FIGURES

Figure 35. Rimov Reservoir computed vs. observed phytoplankton biomass.	50
Figure 36. Rimov Reservoir computed vs. observed phytoplankton biomass.	50
Figure 37. Rimov Reservoir computed vs. observed phytoplankton with wind rotated 90°.....	51
Figure 38. Rimov Reservoir computed vs. observed phytoplankton with wind rotated 90°	52
Figure 39. Rimov Reservoir computed vs. observed phytoplankton with wind rotated 90°.....	52
Figure 40. Rimov Reservoir computed vs. observed phytoplankton with wind rotated 90°.....	53
Figure 41. Rimov Reservoir computed vs. observed phytoplankton with wind rotated 90°.....	53
Figure 42. Rimov Reservoir computed vs. observed phytoplankton with wind rotated 90°.....	54
Figure 43. Rimov Reservoir computed vs. observed phytoplankton with no inflowing phytoplankton.	55
Figure 44. Rimov Reservoir computed vs. observed phytoplankton with no inflowing phytoplankton.	55
Figure 45. Rimov Reservoir computed vs. observed phytoplankton with no inflowing phytoplankton.	56
Figure 46. Rimov Reservoir computed vs. observed phytoplankton with no inflowing phytoplankton.	56
Figure 47. Rimov Reservoir computed vs. observed phytoplankton with no inflowing phytoplankton.	57
Figure 48. Rimov Reservoir computed vs. observed phytoplankton with no inflowing phytoplankton.	57
Figure 49. Water level data versus model predictions for Longview, WA during a 20-day period in 1993.....	60
Figure 50. Model flow predictions versus data for a 20-day period during 1998 at Beaver Army Terminal near Quincy, OR.....	60
Figure 51. Patuxent River computed versus observed vertical salinity distributions.....	62
Figure 52. Patuxent River computed versus observed vertical temperature distributions.	63
Figure 53. Patuxent River computed versus observed nutrient, dissolved oxygen, and chl <i>a</i> time series.....	64
Figure 54. Snake River water level comparison between CE-QUAL-W2 V3 and USGS field data.	66
Figure 55. Channel vertical grid where every slope change is a new branch.	66
Figure 56. Snake River channel slope determination.....	67
Figure 57. Channel slope for the Bull Run system.	68
Figure 58. Vertical grid for W2 model of Bull Run Lower River.	69
Figure 59. Bull Run River computed versus observed tracer at three stations progressing downstream.....	72
Figure 60. Spokane River computed versus observed water surface elevations at Spokane.....	72
Figure 61. Spokane River computed versus observed flows at the city of Spokane.	73
Figure 62. Snake River computed versus observed temperature at six stations.....	74

LIST OF FIGURES

Figure 63. Computed versus observed temperatures for the Spokane River at Stateline Bridge (upstream boundary), City of Spokane, Fort Wright Bridge, and Riverside State Park.....	75
Figure 64. Spokane River computed versus observed conductivity below Nine Mile Dam.....	76
Figure 65. Snake River computed versus observed dissolved oxygen at six stations....	77
Figure 66. Snake River computed versus observed orthophosphorus at six stations. ...	78
Figure 67. Snake River computed versus observed nitrate-nitrite at six stations.	79
Figure 68. Snake River computed versus observed chlorophyll a at six stations.....	80
Figure 69. Snake River computed versus total organic carbon.....	81
Figure 70. Spokane River computed versus observed dissolved oxygen at Riverside State Park.....	81
Figure 71. Spokane River computed versus observed dissolved oxygen below Nine Mile Dam.....	82
Figure 72. Spokane River computed versus observed pH upstream of Nine Mile Dam.	82
Figure 73. Spokane River computed versus observed nitrate-nitrite at Riverside State Park.....	83
Figure 74. Spokane River computed versus observed soluble reactive phosphorus below Nine Mile Dam.....	83
Figure 75. Spokane River computed versus observed total nitrogen below Nine Mile Dam.....	84
Figure A-1. Definition sketch of coordinate system for governing equations where x is oriented east, y is oriented north, and z is oriented upward.....	A-1
Figure A-2. Definition sketch of turbulent time averaging for velocity.	A-2
Figure A-3. Definition sketch of turbulent shear stresses in x-direction.	A-4
Figure A-4. Sketch of turbulent shear stresses in y-direction.	A-5
Figure A-5. Sketch of turbulent shear stresses in z-direction.	A-6
Figure A-6. General coordinate system with z-axis compatible with original derivation of W2 model.	A-7
Figure A-7. Sketch of channel slope and coordinate system for W2 where the x-axis is oriented along the channel slope.....	A-8
Figure A-8. Lateral average and deviation from lateral average components of longitudinal velocity.....	A-11
Figure A-9. Schematization for simplification of pressure term.	A-16
Figure A-10. Coordinate system without channel slope.....	A-18
Figure A-11. Coordinate system with channel slope.....	A-18
Figure A-12. Definition sketch for channel slope.	A-21
Figure A-13. Computational grid variable definitions for arbitrary channel slope.	A-22
Figure A-14. Transfer of mass and momentum between branches with unequal vertical grid spacing.....	A-23
Figure A-15. Linkage of tributary branch coming in at an angle to main branch.....	A-24
Figure A-16. Schematic of x and y velocity components.....	A-25
Figure A-17. Velocity variability with time.....	A-36
Figure A-18. Concentration variability with time.....	A-36
Figure A-19. Lateral average of the velocity field.....	A-38
Figure A-20. Lateral average of the concentration field.....	A-38
Figure A-21. Variable locations in computational grid.....	A-41
Figure A-22. ULTIMATE schematization for positive flow.	A-46

LIST OF FIGURES

Figure A-23. ULTIMATE schematization for negative flow.....	A-47
Figure A-24. Definition sketch for monotonic solution domain.....	A-49
Figure A-25. Comparison of UPWIND, QUICKEST, and ULTIMATE/QUICKEST schemes for conservative tracer transport.....	A-50
Figure A-26. Definition sketch for variable velocity.....	A-52
Figure A-27. Shear stress at the air-water surface.....	A-55
Figure A-28. Segment orientation.....	A-56
Figure A-29. Wind orientation.....	A-57
Figure A-30. Variation of turbulent vertical eddy viscosity for flow of $2574 \text{ m}^3 \text{ s}^{-1}$ flow down a channel of length 30 km and width of 100 m at $x=15 \text{ km}$	A-60
Figure A-31. Variation of turbulent vertical eddy viscosity for flow of $2574 \text{ m}^3 \text{ s}^{-1}$ flow down a channel of length 30 km and width of 100 m measured at $x=15 \text{ km}$	A-60
Figure A-32. Comparison of vertical velocity predictions of W2 model with various eddy viscosity models compared to theory.....	A-61
Figure A-33. Conceptual diagram of wind induced motion.....	A-61
Figure A-34. Mixing length as a function of depth for the Nikuradse formulation.....	A-66
Figure A-35. Variation of A_z with depth for the parabolic model of Englund (1976).....	A-67
Figure A-36. Variation of Manning's friction factor using formulae from Limerinos (1970) and Jarrett (1984) for a channel slope, S , of 0.0005 and 84^{th} percentile diameter of the bed material, d_{84} , of 50	A-69
Figure A-37. Comparison of vertical velocity predictions with one, three, and seven vertical layers.....	A-70
Figure A-38. Comparison of elevation drop of W2 model with one, three, and seven vertical layers with same Manning's friction factor.....	A-71
Figure A-39. Schematic of linkage of model segments with a culvert.....	A-72
Figure A-40. Linkage schematic of model segments with a culvert.....	A-75
Figure A-41. Computed versus observed flow using dynamic culvert model.....	A-75
Figure A-42. Schematic representation of internal weirs.....	A-76
Figure A-43. Tainter gate and spillway flow.....	A-77
Figure A-44. Flow rate over a spillway or weir for submerged and free flow conditions. A- 82	
Figure A-45. Flow rate variation with gate opening.....	A-85
Figure A-46. Selective withdrawal with outflow connected to a valve with a gate.....	A-86
Figure A-47. Schematic of branch connection.....	A-87
Figure A-48. Comparison of the wind speed formulation for Ryan-Harleman and W2 default (for $T_{\text{air}}=15^{\circ}\text{C}$, $T_{\text{dew}}=-5^{\circ}\text{C}$, $T_{\text{surface}}=25^{\circ}\text{C}$).....	A-92
Figure A-49. Schematic of solar altitude, A_o , and azimuth, AZ	A-95
Figure A-50. Schematic of topographic and vegetative shading, solar altitude (α_o), and vegetation height (T) and their affect on shadow length.....	A-96
Figure A-51. Azimuth angle, α_{AZ} , and stream orientation, Θ_o	A-98
Figure A-52. Relationship between azimuth, stream orientation, and shadow length. A- 98	
Figure B-1. Internal flux for generic constituent compartment.....	B-3
Figure B-2. Internal flux for coliform bacteria.....	B-4
Figure B-3. Internal flux for inorganic suspended solids.....	B-5
Figure B-4. Internal flux between labile DOM and other compartments.....	B-6
Figure B-5. Internal flux between refractory DOM and other compartments.....	B-7
Figure B-6. Internal flux between Labile POM and other compartments.....	B-8

LIST OF FIGURES

Figure B-7. Internal flux between refractory POM and other compartments.	B-9
Figure B-8. Internal flux between CBOD and other compartments.	B-10
Figure B-9. Internal flux between algae and other compartments.	B-11
Figure B-10. Internal flux between epiphyton and other compartments.	B-15
Figure B-11. Internal flux between phosphorus and other compartments.	B-20
Figure B-12. Internal flux between ammonium and other compartments.	B-22
Figure B-13. Internal flux between nitrate + nitrite and other compartments.	B-24
Figure B-14. Internal flux between dissolved silica and other compartments.	B-26
Figure B-15. Internal flux between particulate biogenic silica and other compartments. B-27	
Figure B-16. Internal flux between total iron and other compartments.	B-28
Figure B-17. Internal flux between dissolved oxygen and other compartments.	B-29
Figure B-18. Reaeration coefficient as a function of flow rate.	B-33
Figure B-19. Variation of wind speed and KL for lake/reservoir equations.	B-35
Figure B-20. Wind speed of 5 m s^{-1} and a fetch of 5 km corrected to 10 m as a function of measuring height on land.	B-36
Figure B-21. Wind speed of 5 m s^{-1} corrected to 10 m as a function of fetch.	B-36
Figure B-22. Wind corrected to 10 m based on wind measured on land.	B-37
Figure B-23. Variation of K_{LT}/K_{L20} as a function of temperature.	B-38
Figure B-24. Internal flux between 0-order sediment compartment and other compartments.	B-43
Figure B-25. Internal flux between 1st-order sediment compartment and other compartments.	B-43
Figure B-26. Internal flux between inorganic carbon and other compartments.	B-44
Figure B-27. Temperature rate multiplier function.	B-52
Figure C-1. Tree top elevation and vegetation offset from a river.	C-260
Figure C-2. The influence of topographic shading along a river.	C-262
Figure C-3. Topographic slices at three segments along a river.	C-262
Figure C-4. Diagram illustrating unstable water surface elevation solution.	C-330

List of Tables

Table 1. General guidelines for in-pool water quality sampling.....	17
Table 2. Constituent levels and names.	19
Table 3. Coefficients affecting thermal calibration.....	26
Table 4. Reservoir thermal simulations with error statistics for station closest to dam... 28	
Table A-1. Governing equations with and without channel slope.	A-20
Table A-2. Version 3 vertical eddy viscosity formulations.	A-58
Table A-3. HEC-RAS flow rates through weirs and sluice gates.....	A-78
Table A-4. List of weir types (French, 1985; USBR, 1999)	A-80
Table A-5. Typical Evaporation Formulae for Lakes and Reservoirs	A-92
Table A-6. Criteria for determining sunward bank	A-99
Table B-1. CE-QUAL-W2 V3.1 Water Quality State Variables.....	B-2
Table B-2. River reaeration equations.....	B-31
Table B-3. Lake reaeration equations as a function of wind speed at 20°C.....	B-33
Table B-4. Reaeration equations for estuarine waterbody at 20°C.....	B-37
Table B-5. Formulae for small dam or weir reaeration effects.....	B-39
Table B-6. Equations used in CRiSP model for gas production.....	B-40
Table B-7. Equations used in CRiSP model for gas production.....	B-40
Table B-8. Spillways and weirs reaeration.....	B-41
Table C-1. Vertical Eddy Viscosity Formulations.....	C-29
Table C-2. Equations used in CRiSP model for gas production.....	C-51
Table C-3. Equations used in CRiSP model for gas production at Columbia basin dams	C-52
Table C-4. Reaeration Effects of Spillways, Weirs, and Gates.....	C-52
Table C-5. Equations used in CRiSP model for gas production.....	C-62
Table C-6. Equations used in CRiSP model for gas production at Columbia basin dams	C-62
Table C-7. Reaeration effects of gates	C-63
Table C-8. Hydraulic Print Parameters.....	C-88
Table C-9. Extinction Coefficient Literature Values	C-137
Table C-10. <i>In Situ</i> Coliform Decay Rates	C-140
Table C-11. Gross Production Rates of Phytoplankton.....	C-142
Table C-12. Maximum Algal Excretion Rate Literature Values.....	C-144
Table C-13. Algal Dark Respiration Rate Literature Values.....	C-144
Table C-14. Algal settling Velocity Literature Values	C-145
Table C-15. Phosphorus Half-Saturation Constant Literature Values	C-146
Table C-16. Nitrogen Half-Saturation Constant Literature Values	C-146
Table C-17. Literature values for saturating light intensity	C-147
Table C-18. Labile DOM Decay Rate Literature Values.....	C-160

LIST OF TABLES

Table C-19. Detritus Decay Rate Literature Values	C-161
Table C-20. Detritus Settling Velocity Literature Values	C-161
Table C-21. Ammonium Decay Rate Literature Values	C-168
Table C-22. Sediment Oxygen Demand Literature Values	C-181
Table C-23. River Reaeration Equations.....	C-182
Table C-24. Lake, Reservoir, and Estuarine Reaeration Equations	C-183
Table C-25. Estuarine Reaeration Equations	C-184
Table C-26. Description of Dynamic Shading Input Variables	C-259

Model Package

All files on the CE-QUAL-W2 web site (<http://www.ce.pdx.edu/w2>) are archived in compressed zip files. To install CE-QUAL-W2, download the file "w2v3.zip" from the web site to a hard disk, copy over the compressed file "w2v3.zip" onto a hard disk and unzip the file. The "read me file for W2 v3-2.doc" file contains an explanation of the subdirectory structure and files that will be set up on the PC. The "manual.zip" file contains the User's Manual in PDF format and should also be downloaded. The "gui.zip" file includes a GUI preprocessor, a bathymetry editor, and a separate User's Manual for the GUI.

Several example applications are included in the subdirectory "EXAMPLES". The DeGray application is a reservoir with a single branch and a complete water quality application. The Spokane River is an example of a complicated river system with multiple river sections and run-of-the-river dams that flows into Long Lake, a deep-storage reservoir.

Programs

The following FORTRAN files are located in the SOURCE subdirectory:

```

PRE.F90      - preprocessor source code for use in a DOS or Unix environment
PRE_CVF.F90  - preprocessor source code for use in a Windows environment
PRE.EXE      - preprocessor executable for use in a DOS or Unix environment
PRE_CVF.EXE  - preprocessor executable for use in a Windows environment
W2.F90       - CE-QUAL-W2 source code for use in a DOS or Unix environment
W2_CVF.F90   - CE-QUAL-W2 source code for use in a Windows environment
W2.EXE       - CE-QUAL-W2 executable for use in a DOS or Unix environment
W2_CVF.EXE   - CE-QUAL-W2 executable for use in a Windows environment

```

The executables with the "CVF" in the filename are compiled with Compaq Visual FORTRAN and operate in a Windows environment. The `w2_cvf.exe` executable contains code that allows the user to view contour plots of hydrodynamic and water quality variables during program execution. The files without the "CVF" can be run in a DOS or Unix environment with simplified screen output. The `w2.exe` executable does not have code that uses the array visualizer features of the Compaq compiler.

Input Files

The following input files come with each application:

[w2_con.npt](#) - control file for each application

MODEL PACKAGE

[bth.npt](#) - bathymetry file
[met.npt](#) - meteorological file

A subset of the following input files comes with each application:

[qin_br1.npt](#) - inflows
[tin_br1.npt](#) - inflow temperatures
[cin_br1.npt](#) - inflow constituent concentrations
[qtr_tr1.npt](#) - tributary inflows
[ttr_tr1.npt](#) - tributary inflow temperatures
[ctr_tr1.npt](#) - tributary inflow constituent concentrations
[euh_br1.npt](#) - upstream head elevations
[tuh_br1.npt](#) - upstream head boundary temperatures
[cuh_br1.npt](#) - upstream head boundary constituent concentrations
[edh_br1.npt](#) - downstream head elevations
[tdh_br1.npt](#) - downstream head boundary temperatures
[cdh_br1.npt](#) - downstream head boundary constituent concentrations
[got_br1.npt](#) - outflows
[ext_wb1.npt](#) - light extinction
[qwd.npt](#) - withdrawals
[vpr.npt](#) - vertical profile at dam for specifying initial conditions
[lpr.npt](#) - longitudinal and vertical profiles specifying initial conditions for each cell
[wsc.npt](#) - wind sheltering
[shd.npt](#) - solar radiation shading
[qgt.npt](#) - gate flows/operation

If more than one branch or tributary is modeled, then corresponding files using "br2", "br3", etc. (or "TR2", "TR3", etc.) in the filename will also be included.

Output Files

The following output files come with each application:

[snp.sav](#) - snapshot output file in ASCII with interpretation of FORTRAN carriage control characters
[pre.sav](#) - preprocessor output file

The snapshot files are from a short run of the application. Use these files to ensure you obtain the same answers. The FORTRAN compiler used to make these test runs was Compaq Visual FORTRAN V6.6 setup as a QuickWin application using the following options:

```
/check:noflawed_pentium /compile_only /debug:none /fpconstant /include:"Release/"  
/libs:qwin /math_library:fast /nologo /real_size:64 /warn:noalignments /warn:nofileopt  
/warn:nouncalled /warn:nouninitialized /warn:nousage /fast /module:"Release/"  
/object:"Release/"
```

MODEL PACKAGE

The only other PC compiler that will compile the source code is University of Salford's FTN95 compiler, but the executable generated is about 30% slower than the Compaq compiler. Lahey and Absoft FORTRAN are unable to compile the latest version except only with no optimization.

A User's Forum has been set up on the web where support from the developers and other users can be obtained. The forum is located at <http://dneiper.ce.pdx.edu/w2/index.php>.

1 Introduction

Model Overview

CE-QUAL-W2 is a two-dimensional, longitudinal/vertical, hydrodynamic and water quality model. Because the model assumes lateral homogeneity, it is best suited for relatively long and narrow waterbodies exhibiting longitudinal and vertical water quality gradients. The model has been applied to rivers, lakes, reservoirs, estuaries, and combinations thereof.

The application of CE-QUAL-W2 requires knowledge in the following areas:

1. Hydrodynamics
2. Aquatic biology
3. Aquatic chemistry
4. Numerical methods
5. Computers and FORTRAN coding
6. Statistics
7. Data assembly and reconstruction

Water quality modeling is in many ways an art requiring not only knowledge in these areas but also experience in their integration. *A word of caution to the first time user* - model application is a complicated and time-consuming task.

Model Background

Version 1.0. CE-QUAL-W2 has been under continuous development since 1975. The original model was known as LARM (*L*aterally *A*veraged *R*eservoir *M*odel) developed by Edinger and Buchak (1975). The first LARM application was on a reservoir with no branches. Subsequent modifications to allow for multiple branches and estuarine boundary conditions resulted in the code known as GLVHT (*G*eneralized *L*ongitudinal-*V*ertical *H*ydrodynamics and *T*ransport Model). Addition of the water quality algorithms by the Water Quality Modeling Group at the US Army Engineer Waterways Experiment Station (WES) resulted in CE-QUAL-W2 Version 1.0 (Environmental and Hydraulic Laboratories, 1986).

INTRODUCTION

Version 2.0. Version 2.0 was a result of major modifications to the code to improve the mathematical description of the prototype and increase computational accuracy and efficiency. Numerous new capabilities were included in Version 2.0, including:

1. an algorithm that calculated the maximum allowable timestep and adjusted the timestep to ensure hydrodynamic stability requirements were not violated (autostep-ping)
2. a selective withdrawal algorithm that calculated a withdrawal zone based on outflow, outlet geometry, and upstream density gradients
3. a higher-order transport scheme (QUICKEST) that reduced numerical diffusion (Leonard, 1979)
4. time-weighted vertical advection and fully implicit vertical diffusion
5. step function or linear interpolation of inputs
6. improved ice-cover algorithm
7. internal calculation of equilibrium temperatures and coefficients of surface heat exchange or a term-by-term accounting of surface heat exchange
8. variable layer heights and segment lengths
9. surface layer extending through multiple layers
10. generalized time-varying data input subroutine with input data accepted at any frequency
11. volume and mass balances to machine accuracy
12. sediment/water heat exchange

Version 3.1. Version 3.1 is a result of additional improvements to the numerical solution scheme and water quality algorithms, as well as extending the utility of the model to provide state-of-the-art capabilities for modeling entire waterbasins in two-dimensions. The new capabilities include:

1. an implicit solution for the effects of vertical eddy viscosity in the horizontal momentum equation
2. addition of Leonard's ULTIMATE algorithm that eliminates over/undershoots in the transport solution scheme
3. inclusion of momentum transfer between branches
4. the ability to model multiple waterbodies in the same computational grid including multiple reservoirs, steeply sloping riverine sections between reservoirs, and estuaries
5. additional vertical turbulence algorithms for rivers
6. additional reaeration algorithms for rivers
7. variable vertical grid spacing between waterbodies
8. numerical algorithms for pipe, weir, spillway, and pump flow
9. internal weir algorithm for submerged or skimmer weirs
10. any number of user defined arbitrary constituents defined by a decay rate, settling rate, and temperature rate multiplier that can include
 - a. conservative tracers
 - b. coliform bacteria
 - c. water age
 - d. contaminants
11. any number of user defined phytoplankton groups
12. any number of user defined epiphyton groups
13. any number of user defined CBOD groups
14. any number of user defined inorganic suspended solids groups

15. dissolved and particulate biogenic silica
16. derived constituents such as total DOC, organic nitrogen, organic phosphorus, etc. that are not state variables
17. kinetic fluxes
18. graphical preprocessor

Version 3.2. Version 3.2 is a result of additional improvements to the model. These new capabilities include:

1. Internal code rewrite to reduce code size, simplify code maintenance, and improve model execution speed
2. New screen display during model run-time. The new screen display allows for controlling the processor usage, examining output variables, and stopping, starting and restarting a model run on the fly. This allows the model user to stop a code, then make changes in the control file or any input file, and then restart the model at the point that it was stopped.
3. Addition of a new algorithm to estimate suspended solids resuspension as a result of wind-wave action.
4. Reorganization of the graph.npt file to allow more output control formatting possibilities.
5. New turbulent kinetic energy-turbulent dissipation turbulence closure model was added to the model.

Manual

Organization. Chapter 1 consists of an introduction to the model and the user manual. Chapter 2 describes the model's capabilities and limitations. Chapter 3 provides an overview of the steps involved in applying the model including data preparation and model application.

The appendices provide the user with the information necessary to understand the model details. Appendix A describes the theoretical, numerical, and computational basis for the hydrodynamic portion of the model. Appendix B describes the theoretical and computational basis for the water quality algorithms. Appendix C describes input file preparation. References include a partial bibliography of CE-QUAL-W2 applications.

The following concepts have been used in the writing of the User's Manual:

1. Page headers are used to allow the user to easily find major areas in the manual.
2. Where applicable, paragraphs contain descriptive headings for easy reference.
3. Hyperlinks are used when related information is contained elsewhere.

Conventions. References to FORTRAN variables in the manual are made in English and are followed by their FORTRAN name enclosed by brackets (e.g., surface layer [KT]). The user need not first memorize the variable names to comprehend the manual. Potential problem areas in applying the model are emphasized with ***bold italic*** type.

2 Capabilities and Limitations

Capabilities

Hydrodynamic. The model predicts water surface elevations, velocities, and temperatures. Temperature is included in the hydrodynamic calculations because of its effect on water density and cannot be turned off.

Water quality. Any combination of constituents can be included/excluded from a simulation. The effects of salinity or total dissolved solids/salinity on density and thus hydrodynamics are included only if they are simulated in the water quality module. The water quality algorithm is modular allowing constituents to be easily added as additional subroutines. Version 3.2 includes the following water quality state variables in addition to temperature:

1. any number of generic constituents defined by a 0 and/or a 1st order decay rate and/or a settling velocity and/or an Arrhenius temperature rate multiplier that can be used to define any number of the following:
 - a. conservative tracer(s)
 - b. water age or hydraulic residence time
 - c. coliform bacteria(s)
 - d. contaminant(s)
2. any number of inorganic suspended solids groups
3. any number of phytoplankton groups
4. any number of epiphyton groups
5. any number of CBOD groups
6. ammonium
7. nitrate-nitrite
8. bioavailable phosphorus (commonly represented by orthophosphate or soluble reactive phosphorus)
9. labile dissolved organic matter
10. refractory dissolved organic matter
11. labile particulate organic matter
12. refractory particulate organic matter
13. total inorganic carbon
14. alkalinity
15. total iron
16. dissolved oxygen

17. organic sediments
18. gas entrainment

Additionally, over 60 derived variables including pH, TOC, DOC, TON, TOP, DOP, etc. can be computed internally from the state variables and output for comparison to measured data.

Long term simulations. The water surface elevation is solved implicitly, which eliminates the surface gravity wave restriction on the timestep. This permits larger timesteps during a simulation resulting in decreased computational time. As a result, the model can easily simulate long-term water quality responses. The vertical diffusion criteria from stability requirements has also been eliminated allowing for even larger timesteps.

Head boundary conditions. The model can be applied to estuaries, rivers, or portions of a waterbody by specifying upstream or downstream head boundary conditions.

Multiple branches. The branching algorithm allows application to geometrically complex waterbodies such as dendritic reservoirs or estuaries.

Multiple waterbodies. The model can be applied to any number of rivers, reservoirs, lakes, and estuaries linked in series.

Variable grid spacing. Variable segment lengths and layer thicknesses can be used allowing specification of higher resolution where needed. Vertical grid spacing can vary in thickness between waterbodies.

Water quality independent of hydrodynamics. Water quality can be updated less frequently than hydrodynamics thus reducing computational requirements. However, water quality is *not* decoupled from the hydrodynamics (i.e., separate, standalone code for hydrodynamics and water quality where output from the hydrodynamic model is stored on disk and then used to specify advective fluxes for the water quality computations). Storage requirements for long-term hydrodynamic output to drive the water quality model are prohibitive for anything except very small grids. Additionally, reduction in computer time is minimal when hydrodynamic data used to drive water quality are input every timestep.

Autostepping. The model includes a variable timestep algorithm that attempts to help ensure stability requirements for the hydrodynamics imposed by the numerical solution scheme are not violated.

Restart provision. The user can output results during a simulation that can subsequently be used as input. Execution can then be resumed at that point. Note that this feature has not been updated for the latest version but will be included in the next release.

Layer/segment addition and subtraction. The model will adjust surface layer and upstream segment locations for a rising or falling water surface during a simulation.

Multiple inflows and outflows. Provisions are made for inflows and inflow loadings from point/nonpoint sources, branches, and precipitation. Outflows are specified either as releases at a branch's downstream segment or as lateral withdrawals. Although evaporation is not considered an outflow in the strictest sense, it can be included in the water budget.

CAPABILITIES

Ice cover calculations. The model can calculate onset, growth, and breakup of ice cover.

Selective withdrawal calculations. The model can calculate the vertical extent of the withdrawal zone based on outlet geometry, outflow, and density.

Time-varying boundary conditions. The model accepts a given set of time-varying inputs at the frequency they occur independent of other sets of time-varying inputs.

Outputs. The model allows the user considerable flexibility in the type and frequency of outputs. Output is available for the screen, hard copy, plotting, and restarts. The user can specify what is output, when during the simulation output is to begin, and the output frequency. Version 3.1 now includes a graphical pre- and postprocessor for plotting/ visualization.

Details of these capabilities are discussed in Appendix C.

Limitations

Theoretical

Hydrodynamics and transport. The governing equations are laterally and layer averaged. Lateral averaging assumes lateral variations in velocities, temperatures, and constituents are negligible. This assumption may be inappropriate for large waterbodies exhibiting significant lateral variations in water quality. Whether this assumption is met is often a judgment call on the user and depends in large part on the questions being addressed. Eddy coefficients are used to model turbulence. Currently, the user must decide among several vertical turbulence schemes the one that is most appropriate for the type of waterbody being simulated. The equations are written in the conservative form using the Boussinesq and hydrostatic approximations. Since vertical momentum is not included, the model may give inaccurate results where there is significant vertical acceleration.

Water quality. Water quality interactions are, by necessity, simplified descriptions of an aquatic ecosystem that is extremely complex. Improvements will be made in the future as better means of describing the aquatic ecosystem in mathematical terms and time for incorporating the changes into the model become available in this one area. Many of the previous limitations have been addressed in the latest version. The following list describes the major assumptions in the water quality algorithms in the current version.

1. **no zooplankton.** The model does not explicitly include zooplankton and their effects on phytoplankton or recycling of nutrients.
2. **no macrophytes.** The model does not include the effects of macrophytes on hydrodynamics and water quality. In many cases, this is a good assumption. This will be added to the next model release though.
3. **simplistic sediment oxygen demand.** The model does not have a sediment compartment that models kinetics in the sediment and at the sediment-water interface. This places a limitation on long-term predictive capabilities of the water quality portion of the model. If sediments are modeled, then the model is more predictive; however, sediment oxygen demand is still modeled in a simplistic manner.

Future releases will include the following additional capabilities:

1. any number of macrophyte groups and their affects on hydrodynamics and water quality
2. any number of zooplankton groups
3. sediment diagenesis algorithm that will compute SOD and sediment to water column nutrient fluxes based on organic matter delivery to the sediments
4. sediment transport including both cohesive and non-cohesive sediments
5. toxics
6. k- ϵ turbulence algorithm
7. simultaneous water surface elevation solution among all branches in a waterbody
8. downstream segment addition/subtraction between a river and a reservoir and/or estuary
9. Parallel version for use on multiprocessor machines

Numerical

Solution scheme. The model provides three different numerical transport schemes for temperature and constituents - upwind differencing, the higher-order QUICKEST (Leonard, 1979), and Leonard's ULTIMATE algorithm. Upwind differencing introduces numerical diffusion often greater than physical diffusion. The QUICKEST scheme reduces numerical diffusion, but in areas of high gradients generates overshoots and undershoots which may produce small negative concentrations. ULTIMATE, Leonard's solution to the over/undershoots, has been incorporated into Version 3. In addition, discretization errors are introduced as the finite difference cell dimensions or the timestep increase. This is an important point to keep in mind when evaluating model predictions that are spatially and temporally averaged versus observed data collected at discrete points in time and space. A more thorough discussion of the numerical solution and its implementation is found in Appendix A.

Computer limits. A considerable effort has been invested in increasing model efficiency including a vertically implicit solution for vertical turbulence in the horizontal momentum equation. However, the model still places computational and storage burdens on a computer when making long-term simulations. Year long water quality simulations for a single reservoir now typically take less than 5 minutes on a 3 GHz Pentium. However, applications to dynamic river systems can take considerably longer because of much smaller timesteps needed for river numerical stability. Like nearly all new software currently being released, Version 3.1 has added additional computational burdens and memory requirements.

Input Data

The availability of input data is not a limitation of the model itself. However, it is most often the limiting factor in the application or misapplication of the model. This cannot be stressed enough. The user should always keep in mind the adage "garbage in equals garbage out".

3 Model Application

This chapter is intended to present the user with a general overview of the steps involved in a model application. The initial user should read the chapter once to gain a general understanding of these steps setting aside questions that might arise upon initial reading. The user should then reread the chapter and explore the hyperlinks to clarify any questions that arose during the first reading. Filenames are referred to generically (i.e., inflow file, outflow file, withdrawal file). Actual filenames are specified by the user in the control file.

Overview

Data Preparation

The following data are needed for model application:

1. geometric data
2. initial conditions
3. boundary conditions
4. hydraulic parameters
5. kinetic parameters
6. calibration data

A detailed discussion of these data follows.

Geometric Data

The first input task involves assembling geometric data. These data will be used to define the finite difference representation of the waterbody. The following data are needed for setting up input geometry:

1. topographic map and/or sediment range surveys
2. project volume-area-elevation table

The topographic map or sediment range surveys are used to generate bathymetric cross-sections that are input into the model. The project volume-area-elevation table is used for comparison with the volume-area-elevation table generated by the model.

Computational grid. The computational grid is the term used for the finite difference representation of the waterbody. Grid geometry is determined by four parameters:

DATA PREPARATION

1. longitudinal spacing (segment length) [DLX]
2. vertical spacing (layer height) [H]
3. average cross-sectional width (cell width) [B]
4. waterbody slope [SLOPE]

The longitudinal and vertical spacing may vary from segment to segment and layer to layer, but should vary gradually from one segment or layer to the next to minimize discretization errors.

Factors affecting computational grid. A number of factors must be evaluated and weighed against each other when determining longitudinal and vertical spacing. These include:

1. **Areas of strongest gradients.** This factor applies particularly to the metalimnion in freshwater and the pycnocline in saltwater. If the model is not capturing water quality gradients in these regions, then vertical resolution may have to be increased. Similar reasoning applies to areas of longitudinal gradients.
2. **Computational and memory requirements.** The model penalizes the user in two ways when increasing grid resolution. As the number of grid cells goes up, so do computational and memory requirements. In addition, as the dimensions of a grid cell **decrease**, the timestep must also decrease to maintain numerical stability. As a rule of thumb, it is always desirable to err on the side of greater grid resolution, but at some point the user must give way to the reality of the available computer resources and the money and time available for completing the project.
3. **Bottom slope.** For reservoirs and some estuaries, the waterbody bottom slope is more accurately modeled as the ratio of cell thickness to cell length $[H]/[DLX]$ approaches the overall bottom slope. For sloping streams/ivers, the ratio is accurately represented by the slope and is typically not of concern.
4. **Results.** Results should not be a function of the computational grid's resolution. With the development of the bathymetry editor, finely discretized grids can be easily coarsened. The coarser grid will have fewer computational cells and larger average timesteps resulting in decreased runtimes. The computational grid should initially be of high resolution and, if runtimes are excessive, reduced in resolution until the results change substantially. Results should never be a function of the grid resolution.

Previous applications have used a horizontal grid spacing of 100 to 10,000 *m* and a vertical grid spacing of 0.2 to 5 *m*. Regardless of the grid spacing used, the user should check to make certain that model predictions are grid independent. This is usually performed by making model simulations with varying grid resolution and using the largest grid that reproduces essentially the same results as those using the smallest grid.

Bathymetric data. The next step after determining horizontal and vertical cell dimensions is to determine average cross-sectional widths for each cell. This is an iterative procedure whereby initial bathymetry is input into the preprocessor and the volume-area-elevation table is then generated by the preprocessor. This table is compared to the project table and widths are adjusted to better match the project table.

Several methods have been used for determining average widths. Transects along the waterbody centerline can be drawn on a topographic map. A contour at the elevation corresponding to the *center* of a grid cell is located and the area encompassed by the contour line and the upstream and downstream

DATA PREPARATION

transect is determined by planimeter. This area divided by the segment length is the average width of the grid cell. The process is repeated for each grid cell.

When no topographic information is available, the user can determine average widths from sediment range surveys for existing waterbodies. However, this method is generally not as accurate as data obtained from topographic maps since the number of available transects are usually insufficient to adequately describe the complex shape of most waterbodies. If available, sediment range surveys should be used to refine the grid generated from topographic information - particularly where significant sedimentation has occurred.

Other methods by individual investigators have been developed for generating grids using contour plotting packages such as Surfer and AUTOCAD. Eventually, the preprocessor will incorporate an algorithm that will automatically generate the bathymetry based on lateral transects or x-y-z coordinate data.

Sample computational grid. A sample computational grid in the longitudinal/vertical plane with four branches is shown in [Figure 1](#). The FORTRAN variables associated with the grid are also included. The grid consists of 25 longitudinal segments [IMX] and 22 vertical layers [KMX]. They constitute the total number of cells in the computational grid. This is exactly how the model sees the grid layout even though this is not the correct physical representation of the system. In reality, branch two and branch three join branch one. Branch setup is described in more detail below.

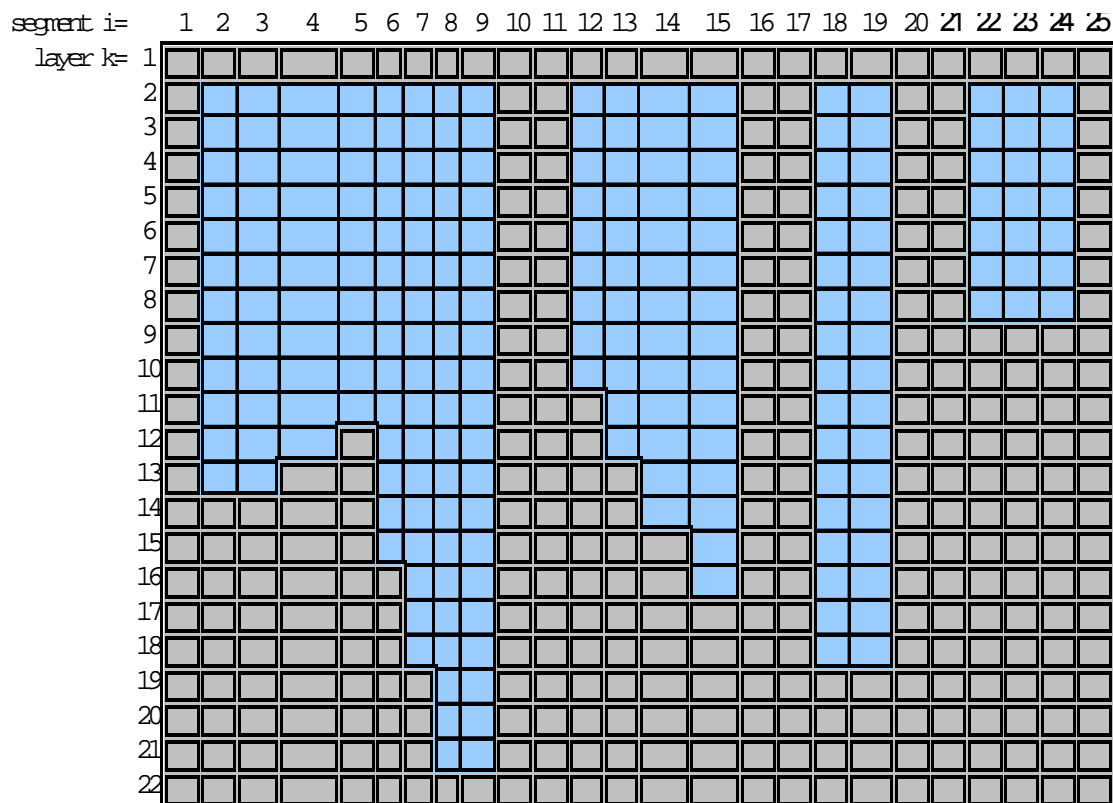


Figure 1. Sample computational grid in the x-z plane showing active and inactive cells.

DATA PREPARATION

Grid cell types. [Figure 1](#) contains two kinds of cells - ones with either a single or a double line border. Cells with a single line border represent cells that may contain water during the simulation. The *active cells* are defined in the bathymetry input as having *non-zero widths*. Cells with a double border represent boundary cells located at or beyond the waterbody boundaries. The *boundary cells* are defined in the bathymetry input as having *zero widths*.

Boundary cells. There are four types of boundary cells:

1. top
2. bottom
3. upstream
4. downstream

Each segment must have a zero width for the cell in layer 1 and a zero width for every cell located below the bottom active cell. For example, cells 1 and 12-22 in segment five would have zero widths. In addition, each branch must have zero widths for upstream boundary and downstream boundary segments. Note this requirement results in *two segments* of boundary cells between each branch (segments 10-11 & 16-17).

Branches. CE-QUAL-W2 can simulate a system with any number of waterbodies containing any number of branches. [Figure 1](#) shows a plan view of the same three branch grid of [Figure 1](#) along with the FORTRAN variables defining the geometry for each branch. For each branch, the upstream segment [US] and the downstream segment [DS] must be defined. The current upstream segment [CUS] is calculated by the model and may vary over time to meet restrictions imposed by the solution scheme.

A branch may connect to other branches at its upstream [UHS] and/or downstream segment [DHS]. In [Figure 1](#), the downstream segment of branch 2 ([DS]=20) connects to branch 1 at segment 3 ([DHS]=3).

DATA PREPARATION

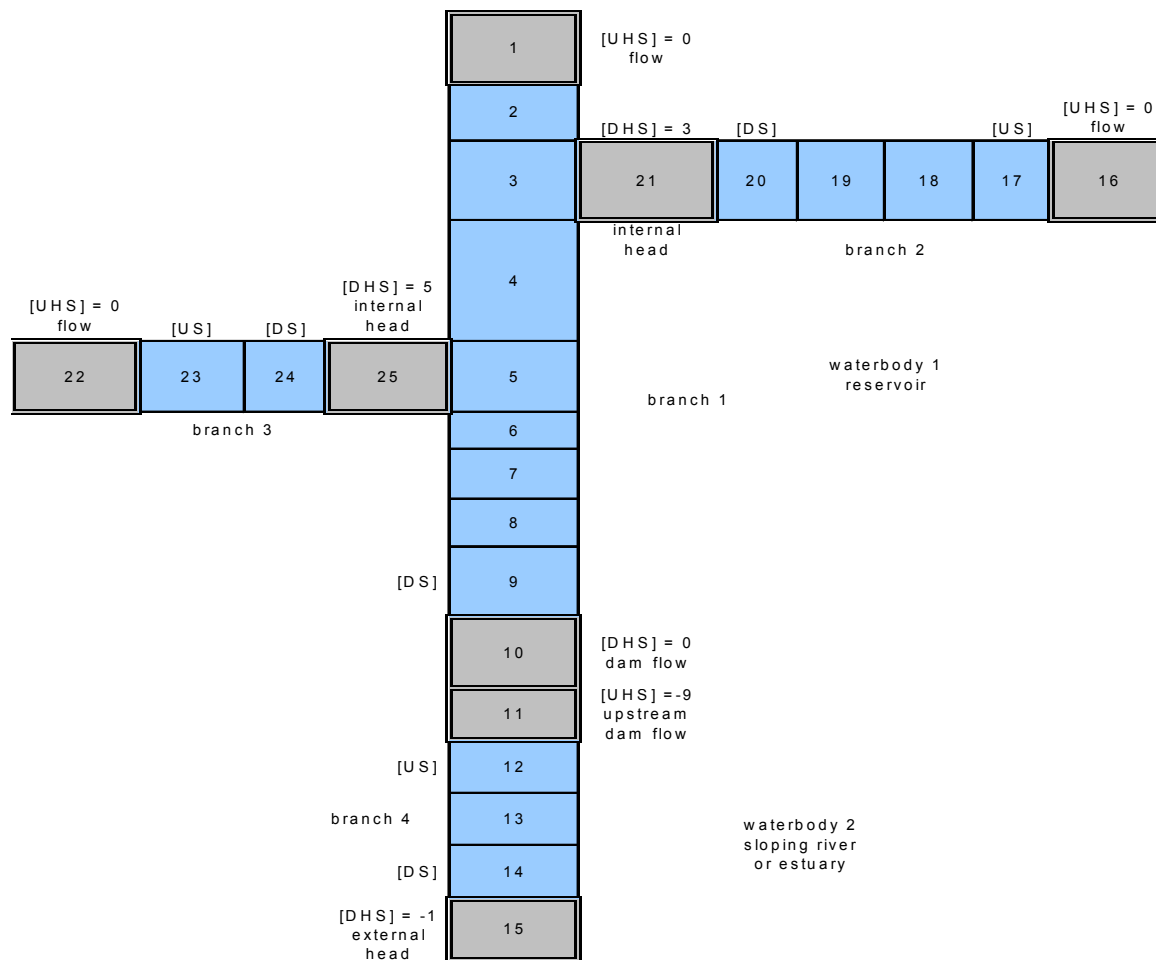


Figure 2. Sample computational grid in the x-y plane showing cell numbering and branch and water body connections.

Grid restrictions. The grid must satisfy the following restrictions:

1. Cell widths *cannot increase* with depth.
2. A **branch** may connect to other branches at its upstream or downstream segment, but a branch *may not enter or leave* itself.
3. Two branches may not connect at the same segment of another branch.

The bathymetry input file contains the longitudinal grid spacing **[DLX]**, initial water surface elevation **[WSEL]**, segment orientations **[PHI0]**, vertical grid spacing **[H]**, bottom friction **[FRICT]**, and average cell widths **[B]**.

After the bathymetry is generated, it should be checked to ensure the bottom elevation varies smoothly and represents the average slope over appropriate portions of the waterbody for reservoirs and estuaries. Oftentimes, minimum bottom widths are set at 5-15 m. This helps increase timesteps with minimal impact on the volume-area-elevation curves. However, increasing widths in the bottom layers can affect water quality since sediment oxygen demand and nutrient fluxes are dependent on

bottom surface areas. Refer to the [bathymetry file](#) and [preprocessor output](#) in the sample applications for additional guidance in setting up the bathymetry.

Initial Conditions

Initial conditions are specified in the control, bathymetry, and vertical and/or longitudinal profile input files. The control file specifies the following initial conditions:

1. **Time (required)**. Starting [\[TMSTRT\]](#) and ending time [\[TMEND\]](#) of the simulation.
2. **Temperatures (required) and concentrations** (optional). The initial temperature [\[IT2\]](#) and constituent concentrations [\[IC2\]](#). If the grid is not initialized to a single value, then a grid-wide vertical profile can be specified in the vertical profile input file [\[VPRFN\]](#). The option is also available to specify a longitudinally and vertically varying initial concentration for temperature and constituents via the longitudinal profile file [\[LPRFN\]](#).
3. **Inflows/outflows** (optional). The number and location of inflows and outflows.
4. **Restart** (optional). If a previous run with the model was made specifying restart conditions were to be written [\[RSOC\]](#) to an output file, then the user can specify the model read the file [\[RSIC\]](#) and continue the simulation from that point. This is not working in the current version, but should be updated sometime in the near future.
5. **Waterbody type (required)**. The waterbody can be specified as either saltwater or freshwater [\[WTYPE\]](#).
6. **Ice thickness** (optional). The initial ice thickness [\[ICETHI\]](#).

Boundary Conditions

Inflows. The model recognizes the following inflows:

1. **Upstream inflows** (optional). Upstream inflows occur only at a branch's current upstream segment [\[CUS\]](#), which may vary during a simulation. The model provides the option to distribute inflows evenly throughout the inflow segment or place inflows according to density [\[PQC\]](#). *If* the upstream inflow option is used, then a separate file for inflow [\[QIN\]](#), a separate file for temperature [\[TIN\]](#), and, *if* constituents are modeled, a separate file containing constituent concentrations [\[CIN\]](#) for *each* branch is required.
2. **Tributary inflows** (optional). Tributary inflows or point source loadings [\[QTR\]](#) may enter any segment of the computational grid. If the current upstream segment [\[CUS\]](#) number is greater than the segment the tributary enters, then the tributary inflows are added into the current upstream segment to maintain the waterbody water balance. As in upstream inflows, the model provides the option to distribute tributary inflows evenly throughout the inflow segment or place inflows according to their density [\[PTRC\]](#). An additional option to place inflows between two specified elevations is also included to better describe point source inflows such as wastewater effluent discharged from a pipe. The number of tributaries [\[NTR\]](#) and their segment location [\[ITR\]](#) are specified in the control file. *If* this option is used, then file requirements for *each* tributary are the same as for upstream inflows.
3. **Distributed tributary inflows** (optional). Distributed tributary inflows or nonpoint source loadings [\[DTRC\]](#) may be specified for any branch. The flow is distributed

DATA PREPARATION

throughout a branch weighted by segment surface areas. *If* this option is used, then file requirements for *each* distributed tributary are the same as for upstream inflows.

4. **Precipitation** (optional). Precipitation [**PRC**] can be specified for each branch and is distributed according to the segment surface areas. *If* this option is used, then file requirements for *each* branch are the same as for upstream inflows.
5. **Internal inflows** (optional). Flows from gates, pipes, and pumps and over spillways and weirs can now be routed internally in the computational grid from one segment to another. This allows application of the model to highly engineered systems.

Outflows. The model recognizes the following outflows:

1. **Downstream outflows** (optional). Downstream outflows [**QOUT**] occur only at the downstream segment [**DS**] of a branch. Selective withdrawal where the vertical extent of and flow distribution in the withdrawal zone is calculated by the model is used for all outflows. Additionally, the bottom [**KBSTR**] and top layers [**KTSTR**] below and above which outflow cannot occur can be specified by the user to include the effects of upstream structures that restrict the selective withdrawal zone. Outflow will occur even if the outlet location is above the current water surface layer [**KT**]. This is a necessity when calibrating water surface elevations. A separate file for *each* branch is required.
2. **Lateral withdrawals** (optional). Lateral withdrawals [**QWD**] may be specified for any active cell. The number of withdrawals [**NWD**], their segment location [**IWD**], and their centerline elevation [**EWD**] must be specified in the control file. *If* this option is used, a separate file for *each* withdrawal is required. Version 3 now uses selective withdrawal for lateral withdrawals.
3. **Evaporation** (optional). Evaporation is calculated by the model from air [**TAIR**] and dewpoint [**TDEW**] temperature and wind speed [**WIND**]. If a waterbody loses a significant amount of water from evaporation that is not accounted for in the inflows, then the user should include evaporation. Evaporative heat loss is *always* included in the heat budget.
4. **Internal outflows** (optional). Flows from gates, pipes, and pumps and over spillways and weirs can now be routed internally in the computational grid from one segment to another. This allows application of the model to highly engineered systems.

Head Boundary Conditions (optional). The model recognizes the following head boundary

1. **External.** The user may specify an external upstream [**UHS**] and/or downstream head [**DHS**] boundary condition for each branch. This boundary specification is intended primarily for estuarine simulations although it has also been used for river and reservoir applications. *If* this option is used, a separate file for time-varying elevations, [**EUH**] and/or [**EDH**], a separate file for vertical temperature profiles, [**TUH**] and/or [**TDH**], and, if constituents are modeled, a separate file containing vertical profiles for each constituent modeled, [**CUH**] and/or [**CDH**], *must* be specified for *each* external head boundary condition.
2. **Internal.** Internal head boundary conditions are specified wherever one branch connects with another branch. The boundary surface elevation, temperatures, and constituent concentrations are calculated internally by the model.

Surface Boundary Conditions (required). The model requires the following surface boundary conditions:

1. **Surface heat exchange.** Surface heat exchange is calculated by either of two methods using the input variable [SLHTC] in the control file. The first method uses equilibrium temperatures [ET] and coefficients of surface heat exchange [CSHE] to calculate surface heat exchange (Brady and Edinger, 1975). The second method uses a term-by-term accounting for calculating surface heat exchange. For both methods, latitude [LAT] and longitude [LONG] are specified in the control file and values for air temperature [TAIR], dew point temperature [TDEW], wind speed [WIND] and direction [PHI], and cloud cover [CLOUD] *must* be included in the meteorological file. If available, short wave solar radiation can be input directly into the model.
2. **Solar radiation absorption.** Distribution of solar radiation in the water column is controlled by the fraction of solar radiation absorbed in the surface layer [BETA] and the attenuation rate due to water [EXH2O], inorganic suspended solids [EXINOR], and organic suspended solids [EXORG]. Values for [EXINOR] and [EXORG] affect solar radiation only if constituents are modeled. These values are specified in the control file.
3. **Wind stress.** Wind speed [WIND] and direction [PHI] must be supplied in the meteorological file [METFN]. Wind stress is an extremely important physical process and should be included in all applications. The model allows the user to specify a wind sheltering coefficient [WSC] which, when multiplied with the wind speed, reduces effects of the wind to take into account differences in terrain from the met station and the prototype site. The sheltering coefficient is specified in the wind sheltering file [WSCFN].
4. **Gas exchange.** The wind speed [WIND] supplied in the meteorological file is also used for computing gas exchange at the water surface if dissolved oxygen and/or total inorganic carbon are simulated. Gas exchange is also affected by the wind sheltering coefficient [WSC].

Temperature transport cannot be turned off in the model. Temperature can be treated conservatively by turning off heat exchange computations [HEATC].

Hydraulic Parameters (required)

Dispersion/diffusion coefficients. The horizontal dispersion coefficients for momentum [AX] and temperature/constituents [DX] are specified in the control file. They are presently time and space invariant. Sensitivity analyses on numerous applications have shown the model is relatively insensitive to variations in the default values for reservoirs, but can be important in rivers and estuaries.

The vertical diffusion coefficients for momentum [AZ] and temperature/constituents [DZ] vary in space and time and are computed by the model. The current version allows for a number of different vertical turbulence algorithms for sloping river sections and estuaries. Work is underway on a $k-\epsilon$ vertical turbulence algorithm that will hopefully replace the various options now available.

Bottom friction. The latest version now allows the user the option of specifying longitudinally varying values for the Chezy coefficient or Manning's N for bottom friction. The friction type is specified in the control file [FRICC]. They are used in calculating boundary friction that varies spatially as

DATA PREPARATION

a function of exposed bottom area and temporally as a function of the flow field. The values are specified in the bathymetry file.

Kinetic Parameters (optional)

There are more than 120 coefficients affecting constituent kinetics, although less than 10 are normally adjusted during water quality calibration. The values are specified in the control file. If simulations include water quality, then the user should see [Appendix C](#) for a detailed discussion of these coefficients.

Calibration Data (required)

Calibration data are used to provide initial and boundary conditions and assess model performance during calibration. A great deal of thought should go into assessing the amount and type of data necessary to adequately characterize and understand the limnology of a waterbody and to develop the database required to support a water quality modeling effort. Gaugush (1986; 1987; 1993) provides detailed information on sampling design and frequency. *Determining the availability of adequate calibration data should be done as early in the study as possible.* If the user determines calibration data are inadequate, then immediate steps should be taken to collect sufficient data. Results will be suspect at best and will not withstand scrutiny at worst if the model is applied with insufficient and/or inadequate calibration data. The following discussion provides an overview of data required for the proper application of CE-QUAL-W2.

In-Pool. Proper application of mechanistic water quality models requires at least one set of in-pool observed data. The preferred method is *at least* two sets of data encompassing different extremes in the prototype (i.e., high and low flow years, warm and cold years, spring phytoplankton bloom and no spring phytoplankton bloom, etc.). In-pool data is used to set initial conditions and assess the model's ability to reproduce observed conditions. Given sufficient time and funding, *all years* in which sufficient data are available should be included during model calibration.

Time-Varying Boundary Conditions. It cannot be overemphasized that data used to drive the model needs to be as accurate as possible. For temperature calibration, this typically means using continuous inflow temperatures or developing regression relationships for inflow temperatures based on flow and air or equilibrium temperature to generate at least daily inflow temperatures (see Ford & Stein, 1984). Equilibrium temperature is preferred since it includes more of the mechanisms affecting water temperature.

For meteorological data, use the most frequent data available. Previously, daily average values were used to drive the model because earlier 1-D models used daily timesteps. Many modelers still take hourly or three-hourly data and generate daily averages for model input. *Any time data is averaged, information is lost.* For most reservoirs, thermocline depth and shape are a function of two physical mechanisms - wind mixing and convective cooling. Using daily average air temperatures eliminates nighttime convective mixing that can be a very important physical process affecting epilimnetic depths and thermocline shapes for reservoirs. As another example, applying a daily average wind speed and direction can generate an artificial water surface slope that incorrectly drives hydrodynamics. Daily averaging of wind speeds can also result in much less energy input into the model since the energy input by wind is a function of the wind speed cubed.

DATA PREPARATION

For water quality simulations, it is important the user provide accurate initial and time-varying boundary conditions. If nutrient loadings are not adequately characterized, then it will be impossible for the model to accurately reproduce phytoplankton/nutrient/DO dynamics. It is a waste of time and effort to collect in-pool data in support of water quality modeling when inflow concentrations/loadings have not been adequately characterized since they often drive the system. As in the development of inflow temperatures, regressions relating concentration/loadings with flow and possibly refined for season should be developed for tributary inflows. Ideally, several storm events should be intensively sampled since this is when loadings are generally highest to a waterbody. Also, point source loadings should be identified and loading estimates obtained. Some estimate of non-point source loadings should also be made. In some cases, meteorological loading estimates should be obtained. A software package, FLUX (Walker, 1986), is useful for generating loadings over time from intermittent samples. [Table 1](#) gives general guidelines for data collection.

Kinetic Rates. Because water quality modeling is still very much an art with numerous rate coefficients available for adjustment during calibration, it is highly preferable to obtain actual measurements of these coefficients used in the water quality formulations. If all of the rate coefficients have been determined for a waterbody, then any discrepancies between computed and observed data highlight the model's shortcomings, help to identify the bounds of the model's predictive capabilities, and provide direction for efficient use of resources to provide a better understanding of the system's water quality dynamics.

Ideally, a model should be used as a starting point for limnological investigations of a waterbody, with the data and formulations continuously refined to reflect the increased understanding of the system and processes gained over time. Unfortunately, this approach is rarely taken in practice due in large part to the expense involved, but also, even more unfortunately, due to the inability of aquatic biologists/limnologists and engineers to collaborate.

This cooperative approach between experimentalists and theoreticians is the main impetus behind the tremendous advances in physics, chemistry, and, to some extent, biology (e.g., genetic research) during the last century, but is seldom seen in the field of water quality modeling. A notable exception is the Chesapeake Bay Modeling Study (Cercio and Cole, 1994). Researchers in the Chesapeake Bay region, including both biologists and engineers, were actively involved in data acquisition and water quality formulations and provided invaluable knowledge and feedback during the course of the study. This cooperative arrangement is continuing and should be a model for all future water quality model development.

Table 1. General guidelines for in-pool water quality sampling.

Boundary Conditions		
Minimum parameters	Additional parameters	Frequency
inflow/outflow temperature	conductivity dissolved oxygen pH total dissolved solids ¹	daily or continuous
total organic carbon	dissolved and/or particulate organic carbon BOD ²	weekly w/ storm sampling
soluble reactive phosphorous total phosphorous	total dissolved phosphorus total inorganic phosphorus dissolved inorganic phosphorus	weekly w/ storm sampling

DATA PREPARATION

nitrate+nitrite nitrogen ammonium nitrogen	total Kjeldahl nitrogen filtered total Kjeldahl nitrogen	weekly w/ storm sampling
	total suspended solids ³ inorganic and/or volatile suspended solids	weekly w/ storm sampling
	chlorophyll a dissolved silica ⁴ alkalinity	weekly w/ storm sampling
In-Pool		
Minimum parameters	Additional parameters	Frequency
Temperature ⁵ Dissolved oxygen ⁵ pH ⁵ Conductivity ⁵	total dissolved solids ¹	monthly ⁶
Chlorophyll a ⁷	phytoplankton biomass and type	monthly
Total organic carbon ⁷	dissolved and/or particulate organic carbon BOD ²	monthly
Soluble reactive phosphorus Total phosphorus ⁷	total dissolved phosphorus total inorganic phosphorus dissolved inorganic phosphorus	monthly
nitrate + nitrite nitrogen ammonium nitrogen ⁷	total Kjeldahl nitrogen filtered total Kjeldahl nitrogen	monthly
	secchi depth/light transmission	monthly
	total inorganic carbon alkalinity	monthly
	total suspended solids ³ inorganic and/or volatile suspended solids	monthly
	dissolved/total iron ⁸ dissolved/total manganese ⁸ dissolved/total silica ⁸ total dissolved sulfide ⁸ sulfate ⁸ iron sulfide ⁸	monthly
¹ enough samples to correlate to conductivity - important for density effects ² used to characterize decay rates of organic matter ³ suspended solids affect phosphorus partitioning, light penetration, and density ⁴ can be limiting for diatom growth ⁵ preferably bi-weekly - samples should be taken at 1m intervals ⁶ 1m intervals ⁷ minimum number of samples includes one each in epilimnion, metalimnion, and hypolimnion - preferred number of samples (depending on depth) would be at 3m intervals with more frequent metalimnetic sampling ⁸ when concerned about sediment release during anoxic periods		

Since water quality compartments are coupled, calibration of one compartment may affect other compartments making calibration difficult. *An understanding of the processes modeled as well as knowledge of the system being simulated is an absolute must if the modeling effort is to succeed.* A complete description of kinetic coefficients along with guidelines for appropriate default and a range of literature values is given in Appendix C.

Constituents are grouped into four levels ([Table 2](#)). Level **I** includes constituents that have no interaction with phytoplankton/nutrient/DO dynamics. Level **II** includes constituents affecting phytoplankton/nutrient/DO dynamics. Level **III** includes constituents that interact with level II constitu-

entnts, but that are not transported. In level **IV**, alkalinity and total inorganic carbon are transported by the model and are thus state variables. They are necessary for computing pH and carbonate species.

Table 2. Constituent levels and names.

Level	Constituent
I	Total dissolved solids (or salinity)
	Generic constituents
	Inorganic suspended solids
II	Dissolved inorganic phosphorus
	Ammonium
	Nitrate-nitrite
	Dissolved silica
	Particulate biogenic silica
	Total Iron
	Labile DOM
	Refractory DOM
	Labile POM
	Refractory POM
	CBOD
	Dissolved oxygen
	Phytoplankton
III	Epiphyton
	Organic sediments
IV	Total inorganic carbon
	Alkalinity

The user should spend time familiarizing himself with the water quality formulations in [Appendix B](#) taking note of the assumptions used.

Data Analysis. An often overlooked step in model applications is plotting and analyzing observed data for all stations and times for which data are available. Do not plot up just the data chosen for calibration as the additional data may reveal important information about the prototype. Unfortunately, most mechanistic water quality modelers come from an engineering background with only cursory exposure to limnology. If a limnologist is available, they should be consulted during this stage to help in identifying the dominant processes occurring in the system. Once these have been identified, then efforts should be made to ensure the dominant forcing functions are represented as accurately as possible in the model, either as accurate boundary conditions or as additional water quality formulations.

For example, phosphorus coprecipitation with calcite is not currently included in the model. If this is known to be an important mechanism for phosphorus removal from the photic zone resulting from pH changes due to phytoplankton primary production, then this mechanism should be included in the kinetic formulations. This is a common mechanism for many freshwater systems located in limestone topography, such as Texas, Tennessee, and Florida. Another example would be the presence of macrophytes that affect hydrodynamics, nutrient uptake rates, phytoplankton primary production, and

CALIBRATION

water column oxygen dynamics. Since macrophytes are not in the current release, then they would have to be included in the hydrodynamic and kinetic formulations.

Another important task in data development and analysis is to analyze the data for reasonableness. Checks for reasonableness should go beyond outlier checks to include checks to see if changes in concentrations over space and time make limnological sense. For example, if reservoir hypolimnetic nitrate concentrations increase during anoxic conditions and inflow temperatures are warmer than epilimnetic temperatures and/or inflow nitrate concentrations are less than the hypolimnetic concentrations, then there is no way for nitrate concentrations to increase during this time in either the prototype or in the model. So, there is no use wasting time during calibration trying to reproduce this behavior and the failure of the model to reproduce this behavior should not be viewed as a shortcoming of the model. Another example would be observed reservoir hypolimnetic release temperatures that were greater than the hypolimnetic temperatures. It would be impossible for the model to match these temperatures during calibration

Simulations

Once the necessary data have been assembled into proper input format, then simulations can begin. This section describes the recommended steps for obtaining meaningful model results.

Model Preparation

Input checks. A preprocessor program, `pre.exe`, performs checks of the control file for many errors that can be detected by the preprocessor. Errors are written to the file [PRE.ERR](#) and warnings are written to the file [PRE.WRN](#). If no errors are detected, then input from the control file is written to the file [PRE.OPT](#). All errors should be corrected before proceeding any further. Warnings should be investigated to ensure that what is being input into the model is what is intended. The preprocessor should be run periodically during the calibration phase to ensure that errors have not been introduced into the input files. However, do not assume that all is necessarily well if no warnings or errors are reported.

Additionally, the user should check preprocessor output against inputs to ensure they are correct. Further evaluation of control file input data must be performed by the user to ensure data the user thinks he has input into the model is what the model is actually receiving. Additionally, *all* time-varying input data should be plotted and screened for errors. These plots will need to be included in any final report and can eliminate a number of problems early on in the project.

Calibration

The next step is to begin calibration runs. Much of the literature refers to this step as calibration and verification in which model coefficients are adjusted to match an observed data set (calibration) and then the model is run on another “independent” data set without adjusting model coefficients to see if the model reproduces observed data in the prototype (verification in most circles, but variously called confirmation, validation, substantiation, etc. as numerous water quality modelers object to the word verification).

CALIBRATION

This separation is artificial and wrong. If a model does not reproduce observed data (and, more importantly, trends in data) for the "verification" data, then any good modeler will adjust coefficients, review model assumptions, include new processes, or collect additional data to adequately match both sets of data. Often, application to additional sets of data improves the fit to the first. The artificiality of this concept has led to applications in which modelers have used May, June, and July data for "calibration" and August, September, and October data of the same year for "verification" so they can state the model has been "calibrated/verified".

The following examples will further illustrate the artificiality of the current concept of "calibration/verification". Consider the following summary of observed data.

Year	Flow	Stratification	Fall algal bloom	Minimum DO at dam
1989	high	weak	yes	0 ppm
1990	low	strong	no	3 ppm
1991	average	medium	yes	1 ppm
1992	average	medium	yes	1 ppm
1993	low	strong	yes	1 ppm
1994	high	weak	no	3 ppm

Based on the currently accepted definition of calibration/verification, which of the years should be chosen for calibration and which should be chosen for verification? A case could be made for 1989 for calibration and 1994 for verification because of a fall phytoplankton bloom in 1989 and its absence in 1994. Additionally, the minimum dissolved oxygen at the dam was different between the years. If the model were to reproduce this behavior, then confidence could be placed in the model's ability to reproduce dissolved oxygen and phytoplankton blooms for the correct reasons. However, both years were years of high flow and using them would not test the model's ability to reproduce prototype behavior under different flow regimes.

Cases could be made for other combinations of calibration/verification years and different modelers would probably choose different calibration/verification years, so there doesn't appear to be one "correct" answer. In actuality, there is a correct answer. Model all the years and model them continuously. Modeling them continuously would eliminate separate calibration and verification years or data sets so the model could not be considered "calibrated and verified". However, if the model reproduces the wide variation in prototype behavior between all the years, a lot more confidence can be placed in the model's ability to reproduce prototype behavior for the "right" reasons than if the model were calibrated for one year and verified for another year.

Another example of the problems with the currently accepted "calibration/verification" approach to establishing model credibility is illustrated in the following table.

Year	Dominant algae	Flow	Minimum DO at dam
1979	diatoms	average	5 ppm
1986	greens	average	3 ppm
1994	bluegreens	average	0 ppm

Which year should be used for calibration and which year should be used for verification? Again, the best approach would be to model all three years, but since data do not exist for all the intervening years from 1979 to 1994, the simulation could not be continuous. An analysis of the data indicates a clear progression of eutrophication from 1979 to 1994 based on phytoplankton progression and increasing hypoxia. According to the current concept of "calibration/verification", all kinetic coeffi-

CALIBRATION

coefficients should be the same for all simulation years. However, the different dominant phytoplankton groups will have different growth, mortality, respiration, excretion, and settling rates and different light and nutrient growth rate half-saturation constants between the years. Keeping these values constant between calibration years would fly in the face of reality.

Additionally, the sediment oxygen demand has clearly changed because of eutrophication, so the values used in the zero-order sediment compartment should be different for the three years. As can be seen from just these two examples, all years should be considered calibration years and rate coefficients in some cases should change between different calibration data sets if the prototype is to be represented accurately.

Another concept associated with “calibration/verification” of a model is a post audit. Post audits are recommended whenever management changes are made as a result of modeling studies. A post audit involves making the management changes and then collecting data to see if the hoped for changes in prototype behavior based on model guidance have taken place. This appears to be a very reasonable concept and straightforward test of a given model’s simulation capabilities and, if the hoped for changes occur, then a great deal of confidence can be placed in the model’s simulative capabilities.

But what if the changes in water quality such as an improvement in minimum dissolved oxygen or extent of hypoxia does not occur? Can one then conclude that the model is not very good and little confidence can be placed in model results? The answer is no and the reason why is that no model can be used to predict the future. A model can only be used to determine what might have occurred if a particular set of boundary forcing functions were to occur in the prototype.

For example, hypoxia in Chesapeake Bay is a result of not only nutrient and organic matter loading, but also the degree of stratification that inhibits vertical mixing and reaeration. The degree of stratification is in large part a function of freshwater inflow. The higher the inflow, the greater the areal extent of density stratification in the Bay resulting in a greater areal extent of hypoxic waters. Suppose a model of the Bay “predicted” that a 40% nitrogen loading reduction decreased the areal extent of hypoxia by 20%. Based on this result, loadings were then reduced by 40% for five years and hypoxia did not decrease but actually increased during this time period.

Since the exact opposite occurred from what the model predicted, can the modeling study be concluded to be a failure? The answer is no. Suppose that the model results assume average freshwater river inflows and the five years after implementing loading reductions were high flow years, which increased the extent of hypoxia compared to an average flow year due strictly to physical effects. The only way to tell if the conclusions based on the model study were erroneous would be to model the five years using observed boundary conditions for this period and see if the model reproduced the observed increase rather than decrease in hypoxia. Thus, if a post audit yielded water quality different from expected water quality based on model results, this has no reflection on a given model’s ability to reproduce water quality in the prototype. Again, models cannot be used to predict the future, only what might have been.

Ideally, calibration should involve multiple data sets encompassing as many variations and extremes as possible in the prototype. A model’s ability to reproduce prototype behavior under a variety of conditions gives the modeler more confidence in the model’s ability to accurately simulate the prototype under proposed conditions. To put it very simply, a model is a theory about behavior in the real world. A theory is continuously tested against *all* observed data, and, if it does not match the data,

then the theory should either be modified or a new one developed that more closely agrees with observed data.

Model data/comparison. The model produces the following output files for displaying results:

1. [Profile file \[PRFFN\]](#). This file is used to plot observed versus predicted vertical profiles for temperature and constituents at a given segment.
2. [Time series file \[TSRFN\]](#). This file is used to plot time histories of water surface elevations, flows, temperatures and constituent concentrations for user specified computational cells. This file also contains information to plot out the time history of the variable timestep and average timestep.
3. [Contour plot file \[CPLFN\]](#). This file is used to plot contours of temperature and constituents along the waterbody length.
4. [Vector plot file \[VPLFN\]](#). This file is used to plot velocity vectors determined from horizontal and vertical velocities. The output is useful in analyzing flow patterns in the waterbody.
5. [Spreadsheet file \[SPRFN\]](#). This file is similar to the profile except the output is suitable for importing into a spreadsheet type database for subsequent plotting.

A description of the output from each file and how to use the information is given in [Appendix C](#). The current release version requires the user to develop plotting capabilities from these files. This is most often done using the [spreadsheet output file](#) and [time series output file](#) and developing macros to process the data.

Calibration is an iterative process whereby model coefficients are adjusted until an adequate fit of observed versus predicted data is obtained. Unfortunately, there are no hard and fast guidelines for determining when an adequate fit is obtained. The user must continually ask himself "is the model giving useful results based on model formulations, assumptions and input data?". If it is not, then the user must determine if the inability of the model to produce useful results is due to the use of the model in an inappropriate manner (i.e., hydrostatic approximation is invalid, one phytoplankton group is not sufficient to capture phytoplankton/nutrient/DO interactions, wind speed function for evaporation is inappropriate for the waterbody, etc.), model formulations are insufficient to describe known prototype behavior, or if input data are insufficient to describe the system dynamics.

Another important point to keep in mind during calibration is that a model may give inadequate results for a given spatial and/or temporal scale, but at another scale may reasonably represent the dynamics of the prototype. For example, the model may fail to predict a short-term phytoplankton bloom using monthly inflowing phytoplankton and nutrient concentrations, but may adequately represent phytoplankton production over the summer stratification period. The model may thus be useful in determining a waterbody's long-term response to nutrient loading reductions but be inadequate in addressing short-term responses to a nutrient reduction strategy. In summary, it is not always necessary for model output to match all of the observed data for the model to provide meaningful results.

The usual sequence for calibration is to first calibrate the water budget (or water surface elevation), then calibrate temperature (preferably salinity for estuarine applications), and finally water quality. Keep in mind water quality calibration can affect temperature/salinity calibration. A description of each follows. Calibration is separated into different sections for river, lake/reservoir, and estuarine applications.

CALIBRATION

Lake/Reservoir

Water budget

The water budget is checked by comparing predicted elevations with observed elevations. Errors in the water budget are generated by the following:

1. **Incorrect bathymetry.** The user should carefully check the volume-area-elevation table produced by the model to ensure it closely matches the project volume-area-elevation table. If it does not, then the bathymetry should be checked carefully to ensure there are no errors. In some cases, additional sediment range surveys may be necessary to adequately define the bathymetry. It may also be necessary to include branches that were not included in the initial bathymetry. Also, keep in mind that development of the original volume-area-elevation table was subject to the same errors used in developing the volume-area-elevation table for the application. In some applications, the new volume-area-elevation table was deemed more accurate than the original.
2. **Storm events.** Errors in the water budget due to storm events can be determined by comparing predicted with observed elevations using output from the time series plots. If the error is generated during storm events, then the user should check to see if precipitation must be included and/or if more tributaries need to be included than were originally specified. The user may need to use a hydrologic model to determine inflows during storm events for ungaged tributaries. An alternative method is to apportion inflows for ungaged tributaries based on their watershed areas.
3. **Incomplete inflow data.** A substantial amount of inflow is often unaccounted for when using gauged inflows. The unaccounted inflows can include minor tributary, precipitation, stormwater, and wastewater treatment plant contributions. The distributed tributary option provides the user with a means to account for these contributions. This option distributes inflows into every branch segment weighted by the segment surface area.
4. **Evaporation.** If evaporation in the region is significant and is not accounted for in inflows, then it should be included using the evaporation option [\[EVC\]](#).
5. **Seepage.** Seepage gains or losses can be significant for some waterbodies. The model does not explicitly handle seepage at present, but the coding is such that seepage can be readily included in the calculations as an additional rate term in the flow source/sink array [QSS]. Several applications required specifying seepage losses through the dam in order to properly calibrate temperature.
6. **Inaccurate Inflow/Outflow Measurements.** Gauged inflows and reservoir outflows are notoriously inaccurate with typical measurement errors of 5-10%. The model is very sensitive to inflow/outflow error measurements that can result in significant errors in water level predictions.

Typically, the user will first plot observed versus predicted water surface elevations for the simulation period after all the inflow/outflow data have been collected and the model is running to completion. The latest version contains a program for computing reservoir water balances that will initially compute the additional flows necessary for reproducing observed water surface elevations, but it will not normally generate a perfect water balance. The computed flows can then be manually adjusted to more closely match observed water surface elevations. Normally, the computed flows are initially incorporated using the distributed tributary option in the model with interpolation turned off so that

the model sees the flows as a step function since this is how the flow is computed by the utility. Using this option, the flows necessary to compute the water balance are distributed into the surface layer weighted according to segment surface area.

Keep in mind that this method only provides the necessary flows to complete the water balance. The user must decide how to incorporate them into the model in a realistic fashion as the method of incorporation can have a large impact on temperature and water quality calibration – another fork in the road in the “art” of water quality modeling. The recommended procedure is to first plot up and analyze the computed flows to see if they provide any information as to the source of the error.

For example, if the majority of the computed flows are negative and the inflows are deemed accurate, then this would indicate that the outflow has been underestimated. It could be due to seepage into groundwater or seepage through the dam. If the hypolimnetic temperatures were also being underpredicted, which would indicate that the hypolimnetic residence time was being overpredicted, then incorporating the computed flows into an additional outflow could solve both problems at once. The point to be made is that various methods of incorporating the computed flows during temperature and water quality calibration should be tried to determine if they have an affect on temperature or water quality. Whichever method improves the calibration is the method to use. The following plot illustrates the accuracy normally expected for a reservoir water surface elevation calibration. The computed elevations overlay the observed elevations.

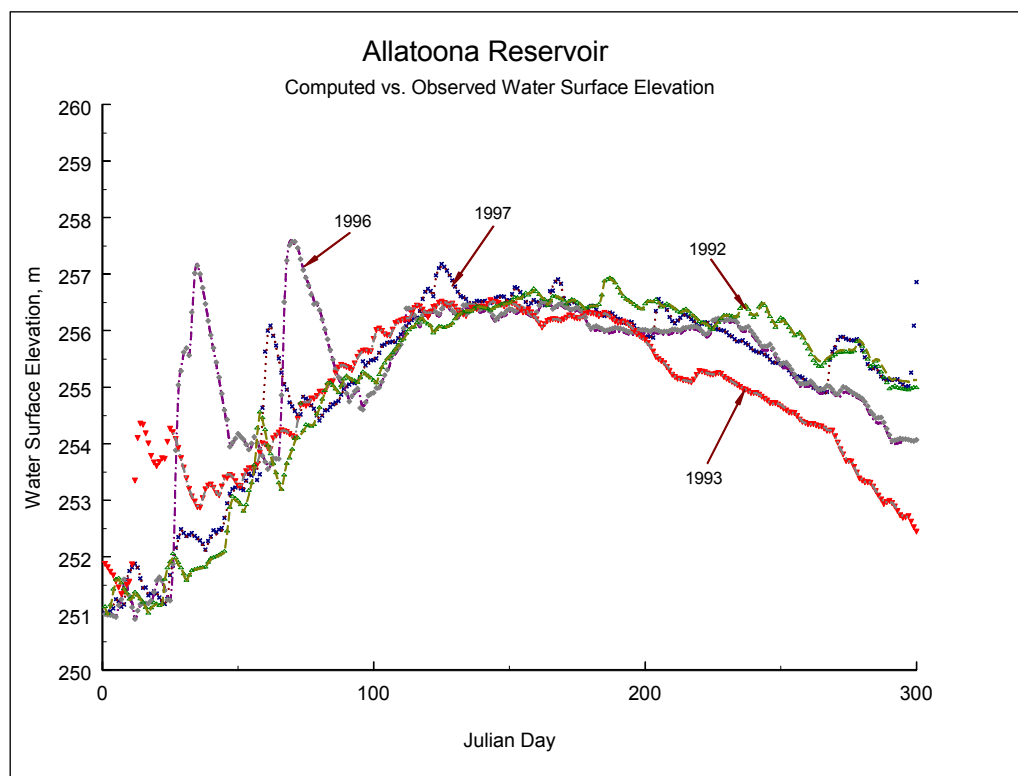


Figure 3. Allatoona Reservoir computed (lines) vs. observed (symbols) water surface elevations for 1992, 1993, 1996, and 1997.

CALIBRATION

Hydrodynamics and Temperature

The earliest one-dimensional mechanistic reservoir models included only temperature. As a result, temperature was the only model prediction that could be used for hydrodynamic calibration. Since temperature is affected by surface and bottom heat exchange and is therefore nonconservative, it is not the best parameter for calibrating hydrodynamics. Salinity, which is conservative, has historically been considered the ideal constituent for hydrodynamic calibration. However, this is generally feasible only for estuarine applications where salinity is routinely monitored. Dissolved solids are not conservative and are generally *not* a good substitute for salinity during calibration except in waterbodies where the conservative assumption is appropriate. The previous three sentences echo the prevailing sentiment of hydrodynamic modelers. In reality, there is no “ideal” constituent that should be used for hydrodynamic calibration. Each constituent can contribute knowledge about the system and can have an impact on the hydrodynamic calibration.

Experience has shown that dissolved oxygen and phytoplankton are often much better indicators of proper hydrodynamic calibration than either temperature or salinity. There are several reasons for this. First, gradients in dissolved oxygen and phytoplankton are often present at different locations in the water column than either temperature or salinity gradients. Consequently, they can provide additional information as to the correctness of the hydrodynamic calibration beyond either temperature and/or salinity alone. Second, dissolved oxygen is much more dynamic than either temperature or salinity and readily responds to wind events including seiching, with the anoxic zone often moving several kilometers over a day in response to the hydrodynamics. Phytoplankton distributions are also affected by the hydrodynamics. Further discussion and examples will be presented in the section on water quality calibration. Nevertheless, temperature and/or salinity should always be the first step during hydrodynamic calibration, with the hydrodynamic calibration further refined during water quality calibration.

Computed velocities can be compared with velocity and flow measurements obtained from an acoustic Doppler current profiler (ADCP) to additionally evaluate the model’s hydrodynamic performance. However, care must be taken when comparing model velocities with observed velocities to ensure ADCP measurements are comparable to the laterally averaged velocities generated by the model.

Coefficients affecting temperature and their default values are given in [Table 3](#). The eddy viscosities, Chezy coefficient, and wind sheltering coefficient directly affect hydrodynamics that affect heat and constituent transport. The remaining coefficients directly affect temperature that affects hydrodynamics. Of these, the last two coefficients affect temperature only if constituents are modeled. See [Appendix C](#) for a more detailed description of these coefficients and their effects.

Table 3. Coefficients affecting thermal calibration

Coefficient	FORTTRAN Name	Default
Longitudinal eddy viscosity	[AX]	1 m ² sec ⁻¹
Longitudinal eddy diffusivity	[DX]	1 m ² sec ⁻¹
Chezy coefficient or Manning’s N	[FRICT]	70 m ² sec ⁻¹
Wind sheltering coefficient	[WSC]	Calibration parameter
Solar radiation absorbed in surface layer	[BETA]	0.45
Extinction coefficient for pure water	[EXH20]	0.45 m ⁻¹

Extinction coefficient for inorganic solids	[EXINOR]	0.01 m ⁻¹
Extinction coefficient for organic solids	[EXORG]	0.2 m ⁻¹

In addition to the above coefficients, temperature predictions are also affected by the surface heat exchange algorithm specified, mainstem and tributary inflows, inflow temperatures and their placement, outlet and withdrawal specifications, the numerical solution scheme, and bathymetric and meteorological data. Again, always represent the prototype as accurately as possible.

Applications on over 400 waterbodies under a wide variety of conditions have shown the model generates remarkably accurate temperature predictions using default values when provided accurate geometry and boundary conditions. The wind-sheltering coefficient [\[WSC\]](#) has the most effect on temperature during calibration and should be adjusted first. Previous applications varied the wind sheltering coefficient from 0.5-0.9 for mountainous and/or dense vegetative canopy and 1.0 for open terrain. In a very few cases, the wind-sheltering coefficient [\[WSC\]](#) has been increased above 1.0 to account for funneling effects on systems with steep banks. The user should also run sensitivity analyses on the other coefficients to gain a "feel" for how they affect temperature predictions.

Calibration problems. Difficulties during temperature calibration can often be traced to the following:

1. **Inflows and Inflow temperatures.** Accurate inflows and inflow temperatures are desirable for all applications, but they are critical for waterbodies with short residence times or during high inflow periods. Temperature calibration will be difficult using monthly inflow temperatures for a waterbody with a one week residence time. Methods exist for generating more frequent inflow temperatures based on flow and meteorological data (Ford and Stein, 1986), but there is no substitute for actual measurements.
2. **Meteorological data.** Many difficulties are associated with extrapolating weather station meteorological data to a waterbody site. Weather stations are typically located in different terrain and at large distances from the prototype. Frontal movements can occur at different times over the waterbody and meteorological station resulting in model predictions that are in closer agreement either earlier or later than the actual comparison date. Methods for addressing these problems include adjustment of the wind sheltering coefficient [\[WSC\]](#), use of an alternative meteorological station, averaging data from several meteorological stations, separating a waterbody into regions applying data from different meteorological stations, and comparison of observed data using model output either before or after the observed date. If the user has the luxury of obtaining calibration data before applying the model, portable weather stations exist which can be deployed on the waterbody. Obviously, this is the preferred method.
3. **Outflow data.** The addition of the selective withdrawal algorithm in Version 2.0 has reduced many of the previous problems of accurately representing outflows. However, problems still arise. In the application of CE-QUAL-W2 to Bluestone Reservoir, Tillman and Cole (1994) were unable to reproduce observed temperature stratification without limiting the lower withdrawal layer. Subsequent investigation showed that withdrawal was limited by trash accumulation that effectively acted as a submerged weir. This was a problem generated by inadequate knowledge of the prototype and not a problem with the model. Indeed, this is an example of a model giving insight into the behavior of the prototype.

CALIBRATION

- Bathymetry.** Several previous applications of the model encountered difficulties during temperature calibration until the bathymetry was revisited. Check the assumptions made during the development of the bathymetry to ensure they are not the source of the problem. Starting points include grid resolution that affects the models ability to define sharp thermal gradients and bottom slope, volume-area-elevation accuracy that can have a marked effect on hypolimnetic temperatures since the volumes are generally small near the bottom, and water surface areas that affect the area available for surface heat exchange. Branch definition has also been found to have an effect on temperature predictions.

In order to illustrate how accurate reservoir temperature modeling has become with CE-QUAL-W2, [Table 4](#) lists calibration results for 70 reservoir thermal simulations. The statistic presented is the absolute mean error (AME) computed as follows:

$$AME = \frac{\sum | Predicted - Observed |}{number\ of\ observations}$$

Although a number of other statistics have been used when evaluating model results, the AME provides the best indication of model performance since it is directly interpretable. For example, an AME of 0.5 °C means that the model results are, on the average, within °0.5 EC of the observed data. As can be seen, model predictions for all the reservoirs are within °1 °C and most of them are much less.

Table 4. Reservoir thermal simulations with error statistics for station closest to dam.

	Reservoir	# years	AME, °C		Reservoir	# years	AME, °C
1	Allatoona	4	0.6	36	Monroe	4	0.7
2	Alum Creek	1	0.5	37	Neely Henry	2	0.6
3	Barklay	1	0.5	38	Neversink	3	0.4
4	Bluestone	2	0.5	39	Norman	3	0.7
5	Brownlee	2	0.6	40	Oxbow	1	0.3
6	Bull Run 1	2	0.5	41	Oahe	2	0.9
7	Bull Run 2	2	0.7	42	Occoquan	1	0.9
8	Burnsville	1	0.9	43	Paint Creek	1	0.4
9	Caesar Creek	1	0.6	44	Paintsville	1	0.4
10	Cannonsville	5	0.7	45	Patoka	3	0.7
11	Cave Run	4	0.8	46	Pepacton	3	0.6
12	C.J. Strike	2	0.7	47	Pineflat	5	0.6
13	Croton	1	0.7	48	Powell	1	0.7
14	Cumberland	1	0.5	49	J. Percy Priest	3	0.8
15	Deer Creek, OH	1	0.4	50	Quabbin	1	0.7
16	Deer Creek, ID	5	0.8	51	Richard B. Russell	3	0.5
17	DeGray	8	0.9	52	Rhodiss	2	0.6
18	Fishtrap	1	0.8	53	Riffe	1	0.7
19	Fort Peck	2	0.7	54	Rimov	1	0.5
20	Francis Case	2	0.7	55	Rondout	3	0.5
21	Herrington	1	0.7	56	Sakakawea	2	0.7
22	Hickory	1	0.5	57	Schoharie	2	0.8
23	J.W. Flanagan	1	0.5	58	Shasta	1	0.6
24	Jordanelle	3	0.7	59	Shepaug	1	0.6
25	J. Strom Thurmond	5	0.9	60	Stonewall Jackson	2	0.5
26	James	1	0.6	61	Toledo Bend	1	0.7
27	Houston	6	0.5	62	Taylorville	2	0.9
28	Lanier	2	0.9	63	Tolt	1	0.5
29	Loch Raven	1	0.9	64	Travis	1	0.3

CALIBRATION

30	Long Lake	1	0.5	65	Wabush	1	0.6
31	Lost Creek	1	0.6	66	Wachusett	4	0.7
32	Maumelle	2	0.7	67	Weiss	2	0.6
33	Mayfield	1	0.6	68	West Point	3	0.8
34	Moehnetalsperre	1	0.4	69	Walter F. George	2	0.6
35	Mountain Island	1	0.7	70	Youghioghenny	2	0.8

The following examples illustrate CE-QUAL-W2's ability to reproduce observed temperatures on a variety of systems with widely varying temperature regimes. On all plots, x's represent observed data and their widths are scaled to represent $\pm 0.5^{\circ}\text{C}$. The dotted lines represent computed model values. The absolute mean error (AME) and root mean square error (RMS) are also included for each date in order to help in interpreting the predictive capability of the model. These statistics should always be included in plots of computed versus observed data since plots can often be misleading depending upon the scale of the x and y axes and the size of the marker used to represent the observed data (a common technique used to make model results appear better than they actually are).

Pineflat Reservoir. Pineflat Reservoir is located in California near the base of the Sierra Madre mountain range. One of its primary uses is for providing irrigation water during the summer growing season. Consequently, the reservoir is drawn down as much as 70 m over the summer during drought years. The model was used to provide operational guidance for a temperature control device that will be installed in the reservoir to optimize the storage of cold water for downstream releases at the end of summer.

[Figure 4](#) shows the results of temperature predictions for 1989. The thermal regime exhibits two thermoclines starting in early spring. As can be seen, the reservoir was drawn down over 40 m during the summer. During 1993, the development of the two thermoclines was delayed until the end of summer ([Figure 5](#)). CE-QUAL-W2 correctly captured the thermal regimes for both years and the differences in the thermal regimes between the two years.

Sensitivity analyses showed that temperature predictions were very sensitive to inflow temperatures. Calibration consisted of adjusting inflow temperatures to more closely match in-pool temperature profiles. Because calibration showed the importance of accurate inflow temperatures in order to properly calibrate the model, additional fieldwork was done to obtain accurate inflow temperatures. During this effort, it was discovered that the location where inflow temperatures were taken showed a lateral variation in the river of over 5°C due to hypolimnetic discharges from an upstream reservoir that did not completely mix laterally. Additionally, during extreme drawdown, it was shown that inflow temperatures increased by nearly 2°C from measured temperatures as the upstream boundary of the model moved downstream approximately 10 km due to the large drawdowns that the reservoir was periodically subjected to.

CALIBRATION

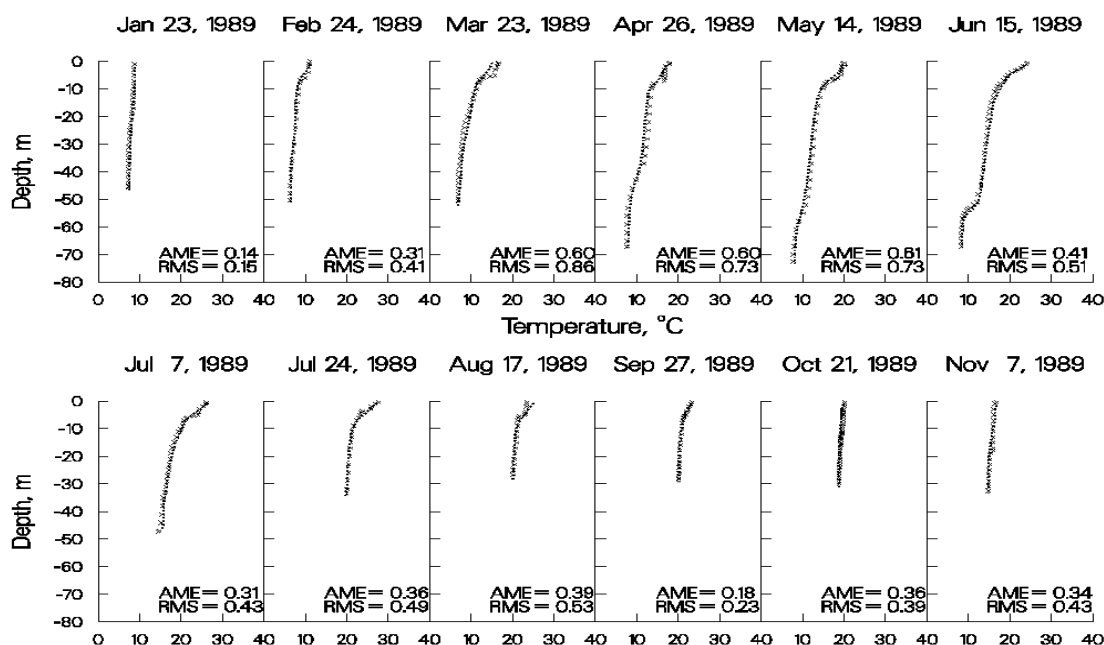


Figure 4. 1989 Pineflat Reservoir computed versus observed temperatures.

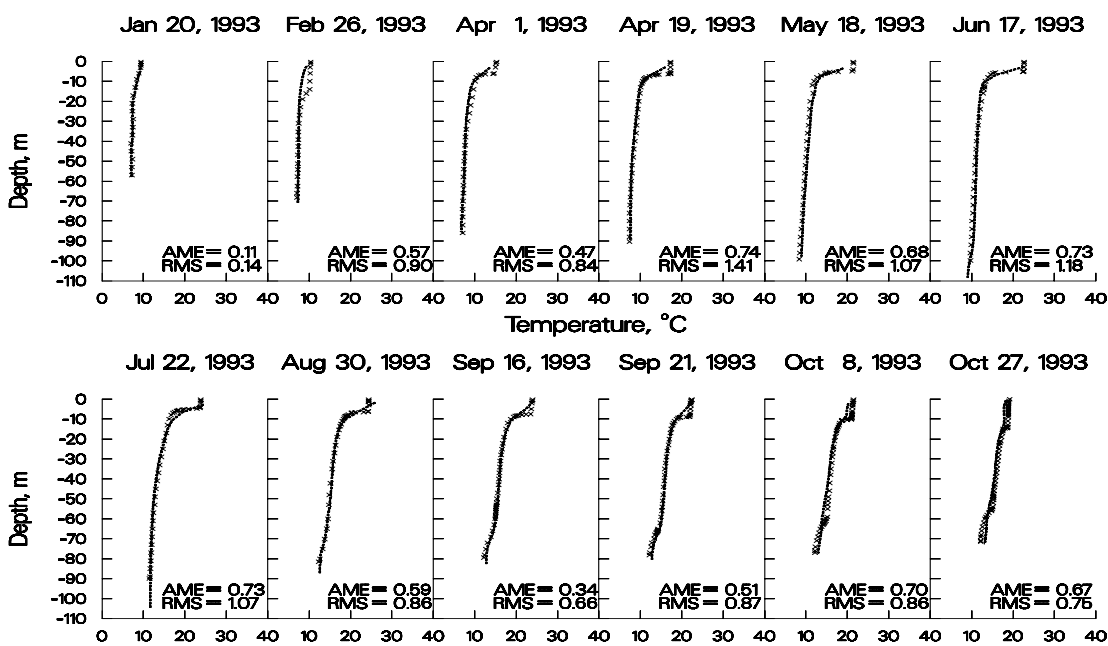


Figure 5. 1993 Pineflat Reservoir computed versus observed temperatures.

Bluestone. Bluestone Reservoir is located in the mountains of West Virginia. The reservoir has an average hydraulic retention time of less than a week during the summer. When first calibrating for temperature, the model predicted essentially no thermal stratification during the summer whereas the observed data showed strong stratification beginning at a depth of about eight meters. Based on the short residence time during the summer, model predictions seemed quite reasonable. However,

stratification was present in both 1981 and 1983 indicating that stratification was not a rare occurrence.

A number of mechanisms were proposed to explain the observed stratification including groundwater seepage and extreme wind sheltering. Including these in the model did not result in any improvements in model predictions. Finally, the lower limit of selective withdrawal was set at the depth corresponding to the outlet elevation. Results of the simulation are shown in [Figure 6](#) and [Figure 7](#). Subsequent investigations at the reservoir revealed that accumulated debris at the level of the trash racks was acting like a submerged weir that limited the bottom of the withdrawal zone to the elevation of the trash racks. This is an example of a model providing insight into previously unknown behavior of the prototype.

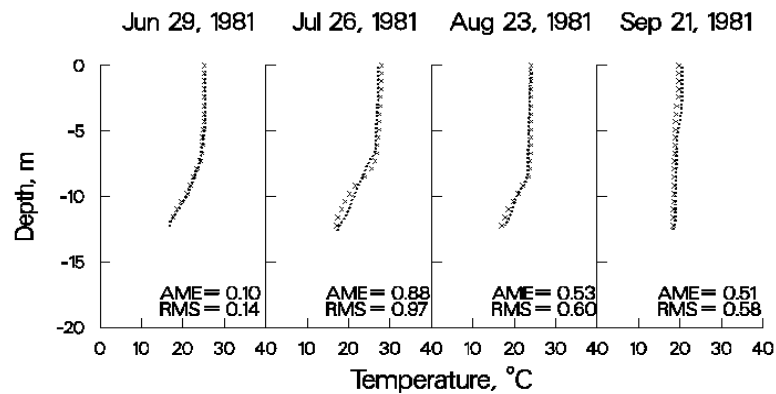


Figure 6. 1981 Bluestone Reservoir computed versus observed temperatures.

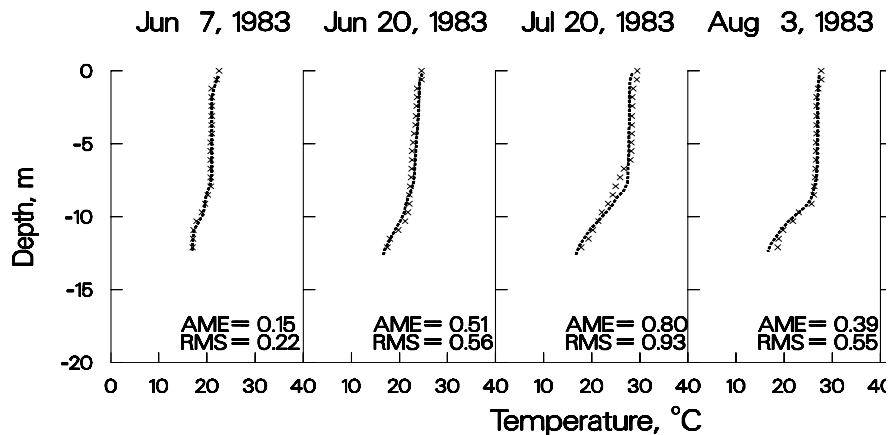


Figure 7. 1983 Bluestone Reservoir computed versus observed temperatures.

Richard B. Russell. Richard B. Russell (RBR) is located immediately upstream of J. Strom Thurmond Reservoir (JST) on the Savannah River bordering Georgia and South Carolina. The model was used to investigate the effects of proposed pump-storage operations in which water would be pumped into RBR from JST and reused for hydropower operations during peak energy demands. An important concern was what effect pump-storage operations would have on the thermal regime in RBR. The model was subsequently applied to 1996, a year in which extensive pump-storage operations oc-

CALIBRATION

curred. In order to simulate the effects of pump-storage, the model code was altered to allow dynamic linkage of RBR and JST reservoirs.

This is a stringent test of the model's simulation capabilities because the dynamic linkage required accurate temperature simulations in RBR in order to provide accurate inflow temperatures to JST. Likewise, accurate temperature predictions were required in JST in order to provide accurate temperatures entering RBR during pumpback.

[Figure 8-Figure 10](#) show the results of the simulations. The model correctly predicted the approximately 4 °C increase in hypolimnetic temperatures compared to previous years that did not have pump-storage operations. No calibration was involved for this simulation. Results are from the first run of the model for 1996 using default hydrodynamic/temperature calibration parameters and a wind-sheltering coefficient determined from calibration to two previous years that did not include pump-storage operations.

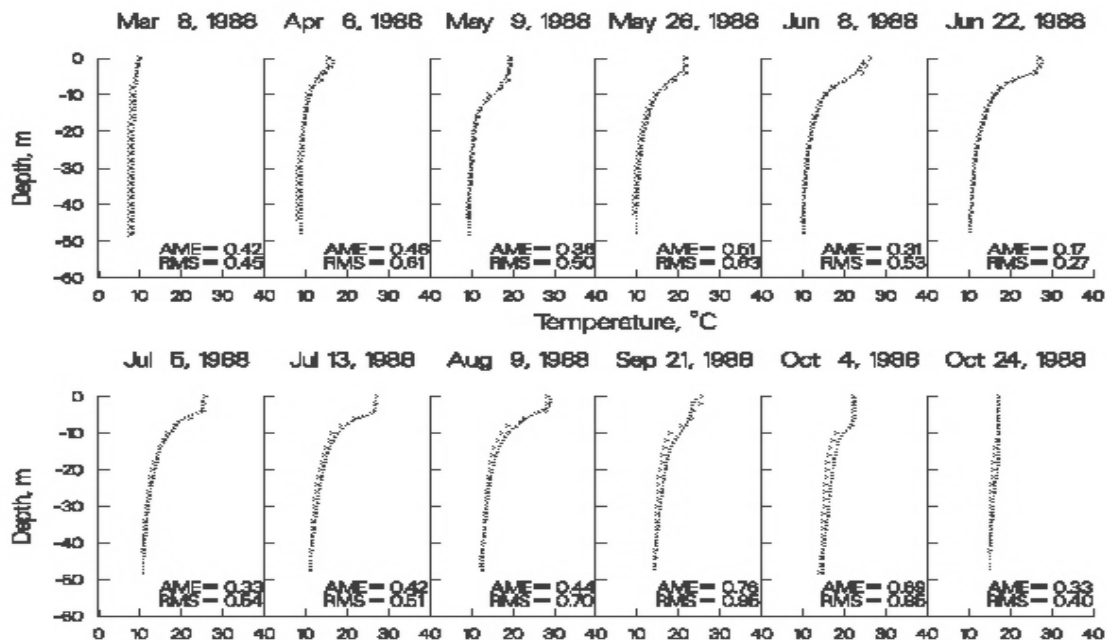


Figure 8. 1988 Richard B. Russell computed versus observed temperatures.

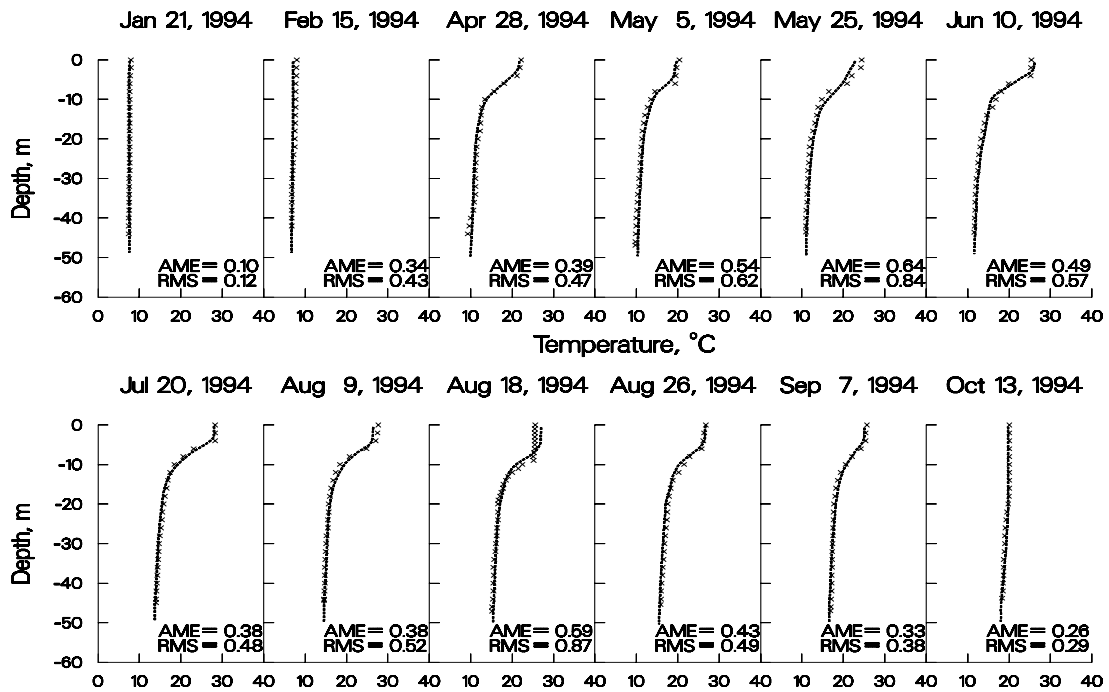


Figure 9. 1994 Richard B. Russell computed versus observed temperatures.

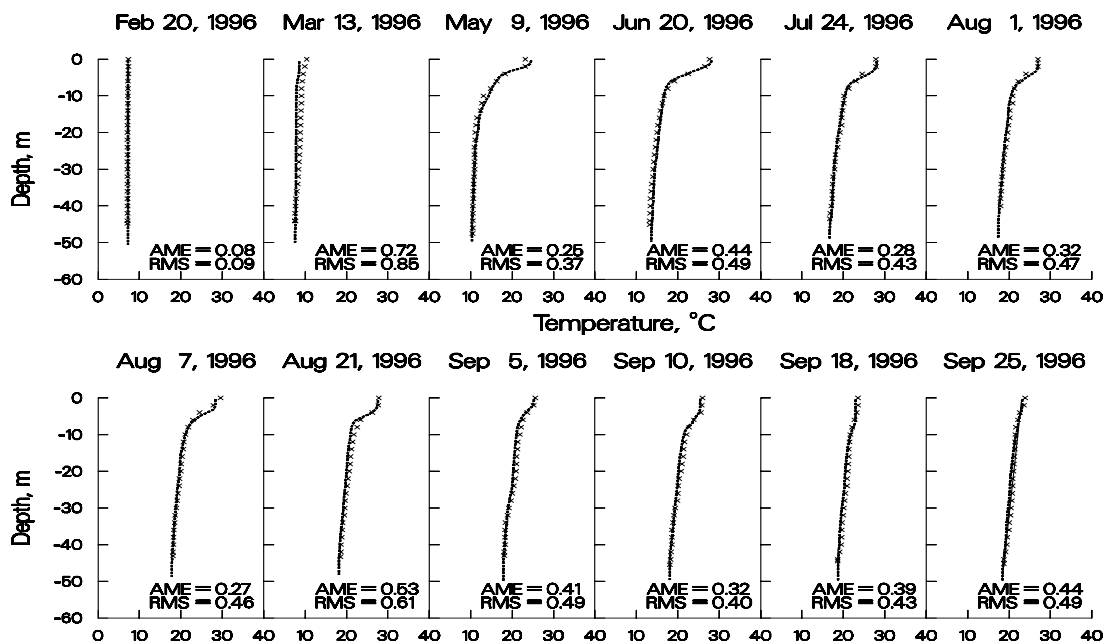


Figure 10. 1996 Richard B. Russell computed versus observed temperatures.

Paintsville Reservoir. Paintsville Reservoir is a US Army Corps of Engineers reservoir located in Kentucky. The reservoir's thermal regime is typical of deep-storage reservoirs with hydraulic retention times greater than four months. [Figure 11](#) illustrates the model's ability to reproduce the spring-

CALIBRATION

time development of the thermocline, the strong thermocline present in late summer, and fall overturn.

During initial calibration, the model consistently overpredicted hypolimnetic temperatures. No parameter adjustment (wind-sheltering or light absorption/extinction) resulted in an acceptable calibration. Realizing that hypolimnetic temperatures are influenced by residence time, a sensitivity analysis was performed in which the widths were increased uniformly (thus increasing hypolimnetic residence time) until the predicted hypolimnetic temperatures matched the observed temperatures. Subsequently, it was determined that the original development of the bathymetry did not include two branches that accounted for approximately 15% of the storage in the reservoir. In this case, calibration consisted of ensuring that the volume-elevation relationship was accurately described.

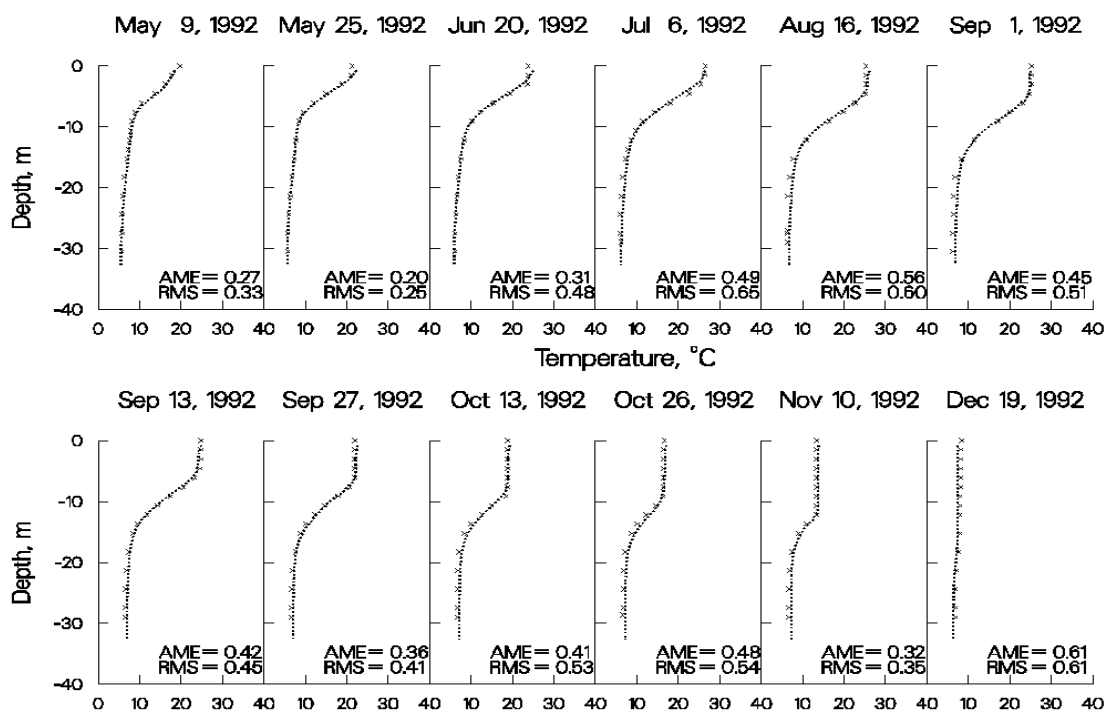


Figure 11. Paintsville Reservoir computed versus observed temperatures.

Brownlee Reservoir. Brownlee Reservoir is located on the Snake River in Idaho and is operated by Idaho Power. Brownlee's thermal regime is very distinctive with the thermocline starting at approximately 30 m below the water surface. [Figure 12](#) and [Figure 13](#) illustrate the model's ability to simulate the thermal regime in Brownlee.

During initial temperature calibration, the model predicted hypolimnetic temperatures greater than 15°C, whereas the observed temperatures were always near 5°C. No parameter adjustment allowed for adequate temperature calibration. An analysis of the system showed that the theoretical residence time during the summer was less than two months indicating that model predictions of warmer hypolimnetic temperatures were more reasonable than the observed data.

Additionally, the thermal structure in Brownlee exhibits a well-mixed epilimnion approximately 30 m in depth. Wind mixing could not supply sufficient energy to account for the depth of the epilimnion. Therefore, it was concluded that outflow dynamics had to be responsible for the observed thermal

regime. As in the Bluestone application, the bottom layer for selective withdrawal was set at approximately the same depth as the thermocline. Subsequent investigations revealed the presence of a ledge below the outlet that was limiting the outflow to the level of the observed thermocline.

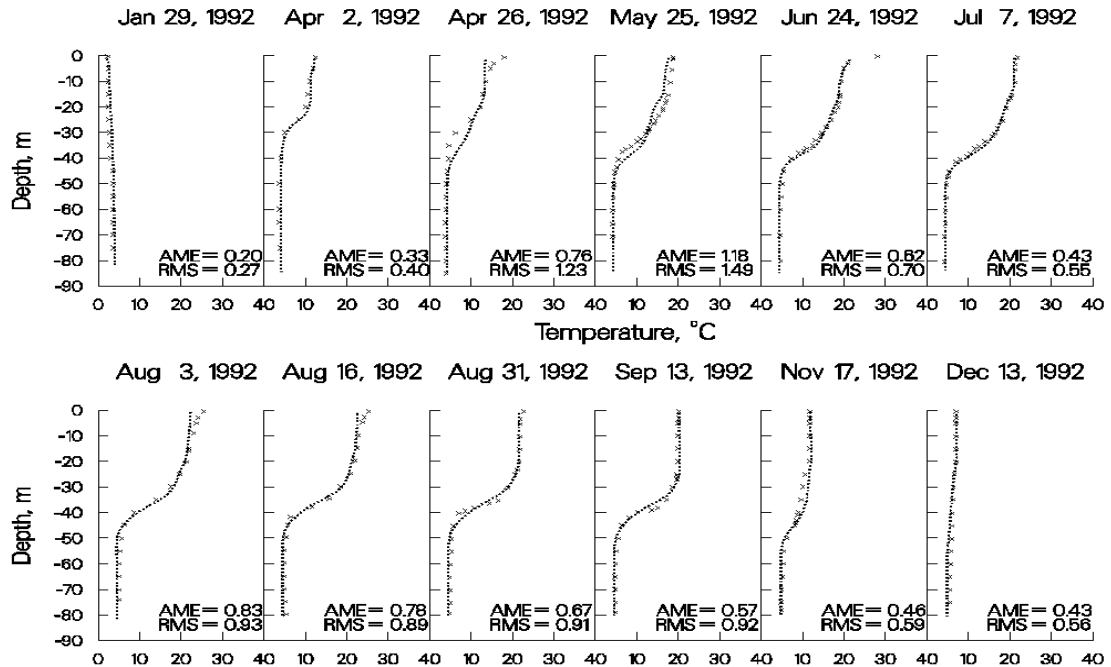


Figure 12. 1992 Brownlee Reservoir computed versus observed temperatures.

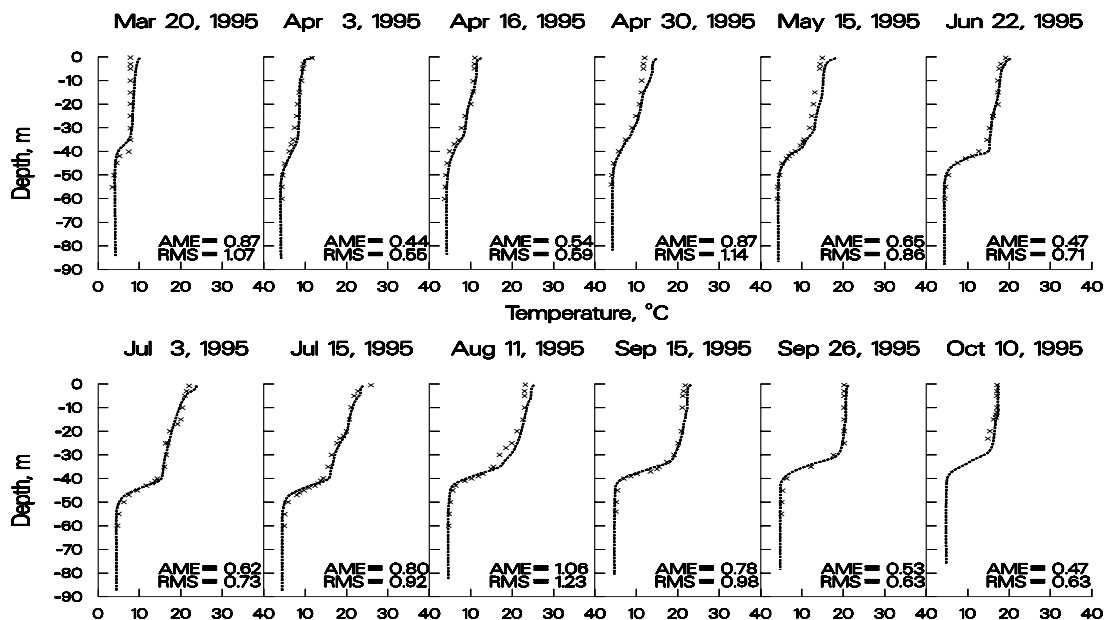


Figure 13. 1995 Brownlee Reservoir computed versus observed temperatures.

CALIBRATION

C.J. Strike Reservoir. C.J. Strike Reservoir is located on the Snake River in Idaho upstream of Brownlee Reservoir and is also operated by Idaho Power. Stratification is not nearly as pronounced as in Brownlee Reservoir due to the smaller volume of C.J. Strike and subsequent shorter residence time.

As noted in the discussion for Brownlee Reservoir, the relatively short residence time during the summer should result in considerable hypolimnetic heating as cold water is withdrawn and replaced by warmer waters from above. Temperature calibration consisted of adjusting the wind-sheltering coefficient until adequate agreement was obtained between computed and observed temperatures.

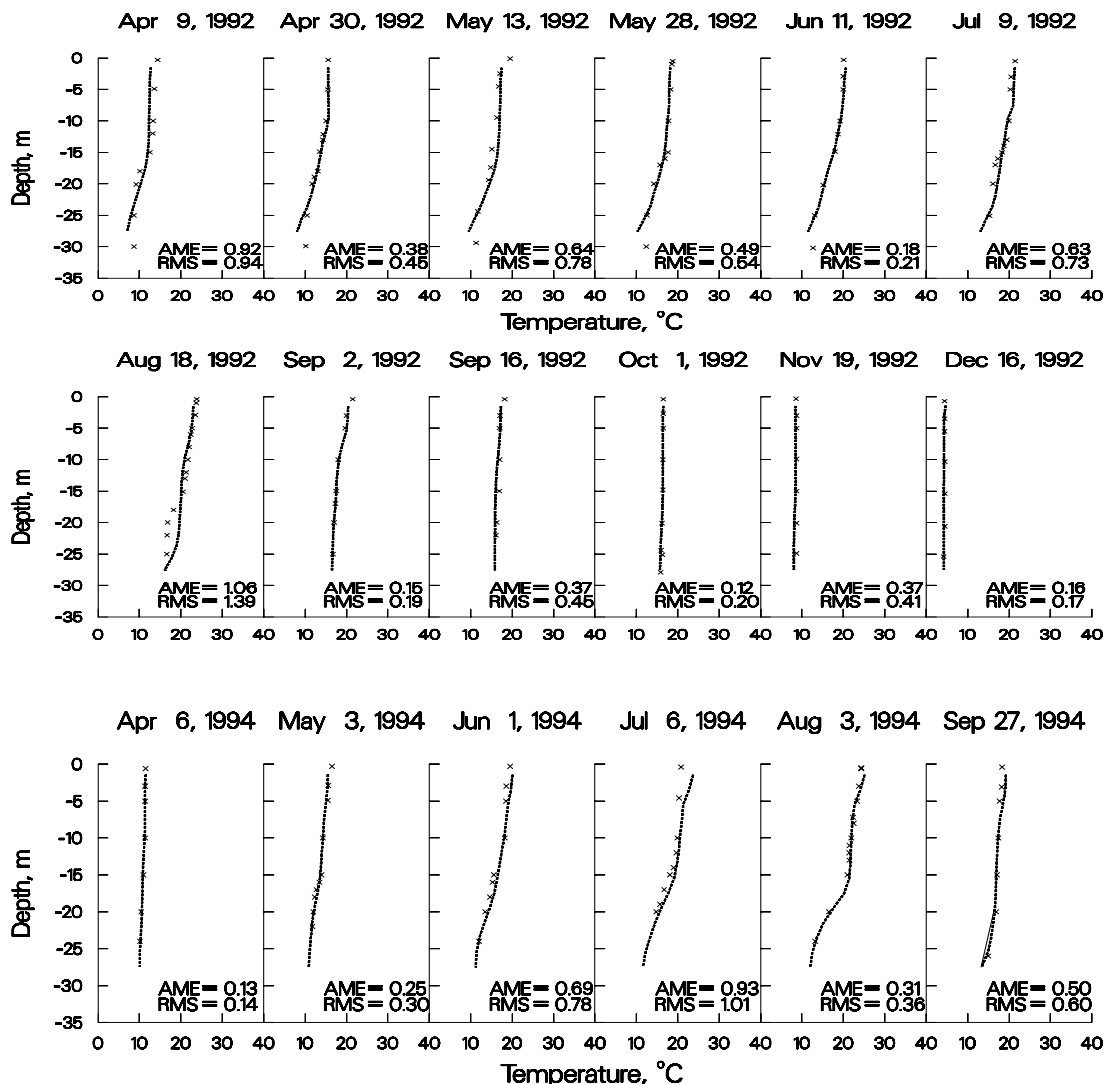


Figure 14. C.J. Strike Reservoir computed versus observed temperatures.

These examples illustrate the model's ability to reproduce complex thermal regimes that differ widely depending upon a particular reservoir's morphometry, location, surrounding terrain, and operations with a minimum of parameter adjustment. The only parameter adjusted was the wind-sheltering coefficient that was used to adjust wind speeds taken at a given meteorological station to the reservoir.

surface. Values ranged from 0.6 for small reservoirs located in mountainous terrains to 1.0 for large reservoirs located in open terrain.

The preceding discussion is not meant to imply that the model is “plug and play” and requires no calibration with regards to temperature. Greater discrepancies between computed and observed temperature profiles were always present at the beginning of thermal calibration for all the presented examples.

Aside from adjustment of wind sheltering, calibration consisted of determining whether known inaccuracies in a given forcing function could be responsible for the discrepancies in the computed temperature profiles and then describing the forcing function more accurately. This procedure included the following:

1. Adjustment of volume-elevation relationship to ensure that residence time was accurately represented
2. Adjustment of bottom elevation to ensure that computed and observed bottom elevations for the deepest station were at least as deep as the observed data
3. Adjustment of inflow temperatures to more closely match temperatures at the most upstream station
4. Generation of more frequent inflow temperatures based on equilibrium temperature
5. Using more frequent outflow data than daily average values, particularly for peaking hydropower systems
6. Ensuring that the outflow distribution for multi-level outlets was accurately described
7. Ensuring sufficient longitudinal/vertical grid resolution
8. Obtaining more frequent meteorological data than daily average values
9. Limiting the bottom zone for selective withdrawal (all instances were eventually physically justified in the prototype)
10. Including additional sources of outflow due to dam leakage or seepage to groundwater
11. Ensuring multiple branch descriptions were accurately represented
12. Using the most accurate numerical scheme (ULTIMATE with [THETA] set to 0) and including the effects of vertical turbulence [VISC] and internal gravity waves [CELC] in the autostepping stability requirements

As a result of the numerous thermal applications of the model, an important concept that has emerged is that the more accurately the behavior of the prototype is described, the more accurately the model responds. Always keep this in mind during model calibration.

Water Quality

The following discussion can serve as a starting point for reservoir water quality calibration. However, each application is different and requires knowledge about prototype behavior and the dominant water quality processes that are occurring in the prototype before ever attempting to model water quality. Black box application of any model is a recipe for failure.

Dissolved Oxygen. Once the user has a good understanding of the dominant water quality processes occurring in the prototype and ensures they are accurately represented in the model, then the user should begin dissolved oxygen calibration. The zero-order SOD should be used initially as it is essentially a pure calibration parameter that allows for back calculating the oxygen uptake rate in the water column. If dissolved oxygen profiles in the water column are exactly matched, then the values

CALIBRATION

for SOD used in calibration are very close to the actual uptake rates of dissolved oxygen in the water column. The problem with using only the zero-order SOD for water column DO calibration is that the model will not be sensitive to load increases/decreases that directly affect water column DO uptake and sediment nutrient recycling that affect phytoplankton primary production.

However, this is seldom the case, particularly where loadings to the system in the form of allochthonous organic matter (or CBOD), autochthonous organic matter due to phytoplankton production, and/or ammonium are important forcing functions for water column dissolved oxygen that are subject to change over time. Unfortunately, for systems where allochthonous loadings of organic matter are important, rarely are there sufficient boundary condition data to adequately represent the loadings to the system.

Particular care should be paid to the timing and duration of events involving phytoplankton, epiphyton, and dissolved oxygen. If the model does not represent the onset, extent, and duration of anoxic conditions, then nutrient dynamics will not be represented either. They in turn affect phytoplankton production that affects dissolved oxygen. Timing of the onset of dissolved oxygen depletion is greatly influenced by the temperature rate multipliers used for organic matter and the sediments. A change in the lower temperature [OMT1] of 1°C in the temperature rate formulation can shift the initial uptake of water column dissolved oxygen by as much as two weeks. The same effect can be obtained by adjusting the value of the multiplier [OMK1]. Much of the art in water quality modeling is involved in calibrating phytoplankton/nutrient/DO dynamics.

The following plots illustrate the model's ability to reproduce widely varying reservoir dissolved oxygen regimes. With the exception of the zero-order SOD rates, all kinetic coefficients were set to their default values thus ensuring that the model was applied with a minimum of "curve fitting". In all likelihood, using the same values for kinetic parameters such as phytoplankton growth and settling rates is not correct. However, the point to be made is that the model is capable of reproducing very different water quality regimes without having to resort to extensive, site-specific parameter manipulations.

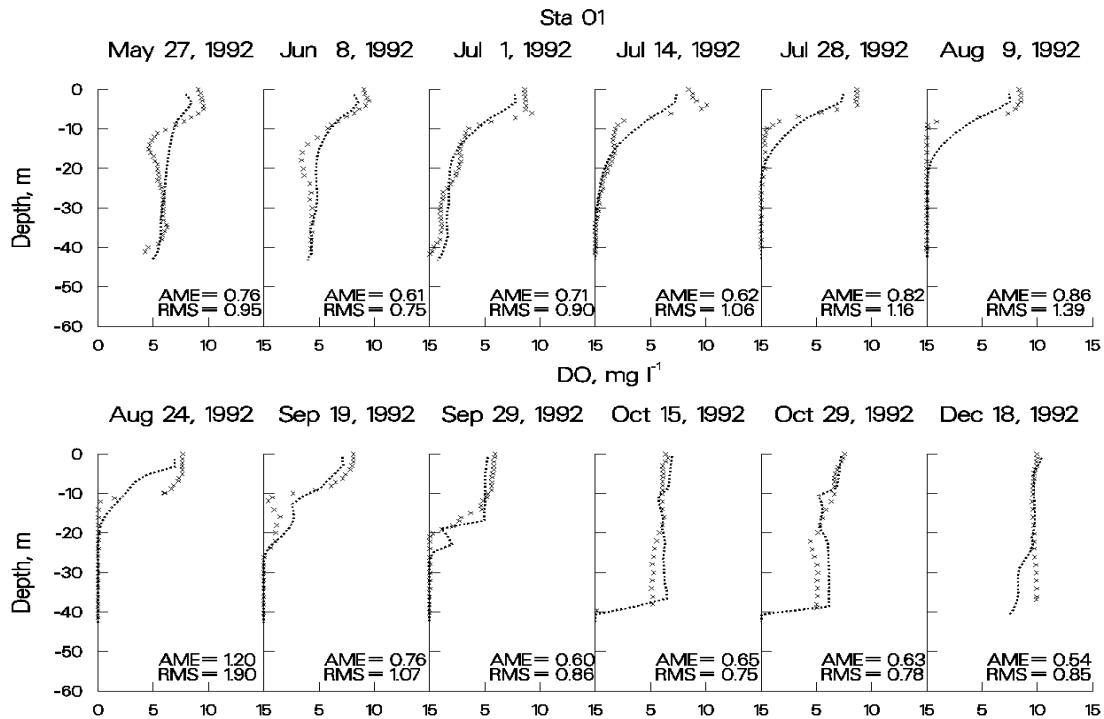


Figure 15. Allatoona Reservoir computed vs. observed DO.

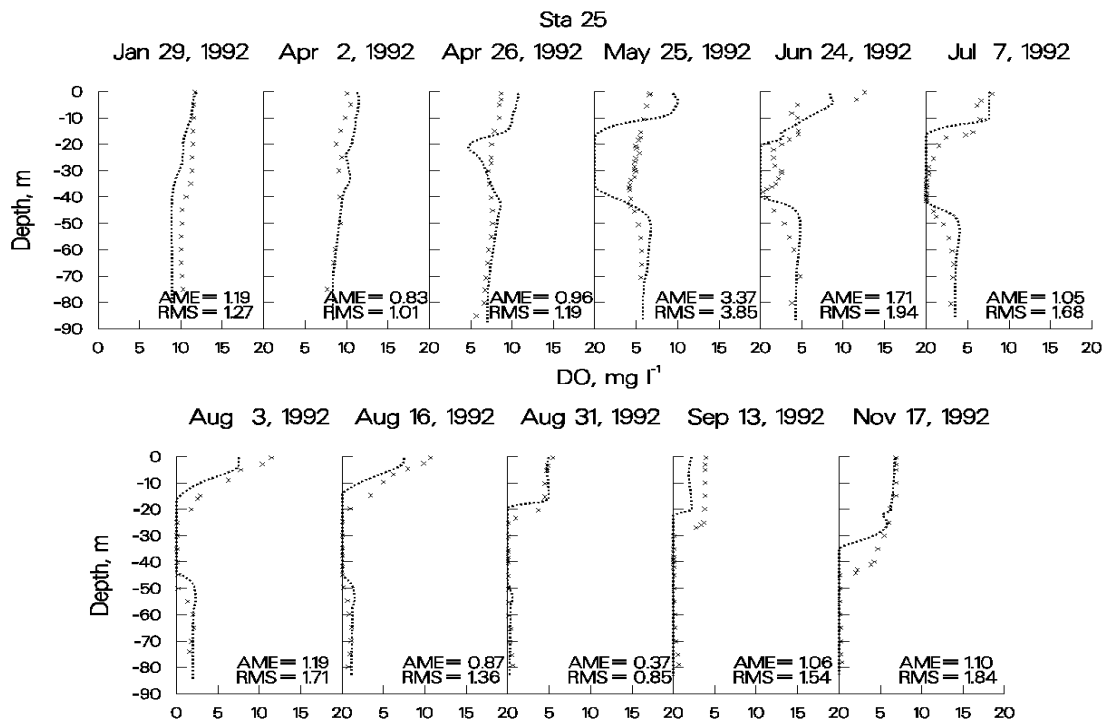


Figure 16. Brownlee Reservoir computed vs. observed DO.

CALIBRATION

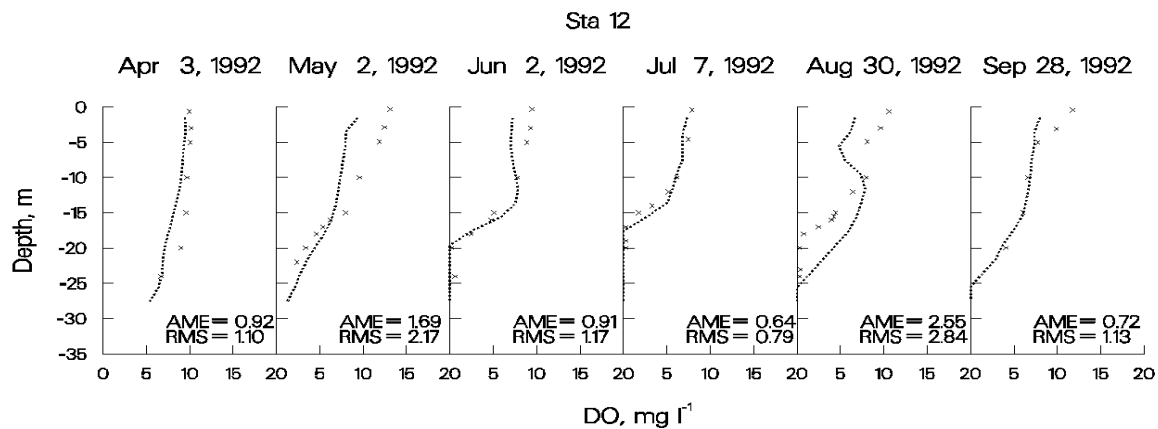


Figure 17. C.J. Strike Reservoir computed vs. observed DO.

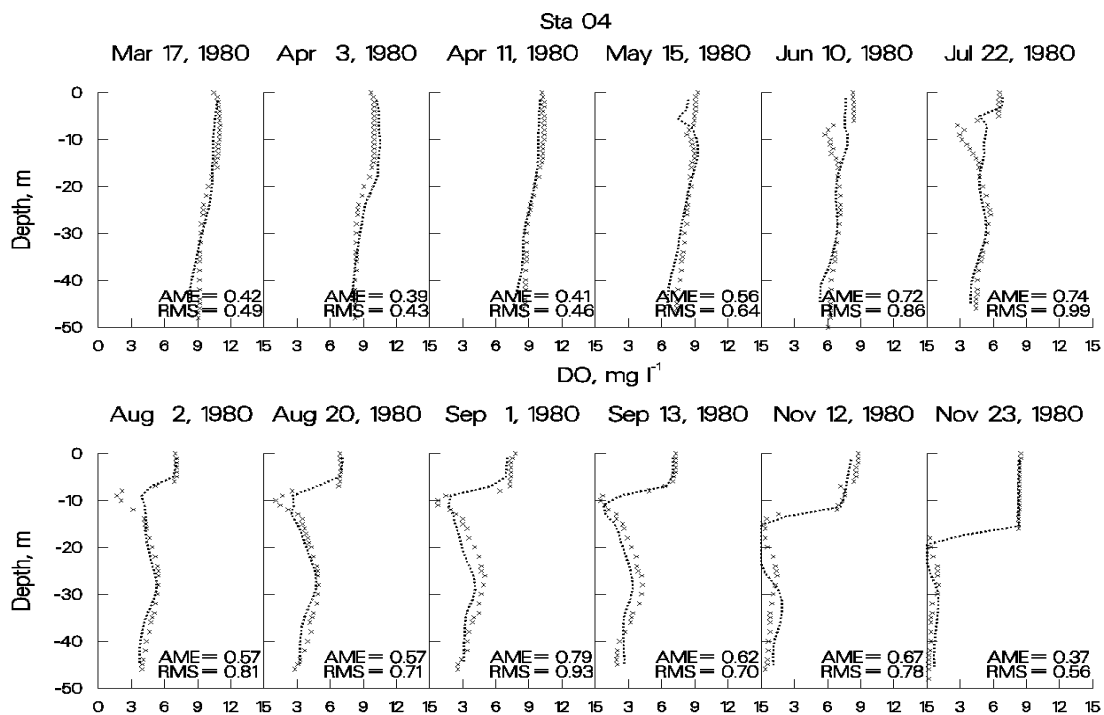


Figure 18. DeGray Reservoir computed vs. observed DO.

CALIBRATION

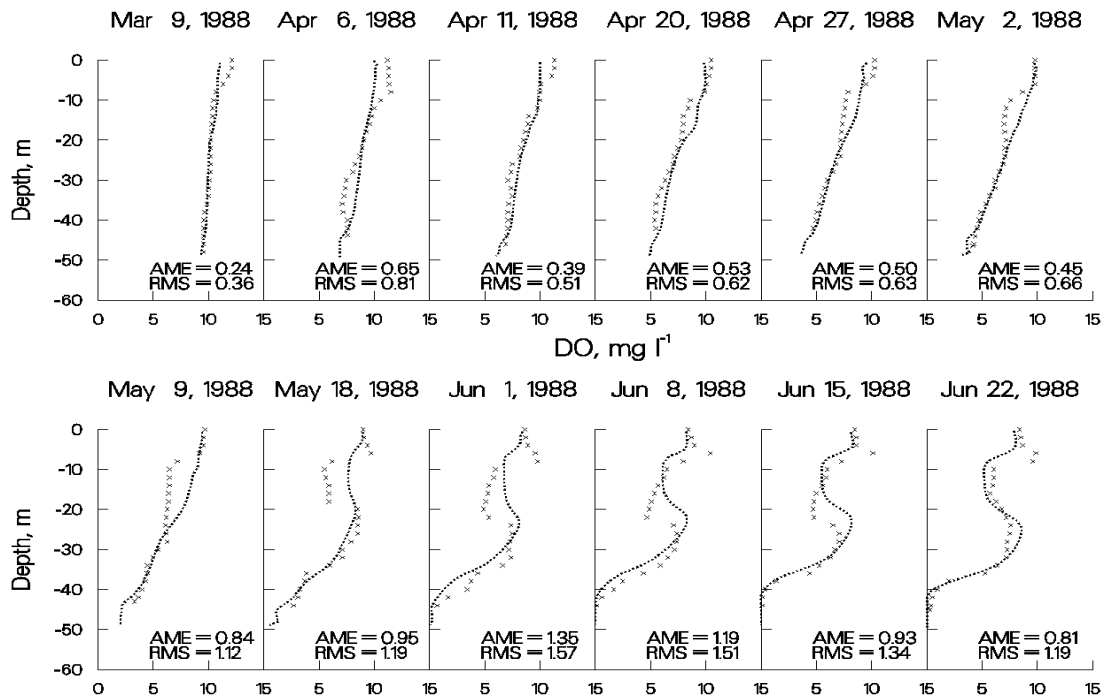


Figure 19. Richard B. Russell Reservoir computed vs. observed DO, March through June, 1988.

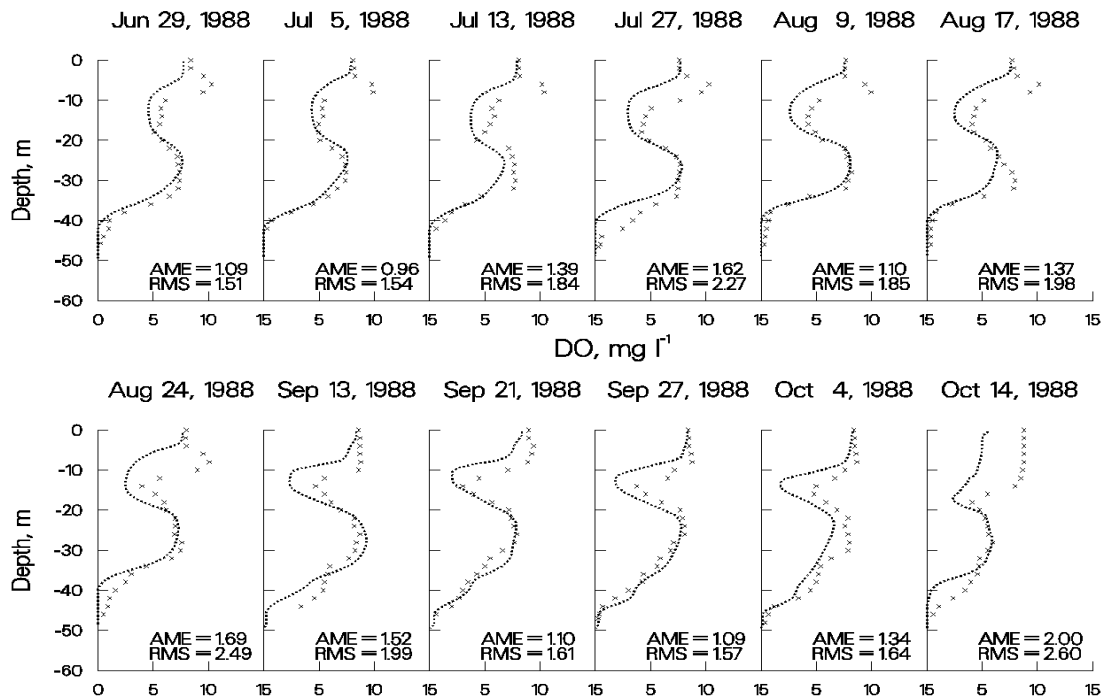


Figure 20. Richard B. Russell Reservoir computed vs. observed DO, June through October, 1988.

CALIBRATION

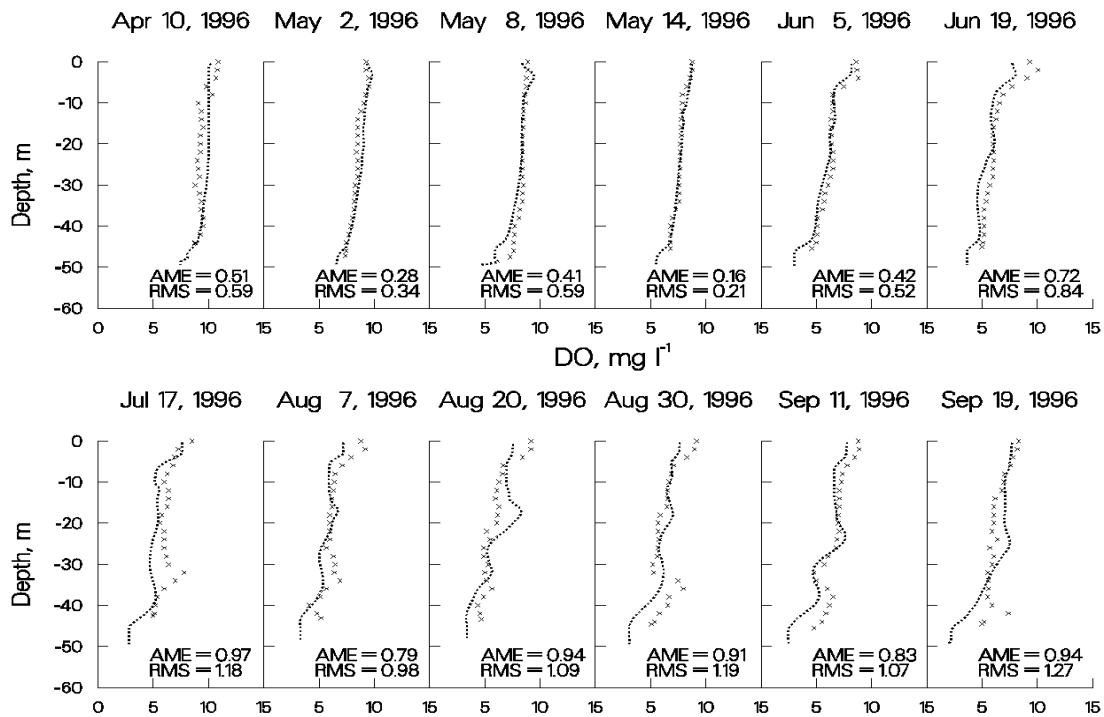


Figure 21. 1996 Richard B. Russell computed vs. observed DO.

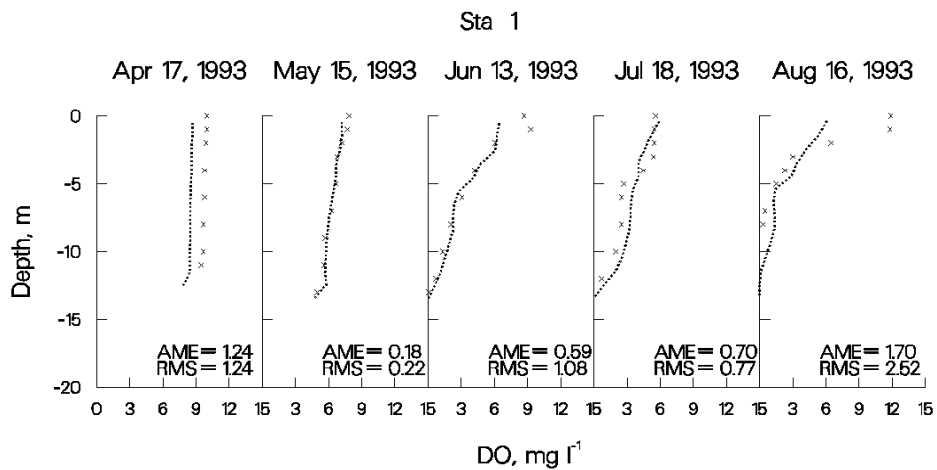


Figure 22. Neely Henry Reservoir computed vs. observed DO.

CALIBRATION

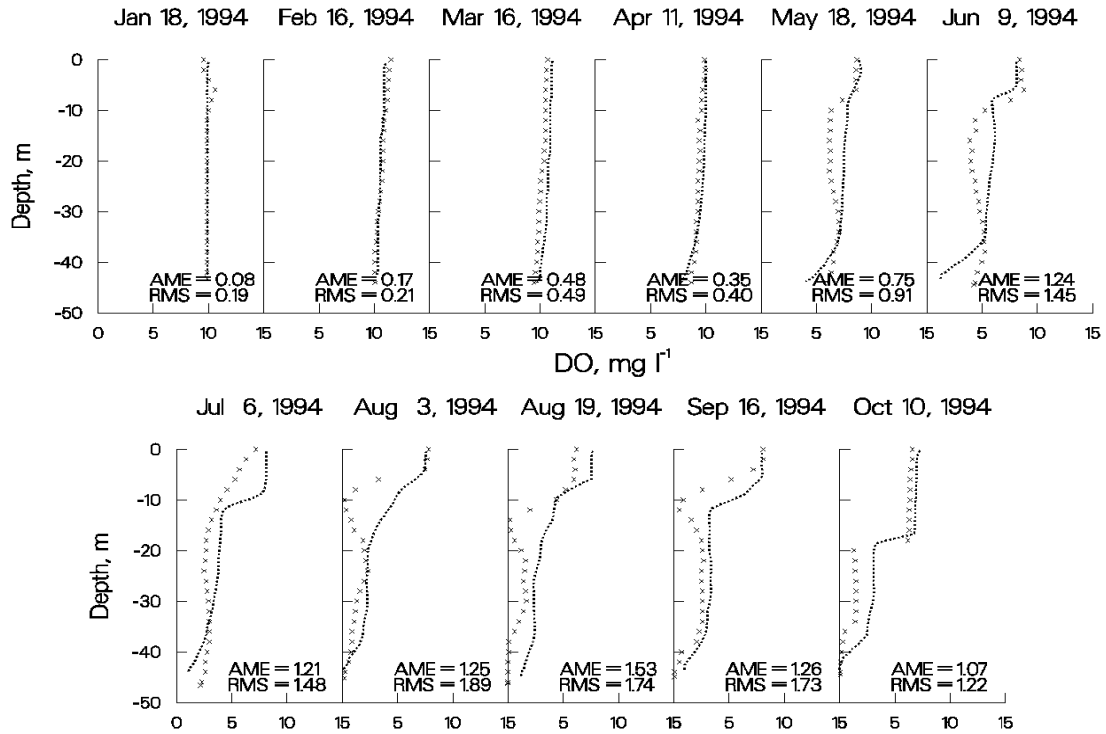


Figure 23. J. Strom Thurmond Reservoir computed vs. observed DO.

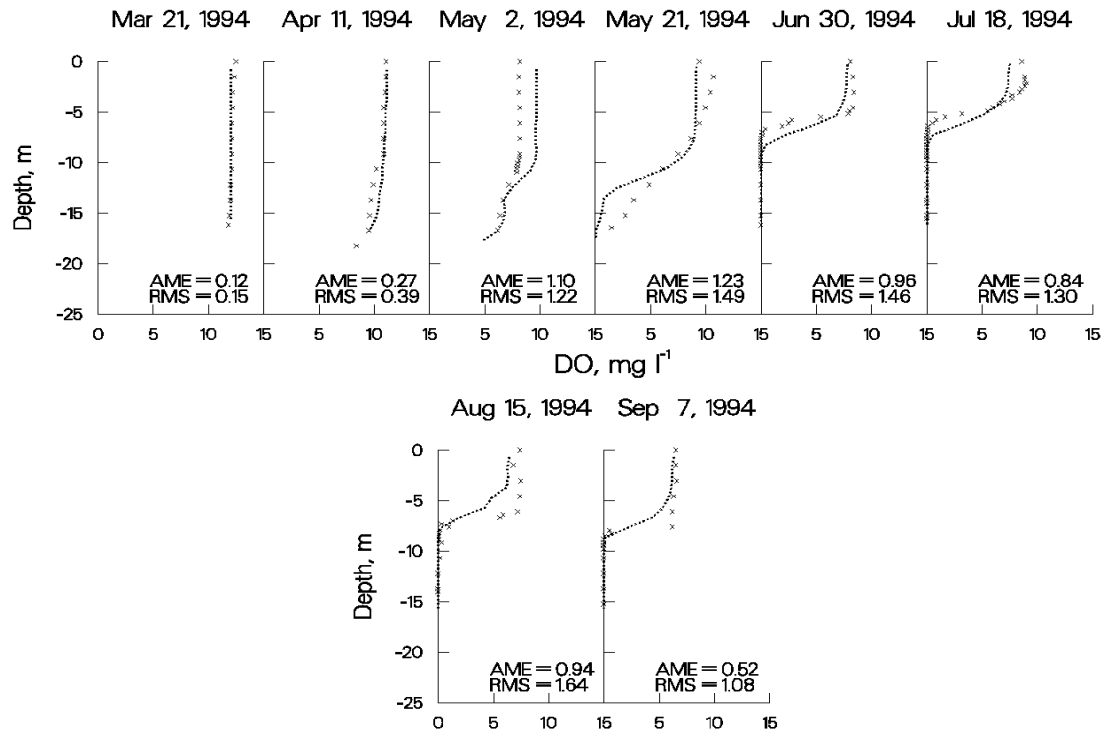


Figure 24. Monroe Reservoir computed vs. observed DO.

CALIBRATION

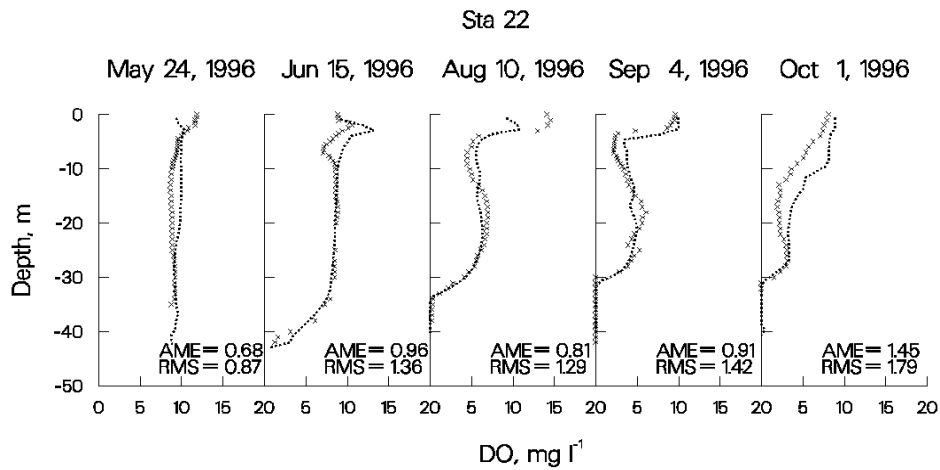


Figure 25. Rimov Reservoir computed vs. observed DO.

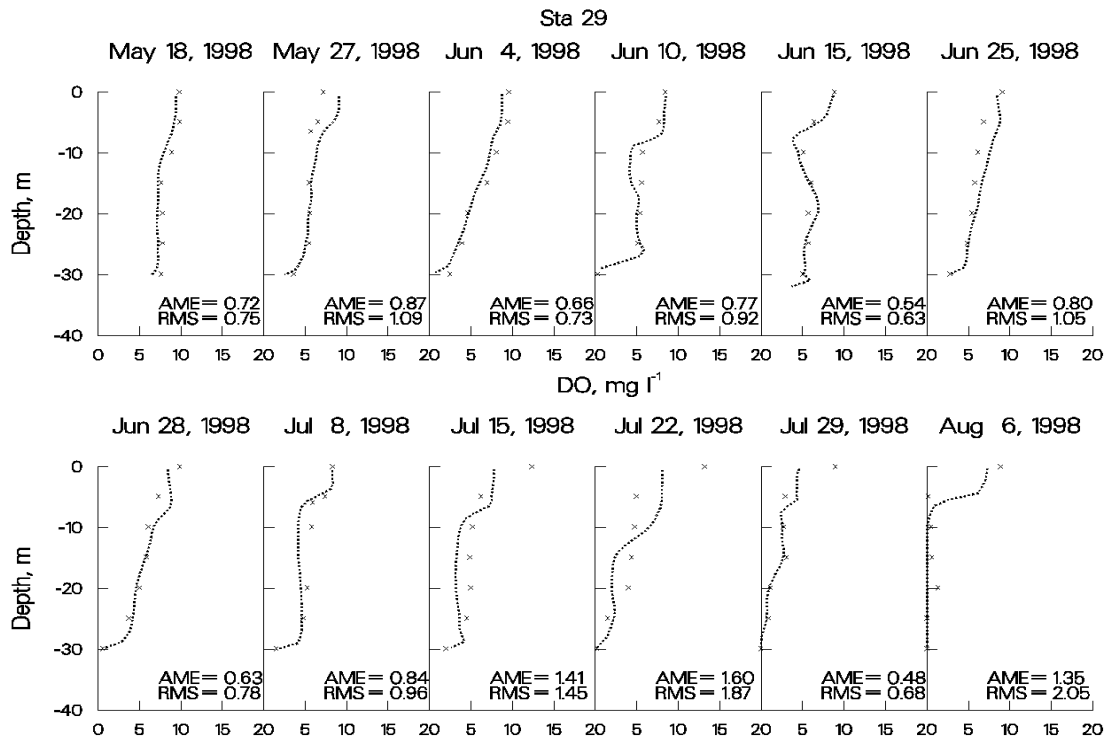


Figure 26. Shepaug Reservoir computed vs. observed DO.

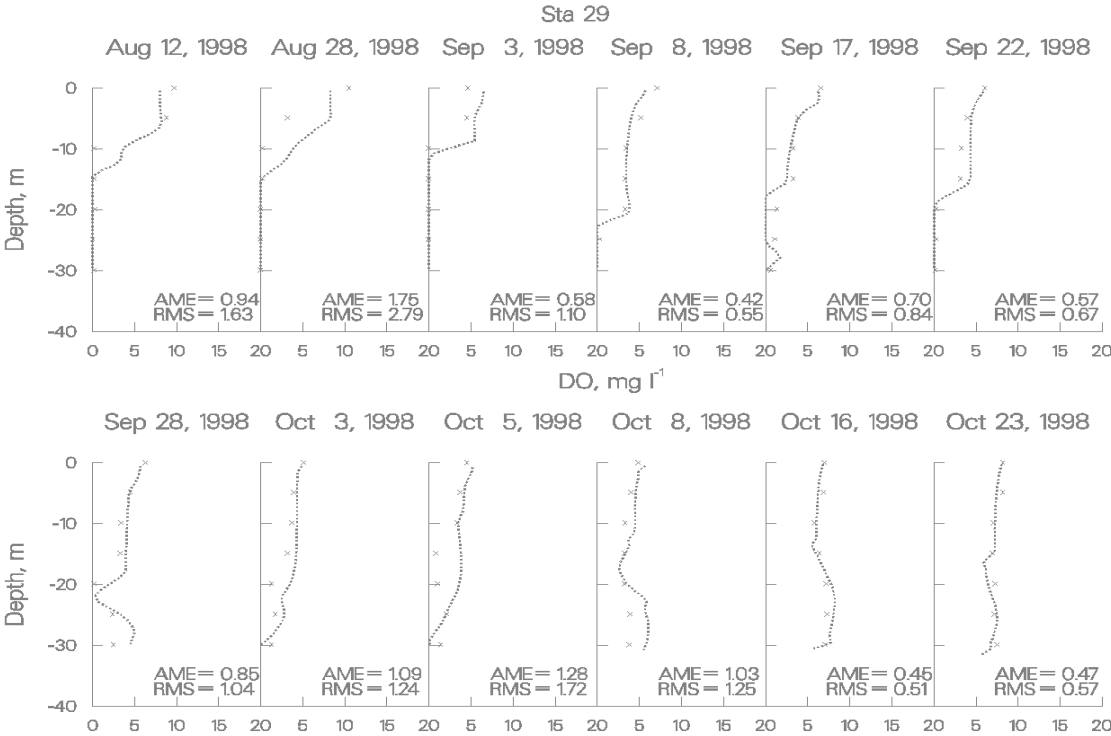


Figure 27. Shepaug Reservoir computed vs. observed DO.

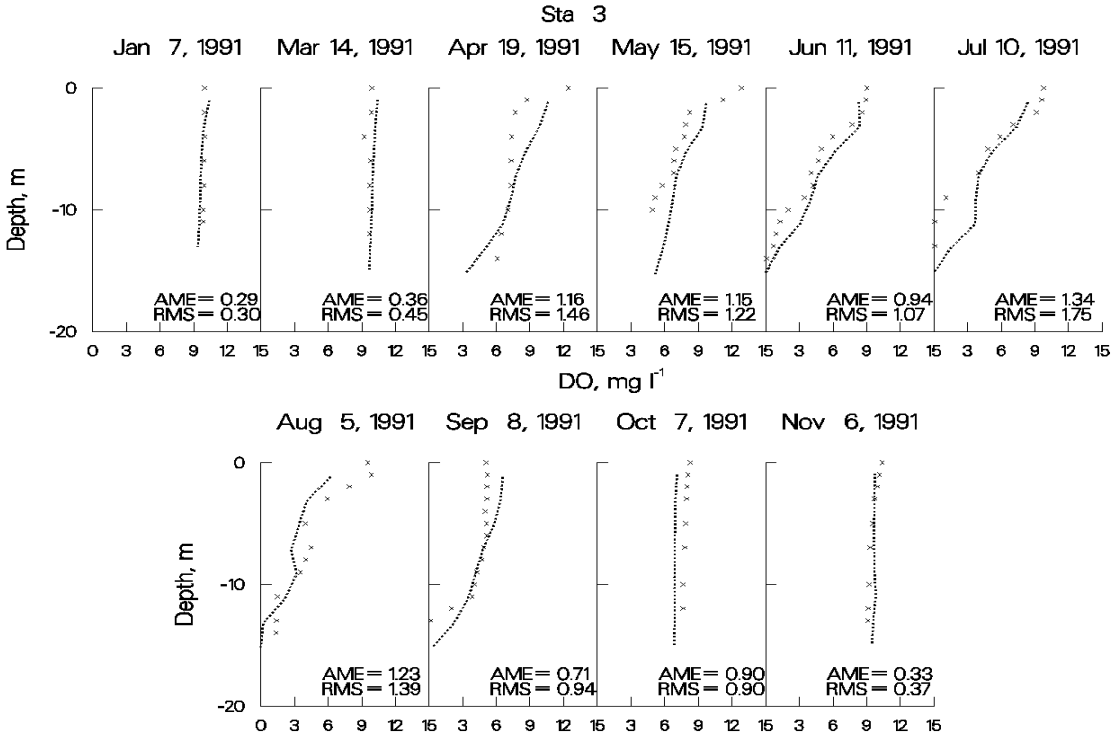


Figure 28. Weiss Reservoir computed vs. observed DO.

CALIBRATION

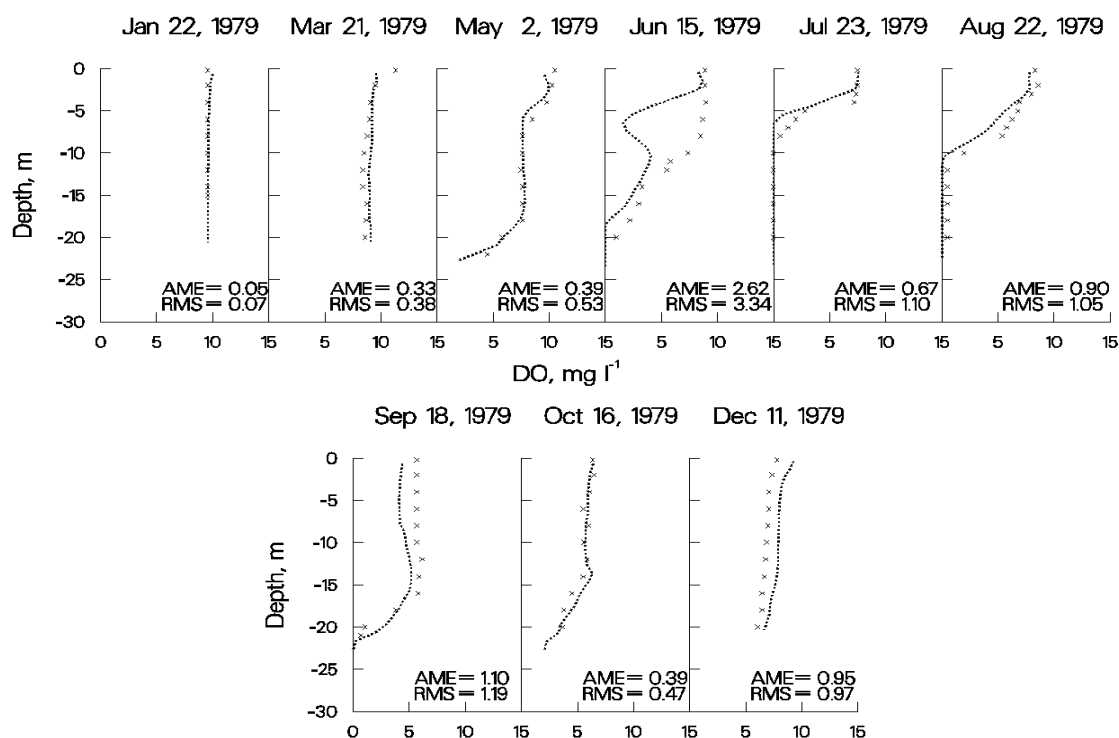


Figure 29. West Point Reservoir computed vs. observed DO.

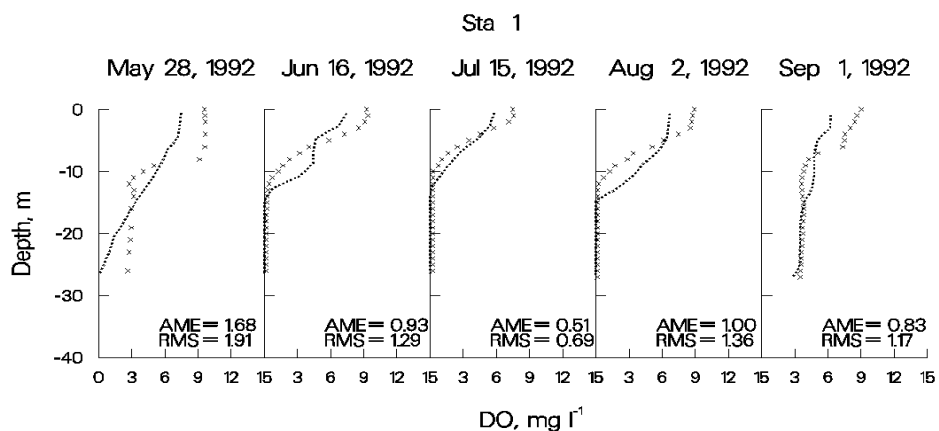


Figure 30. Walter F. George Reservoir computed vs. observed DO.

As can be seen from the previous figures for computed versus observed DO comparisons, the model has reproduced a wide range of DO regimes with a high degree of accuracy using mostly default kinetic parameters. The largest discrepancies between computed and observed DO occur in the epilimnion during middle to late summer where the model consistently underpredicts supersaturated DO. The problem is that if the model is correctly predicting very low nutrient levels during these times (typically at detection levels), then there are insufficient nutrients in the water column to support the observed levels of primary production indicated by supersaturated conditions. This is a shortcoming of all currently used water quality models and indicates insufficient understanding of

phytoplankton/nutrient dynamics in the photic zone. A great deal of research needs to be done in this area in order to improve our ability to model phytoplankton primary productivity.

Another possible problem during dissolved oxygen calibration is during fall overturn when anoxic hypolimnetic water mixes with epilimnetic water. For the most part, the model reproduces dissolved oxygen fairly well during overturn ([Figure 29](#)), but in some applications the model has consistently underpredicted dissolved oxygen and in other applications the model has consistently overpredicted hypolimnetic concentrations.

There are three possible causes for this behavior. The first is the reaeration formula is not appropriate for the waterbody. For reservoirs, the model has accurately reproduced epilimnetic dissolved oxygen concentrations on so many systems that this is probably not the case. The second possibility is that the volumes of epilimnetic and hypolimnetic volumes are sufficiently off to affect the final mixed dissolved oxygen concentration. Depending upon the direction of the volume error, this can result in either over or underprediction. The third possibility in the case of overprediction is that reduced substances including ammonium, iron, manganese, and sulfides have been released from the sediments in sufficient quantities to exert an appreciable oxygen demand. The model includes only the affect of ammonium on dissolved oxygen. In this case, the code would need to be altered to include their effects on dissolved oxygen. All of these scenarios should be investigated if accurate reproduction of dissolved oxygen during fall overturn is important to simulate.

Nutrients. Given accurate boundary conditions for phosphorus, ammonium, and iron and accurate simulations of metalimnetic/hypolimnetic dissolved oxygen, hypolimnetic concentrations of these nutrients are relatively easy to reproduce. Again, this is basically a back calculation of the sediment fluxes to match observed hypolimnetic concentrations.

Epilimnetic concentrations of phosphorus during the growing season are typically at or below detection levels in both the model and the prototype, so they are also relatively easy to reproduce. Fall concentrations can be more complicated, particularly if iron and manganese have built up during the summer in an anoxic hypolimnion. In this case, the iron compartment should be turned on so that iron is released in the hypolimnion. The model includes phosphorus sorption onto iron hydroxides that form during fall overturn and settle into the sediments, thus removing phosphorus from the water column.

Epilimnetic ammonium and nitrate levels are more difficult to reproduce as some phytoplankton show a preference for ammonium over nitrate and the degree to which they exhibit this preference is different between groups. In addition, water column nitrate undergoes denitrification when the water column goes anoxic and also diffuses into the sediments where it undergoes denitrification in the anaerobic layer under both oxic and anoxic conditions. The ammonium preference factor [\[ANPR\]](#), the water column denitrification rate [\[NO3DK\]](#), and the sediment nitrate uptake rate [\[NO3S\]](#) are calibration parameters that can be adjusted to better match observed concentrations of these nutrients.

Phytoplankton. The following plots illustrate the model's ability to reproduce a spring phytoplankton bloom in Rimov Reservoir, Czech Republic. Tremendous amounts of data were collected to analyze the spring bloom. Chlorophyll *a* samples were taken at 1 m depth intervals over upper 10 m of the water column at six stations approximately every three days for over a month. The plots include six stations along the length of the reservoir starting upstream and progressing towards the dam.

CALIBRATION

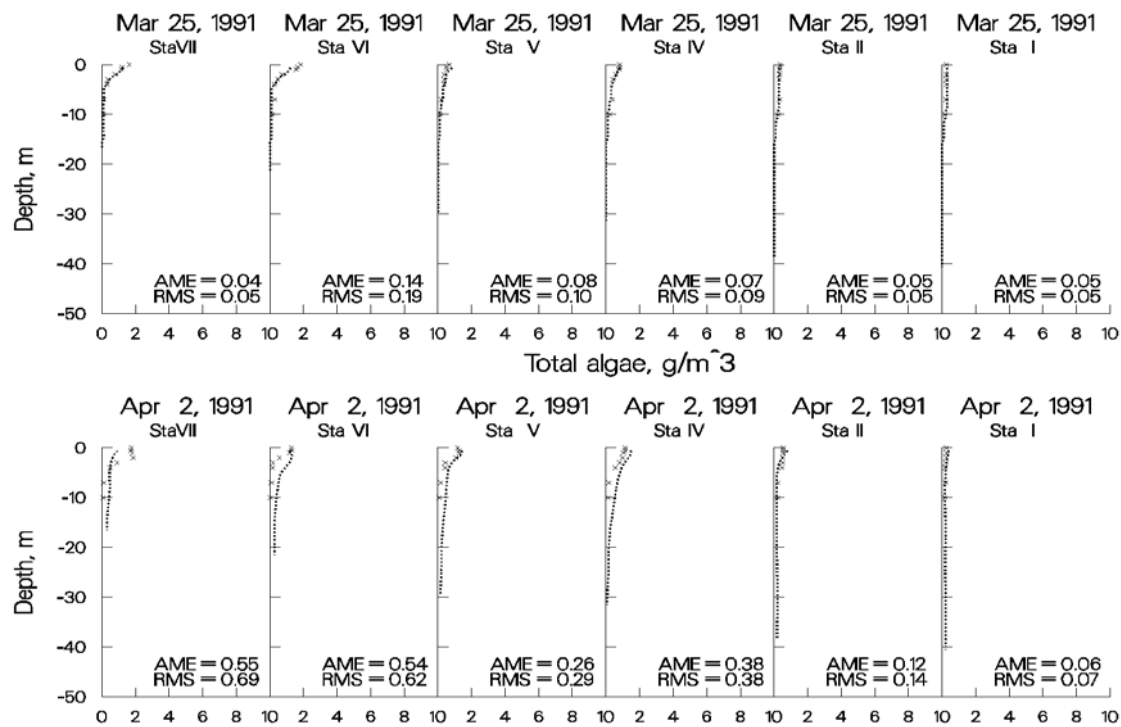


Figure 31. Rimov Reservoir computed vs. observed phytoplankton biomass.

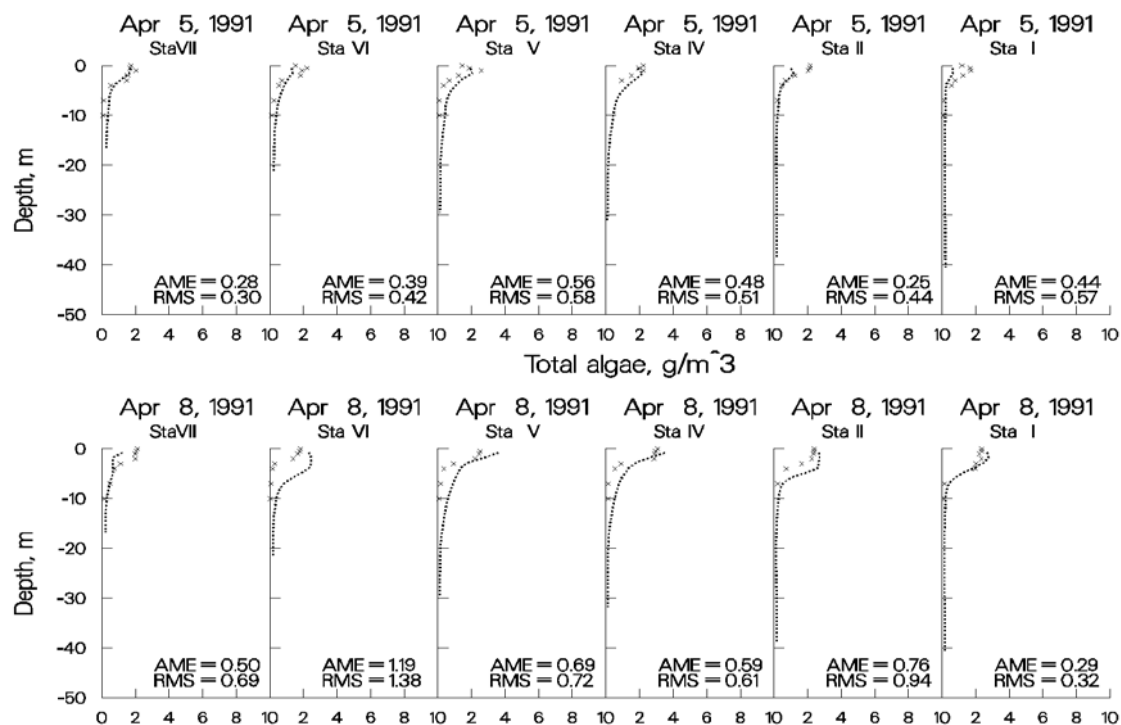


Figure 32. Rimov Reservoir computed vs. observed phytoplankton biomass.

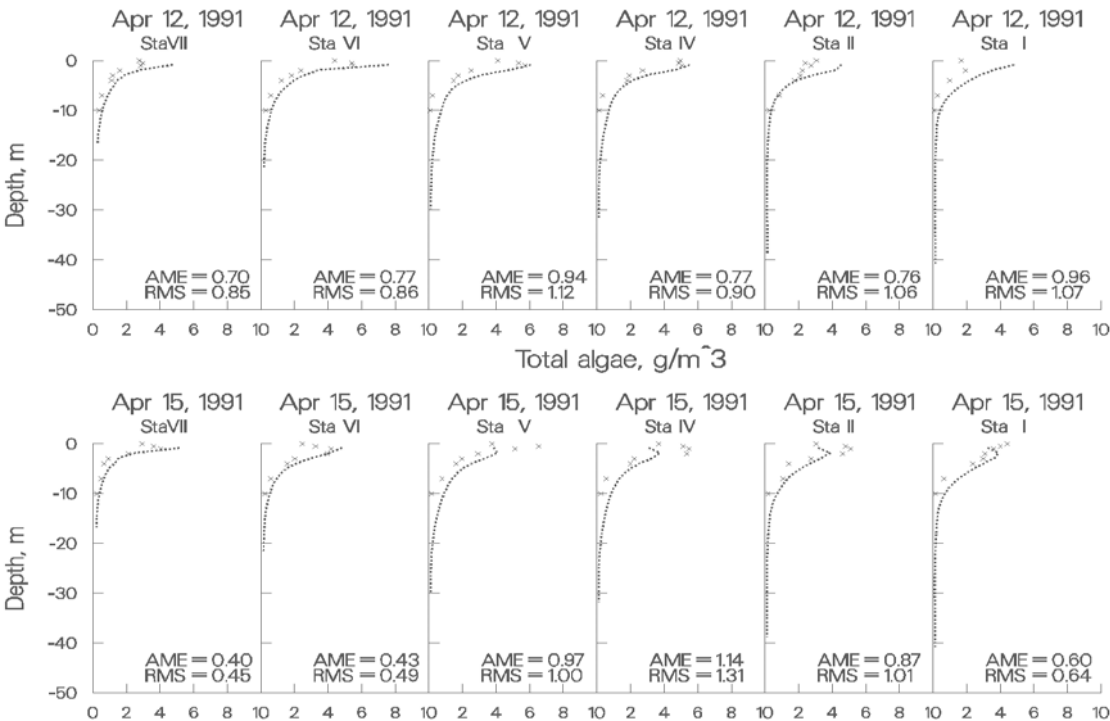


Figure 33. Rimov Reservoir computed vs. observed phytoplankton biomass.

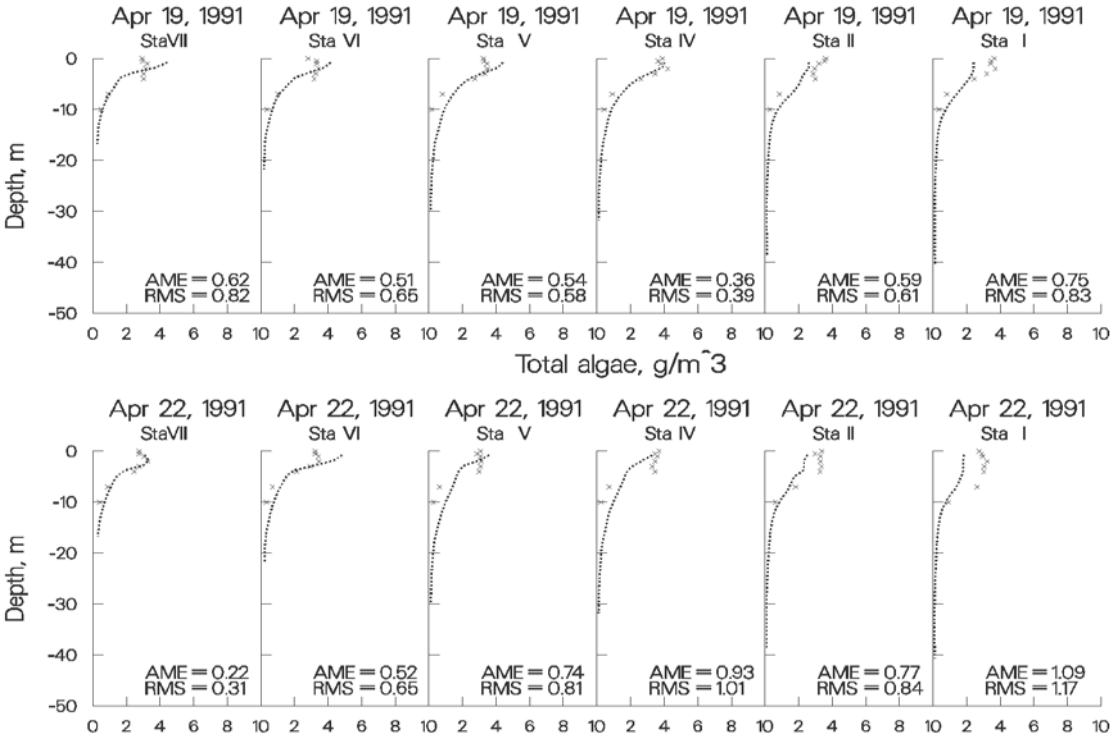


Figure 34. Rimov Reservoir computed vs. observed phytoplankton biomass.

CALIBRATION

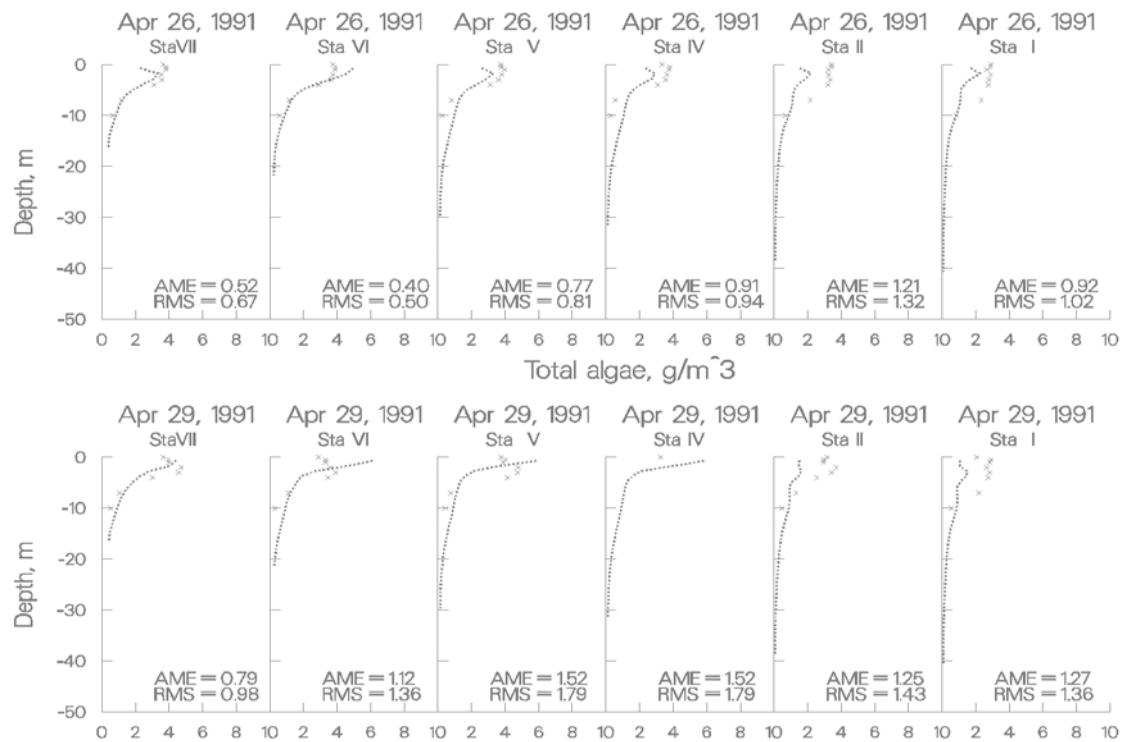


Figure 35. Rimov Reservoir computed vs. observed phytoplankton biomass.

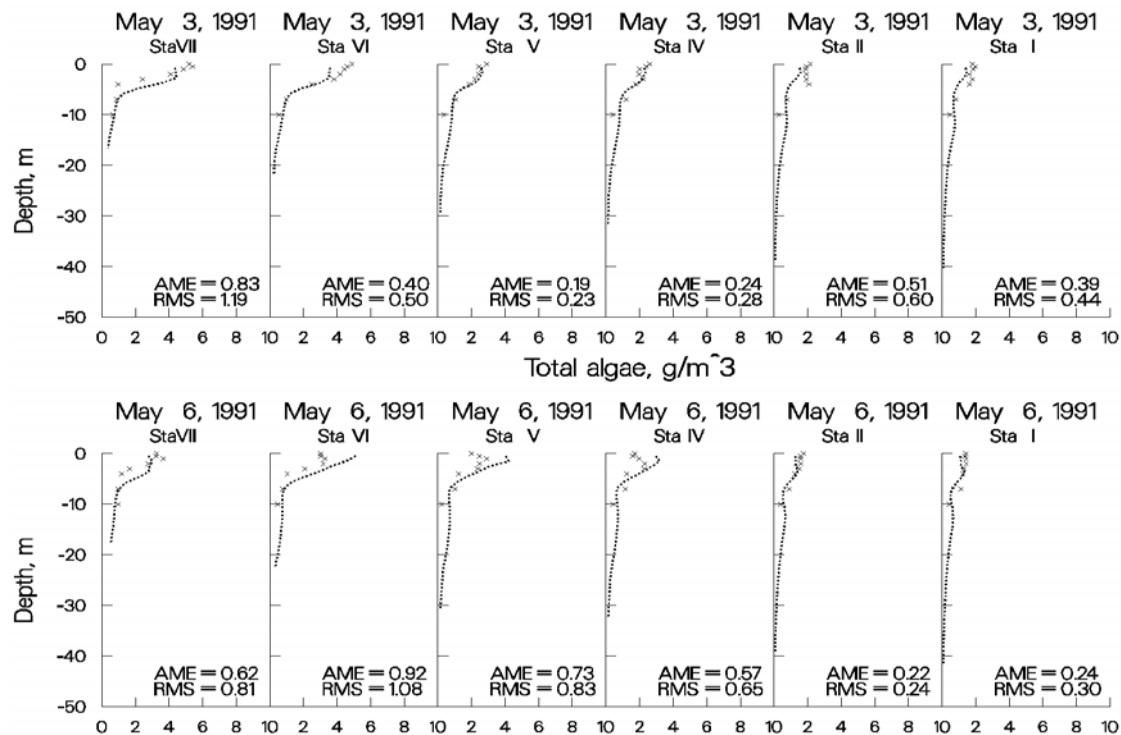


Figure 36. Rimov Reservoir computed vs. observed phytoplankton biomass.

CALIBRATION

The following plots illustrate how important it is to describe the system accurately. The plots show results of the Rimov phytoplankton simulation in which the wind direction was inadvertently changed by 90°. The importance of wind direction and its influence on the spring phytoplankton bloom was noted by limnologists who originally collected the 1991 data. Note the difference at the most downstream station on April 8 compared to the previous plot of April 8 using the correct wind direction. This also illustrates that the model can be a powerful limnological investigative tool when trying to determine how important different forcing functions are to the limnology of a reservoir.

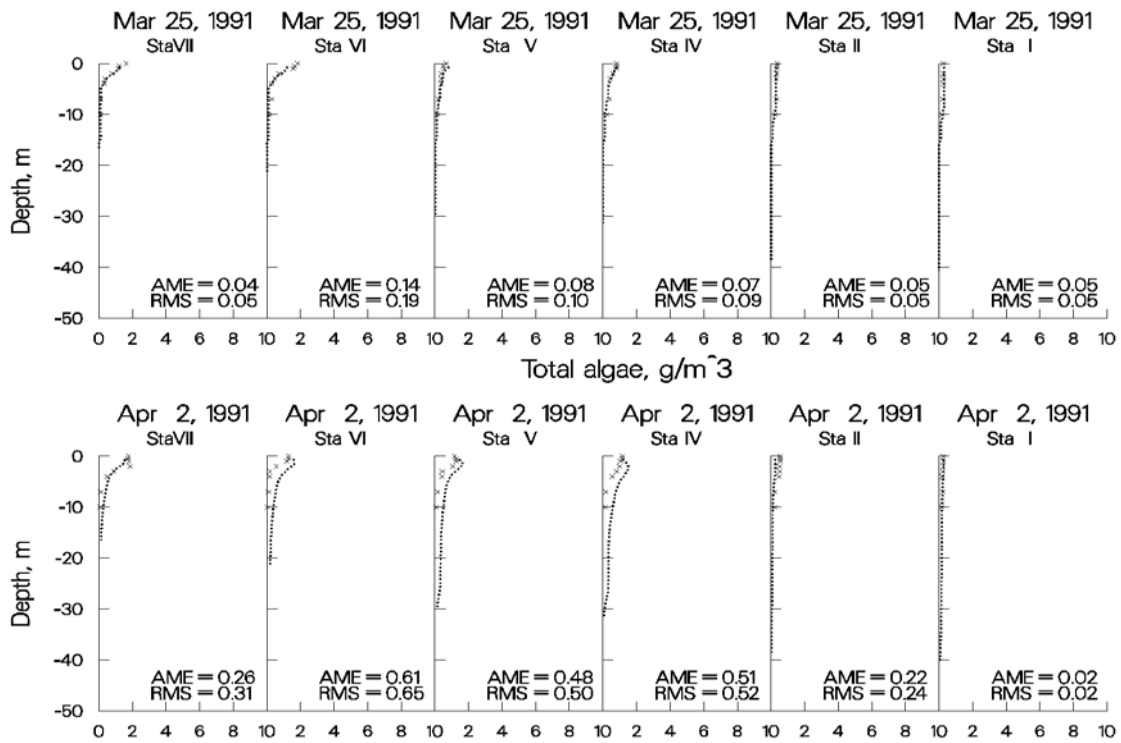


Figure 37. Rimov Reservoir computed vs. observed phytoplankton with wind rotated 90°.

CALIBRATION

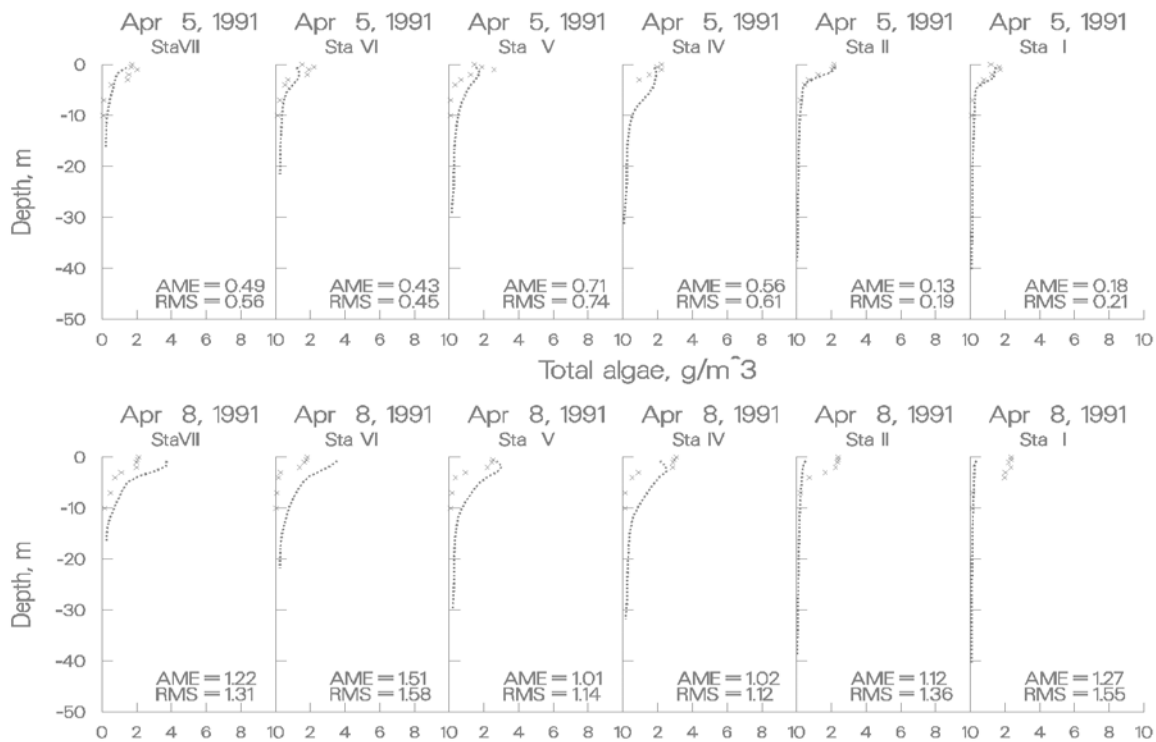


Figure 38. Rimov Reservoir computed vs. observed phytoplankton with wind rotated 90°

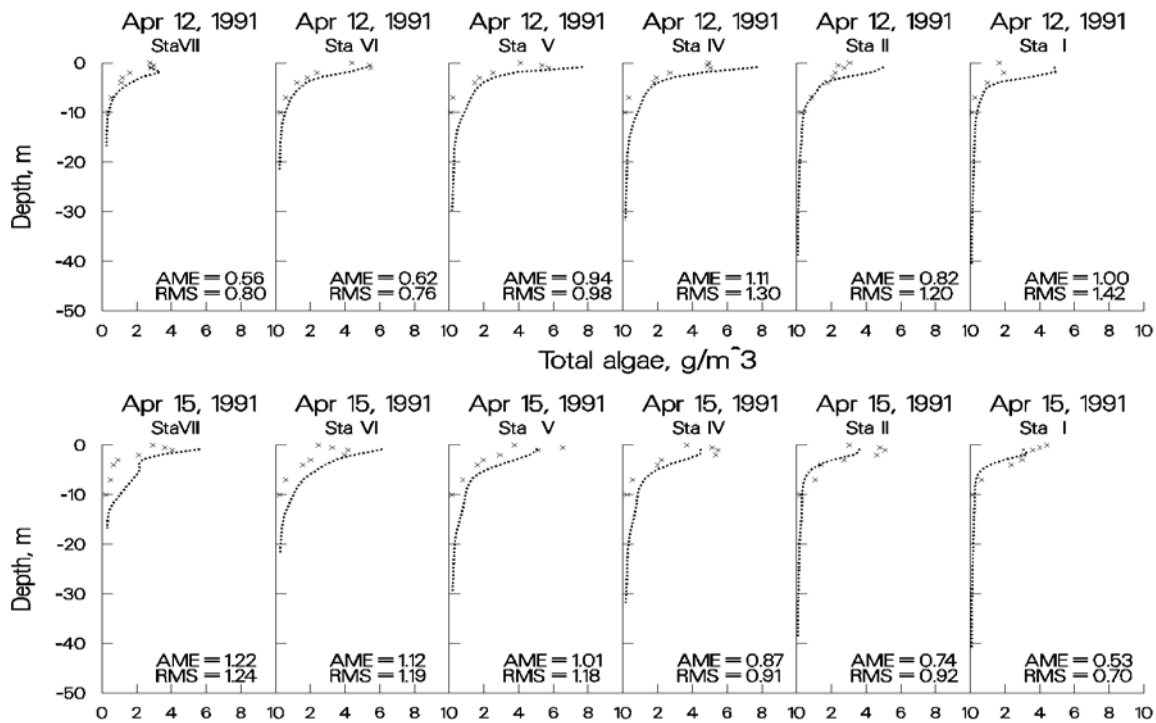


Figure 39. Rimov Reservoir computed vs. observed phytoplankton with wind rotated 90°.

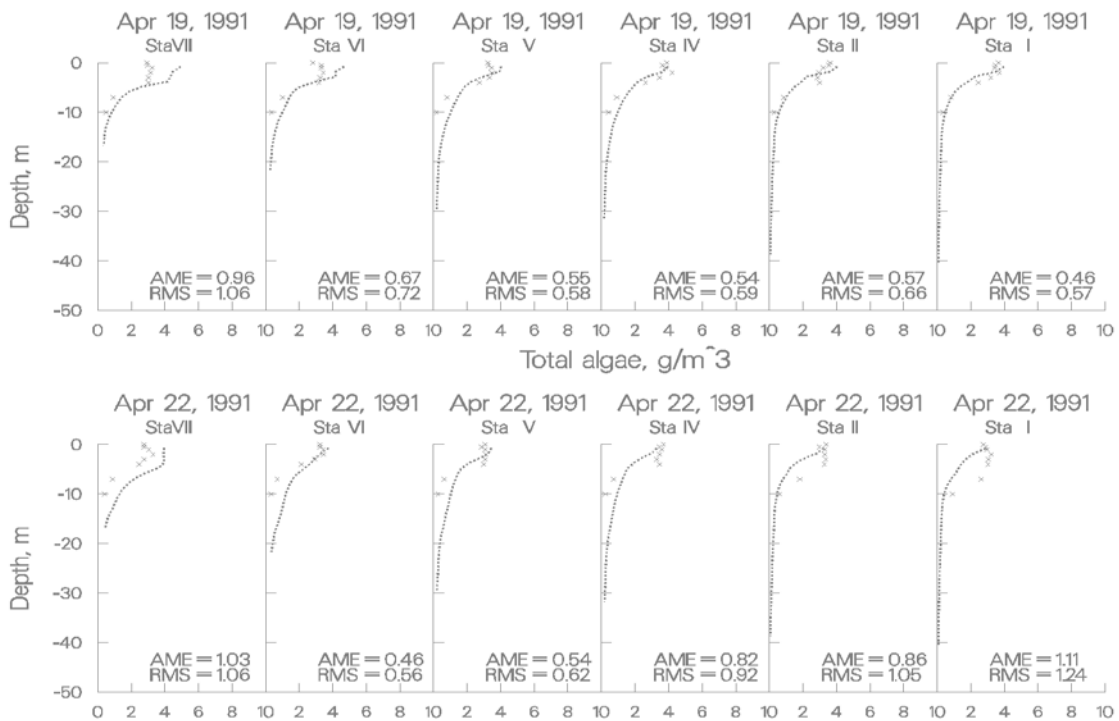


Figure 40. Rimov Reservoir computed vs. observed phytoplankton with wind rotated 90°.

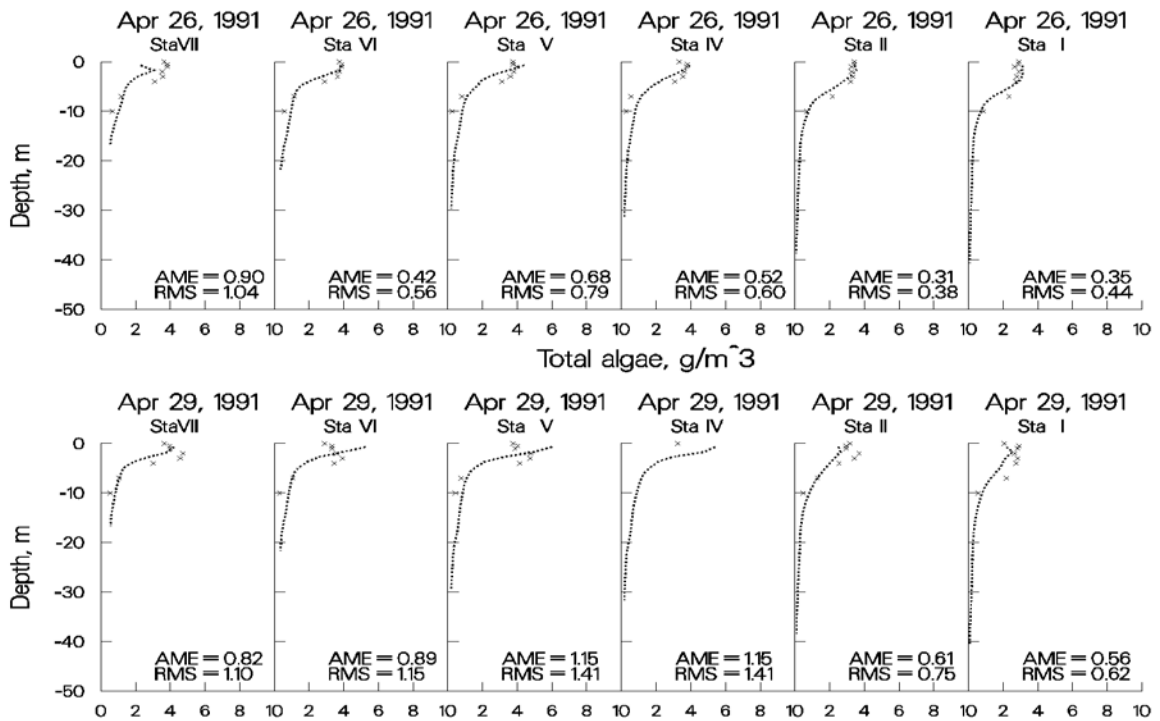


Figure 41. Rimov Reservoir computed vs. observed phytoplankton with wind rotated 90°.

CALIBRATION

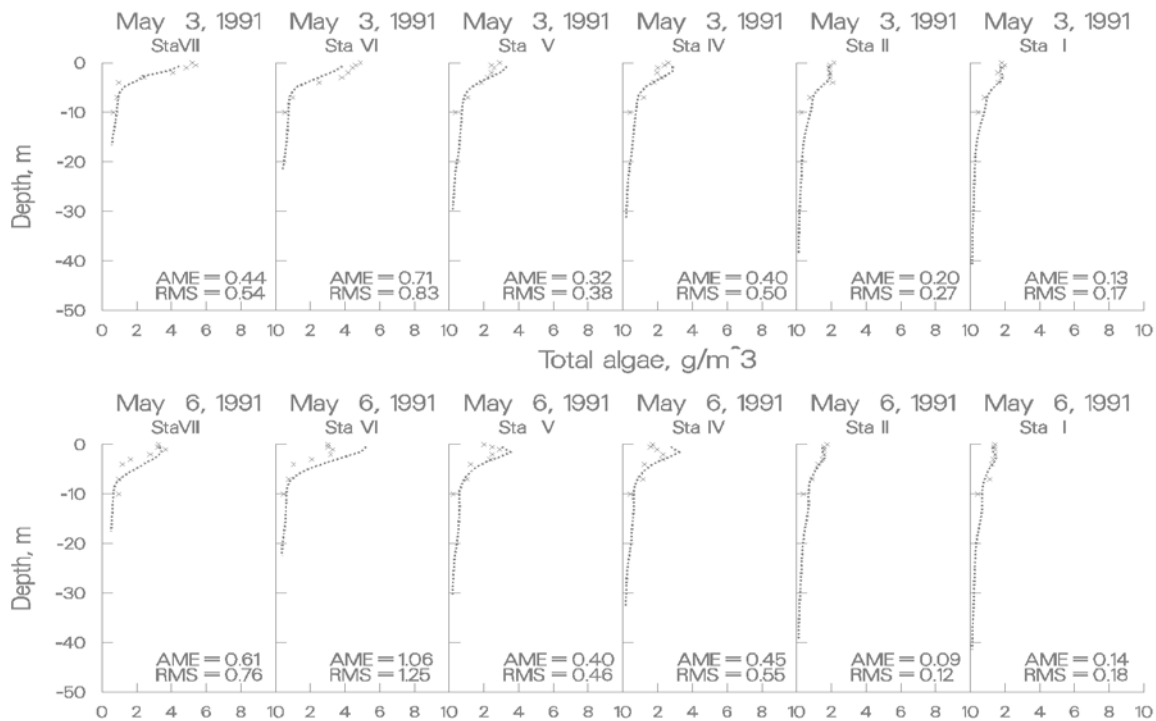


Figure 42. Rimov Reservoir computed vs. observed phytoplankton with wind rotated 90°.

The following plots illustrate the importance of accurate inflow boundary conditions for phytoplankton in Rimov Reservoir. Inflow phytoplankton concentrations were inadvertently set to 0.05 g m^{-3} rather than the observed concentrations when converting from V2 to V3. Again, the researchers who collected the original data concluded that the spring phytoplankton bloom was first initiated in Rimov because of inflowing phytoplankton. The model concurs with this conclusion and again illustrates how powerful a limnological investigative tool the model can be.

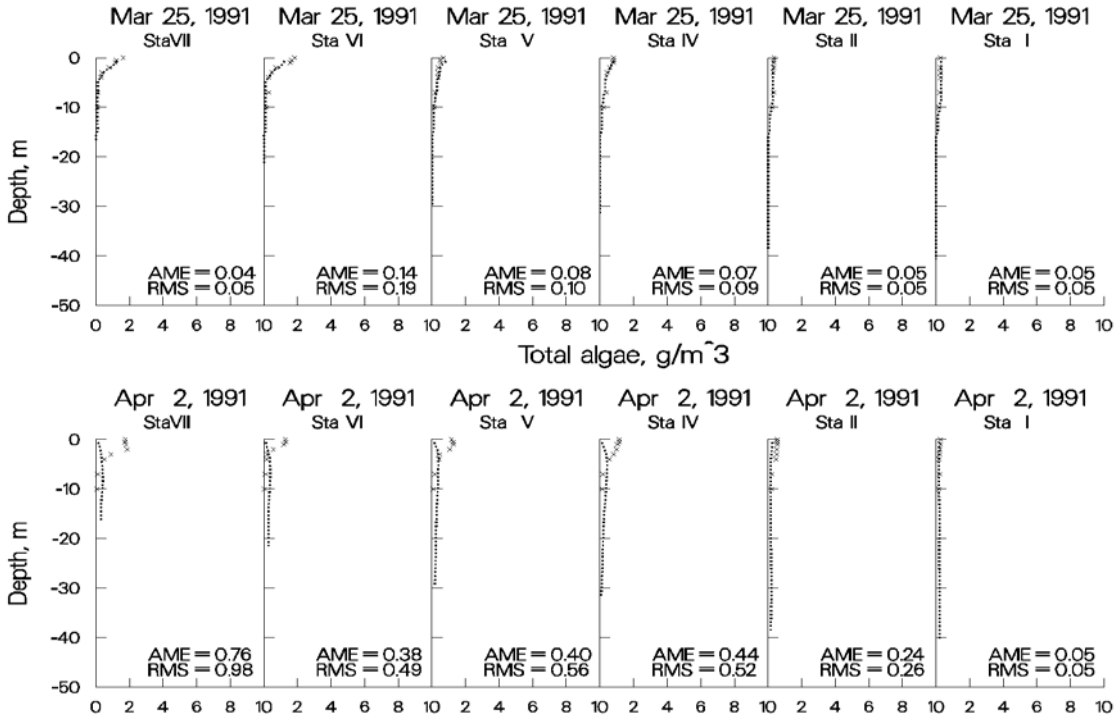


Figure 43. Rimov Reservoir computed vs. observed phytoplankton with no inflowing phytoplankton.

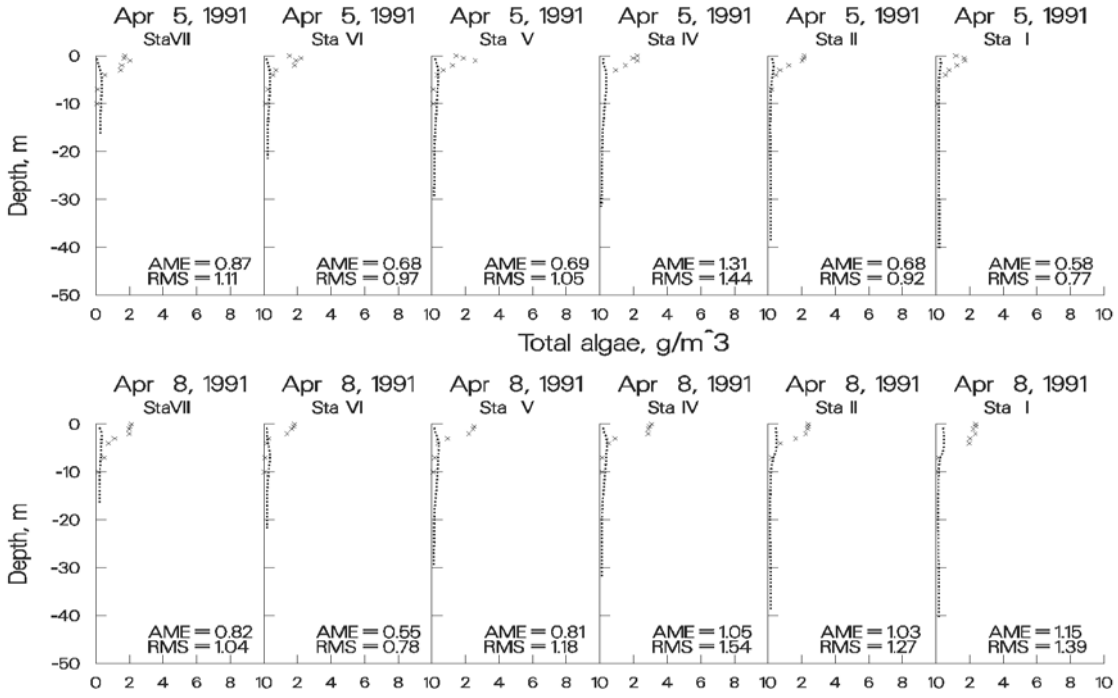


Figure 44. Rimov Reservoir computed vs. observed phytoplankton with no inflowing phytoplankton.

CALIBRATION

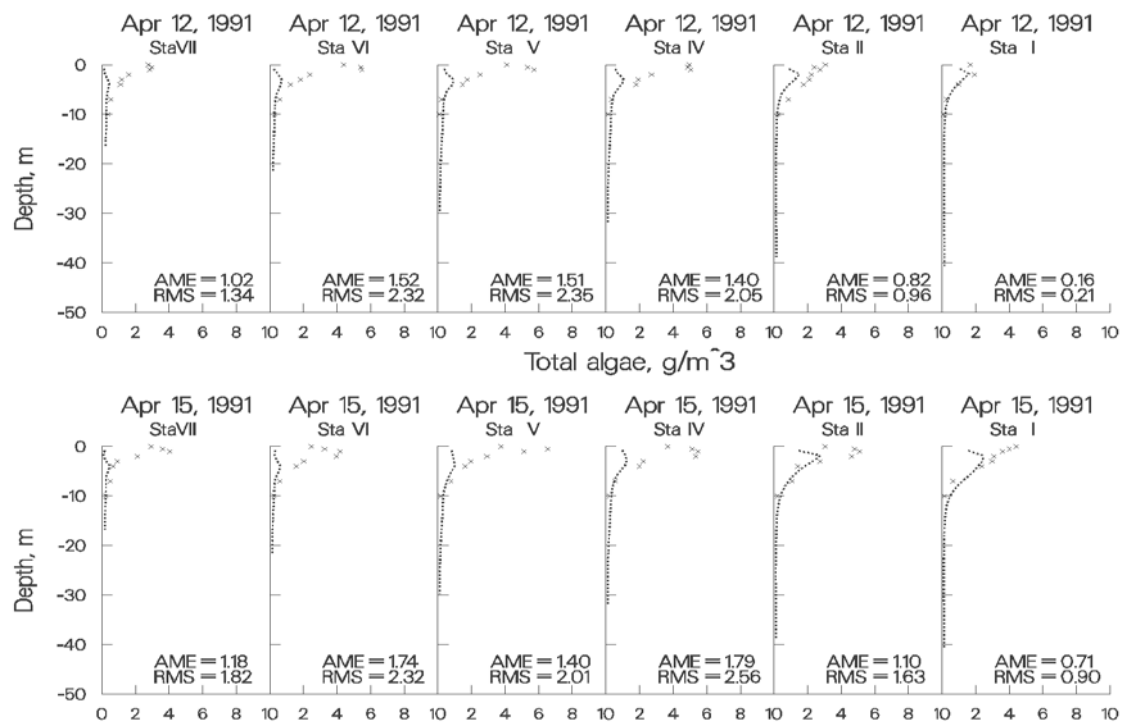


Figure 45. Rimov Reservoir computed vs. observed phytoplankton with no inflowing phytoplankton.

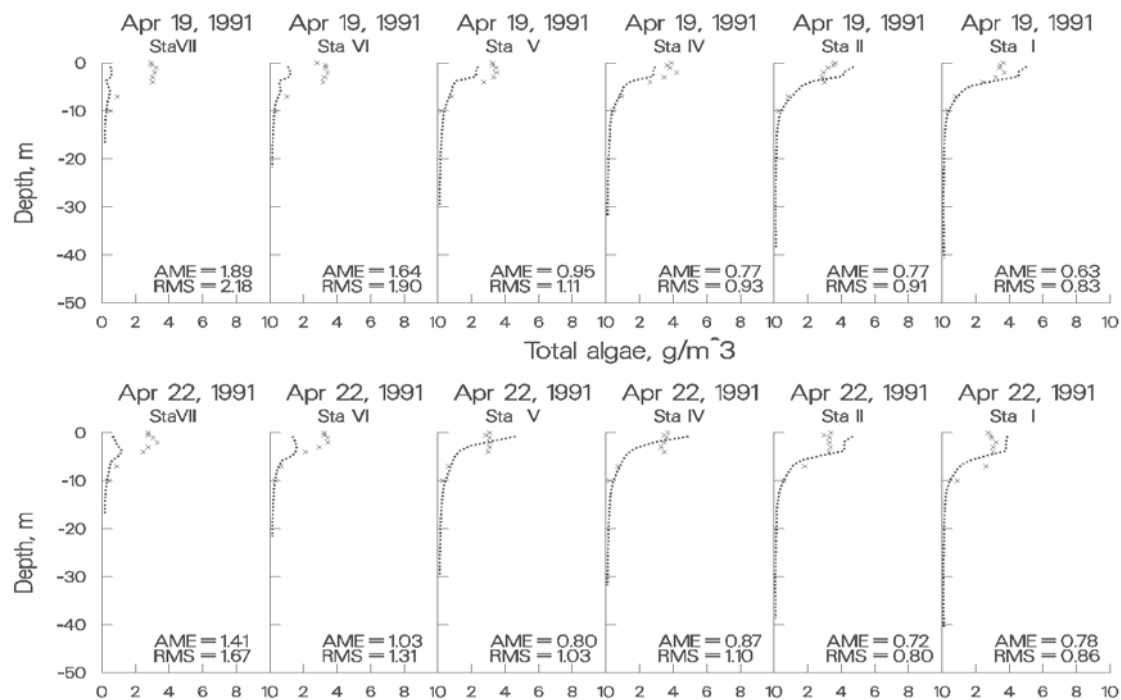


Figure 46. Rimov Reservoir computed vs. observed phytoplankton with no inflowing phytoplankton.

CALIBRATION

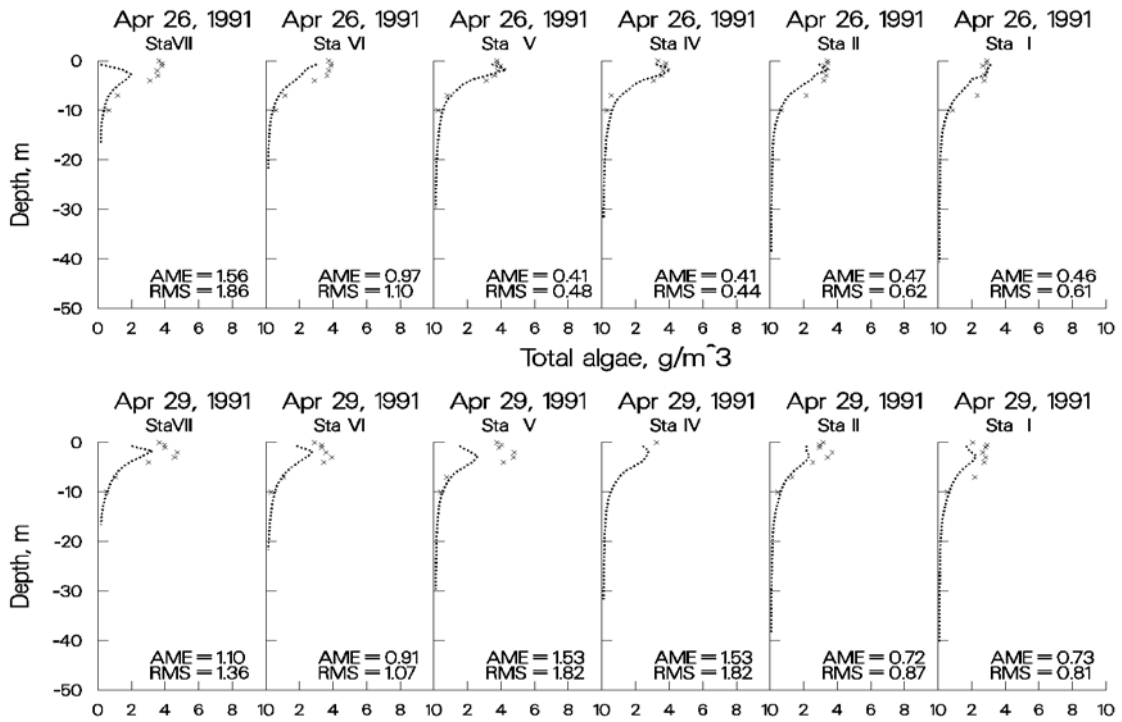


Figure 47. Rimov Reservoir computed vs. observed phytoplankton with no inflowing phytoplankton.

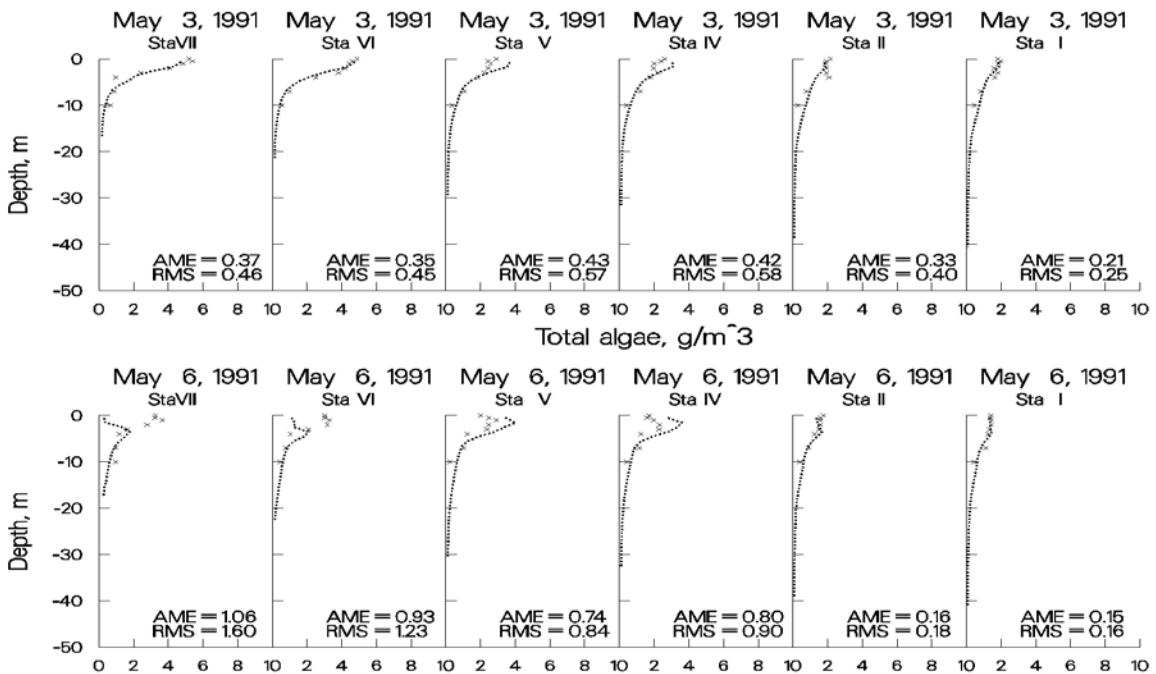


Figure 48. Rimov Reservoir computed vs. observed phytoplankton with no inflowing phytoplankton.

CALIBRATION

Estuary

Estuarine modeling is similar to reservoir and lake modeling for both bathymetry development and water quality modeling, but there are a few important differences in the hydrodynamic calibration. Salinity is commonly used to assess model hydrodynamic performance. However, as with reservoirs, water quality variables such as dissolved oxygen and phytoplankton can be used to also assess the accuracy of the hydrodynamics. When calibrating salinity, it is common practice to plot predicted versus observed time-series of surface and bottom salinity. While plots such as these are useful, vertical plots of computed versus observed salinity, if available, should always be included as part of the calibration process.

Boundary conditions

Ocean boundary conditions play a critical role in estuarine modeling and the data should be frequent and of high quality. At a minimum, downstream head boundary elevations should be available on an hourly basis. The model can be used to linearly interpolate [\[HDIC\]](#) between observed elevations. Alternatively, formulas can be used to compute elevations at any frequency based on various components of the tidal cycle.

Equally important are salinity concentrations specified at the downstream boundary. It is always preferable to set the boundary sufficiently downstream so that there is no vertical variation in salinity and hopefully only small temporal changes. However, the boundary needs to be set where the head elevations are measured, and oftentimes there are significant vertical and temporal variations in salinity at the site. Weekly vertical profiles are usually of insufficient frequency to reproduce the hydrodynamics of the estuary with any accuracy in this case. The same will hold true for temperature and constituents if they exhibit vertical and temporal variations.

Upstream freshwater inflows need to be accurately gaged and evaporation and precipitation should be included in the simulation if possible. Because of the inaccuracies associated with gaged inflows, sensitivity analyses should be run by increasing and decreasing upstream inflows to determine their impacts on hydrodynamics and water quality rather than initially turning to a model “knob” to adjust model results, particularly for vertical salinity distributions in a stratified estuary. Many times the model has provided information as to where forcing functions need to be more accurately measured for a successful model application.

Water surface elevations and flows

In an estuarine system, the first step is to make certain the model correctly replicates tidal elevations and flows at various stations along the length of the system. Usually these stations have continuous data for comparison. Problems in water level and flow calibration can be caused by the following:

1. **Incorrect or inadequate bathymetry.** The user should ensure that the model correctly reproduces cross-sections where these are measured. The model is very sensitive to small changes in the cross-section and more frequent cross-sectional data may be necessary for accurate water level and flow simulations.
2. **Incomplete inflow/outflow data.** A substantial amount of flow can often be unaccounted for as a result of not including tributaries, point sources, precipitation, stormwater, irrigation users, and groundwater. Although precipitation and evaporation will normally be minor sources and sinks, they should be included by turning on the pre-

precipitation [PRC] and evaporation options [EVC]. In an estuary, flow is very dependent on the cross-sectional area at a given location, so grid evaluation should also be part of the calibration process.

3. **Bottom friction.** Bottom friction values [FRICT] for an estuary significantly affect the water level. Bottom friction can be used to calibrate the model to observed water levels at gages along the length of the estuary.

In most cases, the initial water level [WSEL] in the estuary is specified as flat with a velocity field of zero. The model should be run for several days with steady-state inflows [QIN], inflow temperature [TIN], inflow salinity [CIN], meteorology, and downstream head boundary conditions for temperature [TDH] and salinity [CDH]. Once the temperature and salinity distributions are no longer changing, the simulation can continue with observed boundary conditions.

The initial water surface elevation should be the same elevation as the external downstream elevation [EDH] at the start of the simulation. If there is a large elevation difference between the initial condition water level and the first head boundary condition, the model can quickly become unstable because of large flows generated as a result of the water level differences at the head boundary.

Typically, the user will first plot observed versus computed water surface elevations for the simulation period after all the inflow/outflow data have been collected and the model is running to completion. Distributed tributary flows [DTRC] may need to be added or subtracted if the mean flows over a tidal period are not correct. The model user should also check not only instantaneous flow rates, but tidal average rates to make sure the total flow coming into the system at the upstream boundary condition agrees with the net residual flow at different locations downstream. This could point to unaccounted inflows or outflows.

The model user should always take the model segment next to the downstream boundary and compare it to the actual water level data used and the flow rate at the gage, if measured. This checks that the water level in the model is correct and the flow rate predicted by the model agrees with the field data at that location. If the water level matches and the flow does not, this could point to channel bathymetry errors or too high or too low a channel friction near the head boundary condition.

A typical comparison of field data to model predictions of water level are shown in [Figure 49](#) for the Columbia River at Longview, Washington approximately 110 km from the Pacific Ocean. The absolute and root mean square errors were 0.12 m and 0.18 m, respectively, over the period of record with a maximum tidal range of 1.5 m.

CALIBRATION

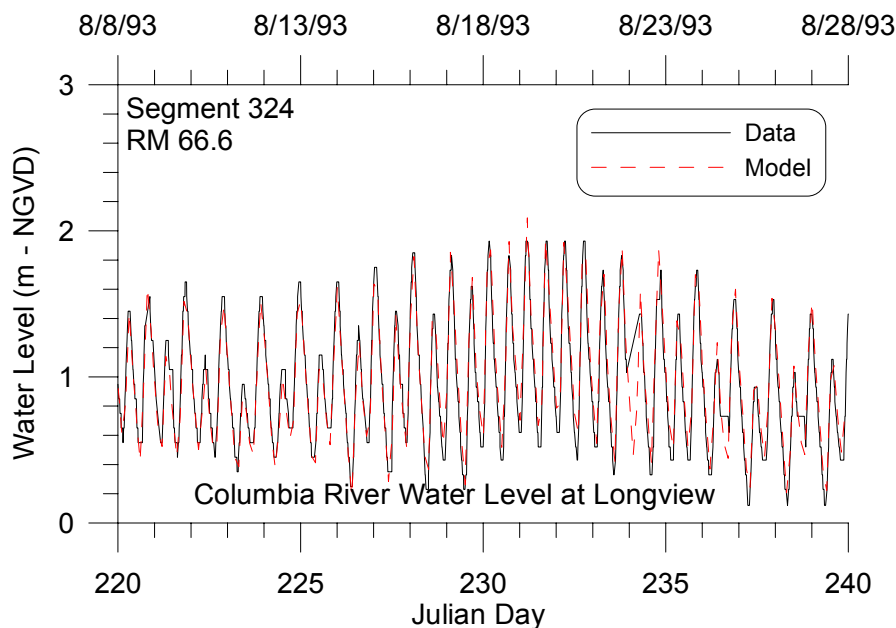


Figure 49. Water level data versus model predictions for Longview, WA during a 20-day period in 1993.

Similarly, a typical comparison of model predictions and field data of flow rate is shown in [Figure 50](#) for the Columbia River approximately 90 km from the Pacific Ocean.

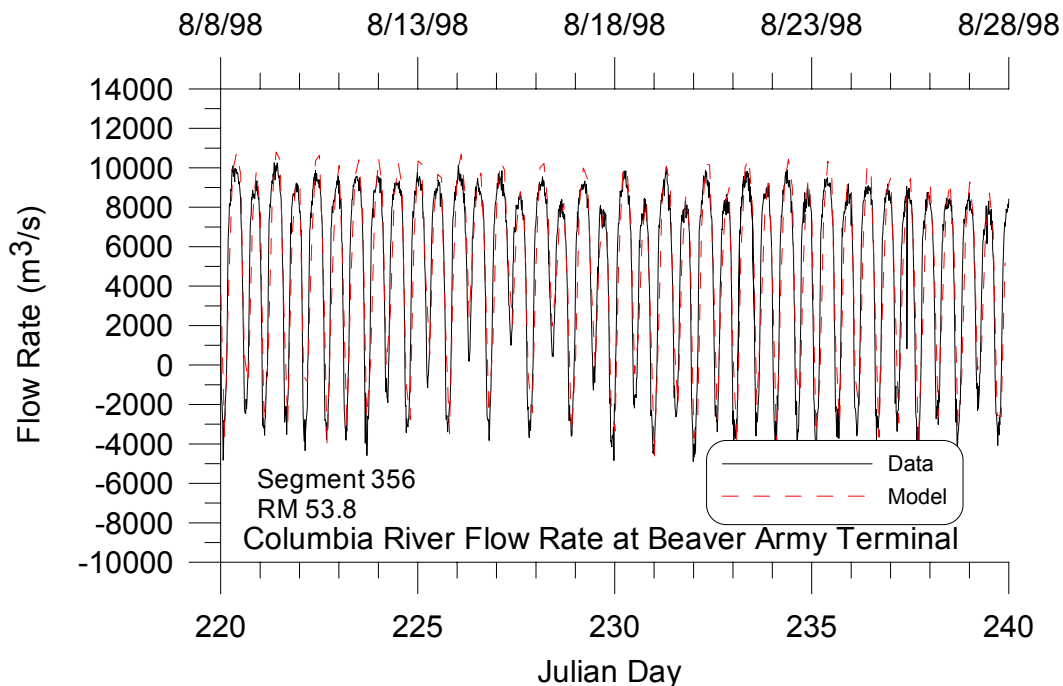


Figure 50. Model flow predictions versus data for a 20-day period during 1998 at Beaver Army Terminal near Quincy, OR.

Time of Travel

If at all possible, the model should be calibrated to a time-of-travel or dye study. This is important to ensure the model represents transport and mixing characteristics of the estuary accurately. Usually, the adjustment of bottom friction is the primary calibration parameter, but in some cases the bathymetry may need revision. The longitudinal eddy viscosity [AX] and diffusivity [DX] can also be adjusted during calibration. Since CE-QUAL-W2 uses a constant value for these coefficients for each waterbody, the user may need to include a longitudinal dispersion algorithm based on theoretical formulae if the constant value is not appropriate.

In many cases a dye release will also vary vertically as a result of stratification. The model internally computes the vertical diffusion coefficient based on the eddy diffusivity using the Reynolds analogy. The model user should ensure that they are using the implicit solution technique for the transport of vertical momentum, [AZSLC]=IMP, and that the maximum value of the vertical eddy viscosity [AZMAX] is at least $1 \text{ m}^2 \text{ s}^{-1}$ for estuarine systems.

Temperature and Salinity

Calibrating the model for estuarine temperature and salinity includes the same caveats as for reservoirs with, as previously mentioned, the additional need for accurate boundary conditions at the ocean boundary. If the user has developed a good hydrodynamic calibration for water surface elevations and flows, then temperature and salinity calibrations should require a minimal effort. However, keep in mind that water surface elevation, flow, and time of travel calibrations are all affected by the adequacy of the temperature and salinity calibration.

[Figure 51](#) and [Figure 52](#) are from an application of CE-QUAL-W2 to the estuarine portion of the Patuxent River that feeds into Chesapeake Bay (Lung and Bai, 2002). They illustrate the model's ability to reproduce vertical profiles of salinity and temperature over time.

CALIBRATION

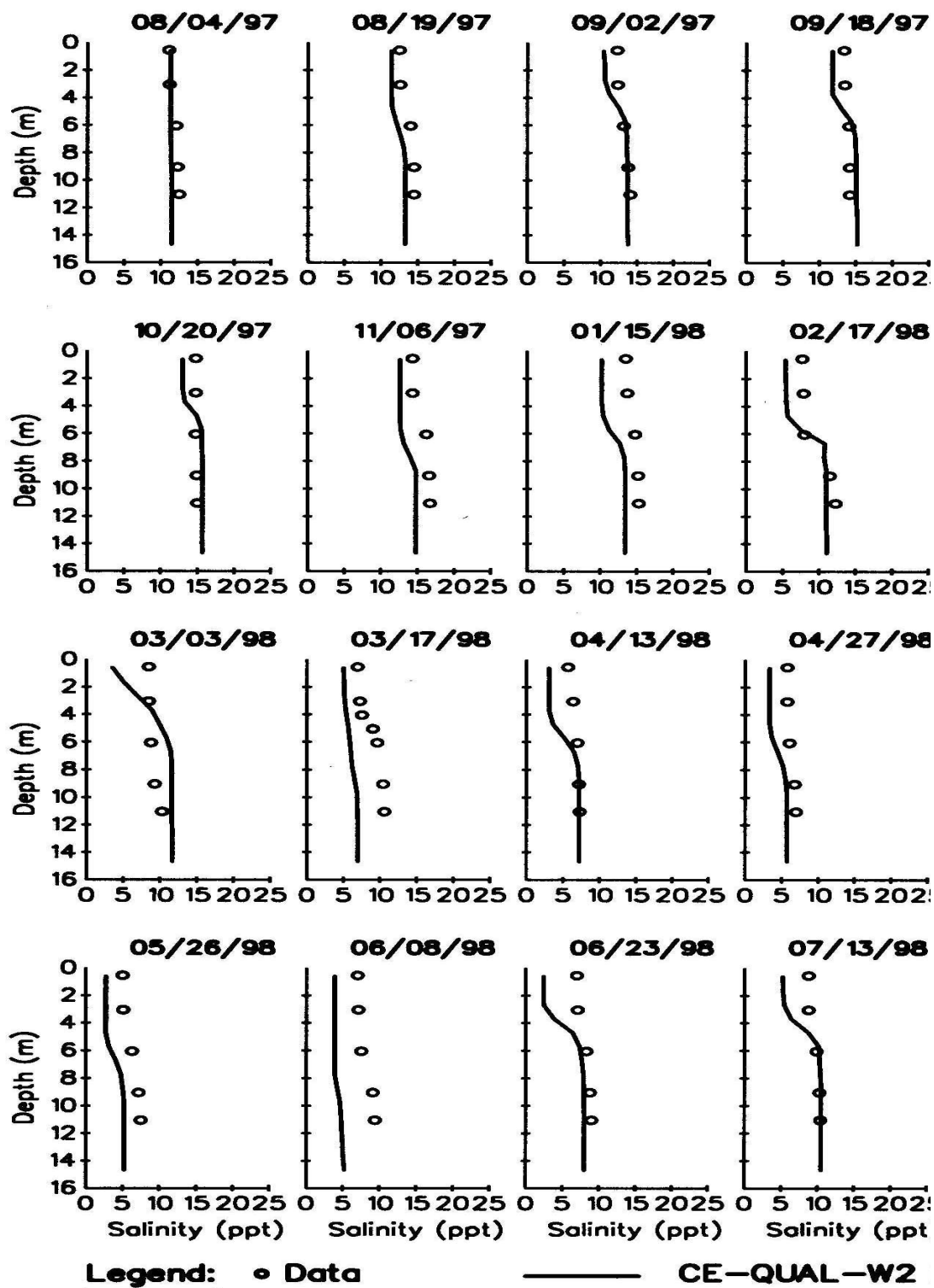


Figure 51. Patuxent River computed versus observed vertical salinity distributions.

CALIBRATION

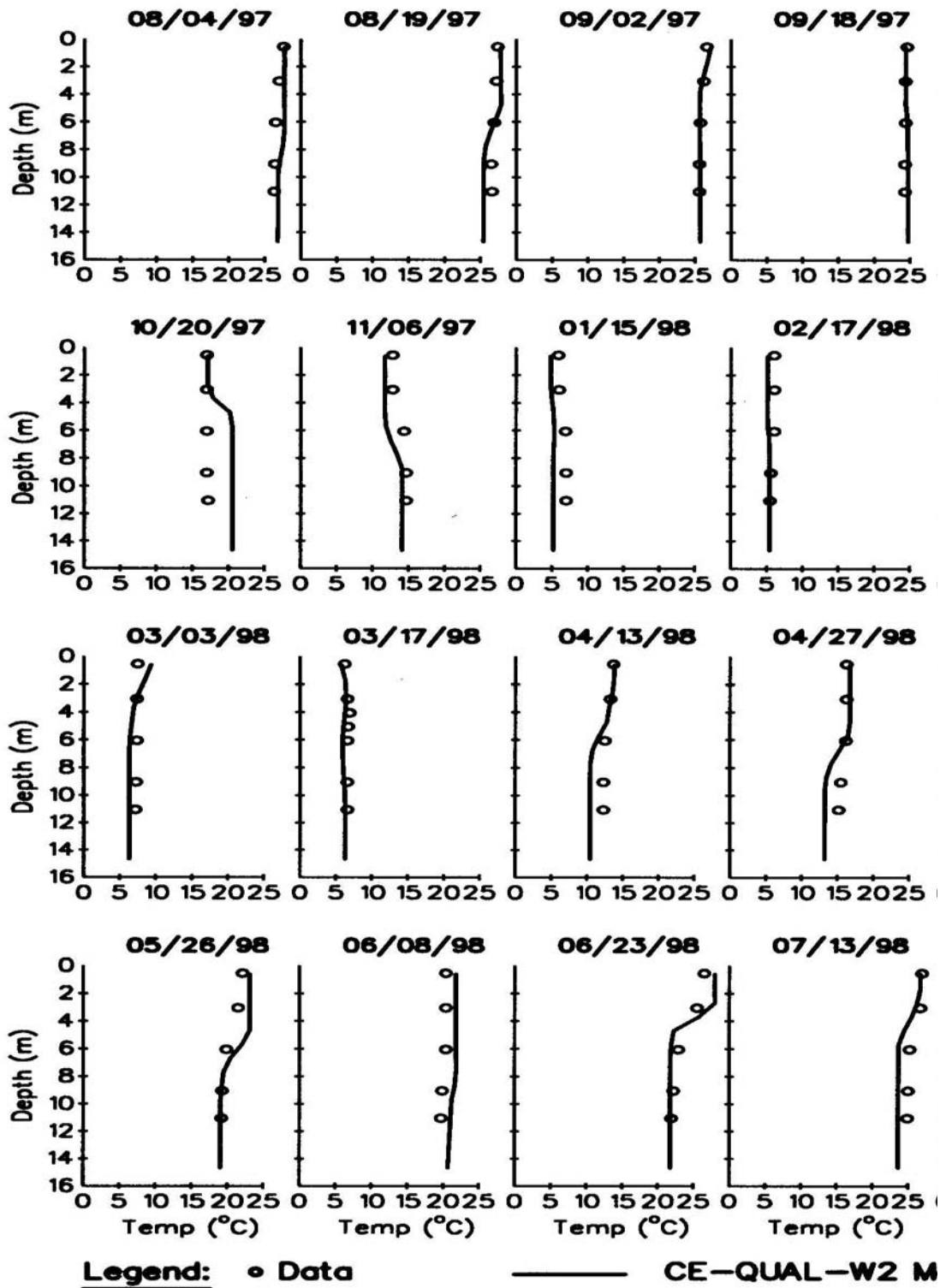


Figure 52. Patuxent River computed versus observed vertical temperature distributions.

CALIBRATION

Water Quality

Water quality calibration for estuaries is again subject to the same caveats as for reservoirs with the additional importance of accurate downstream boundary conditions. Again, if at all possible, the downstream boundary should be located sufficiently downstream where vertical variations in water quality are negligible.

Figure 53 presents results for nutrients, dissolved oxygen, and chl *a* concentrations for Lung and Bai's Patuxent River application of the model.

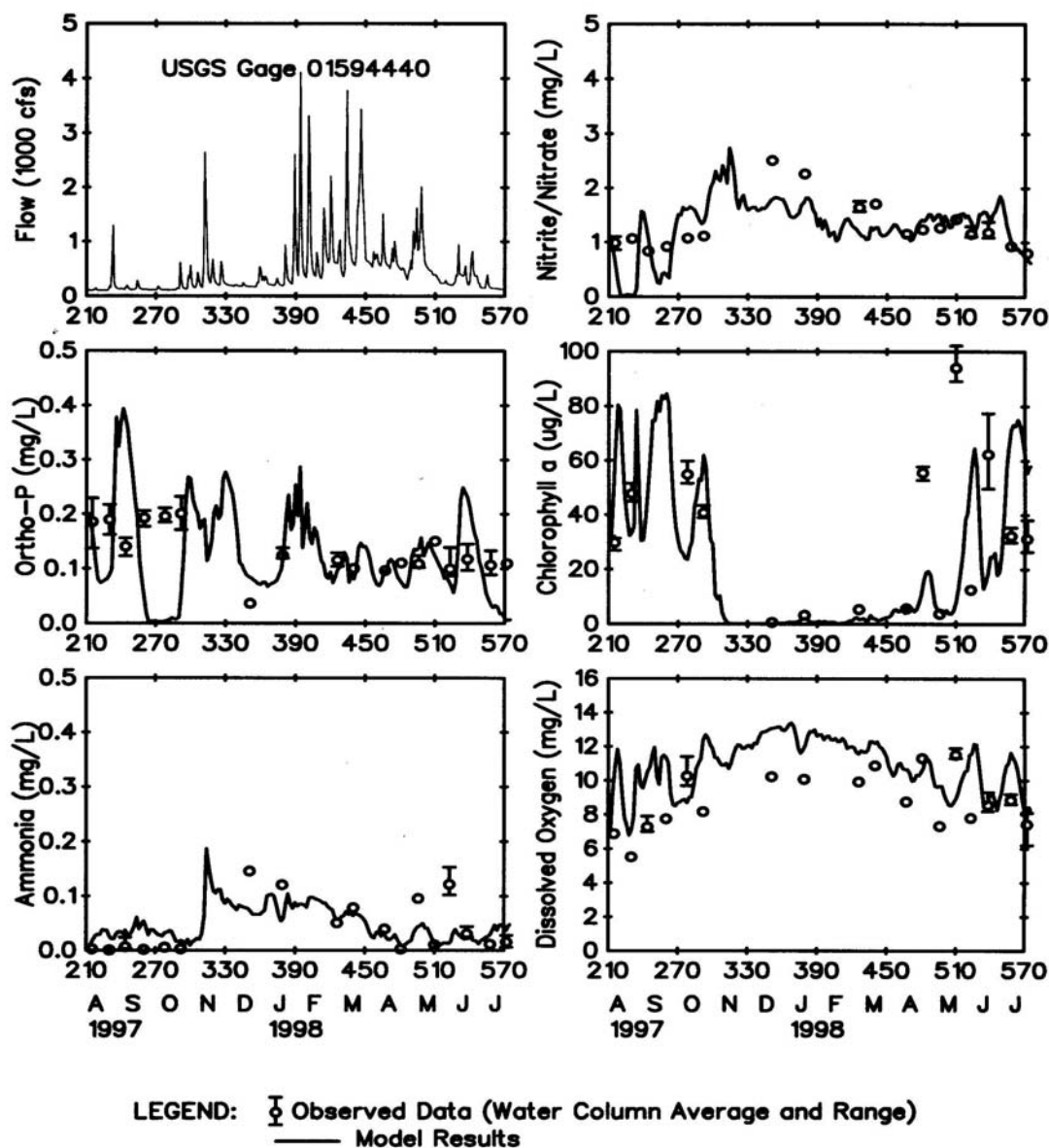


Figure 53. Patuxent River computed versus observed nutrient, dissolved oxygen, and chl *a* time series.

Calibration Problems Modeling an estuarine system requires a tremendous amount of data, expertise, and patience for proper calibration. In previous estuarine applications, calibration consisted mainly of determining whether known inaccuracies in a given forcing function could be responsible for the discrepancies in the model predictions and then describing the forcing function more accurately. This procedure included the following:

1. Ensuring the model reproduces flow and water level at various control points in the model domain and involved detailed evaluation of inflows and outflows, head boundary conditions, channel bathymetry, and channel friction.
3. Adjusting channel friction or longitudinal dispersivity to match time-of-travel data or dye study field data
4. Ensuring accurate vertical profiles for the downstream boundary
5. Ensuring grid refinement does not affect the model results
6. Ensuring accurate meteorological data for the estuary especially if the model domain extends over a large geographical area. Wind variability is extremely important and can be reflected in the wind sheltering coefficient that varies by segment and time.
7. Using an implicit eddy viscosity solution scheme, [AZSLC]=IMP, and a maximum vertical eddy viscosity [AZMAX] of $1 \text{ m}^2 \text{ s}^{-1}$.

Since the model can be susceptible to accuracy issues using an implicit water surface solution scheme with a large time step, the user should ensure results are not impacted by using a smaller maximum time step [DLTMAX]. Again, keep in mind that the more accurately the behavior of the prototype is described, the more accurately the model responds.

River

Dynamic river modeling can be a challenging endeavor because:

1. Velocities are generally high resulting in a lower time step for numerical stability
2. Shear and bottom friction effects are significant requiring a considerable calibration effort
3. Channel slopes accelerate the fluid
4. Changes in river bathymetry can dramatically affect the velocity field
5. Dynamic flow rates at low flows can dry up segments causing the model to stop running

One of the original motivations for development of the capability of modeling sloping rivers was to eliminate vertical accelerations in the fluid since the model does not solve the full vertical momentum equation. Keeping this in mind, the grid slope should be chosen to minimize the vertical fluid acceleration.

Channel Slope

The channel slope is used to compute the gravity force of the channel. This slope should be the slope of the water surface as that is the slope used to accelerate fluid parcels, or the energy grade line, rather than the bottom slope from segment to segment. As an example, consider the slope of a section of the Snake River shown in [Figure 54](#).

CALIBRATION

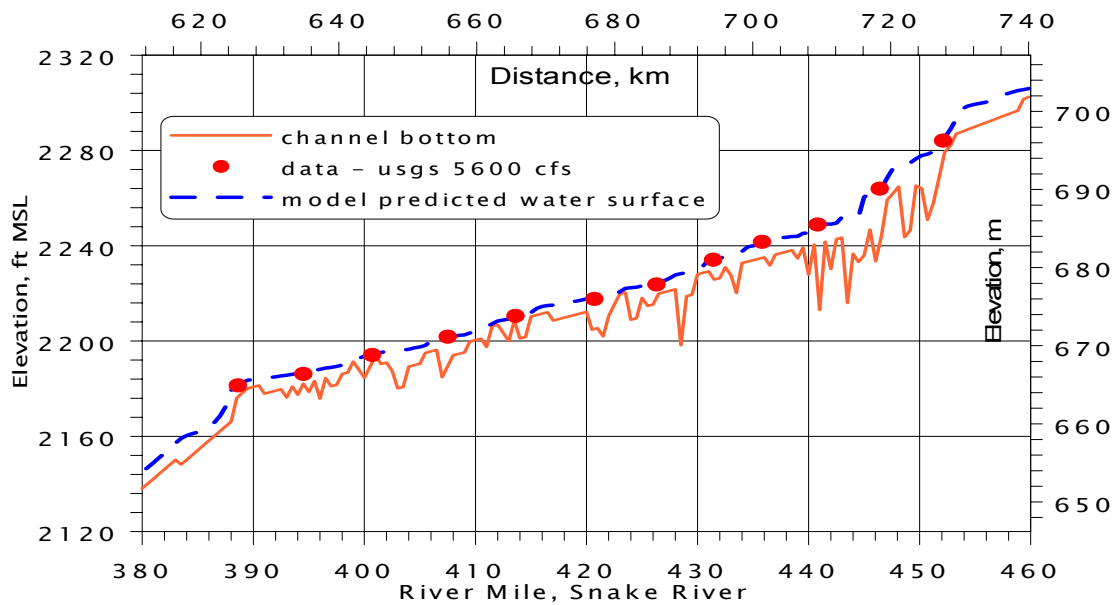


Figure 54. Snake River water level comparison between CE-QUAL-W2 V3 and USGS field data.

The slope of the vertical grid as well as the different branch slopes is shown in [Figure 55](#).

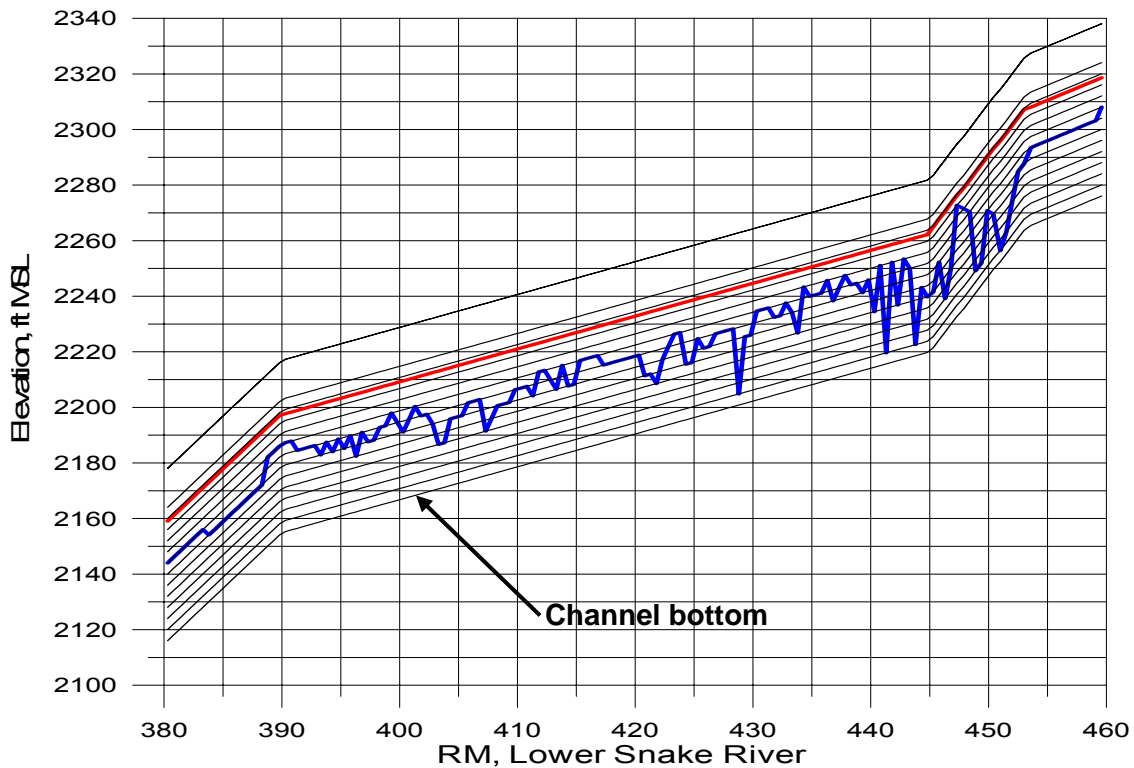


Figure 55. Channel vertical grid where every slope change is a new branch.

Rather than going from segment to segment with varying slopes, a general channel slope is used for a collection of segments with similar water slope. As the variability in water slope changes, so does the grid slope. How can one obtain this slope? [Figure 56](#) illustrates the use of a regression line to fit the channel slope for the section between RM 390 and 445 for the Snake River.

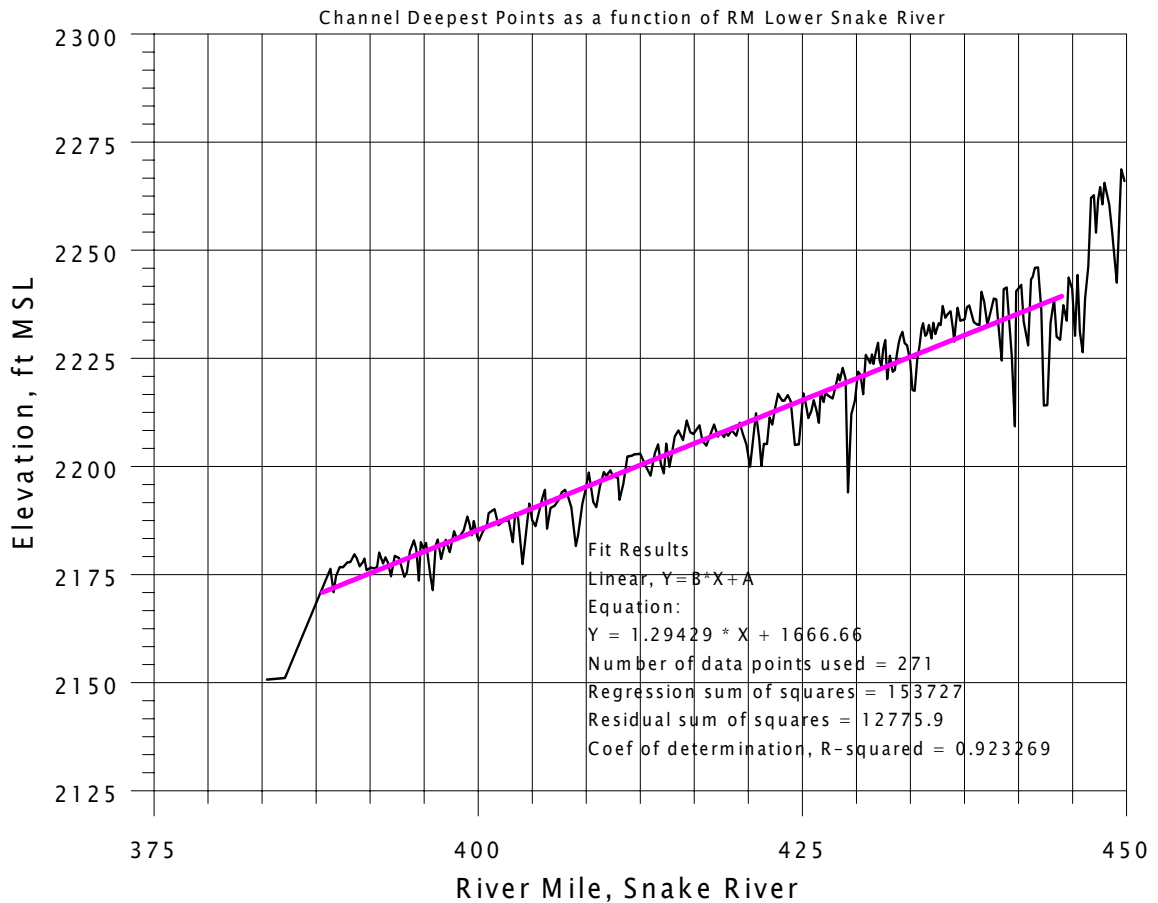


Figure 56. Snake River channel slope determination.

Why does W2 not use a segment-by-segment slope? Consider the “noise” in the cross-sections in [Figure 56](#). Even though the geometry could be set up with a variable channel slope for each segment (in the current application this means creating multiple waterbodies or branches for each slope), setting a general channel grade is often simpler and one still has the noise of the bathymetry represented as shown in [Figure 56](#). Computing the slope from one segment to a deep hole would not be correct since the water is flowing along its energy grade line and not the channel slope. Bottom elevations for many of the channel segments rise or have a negative channel slope following a depression. In using a segment-by-segment slope, these variations become unrealistic when represented using a slope for each segment. Therefore, the proper channel slope should be that of the water surface.

In estuarine flow, one usually uses a channel slope of zero and considers fluid accelerations as a result of water surface elevation changes rather than gravity flow down a slope, at least in the estuary section below the head of tide. This is similar in a reservoir, which may have a sloping channel, but a relatively flat water surface.

CALIBRATION

In some cases, the average channel slope changes and the user must separate the different sections into separate branches or waterbodies. The model can be set up to have almost continuous changes in channel slope by making branches with two segments and changing the slope where it is required. If the choice is to create separate branches, then the surface layer and grid will be the same for all branches. If the choice is to create separate waterbodies, then each waterbody computes a surface layer independently of the other and there can be different vertical grids between water bodies.

When there are problems keeping water in upstream segments, which is a very common problem, the model takes the lowest water level in a waterbody and subtracts layers such that the lowest water level resides in the surface layer. If the surface layer is below the bottom layer in a segment, the model will subtract that segment and all segments above it from the active computational grid. If this occurs in a shallow location in the middle of a branch, the model will not run since it dries up a segment in the middle of a branch.

How can this be corrected? One way is to decouple one branch from another by splitting them into waterbodies. By splitting the system into more than one waterbody, water can be maintained at various levels throughout the domain since each waterbody has its own separate surface layer.

This is another reason why the model does not use segment-by-segment slopes since the surface layer defines the upper layer for a waterbody and in many cases these need to be broken apart into waterbodies to keep water in all segments. In addition, the translation from one waterbody to another introduces some small error into the solution since concentrations, temperatures, and velocities are interpolated from one 2D grid onto another. If the model were run in 1D mode with only one vertical layer, then this problem would not exist.

Consider another case study, the Bull Run system shown in [Figure 57](#).

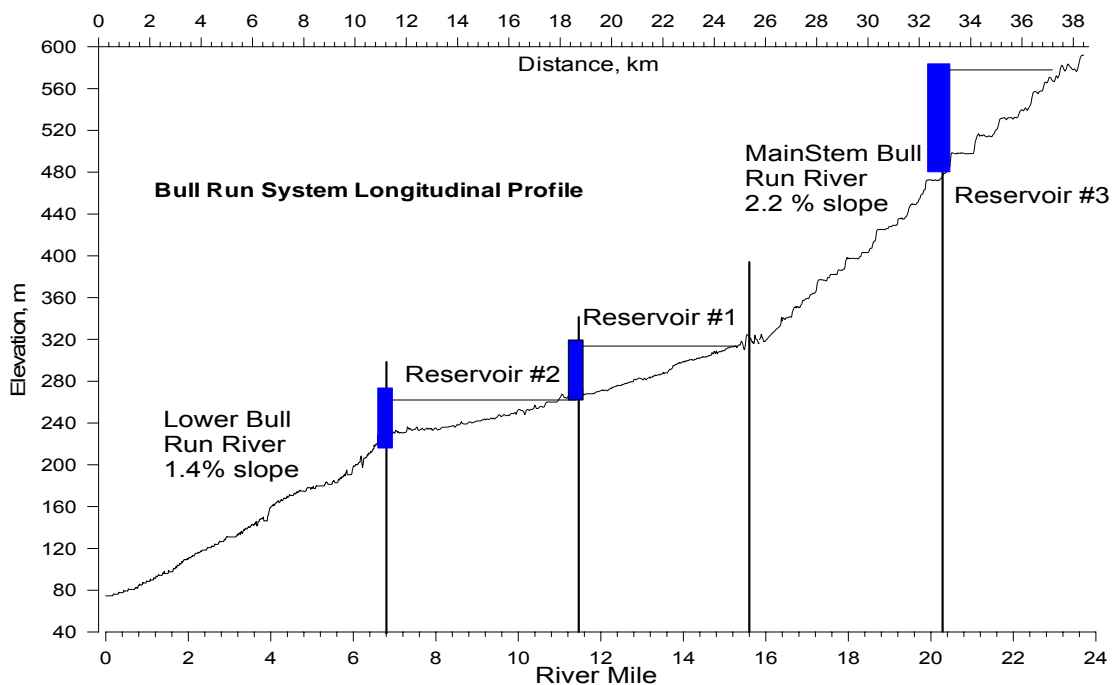


Figure 57. Channel slope for the Bull Run system.

The reservoirs were modeled with a channel slope of zero. Instead of a constant slope of 1.4%, the river is really divided into a large number of small-scale changes including pools and riffles. A section of the river is shown in Figure 58 with the assumed model grid divided into branches and waterbodies. In most cases, different waterbodies were used between branches of different slope. This allowed the water surface layer determination to be based on the water level in the branch with the given slope. However, the steeply sloping section may not have a slope equal to the grid slope shown. This may occur because if the steeply sloping section were modeled in more detail, it would really be a series of “flat” pools with small water drops (or falls) between the pools. If all the fine scale variability is ignored and the system is modeled on a larger scale, the problem becomes one of trying to estimate the “equivalent” channel slope that represents the channel.

This is similar to modeling a network of pipes and ignoring all the details but inserting pipes of “equivalent” slope and diameter. In this case, the channel slope is used as a calibration tool to match water level or dye study data. If channel friction were used to hold the water back, the values would have to be enormous to reproduce the complicated pool-waterfall system.

In addition, if the grid is broken into different waterbodies, discontinuities in the water surface such as waterfalls can be simulated.

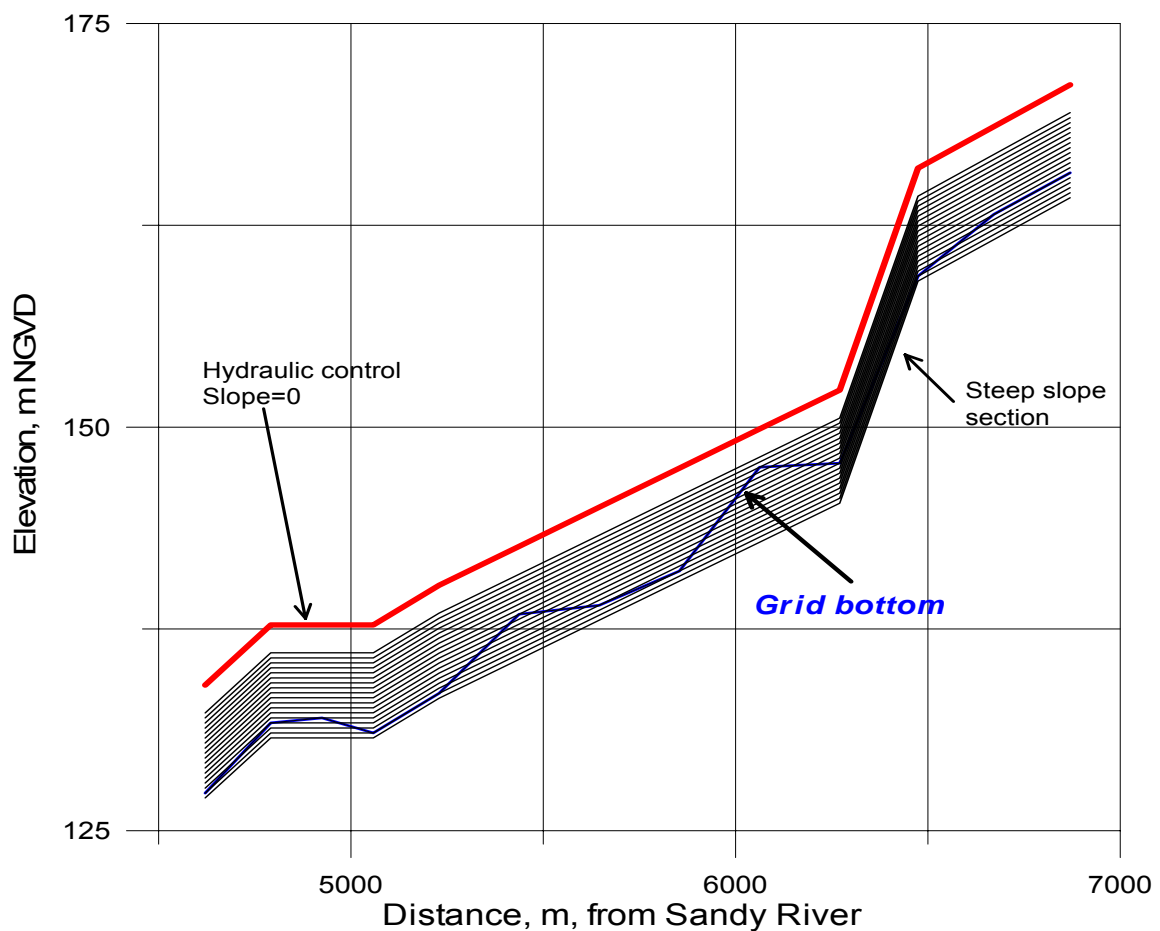


Figure 58. Vertical grid for W2 model of Bull Run Lower River.

CALIBRATION

Modeling of shallow streams with large slopes is difficult and takes patience. The model drying out at intermediate sections is often the cause of problems and can be remedied by breaking the system into smaller pieces or waterbodies and/or by adding additional computational cells below the bottom layer at a given segment. Matching river data is accomplished by adjusting friction factors, refining the geometry, and in some cases refining the “equivalent” channel slope if detail has been sacrificed in setting up the model. The quality of the model geometry is essential for good model-data reproducibility in a river system, especially one that is highly irregular in slope and channel width.

Developing a river model is also difficult at low flows since the model may become either unstable during the initial time steps or become dry in a segment. The reason for this is that, in the beginning, an initial water surface elevation is set and the river is “frozen” at that elevation until the model is started, at which point the water starts moving downstream. If a conservative high water is set initially in all segments, a wall of water will be sent downstream. If inflows are so small that at the upstream edge of this wave there is too little water, segments can dry out. The model includes a warning [w2.wrn] and error file [w2.err] that contains information for debugging a river model problem.

The following are suggestions for setting up a river model:

1. For the first 0.1 JDAY or so of the simulation, choose a maximum timestep **[DLTMAX]** that is small (10 s or less). This should be done only if the code seems to go unstable soon after starting the model. Alternatively, one can lower the fraction of the timestep **[DLTF]** used as this can provide numerical stability and allow for higher timesteps. The maximum timestep should be lowered if the number of time step violations is greater than 10% for an extended period of time.
2. Start with high flow rates gradually approaching the lower flow regime if model stability is a problem at low flows.
3. In order to keep water in the model, friction factors and geometry are very important considerations. The goal is to have sufficient model friction so that water does not quickly drain out of the system.
4. Add active computational cells at the bottom of the grid using small widths to prevent the section of the river from drying up or subtracting segments unnecessarily because the water surface layer [KT] is below the bottom [KB].
4. For a river that has sloping sections followed by flat sections (slope=0), you may want to set the slope to a non-zero value of 0.000001. This activates in the code the ability of the model for KT to be below KB when the segment is still hydrated.
5. If the water surface elevation becomes unstable as evidenced by a negative surface layer thickness, try reducing the maximum timestep **[DLTMAX]** to 5-10 seconds or less during the unstable time period. Alternatively, the fraction of the timestep **[DLTF]** can be set to 0.5 or less during this period.
6. For the end of the river, often a weir/spillway condition is used. This allows the specification of the stage-discharge relationship for the river. See the **Spillways/Weirs** description for an example of how to do this.
7. Set AZSLC=IMP and AZMAX=1.0. Do not use ASC=W2; use one of the other formulations.

The following discussion illustrates the model’s ability to accurately simulate river hydrodynamics, temperature, and water quality and includes a synopsis of the model’s application to the Bull Run River, Snake River, and Spokane River

Bull Run River. The Bull Run River is located in Oregon and the two existing reservoirs located on the river provide water for the city of Portland ([Figure 57](#)). A third reservoir upstream of the existing reservoirs is in the planning stage. The two portions of the free flowing river that were modeled had slopes of 1.4% and 2.2%. The model was used to address temperature and suspended solids questions about the system.

Snake River. The Lower Snake River from C.J. Strike to Brownlee Reservoir suffers from eutrophication problems below the city of Boise. Chlorophyll *a* concentrations in the river often exceed $100 \mu\text{g l}^{-1}$ and ultimately can cause severe dissolved oxygen depletion in the upper reaches of Brownlee Reservoir leading to fish kills. The model was used to determine how inflowing algae and nutrients affect chl *a* and dissolved oxygen concentrations in Brownlee Reservoir.

Spokane River. The Spokane River from the Idaho border to Long Lake was modeled as part of a Total Maximum Daily Load allocation study and was conducted by Portland State University, the Washington State Department of Ecology, and the U.S Army Corps of Engineers. Epiphyton were added to the model because of their importance on nutrient and dissolved oxygen dynamics in the River.

The system is complex hydraulically with three run-of-the-river impoundments used for power generation, significant groundwater inflows during low flow periods, a water fall, and Long Lake, a deep storage impoundment. Although Long Lake is a long and fairly deep reservoir, residence times during the summer are relatively short (< 1 month). Therefore, accurate inflow temperatures and constituent concentrations were crucial for accurate simulations of temperature and water quality in Long Lake, which required accurate simulations of over 40 miles of the Spokane River upstream of Long Lake.

The system is also complex with respect to water quality as epiphyton dominate nutrient and dissolved oxygen dynamics in the river and phytoplankton dominate their dynamics in Long Lake. Additionally, there are four point source discharges including the City of Spokane's wastewater effluent.

Hydrodynamics and Temperature

[Figure 59](#) shows results of a dye study conducted as part of the hydrodynamic calibration for the Bull Run River. Results show that the QUICKEST/ULTIMATE transport algorithm does not suffer from excessive numerical dispersion nor does it generate over/undershoots and that the model is capable of accurate river hydrodynamic simulations.

CALIBRATION

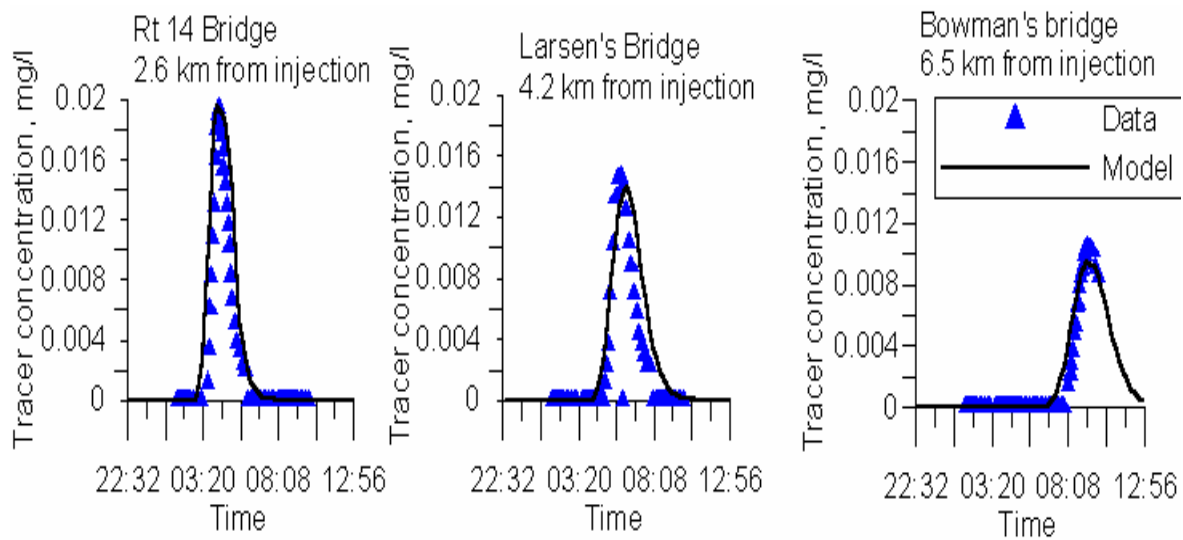


Figure 59. Bull Run River computed versus observed tracer at three stations progressing downstream.

[Figure 60](#) illustrates the accuracy of the water balance at the City of Spokane and [Figure 61](#) shows the accuracy of the computed flows at the same location.

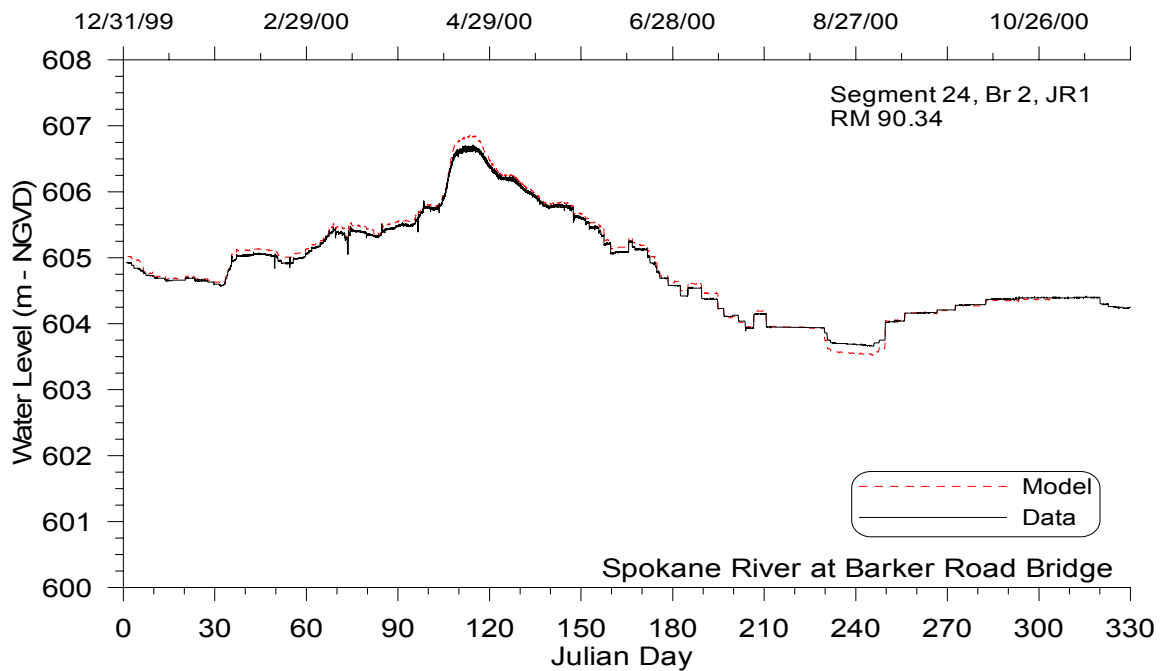


Figure 60. Spokane River computed versus observed water surface elevations at Spokane.

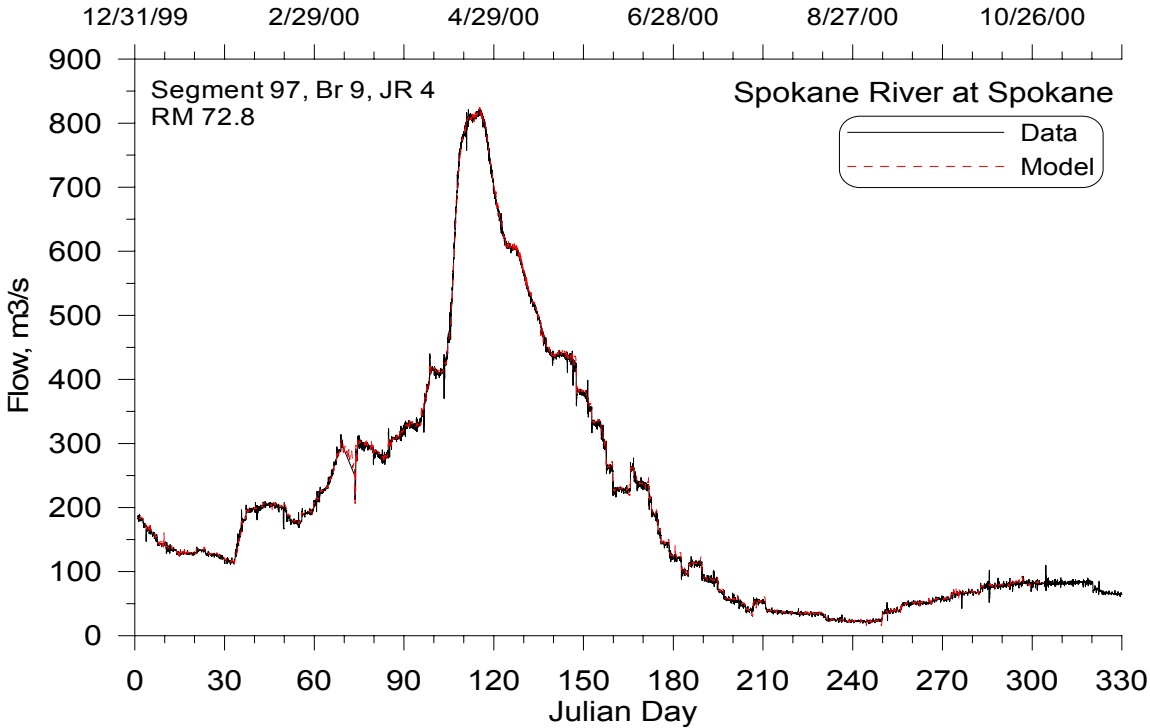


Figure 61. Spokane River computed versus observed flows at the city of Spokane.

Computed versus observed temperatures are shown in [Figure 62](#) and [Figure 63](#) for the Snake and Spokane rivers. As for reservoirs, temperature predictions are in close agreement with observed data.

CALIBRATION

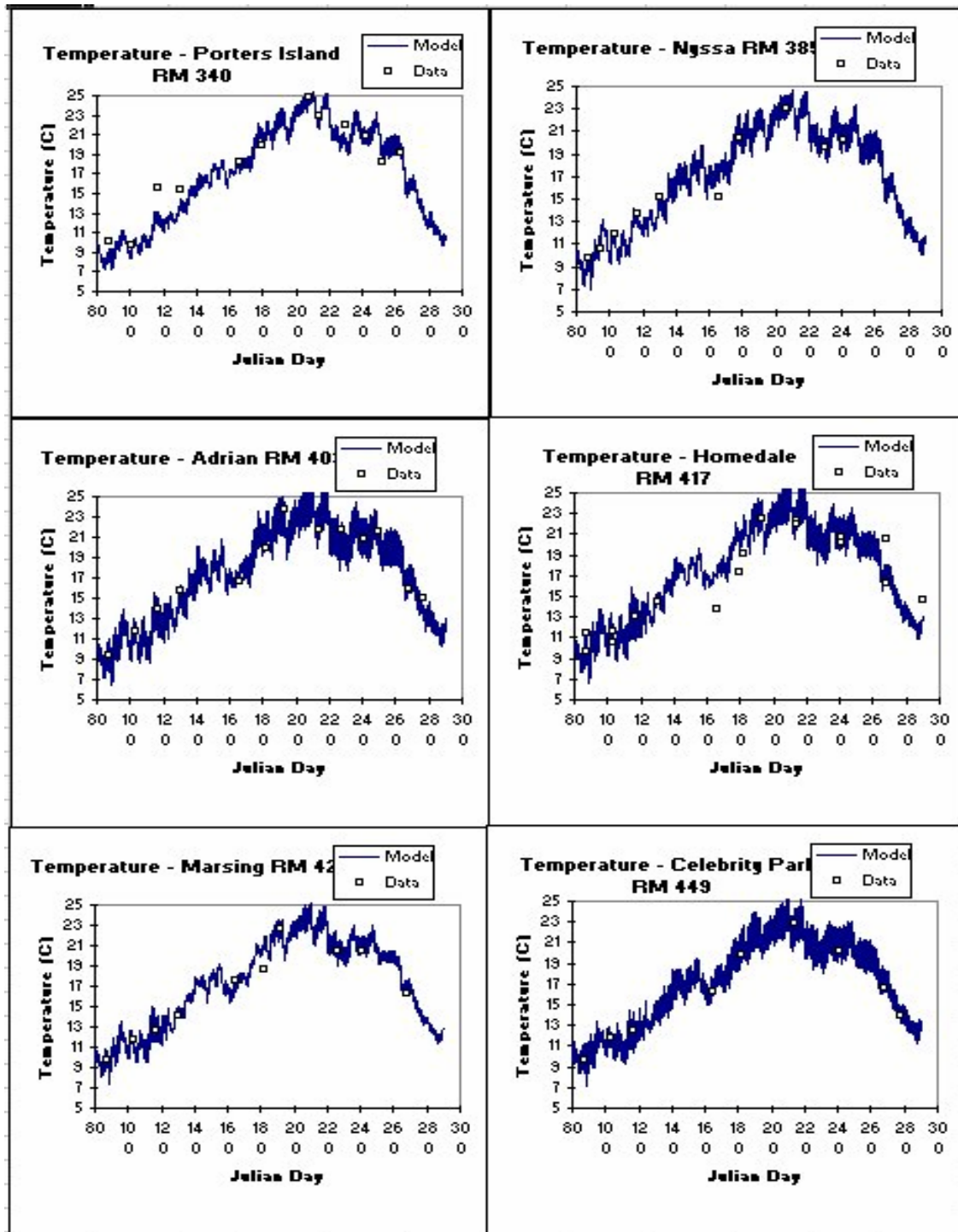


Figure 62. Snake River computed versus observed temperature at six stations.

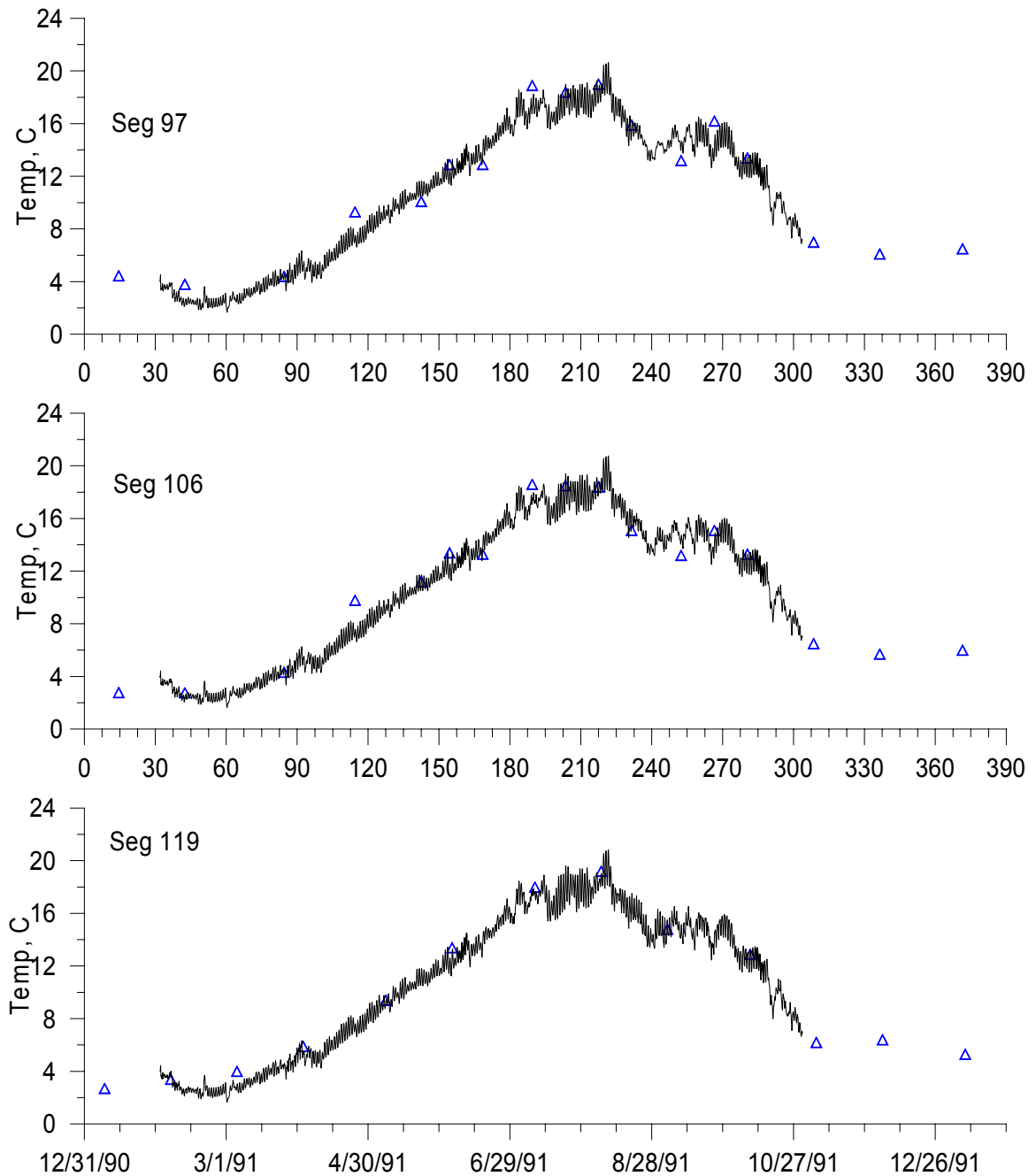


Figure 63. Computed versus observed temperatures for the Spokane River at Stateline Bridge (upstream boundary), City of Spokane, Fort Wright Bridge, and Riverside State Park.

For the Spokane study, conductivity was an important indicator of not only the hydrodynamics but also of the groundwater portion of the water balance. The model is accurately reproducing the temporal variation in conductivity ([Figure 64](#)) and is probably more accurate than any other method for determining groundwater inflows.

CALIBRATION

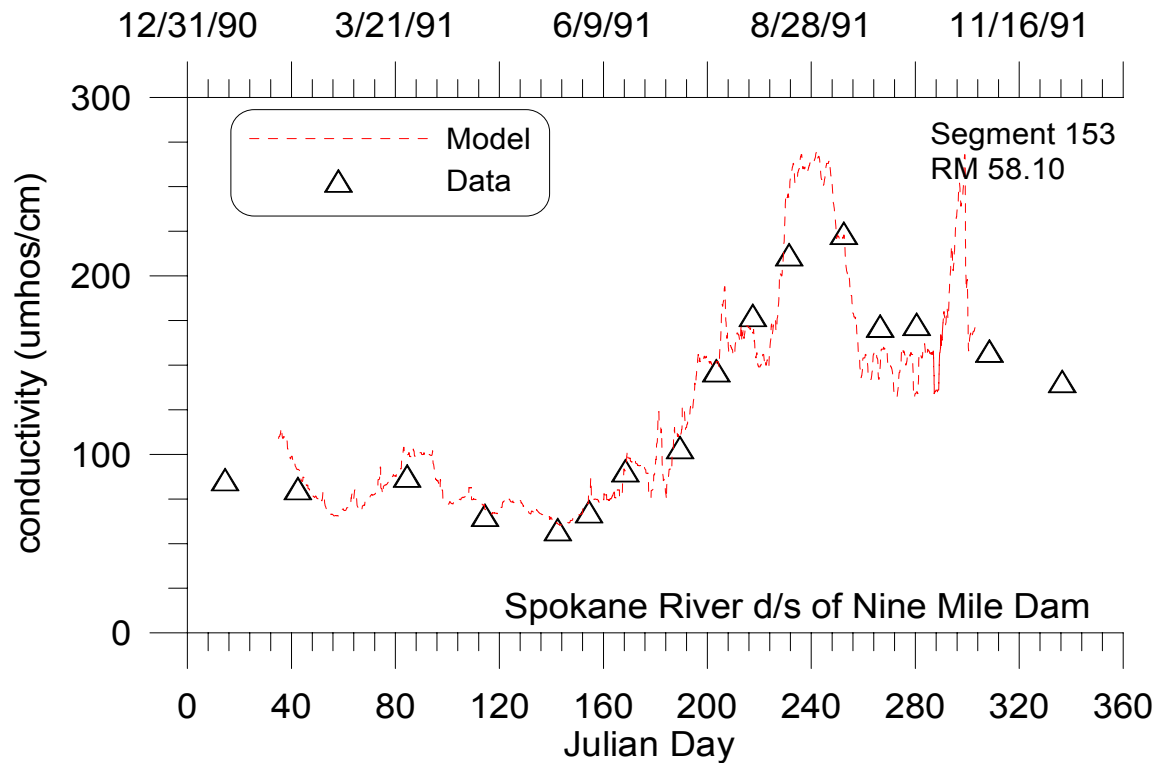


Figure 64. Spokane River computed versus observed conductivity below Nine Mile Dam.

Water Quality

Results for nutrients, dissolved oxygen, and chlorophyll *a* are given in [Figure 65-Figure 69](#) for the Snake River. The model is capturing much of the spatial and temporal changes in water quality for the river section where, unlike the Spokane River, phytoplankton rather than epiphyton dominate dissolved oxygen and nutrient dynamics.

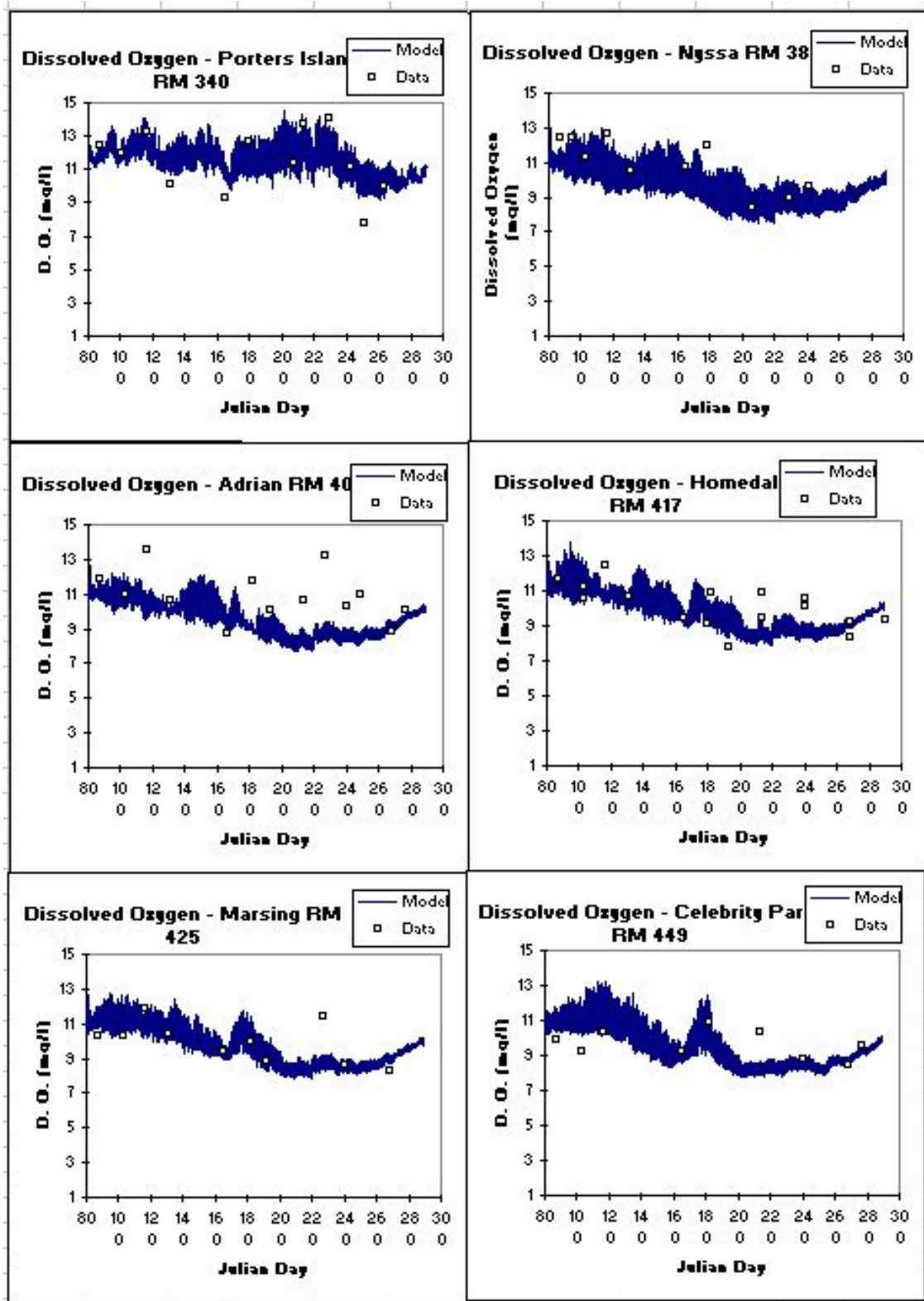


Figure 65. Snake River computed versus observed dissolved oxygen at six stations.

CALIBRATION

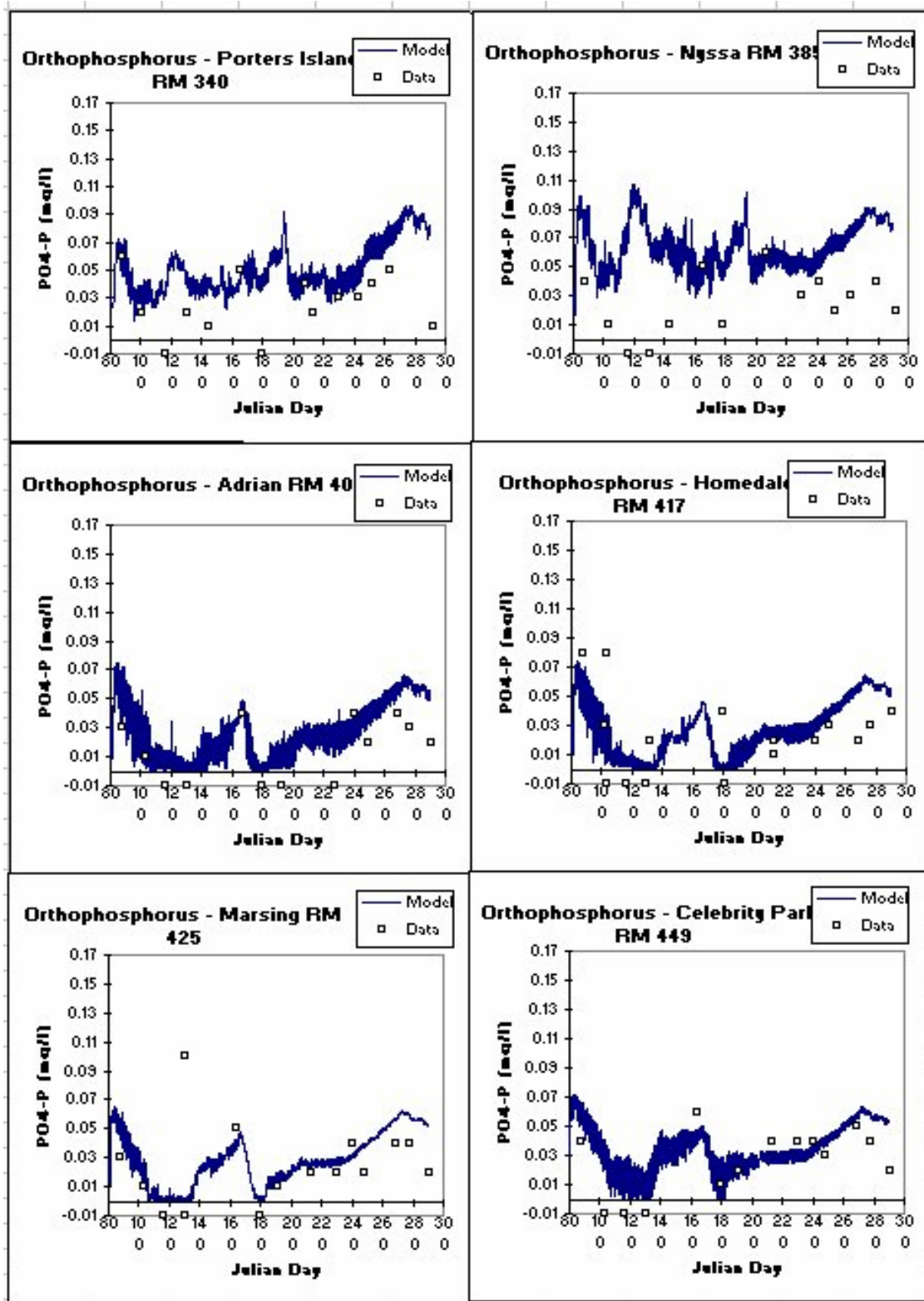


Figure 66. Snake River computed versus observed orthophosphorus at six stations.

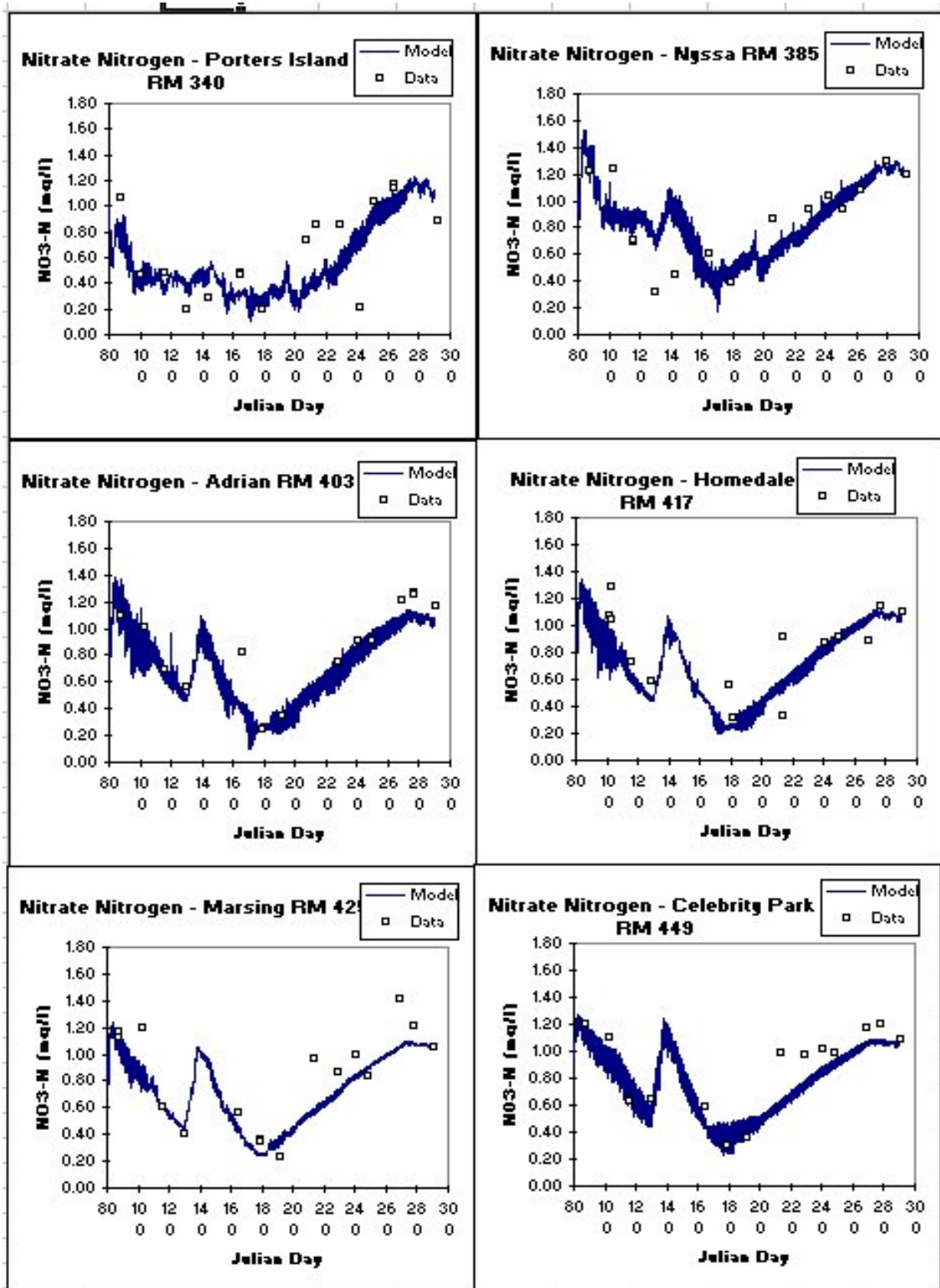


Figure 67. Snake River computed versus observed nitrate-nitrite at six stations.

CALIBRATION

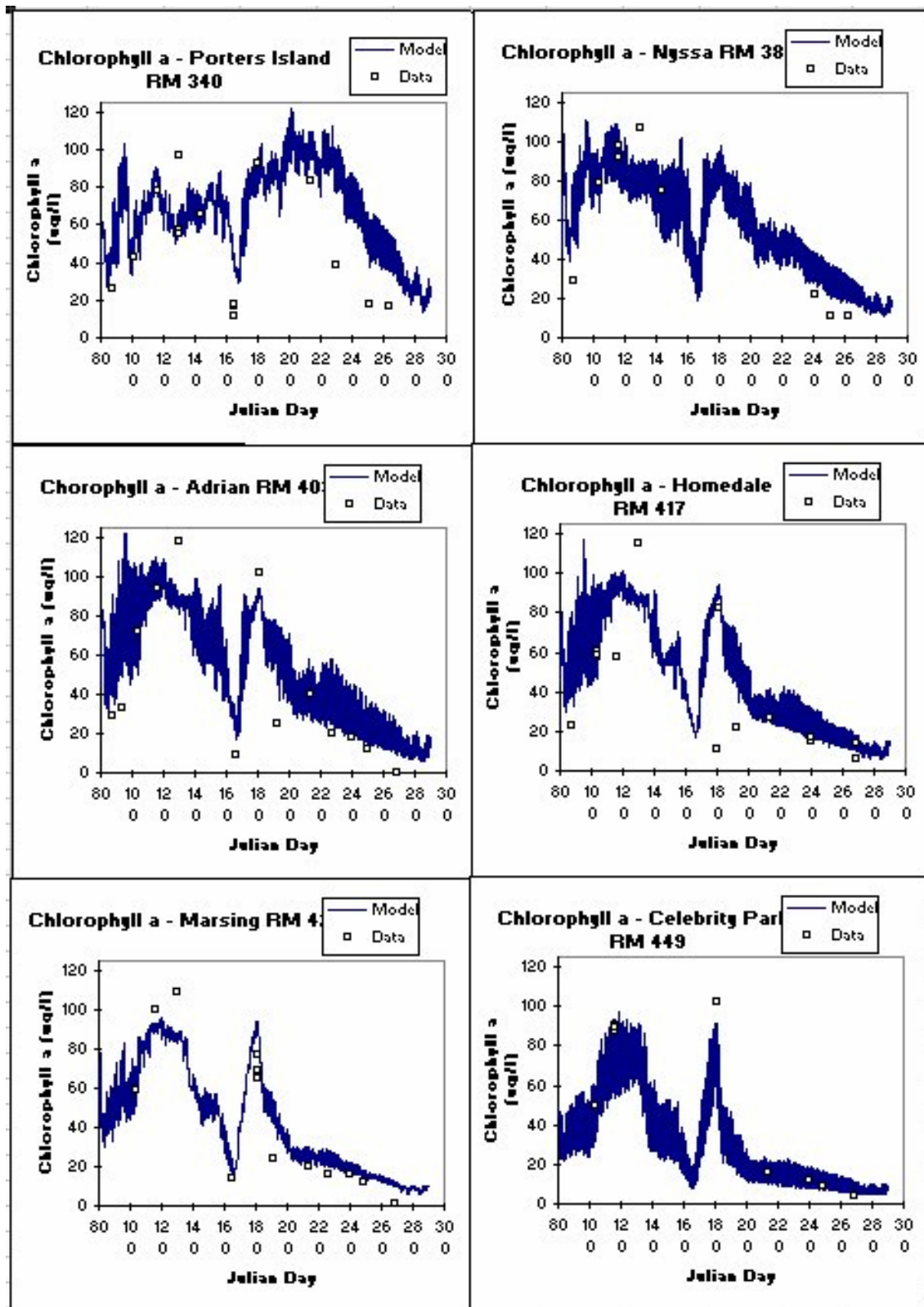


Figure 68. Snake River computed versus observed chlorophyll a at six stations.

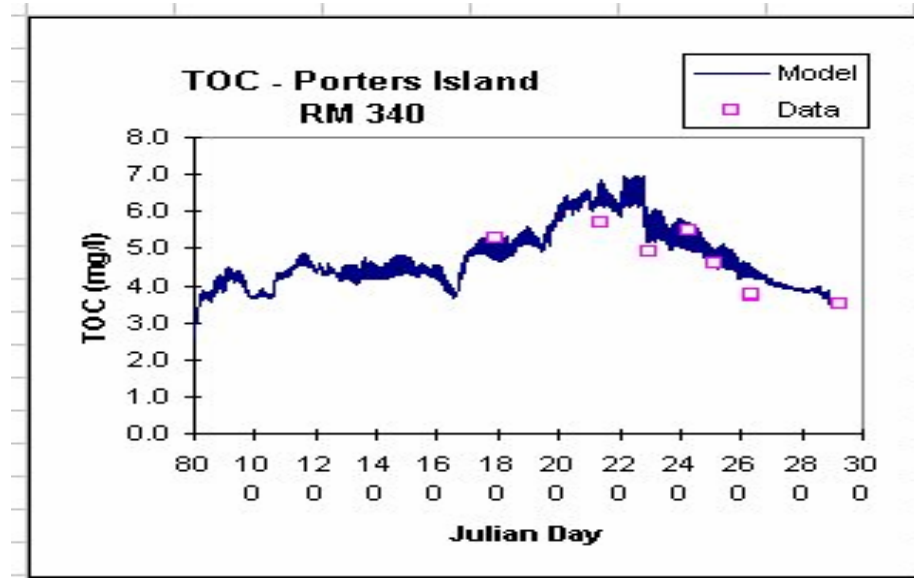


Figure 69. Snake River computed versus total organic carbon.

Figure 70 and Figure 71 illustrate the models ability to reproduce changes in dissolved oxygen over a year and also on a diel basis on the Spokane River. Note how the model has captured not only the diel swings in dissolved oxygen, but also the decrease in the magnitude of the diel variation, which indicates that the model is accurately reproducing epiphyton primary production. This is reinforced in Figure 72 where the model is reproducing diel variations in pH due to epiphyton growth and respiration and the decrease in diel variation over time

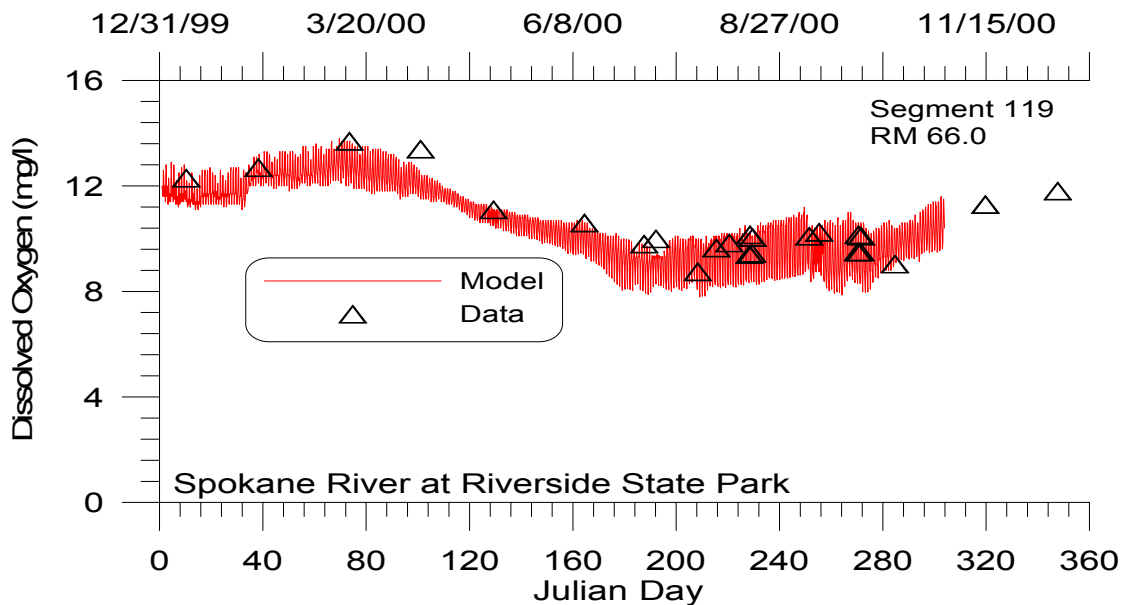


Figure 70. Spokane River computed versus observed dissolved oxygen at Riverside State Park.

CALIBRATION

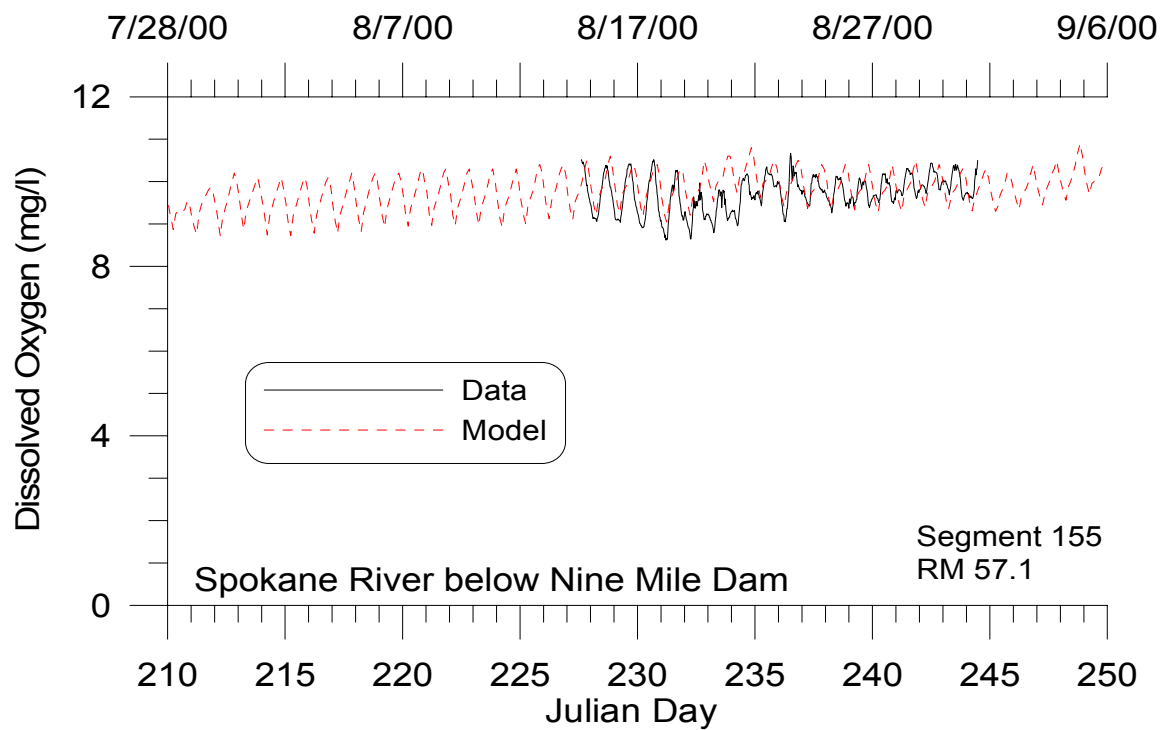


Figure 71. Spokane River computed versus observed dissolved oxygen below Nine Mile Dam.

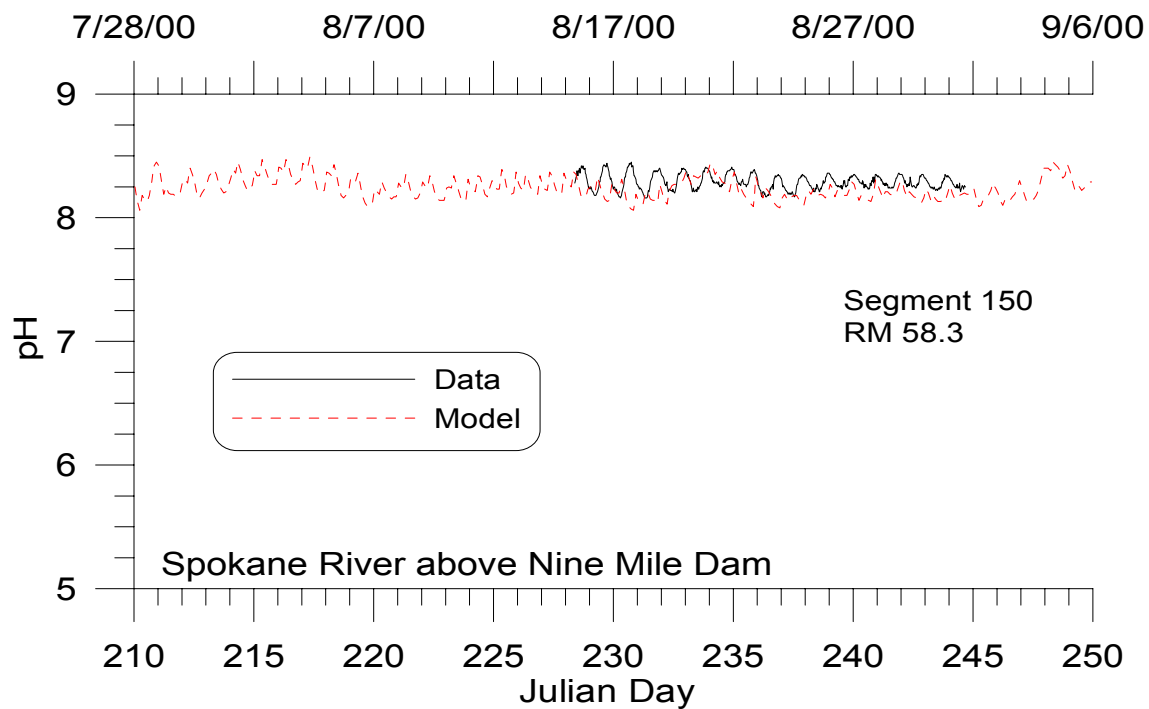


Figure 72. Spokane River computed versus observed pH upstream of Nine Mile Dam.

Figure 73-Figure 75 illustrate the model’s ability to reproduce nutrient dynamics that are impacted by upstream inflows, groundwater inflows, point source loadings, and epiphyton interactions.

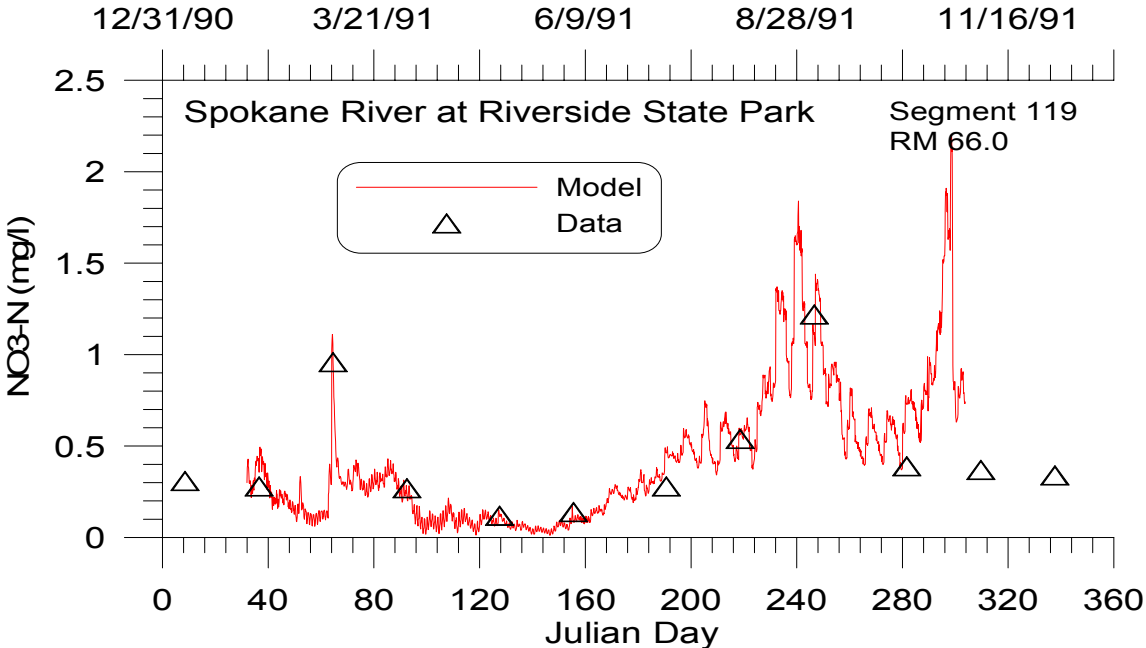


Figure 73. Spokane River computed versus observed nitrate-nitrite at Riverside State Park.

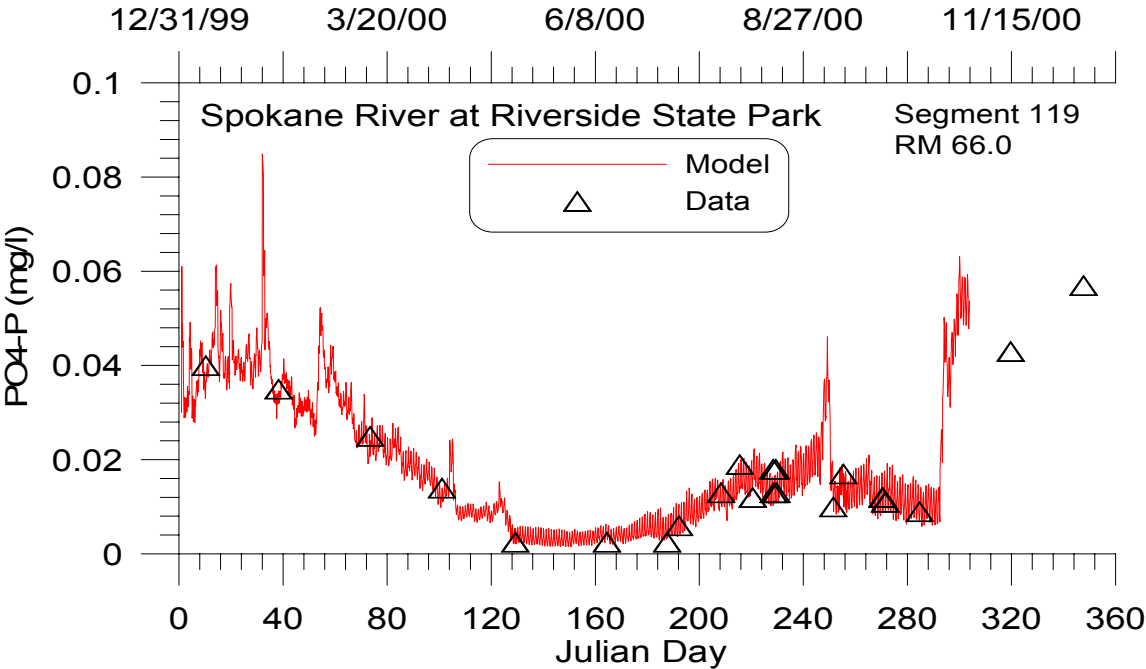


Figure 74. Spokane River computed versus observed soluble reactive phosphorus below Nine Mile Dam.

CALIBRATION

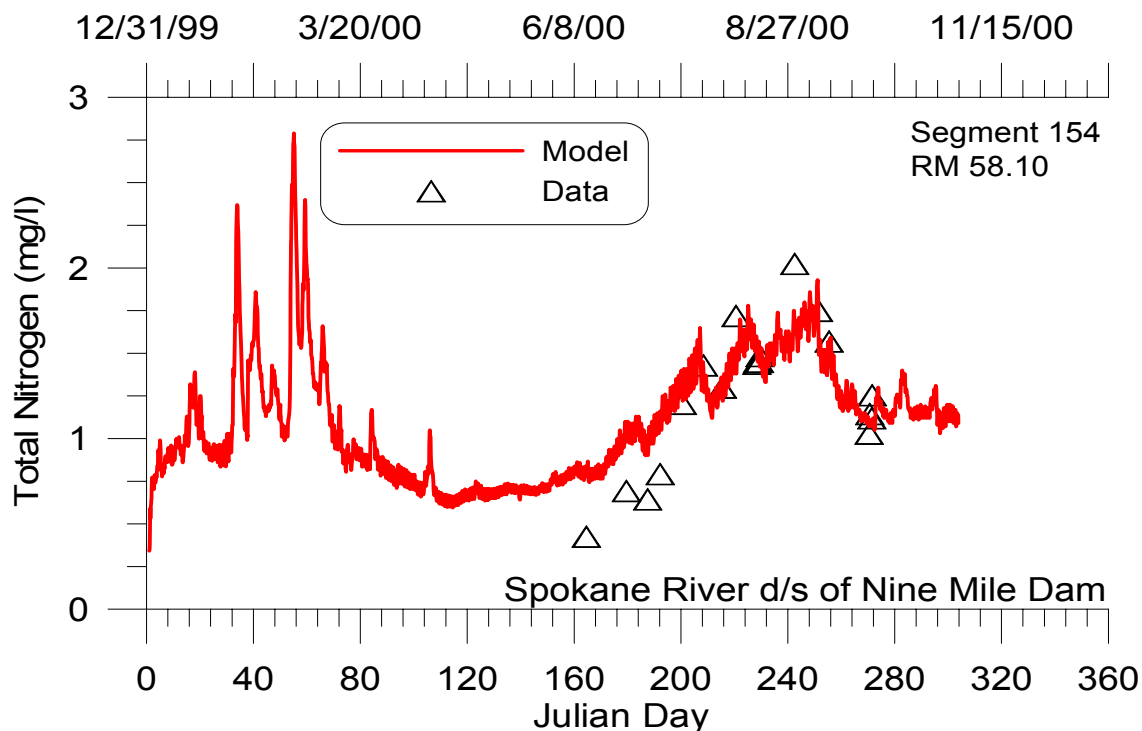


Figure 75. Spokane River computed versus observed total nitrogen below Nine Mile Dam.

Summary

As the preceding figures illustrate, CE-QUAL-W2 is capable of reproducing a wide range of complex hydrodynamics, temperature, dissolved oxygen, nutrient, and phytoplankton and epiphyton regimes in rivers, lakes, reservoirs, and estuaries. If the model is not adequately reproducing prototype behavior, the reason is most likely that the bathymetry or important boundary conditions are not being described with sufficient accuracy. The saying “You cannot make a silk purse out of a sow’s ear” applies equally well to water quality modeling.

A few final words about model calibration. For some applications, no amount of model adjustment or data reconstruction will provide acceptable calibration if data are insufficient to describe the dominant forcing functions in the prototype. For these cases, the model can still be used to provide information about the prototype by pointing out data inadequacies, important mechanisms not included in the model but important in the prototype, or inappropriate assumptions used in the model. In these cases, further fieldwork will be necessary to successfully apply the model.

References

- Alexander, M. 1965. *Microbial Ecology*, John Wiley and Sons, New York.
- Allen, W.E. 1932. "Marine Plankton Diatom of Lower California in 1931", *Botanical Gazette*, Vol 95, pp 485-492.
- Ambrose, R. B.; Wool, T.; Connolly, J. P.; and Schanz, R. W. 1988. "WASP4, A Hydrodynamic and Water Quality Model: Model Theory, User's Manual, and Programmer's Guide," Environmental Research Laboratory, Environmental Protection Agency, EPA 600/3-87/039, Athens, Ga.
- Annear, R., Berger, C. and Wells, S. 2001. "CE-QUAL-W2 Version 3.1 Shading Algorithm," *Technical Report EWR-3-01*, Dept. of Civil and Environmental Engineering, Portland State University, 39 pp.
- APHA 1985. *Standard Methods for the Examination of Water and Wastewater*, APHA, Washington, DC.
- Apstein, C. 1910. "Hat ein Organisms in der Tiefe Gelebt, in der er gefischt ist?", *Internat. Rev. Ges. Hydrobiol. Hydrograph*, Vol 3, pp 17-33.
- Ashton, G.D. 1979. "Suppression of River Ice by Thermal Effluents", *CRREL Rpt. 79-30*, US Army Engineer Cold Regions Research and Engineering Laboratory, Hanover, NH.
- ASCE 1988. "Turbulence Modeling of Surface Water Flow and Transport," *Journal of Hydraulic Engineering, ASCE Committee on Turbulence Models in Hydraulic Computations*, 114(9),970-1073.
- Baca, R.G. and R.C. Arnett. 1976. A Limnological Model for Eutrophic Lakes and Impoundments, Batelle Inc., Pacific Northwest Laboratories, Richland, Washington.
- Banks, R.B. 1975. "Some Features of Wind Action on Shallow Lakes," *ASCE, J. Env. Engr. Div.*, 101(E3), pp. 489-504.
- Banks, R. B. and Herrera, F. F. 1977. Effect of Wind and Rain on Surface Reaeration. *J. Envir. Engr. Div. ASCE*, 101(E5):813-827.
- Bannister, T.T. 1979. "Quantitative Description of Steady State, Nutrient-Saturated Algal Growth, Including Adaptation", *Limnology and Oceanography*, Vol 24, pp 76-96.
- Bansal, M.K. 1976. "Nitrification in Natural Streams", *Water Pollution Control Federation Journal*, Vol 48, pp 2380-2393.

REFERENCES

- Barkau, R. 1997. "UNET One-Dimensional Unsteady Flow Through a Full Network of Open Channels, User's Manual, US Army Corps of Engineers, Hydrologic Engineering Center, Davis, Ca.
- Barrett, M.J.; Gameson, A.L.; and Ogden, C.G. 1960. Aeration Studies of Four Weir Systems, *Water and Water Engineering*, London.
- Batchelor, G. K. 1967. An Introduction to Fluid Dynamics, Cambridge University Press, NY.
- Belay, A. 1981. "An Experimental Investigation of Inhibition of Phytoplankton Photosynthesis at Lake Surfaces", *New Phytologist*, Vol 89, pp 61-74.
- Bella, D. 1970. "Dissolved Oxygen Variations in Stratified Lakes", *ASCE J. of the Sanitary Engineering Division*, Vol 96, No. SA5, pp 1129-1146.
- Berger, C. and Wells, S. A. 1995. "Effects of Management Strategies to Improve Water Quality in the Tualatin River, Oregon," in *Water Resources Engineering, Vol. 2*, ed. by W, Espey Jr. and P. Combs, ASCE, 1360-1364.
- Bernard, F. 1963. "Vitesses de chute chez *Cyclococcolithus fragilis* Lohm", *Consequences Pour le Cycle Vital Des Mers Chaudes*.
- Bloss, S., and Harleman, D.R.F. 1979. "Effect of Wind Mixing on the Thermocline Formation in Lakes and Reservoirs", *R.M. Parsons Laboratory Rpt. 249*, Department of Civil Engineering, Massachusetts Institute of Technology, Cambridge, MA.
- Blum, J.J. 1966. "Phosphate Uptake by Phosphate-Starved *Euglena*", *J. of General Physiology*, Vol 49, pp 1125-1137.
- Bohan, J.P., and Grace, J.L., Jr. 1973. "Selective Withdrawal from Man-Made Lakes: Hydraulic Laboratory Investigation", *Technical Rpt. H-73-4*, US Army Engineer Waterways Experiment Station, Vicksburg, MS.
- Borchardt, J.A. 1966. "Nitrification in the Activated Sludge Process", *The Activated Sludge Process*, Division of Sanitary and Water Resources Engineering, University of Michigan, Ann Arbor, MI.
- Bott, T.L. 1975. "Bacterial Growth Rates and Temperature Optima in a Stream with a Fluctuating Thermal Regime", *Limnology and Oceanography*, Vol 20, pp 191-197.
- Boylen, C.W., and Brock, T.D. 1973. "Bacterial Decomposition Processes in Lake Wingra Sediments During Winter", *Limnology and Oceanography*, Vol 18, pp 628-634.
- Brady, D.K., Graves, W.L., and Geyer, J.C. 1969. "Surface Heat Exchange at Power Plant Cooling Lakes", *Cooling Water 2, Discharge Project No. 5, Publication No. 69-901*, Edison Electric Institute, New York, NY.
- Bramlette, M.N. 1961. In. *Oceanography, No. 67*, M. Sears, ed., American Association of Science, Washington, DC., pp 345-366

REFERENCES

- Broecker, H. C., Petermann, J., and Siems, W. 1978. The Influence of Wind on CO₂ Exchange in a Wind-Wave Tunnel, *J. Marine Res.*, 36(4):595-610.
- Brown, L. C. and Barnwell, T. O. 1987. "The Enhanced Stream water Quality Models QUAL2E and QUAL2E-UNCAS: Documentation and User Manual," *Environmental Research Laboratory, EPA/600/3-87/007*, Athens, Ga.
- Butler, D.; Rock, S. P.; and West, J. R. 1978) "Friction Coefficient Variation with Flow in an Urban Stream," *J. of the Institution of Water Engineers and Scientists*, Vol 32, No 3, pp. 227-232.
- Butts, T.A. and Evans, R.L. 1983. "Small Stream Channel Dam Aeration Characteristics," *ASCE J. Env. Engr.*, Vol 109, No 3, pp. 555-573, June 1983.
- Buchak, E.M., and Edinger, J.E. 1982a. "Hydrothermal Simulation of Quabbin Reservoir Using Longitudinal-Vertical Hydrodynamics, Interim Report", prepared for Wallace, Floyd Associates, Inc., Cambridge, MA.
- 1982b. "User's Guide for LARM2: A Longitudinal-Vertical, Time-Varying Hydrodynamic Reservoir Model", *Instruction Rpt. E-82-3*, US Army Engineer Waterways Experiment Station, Vicksburg, MS.
- _____. 1984. "Generalized Longitudinal-Vertical Hydrodynamics and Transport: Development, Programming and Applications", *Contract No. DACW39-84-M-1636*, prepared for US Army Engineer Waterways Experiment Station, Vicksburg, MS.
- Burns, N.M. 1976. "Nutrient Budgets for Lake Erie", *J. of the Fisheries Research Board of Canada*, Vol 33, pp 520-536.
- Burns, N.M., and Rosa, F. 1980. "In situ Measurement of Settling Velocity of Organic Carbon Particles and 10 Species of Phytoplankton", *Limnology and Oceanography*, Vol 25, pp 855-864.
- Caperon, J., and Meyer, J. 1972. "Nitrogen-Limited Growth of Marine Phytoplankton; I. Changes in Population Characteristics with Steady-State Growth Rate", *Deepsea Research with Oceanography*, Vol 9, pp 601-618.
- Carney, J.F., and Colwell, R.R. 1976. "Heterotrophic Utilization of Glucose and Glutamate in an Estuary: Effect of Season and Nutrient Load", *Applied and Environmental Microbiology*, Vol. 31, pp 227-233.
- Carpenter, E.J., and Guillard, R.R.L. 1971. "Intraspecific Differences in Nitrate Half-Saturation Constants for Three Species of Marine Phytoplankton", *Ecology*, Vol 52, pp 183-185.
- Castenholz, R. W. 1964. "The Effect of Daylength and Light Intensity on the Growth of Littoral Marine Diatoms in Culture", *Physiological Plant*, Vol 17, pp 951-963.
1969. "The Thermophilic Cyanophytes of Iceland and the Upper Temperature Limit", *J. of Phycology*, Vol 5, pp 360-368.

REFERENCES

- Chapman, R.S. 1988. "Analysis and Improvement of the Numerical and Physical Mixing Characteristics of the WASP Box Model", Contract Report Submitted to the US Army Waterway Experiment Station, Vicksburg, MS.
- Chapman, R. 1989. "Review and Recommendation of Estuarine Mixing Parameterizations, with Specific Reference to Vertical Mixing in Multi-Dimensional Boxes," Report prepared for USACE, Waterways Experiments Station, Vicksburg, MS.
- Chapman, R.S. and T.M. Cole. 1992. "Improved Thermal Predictions in CE-QUAL-W2", in *Hydraulic Engineering Saving a Threatened Resource - In Search of Solutions Proceedings of the Hydraulic Engineering sessions at Water Forum '92*, M. Jennings and N. G. Bhowmik, eds.), August 2-6, 1992, Baltimore, MD. American Society of Civil Engineers. New York, NY.
- Chapra, S. 1997. *Surface Water Quality Modeling*, McGraw-Hill, NY
- Chapra, S.C., and Reckhow, K.W. 1983. *Engineering Approaches for Lake Management, Vol 12: Mechanistic Modeling*, Butterworth Publishers, Boston, MA.
- Chen, R.L., Brannon, J.M., and Gunnison, D. 1984. "Anaerobic and Aerobic Rate Coefficients for Use in CE-QUAL-RI", *Miscellaneous Paper E-84-5*, US Army Engineer Waterways Experiment Station, Vicksburg, MS.
- Chen, Yongoin. 1996. "Hydrologic and Water Quality Modeling for Aquatic Ecosystem Protection and Restoration in Forest Watersheds: A Case Study of Stream Temperature in the Upper Grande Ronde River, Oregon," Dissertation submitted to The University of Georgia, Doctor of Philosophy, 268 pp.
- Chiaro, P.S., and Burke, D.A. 1980. "Sediment Oxygen Demand and Nutrient Release", *ASCE J. Env. Engr.*, Vol 106, No. EEL, pp 177-195.
- Chow, V. T. 1959. *Open Channel Hydraulics*, McGraw-Hill, NY.
- Churchill, M.A., Elmore, H. L., and Buckingham, R.A. 1962. "Prediction of Stream Reaeration Rates," *J. San. Engr. Div., ASCE*, SA4:1, Proc. Paper 3199.
- Clay, C.H. 1995. *Design of Fishway and Other Fish Facilities*, Lewis Publishers, Ann Arbor.
- Clendenning, K.A., Brown, T.E., and Eyster, H.C. 1956. *Canadian J. of Botany*, Vol 34, pp 943-966.
- Cloern, J.E. 1977. "Effects of Light Intensity and Temperature on *Cryptomonas* Cryptophyceae. Growth and Nutrient Uptake Rates", *J. of Phycology*, Vol 13, pp 389-395.
- Cole, T. and Buchak, E. 1995. CE-QUAL-W2: A Two-Dimensional, Laterally Averaged, Hydrodynamic and Water Quality Model, Version 2.0, Technical Report EI-95-1, U.S. Army Engineer Waterways Experiment Station, Vicksburg, MS.

REFERENCES

- Collins, C.D., and Boylen, C.W. 1982a. "Physiological Responses of *Anabaena variabilis* Cyanophyceae. to Instantaneous Exposure to Various Combinations of Light Intensity and Temperature", *J. of Phycology*, Vol 18, pp 206-211.
- _____. 1982b. "Ecological Consequences of Long-Term Exposure of *Anabaena variabilis* to Shifts in Environmental Conditions", *Applied and Environmental Microbiology*, Vol 44, pp 141-148.
- Columbia Basin Research 1998. University of Washington, http://www.cqs.washington.edu/d_gas/papers/tdg_manual.html
- Courchaine, R.J. 1968. "Significance of Nitrification in Stream Analysis--Effects on the Oxygen Balance", *J. of the Water Pollution Control Federation*, Vol 40, p 835.
- Covar, A. P. 1976. "Selecting the Proper Reaeration Coefficient for Use in Water Quality Models," presented at the US EPA Conference on Environmental Simulation and Modeling, April 19-22, Cincinnati, OH.
- Cushman-Roisin, B. 1994. *Introduction to Geophysical Fluid Dynamics*, Prentice-Hall, Englewood Cliffs, NJ.
- Davis, J. E., et al. 1987. "SELECT: A Numerical, One-dimensional Model for Selective Withdrawal", *Instruction Rpt. E-87-2*, US Army engineer Waterways Experiment Station, Vicksburg, MS.
- Downing, A.L., and G.A. Truesdale 1955. Some factors affecting the rates of solution of oxygen in water. *J. Applied Chemistry*, Vol. 5, pp.570-581.
- Edinger, J.E., Brady, D.K., and Geyer, J.C. 1974. "Heat Exchange and Transport in the Environment", *Rpt. No. 14, EPRI Publication No. 74-049-00-34*, prepared for Electric Power Research Institute, Cooling Water Discharge Research Project RP-49), Palo Alto, CA.
- Edinger, J.E., and Buchak, E.M. 1975. "A Hydrodynamic, Two-Dimensional Reservoir Model: The Computational Basis", prepared for US Army Engineer Division, Ohio River, Cincinnati, Ohio.
- _____. 1978. "Reservoir Longitudinal and Vertical Implicit Hydrodynamics", *Environmental Effects of Hydraulic Engineering Works*, Proceedings of an International Symposium, Knoxville, TN.
- _____. 1980. "Numerical Hydrodynamics of Estuaries", *Estuarine and Wetland Processes with Emphasis on Modeling*, P. Hamilton and K.B. Macdonald, eds., Plenum Press, New York, pp. 115-146.
- _____. 1983. "Developments in LARM2: A Longitudinal-Vertical, Time-Varying Hydrodynamic Reservoir Model", *Technical Rpt. E-83-1*, US Army Engineer Waterways Experiment Station, Vicksburg, MS.
- Edinger, J. E., D. K. Brady and J. C. Geyer. 1974. "Heat Exchange and Transport in the Environment", *Research Project RP-49, Rpt. 14, EPRI Publication Number 74-049-00-3*, Cooling Water Studies for the Electric Power Research Institute, Palo Alto, CA.

REFERENCES

- Edinger, J.E., Buchak, E.M., and Merritt, D.H. 1983. "Longitudinal-Vertical Hydrodynamics and Transport with Chemical Equilibria for Lake Powell and Lake Mead", *Salinity in Watercourses and Reservoirs*, R.H. French, ed., Butterworth Publishers, Stoneham, MA, pp 213-222.
- Edinger, J.E., and Geyer, J.C. 1965. "Heat Exchange in the Environment", *Publication No. 65-902*, Edison Electric Institute, New York, NY.
- Engelund, F. 1978. Effect of Lateral Wind on Uniform Channel Flow. *Progress Report 45*, Inst. of Hydrodynamic and Hydraulic Engr., Tech. Univ. of Denmark.
- Environmental Laboratory. 1985. "CE-QUAL-R1: A Numerical One-Dimensional Model of Reservoir Water Quality; User's Manual", *Instruction Rpt. E-82-1*, US Army Engineer Waterways Experiment Station, Vicksburg, MS.
- Environmental Laboratory 1995. "CE-QUAL-RIV1: A Dynamic, One-Dimensional Longitudinal Water Quality Model for Streams: User's Manual," *Instruction Report EL-95-2*, USACE Waterways Experiments Station, Vicksburg, MS.
- Eppley, R.W., Holmes, R.W., and Strickland, J.D.H. 1967b. "Sinking Rates of Marine Phytoplankton Measured with a Fluorometer", *J. of Experimental Marine Biology and Ecology*, Vol 1, pp 191-208.
- Eppley, R.W., Rogers, J.N., and McCarthy, J.J. 1969. "Half-Saturation Constants for Uptake of Nitrate and Ammonia by Marine Phytoplankton", *Limnology and Oceanography*, Vol 14, pp 912-920.
- Eppley, R.W., and Sloan, P.R. 1966. "Growth Rates of Marine Phytoplankton: Correlation with Light Adsorption by Cell Chlorophyll-a", *Physiological Plant*, Vol 19, pp 47-59.
- Eppley, R.W., and Thomas, W.H. 1969. "Comparison of Half-Saturation Constants for Growth and Nitrate Uptake of Marine Phytoplankton", *J. of Phycology*, Vol 5, pp 375-379.
- Evans, F.C., Goldreich, E.C., Weibel, S.R., and Robeck, G.G. 1968. "Treatment of Urban Storm Runoff", *J. of the Water Pollution Control Federation*, Vol 40, pp 162-170.
- Fang, X. and Stefan, H. G. 1994. "Modeling Dissolved Oxygen Stratification Dynamics in Minnesota Lakes under Different Climate Scenarios," *Project Report 339*, St. Anthony Falls Hydraulic Laboratory, University of Minnesota, Minneapolis.
- Fenchel, T. 1970. "Studies of the Decomposition of Organic Detritus Derived from Turtle Grass *Thalassia testudinum*", *Limnology and Oceanography*, Vol 15, pp 14-20.
- Finenko, Z.Z., and Krupatkina-Aki-Nina, D.K. 1974. "Effect of Inorganic Phosphorus on the Growth Rate of Diatoms", *Marine Biology*, Vol 26, pp. 193-201.
- Fischer, H. B.; E. List; R. Koh; J. Imberger; N. Brooks 1979. *Mixing in Inland and Coastal Waters*, Academic Press, NY.

REFERENCES

- Fitzgerald, G.P. 1964. "The Effect of Algae on BOD Measurements", *National Pollution Control Federation J.*, Vol 36, pp 1524-1542.
- Fogg, G.E. 1969. "The Physiology of an Algal Nuisance", *Proc. R. Soc.B.*, Vol 173, pp 175-189.
- _____. 1973. "Phosphorus in Primary Aquatic Plants", *Water Research*, Vol 7, pp 77-91.
- Ford, B. and A. B. Stein. 1984. "The Hydrometeorology of DeGray Lake, Arkansas", *Miscellaneous Paper E-84-3*, U.S. Army Engineer Waterways Experiment Station, Vicksburg, MS.
- Ford, D.E., and Johnson, M.C. 1983. "An Assessment of Reservoir Density Currents and Inflow Processes", *Technical Rpt. E-83-7*, US Army Engineer Waterways Experiment Station, Vicksburg, MS.
- Fowler, S.W., and Small, L.F. 1972. *Limnology and Oceanography*, Vol 17, pp 293-296.
- French, R. H. 1985. *Open-Channel Hydraulics*, McGraw-Hill, New York.
- Frost, W.H., and Streeter, H.W. 1924. "Bacteriological Studies", *Public Health Bulletin 143*, US Public Health Service, Washington, DC.
- Fuhs, G.W., Demmerle, S.D., Canelli, E., and Chen, M. 1972. "Characterization of Phosphorus--Limited Plankton Algae", *Limnol. Oceanogr. Special Symposia*, Vol 1, pp 113-133.
- Gaugush, R. F., tech. ed. 1986. "Statistical Methods for reservoir water quality investigations", *Instruction Rpt. E-86-2*, U.S. Army Engineer Waterways Experiment Station, Vicksburg, MS.
- _____. 1987. "Sampling Design for Reservoir Water Quality Investigations", *Instruction Report E-87-1*, U.S. Army Engineer Waterways Experiment Station, Vicksburg, MS.
- _____. 1993. "Sampling Design Software User's Manual", *Instruction Report W-93-1*, U.S. Army Engineer Waterways Experiment Station, Vicksburg, MS.
- Gebhart, B.; Jaluria, Y.; Mahajan, R.; and Sammakia, B. 1988. *Buoyancy-Induced Flows and Transport*, Hemisphere Publishing Co., NY.
- Gelda, R. K., Auer, M. T., Effler, S. W., Chapra, S. C., and Storey, M. L. 1996. Determination of Reaeration Coefficients: A Whole Lake Approach. *ASCE J. Envir. Engr.*
- Geldreich, E.E., Best, L.C., Kenner, B.A., and Van Donsel, D.J. 1968. "The Bacteriological Aspects of Stormwater Pollution", *J. of the Water Pollution Control Federation*, Vol 40, p 1861.
- Giese, A.C. 1968. *Cell Physiology*, 3d ed., W.B. Saunders Co., Philadelphia, PA.
- Gill, A.E. 1982. "Appendix 3, Properties of Seawater", *Atmosphere-Ocean Dynamics*, Academic Press, New York, NY, pp 599-600.
- Goldman, J.C., and Graham, S.J. 1981. "Inorganic Carbon Limitation and Chemical Composition of Two Freshwater Green Microalgae", *Applied and Environmental Microbiology*, Vol 41, pp 60-70.

REFERENCES

- Goldman, J.C., Porcella, D.B., Middlebrooks, E.J., and Toerien, D.F. 1972. "The Effects of Carbon on Algal Growth--Its Relationship to Eutrophication", *Water Research*, Vol 6, pp 637-679.
- Golterman, H.L. 1975. *Physiological Limnology*, Elsevier, Amsterdam.
- Gordon, J.A. 1980. "An Evaluation of the LARM Two-Dimensional Model for Water Quality Management Purposes", *Proceedings of the Symposium on Surface-Water Impoundments*, Minneapolis, MN, June 2-5, 1980, Vol 1, Paper 4-34, pp 518-527, American Society of Civil Engineers, New York, NY.
- _____. 1981. "LARM Two-Dimensional Model: An Evaluation", *ASCE J. of the Environmental Engineering Division*, 107(EE5), pp 877-886.
- _____. 1983. "Short-Term Hydrodynamics in a Stratified Reservoir", *Environmental Engineering, Proceedings of the ASCE Specialty Conference, Hilton Harvest House, Boulder, Colo.*, July 6-8, 1983, pp 524-531, American Society of Civil Engineers, New York, NY.
- Green, D.B., Logan, J., and Smeck, N.E. 1978. "Phosphorus Adsorption-Desorption Characteristics of Suspended Sediments in the Maumee River of Ohio", *J. of Environmental Quality*, Vol 7, pp 208-212.
- Guillard, R.R.L., and Ryther, J.H. 1962. "Studies on the Marine Planktonic Diatoms; I. *Cyclotella nana* Hustedt and *Detonula confervacea* Cleve)", *Canadian J. of Microbiology*, Vol 8, pp 229-239.
- Gunnison, D., and Alexander, M. 1975. "Resistance and Susceptibility of Algae to Decomposition by Natural Microbial Communities", *Limnology and Oceanography*, Vol 20, pp 64-70.
- Gunnison, D., Chen, R.L., and Brannon, J.M. 1983. "Relationship of Materials in Flooded Soils and Sediments to the Water Quality of Reservoir; I. Oxygen Consumption Rates", *Water Research*, Vol 17, No. 11, pp 1609-1617.
- Hall, G.H. 1982. "Apparent and Measured Rates of Nitrification in the Hypolimnion of a Mesotrophic Lake", *Applied and Environmental Microbiology*, Vol 43, pp 542-547.
- Halmann, M., and Stiller, M. 1974. "Turnover and Uptake of Dissolved Phosphate in Freshwater; A Study in Lake Kinneret", *Limnology and Oceanography*, Vol 19, pp 774-783.
- Hanlon, R.D.G. 1982. "The Breakdown and Decomposition of Allochthonous and Autochthonous Plant Litter in an Oligotrophic Lake Llyn Frongoch)", *Hydrobiologia*, Vol 88, pp 281-288.
- Harbeck, G.E., Koberg, G.E., and Hughes, G.H. 1959. "The Effect of Addition of Heat...on Lake Colorado City, Texas", *USGS Professional Paper 272-B*, US Government Printing Office, Washington, DC.
- Hargrave, B.T. 1972a. "Aerobic Decomposition of Sediment and Detritus as a Function of Particle Surface Area and Organic Content", *Limnology and Oceanography*, Vol 17, pp 582-597.

REFERENCES

- 1972b. "Oxidation-Reduction Potentials, Oxygen Concentration and Oxygen Uptake of Profundal Sediments in a Eutrophic Lake", *Oikos*, Vol 23, pp 167-177.
- Hattori, A. 1962. "Light-Induced Reduction of Nitrate, Nitrite and Hydroxylamine in a Blue-green Alga, *Anabaena cylindrica*", *Plant Cell Physiology*, Vol 3, pp 355-369.
- HEC 1997a. "UNET One-Dimensional Unsteady-Flow Through a Full Network of Open Channels, User's Manual," US Army Corps of Engineers, Hydrologic Engineering Center, Davis, CA.
- HEC 1997b. "HEC-RAS River Analysis System Hydraulic Reference Manual Version 2.0," US Army Corps of Engineers, Hydrologic Engineering Center, Davis, CA.
- HEC 1977. "HEC-6 Scour and Deposition in Rivers and Reservoirs," US Army Corps of Engineers, Hydrologic Engineering Center, Davis, CA.
- Hecky, R.E., and Kilham, P. 1974. "Environmental Control of Phytoplankton Cell Size", *Limnology and Oceanography*, Vol 19, No. 2, pp 361-365.
- Henderson, H. 1966. *Open Channel Flow*, The MacMillan Company, NY.
- Hendry, G.R., and Welch, E. 1973. "The Effects of Nutrient Availability and Light Intensity on the Growth Kinetics of Natural Phytoplankton Communities", presented at American Society of Limnology and Oceanography, 36th Annual Meeting, Salt Lake City, UT.
- Henrici, P. 1964. *Elements of Numerical Analysis*, John Wiley & Sons, Inc., New York.
- Holley, E. R. and Jirka, G. 1986. "Mixing in Rivers," *Technical Report E-86-11*, US Army Engineer Waterways Experiment Station, Vicksburg, MS.
- Holm, N.P., and Armstrong, D.E. 1981. "Role of Nutrient Limitation and Competition in Controlling the Populations of *Asterionella formosa* and *Microcystis aeruginosa* in Semicontinuous Culture", *Limnology and Oceanography*, Vol 26, pp 622-634.
- Hoogenhout, H., and Ames, J. 1965. "Growth Rates of Photosynthetic Microorganisms in Laboratory Studies", *Archives of Microbiology*, Vol 50, pp 10-24.
- Hoskins, J.K., Ruchhoft, C.C., and Williams, L.G. 1927. "A Study of the Pollution and Natural Purification of the Illinois River; I. Surveys and Laboratory Studies", *Public Health Bulletin No. 171*, Washington, DC.
- Hutchinson, G.E. 1957. *A Treatise on Limnology; I. Geography, Physics and Chemistry*, John Wiley and Sons, New York, NY.
- Hwang, C.P., Lackie, T.H., and Huang, P.M. 1976. "Adsorption of Inorganic Phosphorus by Lake Sediments", *J. of the Water Pollution Control Federation*, Vol 48, pp 2754-2760.
- Hydrologic Engineering Center. 1981. "Geometric Elements from Cross Section coordinates", Computer program description.

REFERENCES

- Ignatiades, L., and Smayda, T.J. 1970. "Autecological Studies on the Marine Diatom *Rhizosolenia fragilissima* Bergon; I. The Influence of Light, Temperature, and Salinity", *J. of Phycology*, Vol 6, pp 332-229.
- Jacoby, G.C., Jr., et al. 1977. "Evaporation, Bank Storage and Water Budget at Lake Powell", *Lake Powell Research Project Bulletin No. 48*, Institute of Geophysics and Planetary Physics, University of California, Los Angeles, CA.
- Janik, J.J., Taylor, W.D., and Lambou, V.W. 1981. "Estimating Phytoplankton Biomass and Productivity", *Miscellaneous Paper E-81-2*, US Army Engineer Waterways Experiment Station, Vicksburg, MS.
- Jeanjean, R. 1969. "Influence de al Carence en Phosphoric sur les Vitesses d'Absorption du Phosphate Par les Chlorelles", *Bull. Soc. Fr. Physiol. Veg.*, Vol 15, pp 159-171.
- Jewell, W.J., and McCarty, P.L. 1971. "Aerobic Decomposition of Algae", *Environment Science and Technology*, Vol 5, pp 1023-1031.
- Jitts, H.R., McAllister, C.D., Stephens, K., and Strickland, J.D.H. 1964. "The Cell Division Rates of Some Marine Phytoplankton as a Function of Light and Temperature", *J. of the Fisheries Research Board of Canada*, Vol 21, pp 139-157.
- Johnson, M.C., et al. 1981 Oct. "Analyzing Storm Event Data from DeGray Lake, Arkansas Using LARM", presented at the American Society of Civil Engineers 1981 Convention and Exposition, St. Louis, MO.
- Jorgensen, E.G. 1968. "The Adaptation of Plankton Algae; II. Aspects of the Temperature and the Temperature Adaptation of *Skeletonema costatum*", *Physiological Plant*, Vol 21, pp 423-427.
- Kamp-Nielson, L. 1974. "Mud-Water Exchange of Phosphate and Other Ions in Undisturbed Sediment Cores and Factors Affecting Exchange Rates", *Archives of Hydrobiologia*, Vol 73, pp 218-237.
- Kanwisher, J. 1963. "On the Exchange of Gases Between the Atmosphere and the Sea", *Deepsea Research with Oceanography*, Vol 10, pp 195-207.
- Ketchum, B.H. 1939. "The Absorption of Phosphate and Nitrate by Illuminated Cultures of *Nitzschia closterium*", *American J. of Botany*, Vol 26, pp 399-407.
- Kinsman, B. 1979. *Wind Waves: Their Generation and Propagation*, Prentice-Hall, Englewood Cliffs, N.J.
- Kirk, J.T.O. 1975. "A Theoretical Analysis of the Contribution of Algal Cells to the Attenuation of Light Within Natural Waters; I. General Treatment of Suspensions of Pigmented Cells", *New Phytology*, Vol 75, pp 11-20.
- Kittrell, F.W., and Furfari, S.A. 1963. "Observations of Coliform Bacteria in Streams", *J. of the Water Pollution Control Federation*, Vol 35, p 1361.

REFERENCES

- Kittrell, F.W., and Koschitzky, O.W., Jr. 1947. "Natural Purification Characteristics of a Shallow Turbulent Stream", *Sewage Works J.*, Vol 19, p 1031.
- Klock, J.W. 1971. "Survival of Coliform Bacteria in Wastewater Treatment Lagoons", *J. of the Water Pollution Control Federation*, Vol 43, p 2071.
- Knowles, G., Downing, A.L., and Barrett, M.J. 1965. "Determination of Kinetic Constants for Nitrifying Bacteria in Mixed Culture, with the Aid of an Electronic Computer", *J. of General Microbiology*, Vol 38, pp 263-278.
- Knudsen, G. 1965. "Induction of Nitrate Reductase in Synchronized Cultures of *Chlorella pipenodosa*", *Biochem. Biophys. Acta.*, Vol 103, pp 495-502.
- Konopka, A. 1983. "The Effect of Nutrient Limitation and Its Interaction with Light upon the Products of Photosynthesis in *Merismopedia tenuissima* (Cyanophyceae)", *J. Phycology*, Vol 19, pp 403-409.
- Koutitas, C. G. 1978. Numerical Solution of the Complete Equations for Nearly Horizontal Flows. *Advances in Water Resources*, 1(4), 213.
- Ku, W.C., Di Giano, F.A., and Feng, T.H. 1978. "Factors Affecting Phosphate Adsorption Equilibria in Lake Sediments", *Water Research*, Vol 12, pp 1069-1074.
- Lane, E.W. 1938. "Notes on Formation of Sand", *Transactions of the American Geophysical Union*, Vol 18, pp 505-508.
- Langbien, W. B. and Durum, W. H. 1967. "The Aeration Capacity of Streams," USGS, Washington, D.C. Circ. 542.
- Laws, E.A., and Wong, D.C. 1978. "Studies of Carbon and Nitrogen Metabolism by Three Marine Phytoplankton Species in Nitrate-Limited Continuous Culture", *J. of Phycology*, Vol 14, pp 406-416.
- Leendertse, J.J., and Liu, S-K. 1977. "Turbulent Energy for Computation; Volume IV, A Three-Dimensional Model for Estuaries and Coastal Seas", Rpt. No. 2-2187-OWRT, The Rand Corporation, Santa Monica, CA.
- Leonard, B. P. 1979. "A Stable and Accurate Convective Modelling Procedure Based on Upstream Interpolation", *Computer Methods in Applied Mechanics and Engineering*, Vol 19, pp. 59-98.
- Leonard, B. P. 1991. "The ULTIMATE conservative difference scheme applied to unsteady one-dimensional advection," *Computer Methods in Applied Mechanics and Engr*, 88 (1991), 17-74.
- Li, W.K.W., and Morris, I. 1982. "Temperature Adaptation in *Phaeodactylum tricorutum* Bohlin: Photosynthetic Rate Compensation and Capacity", *J. of Experimental Marine Biology and Ecology*, Vol 58, pp 135-150.
- Libby, P. A. 1996. *Introduction to Turbulence*, Taylor and Francis, Washington D.C.

REFERENCES

- Lighthill, J. 1978. *Waves in Fluids*, Cambridge University Press, NY.
- Liggett, J. A. 1970. "Cell Method for Computing Lake Circulation," *J. of the Hydraulics Div., ASCE*, 96(HY3), 725.
- Lin, B., and Falconer, R. A. 1997. "Tidal Flow and Transport Modeling Using ULTIMATE QUICKEST Scheme", *J. of Hydraulic Engineering, ASCE*, 123(4), 303-314.
- Lindijer, G. H. 1979. "Three-Dimensional Circulation Models for Shallow Lakes and Seas; Semi-Analytical Steady-State Analysis of Wind-Driven Current Including the effect of Depth-Dependent Turbulent Exchange Coefficient," *Report R 900-11*, Delft Hydraulics Laboratory, Netherlands.
- Liss, P.S. 1973. "Processes of gas exchange across an air-water interface," *Deep Sea Research*, Vol. 20, pp 221-238.
- MacIsaac, J.H., and Dugdale, R.C. 1969. "The Kinetics of Nitrate and Ammonia Uptake by Natural Populations of Marine Phytoplankton", *Deepsea Research with Oceanography*, Vol 16, pp 16-27.
- Mackay, D. 1980. "Solubility, Partition Coefficients, Volatility, and Evaporation Rates", *Reactions and Processes Handbook*, Vol 2, Part A, Springer-Verlag, New York, NY.
- Madsen, O. S. 1977. A Realistic Model of the Wind-Induced Ekman Boundary Layer. *J. Physical Oceanography*, 7(2), 248.
- Mahloch, J.L. 1974. "Comparative Analysis of Modeling Techniques for Coliform Organisms in Streams", *Applied Microbiology*, Vol 27, p 340.
- Mann, K.H. 1972. "Ecology Energetics of the Seaweed Zone in a Marine Bay on the Atlantic Coast of Canada; I. Zonation and Biomass of Seaweeds", *Marine Biology Berlin*, Vol 12, pp 1-10.
- Marais, G.V.R. 1974. "Faecal Bacterial Kinetics in Stabilization Ponds", *ASCE J. of the Sanitation Engineering Division*, Vol 100, No. EEI, p 119.
- Margalef, R. 1961. "Velocidad de Sedimentatlon de Organismos Pasivos del Fitoplancton", *Investigacion Pesq.*, Vol 18, pp 3-8.
- Martin, J.L. 1987. "Application of a Two-Dimensional Model of Hydrodynamics and Water Quality CE-QUAL-W2. to DeGray Lake, Arkansas", *Technical Rpt. E-87-1*, US Army Engineer Waterways Experiment Station, Vicksburg, MS.
- Martin, J. L., McCutcheon, S.C. 1999. *Hydrodynamics and Transport for Water Quality Modeling*, Lewis Publishers, NY.
- Mastropietro, M. A. 1968. "Effects of Dam Reaeration on Waste Assimilation Capacities of the Mohawk River," *Proceedings of the 23rd Industrial Waste Conference, Purdue University*.
- Maykut, G. N. and N. Untersteiner. 1971. "Some results from a time dependent, thermodynamic model of sea ice", *J. Geophys. Res.*, 83: 1550-1575.

REFERENCES

- Megard, R. O., Comles, W.S., Smith, P.D., and Knoll, A.S. 1980. "Attenuation of Light and Daily Integral Rates of Photosynthesis Attained by Planktonic Algae", *Limnology and Oceanography*, Vol 24, pp 1038-1050.
- Melching, C. and Flores, H. 1999. "Reaeration Equations Derived from USGS Database," *J. Envir. Engr., ASCE*, 125(5), 407-414.
- Meyer, A.F. 1928. *The Elements of Hydrology*, John Wiley and Sons, New York, NY.
- Mills, W.B.; Porcella, D.; Unga, M.; Gherini, S.; Summers, K.; Lingfung, M.; Rupp, G.; Bowie, G. Haith, D. 1985. "A Screening Procedure for Toxic and Conventional Pollutants in Surface and Ground Water," *EPA/600/6-85/002a*, Environmental Research Laboratory, Athens, GA.
- Mitchell, R., and Chamberlain, C. 1978. "Survival of Indicator Organisms", *Indicators of Enteric Contamination in Natural Waters*, G. Berg, ed.), Ann Arbor Science Publ., Inc., Ann Arbor, MI, pp 15-38.
- Moog, D.B. and Jirka, G.H. 1998. "Analysis of reaeration equations using multiplicative error," *J. Envir. Engr, ASCE*, 124(2), 104-110.
- Mortimer, C.H. 1981. "The Oxygen Content of Air Saturated Fresh Waters over Ranges of Temperature and Atmospheric Pressure of Limnological Interest", *International Vereinigung Theoretische and Angewandte Limnologie*, Vol 22, pp 2-23.
- Morton, F.I. 1965. "Potential Evaporation and River Basin Evaporation", *ASCE J. of the Hydraulics Division*, Vol 91, No. HY6, pp 67-97.
- Munk, W. H. and Anderson, E. R. 1948. "Notes on the Theory of the Thermocline," *Journal of Marine Research*, Vol 1, p.276.
- Myers, J., and Graham, J. 1961. "On the Mass Culture of Algae; III. Light Diffusers: High vs. Low Temperature Chlorellas", *Plant Physiology*, Vol 36, pp 342-346.
- Nalewajko, C. 1966. "Photosynthesis and Excretion in Various Planktonic Algae", *Limnology and Oceanography*, Vol 11, pp 1-10.
- Neumann, G. and Pierson, W. J. 1966. *Principles of Physical Oceanography*. Prentice-Hall Inc. Englewood Cliffs, N. J.
- Newbold, J.D., and Liggett, D.S. 1974. "Oxygen Depletion Model for Cayuga Lake", *ASCE J. of the Environmental Engineering Division*, Vol 100, No. EEL, pp 41-59.
- O'Connor, D. J. and Dobbins, W.E. 1958. "Mechanism of Reaeration in Natural Streams," *ASCE Trans.*, 86(SA3):35-55.
- O'Connor, D.J. 1983. "Wind Effects on Gas-Liquid Transfer Coefficients" *J. Envir Engr ASCE*, Vol. 109, pp. 731-752.

REFERENCES

- Odum, E.P., and de la Cruz, A.A. 1967. "Particulate Organic Detritus in a Georgia Salt Marsh-- Estuarine Ecosystem", *Estuaries*, G.H. Lauff, ed., American Association for the Advancement of Sciences, Washington, DC, pp 383-388.
- Olson, R. M. and Wright, S. J. 1990. *Essentials of Engineering Fluid Mechanics*, 5th edition, Harper and Row, NY.
- Osterberg, C., Casey, A.G., and Curl, H. 1963. In *Nature*, Vol 200, pp 1276-1277.
- Otsuki, A., and Hanya, T. 1972. "Production of Dissolved Organic Matter from Dead Green Algal Cells; I. Aerobic Microbial Decomposition", *Limnology and Oceanography*, Vol 17, pp 248-257.
- Owens, M., Edwards, R., and Gibbs, J. 1964. "Some Reaeration Studies in Streams," *Int. J. Air Water Poll.*, 8:469-486.
- Paasche, E. 1968. "Marine Plankton Algae Grown with Light-Dark Cycles; II. *Ditylum brightwellii* and *Nitzschia turgidula*", *Physiological Plant*, Vol 21, pp 66-77.
- Parson, T.R., and Strickland, J.D.H. 1963. "On the Production of Particulate Organic Carbon by Heterotrophic Processes in Sea Water", *Deepsea Research with Oceanography*, Vol 8, pp 211-222.
- Patterson, J.C. and Hamblin, P.F., "Thermal Simulation of a Lake with Winter Ice Cover", *Limnology and Oceanography*, 33(3), 1988, P. 323-338.
- Pickett, J.M. 1975. "Growth of *Chlorella* in a Nitrate-Limited Chemostat", *Plant Physiology*, Vol 55, pp 223-225.
- Piecznska. 1972. *Wiadomosci Ekologiczne*, Vol 18, pp 131-140.
- Quasim, S.Z., Bhattathiri, P.M.A., and Dovassoy, V.P. 1973. *Marine Biology*, Vol 21, pp 299-304.
- Rhee, G-Yull. 1973. "A Continuous Culture Study of Phosphate Uptake, Growth Rate and Polyphosphate in *Scenedesmus sp.*", *J. of Phycology*, Vol 9, pp 495-506.
- Rhee, G-Yull, and Gotham, I.J. 1981a. "The Effects of Environmental Factors on Phytoplankton Growth: Temperature and the Interaction of Temperature with Nutrient Limitation", *Limnology and Oceanography*, Vol 26, pp 635-648.
- _____. 1981b. "The Effects of Environmental Factors on Phytoplankton Growth: Light and the Interaction of Light with Nitrate Limitation", *Limnology and Oceanography*, Vol 26, pp 649-659.
- Riley, G.A. 1943. *Bulletin of the Bingham Oceanography College*, Vol 8, Art. 4, p 53.
- Riley, G.A., H. Stommel, and D.F. Bumpus. 1949. "Quantitative Ecology of the Plankton of the Western North Atlantic", *Bulletin of the Bingham Oceanography College*, Vol 12, pp 1-169.
- Riley, G.A., and von Aux, R. 1949. In *J. of Marine Research*, Vol 8, No. 11, pp 60-72.

REFERENCES

- Roache, P.J. 1982. *Computational Fluid Dynamics*, Hermosa Publishers, Albuquerque, NM.
- Rodi, W. 1993. *Turbulence Models and Their Application in Hydraulics, 3rd edition*, IAHR, A.A. Balkema, Rotterdam.
- Rogers, K.H., and C.M. Breen. 1982. "Decomposition of *Potamogeton crispus*; I. Effects of Drying on the Pattern of Mass and Nutrient Loss", *Aquatic Botany*, Vol 12, pp 1-12.
- Ryan, P.J. and D.R.F. Harleman. 1974. "Surface Heat Losses from Cooling Ponds," *Water Resources Research*, Vol 10, No 5, Oct 1974, pp. 930-938.
- Ryan, Patrick J. and Keith D. Stolzenbach. 1972. Chapter 1: "Environmental Heat Transfer" in *Engineering Aspects of Heat Disposal from Power Generation*, D. R. F. Harleman, ed.. R. M. Parson Laboratory for Water Resources and Hydrodynamics, Department of Civil Engineering, Massachusetts Institute of Technology, Cambridge, MA.
- Ryding, S.O., and C. Forsberg. 1977. "Sediments as a Nutrient Source in Shallow Polluted Lakes", *Interactions Between Sediments and Freshwater*, H.L. Golterman, ed.), Junk, The Hague.
- Ryther, J.H. 1954. "Inhibitory Effects of Phytoplankton upon the Feeding of *Daphnia magna* with Reference to Growth, Reproduction, and Survival", *Ecology*, Vol 35, pp 522-533.
- Sabersky, R.; A. Acosta, E. Haupmann 1989. *Fluid Flow A First Course in Fluid Mechanics*, Macmillan Publishing Co., NY.
- Saunders, G.W. 1972. "The Transformation of Artificial Detritus in Lake Water", *Mem. Ist. Ital. Idrobiol. Dott Marco de Marchi*, Pallanza, Italy 29 Suppl), pp 261-288.
- Sawyer, C.N., and McCarty, P.L. 1967. *Chemistry for Sanitary Engineers*, 2d ed., McGraw-Hill, St. Louis, MO.
- Schindler, D.W. 1971. "Food Quality and Zooplankton Nutrition", *J. of Animal Ecology*, Vol 40, pp 598-595.
- Schindler, D.W., et al. 1973. "Eutrophication of Lake 227 by Addition of Phosphate and Nitrate: The Second, Third and Fourth Years of Enrichment, 1970, 1971, 1972", *J. of the Fisheries Research Board of Canada*, Vol 30, pp 1415-1428.
- Schlichting, H. 1962. *Boundary Layer Theory*, McGraw-Hill, NY.
- Schnoor, J.L., and Fruh, E.G. 1979. "Dissolved Oxygen Model of a Short Detention Time Reservoir with Anaerobic Hypolimnion", *Water Resources Bulletin*, Vol 15, No. 2, pp 506-518.
- Sedell, J.R., Triska, F.J., and Triska, N.S. 1975. "The Processing of Conifer and Hardwood Leaves in Two Coniferous Forest Streams; I. Weight Loss and Associated Invertebrates", *Verh. Internat. Verein. Limnol.*, Vol 19, pp 1617-1627.

REFERENCES

- Shanahan, P. and Harleman, D. 1982. "Linked Hydrodynamic and Biogeochemical Models of Water Quality in Shallow Lakes," *Technical Report 268*, R. M. Parson Laboratory, MIT, Cambridge, MA.
- Shelef, G. 1968. "Kinetics of Algal Systems in Waste Treatment; Light Intensity and Nitrogen Concentration as Growth-Limiting Factors", Ph.D. Thesis, University of California, Berkeley, CA.
- Simoës, F. 1998. "An Eddy Viscosity Model for Shallow-Water Flows," *Water Resources Engineering 98*, ASCE, NY, 1858-1863.
- Smayda, T.J. 1969. "Experimental Observations on the Influence of Temperature, Light, and Salinity on Cell Division of the Marine Diatom *Detonula cofervacea* Cleve. Gran", *J. of Phycology*, Vol 5, pp 150-157.
- _____. 1971. "Normal and Accelerated Sinking of Phytoplankton in the Sea", *Marine Geology*, Vol 11, pp 105-122.
- _____. 1974. "Some Experiments on the Sinking Characteristics of Two Freshwater Diatoms", *Limnology and Oceanography*, Vol 19, No. 4, pp 628-635.
- Smayda, T.J., and Boleyn, B.J. 1965. "Experimental Observations on the Flotation of Marine Diatoms; I. *Thalassiosira* cf. *nana*, *Thalassiosira rotula* and *Nitzschia seriata*", *Limnology and Oceanography*, Vol 10, pp 499-509.
- _____. 1966. "Experimental Observations on the Flotation of Marine Diatoms; III. *Bacteriastrum hyalinum* and *Chaetoceros lauderi*", *Limnology and Oceanography*, Vol 11, pp 35-43.
- Smith, D.J. 1978. "WQRRS, Generalized computer program for River-Reservoir systems," *USACE Hydrologic Engineering Center HEC*, Davis, California. User's Manual 401-100, 100A, 210 pp.
- Smith, W.O. 1979. "A Budget for the Autotrophic Ciliate *Mesodinium rubrum*", *J. of Phycology*, Vol 15, pp 27-33.
- Smith, R.C., and Baker, K.S. 1978. "The Bio-optical State of Ocean Waters and Remote Sensing", *Limnology and Oceanography*, Vol 23, pp 247-259.
- Snow, P.D., and Di Giano, F.A. 1976. "Mathematical Modeling of Phosphorus Exchange Between Sediments and Overlaying Water in Shallow Eutrophic Lakes", *Rpt. 54-76-3*, Department of Civil Engineering, University of Massachusetts, Amherst, MA.
- Sorokin, C., and Krauss, R.W. 1962. "Effects of Temperature and Illumination on *Chorella* Growth Uncoupled from Cell Division", *Plant Physiology*, Vol 37, pp 37-42.
- Sorokin, C., and Meyers, J. 1953. "A High Temperature Strain of *Chlorella*", *Science*, Washington, D.C., Vol 117, pp 330-331.
- Soong, T. W., DePue, M.; D. Anderson 1995. "The Changes of Manning's Roughness Coefficient with River Stages," *Water Resources Engineering*, ed. by W. H. Epsey and P. Combs, ASCE, pp.1759-1763.

REFERENCES

- Spence, D.H.N. 1981. "Light Quality and Plant Responses Underwater", *Plants and the Daylight Spectrum*, H. Smith, ed., Academic Press, New York, NY, pp 245-276.
- Spencer, D.F., and Lembi, C.A. 1981. "Factors Regulating the Spatial Distribution of the Filamentous Alga *Pithophora oedoga* Chlorophyceae. in an Indiana Lake", *J. of Phycology*, Vol 17, pp 168-173.
- Steele, J.H. 1962. "Environmental Control of Photosynthesis in the Sea", *Limnology and Oceanography*, Vol 7, pp 137-150.
- Steemann-Nielsen, E. 1952. "On Detrimental Effects of High Light Intensities on the Photosynthetic Mechanism", *Physiological Plant*, Vol 5, pp 334-344.
- Steemann-Nielsen, E., and Jorgensen, E.G. 1968. "The Adaptation of Plankton Algae; I. General Part", *Physiological Plant*, Vol 21, pp 401-413.
- St. John, et . al. 1984. in *International Symposium on Gas Transfer*, ed by W. Brutsart and G. Jirka, ASCE, New York, NY.
- Stumm, W., and Morgan, J.J. 1981. *Aquatic Chemistry*, Wiley Interscience, New York, NY.
- Tailing, J.F. 1955. "The Relative Growth Rates of Three Plankton Diatoms in Relation to Underwater Radiation and Temperature", *Ann. Bot. N. S.*, Vol 19, pp 329-341.
- Tamiya, H.T., Sasa, T., Nikei, T., and Ishibashi, S. 1965. "Effects of Variation of Daylength, Day and Night Temperatures, and Intensity of Daylight on the Growth of *Chlorella*", *J. of General and Applied Microbiology*, Vol 4, pp 298-307.
- Tanaka, N., Nakanishi, M., and Kadota, H. 1974. "Nutritional Interrelation Between Bacteria and Phytoplankton in a Pelagic Ecosystem", *Effects of the Ocean Environment on Microbial Activities*, R.R. Colwell and R.V. Mouta, eds., University Park Press, Baltimore, MD, pp 495-509.
- Thackston, E. L. and Krenkel, P. A. 1966. "Reaeration Predictions in Natural Streams," *J. San. Engr. Div., ASCE*, 89(SA5):1-30.
- Thibodeaux, L. 1996. *Environmental Chemodynamics*, Wiley-Interscience, NY.
- Thomann, R.V. 1971. "The Effect of Nitrification on the Dissolved Oxygen of Streams and Estuaries", Environmental Engineering and Scientific Program, Manhattan College, Bronx, New York, NY.
- Thomann, R. V. and Fitzpartrick, J. F. 1982. "Calibration and Verification of a Mathematical Model of the Eutrophication of the Potomac Estuary," report by HydroQual, Inc. Mahwah, NJ, to DES, District of Columbia.
- Thomann, R. V. and Mueller, J. A. 1987. *Principles of Surface Water Quality Modeling and Control*, Harper and Row, NY.

REFERENCES

- Thomas, J. H. 1975. "A Theory of Steady Wind-Driven Current in Shallow Water with Variable Eddy Viscosity," *J. Physical Oceanography*, 5(1), 136.
- Thomas, W.H., and Dodson, A.N. 1968. "Effects of Phosphate Concentration on Cell Division Rates and Yield of a Tropical Oceanic Diatom", *Biological Bulletin*, Vol 134, pp 199-208.
- Thompson, J.R., and Bernard, R.S. 1985. "WESSEL: Code for Numerical Simulation of Two--Dimensional Time-Dependent, Width-Averaged Flows with Arbitrary Boundaries", *Technical Rpt. E-85-8*, US Army Engineer Waterways Experiment Station, Vicksburg, MS.
- Thornton, K.W., and Lessem, A.S. 1978. "A Temperature Algorithm for Modifying Biological Rates", *Transactions of the American Fisheries Society*, Vol 107, No. 2, pp 284-287.
- Thornton, K.W., Nix, J.F., and Bragg, J.D. 1980. "Coliforms and Water Quality: Use of Data in Project Design and Operation", *Water Resources Bulletin*, No. 16, pp 86-92.
- Tison, D.L., and Pope, D.H. 1980. "Effect of Temperature on Mineralization by Heterotrophic Bacteria", *Applied and Environmental Microbiology*, Vol 39, pp 584-587.
- Tison, D.L., Pope, D.P., and Boylen, C.W. 1980. "Influence of Seasonal Temperature on the Temperature Optima of Bacteria in Sediments of Lake George, New York", *Applied and Environmental Microbiology*, Vol 39, pp 675-677.
- Titman, D., and Kilham, P. 1976. "Sinking in Freshwater Phytoplankton: Some Ecological Implications of Cell Nutrient Status and Physical Mixing Processes", *Limnology and Oceanography*, Vol 21, No. 3, pp 109-117.
- Toerien, D.F., and Cavari, B. 1982. "Effect of Temperature on Heterotrophic Glucose Uptake, Mineralization, and Turnover Rates in Lake Sediment", *Applied and Environmental Microbiology*, Vol 43, pp 1-5.
- Toetz, D., Varga, L., and Loughran, D. 1973. "Half-Saturation Constants for Uptake of Nitrate and Ammonia by Reservoir Plankton", *Ecology*, Vol 54, pp 903-908.
- Trussell, R.P. 1972. "The Percent Un-ionized Ammonia in Aqueous Ammonia Solutions at Different pH Levels and Temperature", *J. of the Fisheries Research Board of Canada*, Vol 29, pp 1505-1507.
- Tsivoglou, E. C. and Wallace, S. R. 1972. "Characterization of Stream Reaeration Capacity," *USEPA, Report No. EPA-R3-72-012*.
- Turner, J. S. 1979. *Buoyancy Effects in Fluids*, Cambridge University Press, NY.
- Turner, J.T. 1977. "Sinking Rates of Fecal Pellets from the Marine Copepod *Pontella meadii*", *Marine Biology*, Vol 40, No. 3, pp 249-259.
- Underhill, P.A. 1977. "Nitrate Uptake Kinetics and Clonal Variability in the Neritic Diatom *Biddulphia aurita*", *J. of Phycology*, Vol 13, pp 170-176.

REFERENCES

- Ugarte, A. and M. Madrid 1994. "Roughness Coefficient in Mountain Rivers," *Proceedings National Conference on Hydraulic Engineering, ASCE*, pp. 652-656.
- USBR 1999. Water Measurement Manual, <http://ogee.do.usbr.gov/fmt/wmm>.
- US Army Engineer District, Baltimore. 1977. "Thermal Simulation of Lakes; User's Manual for Program Numbers 722-F5-E1010 and 722-F5-E1011", Baltimore, MD.
- Vaccaro, R.F. 1969. "The Response of Natural Microbial Populations in Seawater to Organic Enrichment", *Limnology and Oceanography*, Vol 14, pp 726-735.
- van Lierre, L., Zevenboom, W., and Mur, L.R. 1977. "Nitrogen as a Limiting Factor for the Growth of the Blue Green Alga *Oscillatoria*", *Progressive Water Technology*, Vol 8, pp 301-312.
- Verduin, J. 1952. "Photosynthesis and Growth Rates of Live Diatom Communities in Western Lake Erie", *Ecology*, Vol 33, pp 163-169.
- _____. 1982. "Components Contributing to Light Extinction in Natural Waters: Methods of Isolation", *Archives of Hydrobiology*, Vol 93, pp 303-312.
- Verity, P.G. 1981. "Effects of Temperature, Irradiance and Daylength on the Marine Diatom *Leptocylindrus danicus* Cleve; I. Photosynthesis and Cellular Composition", *J. of Experimental Marine Biology and Ecology*, Vol 55, pp 79-91.
- Vollenweider, R.A. 1968. "Scientific Fundamentals of the Eutrophication of Lakes and Flowing Waters, with Particular Reference to Nitrogen and Phosphorus as Factors in Eutrophication", *Tech. Rept. OECD, DAS/CSI/68.27*, Paris, France.
- _____. 1976. "Advances in Defining Critical Loading Levels for Phosphorus in Lake Eutrophication", *Mem. Inst. Ital. Idrobiol.*, Vol 33, pp 53-83.
- Von Muller, H. 1972. "Wachstum und Phosphatbedarf von *Nitzschia octinastroides* Lemm.. V. Goor in Statischer and Homokontinuierlicher Kultur unter Phosphatlimitierung", *Arch. Hydrobiol. Suppl.*, Vol 38, pp 399-484.
- Wallen, D.G., and Cartier, L.D. 1975. "Molybdenum Dependence, Nitrate Uptake and Photosynthesis of Freshwater Plankton Algae", *J. of Phycology*, Vol 11, pp 345-349.
- Wake, A. 1977. "Development of a Thermodynamic Simulation Model for the Ice Regime of Lake Erie", Ph.D. thesis, SUNY at Buffalo, Buffalo, NY.
- Wang, L.K., Poon, C.P., Wang, M.H., and Bergenthal, J. 1978. "Chemistry of Nitrification-Denitrification Process", *J. of Environmental Sciences*, Vol 21, pp 23-28.
- Wannikof, R., Ledwell, J. R., and Crusius, J. 1991. "Gas Transfer Velocities on Lakes measured with Sulfur Hexafluoride," In *Symposium Volume of the Second International Conference on Gas Transfer at Water Surfaces*, S. C. Wilhelms and J. S. Gulliver, eds., Minneapolis, MN.

REFERENCES

- Watts, F. J. 1993. "n Values for Shallow Flow in Rough Channels," *Proceedings National Conference on Hydraulic Engineering, Part 1, ASCE*, pp. 995-1000.
- Weiler, R.R. 1974. "Carbon dioxide exchange between water and atmosphere," *Journal of Fisheries Research, Board Committee*, Vol. 31, pp. 329-332.
- Wells, S. A. and Berger, C. J. 1995. "Hydraulic and Water Quality Modeling of Wahiawa Reservoir," prepared for R. M. Towill Corporation, Honolulu, HA.
- Wells, S. A. 1997. "Theoretical Basis for the CE-QUAL-W2 River Basin Model," Department of Civil Engineering, *Technical Report EWR-6-97*, Portland State University, Portland, OR.
- Wells, S. A. and Berger, C. 1997. "Modeling the Lower Snake River," report prepared for HDR Engineering, Inc., Boise, ID.
- Wells, S. A. and Berger, C. 1998. "The Lower Snake River Model," report prepared for HDR Engineering, Inc., Boise, ID.
- WES. 1996. Evaluation and Analysis of Historical Dissolved Gas Data from the Snake and Columbia Rivers, Waterways Experiments Station, *ACOE Dissolved Gas Abatement Study Phase 1 Technical Report*, Vicksburg, MS.
- WES. 1997. "Total Dissolved Gas Production at Spillways on the Snake and Columbia Rivers, Memorandum for Record," Waterways Experiments Station, *ACOE Dissolved Gas Abatement Study Phase 1 Technical Report*, Vicksburg, MS.
- Wetzel, R.G. 1975. *Limnology*, W.B. Saunders, Philadelphia, PA.
- Wetzel, R.G., Rich, P.H., Miller, M.C., and Allen, H.L. 1972. "Metabolism of Dissolved Particulate Detrital Carbon in a Temperate Hardwater Lake", *Mem. Ist Ital. Idrobiol. Suppl.*, Vol 29, pp 185-243.
- Whittaker, R.H. 1975. *Communities and Ecosystems*, MacMillan, New York, NY.
- Wiegel, R.L. 1964. *Oceanographical Engineering*, Prentice-Hall, Englewood Cliffs, NJ.
- Wild, H.E., Sawyer, C.N., and McMahon, T.C. 1971. "Factors Affecting Nitrification Kinetics", *J. of the Water Pollution Control Federation*, Vol 43, pp 1845-1854.
- Williams, D.T., et al. 1980. "Determination of Light Extinction Coefficients in Lakes and Reservoirs", *Surface Water Impoundments, Proceedings of the Symposium on Surface Water Impoundments*, American Society of Civil Engineers, H.G. Stefan, ed..
- Williams, P.J., Yentsch, L.B., and Yentsch, C.S. 1976. "An Examination of Photosynthetic Production, Excretion of Photosynthetic Products and Heterotrophic Utilization of Dissolved Organic Compounds with Reference to Results from a Coastal Subtropical Sea", *Marine Biology*, Vol 35, pp 31-40.

REFERENCES

- Witten, A. J. and J. H. Thomas 1976. "Steady Wind-Driven Currents in a Large Lake with Depth Dependent Eddy Viscosity," *J. Physical Oceanography*, 6(1), 85.
- Wright, R.T. 1975. "Studies on Glycolic Acid Metabolism by Freshwater Bacteria", *Limnology and Oceanography*, Vol 20, pp 626-633.
- Wuhrmann, K. 1972. "Stream Purification", *Water Pollution Microbiology*, R. Mitchell, ed.), Interscience, New York, NY.
- Wunderlich, W. 1972. "Heat and Mass Transfer between a Water Surface and the Atmosphere", *Rpt. No. 14, Rpt. Publication No. 0-6803*, Water Resources Research Laboratory, Tennessee Valley Authority, Division of Water Control Planning, Engineering Laboratory, Norris, TN.
- Zimmerman, U. 1969. "Okologische and Physiologische Untersuchungen an der Planktonischen Blaualge *Oscillatoria Rubescens*, D.C., unter Besonderer Berücksichtigung von Licht and Temperatur", *Schweiz. Z. Hydrol.*, Vol 31, pp 1-58.
- Yakhot, V. and Orszag, S. 1986. "Renormalization Group Analysis of Turbulence 1: Basic Theory," *J. Sci. Comput.* 1(1), 3-51.
- Yen, B. C. 1992. *Hydraulic Resistance of Open Channels in Channel Flow: Centennial of Manning's Formula*, ed. B.C. Yen, Water Resources Publications, Littleton, CO.
- Yu, S.L., T.J. Tuffy, and D.S. Lee. 1977. "Atmosphere Reaeration in a lake," *Office of Water Resources and Technology*, U.S. Department of the Interior.
- Zison, S.W., Mills, W.B., Deimer, B., and Chen, C.W. 1978. "Rates, Constants, and Kinetics Formulations in Surface Water Quality Modeling", *EPA-600/3-68-105*, US Environmental Protection Agency, Washington, DC.

CE-QUAL-W2 Publications

Peer Reviewed Publications

- Bartholow, J., R.B. Hanna, L. Saito, D. Lieberman, and M. Horn. 2001. "Simulated Limnological Effects of the Shasta Lake Temperature Control Device". *Environmental Management*, Vol. 27, No. 4, pp. 609-626. http://smig.usgs.gov/SMIG/uo/features_0999/shasta_tcd.html.
- Bath, A.J., and T.D. Timm. 1994. "Hydrodynamic Simulation of Water Quality in Reservoirs of South Africa", *Commission Internationale Des Grands Barrages*, Q.69 R. 39, 625-633.
- Boatman, C.D., and E.M. Buchak. 1987. "Application of an Ecosystem/Water Quality Model as a Tool for Managing Estuarine Water Quality". In *Proceedings Fifth Symposium on Coastal Ocean Management, ASCE, Vol. 3*, Seattle, Washington, 3932-3945.
- Boegman, L., M.R. Loewen, D.A. Culver, P.F. Hamblin and M.N. Charlton. 2002. "A two-dimensional model coupling pelagic dynamics to benthic grazing by zebra mussels in western Lake Erie: Relative impacts of nutrient load abatement and mussel invasion, 1960s to 1994". (Under consideration for submission to *Can. J. Fish. Aquat. Sci.*).
- Boegman, L., M.R. Loewen, P.F. Hamblin and D.A. Culver. 2002. "A Two-Dimensional Model Coupling Pelagic Dynamics to Benthic Grazing by Zebra Mussels in Western Lake Erie: Spatial-Dynamic Responses". (Under consideration for submission to *Canadian Journal of Fisheries and Aquatic Sciences*).
- Boegman, L., M.R. Loewen, P.F. Hamblin and D.A. Culver. 2001. Application of a Two-Dimensional Hydrodynamic Reservoir Model to Lake Erie". *Canadian Journal of Fisheries and Aquatic Sciences*, 58: 858-869.
- Crain, A. S., G. L. Jarrett, and P. A. Bukaveckas. 1997. "Development And Calibration Of A Water Quality Model For Herrington Lake". *Waterworks* 3(1):1-3.
- Deliman, P.N. and J.A. Gerald. 2002. "Application of the Two-Dimensional Hydrothermal and Water Quality Model, CE-QUAL-W2, to the Chesapeake Bay – Conowingo Reservoir". *Journal of Lake and Reservoir Management*, Vol. 18, No. 1, pp. 1-9.

CE-QUAL-W2 BIBLIOGRAPHY

- Dortch, M. S., and W. L. Boyt. 1983. "Simulating Advective Transport in Reservoirs". In *Proceedings of the Conference on Frontiers in Hydraulic Engineering*, H. T. Shen, ed., August 9-12, 1983. Hydraulics Division of the American Society of Civil Engineers in conjunction with Massachusetts Institute of Technology and the Boston Society of Civil Engineers. Cambridge, MA.
- Edinger, J. E., and E. M. Buchak. 1980. "Numerical Hydrodynamics of Estuaries" in *Estuarine and Wetland Processes with Emphasis on Modeling*, P. Hamilton and K. B. MacDonald eds., Plenum Press, New York, NY, 115-146.
- Edinger, J. E., E. M. Buchak, and D. H. Merritt. 1983. "Longitudinal-Vertical Hydrodynamics and Transport with Chemical Equilibria for Lake Powell and Lake Mead", in *Salinity in Watercourses and Reservoirs*, R. H. French, ed., Butterworth Publishers, Stoneham, MA, pp. 213-222.
- Edinger, J. E., E. M. Buchak, and S. Rives. 1987. "GLVHT Model Verification Using Field Data", in *Proc. 1987 National Conference on Hydraulic Engineering*, R. M. Ragan, ed., August 3-7, 1987. Hydraulics Division of the American Society of Civil Engineers. Williamsburg, VA.
- Garvey, E., J.E. Tobiasson, M. Hayes, E. Wolfram, D.A. Reckhow, and J.W. Male. 1998. "Coliform Transport in a Pristine Reservoir: Modeling and Field Studies". *Water Science and Technology*, Vol. 37, No. 2, pp. 137-144.
- Gelda, R. K. and S. W. Effler. 2000. "A River Water Quality Model for Chlorophyll and Dissolved Oxygen that Accommodates Zebra Mussel Metabolism". *Water Quality and Ecosystem Modeling* 1:271-309.
- Gelda, R. K., S. W. Effler and E. M. Owens. 2001. "River Dissolved Oxygen Model with Zebra Mussel Oxygen Demand (ZOD)". *Journal of Environmental Engineering Division, ASCE* 127:790-801.
- Gelda, R. K., E. M. Owens and S. W. Effler. 1998. "Calibration, Verification, and an Application of a Two-Dimensional Hydrothermal Model [CE-QUAL-W2] for Cannonsville Reservoir". *Journal of Lake and Reservoir Management*, 14:186-196.
- Gordon, J. A. 1980. "An Evaluation of the LARM Two-Dimensional Model for Water Quality Management Purposes", in *Proceedings of the Symposium on Surface-Water Impoundments*, H. G. Stefan, ed., Minneapolis, Minnesota, June 2-5, 1980, Vol. 1, Paper 4-34, pp. 518-527. American Society of Civil Engineers, New York, NY.
- Gordon, J. A. 1981. "LARM Two-Dimensional Model: An Evaluation". *Journal of Environmental Engineering*, 107(5), 77-886.
- Gordon, J. A., and J. S. Lane. 1983. "Short-Term Hydrodynamics in a Stratified Reservoir", in *Proceedings of the 1983 National Conference on Environmental Engineering*, A. Medine and M. Anderson, eds., Boulder, Colorado, July 6-8, 1983, pp. 524-531. American Society of Civil Engineers, New York, NY.
- Gündüz, O., S. Soyupak, and C. Yurteri. 1998. Development of Water Quality Management Strategies for the Proposed Isikli Reservoir". *Water Science and Technology*, Vol. 37, No. 2, pp. 369-376

CE-QUAL-W2 BIBLIOGRAPHY

- Hanna, R.B., L. Saito, J.M. Bartholow, and J. Sandelin. 1999. "Results of Simulated Temperature Control Device Operations on In-Reservoir and Discharge Water Temperatures Using CE-QUAL-W2". *Journal of Lake and Reservoir Management* 15(2):87-102. <http://www.fort.usgs.gov/>.
- Johnson, B. H., M. B. Boyd and R. R. Copeland. 1987. "Lower Mississippi River Salt Intrusion Modeling", in *Proceedings 1987 National Conference on Hydraulic Engineering*, R. M. Ragan, ed.), 3-7 August 1987. Hydraulics Division of the American Society of Civil Engineers. Williamsburg, VA.
- Kim, B. R., J. M. Higgins and D. J. Bruggink. 1983. "Reservoir Circulation Patterns and Water Quality". *Journal of Environmental Engineering, ASCE*, 109(6), 1284-1294.
- Kurup, R.G., D.P. Hamilton, and R.L. Phillips. 2000. "Comparison of Two 2-Dimensional, Laterally Averaged Hydrodynamic Model Applications to the Swan River Estuary". *Mathematics and Computers in Simulation*, 51(6): 627-639. <http://www.cwr.uwa.edu.au/cwr/publications/papers1500/1536.html>
- Martin, J. L. 1988. "Application of Two-Dimensional Water Quality Model". *Journal of Environmental Engineering, ASCE*, 114(2), 317-336.
- Saito, L. B.M. Johnson, J. Bartholow, R. B. Hanna. 2001. "Assessing Ecosystem Effects of Reservoir Operations Using Food Web-Energy Transfer and Water Quality Models". *Ecosystems* 4(2):105-125. <http://link.springer-ny.com/link/service/journals/10021/bibs/1004002/10040105.html>
- Saito, Laurel, Brett M. Johnson, John M. Bartholow, and Darrell G. Fontane. 2001. Interdisciplinary modeling to assess ecosystem effects of reservoir operations. Pp. 373-377 in Marino, Miguel A., and Slobodan P. Simonovic, editors. *Integrated Water Resources Management*. IAHS Publication no. 272. Oxfordshire (UK): International Association of Hydrologic Sciences Press.

Presentations at Scientific Meetings

- Annear, R. and S. Wells. 2002. "The Bull Run Reservoir River System Model". *Proceedings Research and Extension Regional Water Quality Conference 2002* [on CD], Vancouver, Washington.
- Annear, R. and S. Wells. 2002. "The Bull Run River – Reservoir System Model". *Proceedings 2nd Federal InterAgency Hydrologic Modeling Conference*, Las Vegas, July 28-Aug 1, 2002.
- Atkins, D., T. Martin, and M. Bennett. 1998. "Pitlake Limnology". In *Proceedings of the 1998 Conference on Hazardous Waste Research: Bridging Gaps in Technology and Culture*, Snowbird, Utah, May 18-21, 1998.
- Atkins, D., J.H. Kempton, T. Martin, and P. Maley. 1997. "Limnologic Conditions in Three Existing Nevada Pit Lakes: Observations and Modeling Using CE-QUAL-W2". in *Proceedings - Fourth International Conference on Acid Rock Drainage*, Vancouver, B.C., Canada, May 31 - June 6, 1997.

CE-QUAL-W2 BIBLIOGRAPHY

- Bales, J.D. 2001. "Data Quality and Uncertainty in Reservoir Water-Quality Modeling Carolina". In *Warwick, J.J., ed., Water Quality Monitoring and Modeling—Proceedings of the AWRA Annual Spring Specialty Conference*, p. 113.
- Bales, J.D. 2001. Dynamic Water-Quality Models of Catawba River Basin Reservoirs, North Carolina". In *NALMS 10th Annual Southeastern Lakes Conference*, Knoxville, TN, p. 28.
- Bales, J.D. 1998. "Dynamic Water-Quality Modeling of Catawba River Reservoirs". In *Water resources protection: understanding and management, Institute Proceedings Series No. 11*, Raleigh, NC, University of North Carolina Water Resources Research Institute, p. 23 [abs].
- Bales, J.D. 1997. "Modeling estuarine effects of nitrogen loading reduction". In *Tanner, J., ed., Nutrients in the Neuse River--Working Toward Solutions*. New Bern, NC, Confere, North Carolina State University, p. 11 [abs].
- Bales, J.D., and M.L. Jaynes. 1995. "Dynamic Modeling of Circulation and Water Quality in a Narrow Piedmont Reservoir". *4th Annual Southeastern Lakes Management Conference*, North American Lake Management Society, Charlotte, North Carolina.
- Bales, J.D. 1993. U.S. Geological Survey Reservoir Studies in North Carolina". *2nd Annual Southeastern Lakes Management Conference*, North American Lake Management Society Chattanooga, Tennessee.
- Bales, J.D., 1993, The role of models in evaluating water quality in Proceedings of the Conference on Water Issues in the 1990's: Hickory, NC, Environmental Policy Studies Center, Catawba Valley Community College, p. 1-2.
- Bales, J.D. and M.J. Diorgino. 1998. "Dynamic Modeling of Water Supply Reservoir Physical and Chemical Processes". In *Proceedings of the First Federal Interagency Hydrologic Modeling Conference*, April 19-23, 1998, Las Vegas, NV: Subcommittee on Hydrology of the Interagency Advisory Committee on Water Data, p. 2-61 to 2-67. http://smig.usgs.gov/SMIG/features_0998/rhodhiss.html.
- Bartholow, J., L. Saito, B. Hanna, B. Johnson, D. Lieberman, and M. Horn. 2000. "Predicting the Effects of Shasta's Temperature Control Device on In-Reservoir Limnology and Fish". *Bay Delta Modeling Forum/Interagency Ecological Program*, Pacific Grove, California, February 29-March 3, 2000.
- Bartholow, J.M., B. Hanna, L. Saito, D. Lieberman, and M. Horn. 1999. "Simulated effects of a temperature control device on Shasta Lake". *North American Lake Management Society Symposium '99*. Reno, Nevada, December 1-4, 1999.
- Bartholow, J., D. Lieberman, M. Horn, B. Hanna, and L. Saito. 1998. "Effects of Dam Reoperation on Reservoir Limnology and Fishery Energetics". *North American Lake Management Society Conference*, Banff, Alberta, Canada.
- Berger, C. and S. Wells. 1995. "Effects of Management Strategies to Improve Water Quality in the Tualatin River, Oregon," in *Water Resources Engineering, Vol. 2*, ed. by W. Espey Jr. and P. Combs, ASCE, 1360-1364.

CE-QUAL-W2 BIBLIOGRAPHY

- Berger, C. and S. Wells. 1999. "Macrophyte Modeling in the Columbia Slough," *Proceedings International Water Resources Engineering Conference, ASCE*, Seattle, Wa, Aug.8-11.
- Berger, C., R. Annear, and S. Wells. 2002. "Willamette River and Columbia River Waster Load Allocation Model". In *Proceedings 2nd Federal InterAgency Hydrologic Modeling Conference*, Las Vegas, July 28-Aug 1, 2002.
- Bowen, J.D. 1998. "Using Eutrophication Modeling to Predict the Effectiveness of River Restoration Efforts". In *Proceedings Wetlands Engineering and River Restoration Conference*", ASCE
- Buchak, E. M., and J. E. Edinger. 1989. "Comparison of Computed and Observed Velocities at Three Estuarine Sites". Presented at the *Estuarine and Coastal Circulation and Pollutant Transport Modeling: Model-Data Comparison*. Waterway, Port, Coastal and Ocean Division, American Society of Civil Engineers, November 17, Newport, RI.
- Buchak, E.M., J.E. Edinger, J.J. Loos and E.S. Perry. 1989. "Larval Transport and Entrainment Modeling for the Patuxent Estuary". Presented at the *Tenth Biennial International Estuarine Research Conference*, Estuarine Research Federation, October 11, Baltimore, MD.
- Buchak, E. M., C. B. James and A. C. Mitchell. 1991. "Nechako Reservoir Mathematical Modelling Studies". Presented at the *1991 Annual Conference of the Canadian Society for Civil Engineering, 10th Canadian Hydrotechnical Conference and Engineering Mechanics Symposium*, May 29, Vancouver, BC.
- Boegman, L., P.F. Hamblin and M.R. Loewen. Two-Dimensional Modelling of Zebra Mussel Effects in Lake Erie, Stage One: Validation of Temperature, Currents and Water Levels. In *Proceedings of the 42nd Conference of the International Association of Great Lakes Research*, May 24-28, 1999, Case Western Reserve University, Cleveland, Ohio USA.
- Boegman, L., M.R. Loewen, P.F. Hamblin and D.A. Culver. Application of a Two-Dimensional Hydrodynamic and Water Quality Model to Lake Erie. Abstract in proceedings 2000 Ocean Sciences Meeting, Jan. 24-28, 2000, San Antonio, Texas USA.
- Chapman, R.S. and T.M. Cole. 1992. "Improved Thermal Predictions in CE-QUAL-W2". In *Hydraulic Engineering: Saving a Threatened Resource—In Search of Solutions, Water Forum '92*, Baltimore, Maryland.
- Chow, I.B. 2002 "A Two-Dimensional Model Application for Manatee Protection". *Charlotte Harbor Watershed Summit*, IMPAC University in Punta Gorda, Florida, February 7-9, 2002.
- Cole, T. M., and Hannan, H. H. 1979. "Computer Simulations of Canyon Reservoir". Presented at the *Texas Academy of Sciences Annual Meeting*. Austin, TX.
- Cole, T.M. 1995. "The Future Role of Sophisticated Models in Reservoir Management". *Lake and Reservoir Management V9 No. 2, NALMS 14th Annual International Symposium*, Orlando, FL.
- Cole, T. M. (2000) "Temperature Modeling Using CE-QUAL-W2". In *Proceedings HydroInformatics 2000, IAHR*, CDROM EW4.

CE-QUAL-W2 BIBLIOGRAPHY

- Cole, T.M. 2002. "CE-QUAL-W2 – A 2D Hydrodynamic and Water Quality Model for Rivers, Lakes, Reservoirs, and Estuaries". In *4th International Conference on Reservoir Limnology and Water Quality*, Ceshe Budejovice, Czech Republic, August 12-16, 2002.
- Devine, G., M. French, And G. L. Jarrett. 1997. "Neural Networks As A Tool To Calibrate Reservoir Water Quality Models". In *Proceedings Of The Kentucky Water Resources Research Institute*.
- Easley, W.S., L.E. Barness-Walz, P.L. Neichter, and J.A. Bohannon. 1995. "Evaluation of Water Quality in Taylorsville Lake, Kentucky: Using CE-QUAL-W2 Water Quality Model". *Lake and Reservoir Management V9 No. 2, NALMS 14th Annual International Symposium*, Orlando, FL.
- Edinger, J. E., and E. M. Buchak. 1978. "Reservoir Longitudinal and Vertical Implicit Hydrodynamics". Presented at the international conference *Environmental Effects of Hydraulic Engineering Works, ASCE*, September, Knoxville, TN.
- Goodwin, R.A., J.M. Nestler, and D. Degan. 2000. "Simulating Movement of Cool Water Fish in a Stratified Southern Impoundment". *American Fisheries Society Annual Meeting: Reflections*, St. Louis, Missouri, August 20-24, 2000.
- Hanna, B., L. Saito, J. Bartholow, and J. Sandelin. 1997. "Results of Mock 1995 Shasta TCD Operations on In-Reservoir and Discharge Water Quality Parameters using CE-QUAL-W2". *17th International Symposium of the North American Lake Management Society*, Houston, TX. page 54. <http://www.fort.usgs.gov/>.
- Johnson, M. C., D. E. Ford, J. E. Edinger and E. M. Buchak. 1981. "Analyzing Storm Event Data from DeGray Lake, Arkansas Using LARM". Presented at the *American Society of Civil Engineers Convention and Exposition*, October, St. Louis, MO.
- Hejzlar J., M. Růžička, and P. A. Diogo. 1999. "The Use of water quality modelling for optimising operation of a drinking water reservoir" *Proceedings International Conference on Fluid Mechanics and Hydrology*, June 23-26, 1999, Prague, Czech Republic, Institute of Hydrodynamics AS CR, Prague, 475-482.
- Jain, R., G. L. Jarrett, and E. M. Buchak. 2002. "Watershed and Reservoir Modeling in the Crum Creek Watershed". *AWRA Annual 2002 Conference*. Philadelphia, Pennsylvania. November 3-7.
- Jarrett, G. L, L. Curry, and J. Overing. 2001. Herrington Lake - Dix River Watershed (HSPF CEQUAL-W2 linkage). *Kentucky Water Resources Symposium*, Lexington, KY, Feb. 23.
- Kennedy, R.H., T. Cole, W. Boyd, K. Barko. 2002. Operational Influences on the Limnological Characteristics of Reservoirs: A Model Study. 2002. In *4th International Conference on Reservoir Limnology and Water Quality*, Ceshe Budejovice, Czech Republic, August 12-16, 2002.
- Lieberman, D., J. Bartholow, M. Horn, B. Hanna, and L. Saito. 1999. "Effects of Dam Reoperation on Reservoir Limnology and Fishery Energetics". *North American Lake Management Society Conference*, Banff, Alberta, Canada.

CE-QUAL-W2 BIBLIOGRAPHY

- Little, J.C. and McGinnis, D. F. "Hypolimnetic Oxygenation: Predicting Performance Using a Discrete-Bubble Model". In *Proceedings of 1st World Water Congress, International Water Association (IWA)*, Paris, France, July 3-7, 2000.
- Makinia, J., Wells, S. A., Crawford, D., and Kulbik, M. 1998. "Application of Mathematical Modeling and Computer Simulation for Solving Water Quality Problems," *Proceedings of the Fourth International Symposium and Exhibition on Environmental Contamination in Central and Eastern Europe Warsaw '98*, Warsaw, Poland, September 15-17, #233 CD-ROM.
- McGinnis, D.F., Little, J.C. and Wüest, A. "Hypolimnetic oxygenation: Coupling bubble-plume and reservoir models" submitted to *Asian Waterqual 2001, First IWA Asia-Pacific Regional Conference*, Fukuoka, Japan.
http://www.eawag.ch/research_e/apec/Scripts/IWA%20Japan%20v6.pdf
- McGinnis, D., J. Little, A. Wuest. 2002. "Coupling Bubble-Plume and Reservoir Models for Optimization of Hypolimnetic Oxygenation". In *4th International Conference on Reservoir Limnology and Water Quality*, Ceshe Budejovice, Czech Republic, August 12-16, 2002.
- Müller M., F. Werner, and L. Luckner. 2002. "A Tool for Conjunctive Groundwater and Surface Water Quality Modeling in Post Mining Areas". In *Proceedings of Third International Conference on Water Resources and Environment Research*, Dresden, Germany. Vol. I. pp.136-141.
- Růžička, M., J. Hejzlar, and T.M. Cole. 2002. "Impacts of Climate Change on the Water Quality in a Dimictic Reservoir". In *4th International Conference on Reservoir Limnology and Water Quality*, Ceshe Budejovice, Czech Republic, August 12-16, 2002.
- Růžička M., J. Hejzlar, P. Mikešová, and T. M. Cole. 2000. "2-D Water Quality Modelling of a Drinking Water Reservoir: Římov Reservoir, Czech Republic". In *Proceedings 5th International Symposium on Systems Analysis and Computing in Water Quality Management WATERMATEX 2000*, Gent, Belgium, 18-20 September 2000. Gent University, Gent, pp. 1.59-1.66.
- Ruzicka, M., J. Hejzlar, M. Dubrovsky, J. Buchtele, T.M. Cole. 2001. "A Scenario Study of Water Quality in a Drinking Water Supply Reservoir in Response to Climate Change". In *Detecting Environmental Change*, London, 17-20 July 2001, London, UK.
<http://www.ufa.cas.cz/dub/dub.htm>
- Rounds, S.A. 2001. "Modeling water quality in the Tualatin River: Achievements and limitations". In *AWRA Annual Spring Specialty Conference Proceedings, "Water Quality Monitoring and Modeling"*. Warwick, John J., ed., American Water Resources Association, Middleburg, Virginia, TPS-01-1, p. 115-120.
- Saito, L., B. Johnson, J. Bartholow, and Blair Hanna. 2001. "Assessing Effects of Reservoir Operations on the Reservoir Ecosystem Using Food Web-Energy Transfer and Water Quality Models". *21st Annual American Geophysical Union Hydrology Days*, April 2-5, 2001, Colorado State University, Fort Collins, Colorado, USA.
- Saito, L., B. Johnson, J. Bartholow, and D. Fontane. 2000. "Interdisciplinary modeling to assess ecosystem effects of reservoir operations". *International Symposium on Integrated Water Resources Management*. Davis, CA. April 2000.

CE-QUAL-W2 BIBLIOGRAPHY

- Smemoe, C.M., E.J. Nelson, and T.M. Cole. 2000. "A Conceptual Modeling Approach to CEQUAL-W2 Using the Watershed Modeling System". In *Proceedings of the Hydroinformatics Conference*, Iowa City, Iowa, July 2000.
- Wells, S.A. 1995. "Management of the Water Quality of the North Slough Adjacent to the St. John's Landfill". In *Proceedings First Annual Pacific Northwest Water Issues and 1995 Pacific Northwest/Oceania Conference*, Portland, Oregon.
- Wells, S.A. 1999. "River Basin Modeling Using CE-QUAL-W2". In *Proceedings International Water Resources Engineering Conference, ASCE*, Seattle, WA, Aug.8-11.
- Wells, S.A. 2000. "Hydrodynamic and Water Quality River Basin Modeling Using CE-QUAL-W2 Version 3". In *Development and Application of Computer Techniques to Environmental Studies VIII*, ed. G. Ibarra-Berastegi, C. Brebbia, P. Zannetti, WIT Press, Boston, 195-204.
- Wells, S. A. 2000. "CE-QUAL-W2 Version 3: Hydrodynamic and Water Quality River Basin Modeling". In *Proceedings Hydroinformatics 2000, IAHR*, CDROM EW4.
- Wells, S.A. 2002. "Validation of the CE-QUAL-W2 Version 3 River Basin Hydrodynamic and Water Quality Model". *Proceedings Hydroinformatics 2002, IAHR*, Cardiff, England.
- Wells, S.A. 2002. "Basis of the CE-QUAL-W2 Version 3 River Basin Hydrodynamic and Water Quality Model.". In *Proceedings 2nd Federal InterAgency Hydrologic Modeling Conference*, Las Vegas, July 28-Aug 1, 2002.
- Wells, S. A. and Annear, R. A. (2002) "River Basin Modeling Using CE-QUAL-W2 Version 3: The Bull Run River-Reservoir System Model". In *Proceedings 4th International Conference on Reservoir Limnology and Water Quality*, Ceske Budejovice, Czech Republic, August 12-16, 2002.
- Wells, S.A. and C. Berger. 1995. "Management Strategies to Improve Water Quality in the Tualatin River, Oregon". In *Proceedings NCASI Conference*, September 27-28, 1995, Portland, OR.
- Wells, S.A. and C. Berger. 1995. "Management of the Water Quality of the Upper and Lower Columbia Slough System". In *Proceedings First Annual Pacific Northwest Water Issues and 1995 Pacific Northwest/Oceania Conference*, Portland, OR.
- Wells, S. A., C. Berger, and M. Abrams. 1996. "Winter Storm Event Impacts on Dissolved Oxygen Levels in the Columbia Slough System". In *The Pacific Northwest Floods of February 6-11, 1996, Proceedings of the Pacific Northwest Water Issues Conference*, ed. by A. Laenen, American Institute of Hydrology, pp.107-126.
- Wells, S.A. and C. Berger. 1998. "Water Quality Impacts of Urban Stormwater Runoff from the Portland International Airport on the Columbia Slough". In *Proceedings Gdanska Fundacja Wody, Podczyszczenie Wod Opadowych Wymagania Formalnoprawne I Mozliwosci Techniczne*, [in Polish], Gdansk, Poland.
- Wells, S.A. and T.M. Cole. 2002. "TMDLS: Statistical Correlations or Mechanistic Modeling?". In *Proceedings National TMDL Science and Policy Conference*, Phoenix, AR, November 13-16, 2002.

CE-QUAL-W2 BIBLIOGRAPHY

- Wells, S.A. and R. Annear. 2002. "River Basin Modeling Using CE-QUAL-W2 V3: The Bull Run River-Reservoir System Model". In *4th International Conference on Reservoir Limnology and Water Quality*, Ceshe Budejovice, Czech Republic, August 12-16, 2002.
- Wood, T.M. and Rounds, S.A. 1998. "Using CE-QUAL-W2 to Assess the Effect of Reduced Phosphorus Loads on Chlorophyll-a and Dissolved Oxygen in the Tualatin River, Oregon". In *Proceedings of the First Federal Interagency Hydrologic Modeling Conference*, Las Vegas, Nevada, April 19-23, 1998: U.S. Geological Survey, p. 2-149 - 2-156. http://smig.usgs.gov/SMIG/features_0398/phos_tual.html
- Rounds, S.A. and Wood, T.M. 1998. "Using CE-QUAL-W2 to Assess the Ammonia Assimilative Capacity of the Tualatin River, Oregon". In *Proceedings of the First Federal Interagency Hydrologic Modeling Conference*, Las Vegas, Nevada, April 19-23, 1998: U.S. Geological Survey, p. 2-133 - 2-140. http://smig.usgs.gov/SMIG/features_0398/ammonia_tual.html
- Yager, R.E. B.R. Hayes, and M.J. Sale. 1995. "Modeling of Reservoir Release Temperature for Protecting Downstream Fish Habitat". In *Lake and Reservoir Management V9 No. 2, NALMS 14th Annual International Symposium*, Orlando, FL.
- Young, W.S., B.R. Schachte, and J.D. Bales. 1996. "Customized Software for Model Calibration and Visualization of Reservoir Water-Quality Model Results". In *Babcock, C.A., ed., Proceedings 1996 USGS National Computer Technology Meeting*.

Reports and Miscellaneous Articles

- Adams, R. W., Thackston, E. L., Speece, R. E., Wilson, D. J., and Cardozo, R. 1993. "Effect of Nashville's Combined Sewer Overflows on the Water Quality of the Cumberland River", *Technical Rpt. No. 42*, Environmental and Water Resources Engineering, Vanderbilt University, Nashville, TN.
- Bales, J.D., K.M. Sarver, and M.J. Giorgino. 2001. "Mountain Island Lake, North Carolina: Analysis of Ambient Conditions and Simulation of Hydrodynamics, Constituent Transport, and Water-Quality Characteristics, 1996-97". *U.S. Geological Survey Water-Resources Investigations Report 01-4138*.
- Bales, J.D., and J.C. Robbins. 1999. "A Water-Quality Modeling Framework for the Neuse River Estuary, North Carolina". *U.S. Geological Survey Water-Resources Investigations Report 99-4017*, 35 p.
- Bales, J.D., and M.J. Giorgino. 1998. "Lake Hickory, North Carolina: Analysis of Ambient Conditions and Simulation of Hydrodynamics, Constituent Transport, and Water-Quality Characteristics, 1993-94". *U.S. Geological Survey Water-Resources Investigations Report 98-4189*, 62 p.
- Barnese, Lisa E., Neichter, Patrick L., and Bohanon, Joseph A. 1993. "Evaluation of Water Quality in Caesar Creek Lake, Ohio using the CE-QUAL-W2 Water Quality Model", U.S. Army Corps of Engineers, Louisville, KY.

CE-QUAL-W2 BIBLIOGRAPHY

- Bartholow, J. 1998. "Animation of 'Age of Water' in Shasta Lake for 1995". <http://www.fort.usgs.gov/>.
- Buchak, E. M. and J. E. Edinger. 1982. "Hydrothermal Simulation of Quabbin Reservoir Using Longitudinal-Vertical Hydrodynamics", Final Report, prepared for Wallace, Floyd Associates, Inc., Cambridge, MA.
- _____. 1982. "Hydrothermal Simulations of Pool 3, Monongahela River Using Longitudinal-Vertical Numerical Hydrodynamics", prepared for Energy & Environmental Management, Inc., Murrysville, PA 15668-1809. Prepared by J. E. Edinger Associates, Inc., Wayne, Pennsylvania 19087-3226.
- _____. 1982. "User Guide for CE-QUAL-ELV2: A Longitudinal-Vertical, Time-Varying Estuarine Water Quality Model", *Instruction Rpt. EL-82-1*, U.S. Army Engineer Waterways Experiment Station, Vicksburg, MS.
- _____. 1982. "User Guide for LARM2: A longitudinal-Vertical, Time-Varying Hydrodynamic Reservoir Model", *Instruction Rpt. E-82-3*, U.S. Army Engineer Waterways Experiment Station, Vicksburg, MS.
- _____. 1985. "Simulation of Cooling Operations at Oak Knoll Reservoir, Phase II of Cooling Reservoir Modeling Program", *Document No. 85-41-R*, prepared for Environmental Department, Texas Utilities Generating Company, Dallas, Texas 75201 by J. E. Edinger Associates, Inc., Wayne, PA.
- _____. 1988. "Hydrothermal Analysis of Jersey Central Power and Light Sayreville and Werner Generating Stations", *Document No. 88-103-R/L*, prepared for EA Engineering, Science, and Technology, Inc., Hunt Valley/Loveton Center, Sparks, Maryland by J. E. Edinger Associates, Inc., Wayne, PA.
- Buchak, E. M., J. E. Edinger, and N. C. Huang. 1989. "Hydrothermal Analysis of Public Service Electric and Gas Linden and Sewaren Generating Stations", *Document No. 89-79-R*, prepared for EA Engineering, Science, and Technology, Inc., Hunt Valley/Loveton Center, Sparks, Maryland by J. E. Edinger Associates, Inc., Wayne, PA.
- _____. 1990. "Stationary State Dilution Studies of Lake Sinclair and Plant Harlee Branch", *Document No. 90-068-R*, prepared for Georgia Power Company Environmental Affairs, Atlanta, Georgia 30302. Prepared by J. E. Edinger Associates, Inc., Wayne, PA.
- Cole, T. M. 1982. "Application of the LARM Two-Dimensional Computer Model to Canyon Reservoir", M.S. Thesis, Southwest Texas State University, San Marcos, TX.
- Cole, T.M. and D.H. Tillman. 2001. "Water Quality Modeling of Allatoona and West Point Reservoirs Using CE-QUAL-W2". ERDC/EL SR-01-3, U.S. Army Engineer Research and Development Center, Vicksburg, MS.
- Crain, A. S., A. A. Shipp, T. Mesko, and G. L. Jarrett. 1999. Modeling Hydrodynamics and Water Quality in Herrington Lake, Kentucky. U.S. Geological Survey, *Water-Resources Investigations Report, 99-4281*. pp. 84.

CE-QUAL-W2 BIBLIOGRAPHY

- EA Engineering, Science, and Technology, Inc. 1987. "Perryman Site Cooling Water Alternatives Study", *Rpt. No. BSC43D*, prepared for Baltimore Gas and Electric Company, Baltimore, MD.
- EA Engineering, Science, and Technology, Inc. 1993. "Lake Intrusion Modeling Study of the Black River", prepared for USS/KOBE, Loraine, OH.
- EA Engineering, Science, and Technology, Inc. 1994. "Shellfish Harvesting Exclusion Zone for the proposed Tolchester Outfall", prepared for McCrone, Inc., Annapolis, MD.
- _____. 1993. "Comparison of the Lake Sinclair GLVHT Model Predictions with Current Meter Measurements", *EA Project No. 11987.01*, prepared for Georgia Power Company.
- Edinger, J. E. and E. M. Buchak. 1978. "Hydrodynamics and Transport of Chlorine in Panther Branch Arm, Squaw Creek Reservoir for Comanche Peak S. E. S., Development Document", prepared for Texas Utilities Services, Inc., Dallas, TX.
- _____. 1981. "Estuarine Laterally Averaged Numerical Dynamics: The Development and Testing of Estuarine Boundary conditions in the LARM Code", *Miscellaneous Paper EL-81-9*, U.S. Army Engineer Waterways Experiment Station, CE, Vicksburg, MS.
- _____. 1982. "Analysis and Development of Carbonate-Bicarbonate Chemical Subroutine", Phase II, Development, Verification, and Use of Methods to Model Chemical and Thermal Processes for Lakes Mead and Powell. *Contract No. 2-07-DV-00131*, United States Department of the Interior, Bureau of Reclamation, Denver, CO.
- _____. 1983. "Developments in LARM2: A Longitudinal-Vertical, Time-Varying Hydrodynamic Reservoir Model", *Technical Rpt. E-83-1*, U.S. Army Engineer Waterways Experiment Station, Vicksburg, MS.
- _____. 1987. "Summary of Plant Hammond Coosa River - Weiss Reservoir Hydrothermal Analysis and Compliance Temperatures Reporting Procedures", *Document No. 87-119-R*, prepared for Georgia Power Company by J. E. Edinger Associates, Inc., Wayne, PA.
- _____. 1989. "Probabilistic Hydrothermal Modeling Study of Clinton Lake, Exhibit D", *Document No. 89-15-R*, prepared for Illinois Power Company, Decatur, IL 62525. Prepared by J. E. Edinger Associates, Inc., Wayne, PA.
- _____. 1993. "Harlee Branch Impact on Dissolved Oxygen of Lake Sinclair", *Document No. January 18*, prepared for Georgia Power Company Environmental Affairs, Atlanta, Georgia. Prepared by J. E. Edinger Associates, Inc., Wayne, PA.
- Edinger, J. E., E. M. Buchak, J. Loos, and E. Krueger. 1986. "Effects of the Chalk Point Steam Electric Station on BOD and DO in the Patuxent Estuary", *Document No. 86-56-R*, Potomac Electric Power Company, Environmental Affairs Group, Water and Land Use Department, Washington, DC 20068, prepared by J. E. Edinger Associates, Inc., Wayne, PA.

CE-QUAL-W2 BIBLIOGRAPHY

- Edinger, J.E., E.M. Buchak, and N.C. Huang. 1988. "Chalk Point Steam Electric Station Patuxent Estuary Hydrodynamic and Transport Model Verification and Real Time Intake Entrainment Rates for 1985 Larval Sampling", *Document No. 88-77-R*, prepared for Potomac Electric Power Company, Environmental Affairs Group, Water and Land Use Department, Washington, D.C. 20068. Prepared by J. E. Edinger Associates, Inc., Wayne, PA.
- _____. 1989. "Verification of Nechako Reservoir Hydrothermal Model", *Document No. 89-130-R*, prepared for Triton Environmental Consultants, Ltd., Burnaby, British Columbia V5M 3Z3. Prepared by J. E. Edinger Associates, Inc., Wayne, PA.
- Edward K. Noda and Associates, Inc. 1992. "Ala Wai Canal Improvement, Feasibility Report", prepared for Hawaii Department of Land and Natural Resources, Division of Water and Land Development.
- Energy & Environmental Management, Inc. 1990. "Gorge Power Station Load Management Project", prepared for Ohio Edison Company, Ohio.
- Envirocon Pacific Limited and J. E. Edinger Associates, Inc. 1989. "Nechako Reservoir Mathematical Modeling Program Preliminary Results and Conclusions", prepared for Alcan Smelters & Chemicals Ltd., Vancouver, British Columbia.
- Environmental Consulting & Technology, Inc. 1999. "Thermal Modeling Report: Fort Myers Power Plant Repowering Project". ECT No. 98615-0100. Prepared for Florida Power & Light Company, Juno Beach, FL.
- Environmental Consulting & Technology, Inc. 1999. "Thermal Impact Study for S-79 Lock Operation: Fort Myers Power Plant Repowering Project". ECT No. 98615-0100. Prepared for Florida Power & Light Company, Juno Beach, FL.
- Environmental Consulting & Technology, Inc. 1999. "Manatee Protection Modeling Report: Fort Myers Power Plant Repowering Project". ECT No. 98615-0100. Prepared for Florida Power & Light Company, Juno Beach, FL.
- Environmental and Hydraulics Laboratory. 1986. "CE-QUAL-W2: A Numerical Two-Dimensional, Laterally Averaged Model of Hydrodynamics and Water Quality; User's Manual", *Instruction Rpt. E-86-5*. U.S. Army Engineer Waterways Experiment Station, Vicksburg, MS.
- EPA. 1994. "Alaska Juneau Gold Mine Project", Technical Assistance Report for the U.S. Army Corps of Engineers Alaska District, EPA 910/B-94-007.
- FERC. 1992. "Proposed Modifications to the Lower Mokelumne River Project, California", Draft Environmental Impact Statement, Federal Energy Regulatory Commission Office of Hydropower Licensing, FERC Project No. 2916-004.
- Flowers, J.D., L.M. Hauch, and R.L. Kiesling. 2001. "Water Quality Modeling of Lake Waco Using CE-QUAL-W2 for Assessment of Phosphorus Control Strategies". *TR0114*, Texas Institute for Applied Environmental Research, Tarleton State University, Stephenville, Texas.

CE-QUAL-W2 BIBLIOGRAPHY

- FTN Associates. 2001. "Center Hill Lake CE-QUAL-W2 Water Quality Model". Prepared for U.S. Army Corps of Engineers, Nashville District, Contract DACW 62-98-D-0002, Delivery Order No. 0011.
- FTN Associates. 1998. "Taylorsville Lake Water Quality Model Study". Prepared for U.S. Army Corps of Engineers, Louisville District, Louisville, KY.
- Georgia Power Company. 1992. "Hydrological and Limnological Study of Lake Sinclair in Support of Application for Renewal and Modification of a Thermal Variance for Plant Branch NPDES Permit No. GA00026051)", prepared for Georgia Power Company, Atlanta, Georgia by EA Engineering Science and Technology, Atlanta, Georgia and J. E. Edinger Associates, Inc., Wayne, PA.
- Giorgino, M.J., J.D. and Bales. 1997. "Rhodhiss Lake, North Carolina: Analysis of Ambient Conditions and Simulation of Hydrodynamics, Constituent Transport, and Water-Quality Characteristics, 1993-94". *U.S. Geological Survey Water-Resources Investigations Report 97-4131*, 62 p.
- Gorgens, A.H.M, A.J. Bath, A. Venter, K. De Smidt, G.v.R. Marais. 1993. "The Applicability of Hydrodynamic Reservoir Models for Water Quality Management of Stratified Water Bodies in South Africa", Report to the Water Research Commission, WRC Report No. 304/1/93.
- Green, W.R. 2001. "Analysis of Ambient Conditions and Simulation of Hydrodynamics, Constituent Transport, and Water-Quality Characteristics in Lake Maumelle, Arkansas, 1991-92. *USGS Water-Resources Investigations Report 01-4045*.
- Hall, R. W. 1987. "Application of CE-QUAL-W2 to the Savannah River Estuary", *Technical Rpt. EL-87-4*, U.S. Army Engineer Waterways Experiment Station, Vicksburg, MS.
- Jain, R., G. A. Krallis and E. M. Buchak. 2000. "Sammamish River Temperature Study: 1998 and 1999 CE-QUAL-W2 Calibration and Management Scenarios". Prepared for Seattle District, Corps of Engineers, Seattle, Washington. Prepared by J. E. Edinger Associates, Inc., Wayne, Pennsylvania. 15 September.
- Johnson, B. H. 1981. "A Review of Numerical Reservoir Hydrodynamic Modeling", *Technical Rpt. E-81-2*, U.S. Army Engineer Waterways Experiment Station, Vicksburg, MS.
- Johnson, B. H., M. J. Trawle and P. G. Kee. 1989. "A Numerical Model Study of the Effect of Channel Deepening on Shoaling and Salinity Intrusion in the Savannah Estuary", *Technical Rpt. HL-89-26*, Hydraulics Laboratory, Department of the Army, Waterways Experiment Station, Vicksburg, MS.
- Kinhill Cameron McNamara Pty Ltd. 1991. Proposed Third Runway Sydney Kingsford-Smith. Airport, Botany Bay Borrow Pit, Water Quality", Milton Queensland, Australia.
- Martin, J. L. 1988. "Application of a Two-Dimensional Model of Hydrodynamics and Water Quality CE-QUAL-W2. to DeGray Lake, Arkansas", *Technical Rpt. E-87-1*, U.S. Army Engineer Waterways Experiment Station, Vicksburg, MS.

CE-QUAL-W2 BIBLIOGRAPHY

- McKee, C. P., Thackston, E. L., Speece, R. E., Wilson, D. J., Cardozo, R. J. 1992. "Modeling of Water Quality in Cheatham Lake", *Technical Rpt. No. 42*, Environmental and Water Resources Engineering, Vanderbilt University, Nashville, TN.
- Mobley, M.H., D. McGinnis, and R.J. Ruane. 1999. "Conceptual Design Report for the Shepaug Oxygen Diffuser System". Tennessee Valley Authority report WR99-1-760-128.
- Ormsbee, L., L. Jarrett, and B. Perkins. 1998. Kentucky River Basin Water Quality Assessment Study. *Kentucky Water Resources Institute (KWRI) Technical Report*. pp. 110.
- Owoputi, L. 1998. "Water Quality Model Development for Stonewall Jackson Lake and the West Fork River". Prepared for USACE Pittsburg District, Contract No. DACW59-96-D-0005, Delivery Order No. 6.
- Risley, J.C. 2000. "Effects of Hypothetical Management Scenarios on Water Temperatures in the Tualatin River, Oregon", U.S. Geological Survey Water-Resources Investigations Report 00-4071 (supplement to Water-Resources Investigations Report 97-4071), 110 p. http://oregon.usgs.gov/pubs_dir/Online/Pdf/00-4071.pdf
- Risley, J.C. 1997. Relations of Tualatin River Water Temperatures to Natural and Human-Caused Factors: U.S. Geological Survey Water-Resources Investigations Report 97-4071, 143 p. http://oregon.usgs.gov/pubs_dir/Online/Pdf/97-4071.pdf
- Rounds, S.A. and T.M. Wood. 2001. "Modeling Water Quality in the Tualatin River, Oregon, 1991-1997". USGS Water Resources Investigations Report 01-4041.
- Rounds, S.A., T.M. Wood, and D.D. Lynch. 1998. "Modeling Discharge, Temperature, and Water Quality in the Tualatin River, Oregon". USGS Open-File Report 98-186.
- Tetra Tech. 2002. "Pineview Reservoir TMDL". Prepared for Utah Department of Environmental Quality.
- Tillman, D. H., and Cole, T. M. 1993. "Bluestone Phase 2 Temperature and Dissolved Oxygen Modeling Study", *Technical Rpt. EL-93-*, U.S. Army Engineer Waterways Experiment Station, Vicksburg, MS.
- Tillman, D.H., T.M. Cole, and B.W. Bunch. 1999. "Detailed Reservoir Water Quality Modeling (CE-QUAL-W2), Alabama-Coosa-Tallapoosa/Apalachicola-Chattahoochee-Flint (ACT-ACF) Comprehensive Water Resource Study". Technical Report EL-99-XXX, U.S. Army Engineer Waterways Experiment Station, Vicksburg, MS.
- URS Corporation. 1986. "Southern Puget Sound Water Quality Assessment Study, Final Report, Comprehensive Circulation and Water Quality Study of Budd Inlet", prepared for Washington State Department of Ecology. By URS Corporation, Seattle, WA.
- Waide, J. B., Dortch, M. S., and Cole, T. M., 1984. "Two-Dimensional Reservoir Model", *EWQOS Information Exchange Bulletin, Vol. E-84-3*, U.S. Army Engineer Waterways Experiment Station, Vicksburg, MS.

CE-QUAL-W2 BIBLIOGRAPHY

- Wells, S. A. 1992. "Assessment of Management Alternatives for Water Quality Improvement in the Columbia Slough System, Volume 1: Technical Report", *Technical Rpt. EWR-001-92*, Department of Civil Engineering, Portland State University, Portland, OR.
- _____. 1992. "User Manual for the Columbia Slough Model using CE-QUAL-W2", *Technical Rpt. EWR-003-92*, Department of Civil Engineering, Portland State University, Portland, OR.
- Wells, S. A., Berger, C., and Knutson, M. 1992. "Modeling the Tualatin River System Including Scoggins Creek and Hagg Lake: Model Description, Geometry, and Forcing Data", *Technical Rpt. EWR-010-92*, Department of Civil Engineering, Portland State University, Portland, OR.
- Wells, S.A. and T.M. Cole. 2000. "Theoretical Basis for the CE-QUAL-W2 River Basin Model." ERDC/EL TR-00-7, U.S. Army Engineer Research and Development Center, Vicksburg, MS.
- Yager, R.E. 1996. "Application of CE-QUAL-W2 to Lake Cumberland". Report prepared by Environmental Consulting Engineers for U.S. Army Corps of Engineers, Nashville District, Nashville, Tennessee.

Appendix A Hydrodynamics and Transport

CE-QUAL-W2 uses the laterally averaged equations of fluid motion derived from the three dimensional equations, which consist of six equations and six unknowns. Their development is described below.

Coordinate System

The general coordinate system used in the development of the laterally averaged equations of fluid motion is shown in [Figure A-1](#).

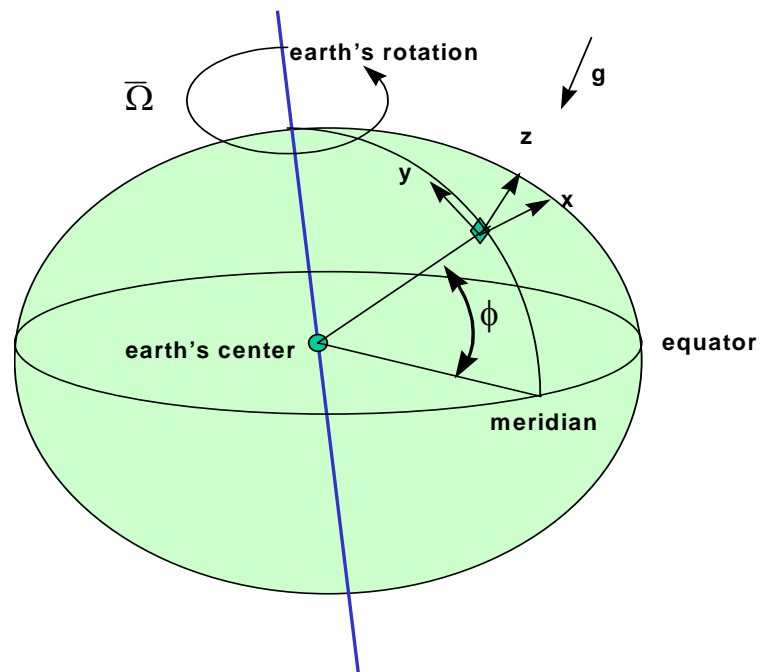


Figure A-1. Definition sketch of coordinate system for governing equations where x is oriented east, y is oriented north, and z is oriented upward.

Note that Ω is a vector that represents the angular velocity of the earth spinning on its axis. The rotation of the coordinate system can result in significant horizontal accelerations of fluids. This is usually restricted to large water bodies such as large lakes and ocean systems. The force that causes horizontal accelerations because of the spinning coordinate system is termed the Coriolis force.

Turbulent Time-Averaged Equations

The governing equations are obtained by performing a mass and a momentum balance of the fluid phase about a control volume. The resulting equations are the continuity (or conservation of fluid mass) and the conservation of momentum equations for a rotating coordinate system (Batchelor, 1967; Sabersky et al., 1989; Cushman-Roisin, 1994). After using the coordinate system in [Figure A-1](#), applying the following assumptions:

1. incompressible fluid
2. centripetal acceleration is a minor correction to gravity
3. Boussinesq approximation
4. $\frac{1}{\rho} = \frac{1}{\rho_o + \Delta\rho} \approx \frac{1}{\rho_o}$ where $\rho = \rho_o + \Delta\rho$; ρ_o is a base value
and $\Delta\rho$ has all variations in ρ

and substituting the turbulent time averages of velocity and pressure as defined below:

all velocities and pressure are considered the sum of turbulent time averages and deviations from that average, i.e., $u = \bar{u} + u'$, where $\bar{u} = \frac{1}{T} \int_t^{t+T} u dt$ as shown in [Figure A-2](#). The other terms are $v = \bar{v} + v'$; $w = \bar{w} + w'$ and $p = \bar{p} + p'$ where the overbar represents time averaged and the prime represents deviation from the temporal average;

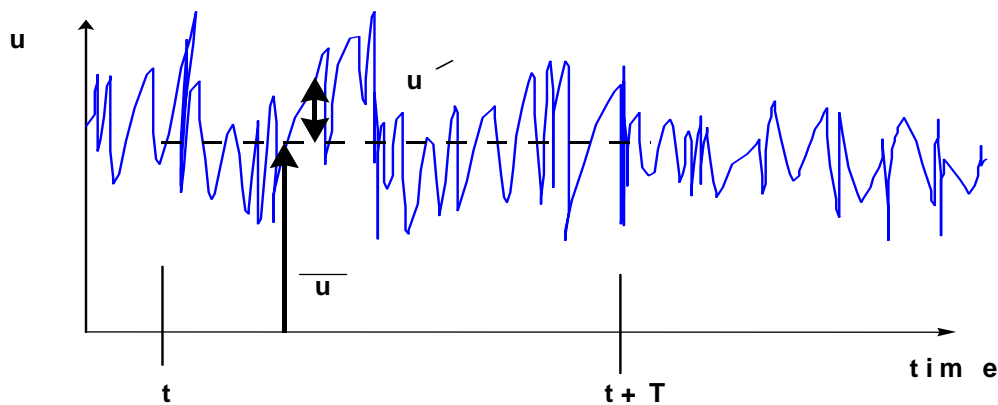


Figure A-2. Definition sketch of turbulent time averaging for velocity.

The governing equations become after simplification:

Continuity

$$\frac{\partial \bar{u}}{\partial x} + \frac{\partial \bar{v}}{\partial y} + \frac{\partial \bar{w}}{\partial z} = 0 \quad (\text{A-1})$$

where:

- u = x-direction velocity
- v = y-direction velocity
- w = z-direction velocity

x-Momentum Equation

$$\underbrace{\frac{\partial \bar{u}}{\partial t}}_{\text{unsteady acceleration}} + \underbrace{\bar{u} \frac{\partial \bar{u}}{\partial x} + \bar{v} \frac{\partial \bar{u}}{\partial y} + \bar{w} \frac{\partial \bar{u}}{\partial z}}_{\text{convective acceleration}} - \underbrace{2\Omega_z \bar{v} + 2\Omega_y \bar{w}}_{\text{Coriolis acceleration}} = - \underbrace{\frac{1}{\rho} \frac{\partial \bar{p}}{\partial x}}_{\text{pressure gradient}} + \underbrace{\frac{\mu}{\rho} \left(\frac{\partial^2 \bar{u}}{\partial x^2} + \frac{\partial^2 \bar{u}}{\partial y^2} + \frac{\partial^2 \bar{u}}{\partial z^2} \right)}_{\text{viscous stresses}} + \underbrace{\frac{1}{\rho} \left(\frac{\partial \tau_{xx}}{\partial x} + \frac{\partial \tau_{xy}}{\partial y} + \frac{\partial \tau_{xz}}{\partial z} \right)}_{\text{turbulent stresses}} \quad (\text{A-2})$$

where:

- τ_{xx} = turbulent shear stress acting in x direction on the x-face of control volume
- τ_{xy} = turbulent shear stress acting in x direction on the y-face of control volume
- τ_{xz} = turbulent shear stress acting in x direction on the z-face of control volume
- μ = dynamic viscosity
- Ω = component of Coriolis acceleration where:
 - $\Omega_z = \Omega_E \sin \phi$
 - $\Omega_y = \Omega_E \cos \phi$
 - ϕ = latitude
 - Ω_E = earth's rotation rate

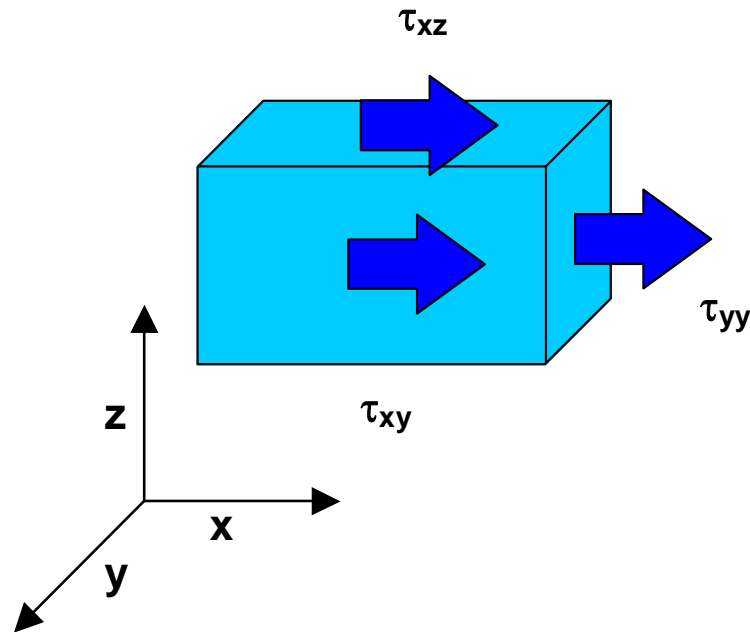


Figure A-3. Definition sketch of turbulent shear stresses in x-direction.

y-Momentum Equation

$$\begin{aligned} \frac{\partial \bar{v}}{\partial t} + \bar{u} \frac{\partial \bar{v}}{\partial x} + \bar{v} \frac{\partial \bar{v}}{\partial y} + \bar{w} \frac{\partial \bar{v}}{\partial z} + 2\Omega_z \bar{u} - 2\Omega_x \bar{w} = \\ -\frac{1}{\rho} \frac{\partial \bar{p}}{\partial y} + \frac{\mu}{\rho} \left(\frac{\partial^2 \bar{v}}{\partial x^2} + \frac{\partial^2 \bar{v}}{\partial y^2} + \frac{\partial^2 \bar{v}}{\partial z^2} \right) + \frac{1}{\rho} \left(\frac{\partial \tau_{yx}}{\partial x} + \frac{\partial \tau_{yy}}{\partial y} + \frac{\partial \tau_{yz}}{\partial z} \right) \end{aligned} \quad (\text{A-3})$$

where:

τ_{yx} = turbulent shear stress acting in y direction on the x-face of control volume

τ_{yy} = turbulent shear stress acting in y direction on the y-face of control volume

τ_{yz} = turbulent shear stress acting in y direction on the z-face of control volume

$\Omega_x = 0$

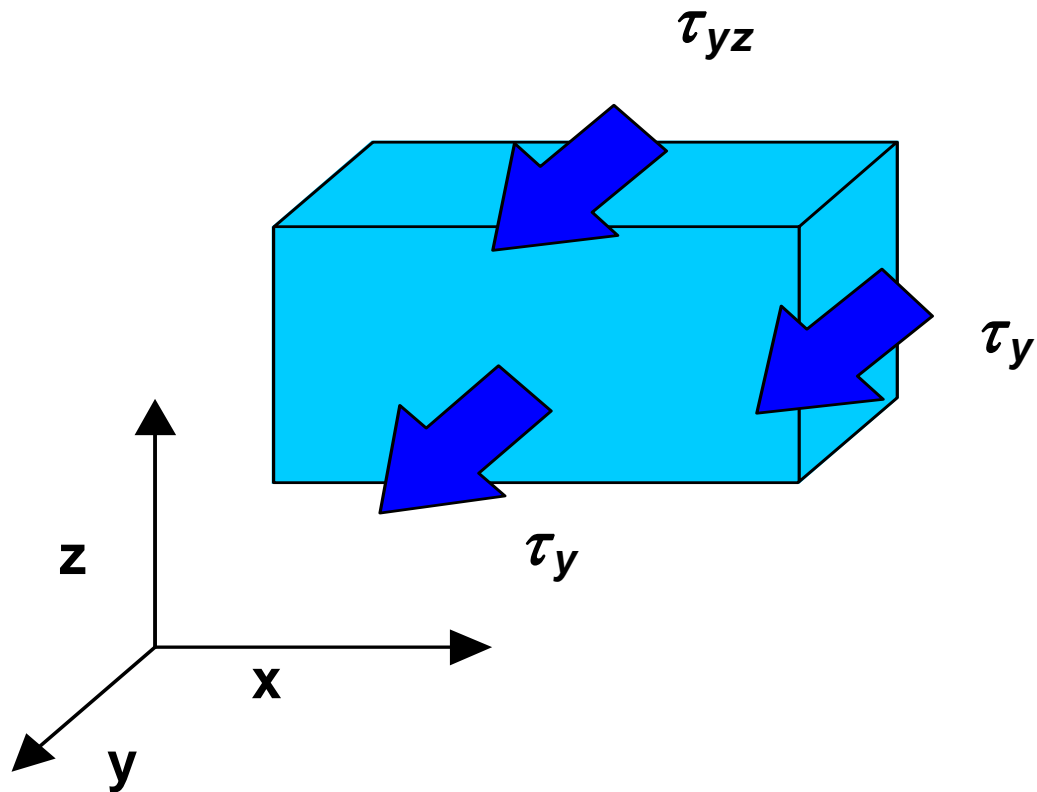


Figure A-4. Sketch of turbulent shear stresses in y-direction.

z-Momentum Equation

$$\frac{\partial \bar{w}}{\partial t} + \bar{u} \frac{\partial \bar{w}}{\partial x} + \bar{v} \frac{\partial \bar{w}}{\partial y} + \bar{w} \frac{\partial \bar{w}}{\partial z} - 2\Omega_y \bar{u} + 2\Omega_x \bar{v} = -g \tag{A-4}$$

$$- \frac{1}{\rho} \frac{\partial \bar{p}}{\partial z} + \frac{\mu}{\rho} \left(\frac{\partial^2 \bar{w}}{\partial x^2} + \frac{\partial^2 \bar{w}}{\partial y^2} + \frac{\partial^2 \bar{w}}{\partial z^2} \right) + \frac{1}{\rho} \left(\frac{\partial \tau_{zx}}{\partial x} + \frac{\partial \tau_{zy}}{\partial y} + \frac{\partial \tau_{zz}}{\partial z} \right)$$

where:

- τ_{zx} = turbulent shear stress acting in z direction on the x-face of control volume
- τ_{zy} = turbulent shear stress acting in z direction on the y-face of control volume
- τ_{zz} = turbulent shear stress acting in z direction on the z-face of control volume
- $\Omega_x = 0$

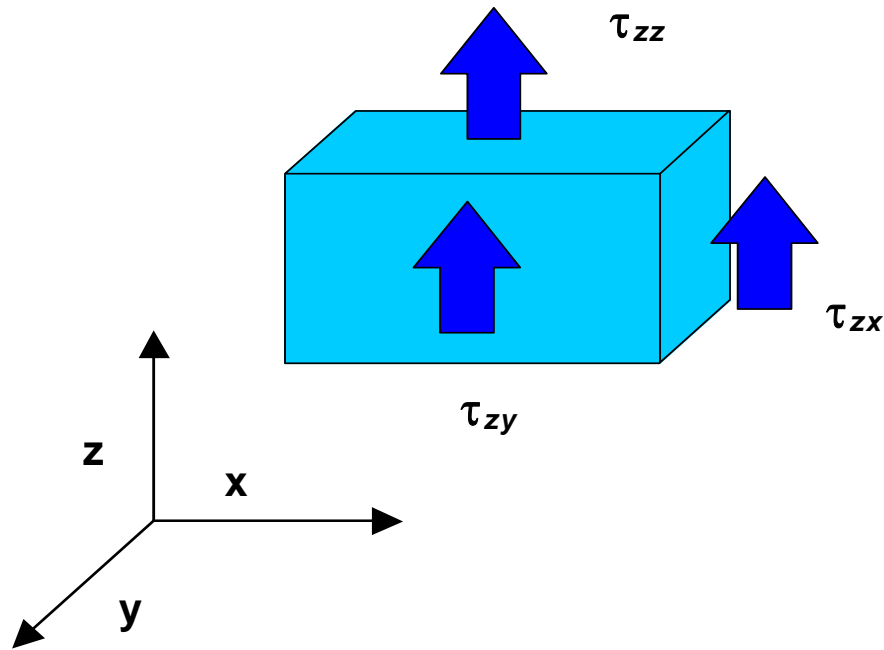


Figure A-5. Sketch of turbulent shear stresses in z-direction.

Note that the turbulent shear stresses are defined as follows:

$$\begin{aligned} \tau_{xx} &= \rho \overline{u'u'} \\ \tau_{xy} &= \rho \overline{u'v'} \text{ is the same as } \tau_{yx} = \rho \overline{v'u'} \\ \tau_{xz} &= \rho \overline{u'w'} \text{ is the same as } \tau_{zx} = \rho \overline{w'u'} \\ \tau_{yy} &= \rho \overline{v'v'} \\ \tau_{yz} &= \rho \overline{v'w'} \text{ is the same as } \tau_{zy} = \rho \overline{w'v'} \\ \tau_{zz} &= \rho \overline{w'w'} \end{aligned}$$

Coriolis Effect

As noted above, all the Ω_x terms are zero and can be eliminated from the y and z-momentum equations. If one integrates over the y-direction (therefore assuming the net velocity in y is zero) and assumes that the horizontal length scale is much greater than vertical length scale, it can be shown by using scaling arguments that the Coriolis acceleration forces are negligible (Cushman-Roisin, 1994). Hence, prior to lateral averaging, the Coriolis acceleration terms will be neglected.

Adjusting the Coordinate System

The coordinate system is transformed into a form compatible with the original W2 development where the vertical axis is in the direction of gravity. In addition, as shown in [Figure A-6](#), the coordinate system is oriented along an arbitrary slope.

Coordinate System

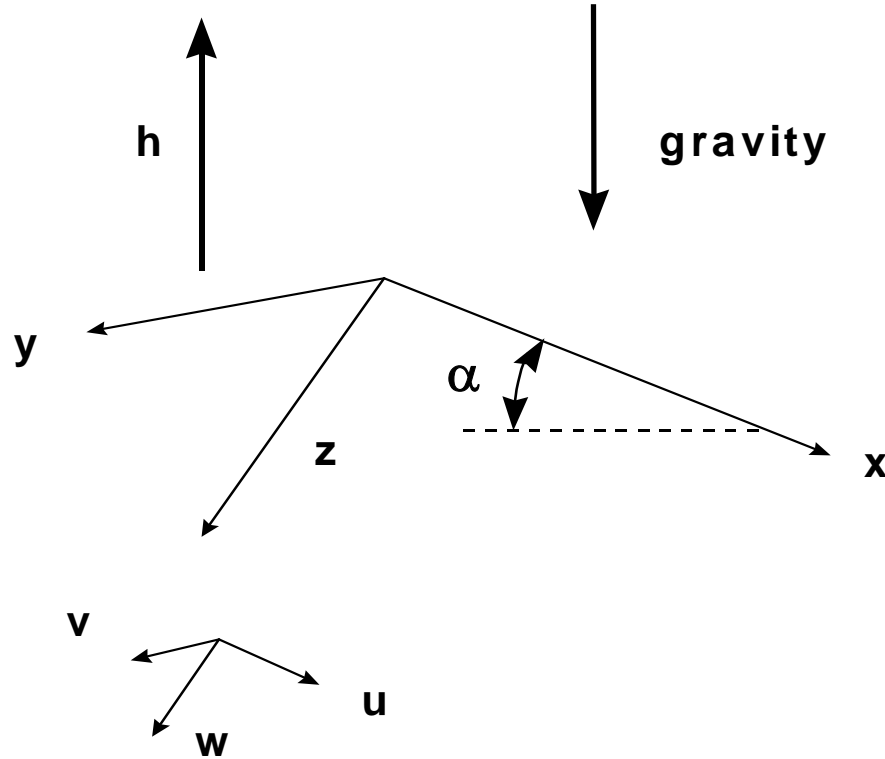


Figure A-6. General coordinate system with z-axis compatible with original derivation of W2 model.

The gravity acceleration is a body force that is then represented by a vector:

$$\vec{g} = -g\vec{\nabla}h \tag{A-5}$$

where:

- h = surface normal from the earth's surface
- g = gravitational acceleration, 9.8 m s^{-2} .

This term can be written as three vector components:

$$g_x = -g \frac{\partial h}{\partial x} \quad (\text{A-6})$$

$$g_y = -g \frac{\partial h}{\partial y} \quad (\text{A-7})$$

$$g_z = -g \frac{\partial h}{\partial z} \quad (\text{A-8})$$

These gravity components can be applied to an arbitrary channel slope as shown in [Figure A-7](#).

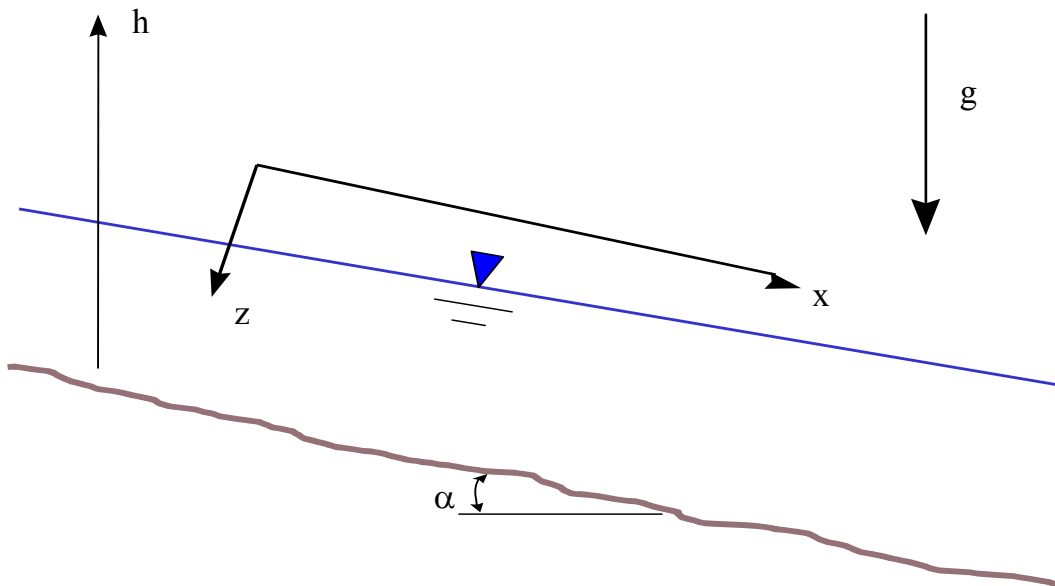


Figure A-7. Sketch of channel slope and coordinate system for W2 where the x-axis is oriented along the channel slope.

The channel slope can also be incorporated into the definition of the gravity vector if the x-axis is chosen parallel to the channel slope as:

The channel slope is defined as:

$$S_o = \tan \alpha \quad (\text{A-9})$$

and also:

$$g_x = -g \frac{\partial h}{\partial x} = g \sin \alpha \quad (\text{A-10})$$

$$g_z = -g \frac{\partial h}{\partial z} = g \cos \alpha \quad (\text{A-11})$$

The gravity acceleration in y is assumed negligible since $\frac{\partial h}{\partial y} = 0$ in the lateral direction of the channel.

Governing Equations for General Coordinate System

After redefining the coordinate system, eliminating Coriolis effects, and neglecting viscous shear stresses the governing equations become:

Continuity

$$\frac{\partial \bar{u}}{\partial x} + \frac{\partial \bar{v}}{\partial y} + \frac{\partial \bar{w}}{\partial z} = 0 \quad (\text{A-12})$$

x-Momentum Equation

$$\underbrace{\frac{\partial \bar{u}}{\partial t}}_{\text{unsteady acceleration}} + \underbrace{\bar{u} \frac{\partial \bar{u}}{\partial x} + \bar{v} \frac{\partial \bar{u}}{\partial y} + \bar{w} \frac{\partial \bar{u}}{\partial z}}_{\text{convective acceleration}} = \underbrace{g \sin \alpha}_{\text{gravity}} - \underbrace{\frac{1}{\rho} \frac{\partial \bar{p}}{\partial x}}_{\text{pressure gradient}} + \underbrace{\frac{1}{\rho} \left(\frac{\partial \tau_{xx}}{\partial x} + \frac{\partial \tau_{xy}}{\partial y} + \frac{\partial \tau_{xz}}{\partial z} \right)}_{\text{turbulent shear stresses}} \quad (\text{A-13})$$

y-Momentum Equation

$$\underbrace{\frac{\partial \bar{v}}{\partial t}}_{\text{unsteady acceleration}} + \underbrace{\bar{u} \frac{\partial \bar{v}}{\partial x} + \bar{v} \frac{\partial \bar{v}}{\partial y} + \bar{w} \frac{\partial \bar{v}}{\partial z}}_{\text{convective acceleration}} = - \underbrace{\frac{1}{\rho} \frac{\partial \bar{p}}{\partial y}}_{\text{pressure gradient}} + \underbrace{\frac{1}{\rho} \left(\frac{\partial \tau_{yx}}{\partial x} + \frac{\partial \tau_{yy}}{\partial y} + \frac{\partial \tau_{yz}}{\partial z} \right)}_{\text{turbulent shear stresses}} \quad (\text{A-14})$$

z-Momentum Equation

$$\underbrace{\frac{\partial \bar{w}}{\partial t}}_{\text{unsteady acceleration}} + \underbrace{\bar{u} \frac{\partial \bar{w}}{\partial x} + \bar{v} \frac{\partial \bar{w}}{\partial y} + \bar{w} \frac{\partial \bar{w}}{\partial z}}_{\text{convective acceleration}} = \underbrace{g \cos \alpha}_{\text{gravity}} - \underbrace{\frac{1}{\rho} \frac{\partial \bar{p}}{\partial z}}_{\text{pressure gradient}} + \underbrace{\frac{1}{\rho} \left(\frac{\partial \tau_{zx}}{\partial x} + \frac{\partial \tau_{zy}}{\partial y} + \frac{\partial \tau_{zz}}{\partial z} \right)}_{\text{turbulent shear stresses}} \quad (\text{A-15})$$

Simplification of z-Momentum Equation

If the longitudinal length scale is much greater than the vertical length scale, then this makes all vertical velocities \ll horizontal velocities. A result of this assumption is that vertical velocities are very small such that the z-momentum equation becomes the hydrostatic equation:

$$\frac{1}{\rho} \frac{\partial \bar{p}}{\partial z} = g \cos \alpha \quad (\text{A-16})$$

This assumption prevents the model from accurately modeling vertical accelerations of the fluid because of convective cooling at night and other such vertical accelerations.

Lateral Averaging

The governing equations above will be laterally averaged after decomposing all velocities and pressure into a lateral average and a deviation from the lateral average. The lateral, longitudinal, and vertical velocities and pressure are defined as follows:

$$\bar{v} = \bar{\bar{v}} + v'' \quad (\text{A-17})$$

$$\bar{u} = \bar{\bar{u}} + u'' \quad (\text{A-18})$$

$$\bar{w} = \bar{\bar{w}} + w'' \quad (\text{A-19})$$

$$\bar{p} = \bar{\bar{p}} + p'' \quad (\text{A-20})$$

where:

$$\bar{\bar{u}} = \frac{1}{B} \int_{y_1}^{y_2} \bar{u} dy$$

B = control volume width, *m*

*y*₁ = left bank coordinate

*y*₂ = right bank coordinate

The double overbars represent the spatial average of the temporal average quantity. The double prime represents the deviation from the lateral average and is a function of y . This is shown in [Figure A-8](#).

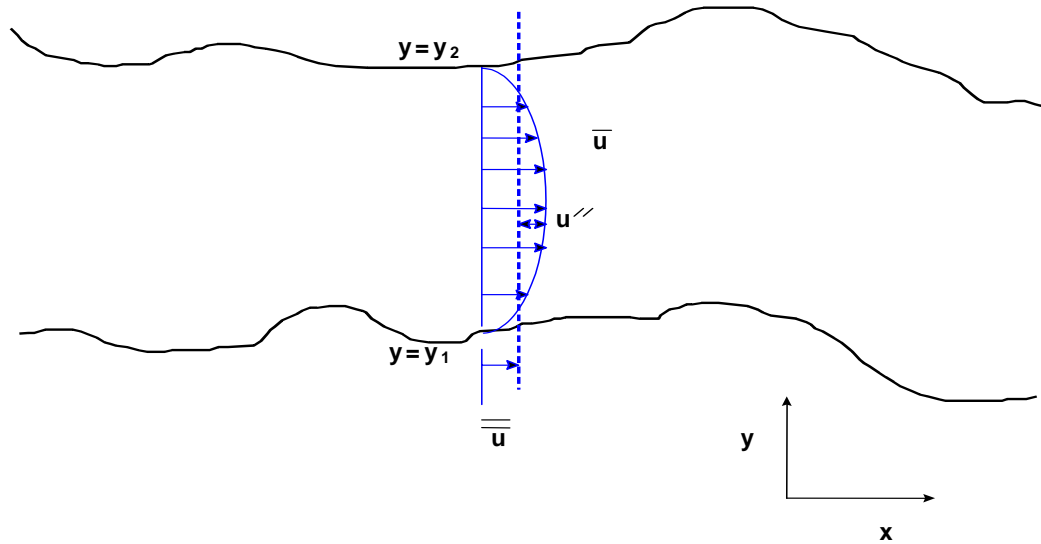


Figure A-8. Lateral average and deviation from lateral average components of longitudinal velocity.

These definitions are substituted into the turbulent time-average governing equations and then laterally averaged. The y -momentum equation is neglected since the average lateral velocities are zero ($\bar{v} = 0$) and cross shear stresses that contribute to vertical mixing will be computed from the analysis of wind stress. The equations that remain are the continuity, x -momentum, and z -momentum equations.

Continuity Equation

The continuity equation becomes after substituting the above velocity components and laterally averaging

$$\frac{\partial(\bar{\bar{u}} + u'')}{\partial x} + \frac{\partial(\bar{\bar{v}} + v'')}{\partial y} + \frac{\partial(\bar{\bar{w}} + w'')}{\partial z} = 0 \tag{A-21}$$

The lateral average of a double primed variable is by definition zero:

$$\bar{\bar{u}}'' = \frac{1}{B} \int_{y_1}^{y_2} u'' dy = 0 \tag{A-22}$$

Also, note that:

$$\begin{aligned}
 \frac{\partial(\bar{\bar{v}} + v'')}{\partial y} &= \frac{1}{B} \int_{y_1}^{y_2} \frac{\partial(\bar{\bar{v}} + v'')}{\partial y} dy \\
 &= \frac{(\bar{\bar{v}} + v'')}{B} \Big|_{y_1}^{y_2} \\
 &= \frac{v''}{B} \Big|_{y_1}^{y_2} \\
 &= q
 \end{aligned} \tag{A-23}$$

where q is defined as the net lateral inflow per unit volume of cell [T^{-1}], and:

$$\begin{aligned}
 \frac{\partial(\bar{\bar{u}} + u'')}{\partial x} &= \frac{1}{B} \int_{y_1}^{y_2} \frac{\partial(\bar{\bar{u}} + u'')}{\partial x} dy \\
 &= \frac{1}{B} \int_{y_1}^{y_2} \frac{\partial \bar{\bar{u}}}{\partial x} dy + \frac{1}{B} \int_{y_1}^{y_2} \frac{\partial u''}{\partial x} dy \\
 &= \frac{1}{B} \frac{\partial}{\partial x} \int_{y_1}^{y_2} \bar{\bar{u}} dy \\
 &= \frac{1}{B} \frac{\partial B \bar{\bar{u}}}{\partial x}
 \end{aligned} \tag{A-24}$$

and:

$$\begin{aligned}
 \frac{\partial(\bar{\bar{w}} + w'')}{\partial z} &= \frac{1}{B} \int_{y_1}^{y_2} \frac{\partial(\bar{\bar{w}} + w'')}{\partial z} dy \\
 &= \frac{1}{B} \int_{y_1}^{y_2} \frac{\partial \bar{\bar{w}}}{\partial z} dy + \frac{1}{B} \int_{y_1}^{y_2} \frac{\partial w''}{\partial z} dy \\
 &= \frac{1}{B} \frac{\partial}{\partial z} \int_{y_1}^{y_2} \bar{\bar{w}} dy \\
 &= \frac{1}{B} \frac{\partial B \bar{\bar{w}}}{\partial z}
 \end{aligned} \tag{A-25}$$

Combining terms, the continuity equation becomes:

$$\frac{\partial B \bar{\bar{u}}}{\partial x} + \frac{\partial B \bar{\bar{w}}}{\partial z} = qB \tag{A-26}$$

x-Momentum Equation

The laterally-averaged x-momentum equation is more easily simplified by writing it in conservative form (this can be verified by using the continuity equation with the x-momentum equation),

$$\begin{aligned} \frac{\partial(\bar{u} + u'')}{\partial t} + \frac{\partial(\bar{u} + u'')(\bar{u} + u'')}{\partial x} + \frac{\partial(\bar{v} + v'')(\bar{u} + u'')}{\partial y} + \frac{\partial(\bar{w} + w'')(\bar{u} + u'')}{\partial z} \\ = \overline{g \sin \alpha} - \frac{1}{\rho} \frac{\partial(\bar{p} + p'')}{\partial x} + \frac{1}{\rho} \left(\frac{\partial \tau_{xx}}{\partial x} + \frac{\partial \tau_{xy}}{\partial y} + \frac{\partial \tau_{xz}}{\partial z} \right) \end{aligned} \quad (\text{A-27})$$

Each term in this equation can be simplified as follows (note that the spatial average of any double primed variable goes to zero by definition).

The unsteady acceleration term:

$$\begin{aligned} \frac{\partial(\bar{u} + u'')}{\partial t} &= \frac{1}{B} \int_{y_1}^{y_2} \frac{\partial(\bar{u} + u'')}{\partial t} dy \\ &= \frac{1}{B} \int_{y_1}^{y_2} \frac{\partial \bar{u}}{\partial t} dy + \frac{1}{B} \int_{y_1}^{y_2} \frac{\partial u''}{\partial t} dy \\ &= \frac{1}{B} \frac{\partial}{\partial t} \int_{y_1}^{y_2} \bar{u} dy + \frac{1}{B} \frac{\partial}{\partial t} \int_{y_1}^{y_2} u'' dy \\ &= \frac{1}{B} \frac{\partial B \bar{u}}{\partial t} \end{aligned} \quad (\text{A-28})$$

The convective acceleration terms:

$$\begin{aligned} \frac{\partial(\bar{u} + u'')(\bar{u} + u'')}{\partial x} &= \frac{1}{B} \int_{y_1}^{y_2} \frac{\partial(\bar{u} + u'')(\bar{u} + u'')}{\partial x} dy \\ &= \frac{1}{B} \int_{y_1}^{y_2} \frac{\partial \bar{u} \bar{u}}{\partial x} dy + \frac{1}{B} \int_{y_1}^{y_2} \frac{\partial 2\bar{u} u''}{\partial x} dy + \frac{1}{B} \int_{y_1}^{y_2} \frac{\partial u'' u''}{\partial x} dy \\ &= \frac{1}{B} \frac{\partial}{\partial x} \int_{y_1}^{y_2} \bar{u} \bar{u} dy + \frac{1}{B} \frac{\partial}{\partial x} \int_{y_1}^{y_2} u'' u'' dy \\ &= \frac{1}{B} \frac{\partial B \bar{u} \bar{u}}{\partial x} + \underbrace{\frac{1}{B} \frac{\partial}{\partial x} \int_{y_1}^{y_2} u'' u'' dy}_{\text{dispersion term}} \end{aligned} \quad (\text{A-29})$$

Similarly for the other two terms:

$$\frac{\overline{\overline{\partial(\bar{u} + u'')(\bar{w} + w'')}}}{\partial z} = \frac{1}{B} \frac{\partial B \bar{u} \bar{w}}{\partial z} + \underbrace{\frac{1}{B} \frac{\partial}{\partial z} \int_{y1}^{y2} u'' w'' dy}_{\text{dispersion term}} \quad (\text{A-30})$$

$$\frac{\overline{\overline{\partial(\bar{u} + u'')(\bar{v} + v'')}}}{\partial y} = u'' v''|_{y2} - u'' v''|_{y1} = 0 \quad (\text{A-31})$$

The gravity term:

$$\overline{\overline{g \sin \alpha}} = \frac{1}{B} \int_{y1}^{y2} g \sin \alpha dy = \frac{1}{B} (g \sin \alpha) \int_{y1}^{y2} dy = g \sin \alpha \quad (\text{A-32})$$

The pressure gradient term:

$$\begin{aligned} \frac{\overline{\overline{\partial(\bar{p} + p'')}}}{\partial x} &= \frac{1}{B} \int_{y1}^{y2} \frac{\partial(\bar{p} + p'')}{\partial x} dy \\ &= \frac{1}{B} \int_{y1}^{y2} \frac{\partial \bar{p}}{\partial x} dy + \frac{1}{B} \int_{y1}^{y2} \frac{\partial p''}{\partial x} dy \\ &= \frac{1}{B} \frac{\partial}{\partial x} \int_{y1}^{y2} \bar{p} dy + \frac{1}{B} \frac{\partial}{\partial x} \int_{y1}^{y2} p'' dy \\ &= \frac{1}{B} \frac{\partial B \bar{p}}{\partial x} \end{aligned} \quad (\text{A-33})$$

or the above equation can be written, assuming that the derivative of the lateral average pressure gradient in the x-direction is not a function of y:

$$\begin{aligned} \frac{\overline{\overline{\partial(\bar{p} + p'')}}}{\partial x} &= \frac{1}{B} \int_{y1}^{y2} \frac{\partial(\bar{p} + p'')}{\partial x} dy \\ &= \frac{1}{B} \frac{\partial \bar{p}}{\partial x} \int_{y1}^{y2} dy + \frac{1}{B} \int_{y1}^{y2} \frac{\partial p''}{\partial x} dy \\ &= \frac{1}{B} \frac{\partial \bar{p}}{\partial x} B + \frac{1}{B} \frac{\partial}{\partial x} \int_{y1}^{y2} p'' dy \\ &= \frac{\partial \bar{p}}{\partial x} \end{aligned} \quad (\text{A-34})$$

Shear stresses

$$\begin{aligned}
 \overline{\left(\frac{\partial \tau_{xx}}{\partial x} + \frac{\partial \tau_{xy}}{\partial y} + \frac{\partial \tau_{xz}}{\partial z} \right)} &= \frac{1}{B} \int_{y1}^{y2} \frac{\partial \tau_{xx}}{\partial x} dy + \frac{1}{B} \int_{y1}^{y2} \frac{\partial \tau_{xy}}{\partial y} dy + \frac{1}{B} \int_{y1}^{y2} \frac{\partial \tau_{xz}}{\partial z} dy \\
 &= \frac{1}{B} \frac{\partial}{\partial x} \int_{y1}^{y2} \tau_{xx} dy + \frac{1}{B} \frac{\partial}{\partial x} \int_{y1}^{y2} \tau_{xy} dy + \frac{1}{B} \frac{\partial}{\partial z} \int_{y1}^{y2} \tau_{xz} dy \\
 &= \frac{1}{B} \left(\frac{\partial \overline{\tau_{xx}}}{\partial x} + \frac{\partial \overline{\tau_{xy}}}{\partial y} + \frac{\partial \overline{\tau_{xz}}}{\partial z} \right) = \frac{1}{B} \left(\frac{\partial \overline{\tau_{xx}}}{\partial x} + \frac{\partial \overline{\tau_{xz}}}{\partial z} \right)
 \end{aligned} \tag{A-35}$$

Collecting all terms and neglecting all dispersion terms, the final x-momentum equation is:

$$\frac{\partial \overline{B\bar{u}}}{\partial t} + \frac{\partial \overline{B\bar{u}\bar{u}}}{\partial x} + \frac{\partial \overline{B\bar{u}\bar{w}}}{\partial z} = Bg \sin \alpha - \frac{B}{\rho} \frac{\partial \bar{p}}{\partial x} + \frac{1}{\rho} \left(\frac{\partial \overline{\tau_{xx}}}{\partial x} + \frac{\partial \overline{\tau_{xz}}}{\partial z} \right) \tag{A-36}$$

Summary of Laterally Averaged Equations

In the development of CE-QUAL-W2 in Cole and Buchak (1995), the lateral average terms were represented by uppercase characters, such that $\bar{u} = U$, $\bar{w} = W$, and $\bar{p} = P$. The shear stress terms will be assumed lateral averages and the double overbars will be dropped for convenience. Making these simplifications, the governing equations become:

Continuity Equation

$$\frac{\partial UB}{\partial x} + \frac{\partial WB}{\partial z} = qB \tag{A-37}$$

x-Momentum Equation

$$\frac{\partial UB}{\partial t} + \frac{\partial UUB}{\partial x} + \frac{\partial WUB}{\partial z} = gB \sin \alpha - \frac{B}{\rho} \frac{\partial P}{\partial x} + \frac{1}{\rho} \frac{\partial B\tau_{xx}}{\partial x} + \frac{1}{\rho} \frac{\partial B\tau_{xz}}{\partial z} \tag{A-38}$$

z-Momentum Equation

$$\frac{1}{\rho} \frac{\partial P}{\partial z} = g \cos \alpha \tag{A-39}$$

There are now three equations and three unknowns - U , W , and P .

Simplification of Pressure Term

The z-momentum equation reduces to:

$$P = P_a + g \cos \alpha \int_{\eta}^z \rho dz \quad (\text{A-40})$$

after integration from a depth z to the water surface defined as $z=\eta$. P_a is the atmospheric pressure at the water surface ([Figure A-9](#)).

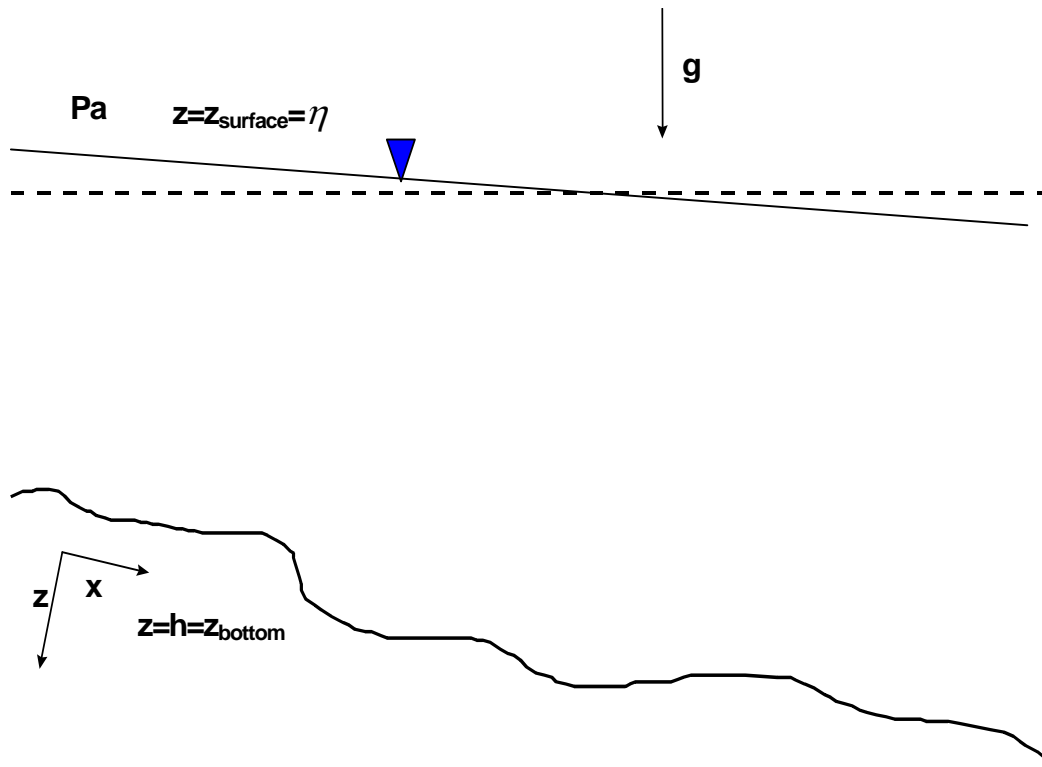


Figure A-9. Schematization for simplification of pressure term.

This equation for pressure is now substituted into the x-momentum equation and simplified using Leibnitz rule. The pressure gradient term in the x-momentum equation then becomes:

$$-\frac{1}{\rho} \frac{\partial P}{\partial x} = -\frac{1}{\rho} \frac{\partial P_a}{\partial x} + g \cos \alpha \frac{\partial \eta}{\partial x} - \frac{g \cos \alpha}{\rho} \int_{\eta}^z \frac{\partial \rho}{\partial x} dz \quad (\text{A-41})$$

The first term on the RHS is the atmospheric pressure term (accelerations due to atmospheric pressure changes over the water surface), the second is the barotropic pressure term (accelerations due to water surface variations), and the third is the baroclinic pressure term (accelerations due to density driven currents).

In CE-QUAL-W2, the atmospheric pressure term is assumed zero and is neglected. This implies that for long systems during severe storms the model will not be able to account for accelerations because of atmospheric changes. For a large physical domain, variations in meteorological forcing may be significant. This is discussed in the section on Variability in Meteorological Forcing. The pressure term then becomes:

$$-\frac{1}{\rho} \frac{\partial P}{\partial x} = g \cos \alpha \frac{\partial \eta}{\partial x} - \frac{g \cos \alpha}{\rho} \int_{\eta}^z \frac{\partial \rho}{\partial x} dz \quad (\text{A-42})$$

The revised form of the x-momentum equation is then:

$$\begin{aligned} \frac{\partial UB}{\partial t} + \frac{\partial UUB}{\partial x} + \frac{\partial WUB}{\partial z} = gB \sin \alpha + g \cos \alpha B \frac{\partial \eta}{\partial x} - \frac{g \cos \alpha B}{\rho} \int_{\eta}^z \frac{\partial \rho}{\partial x} dz \\ + \frac{1}{\rho} \frac{\partial B \tau_{xx}}{\partial x} + \frac{1}{\rho} \frac{\partial B \tau_{xz}}{\partial z} \end{aligned} \quad (\text{A-43})$$

Effectively, pressure has been removed from the unknowns by combining the z-momentum and x-momentum equations, but η has been added as an unknown.

Free Water Surface

This equation is a simplification of the continuity equation. The continuity equation integrated over the depth from the water surface to the bottom is called the free water surface equation. [Figure A-10](#) and [Figure A-11](#) are definition sketches for the computational grid without and with a channel slope, respectively.

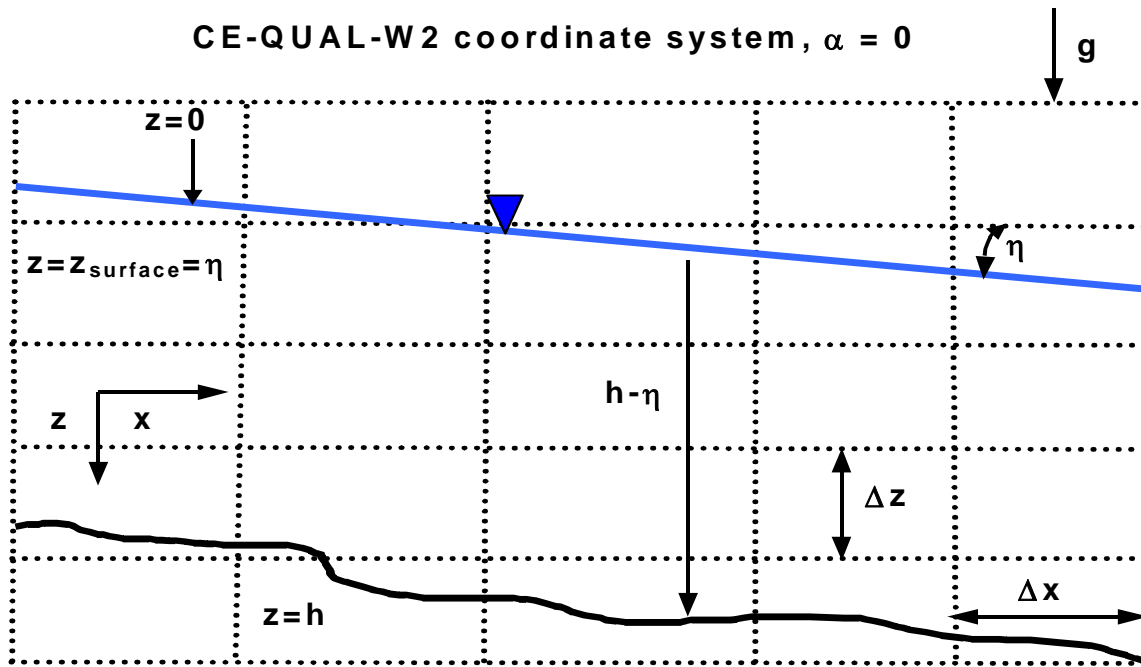


Figure A-10. Coordinate system without channel slope.

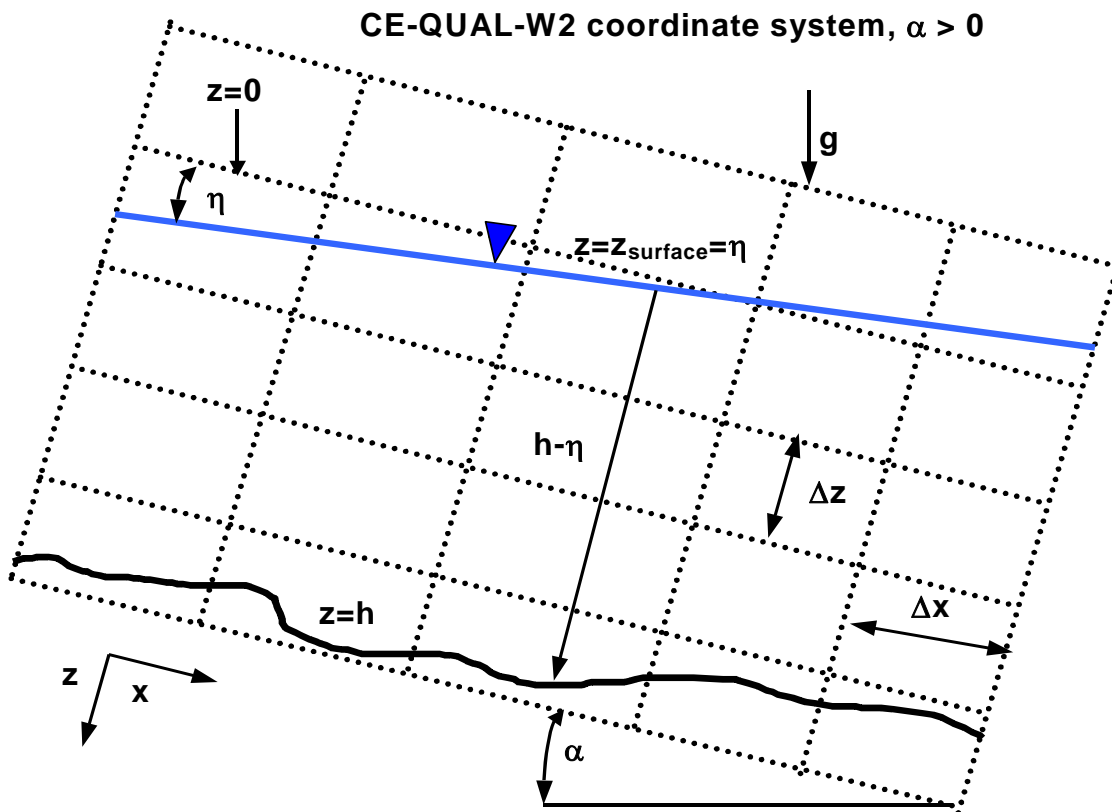


Figure A-11. Coordinate system with channel slope.

The continuity equation is integrated over the depth as follows:

$$\int_{\eta}^h \frac{\partial UB}{\partial x} dz + \int_{\eta}^h \frac{\partial WB}{\partial z} dz = \int_{\eta}^h qB dz \quad (\text{A-44})$$

The first term can be expanded as follows using Leibnitz's rule:

$$\int_{\eta}^h \frac{\partial UB}{\partial x} dz = \frac{\partial}{\partial x} \int_{\eta}^h UB dz - \frac{\partial h}{\partial x} UB|_h + \frac{\partial \eta}{\partial x} UB|_{\eta} \quad (\text{A-45})$$

The integral of the vertical flow rate over z relates to changes in water surface elevation as shown below:

$$\int_{\eta}^h \frac{\partial WB}{\partial z} dz = WB|_h - WB|_{\eta} \quad (\text{A-46})$$

where:

$$W_h = \frac{\partial h}{\partial t} + U_h \frac{\partial h}{\partial x}$$

$$W_{\eta} = \frac{\partial \eta}{\partial t} + U_{\eta} \frac{\partial \eta}{\partial x}$$

Combining these terms together, the free surface equation becomes:

$$\int_{\eta}^h qB dz = \frac{\partial}{\partial x} \int_{\eta}^h UB dz - \frac{\partial h}{\partial x} UB|_h + \frac{\partial \eta}{\partial x} UB|_{\eta} + U_h B_h \frac{\partial h}{\partial t} + U_h B_h \frac{\partial h}{\partial x} - B_{\eta} \frac{\partial \eta}{\partial t} - B_{\eta} U_{\eta} \frac{\partial \eta}{\partial x} \quad (\text{A-47})$$

Canceling out terms and applying the no-slip boundary condition that U_h is zero:

$$\frac{\partial}{\partial x} \int_{\eta}^h UB dz - B_{\eta} \frac{\partial \eta}{\partial t} = \int_{\eta}^h qB dz \quad (\text{A-48})$$

or

$$B_{\eta} \frac{\partial \eta}{\partial t} = \frac{\partial}{\partial x} \int_{\eta}^h UB dz - \int_{\eta}^h qB dz \quad (\text{A-49})$$

where B_η is the width at the surface.

Equation of State

The density must be known for solution of the momentum equations. The equation of state is an equation that relates density to temperature and concentration of dissolved substances. This equation is given by:

$$\rho = f(T_w, \Phi_{TDS}, \Phi_{ISS}) \quad (\text{A-50})$$

where $f(T_w, \Phi_{TDS}, \Phi_{ISS})$ is a density function dependent upon temperature, total dissolved solids or salinity, and inorganic suspended solids.

Summary of Governing Equations

Table A-1 shows the governing equations after lateral averaging for a channel slope of zero (original model formulation) and for an arbitrary channel slope. Parameters used in [Table A-1](#) are illustrated in [Figure A-12](#).

Table A-1. Governing equations with and without channel slope.

Equation	Governing equation assuming no channel slope and no momentum conservation at branch intersections	Governing equation assuming an arbitrary channel slope and conservation of momentum at branch intersections
x-momentum	$\frac{\partial UB}{\partial t} + \frac{\partial UUB}{\partial x} + \frac{\partial WUB}{\partial z} =$ $gB \frac{\partial \eta}{\partial x} - \frac{gB}{\rho} \int_{\eta}^z \frac{\partial \rho}{\partial x} dz +$ $\frac{1}{\rho} \frac{\partial B \tau_{xx}}{\partial x} + \frac{1}{\rho} \frac{\partial B \tau_{xz}}{\partial z}$	$\frac{\partial UB}{\partial t} + \frac{\partial UUB}{\partial x} + \frac{\partial WUB}{\partial z} = gB \sin \alpha$ $+ g \cos \alpha B \frac{\partial \eta}{\partial x} - \frac{g \cos \alpha B}{\rho} \int_{\eta}^z \frac{\partial \rho}{\partial x} dz +$ $\frac{1}{\rho} \frac{\partial B \tau_{xx}}{\partial x} + \frac{1}{\rho} \frac{\partial B \tau_{xz}}{\partial z} + qBU_x$
z-momentum	$0 = g - \frac{1}{\rho} \frac{\partial P}{\partial z}$	$0 = g \cos \alpha - \frac{1}{\rho} \frac{\partial P}{\partial z}$
continuity	$\frac{\partial UB}{\partial x} + \frac{\partial WB}{\partial z} = qB$	$\frac{\partial UB}{\partial x} + \frac{\partial WB}{\partial z} = qB$
state	$\rho = f(T_w, \Phi_{TDS}, \Phi_{ss})$	$\rho = f(T_w, \Phi_{TDS}, \Phi_{ss})$
free surface	$B_\eta \frac{\partial \eta}{\partial t} = \frac{\partial}{\partial x} \int_{\eta}^h UB dz - \int_{\eta}^h qB dz$	$B_\eta \frac{\partial \eta}{\partial t} = \frac{\partial}{\partial x} \int_{\eta}^h UB dz - \int_{\eta}^h qB dz$

U = horizontal velocity, $m s^{-1}$	τ_x = x-direction lateral average shear stress
W = vertical velocity, $m s^{-1}$	τ_y = y-direction lateral average shear stress
B = channel width	ρ = density
P = pressure	η = water surface

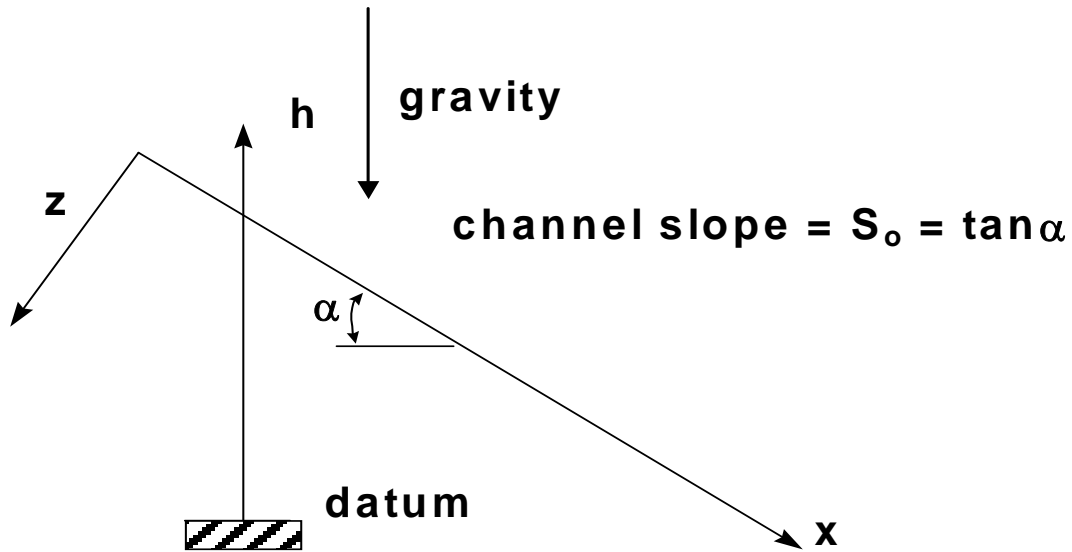


Figure A-12. Definition sketch for channel slope.

Branch Linkage with Internal Head Boundary Conditions

Linkage of Mainstem Branches

One issue in the development of the river basin model is the linkage of branches with different vertical grids. [Figure A-13](#) shows variable definitions for a sloping channel.

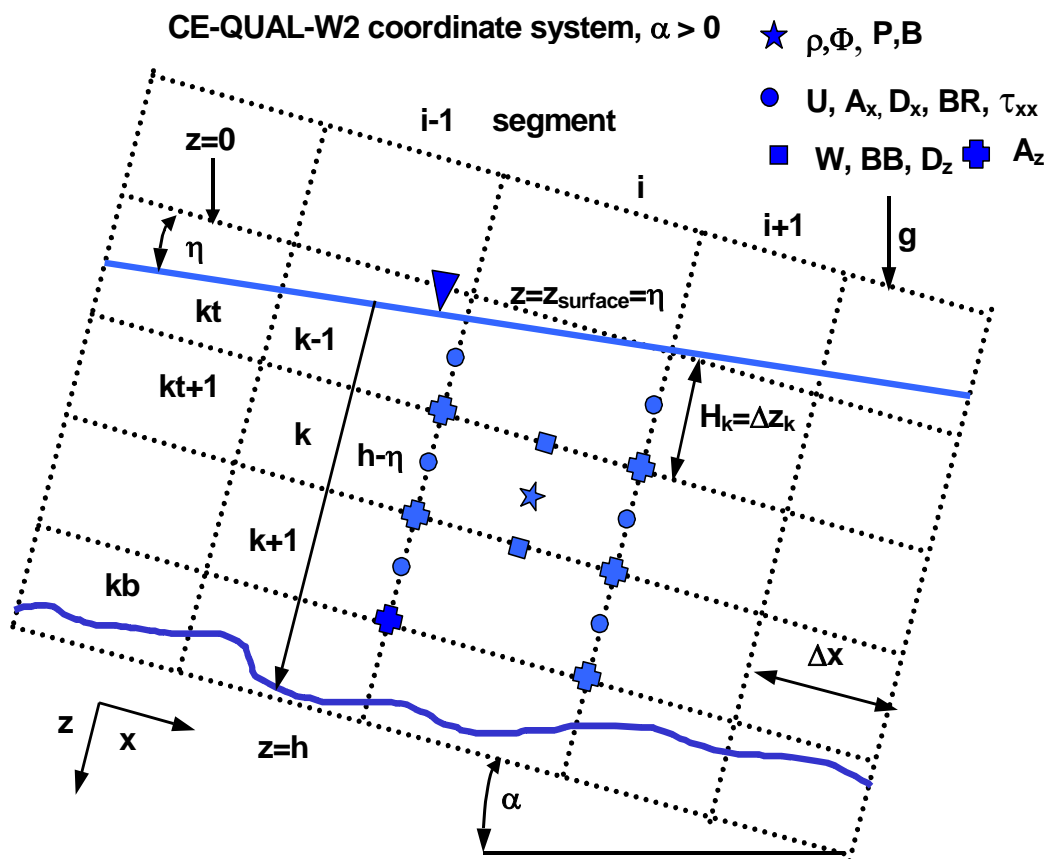


Figure A-13. Computational grid variable definitions for arbitrary channel slope.

However, the vertical velocity of a cell is not determined at the side edge of a segment, but at the bottom of the segment. In order for all the volume to be passed from one cell to another, all the flow from the downstream segment [ID] should be transferred to the upstream segment [IU]. Since the model does not assume strong vertical accelerations, we may be forced to neglect the vertical component of velocity at this transition and assume that the longitudinal velocity entering the upstream segment is U_{ID} .

The model ensures that flow and mass are conserved between branches when the vertical spacing is different between the upstream and downstream grid. Spatial averaging to conserve flow, heat, and mass is illustrated in [Figure A-14](#).

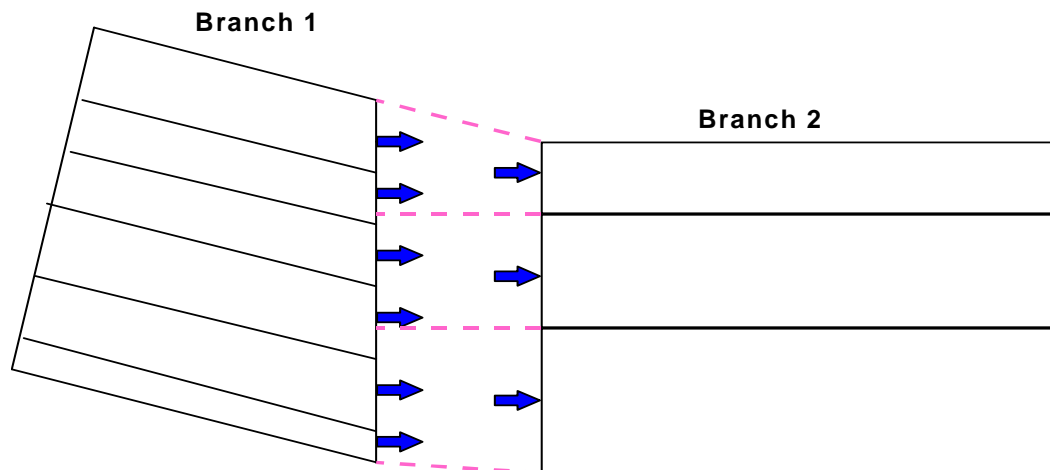


Figure A-14. Transfer of mass and momentum between branches with unequal vertical grid spacing.

Linkage of Tributary Branches

Version 2 assumed all tributary branches came in at right angles to the main channel resulting in no longitudinal momentum exchange between the branches. In many cases, this was appropriate, but in certain cases prevented a realistic depiction of the physics of the prototype. Version 3 now includes momentum transfer between branches that do not enter perpendicular to each other ([Figure A-15](#)).

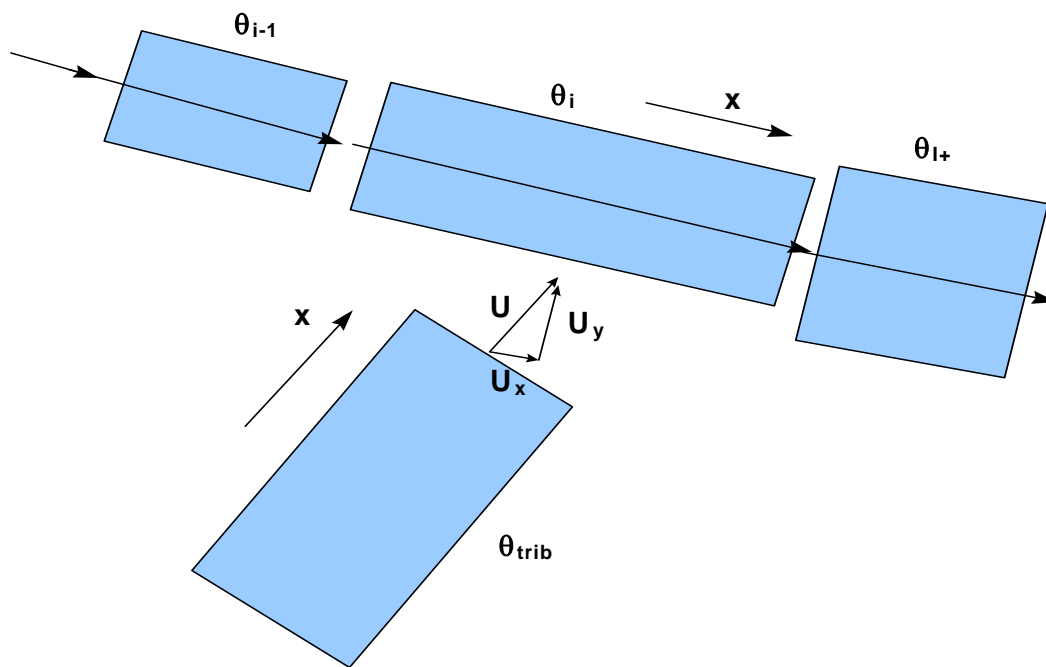


Figure A-15. Linkage of tributary branch coming in at an angle to main branch.

The tributary inflow can create shear stress along both the longitudinal axis of the main stem branch and along the y-axis of the segment. For the new formulation, the cross-shear mixing has been added to the cross-shear wind stress for the computation involving the vertical eddy viscosity and vertical diffusivity. This involves determining the y and x velocity components of the entering branch ([Figure A-16](#)).

Longitudinal Momentum

The vector component of velocity in the x-direction of the main channel, U_x , can be computed by analysis of the channel orientations. This component in the x-direction would be:

$$U_x = U \cos \beta \quad (\text{A-51})$$

where:

U = longitudinal velocity of the tributary at segment ID for the tributary branch

β = difference in the angle between the main stem and tributary segments ([Figure A-16](#)).

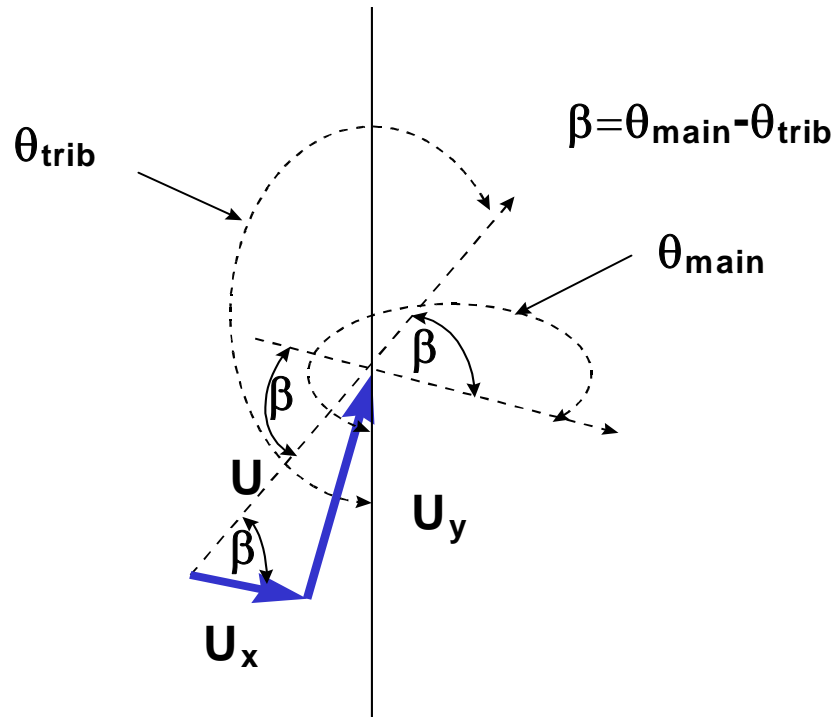


Figure A-16. Schematic of x and y velocity components.

The conservation of momentum about a control volume, the main stem segment, would result in an additional source of momentum. Lai (1986) shows that the correction to the x-momentum equation would be:

$$qBU_x \tag{A-52}$$

where:

q = lateral inflow per unit length.

This arises from re-deriving the momentum equations and assuming that all the fluid (q) entering the segment is moving at the velocity U_x . This correction to the x-momentum equation would be

$$\begin{aligned} \frac{\partial UB}{\partial t} + \frac{\partial UUB}{\partial x} + \frac{\partial WUB}{\partial z} = & gB \sin \alpha + g \cos \alpha B \frac{\partial \eta}{\partial x} - \frac{g \cos \alpha B}{\rho} \int_{\eta}^z \frac{\partial \rho}{\partial x} dz \\ & + \frac{1}{\rho} \frac{\partial B \tau_{xx}}{\partial x} + \frac{1}{\rho} \frac{\partial B \tau_{xz}}{\partial z} + \underbrace{qBU_x}_{\text{momentum from side tributaries}} \end{aligned} \tag{A-53}$$

Cross-shear of Tributary Inflow

The y-velocity coming into a reservoir may also contribute to vertical mixing. The y component of a tributary inflow is $U_y = U \sin \beta$ (Figure A-16). Since there is no y-momentum equation, the only

mechanism for mixing energy with the present formulation of the vertical shear stress is the cross-shear stress from the wind given as $\tau_{wy} \cong C_D \rho_a W_h^2 \sin(\Theta_1 - \Theta_2)$. The cross-shear stress accounts for the shear stress and mixing that results from wind blowing across the y-axis of the segment. The lateral branch inflow at a velocity, U_y , could be thought of as an additional component of the stress under the current context of the turbulence closure approximations.

If the water in the y-direction has zero velocity, the additional shear stress can be parameterized as an interfacial shear:

$$\tau_{ytrib} \cong \rho \frac{f}{8} U_y^2 \quad (\text{A-54})$$

where:

f = interfacial friction factor

For two-layer flow systems, f has been found to be of order 0.01. The value of f for this non-ideal approach could be determined by numerical computation. Therefore, the value of the cross-shear term would be increased by a lateral tributary inflow. This can be evaluated by numerical experiments computing the magnitude of the cross-shear term from wind and from lateral inflow. A more robust theoretical approach may be needed to account for this increase in lateral shear, but that may be necessary only if the model includes the y-momentum equation.

River Basin Theory

The corrections to the governing equations incorporating the sloping channel and the transfer of momentum from a side tributary are incorporated in the new solution technique as described below.

Free-Water Surface Numerical Solution

The free surface equation:

$$B_\eta \frac{\partial \eta}{\partial t} = \frac{\partial}{\partial x} \int_\eta^h UB dz - \int_\eta^h qB dz \quad (\text{A-55})$$

is solved by substituting the momentum equation:

$$\begin{aligned} \frac{\partial UB}{\partial t} + \frac{\partial UUB}{\partial x} + \frac{\partial WUB}{\partial z} &= gB \sin \alpha + g \cos \alpha B \frac{\partial \eta}{\partial x} - \frac{g \cos \alpha B}{\rho} \int_\eta^z \frac{\partial \rho}{\partial x} dz \\ &+ \frac{1}{\rho} \frac{\partial B \tau_{xx}}{\partial x} + \frac{1}{\rho} \frac{\partial B \tau_{xz}}{\partial z} + qBU_x \end{aligned} \quad (\text{A-56})$$

in finite difference form and then simplifying. The finite difference form of the momentum equation is:

$$UB_i^{n+1} = UB_i^n + \Delta t \left[-\frac{\partial UUB}{\partial x} - \frac{\partial WUB}{\partial z} + gB \sin \alpha + g \cos \alpha B \frac{\partial \eta}{\partial x} - \frac{g \cos \alpha B}{\rho} \int_{\eta}^z \frac{\partial \rho}{\partial x} dz + \frac{1}{\rho} \frac{\partial B \tau_{xx}}{\partial x} + \frac{1}{\rho} \frac{\partial B \tau_{xz}}{\partial z} + qBU_x \right]_i \quad (\text{A-57})$$

Defining for simplicity the term F as:

$$F = -\frac{\partial UUB}{\partial x} - \frac{\partial WUB}{\partial z} + \frac{1}{\rho} \frac{\partial B \tau_{xx}}{\partial x} \quad (\text{A-58})$$

and substituting in for τ_{xx} , F becomes:

$$F = -\frac{\partial UUB}{\partial x} - \frac{\partial WUB}{\partial z} + \frac{\partial \left(BA_x \frac{\partial U}{\partial x} \right)}{\partial x} \quad (\text{A-59})$$

Substituting in the term UB_i^{n+1} in the free surface equation for UB , the free surface equation becomes:

$$\begin{aligned} B_{\eta} \frac{\partial \eta}{\partial t} &= \frac{\partial}{\partial x} \int_{\eta}^h UB_i^n dz + \Delta t \frac{\partial}{\partial x} \int_{\eta}^h F^n dz + \Delta t \frac{\partial}{\partial x} \int_{\eta}^h gB \sin \alpha dz \\ &+ \Delta t \frac{\partial}{\partial x} \int_{\eta}^h g \cos \alpha B \frac{\partial \eta}{\partial x} dz - \Delta t \frac{\partial}{\partial x} \int_{\eta}^h \frac{g \cos \alpha B}{\rho} \int_{\eta}^z \frac{\partial \rho}{\partial x} dz dz \\ &+ \Delta t \frac{\partial}{\partial x} \int_{\eta}^h \frac{1}{\rho} \frac{\partial B \tau_{xz}}{\partial z} dz + \Delta t \frac{\partial}{\partial x} \int_{\eta}^h qBU_x^n dz \\ &- \int_{\eta}^h q^n B dz \end{aligned} \quad (\text{A-60})$$

Some of these terms can be simplified as follows:

$$\frac{\partial}{\partial x} \int_{\eta}^h gB \sin \alpha dz = g \sin \alpha \frac{\partial}{\partial x} \int_{\eta}^h B dz \quad (\text{A-61})$$

$$\frac{\partial}{\partial x} \int_{\eta}^h g \cos \alpha B \frac{\partial \eta}{\partial x} dz = g \cos \alpha \frac{\partial}{\partial x} \left(\frac{\partial \eta}{\partial x} \int_{\eta}^h B dz \right) \quad (\text{A-62})$$

$$\frac{\partial}{\partial x} \int_{\eta}^h \frac{g \cos \alpha B}{\rho} \int_{\eta}^z \frac{\partial \rho}{\partial x} dz dz = \frac{g \cos \alpha}{\rho} \frac{\partial}{\partial x} \int_{\eta}^h B \int_{\eta}^z \frac{\partial \rho}{\partial x} dz dz \quad (\text{A-63})$$

$$\frac{\partial}{\partial x} \int_{\eta}^h \frac{1}{\rho} \frac{\partial B \tau_{xz}}{\partial z} dz = \frac{1}{\rho} \frac{\partial}{\partial x} \left(B \tau_{xz} \Big|_h - B \tau_{xz} \Big|_{\eta} \right) \quad (\text{A-64})$$

Then substituting these into the above equation:

$$\begin{aligned} B_{\eta} \frac{\partial \eta}{\partial t} &= \frac{\partial}{\partial x} \int_{\eta}^h UB_i^n dz + \Delta t \frac{\partial}{\partial x} \int_{\eta}^h F^n dz + \Delta t g \sin \alpha \frac{\partial}{\partial x} \int_{\eta}^h B dz \\ &+ \Delta t g \cos \alpha \frac{\partial}{\partial x} \left(\frac{\partial \eta}{\partial x} \Big|_{\eta} \int_{\eta}^h B dz \right) - \Delta t \frac{g \cos \alpha}{\rho} \frac{\partial}{\partial x} \int_{\eta}^h B \int_{\eta}^z \frac{\partial \rho}{\partial x} \Big| dz dz \\ &+ \Delta t \frac{\partial}{\partial x} \frac{1}{\rho} \left(B \tau_{xz} \Big|_h - B \tau_{xz} \Big|_{\eta} \right)^n + \Delta t \frac{\partial}{\partial x} \int_{\eta}^h q B U_x^n dz - \int_{\eta}^h q^n B dz \end{aligned} \quad (\text{A-65})$$

All terms with η are grouped on the LHS such that:

$$\begin{aligned} B_{\eta} \frac{\partial \eta}{\partial t} - \Delta t g \cos \alpha \frac{\partial}{\partial x} \left(\frac{\partial \eta}{\partial x} \Big|_{\eta} \int_{\eta}^h B dz \right) &= \frac{\partial}{\partial x} \int_{\eta}^h UB_i^n dz + \Delta t \frac{\partial}{\partial x} \int_{\eta}^h F^n dz \\ &+ \Delta t g \sin \alpha \frac{\partial}{\partial x} \int_{\eta}^h B dz \\ &- \Delta t \frac{g \cos \alpha}{\rho} \frac{\partial}{\partial x} \int_{\eta}^h B \int_{\eta}^z \frac{\partial \rho}{\partial x} \Big| dz dz \\ &+ \Delta t \frac{\partial}{\partial x} \frac{1}{\rho} \left(B \tau_{xz} \Big|_h - B \tau_{xz} \Big|_{\eta} \right)^n \\ &+ \Delta t \frac{\partial}{\partial x} \int_{\eta}^h q B U_x^n dz \\ &- \int_{\eta}^h q^n B dz \end{aligned} \quad (\text{A-66})$$

The first term on the LHS can be put into a backward finite difference form as:

$$B_{\eta} \frac{\partial \eta}{\partial t} \approx B_{\eta} \frac{\eta_i^n - \eta_i^{n-1}}{\Delta t} \quad (\text{A-67})$$

The second term, $-\Delta t g \cos \alpha \frac{\partial}{\partial x} \left(\frac{\partial \eta}{\partial x} \int_{\eta}^h B dz \right)^n$, can be simplified using the chain rule for partial differential equations to:

$$-\Delta t g \cos \alpha \frac{\partial \eta}{\partial x} \left| \frac{\partial}{\partial x} \int_{\eta}^h B dz - \Delta t g \cos \alpha \int_{\eta}^h B dz \frac{\partial^2 \eta}{\partial x^2} \right|^n \quad (\text{A-68})$$

Then using a second-order central difference for the second derivative and a first order backward difference for the first derivative such that:

$$\begin{aligned} & -\Delta t g \cos \alpha \frac{\partial \eta}{\partial x} \left| \frac{\partial}{\partial x} \int_{\eta}^h B dz - \Delta t g \cos \alpha \int_{\eta}^h B dz \frac{\partial^2 \eta}{\partial x^2} \right|^n \\ & \approx -\Delta t g \cos \alpha \frac{\eta_i^n - \eta_{i-1}^n}{\Delta x} \frac{\partial}{\partial x} \int_{\eta}^h B dz \\ & \quad - \Delta t g \cos \alpha \int_{\eta}^h B dz \frac{\eta_{i+1}^n - 2\eta_i^n + \eta_{i-1}^n}{\Delta x^2} \end{aligned} \quad (\text{A-69})$$

Also using a backward difference:

$$\frac{\partial}{\partial x} \int_{\eta}^h B dz = \frac{1}{\Delta x} \left(\int_{\eta}^h B dz \Big|_i - \int_{\eta}^h B dz \Big|_{i-1} \right). \quad (\text{A-70})$$

Grouping and collecting terms and multiplying through by $\Delta t \Delta x$, the LHS becomes after simplification:

$$\begin{aligned} & \eta_{i-1}^n \left[\frac{-g \cos \alpha \Delta t^2}{\Delta x} \int_{\eta}^h B dz \Big|_{i-1} \right] + \eta_i^n \left[B_{\eta} \Delta x + \frac{g \cos \alpha \Delta t^2}{\Delta x} \left\{ \int_{\eta}^h B dz \Big|_i + \int_{\eta}^h B dz \Big|_{i-1} \right\} \right] \\ & + \eta_{i+1}^n \left[\frac{-g \cos \alpha \Delta t^2}{\Delta x} \int_{\eta}^h B dz \Big|_i \right] = (RHS)_i^n \Delta x \Delta t + B_{\eta} \eta_i^{n-1} \Delta x \end{aligned} \quad (\text{A-71})$$

where the RHS is defined as:

$$\begin{aligned}
 RHS = & \frac{\partial}{\partial x} \int_{\eta}^h UB_i^n dz + \Delta t \frac{\partial}{\partial x} \int_{\eta}^h F dz + \Delta t g \sin \alpha \frac{\partial}{\partial x} \int_{\eta}^h B dz \\
 & - \Delta t \frac{g \cos \alpha}{\rho} \frac{\partial}{\partial x} \int_{\eta}^h B \int_{\eta}^z \frac{\partial \rho}{\partial x} dz dz + \Delta t \frac{\partial}{\partial x} \frac{1}{\rho} \left(B \tau_{xz} \Big|_h - B \tau_{xz} \Big|_{\eta} \right) \\
 & + \Delta t \frac{\partial}{\partial x} \int_{\eta}^h q B U_x dz - \int_{\eta}^h q B dz
 \end{aligned} \tag{A-72}$$

and is evaluated at time level n.

The integral of the cell widths can be put into a summation over the vertical layers as:

$$\int_{\eta}^h B dz \Big|_i = \sum_{kb}^{kt} BH_{ri} \tag{A-73}$$

$$\int_{\eta}^h B dz \Big|_{i-1} = \sum_{kb}^{kt} BH_{ri-1} \tag{A-74}$$

where BH_r is the value of the width times the layer depth for the right-hand side of a cell. In the code, this is the variable BR(I,K) times H(K), or the derived variable BHR(I,K).

Some of the right hand side terms can be put into a format compatible with the model schematization such as:

$$\begin{aligned}
 \frac{\partial}{\partial x} \int_{\eta}^h (UB)_i^n dz & \approx \frac{\partial}{\partial x} \sum_{kt}^{kb} UBH_r \\
 & \approx \frac{1}{\Delta x} \left(\sum_{kt}^{kb} UBH_r \Big|_i - \sum_{kt}^{kb} UBH_r \Big|_{i-1} \right) \\
 & = \frac{1}{\Delta x} \sum_{kt}^{kb} \left(UBH_r \Big|_i - UBH_r \Big|_{i-1} \right)^n
 \end{aligned} \tag{A-75}$$

$$\begin{aligned}
 \Delta t \frac{\partial}{\partial x} \int_{\eta}^h F^n dz & \approx \Delta t \frac{\partial}{\partial x} \sum_{kt}^{kb} FH_r \\
 & \approx \frac{\Delta t}{\Delta x} \left(\sum_{kt}^{kb} FH_r \Big|_i - \sum_{kt}^{kb} FH_r \Big|_{i-1} \right) \\
 & = \frac{\Delta t}{\Delta x} \sum_{kt}^{kb} \left(FH_r \Big|_i - FH_r \Big|_{i-1} \right)^n
 \end{aligned} \tag{A-76}$$

$$\begin{aligned} \Delta t g \sin \alpha \frac{\partial}{\partial x} \int_{\eta}^h B dz &\approx \Delta t g \sin \alpha \frac{\partial}{\partial x} \sum_{kt}^{kb} B H_r \\ &\approx \frac{\Delta t g \sin \alpha}{\Delta x} \left(\sum_{kt}^{kb} B H_r \Big|_i - \sum_{kt}^{kb} B H_r \Big|_{i-1} \right) \\ &= \frac{\Delta t g \sin \alpha}{\Delta x} \sum_{kt}^{kb} (B H_r \Big|_i - B H_r \Big|_{i-1}) \end{aligned} \quad (\text{A-77})$$

$$\begin{aligned} \Delta t \frac{g \cos \alpha}{\rho} \frac{\partial}{\partial x} \int_{\eta}^h B \int_{\eta}^z \frac{\partial \rho}{\partial x} dz dz &\approx \Delta t \frac{g \cos \alpha}{\rho} \frac{\partial}{\partial x} \int_{\eta}^h B \sum_{kt}^{kb} \frac{\partial \rho}{\partial x} H_r dz \\ &\approx \Delta t \frac{g \cos \alpha}{\rho \Delta x} \sum_{kt}^{kb} \frac{\partial \rho}{\partial x} H_r \sum_{kt}^{kb} (B H_r \Big|_i - B H_r \Big|_{i-1}) \end{aligned} \quad (\text{A-78})$$

$$\Delta t \frac{\partial}{\partial x} \frac{1}{\rho} (B \tau_{xz} \Big|_h - B \tau_{xz} \Big|_{\eta}) \approx \frac{\Delta t}{\rho \Delta x} \left\{ (B \tau_{xz} \Big|_h - B \tau_{xz} \Big|_{\eta})_i - (B \tau_{xz} \Big|_h - B \tau_{xz} \Big|_{\eta})_{i-1} \right\} \quad (\text{A-79})$$

The lateral inflow of momentum term represents the gradient over x of the inflow momentum:

$$\Delta t \frac{\partial}{\partial x} \int_{\eta}^h q B U_x dz \approx \Delta t \frac{\partial}{\partial x} \sum_{kt}^{kb} q U_x B H_r \quad (\text{A-80})$$

$$\int_{\eta}^h q B dz \approx \sum_{kt}^{kb} q B H_r \quad (\text{A-81})$$

Combining these terms into one equation:

$$A \eta_{i-1}^n + X \eta_i^n + C \eta_{i+1}^n = D \quad (\text{A-82})$$

where:

$$\begin{aligned} A &= \left[\frac{-g \cos \alpha \Delta t^2}{\Delta x} \sum_{kt}^{kb} B H_r \Big|_{i-1} \right] \\ X &= \left[B_{\eta} \Delta x + \frac{g \cos \alpha \Delta t^2}{\Delta x} \left\{ \sum_{kt}^{kb} B H_r \Big|_i + \sum_{kt}^{kb} B H_r \Big|_{i-1} \right\} \right] \\ C &= \left[\frac{-g \cos \alpha \Delta t^2}{\Delta x} \sum_{kt}^{kb} B H_r \Big|_i \right] \end{aligned}$$

$$\begin{aligned}
D = & \Delta t \sum_{kt}^{kb} (UBH_r|_i - UBH_r|_{i-1}) + B_\eta \eta_i^{n-1} \Delta x + \Delta t^2 \sum_{kt}^{kb} (FH_r|_i - FH_r|_{i-1}) \\
& + \Delta t^2 g \sin \alpha \sum_{kt}^{kb} (BH_r|_i - BH_r|_{i-1}) + \Delta t^2 \frac{g \cos \alpha}{\rho} \sum_{kt}^{kb} (BH_r|_i - BH_r|_{i-1}) \sum_{kt}^{kb} \frac{\partial \rho}{\partial x} H_r \\
& + \Delta x \Delta t \sum_{kt}^{kb} qBH_r + \Delta x \Delta t^2 \frac{\partial}{\partial x} \sum_{kt}^{kb} qU_x BH_r \\
& + \frac{\Delta t^2}{\rho} \left[(B\tau_{xz}|_h - B\tau_{xz}|_\eta)_i - (B\tau_{xz}|_h - B\tau_{xz}|_\eta)_{i-1} \right]
\end{aligned}$$

This equation is solved for the water surface elevation at the n+1 time level using the Thomas algorithm. The boundary condition implementation is the same as described in Cole and Buchak (1995).

Horizontal Momentum Numerical Solution

The x-momentum equation:

$$\begin{aligned}
\frac{\partial UB}{\partial t} + \frac{\partial UUB}{\partial x} + \frac{\partial WUB}{\partial z} = & gB \sin \alpha + g \cos \alpha B \frac{\partial \eta}{\partial x} - \frac{g \cos \alpha B}{\rho} \int_\eta^z \frac{\partial \rho}{\partial x} dz \\
& + \frac{1}{\rho} \frac{\partial B \tau_{xx}}{\partial x} + \frac{1}{\rho} \frac{\partial B \tau_{xz}}{\partial z} + qBU_x
\end{aligned} \tag{A-83}$$

is solved using either a fully explicit or an explicit/implicit finite difference solution technique specified by the user.

Explicit Solution

This scheme is based on solving the partial differential terms using an explicit finite difference technique where:

$$\begin{aligned}
U_i^{n+1} B_i^{n+1} = & U_i^n B_i^n + \Delta t \left\{ -\frac{\partial UUB}{\partial x} - \frac{\partial WUB}{\partial z} + gB \sin \alpha + g \cos \alpha B \frac{\partial \eta}{\partial x} \right. \\
& \left. - \frac{g \cos \alpha B}{\rho} \int_\eta^z \frac{\partial \rho}{\partial x} dz + \frac{1}{\rho} \frac{\partial B \tau_{xx}}{\partial x} + \frac{1}{\rho} \frac{\partial B \tau_{xz}}{\partial z} + qBU_x \right\}_i^n
\end{aligned} \tag{A-84}$$

The various terms are put into finite difference form as follows. The longitudinal advection of momentum is an upwind difference scheme where the order of differencing is dependent on the sign of U , e.g., for $U > 0$

$$\left. \frac{\partial UUB}{\partial x} \right|_{i,k} \cong \frac{1}{\Delta x_i} [B_{i,k}^n U_{i+1/2,k}^n U_{i,k}^n - B_{i-1,k}^n U_{i-1/2,k}^n U_{i-1,k}^n] \tag{A-85}$$

The vertical advection of momentum is also an upwind scheme based on the velocity of W . For $W > 0$ or downward flow

$$\left. \frac{\partial WUB}{\partial z} \right|_{i,k} \cong \frac{1}{\Delta z_k} \left[(W_{i,k}^n U_{i,k}^n B_{i,k}^n) - (W_{i,k-1}^n U_{i,k-1}^n B_{i,k-1}^n) \right] \quad (\text{A-86})$$

The gravity force is:

$$gB \sin \alpha = g \sin \alpha B_i^n \quad (\text{A-87})$$

The pressure gradient is:

$$\begin{aligned} g \cos \alpha B \frac{\partial \eta}{\partial x} - \frac{g \cos \alpha B}{\rho} \int_{\eta}^z \frac{\partial \rho}{\partial x} dz &= \frac{g \cos \alpha B_i^n}{\Delta x} (\eta_{i+1} - \eta_i)^n \\ &\quad - \frac{g \cos \alpha B_i^n}{\rho \Delta x} (\rho_{i+1,k} - \rho_{i,k})^n \Delta z_k \end{aligned} \quad (\text{A-88})$$

The horizontal advection of turbulent momentum is:

$$\begin{aligned} \frac{1}{\rho} \frac{\partial B \tau_{xx}}{\partial x} &= \frac{\partial B A_x}{\partial x} \frac{\partial U}{\partial x} = \left(\frac{B_{i+1/2}^n A_x}{\Delta x_i \Delta x_{i+1/2}} \right) (U_{i+1,k}^n - U_{i,k}^n) \\ &\quad - \left(\frac{B_{i-1/2}^n A_x}{\Delta x_i \Delta x_{i-1/2}} \right) (U_{i,k}^n - U_{i-1,k}^n) \end{aligned} \quad (\text{A-89})$$

The contribution to longitudinal momentum by lateral branch inflows is:

$$qBU_x = qBU_x|_{i,k}^n \quad (\text{A-90})$$

Using the definition of the shear stress:

$$\tau_{xz} = \left[\tau_w + \tau_b + A_z \frac{\partial U}{\partial z} \right] \quad (\text{A-91})$$

the vertical transport of momentum is:

$$\begin{aligned} \frac{1}{\rho} \frac{\partial B}{\partial z} \tau_{xz} = \frac{\partial}{\partial z} \frac{B}{\rho} \left[\tau_w + \tau_b + A_z \frac{\partial U}{\partial z} \right] = & \left(\frac{B_{i,k+1/2}^n}{\Delta z_k \Delta z_{k+1/2} \rho} \right) \\ & \left[\tau_w \Big|_{i,k+1/2}^n + \tau_b \Big|_{i,k+1/2}^n + \frac{A_{z,i,k+1/2}}{\Delta z_{k+1/2}} (U_{i,k+1}^n - U_{i,k}^n) \right] \\ & - \left(\frac{B_{i,k-1/2}^n}{\Delta z_k \Delta z_{k-1/2} \rho} \right) \left[\tau_w \Big|_{i,k-1/2}^n + \tau_b \Big|_{i,k-1/2}^n + \frac{A_{z,i,k-1/2}}{\Delta z_{k-1/2}} (U_{i,k}^n - U_{i,k-1}^n) \right] \end{aligned} \quad (\text{A-92})$$

Implicit Solution

The implicit technique was utilized to reduce the time step limitation for numerical stability when values of A_z were large, as for an estuary or a river system. This occurs because the time step limitation is a function of A_z . Only the vertical transport of momentum term was solved implicitly. All other terms for the solution of the horizontal momentum equation were the same as the explicit scheme.

The horizontal momentum equation can be separated into the following two equations:

$$\begin{aligned} \frac{\partial UB}{\partial t} + \frac{\partial UUB}{\partial x} + \frac{\partial WUB}{\partial z} = gB \sin \alpha + g \cos \alpha B \frac{\partial \eta}{\partial x} - \frac{g \cos \alpha B}{\rho} \int_{\eta}^z \frac{\partial \rho}{\partial x} dz \\ + \frac{1}{\rho} \frac{\partial B \tau_{xx}}{\partial x} + \frac{1}{\rho} \frac{\partial B(\tau_b + \tau_w)}{\partial z} + qBU_x \end{aligned} \quad (\text{A-93})$$

$$\frac{\partial UB}{\partial t} = \frac{1}{\rho} \frac{\partial}{\partial z} \left(BA_z \frac{\partial U}{\partial z} \right) \quad (\text{A-94})$$

Equation A-93 is written as:

$$\begin{aligned} U_i^* B_i^{n+1} = U_i^n B_i^n + \Delta t \left\{ - \frac{\partial UUB}{\partial x} - \frac{\partial WUB}{\partial z} + gB \sin \alpha + g \cos \alpha B \frac{\partial \eta}{\partial x} \right. \\ \left. - \frac{g \cos \alpha B}{\rho} \int_{\eta}^z \frac{\partial \rho}{\partial x} dz + \frac{1}{\rho} \frac{\partial B \tau_{xx}}{\partial x} + \frac{1}{\rho} \frac{\partial B(\tau_b + \tau_w)}{\partial z} + qBU_x \right\}_i^n \end{aligned} \quad (\text{A-95})$$

where U^* is the velocity at the new time level before the application of equation A-94. Equation A-92 is solved similarly to the solution of the fully explicit technique outlined above.

Equation A-94 is then solved using a fully implicit technique as:

$$\begin{aligned} \frac{\partial UB}{\partial t} &= \frac{(U_i^{n+1} B_i^{n+1} - U_i^* B_i^{n+1})}{\Delta t} \\ &= \frac{I}{\rho} \frac{\partial}{\partial z} \left(B^{n+1} A_z \frac{\partial U^{n+1}}{\partial z} \right) \end{aligned} \quad (\text{A-96})$$

This can be rewritten as:

$$\begin{aligned} U_i^{n+1} B_i^{n+1} &= U_i^* B_i^{n+1} + \left(\frac{\Delta t B_{i,k+1/2}^{n+1}}{\Delta z_k \rho} \right) \left[\frac{A_{z_{i,k+1/2}}}{\Delta z_{k+1/2}} (U_{i,k+1}^{n+1} - U_{i,k}^{n+1}) \right] \\ &\quad - \left(\frac{\Delta t B_{i,k-1/2}^{n+1}}{\Delta z_k \rho} \right) \left[\frac{A_{z_{i,k-1/2}}}{\Delta z_{k-1/2}} (U_{i,k}^{n+1} - U_{i,k-1}^{n+1}) \right] \end{aligned} \quad (\text{A-97})$$

Regrouping terms at n+1 time level on the LHS, the equation can be written as

$$AU_{i,k-1}^{n+1} + VU_{i,k}^{n+1} + CU_{i,k+1}^{n+1} = DU_{i,k}^* \quad (\text{A-98})$$

where:

$$\begin{aligned} A &= \left(\frac{-\Delta t B_{i,k-1/2}^{n+1}}{B_{i,k}^{n+1} \Delta z_k \rho} \right) \left[\frac{A_{z_{i,k-1/2}}}{\Delta z_{k-1/2}} \right] \\ V &= 1 + \left(\frac{\Delta t B_{i,k+1/2}^{n+1}}{B_{i,k}^{n+1} \Delta z_k \rho} \right) \left[\frac{A_{z_{i,k+1/2}}}{\Delta z_{k+1/2}} \right] + \left(\frac{\Delta t B_{i,k-1/2}^{n+1}}{B_{i,k}^{n+1} \Delta z_k \rho} \right) \left[\frac{A_{z_{i,k-1/2}}}{\Delta z_{k-1/2}} \right] \\ C &= \left(\frac{-\Delta t B_{i,k+1/2}^{n+1}}{B_{i,k}^{n+1} \Delta z_k \rho} \right) \left[\frac{A_{z_{i,k+1/2}}}{\Delta z_{k+1/2}} \right] \\ D &= 1 \end{aligned}$$

The resulting simultaneous equations are solved for U^{n+1} using the Thomas algorithm.

Turbulent Advection-Diffusion Equation

As in the momentum equation, time-averaged variables for velocity are introduced ([Figure A-17](#)) and concentration ([Figure A-18](#)).

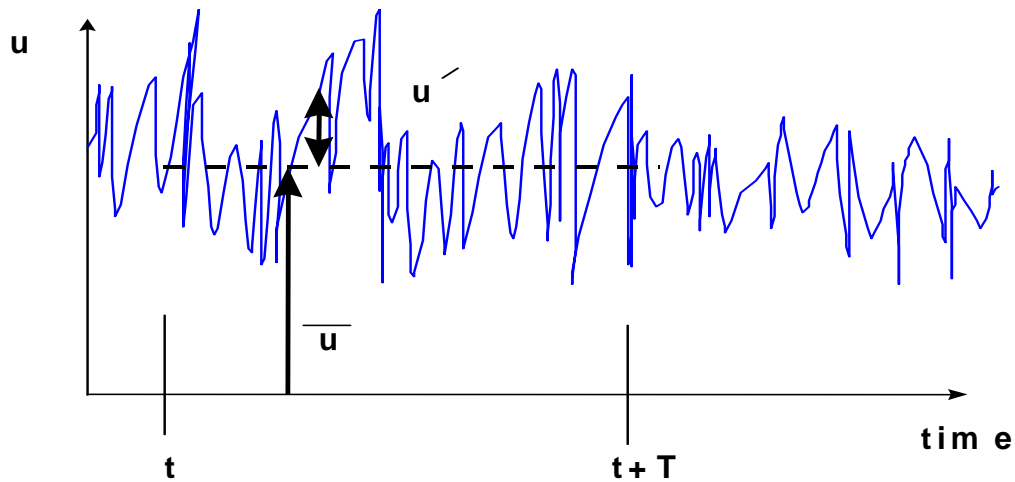


Figure A-17. Velocity variability with time.

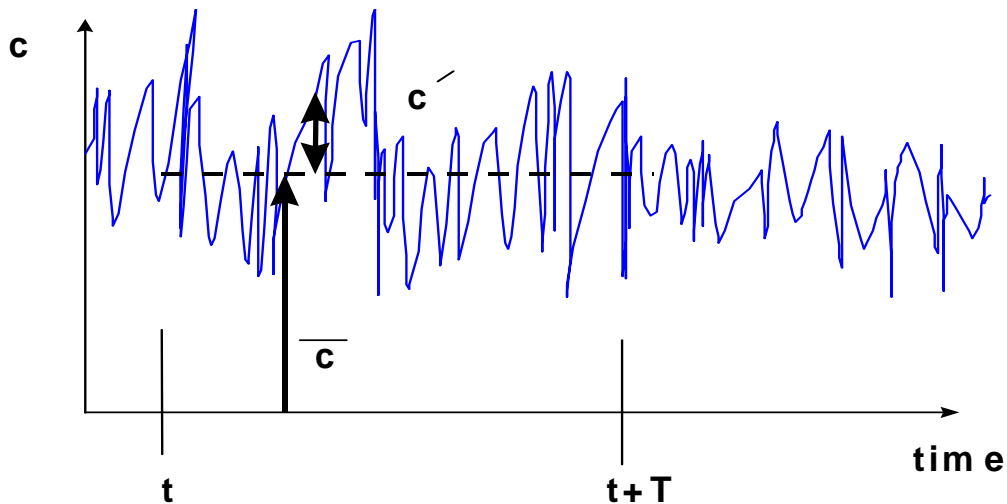


Figure A-18. Concentration variability with time.

The instantaneous velocity and concentration are decomposed into a mean and an unsteady component:

$$u(t) = \bar{u} + u'(t) \text{ where } \bar{u} = \frac{1}{T} \int_t^{t+T} u(t) dt \quad (\text{A-99})$$

Similarly for w , v , and c :

$$\begin{aligned} v &= \bar{v} + v' \\ w &= \bar{w} + w' \\ c &= \bar{c} + c' \end{aligned} \quad (\text{A-100})$$

Substituting these into the 3D governing equation and time averaging:

$$\underbrace{\frac{\partial \bar{c}}{\partial t} + \bar{u} \frac{\partial \bar{c}}{\partial x} + \bar{v} \frac{\partial \bar{c}}{\partial y} + \bar{w} \frac{\partial \bar{c}}{\partial z}}_{\text{transport by mean advection}} = D \underbrace{\left[\frac{\partial^2 \bar{c}}{\partial x^2} + \frac{\partial^2 \bar{c}}{\partial y^2} + \frac{\partial^2 \bar{c}}{\partial z^2} \right]}_{\text{molecular diffusive transport}} \tag{A-101}$$

$$- \underbrace{\frac{\partial}{\partial x} (\overline{u'c'}) - \frac{\partial}{\partial y} (\overline{v'c'}) - \frac{\partial}{\partial z} (\overline{w'c'})}_{\text{turbulent mass transport}} + \bar{S}$$

The new terms in the governing equation represent mass transport by turbulent eddies. As the intensity of turbulence increases, turbulent mass transport increases. Notice also that all velocities and concentrations are time averaged. The following turbulent mass fluxes are defined as:

$$\bar{J}_i = (\overline{u'c'}, \overline{v'c'}, \overline{w'c'}) \tag{A-102}$$

where:

$$\begin{aligned} (\overline{u'c'}) &= - E_x \frac{\partial \bar{c}}{\partial x} \\ (\overline{v'c'}) &= - E_y \frac{\partial \bar{c}}{\partial y} \\ (\overline{w'c'}) &= - E_z \frac{\partial \bar{c}}{\partial z} \end{aligned}$$

Substituting into the above equation:

$$\begin{aligned} \frac{\partial \bar{c}}{\partial t} + \bar{u} \frac{\partial \bar{c}}{\partial x} + \bar{v} \frac{\partial \bar{c}}{\partial y} + \bar{w} \frac{\partial \bar{c}}{\partial z} &= \frac{\partial}{\partial x} \left[(E_x + D) \frac{\partial \bar{c}}{\partial x} \right] + \frac{\partial}{\partial y} \left[(E_y + D) \frac{\partial \bar{c}}{\partial y} \right] \\ &+ \frac{\partial}{\partial z} \left[(E_z + D) \frac{\partial \bar{c}}{\partial z} \right] + \bar{S} \end{aligned} \tag{A-103}$$

In turbulent fluids, $E_x, E_y,$ and $E_z \gg D$, and D can be neglected except at interfaces where turbulence goes to zero. The turbulent diffusion coefficients can be thought of as the product of the velocity scale of turbulence and the length scale of that turbulence. These coefficients are related to the turbulent eddy viscosity. One is turbulent mass transport, the other is turbulent momentum transport between adjacent control volumes. In general, these turbulent diffusion coefficients are non-isotropic and non-homogeneous.

Water Quality Transport

Spatial averages across the lateral dimension of the channel of the turbulent time-averaged quantities can now be introduced:

$$\begin{aligned}\bar{c} &= \overline{c} \\ \bar{u} &= \overline{u} \\ \bar{w} &= \overline{w}\end{aligned}\quad (\text{A-104})$$

where the double overbar is a spatial average over y and the double prime is the deviation from the spatial mean as illustrated in [Figure A-19](#) for velocity and [Figure A-20](#) for constituent concentrations.

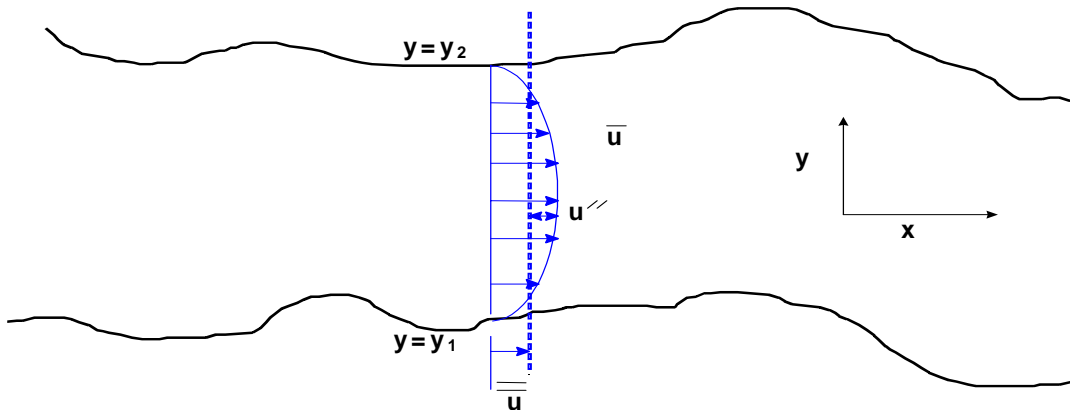


Figure A-19. Lateral average of the velocity field.

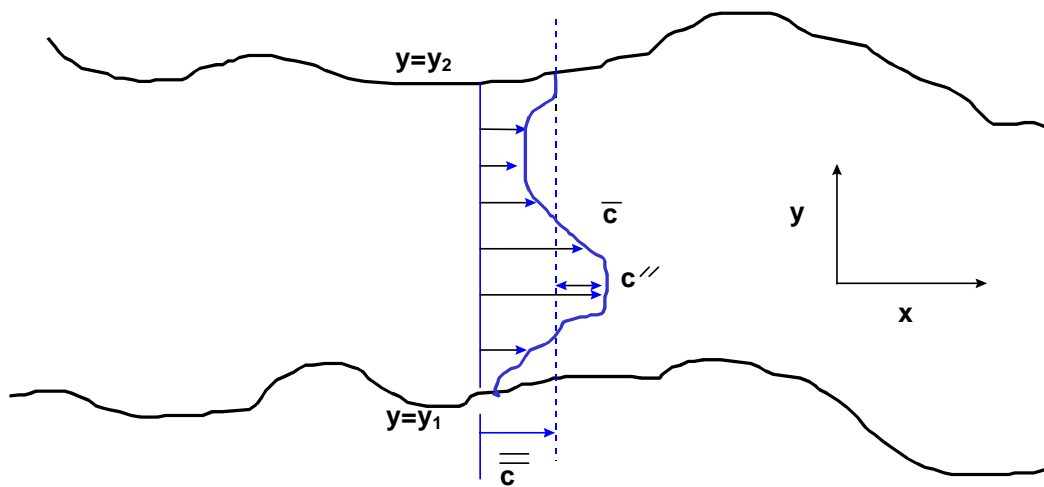


Figure A-20. Lateral average of the concentration field.

These are substituted into the governing equation and then the governing equation is integrated over the width such that:

$$\begin{aligned} \frac{\partial B\bar{c}}{\partial t} + \frac{\partial B\bar{u}\bar{c}}{\partial x} + \frac{\partial B\bar{w}\bar{c}}{\partial z} &= -B \overbrace{\left(\bar{v}\bar{c} \Big|_{y_2} - \bar{v}\bar{c} \Big|_{y_1} + \bar{c}'v' \Big|_{y_2} - \bar{c}'v' \Big|_{y_1} \right)}^{\text{mass transfer at side boundaries}} \\ &+ \frac{\partial}{\partial x} \left((D + E_x)B \frac{\partial \bar{c}}{\partial x} \right) + \frac{\partial}{\partial z} \left((D + E_z)B \frac{\partial \bar{c}}{\partial z} \right) \\ &- \left[\frac{\partial B\overline{u''c''}}{\partial x} + \frac{\partial B\overline{w''c''}}{\partial z} \right] + rB \end{aligned} \quad (\text{A-105})$$

Note how the following terms are simplified:

$$\begin{aligned} \frac{1}{B} \int_{y_1}^{y_2} \frac{\partial(\bar{c} + c'')}{\partial t} dy &= \frac{1}{B} \int_{y_1}^{y_2} \frac{\partial(\bar{c})}{\partial t} dy + \frac{1}{B} \int_{y_1}^{y_2} \frac{\partial(c'')}{\partial t} dy \\ &= \frac{1}{B} \frac{\partial}{\partial t} \int_{y_1}^{y_2} \bar{c} dy + \frac{1}{B} \frac{\partial}{\partial t} \int_{y_1}^{y_2} c'' dy \\ &= \frac{1}{B} \frac{\partial B\bar{c}}{\partial t} \end{aligned} \quad (\text{A-106})$$

$$\begin{aligned} \frac{1}{B} \int_{y_1}^{y_2} \frac{\partial(\bar{u} + u'')(\bar{c} + c'')}{\partial x} dy &= \frac{1}{B} \int_{y_1}^{y_2} \frac{\partial(\bar{c}\bar{u})}{\partial x} dy + \frac{1}{B} \int_{y_1}^{y_2} \frac{\partial(c''u'')}{\partial x} dy \\ &= \frac{1}{B} \frac{\partial}{\partial x} \int_{y_1}^{y_2} \bar{c}\bar{u} dy + \frac{1}{B} \frac{\partial}{\partial x} \int_{y_1}^{y_2} c''u'' dy \\ &= \frac{1}{B} \frac{\partial B\bar{u}\bar{c}}{\partial x} + \frac{1}{B} \frac{\partial B\overline{u''c''}}{\partial x} \end{aligned} \quad (\text{A-107})$$

The spatial average of any double primed variable goes to zero by definition.

The turbulent dispersion coefficients are defined as:

$$\begin{aligned} \overline{u''c''} &= -D_x \frac{\partial \bar{c}}{\partial x} \\ \overline{w''c''} &= -D_z \frac{\partial \bar{c}}{\partial z} \end{aligned} \quad (\text{A-108})$$

The dispersion terms are a result of lateral averaging of the velocity field. In general, except at an interface, $D_x \gg E_x \gg D$ and similarly for $D_z \gg E_z \gg D$. Substituting in for the dispersion coefficients and using q to be the net mass transport from lateral boundaries, this equation becomes:

$$\frac{\partial \overline{B\bar{c}}}{\partial t} + \frac{\partial \overline{B\bar{u}c}}{\partial x} + \frac{\partial \overline{B\bar{w}c}}{\partial z} = qB + \frac{\partial}{\partial x} \left(D_x B \frac{\partial \bar{c}}{\partial x} \right) + \frac{\partial}{\partial z} \left(D_z B \frac{\partial \bar{c}}{\partial z} \right) + rB \quad (\text{A-109})$$

If the overbars are dropped and replaced with capitals, c is replaced with Φ , then the following equation is obtained:

$$\frac{\partial B\Phi}{\partial t} + \frac{\partial UB\Phi}{\partial x} + \frac{\partial WB\Phi}{\partial z} - \frac{\partial \left(BD_x \frac{\partial \Phi}{\partial x} \right)}{\partial x} - \frac{\partial \left(BD_z \frac{\partial \Phi}{\partial z} \right)}{\partial z} = q_\Phi B + S_\Phi B \quad (\text{A-110})$$

where:

- Φ = laterally averaged constituent concentration, $g\ m^{-3}$
- D_x = longitudinal temperature and constituent dispersion coefficient, $m^2\ sec^{-1}$
- D_z = vertical temperature and constituent dispersion coefficient, $m^2\ sec^{-1}$
- q_Φ = lateral inflow or outflow mass flow rate of constituent per unit volume, $g\ m^{-3}\ sec^{-1}$
- S_Φ = laterally averaged source/sink term, $g\ m^{-3}\ sec^{-1}$

Note that this can be concentration or temperature since the concentration of heat can be determined to be $\rho c_p T$ where ρ is the fluid density, c_p is the specific heat of water, and T is the temperature.

The following must be determined in order to solve the equation:

1. laterally-averaged velocity field from momentum equations
2. appropriate boundary and initial conditions
3. D_x and D_z
4. laterally-averaged source/sink terms

Numerical Solution

The first step in the numerical solution is to define the computational grid ([Figure A-21](#)). The grid is space-staggered since some variables are defined at one location and the remainder are displaced by $\Delta x/2$ or $\Delta z/2$. The grid discretizes a waterbody into computational cells whose locations are defined by their segment [I] and layer number [K], i.e., cell (K,I). Variables are located at either the center or boundary of a cell. Variables defined at the boundary include the horizontal and vertical velocities, U and W , longitudinal eddy viscosity and diffusivity, A_x and D_x , vertical eddy viscosity and diffusivity, A_z and D_z , and internal shear stress τ_x . The density, ρ , temperature, T , constituent concentration, Φ , pressure, P , and average cell width, B are defined at the cell center.

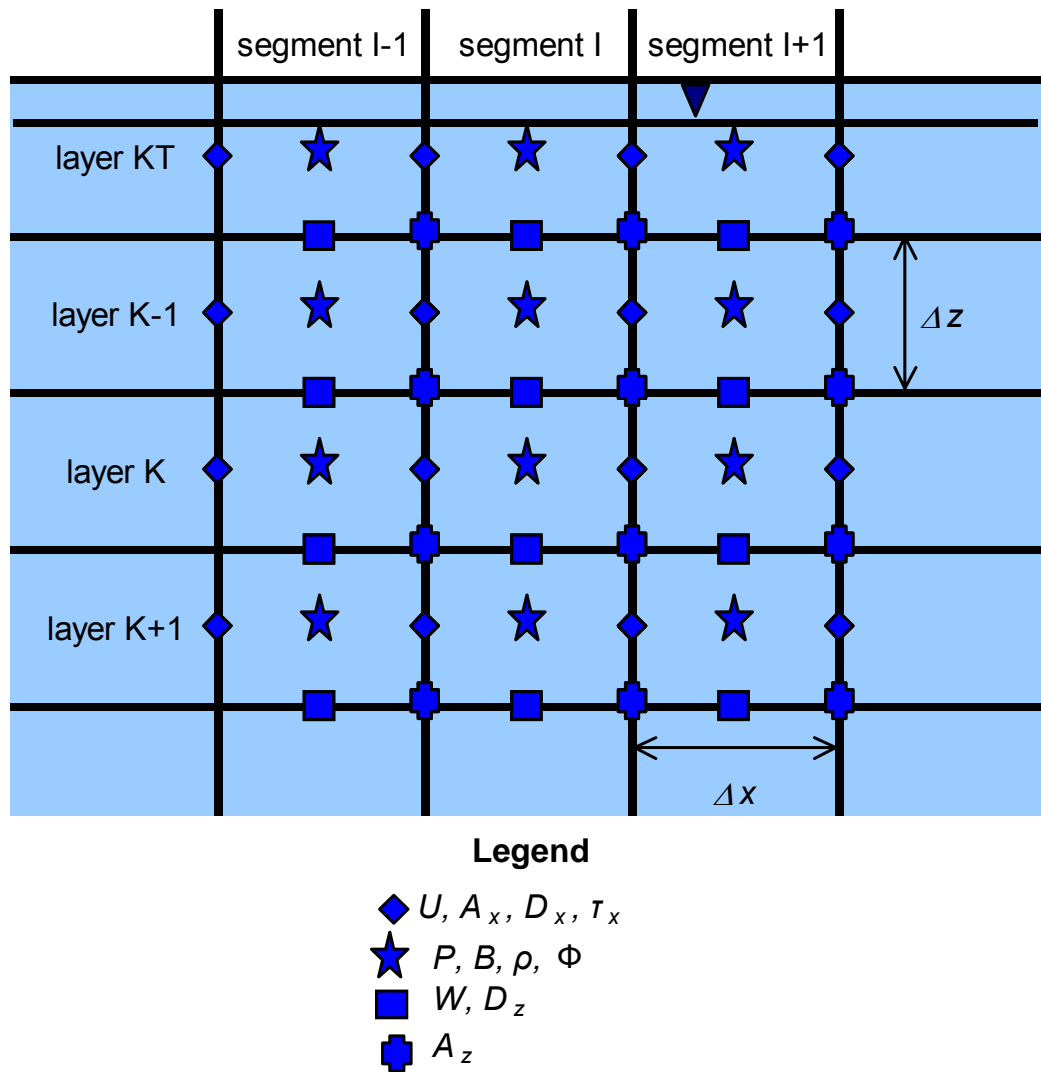


Figure A-21. Variable locations in computational grid.

There is a rational basis for choosing variable locations. Since the constituent concentration is defined at the center and velocities are defined at the boundaries, spatial averaging of velocities is not required to determine changes in concentration over time. In addition, the horizontal velocity is surrounded by a cell with water surface elevations and densities defined on either side. Thus, the horizontal velocity is computed from horizontal gradients of the surface slope and densities without requiring spatial averaging of these variables.

The geometry is specified by a cell width, B , thickness, H , and length, Δx . Several additional geometric variables are used in the calculations. These include the average cross-sectional area between two cells (k,i) and ($k,i+1$)

$$BH_{r_{k,i}} = \frac{B_{k,i} H_{k,i} + B_{k,i} H_{k,i+1}}{2} \tag{A-111}$$

the average widths between two cells (k,i) and (k+1,i)

$$B_{b_{k,i}} = \frac{B_{k,i} + B_{k+1,i}}{2} \quad (\text{A-112})$$

and the average layer thickness between layers k and k+1

$$\bar{H}_{k,i} = \frac{H_k + H_{k+1}}{2} \quad (\text{A-113})$$

The numerical procedure for solving the six unknowns at each timestep is to first compute water surface elevations. With the new surface elevations, new horizontal velocities can be computed. With new horizontal velocities, the vertical velocities can be found from continuity. New constituent concentrations are computed from the constituent balance. Using new horizontal and vertical velocities, the water surface elevation equation can be solved for η simultaneously. The solution for η is thus spatially implicit at the same time level and eliminates the surface gravity wave speed criterion:

$$\Delta t < \frac{\Delta x}{\sqrt{g H_{max}}} \quad (\text{A-114})$$

that can seriously limit timesteps in deep waterbodies.

Version 1.0 used upwind differencing in the constituent transport advective terms in which the cell concentration immediately upstream of the velocity is used to calculate fluxes. A major problem with upwind differencing is the introduction of numerical diffusion given by (for longitudinal advection):

$$\alpha_e = \frac{u \Delta x}{2} (1 - c) \quad (\text{A-115})$$

where:

α_e = numerical diffusion

$c = \frac{U \Delta t}{\Delta x}$ = Courant number

A similar condition holds for vertical advection. In many cases, numerical diffusion can overwhelm physical diffusion producing inaccurate results when strong gradients are present. The problem is particularly pronounced for stratified reservoirs and estuaries.

Numerical diffusion has been reduced by implementing an explicit, third-order accurate QUICKEST horizontal/vertical transport scheme (Leonard, 1979), and time-weighted, implicit vertical advection. Tests of this scheme are reported in Chapman and Cole (1992).

QUICKEST uses an additional spatial term to estimate concentrations used in computing horizontal and vertical fluxes. A nonuniform grid QUICKEST scheme was developed using a three-point Lagrangian interpolation function to estimate constituent values at grid cell interfaces. Specifically,

advective multipliers for each of three upstream weighted grid cells are derived in terms of cell lengths and the local cell interface velocity. Time invariant parts of the interpolation functions are calculated once thus minimizing computations for additional constituents.

Implicit vertical transport including variable layer heights has also been implemented. Vertical diffusion is fully implicit and advection employs a time-weighted, central difference, implicit scheme. A unique feature of vertical advection, in the explicit part of the time-weighted scheme, is QUICKEST which increases overall accuracy.

As implemented in the code, the new transport scheme is a two-part solution for constituent concentrations at the new timestep. First, horizontal advection is computed using QUICKEST and diffusion is computed using central differencing. This part also includes the explicit vertical advection contribution (which utilizes QUICKEST) and all sources and sinks.

Next, the implicit part of vertical advection and diffusion are included. Diffusion is always fully implicit. The user can time-weight advection by specifying a value for **[THETA]** which varies from 0 to 1. For **[THETA]** equal to 0, the solution is explicit in time and vertical advection is accounted for in the first part of the algorithm. For **[THETA]** equal to 1, the solution is fully implicit in time and vertical advection is accounted for in this part of the algorithm. A Crank-Nicholson scheme where vertical advection is time-weighted between the explicit (using QUICKEST) and implicit parts results if **[THETA]** is set to 0.5 or greater. The following is a description of QUICKEST, the preferred transport scheme.

Non-Uniform Grid QUICKEST Formulation

In one dimension, the conservative control volume advective transport of a constituent Φ integrated over a timestep is:

$$\Phi_i^{n+1} = \Phi_i^n - \frac{\Delta t}{\Delta x} (U_r \Phi_r^n - U_l \Phi_l^n) \quad (\text{A-116})$$

where:

- Φ_i = constituent concentration at a grid point, $g\ m^{-3}$
- $\Phi_{r,l}$ = right and left cell face constituent concentrations, $g\ m^{-3}$
- $U_{r,l}$ = right and left cell face velocity, $m\ s^{-1}$
- t = time, s

The QUICKEST algorithm was originally derived using an upstream weighted quadratic interpolation function defined over three uniformly spaced grid points. This interpolation function estimates cell face concentrations required by the conservative control volume transport scheme. For example, the right cell face concentration estimate for a flow positive to the right is:

$$\Phi_r = T_{i-1} \Phi_{i-1} + T_i \Phi_i + T_{i+1} \Phi_{i+1} \quad (\text{A-117})$$

where T are advective multipliers which weight the contribution of three adjacent grid point concentrations.

The advective multipliers are obtained by collecting terms associated with each constituent defined by the QUICKEST advection operator. For a non-uniform grid, a combination of two and three point Lagrangian interpolation functions (Henrici, 1964) are used to compute the QUICKEST estimate for the right cell face concentration centered about cells i and $i+1$:

$$\Phi_r = P_1(x) - \frac{U\Delta t}{2} P_2(x) + \left[D_x \Delta t - \frac{1}{6} \left[\Delta x^2 - (U\Delta t)^2 \right] \right] P_2''(x) \quad (\text{A-118})$$

where:

x = the local right cell face position

D_x = diffusion coefficient

Defining a local coordinate system of three non-uniformly spaced grid cells denoted by x_{i-1} , x_i and x_{i+1} with corresponding constituent values, the interpolation functions required in equation A-118 are:

$$P_1(x) = \frac{(x - x_i)}{(x_{i+1} - x_i)} \Phi_{i+1} + \frac{(x_{i+1} - x)}{(x_{i+1} - x_i)} \Phi_i \quad (\text{A-119})$$

$$P_2(x) = \frac{(x - x_i)(x - x_{i-1})}{(x_{i+1} - x_i)(x_{i+1} - x_{i-1})} \Phi_{i+1} + \frac{(x - x_{i+1})(x - x_{i-1})}{(x_i - x_{i+1})(x_i - x_{i-1})} \Phi_i \quad (\text{A-120})$$

$$+ \frac{(x - x_{i+1})(x - x_i)}{(x_{i-1} - x_{i+1})(x_{i-1} - x_i)} \Phi_{i-1}$$

Taking the first derivative of $P_1(x)$ and the second derivative of $P_2(x)$ and substituting into equation A-118, it is then possible to group terms and obtain the advective multipliers. For example, the T_{i+1} multiplier is:

$$T_{i+1} = \frac{(x - x_i)}{(x_{i+1} - x_i)} - \frac{U \Delta t}{2} \frac{[(x - x_i) + (x - x_{i-1})]}{(x_{i+1} - x_i)(x_{i+1} - x_{i-1})} \quad (\text{A-121})$$

$$+ \frac{2 \left(D_x \Delta t - \frac{1}{6} \left[\Delta x_i^2 - (U \Delta t)^2 \right] \right)}{(x_{i+1} - x_i)(x_{i+1} - x_{i-1})}$$

Similar functions are obtained for T_i and T_{i-1} multipliers that complete the formulation for the QUICKEST algorithm.

From a computational standpoint, most geometric components of the multipliers are time-invariant and are computed once and stored in arrays. The time-varying part of the multipliers (U , Δt , D_x) are updated each timestep during computation of the T arrays. However, when the QUICKEST scheme is applied vertically, the spatial part of the multipliers for layers [KT] and [KT]+1 are updated each timestep to accommodate the surface elevation fluctuation.

ULTIMATE/QUICKEST Numerical Transport Solution Scheme

In Version 2, the QUICKEST numerical scheme replaced the upwind numerical scheme used in Version 1 for solving the advective terms in the advection-diffusion equation. Compared to the upwind scheme, QUICKEST resulted in improved numerical accuracy in simulating sharp fronts since the upwind transport scheme adds excessive numerical diffusion.

A problem with the QUICKEST scheme is that it can give rise to spurious oscillations at the leading and trailing edge of a sharp front or gradient. This can occur where there are fresh/salt water interfaces, point source discharges, or cases of strong temperature stratification. Even though the upwind scheme always gives physically realistic solutions, it introduces numerical diffusion that artificially reduces sharp gradients.

An improvement was introduced by Leonard (1991) that eliminated spurious oscillations but preserved the higher-order solution scheme of QUICKEST. This technique is a universal (in the sense that it can be applied to numerical schemes other than QUICKEST) limiter for maintaining monotonic profiles near a gradient and is called the ULTIMATE solution scheme.

In order to illustrate the scheme, consider the solution of the unsteady advective equation:

$$\frac{\partial B\Phi}{\partial t} + \frac{\partial BU\Phi}{\partial x} = 0 \quad (\text{A-122})$$

where:

- Φ = concentration, $g\ m^{-3}$
- B = width, m
- U = velocity, $m\ s^{-1}$
- x = longitudinal coordinate, m
- t = time, s

The finite difference scheme for this based on a positive flow ($U > 0$) is:

$$\Phi_i^{n+1} = \frac{1}{B_i^{n+1}} \left(B_i^n \Phi_i^n - \left\{ \left[\frac{UB\Delta t}{\Delta x} \right]_R \Phi_R - \left[\frac{UB\Delta t}{\Delta x} \right]_L \Phi_L \right\} \right) \quad (\text{A-123})$$

The value i refers to the center grid point, R is the right-hand face value, and L is the left hand face value ([Figure A-22](#)).

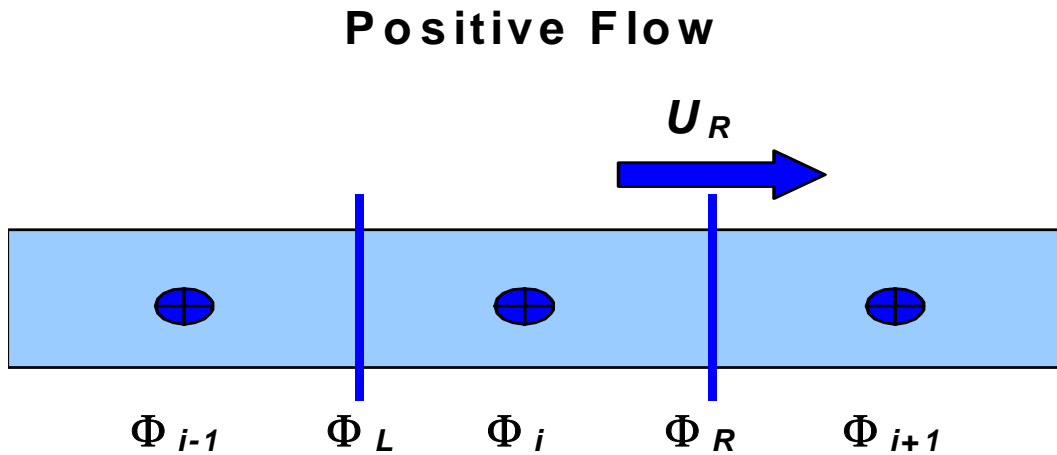


Figure A-22. ULTIMATE schematization for positive flow.

where:

- Φ_{i-1} = upstream concentration, $g\ m^{-3}$
- Φ_i = center concentration, $g\ m^{-3}$
- Φ_{i+1} = downstream concentration, $g\ m^{-3}$
- Φ_L = left face concentration, $g\ m^{-3}$
- Φ_R = right face concentration, $g\ m^{-3}$
- U_r = right face horizontal velocity, $m\ s^{-1}$

Figure A-23 shows a sketch of variables used for a negative flow. The term $U\Delta t / \Delta x$ is called the Courant number. The problem to resolve is how to choose the concentrations at the “face” values since concentrations are defined at the center of a cell. An upwinding scheme would say that the concentration at the left face is Φ_{i-1} and the concentration at the right face is Φ_i for positive flow. In order to improve numerical accuracy, there are other higher-order numerical techniques, such as QUICKEST (Leonard, 1979), to estimate these face values. In CE-QUAL-W2, Φ_R and Φ_L are initially computed based on the QUICKEST method. However, if the criteria for a monotonic solution are violated, the values for Φ_R and Φ_L are revised to assure a monotonic solution. This is the essence of the ULTIMATE algorithm that eliminates over/undershoots in the numerical transport scheme.

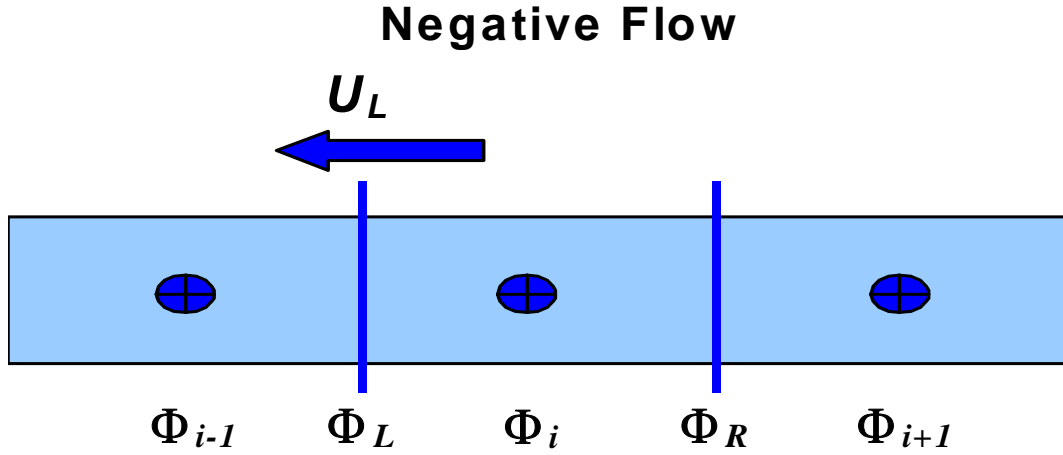


Figure A-23. ULTIMATE schematization for negative flow.

where:

- Φ_{i-1} = downstream concentration, $g\ m^{-3}$
- Φ_i = center concentration, $g\ m^{-3}$
- Φ_{i+1} = upstream concentration, $g\ m^{-3}$
- Φ_L = left face concentration, $g\ m^{-3}$
- Φ_R = right face concentration, $g\ m^{-3}$
- U_L = left face horizontal velocity, $m\ s^{-1}$

To outline the procedure for simple conditions, the velocity, segment spacing and segment widths are assumed constant, so that Equation A-123 can be written as:

$$\Phi_i^{n+1} = \left(\Phi_i^n - \left\{ \left[\frac{U\Delta t}{\Delta x} \right] \Phi_R - \left[\frac{U\Delta t}{\Delta x} \right] \Phi_L \right\} \right) \quad (\text{A-124})$$

Defining normalized variables based on:

$$\tilde{\Phi} = \frac{\Phi - \Phi_{i-1}^n}{\Phi_{i+1}^n - \Phi_{i-1}^n}, \quad (\text{A-125})$$

for location i (the center location) and the right face value for positive flow as in [Figure A-22](#), we have the following:

$$\tilde{\Phi}_i^n = \frac{\Phi_i^n - \Phi_{i-1}^n}{\Phi_{i+1}^n - \Phi_{i-1}^n} \quad (\text{A-126})$$

$$\tilde{\Phi}_R = \frac{\Phi_R - \Phi_{i-1}^n}{\Phi_{i+1}^n - \Phi_{i-1}^n} \quad (\text{A-127})$$

$$\text{If } \tilde{\Phi}_R \leq \left[\frac{\tilde{\Phi}_i^n}{U\Delta t / \Delta x} \right]_R \text{ for } 0 < \tilde{\Phi}_i^n \leq 1 \quad (\text{A-128})$$

$$\tilde{\Phi}_i^n \leq \tilde{\Phi}_R \leq 1 \text{ for } 0 < \tilde{\Phi}_i^n \leq 1 \quad (\text{A-129})$$

$$\tilde{\Phi}_i^n = \tilde{\Phi}_R \text{ for } \tilde{\Phi}_i^n < 0 \text{ or } \tilde{\Phi}_i^n > 1 \quad (\text{A-130})$$

The face value is unadjusted from that computed by the numerical scheme and the QUICKEST value of Φ_R is used without alteration. These conditions are shown as the shaded region in [Figure A-24](#).

If these conditions are not met, then Φ_R is adjusted to force a monotonic solution. The value of the face is replaced with the nearest allowable value of $\tilde{\Phi}_R$ based on the above criteria that will ensure these criteria are met. The face value is determined by using:

$$\Phi_R = \Phi_{i-1}^n + \tilde{\Phi}_R (\Phi_{i+1}^n - \Phi_{i-1}^n) \quad (\text{A-131})$$

This procedure is applied to all the faces and then Equation A-124 is solved to update the concentration at the next time level. This means that the right face concentration will be the left face concentration for the next segment thus ensuring mass conservation.

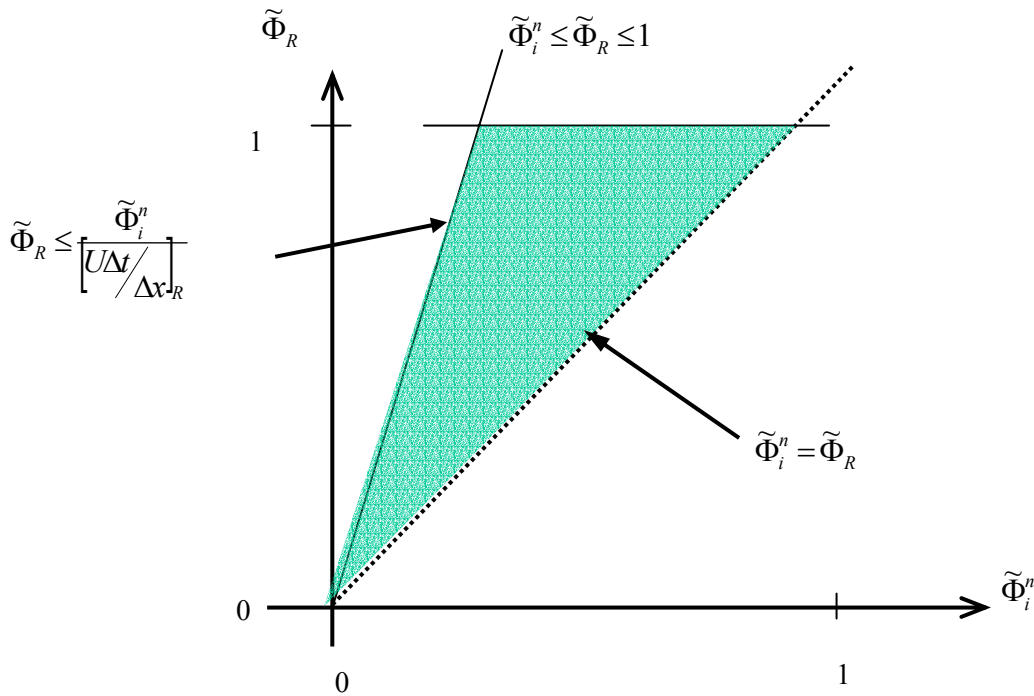


Figure A-24. Definition sketch for monotonic solution domain.

According to tests performed by Lin and Falconer (1997), the QUICKEST-ULTIMATE scheme with splitting of the diffusion and source/sink terms conserved mass and eliminated numerical oscillations. Leonard (1991) also indicated that the QUICKEST scheme coupled with the ULTIMATE scheme was numerically accurate and cost-effective in terms of computational time.

[Figure A-25](#) shows the results of a square pulse of 100 g m^{-3} moving downstream using the UPWIND, QUICKEST, and ULTIMATE/QUICKEST numerical transport schemes. The UPWIND scheme has a large amount of numerical diffusion whereas the QUICKEST scheme has non-physical oscillations about the leading and trailing edge of the solution. The ULTIMATE/QUICKEST numerical solution greatly reduces numerical diffusion and eliminates the over and undershoots.

For any case of unequal grid spacing, the order of accuracy diminishes. Leonard (1991) recommends that if used with non-uniform grid spacing, the formal accuracy of the method is only preserved if the grid does not expand or contract more than about 125%.

Even though the ULTIMATE scheme can be used with any suitable numerical technique, Leonard (1991) indicates that when coupled with the 3rd order QUICKEST scheme and a 2nd order central difference diffusion operator, the results are virtually indistinguishable from other higher-order advection solvers.

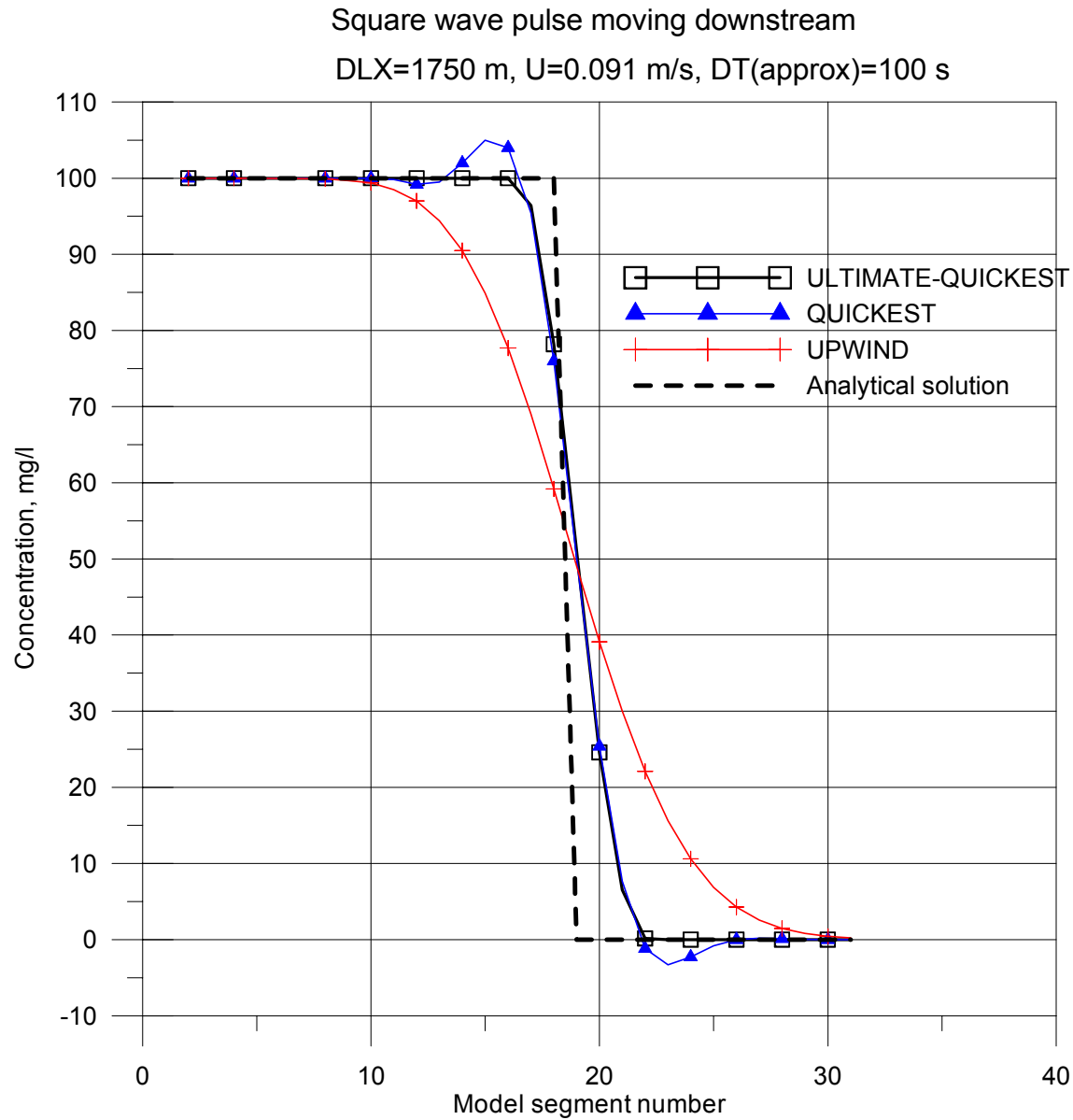


Figure A-25. Comparison of UPWIND, QUICKEST, and ULTIMATE/QUICKEST schemes for conservative tracer transport.

The following shows a straightforward procedure by Leonard to compute the right and left face values if they do not meet the monotonic criteria, as well as a procedure for variable velocities.

Based on the sign of the velocity for each face, compute DEL:

$$DEL = \Phi_{i+1}^n - \Phi_{i-1}^n \tag{A-132}$$

If $|DEL| < 10^{-5}$ set $\Phi_{face} = \Phi_i^n$ and proceed to the next face (the face value is the L or R face as shown in). Otherwise, compute:

$$\tilde{\Phi}_i^n = \frac{\Phi_i^n - \Phi_{i-1}^n}{\Phi_{i+1}^n - \Phi_i^n} = \frac{\Phi_i^n - \Phi_{i-1}^n}{DEL} \quad (\text{A-133})$$

If $\tilde{\Phi}_i^n < 0$ or $\tilde{\Phi}_i^n > 1$, set $\Phi_{face} = \Phi_i^n$ and proceed to the next face. If not, compute:

$$\tilde{\Phi}_{face} = \frac{\Phi_{face} - \Phi_{i-1}^n}{\Phi_{i+1}^n - \Phi_{i-1}^n} = \frac{\Phi_{face} - \Phi_{i-1}^n}{DEL} \quad (\text{A-134})$$

where Φ_{face} is computed based on the user's chosen numerical scheme (such as QUICKEST or another scheme).

1. If $\tilde{\Phi}_{face} < \tilde{\Phi}_i^n$, $\tilde{\Phi}_{face} = \tilde{\Phi}_i^n$
2. if $\tilde{\Phi}_{face} > \frac{\tilde{\Phi}_i^n}{\left(\frac{U\Delta t}{\Delta x}\right)}$, $\tilde{\Phi}_{face} = \frac{\tilde{\Phi}_i^n}{\left(\frac{U\Delta t}{\Delta x}\right)}$
3. if $\tilde{\Phi}_{face} > 1$, $\tilde{\Phi}_{face} = 1$

Then recompute the face value according to $\Phi_{face} = \tilde{\Phi}_{face} DEL + \Phi_i^n$.

Once all the face values are determined, use the finite difference form of the solution to determine the solution (Equation A-123)

Leonard (1991) also showed a numerical technique that minimized the computational burden when using ULTIMATE with the QUICKEST scheme. This technique is described as follows.

Based on the sign of the velocity for each face, define C, D, and U nodes (center, downstream, and upstream) corresponding for positive flow to i, i+1, and i-1, respectively.

Compute DEL and CURV, where $DEL = \Phi_{i+1}^n - \Phi_i^n$ and $CURV = \Phi_{i+1}^n - 2\Phi_i^n + \Phi_{i-1}^n$

1. If $|CURV| \leq 0.6|DEL|$, then use the QUICKEST computed value for the face value, Φ_{face} (the face value is the R or L face as shown in).
2. If not, and if $|CURV| \geq |DEL|$, then set $\Phi_{face} = \Phi_i^n$
3. If not, and $DEL > 0$, limit Φ_{face} by Φ_i^n below, or the smaller of

$$\Phi_{reference} = \Phi_{i-1}^n + \frac{(\Phi_i^n - \Phi_{i-1}^n)}{\left(\frac{U\Delta t}{\Delta x}\right)} \text{ and } \Phi_{i+1}^n$$

4. If not, and $DEL < 0$, limit Φ_{face} by Φ_i^n , or the larger of $\Phi_{reference} = \Phi_{i-1}^n + \frac{(\Phi_i^n - \Phi_{i-1}^n)}{\left(\frac{U\Delta t}{\Delta x}\right)}$

and Φ_{i+1}^n

5. Once all the face values are determined, use Equation A-123 to obtain the solution .

The procedure outlined above is based on unidirectional and uniform magnitude velocity and segment widths. If the velocity regime and widths are variable, then the following procedure is followed in order to maintain a monotonic solution. Consider the following limitations based on definitions shown in [Figure A-26](#).

Positive flow at right face, $U > 0$

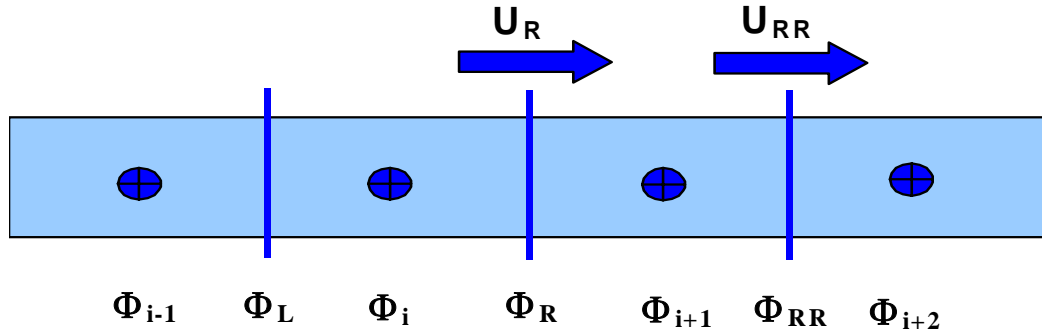


Figure A-26. Definition sketch for variable velocity.

where:

- Φ_{i-1} = upstream concentration
- Φ_i = center concentration
- Φ_{i+1} = center concentration
- Φ_L = left face concentration at i
- Φ_R = right face concentration at i
- Φ_{RR} = right face concentration at $i+1$

Assuming that U_R is positive and the concentration times width (ΦB) increases monotonically, i.e., $(B\Phi)_{i-1}^n < (B\Phi)_i^n < (B\Phi)_{i+1}^n < (B\Phi)_{i+2}^n$, between segment $i-1$ and $i+2$, then the goal of the technique is to estimate Φ_R , or really $B_R \Phi_R$, and to update the concentration using Equation A-123. Equation A-123 can be written as a condition for Φ_R as:

$$\left[\frac{UB\Delta t}{\Delta x} \right]_R \Phi_R = B_i^n \Phi_i^n - \Phi_i^{n+1} B_i^{n+1} + \left[\frac{UB\Delta t}{\Delta x} \right]_L \Phi_L \tag{A-135}$$

If it is assumed that $B_i^n \Phi_i^n \leq B_R \Phi_R \leq B_{i+1}^n \Phi_{i+1}^n$, then this is equivalent to saying that $B_i^n U_i^n \Phi_i^n \leq B_R^n U_R^n \Phi_R \leq B_{i+1}^n U_{i+1}^n \Phi_{i+1}^n$ or that the net flux into a segment is increasing.

Using the monotonic limitation that $B_i^{n+1} \Phi_i^{n+1} \geq B_{i-1}^n \Phi_{i-1}^n$ then Equation A-135 becomes:

$$\left[\frac{UB\Delta t}{\Delta x} \right]_R \Phi_R \leq B_i^n \Phi_i^n - \Phi_{i-1}^n B_{i-1}^n + \left[\frac{UB\Delta t}{\Delta x} \right]_L \Phi_L \quad (\text{A-136})$$

Then making a conservative assumption that $B_L \Phi_L \geq B_{i-1}^n \Phi_{i-1}^n$, Equation A-136 becomes:

$$\left[\frac{UB\Delta t}{\Delta x} \right]_R \Phi_R \leq B_i^n \Phi_i^n - \Phi_{i-1}^n B_{i-1}^n + \left[\frac{UB\Delta t}{\Delta x} \right]_{i-1}^n \Phi_{i-1}^n \quad (\text{A-137})$$

Another condition is also imposed on $B_R \Phi_R$ by looking at the control volume segment centered at $i+1$. Using similar reasoning as above and assuming that $U_{RR} > 0$, the other criterion for $B_R \Phi_R$ is

$$\left[\frac{UB\Delta t}{\Delta x} \right]_R \Phi_R \leq B_{i+2}^n \Phi_{i+2}^n - \Phi_{i+1}^n B_{i+1}^n + \left[\frac{UB\Delta t}{\Delta x} \right]_{RR} \Phi_{i+1}^n \quad (\text{A-138})$$

These criteria would be altered appropriately if the function were monotonically decreasing rather than increasing.

Vertical Implicit Transport

Focusing on vertical advective and diffusive transport, constituent transport can be written as:

$$\frac{\partial B\Phi}{\partial t} + \frac{\partial WB\Phi}{\partial z} - \frac{\partial}{\partial z} \left(BD_z \frac{\partial \Phi}{\partial z} \right) = RHS \quad (\text{A-139})$$

where RHS represents horizontal transport and all sources/sinks. Integrating the transport equation vertically and over time gives:

$$BH \Phi^{n+1} + \theta H \Delta t \delta_z (WB \Phi^{n+1}) - H \Delta t \delta_z \left(BD_z \frac{\partial \Phi^{n+1}}{\partial z} \right) = BH \Phi^* \quad (\text{A-140})$$

where:

- Φ^* = all n-time level horizontal and explicit vertical transport and sources/sinks
- θ = time-weighting for vertical advection; 0 for fully explicit, 0.55 for Crank-Nicholson, and 1 for fully implicit

Expanding the differential operators in terms of central differences and collecting terms, the above equation can be recast as:

$$A_{t,i} \Phi_{i-1}^{n+1} + V_{t,i} \Phi_i^{n+1} + C_{t,i} \Phi_{i+1}^{n+1} = D_{t,i} \quad (\text{A-141})$$

where:

$$V_{t,i} = 1 + \frac{\Delta t}{BH_{ki}} \left[\theta \left(\frac{W_{ki} B_{bki} - W_{k-1,i} B_{bk-1,i}}{2} \right) + \frac{B_{bki} D_{zki}}{\bar{H}_k} + \frac{B_{bk-1,i} D_{zk-1,i}}{\bar{H}_{k-1}} \right]$$

$$A_{t,i} = \frac{\Delta t B_{bki}}{BH_{ki}} \left(\theta \frac{W_{k,i}}{2} - \frac{D_{zki}}{\bar{H}_k} \right)$$

$$C_{t,i} = - \frac{\Delta t B_{bk-1,i}}{BH_{ki}} \left(\theta \frac{W_{k-1,i}}{2} + \frac{D_{zk-1,i}}{\bar{H}_{k-1}} \right)$$

The coefficients are computed once, stored in arrays, and used to update each constituent. This is accomplished by loading the explicit part of the solution, Φ^* , with each successive constituent and inverting the resulting matrix via a Thomas tridiagonal solver.

Auxiliary Functions

Auxiliary functions are relationships that describe processes independent of basic hydrodynamic and transport computational schemes in the model. Auxiliary functions include turbulent dispersion and wind shear processes, heat exchange (including ice cover), evaporation, hydraulic structures, density, and selective withdrawal.

Surface Shear Stress

Referring to [Figure A-27](#), the shear stress at the water surface is defined as

$$\tau_s = C_D \rho_a (W_h - u_s)^2 \cong C_D \rho_a (W_h)^2 \quad (\text{A-142})$$

where:

- τ_s = surface shear stress at water surface
- u_s = surface velocity in water
- W_h = wind velocity measured at a distance h above water surface in direction of shear
- C_D = drag coefficient
- ρ_a = air density

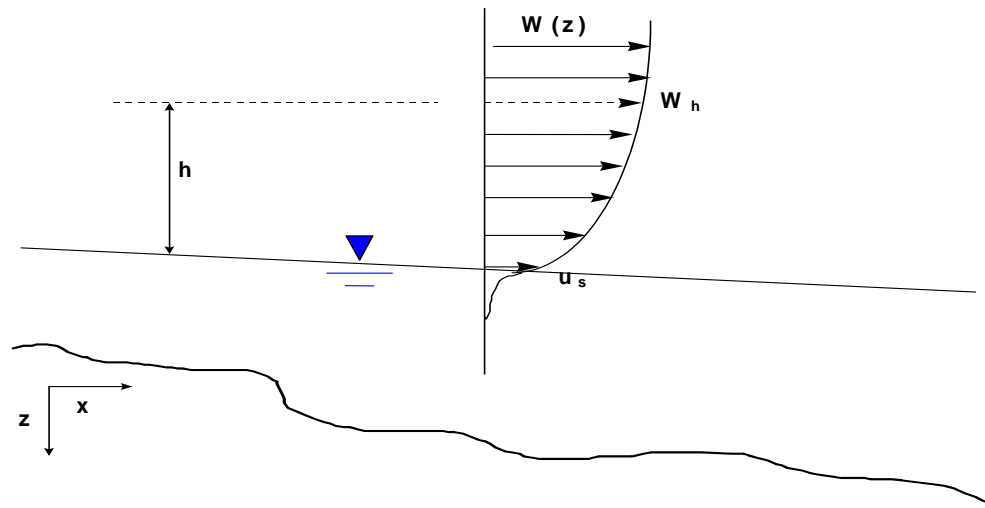


Figure A-27. Shear stress at the air-water surface.

Note that this relationship leads to the “3% rule” for surface currents:

$$\tau_s = \underbrace{C_D \rho_a}_{\text{air}} (W_h - u_s)^2 = \underbrace{C_D \rho_w}_{\text{water}} u_s^2 \quad (\text{A-143})$$

$$\text{if } C_{D_{\text{air}}} \sim C_{D_{\text{water}}}, \text{ then } \underbrace{u_s}_{\text{3\% rule}} \sim 0.03 W_h$$

Usually the drag coefficient is a function of the measurement height, h , above the water surface. Most drag coefficient formulae have been determined based on a 10 m wind speed measurement height. If wind speeds are taken at other measurement heights for the shear stress calculation, these should be corrected to 10 m .

The wind speed is a function of measurement height. To correct the measurement height to an elevation z , use the following approach.

Assuming a logarithmic boundary layer:

$$\frac{W_z}{W_{z_1}} = \frac{\ln\left(\frac{z}{z_0}\right)}{\ln\left(\frac{z_1}{z_0}\right)} \quad (\text{A-144})$$

where:

W_z = desired wind speed at elevation z

W_{z_1} = known wind speed at height z_1

z_0 = wind roughness height (assume 0.003 ft for wind < 5 mph and 0.015 for wind > 5 mph , range 0.0005 to 0.03 ft)

This term can then be used to compute the surface stress in the direction of the x-axis and the cross-shear (the cross-shear term will be used in the turbulent shear stress algorithm) as follows:

$$\tau_{wx} \cong C_D \rho_a W_h^2 \cos(\Theta_1 - \Theta_2) \tag{A-145}$$

$$\tau_{wy} \cong C_D \rho_a W_h^2 \sin(\Theta_1 - \Theta_2) \tag{A-146}$$

where:

- τ_{wx} = surface shear stress along x-axis due to wind
- τ_{wy} = surface shear stress along lateral direction due to wind
- Θ_1 = wind orientation relative to North, radians

Segment and wind orientation are illustrated in [Figure A-28](#) and [Figure A-29](#). The angles are measured in radians clockwise from north. A wind from the east would have an angle of $\pi/2$ radians, π radians from the south, $3\pi/2$ radians from the west, and 0 or 2π radians from the north.

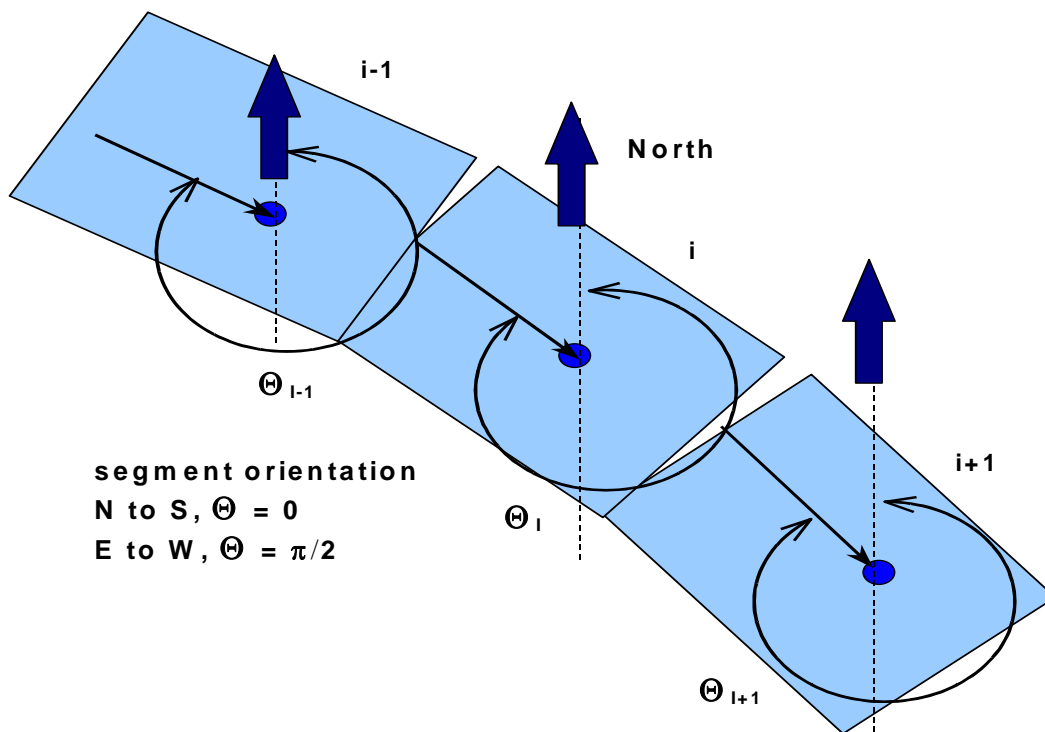


Figure A-28. Segment orientation.

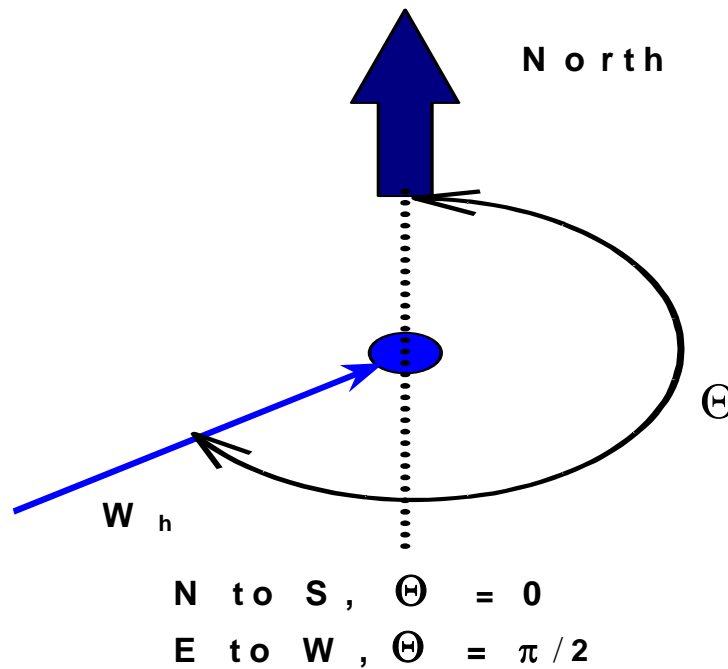


Figure A-29. Wind orientation.

The drag coefficient based on a 10 m measurement height, C_D , is defined as:

1. For $W_h < 1 \text{ m s}^{-1}$, $C_D = 0.0$
2. For $1 \leq W_h < 15 \text{ m s}^{-1}$, $C_D = 0.0005 W_h^{0.5}$
3. For $W_h \geq 15 \text{ m s}^{-1}$, $C_D = 0.0026$

In addition, a fetch correction to the wind velocity can be used as determined by Fang and Stefan (1994). This correction is described in Appendix B under [Dissolved Oxygen](#), but is not applicable to rivers.

Bottom Shear Stress

The shear stress is defined along the bottom of each cell (or for each cell in contact with side walls or channel bottom) as

$$\tau_b = \frac{\rho_w g}{C^2} U |U| \quad (\text{A-147})$$

where:

- C = Chezy friction coefficient
- U = longitudinal velocity
- ρ_w = density of water

Also, the model user can specify a Manning’s friction factor where the Chezy coefficient is related to the Manning’s friction factor (SI units) as

$$C = (1/n)R^{1/6} \tag{A-148}$$

where:

- n = Manning’s friction factor
- R = hydraulic radius

In Version 2, the bottom shear stress was applied only to the bottom of each layer. In the new version, the sidewall friction is accounted for because of its greater importance in river systems. The user can input either the Chezy or Manning’s coefficient for each model segment.

Vertical Shear Stress

The algorithm for the vertical shear stress is

$$\frac{\tau_{xz}}{\rho} = \nu_t \frac{\partial U}{\partial z} = A_z \frac{\partial U}{\partial z} \tag{A-149}$$

In Version 3, the user must specify which formulation to use for A_z or ν_t . The formulations are shown in [Table A-2](#).

Table A-2. Version 3 vertical eddy viscosity formulations.

Formulation	Formula	Reference
Nickuradse (NICK)	$\nu_t = \ell_m^2 \left \frac{\partial u}{\partial z} \right e^{-CR_i}$ $\ell_m = H \left[0.14 - 0.08 \left(1 - \frac{z}{H} \right)^2 - 0.06 \left(1 - \frac{z}{H} \right)^4 \right]$	Rodi (1993)
Parabolic (PARAB)	$\nu_t = \kappa U_* z \left(1 - \frac{z}{H} \right) e^{-CR_i}$	Engelund (1976)
W2 (used in Version 2)	$\nu_t = \kappa \left(\frac{l_m^2}{2} \right) \sqrt{\left(\frac{\partial U}{\partial z} \right)^2 + \left(\frac{\tau_{wy} e^{-2kz} + \tau_{y \text{ tributary}}}{\rho \nu_t} \right)^2} e^{-(CR_i)}$ $\ell_m = \Delta z_{\max}$	Cole and Buchak (1995)
W2 with mixing length of Nickuradse (W2N)	$\nu_t = \kappa \left(\frac{l_m^2}{2} \right) \sqrt{\left(\frac{\partial U}{\partial z} \right)^2 + \left(\frac{\tau_{wy} e^{-2kz} + \tau_{y \text{ tributary}}}{\rho \nu_t} \right)^2} e^{-(CR_i)}$ $\ell_m = H \left[0.14 - 0.08 \left(1 - \frac{z}{H} \right)^2 - 0.06 \left(1 - \frac{z}{H} \right)^4 \right]$	Cole and Buchak (1995) and Rodi (1993)

Formulation	Formula	Reference															
RNG (re-normalization group)	$v_t = \nu \left[1 + \Psi \left(3\kappa \left(\frac{zu_*}{\nu} \right)^3 \left(1 - \frac{z}{H} \right)^3 - C_1 \right) \right]^{1/3} e^{-CRi}$	Simoes (1998)															
TKE (Turbulent kinetic energy)	$v_t = C_\mu \frac{k^2}{\varepsilon}$ <p>where k and ε are defined from</p> $\frac{\partial k B}{\partial t} + \frac{\partial k B U}{\partial x} + \frac{\partial k B W}{\partial z} - \frac{\partial}{\partial z} \left(B \frac{v_t}{\sigma_k} \frac{\partial k}{\partial z} \right) - \frac{\partial}{\partial x} \left(B \frac{v_t}{\sigma_k} \frac{\partial k}{\partial x} \right) = B(P + G - \varepsilon + P_k)$ $\frac{\partial \varepsilon B}{\partial t} + \frac{\partial \varepsilon B U}{\partial x} + \frac{\partial \varepsilon B W}{\partial z} - \frac{\partial}{\partial z} \left(B \frac{v_t}{\sigma_\varepsilon} \frac{\partial \varepsilon}{\partial z} \right) - \frac{\partial}{\partial x} \left(B \frac{v_t}{\sigma_\varepsilon} \frac{\partial \varepsilon}{\partial x} \right) = B \left(C_{\varepsilon 1} \frac{\varepsilon}{k} P + C_{\varepsilon 2} \frac{\varepsilon^2}{k} + P_\varepsilon \right)$	Wells (2003)															
<p>where:</p> <table style="width:100%; border:none;"> <tr> <td>ℓ_m = mixing length</td> <td>C = constant (assumed 0.15)</td> <td>k = wave number</td> </tr> <tr> <td>z = vertical coordiante</td> <td>u = shear velocity</td> <td>ρ = liquid density</td> </tr> <tr> <td>H = depth</td> <td>κ = von Karman constant</td> <td>$\Psi(x) = \max(0,x)$</td> </tr> <tr> <td>u = horizontal velocity</td> <td>τ_{wy} = cross-shear from wind</td> <td>ν = molecular viscosity</td> </tr> <tr> <td>Ri = Richardson number</td> <td>ΔZ_{max} = maximum vertical grid spacing</td> <td>C_1 = empirical constant, 100</td> </tr> </table>			ℓ_m = mixing length	C = constant (assumed 0.15)	k = wave number	z = vertical coordiante	u = shear velocity	ρ = liquid density	H = depth	κ = von Karman constant	$\Psi(x) = \max(0,x)$	u = horizontal velocity	τ_{wy} = cross-shear from wind	ν = molecular viscosity	Ri = Richardson number	ΔZ_{max} = maximum vertical grid spacing	C_1 = empirical constant, 100
ℓ_m = mixing length	C = constant (assumed 0.15)	k = wave number															
z = vertical coordiante	u = shear velocity	ρ = liquid density															
H = depth	κ = von Karman constant	$\Psi(x) = \max(0,x)$															
u = horizontal velocity	τ_{wy} = cross-shear from wind	ν = molecular viscosity															
Ri = Richardson number	ΔZ_{max} = maximum vertical grid spacing	C_1 = empirical constant, 100															

The model user can also specify the maximum value of the vertical eddy viscosity **AZMAX1**, but this value is only used with the W2N and W2 formulations. This value is specified because the time step for numerical stability is greatly reduced when solving the momentum equations using an explicit numerical technique. In addition, the model user can choose whether to compute the vertical momentum transfer with the longitudinal momentum equation using an implicit or an explicit numerical technique. The explicit formulation was used in Version 2 with a fixed **AZMAX1** of $1.0 \times 10^{-5} m^2 s^{-1}$. The implicit solution code was originally developed by Chapman and Cole and revised for Version 3.

Note that only the W2 and W2N include the effects of cross-shear from wind and from tributary or branch inflows. Hence, it is recommended to use either W2 or W2N for waterbodies with deep sections that could be stratified. The other formulations should be used for estuary or river systems where the maximum computed **AZMAX1** could be as high as 1 to $5 m^2 s^{-1}$. For the river model, the model user should use the implicit solution technique. To reproduce results from Version 2 in a stratified reservoir, set **AZMAX1** to $1.0 \times 10^{-5} m^2 s^{-1}$ and use the explicit solution.

How does one know which turbulent closure scheme to use for τ_{xz} since, according to Hamblin and Salmon (1975), "the vertical diffusion of momentum is probably the most important internal parameter" for predicting internal circulation patterns? Because of the disarray in the literature over which formulation is best, Shanahan (1980) suggested that we "use theory and literature as a guide to develop alternative viscosity functions and then test those functions in calibration runs against field

data." In the absence of expensive-to-obtain current velocity data, the use of temperature profiles is often used to test the adequacy of the hydrodynamic regime against different formulations.

Typical variations of these formulations as predicted by the model are shown in [Figure A-30](#) for Manning's friction factor and in [Figure A-31](#) for a Chezy friction factor. Comparison of the various turbulence closure theories to classical open channel flow theory for seven vertical layers is shown in [Figure A-32](#).

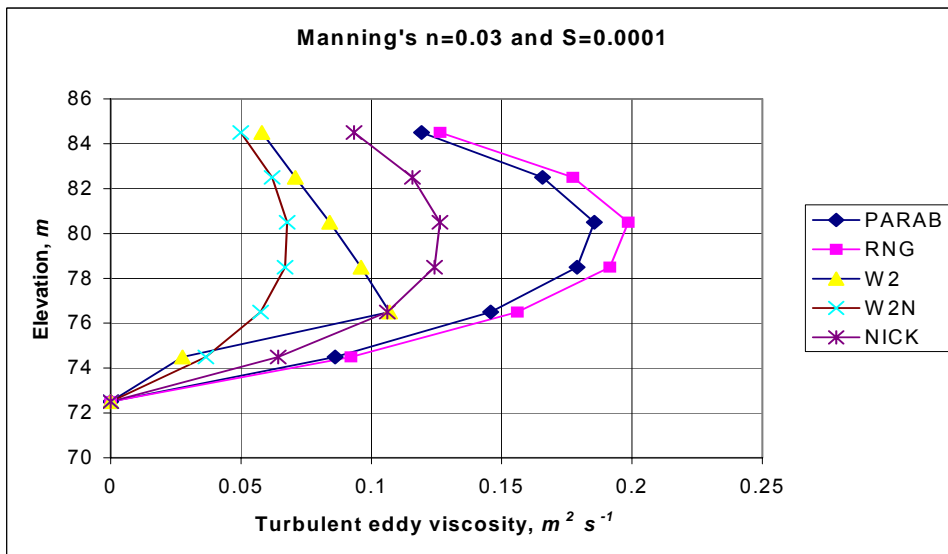


Figure A-30. Variation of turbulent vertical eddy viscosity for flow of $2574 \text{ m}^3 \text{ s}^{-1}$ flow down a channel of length 30 km and width of 100 m at $x=15 \text{ km}$.

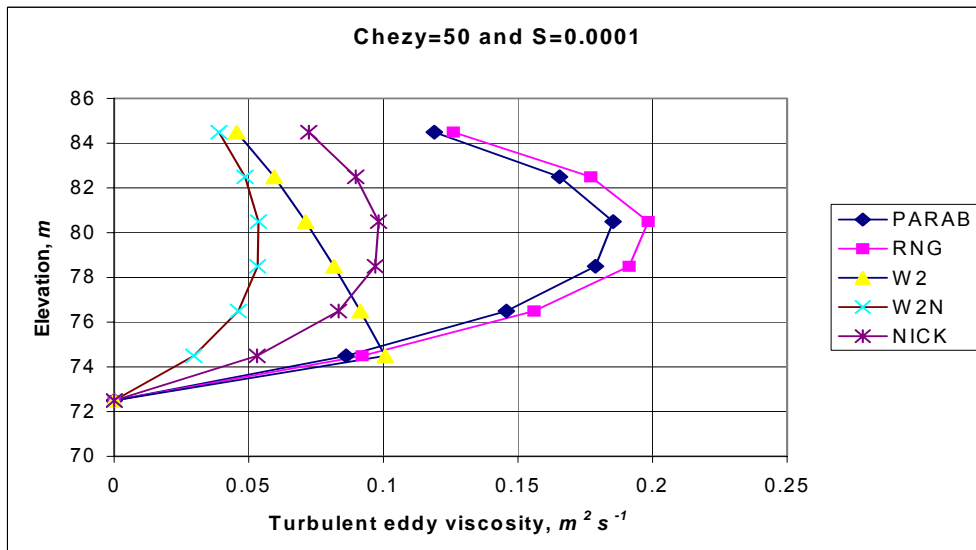


Figure A-31. Variation of turbulent vertical eddy viscosity for flow of $2574 \text{ m}^3 \text{ s}^{-1}$ flow down a channel of length 30 km and width of 100 m measured at $x=15 \text{ km}$.

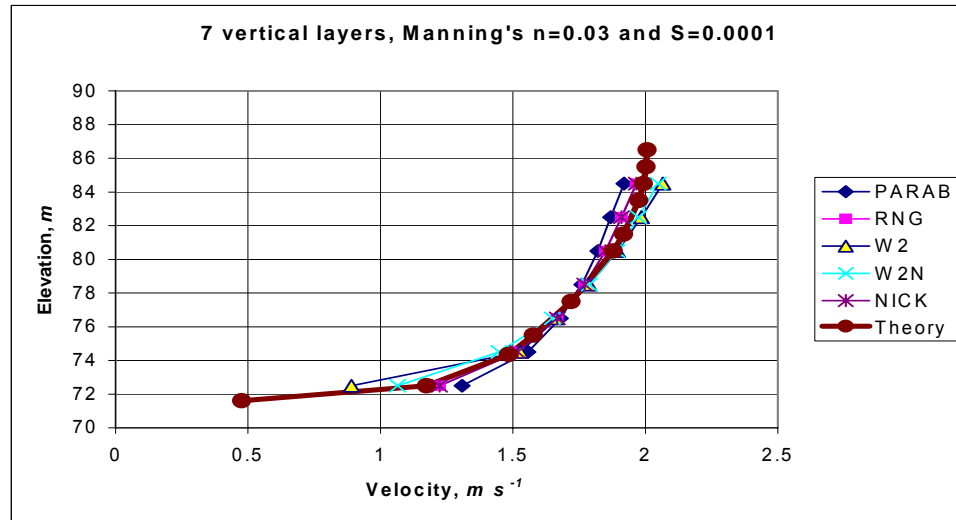


Figure A-32. Comparison of vertical velocity predictions of W2 model with various eddy viscosity models compared to theory.

Formulation

In CE-QUAL-W2, the shear stress term includes the contribution to the shear stress from surface waves induced by the wind. The wind can produce waves that produce decaying motions with depth ([Figure A-33](#)).

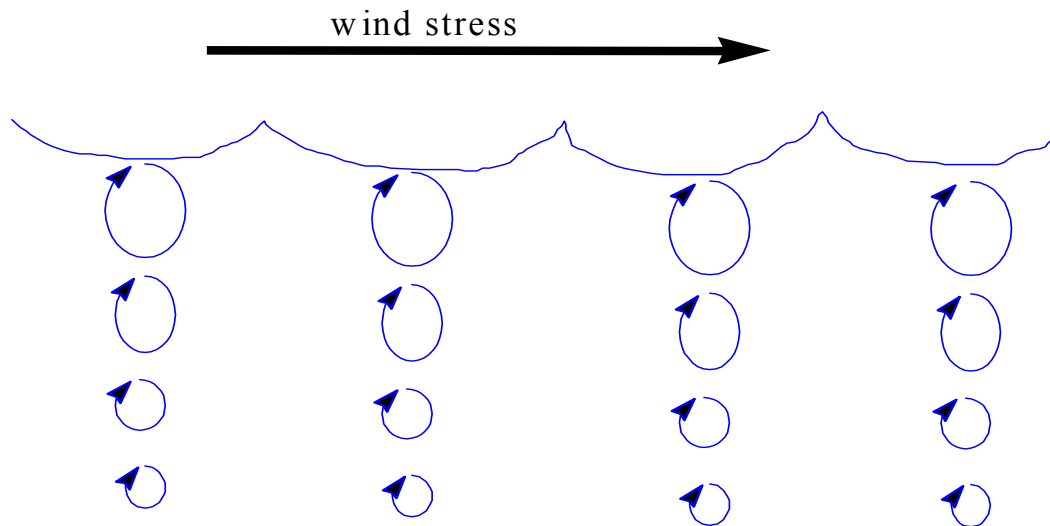


Figure A-33. Conceptual diagram of wind induced motion.

The total longitudinal shear stress for a layer is defined as having contributions from interfacial velocity shear, wind wave generated shear, and friction shear along boundaries:

$$\frac{\tau_{xz}}{\rho} = A_z \frac{\partial U}{\partial z} + \frac{\tau_{wx}}{\rho} e^{-2kz} + \frac{\tau_b}{\rho} \tag{A-150}$$

where:

τ_{wx} = longitudinal wind shear at the surface

$$k = \text{wave number} = \frac{4\pi^2}{gT_w^2}$$

$$T_w = \text{wind wave period} = 6.95E - 2F^{0.233}|W|^{0.534}$$

F = fetch length, m

The turbulent eddy viscosity was conceptualized by Prandtl as:

$$\nu_{turbulent} = \ell^2 \left| \frac{dU}{dz} \right| \quad (\text{A-151})$$

where ℓ is defined as the mixing length and can be interpreted as being proportional to the average size of large eddies or the length scale of a turbulent eddy. This length is a function of distance from a boundary or wall since the eddy sizes vary as a function of distance from a boundary. The goal in most turbulence models is the determination of the mixing length as a function of position in the fluid. Because this concept is not firmly grounded in theory, there have been many published formulations for determination of A_z in the literature (Shanahan and Harleman, 1982).

The mechanism for transporting the wind stress on the surface in the model is based on:

$$A_z = \kappa \frac{\ell^2}{2} \left[\left(\frac{\partial U}{\partial z} \right)^2 + \left(\frac{\partial V}{\partial z} \right)^2 \right]^{1/2} e^{-CRi} \quad (\text{A-152})$$

where:

$$Ri = \text{Richardson number} = \frac{g \frac{\partial \rho}{\partial z}}{\rho \left(\frac{\partial U}{\partial z} \right)^2}$$

κ = von Karman constant, 0.4

C = constant, 1.5

ℓ = vertical length scale chosen as cell thickness, Δz

The formulation is a typical mixing length formulation that is decreased or increased based on the Richardson number. The Richardson number accounts for the impact of density stratification on transfer of momentum between fluid parcels. In regions where there is no stratification, the Richardson number is zero and the exponential term is one. For regions where there is strong stratification, the Richardson number becomes large and the exponential term approaches zero.

In the longitudinal-vertical model, the lateral velocity, V , and its gradient, $\partial V/\partial z$, are due to the lateral component of wind wave motion and are assumed to be zero when averaged laterally, but not neces-

sarily the square $(\partial V/\partial z)^2$. It is assumed that cross wind shear, τ_{wy} , generates lateral wave components and decays exponentially with depth such that

$$\tau_{yz} = \tau_{wy} e^{(-2kz)} \quad (\text{A-153})$$

where:

τ_{wy} = lateral wind shear at the surface

Then using:

$$\frac{\tau_{yz}}{\rho} = A_z \frac{\partial V}{\partial z} \quad (\text{A-154})$$

The lateral velocity gradient squared becomes:

$$\left(\frac{\partial V}{\partial z}\right)^2 = \left[\frac{\tau_{wy} e^{(-2kz)}}{\rho A_z}\right]^2 \quad (\text{A-155})$$

The final equation for the vertical eddy viscosity is then:

$$A_z = \kappa \left(\frac{l^2}{2}\right) \sqrt{\left(\frac{\partial U}{\partial z}\right)^2 + \left(\frac{\tau_{wy} e^{-2kz}}{\rho A_z}\right)^2} e^{(-CR_t)} \quad (\text{A-156})$$

The above equation is implicit. In the model, this equation is explicit since the value of A_z in the lateral wind shear term is used from the previous time step. A_z is never less than the molecular kinematic viscosity for water.

The above formulation of wind shear in horizontal momentum and evaluation of A_z leads to wind driven surface currents that are three to ten percent of the surface wind velocity with higher values appearing at higher wind speeds. This is in accordance with the few attempts to relate wind speed and surface current velocity from field data appearing in the literature. With this formulation, the surface current does not reach abnormal values as it does for the case of wind shear applied only to the surface and as the surface layer thickness decreases. The depth of the wind driven surface layer increases with wind speed, and mass transport due to wind appears to be insensitive to the finite difference layer thickness.

RNG Turbulent Eddy Viscosity Formulation

The RNG model was derived from the RNG model of Yakhot and Orszag (1986) by Simoes (1998). The turbulent eddy viscosity is derived from Yakhot and Orszag (1986) as

$$\nu_t = \nu \left[1 + \Psi \left(a' \frac{\varepsilon \ell_m^4}{\nu^3} - C_1 \right) \right]^{1/3} \quad (\text{A-157})$$

where:

- $\Psi(x) = \max(0,x)$
- ν = molecular viscosity
- ν_t = turbulent eddy viscosity
- ℓ_m = mixing length
- ε = turbulent energy dissipation rate
- $a' \approx 1$
- $C_I \approx 100$

Two additional equations are necessary in determining the mixing length and the turbulent energy dissipation. For the mixing length:

$$\frac{\ell_m}{H} = \kappa \frac{z}{H} \sqrt{1 - \frac{z}{H}} \tag{A-158}$$

and for the turbulent eddy dissipation:

$$\frac{\varepsilon H}{u_*^3} = \frac{3z}{H} \left(1 - \frac{z}{H}\right)^{3/2} \tag{A-159}$$

where:

- u^* = shear velocity, $m s^{-1}$
- H = depth of the channel, m
- Z = vertical coordinate measured from the bottom of the channel, m
- κ = von Karman's constant, 0.41

Substituting these into equation A-157:

$$\nu_t = \nu \left[1 + \Psi \left(3\kappa \left(\frac{zu_*}{\nu} \right)^3 \left(1 - \frac{z}{H} \right)^3 - C_I \right) \right]^{1/3} \tag{A-160}$$

Simoes (1998) states that this model better represents experimental data than the more traditional parabolic eddy viscosity model of

$$\nu_t = \kappa z u_* \left(1 - \frac{z}{H} \right) \tag{A-161}$$

A value of ν was derived as a function of temperature based on values from Batchelor (1966) using a polynomial curve fit between 0 and 30°C.

This model was adjusted to account for stratified flow conditions by using the same Richardson number criteria as used in the original W2 model (the approach of Mamayev as quoted in French, 1985),

$$v_t = \max(v, v_{IRNG} e^{-CRi}) \quad (\text{A-162})$$

where:

$$\text{Ri} = \text{Richardson number} = \frac{g \frac{\partial \rho}{\partial z}}{\rho \left(\frac{\partial U}{\partial z} \right)^2}$$

C = empirical constant, 1.5 (French [1985] shows a value of 0.4)

The Richardson number accounts for the impact of density stratification on transfer of momentum between fluid parcels. In regions where there is no stratification, Ri=0, and the exponential term is 1.

For regions where there is strong stratification (or as $\frac{d\rho}{dz} \rightarrow \infty$), the Richardson number becomes large and the exponential term approaches 0.

Nikuradse Formulation

This model, as noted in Rodi (1993), is a mixing length model where the mixing length, ℓ_m , and eddy viscosity, v_t , are determined from

$$v_t = \ell_m^2 \left| \frac{\partial u}{\partial z} \right| \quad (\text{A-163})$$

$$\ell_m = H \left[0.14 - 0.08 \left(1 - \frac{z}{H} \right)^2 - 0.06 \left(1 - \frac{z}{H} \right)^4 \right] \quad (\text{A-164})$$

This results in a vertical distribution for the mixing length as shown in [Figure A-34](#).

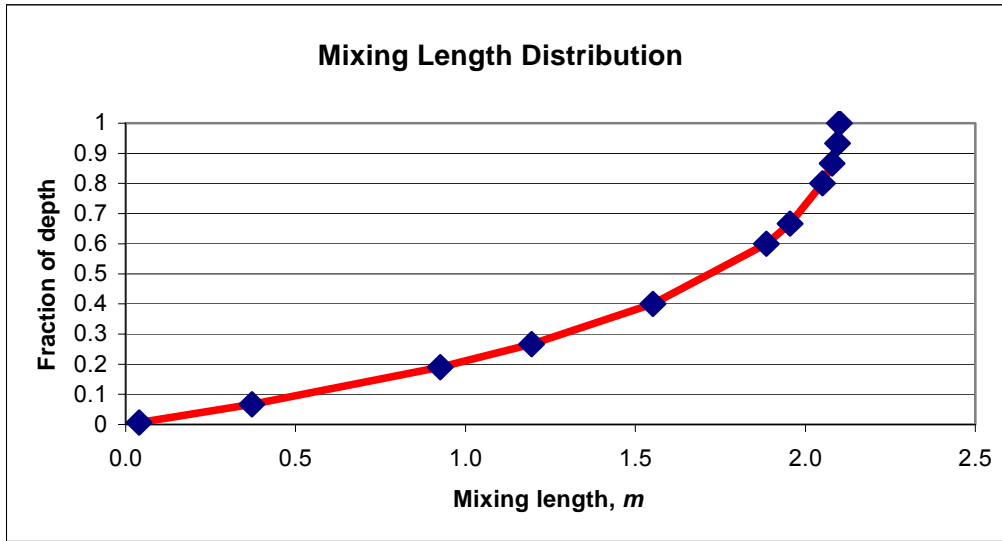


Figure A-34. Mixing length as a function of depth for the Nikuradse formulation.

The stability of the water column affects the mixing length. A Richardson number criteria has been applied to correct the mixing length for stability effects such as

$$\ell_m = \ell_{mo} (1 - 7 Ri) \quad \text{if } Ri \geq 0 \tag{A-165}$$

$$\ell_m = \ell_{mo} (1 - 14 Ri)^{-0.25} \quad \text{if } Ri < 0 \tag{A-166}$$

This is different from the approach of Munk and Anderson (1948) where the Richardson number correction was applied to the value of A_z and not the mixing length directly.

In order to be compatible with the original formulation, the computed value of A_z is corrected using the Mamayev formulation:

$$v_t = \max \left(v, v_{t_{NICK}} e^{-CRi} \right) \tag{A-167}$$

Parabolic Formulation

Another formulation is a parabolic distribution for A_z (Engelund, 1978):

$$v_t = \kappa u_* z \left(1 - \frac{z}{H} \right) \tag{A-168}$$

[Figure A-35](#) shows the spatial distribution of A_z for the parabolic model.

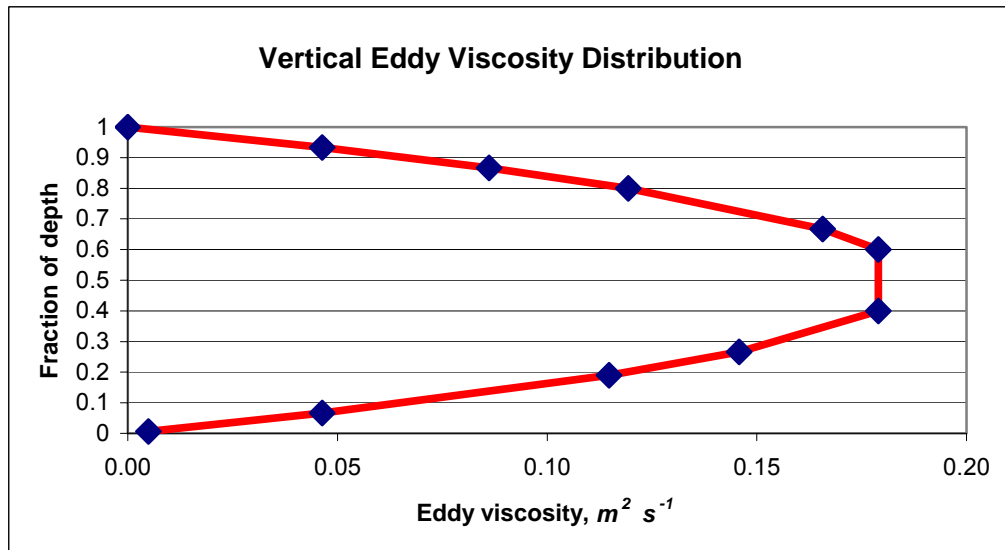


Figure A-35. Variation of A_z with depth for the parabolic model of England (1976).

In order to be compatible with the original formulation in the model, the computed value of A_z is corrected using the Mamayev formulation:

$$v_t = \max(v, v_{t_{PARAB}} e^{-CR_i}) \quad (\text{A-169})$$

W2N Formulation

The W2N formulation is the same as the W2 model except that the mixing length is no longer the layer thickness, but is computed using Nickaradse's mixing length model. The equations for the W2N formulation are:

$$A_z = \kappa \left(\frac{\ell_m^2}{2} \right) \sqrt{\left(\frac{\partial U}{\partial z} \right)^2 + \left(\frac{\tau_{wy} e^{-2kz}}{\rho A_z} \right)^2} e^{(-CR_i)} \quad (\text{A-170})$$

$$\ell_m = H \left[0.14 - 0.08 \left(1 - \frac{z}{H} \right)^2 - 0.06 \left(1 - \frac{z}{H} \right)^4 \right] \quad (\text{A-171})$$

TKE Formulation

The TKE formulation is a typical application of the k - ϵ turbulence model. This model includes both vertical transport of kinetic energy and dissipation by advection and 'diffusion' but also horizontal transport by advection. The model solves 2 partial differential equations for k and ϵ in order to compute the turbulent eddy viscosity:

$$v_t = C_\mu \frac{k^2}{\varepsilon} \quad (\text{A-172})$$

$$\frac{\partial \varepsilon B}{\partial t} + \frac{\partial \varepsilon B U}{\partial x} + \frac{\partial \varepsilon B W}{\partial z} - \frac{\partial}{\partial z} \left(B \frac{v_t}{\sigma_\varepsilon} \frac{\partial \varepsilon}{\partial z} \right) - \frac{\partial}{\partial x} \left(B \frac{v_t}{\sigma_\varepsilon} \frac{\partial \varepsilon}{\partial x} \right) = B \left(C_{\varepsilon 1} \frac{\varepsilon}{k} P + C_{\varepsilon 2} \frac{\varepsilon^2}{k} + P_\varepsilon \right) \quad (\text{A-173})$$

$$\frac{\partial k B}{\partial t} + \frac{\partial k B U}{\partial x} + \frac{\partial k B W}{\partial z} - \frac{\partial}{\partial z} \left(B \frac{v_t}{\sigma_k} \frac{\partial k}{\partial z} \right) - \frac{\partial}{\partial x} \left(B \frac{v_t}{\sigma_k} \frac{\partial k}{\partial x} \right) = B (P + G - \varepsilon + P_k) \quad (\text{A-174})$$

where C_μ is an empirical constant

$$P = v_t \left[\left(\frac{\partial U}{\partial z} \right)^2 \right]$$

$$G = - \frac{v_t}{\sigma_t} N^2$$

$$P_k = \frac{C_f U^3}{(0.5B)} \text{ Production term from boundary friction}$$

$$P_\varepsilon = \frac{10C_f^{1.25} U^4}{(0.5B)^2} \text{ Production term from boundary friction}$$

B is the width, U and W are the advective velocities in x and z respectively, and other terms are empirical constants.

Typical values of the above model constants that have been used in other studies are:

$$\sigma_k = 1.0$$

$$\sigma_\varepsilon = 1.3$$

$$C_\mu = 0.09$$

$$C_{1\varepsilon} = 1.44$$

$$C_{2\varepsilon} = 1.92$$

Turbulent Prandtl/Schmidt number, $\sigma_t = 1.0$.

The solution of the above equations for k and ε is by using a split solution technique: explicit horizontal and source-sink term solution followed by an implicit vertical solution in the vertical.

Effect of Vertical Layer Numbers on Vertical Turbulence

In contrast to other riverine models that assume vertically well-mixed systems, CE-QUAL-W2 accounts for the vertical variation of velocity in a riverine reach. Even though there is an added computational burden of computing the 2D velocity profile, the advantage of making this computation is that the friction factor (Manning's or Chezy) for a segment can be flow or stage invariant depending on the number of vertical layers schematized.

Many 1D hydraulic flow models, such as CE-QUAL-RIV1 and UNET (Barkau, 1997), allow the model user to specify how Manning's friction factor changes with depth. The Manning's friction factor, n , has been thought to vary as a function of depth, Reynolds number, and roughness factor or scale of bed grain size (Ugarte and Madrid, 1994; Soong, et. el., 1995). Some of these formulations for variation of Manning's friction factor with hydraulic radius, R , are shown in [Figure A-36](#):

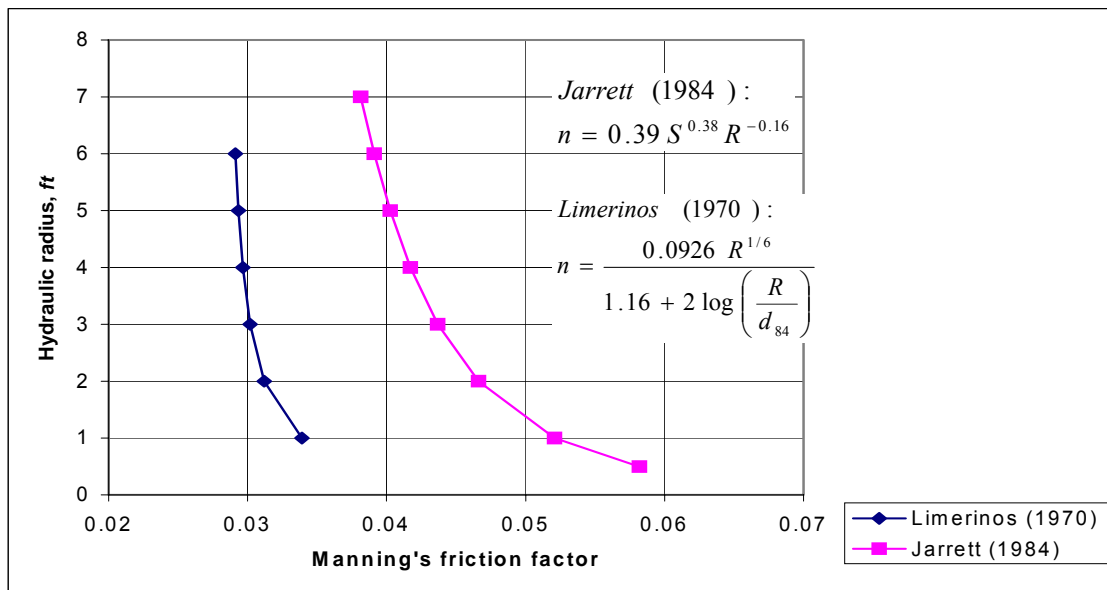


Figure A-36. Variation of Manning's friction factor using formulae from Limerinos (1970) and Jarrett (1984) for a channel slope, S , of 0.0005 and 84th percentile diameter of the bed material, d_{84} , of 50.

Researchers understand that the friction factor, when representing a hydraulic element with uniform roughness, should be flow invariant with depth (Henderson 1966). However, many assert that the friction factor changes with depth because the friction coefficient is variable with the wetted perimeter. Some investigators reason that it is to be expected that at shallow depths the larger size of the bed material produces a higher overall friction factor than a deeper flow where the sidewalls may have a smaller friction.

Since most researchers used 1D, cross-sectionally averaged flow equations such as Manning's Equation or 1D dynamic hydraulic models, this parameterization itself has been responsible for the seeming variation of Manning's friction factor with depth. For example, all 1D hydraulic models implicitly assume that the rate of transfer of momentum from the bottom of the channel to the top is infinite. For these hydraulic models, even as the depth of the channel increases, they still assume an infinite momentum transfer rate over the depth of the channel. Therefore, as the water depth increases, the apparent friction factor must be reduced because of the assumption of infinite momentum transfer between the bottom and the surface.

However, in a longitudinal-vertical river model, Manning's friction factor does not have to vary with stage in order to produce the effect that as the river stage increases, the apparent friction decreases. The water surface set-up changes significantly as the layer numbers increase. In general, the water surface slope increases as the number of computational layers decreases. This is because the average eddy viscosity in the water column increases as the number of layers decrease until at the limit of a

one-layer system, the average vertical eddy viscosity is infinite. The fact that the Manning’s friction factor seems to decrease with depth in 1D models is accounted for in modeling the river channel as a 2D, longitudinal-vertical system.

Version 3 allows choosing between five different vertical eddy viscosity formulations. These formulations are shown in [Table A-2](#). Typical variation of these formulations is shown in [Figure A-32](#) for Manning’s friction factor for an open-channel, non-stratified flow regime as compared to theory of steady, uniform channel flow.

The number of vertical layers significantly affects model predictions. For example, [Figure A-37](#) shows a comparison of vertical velocity profiles from a model with one, three, and seven vertical layers using the parabolic eddy viscosity model.

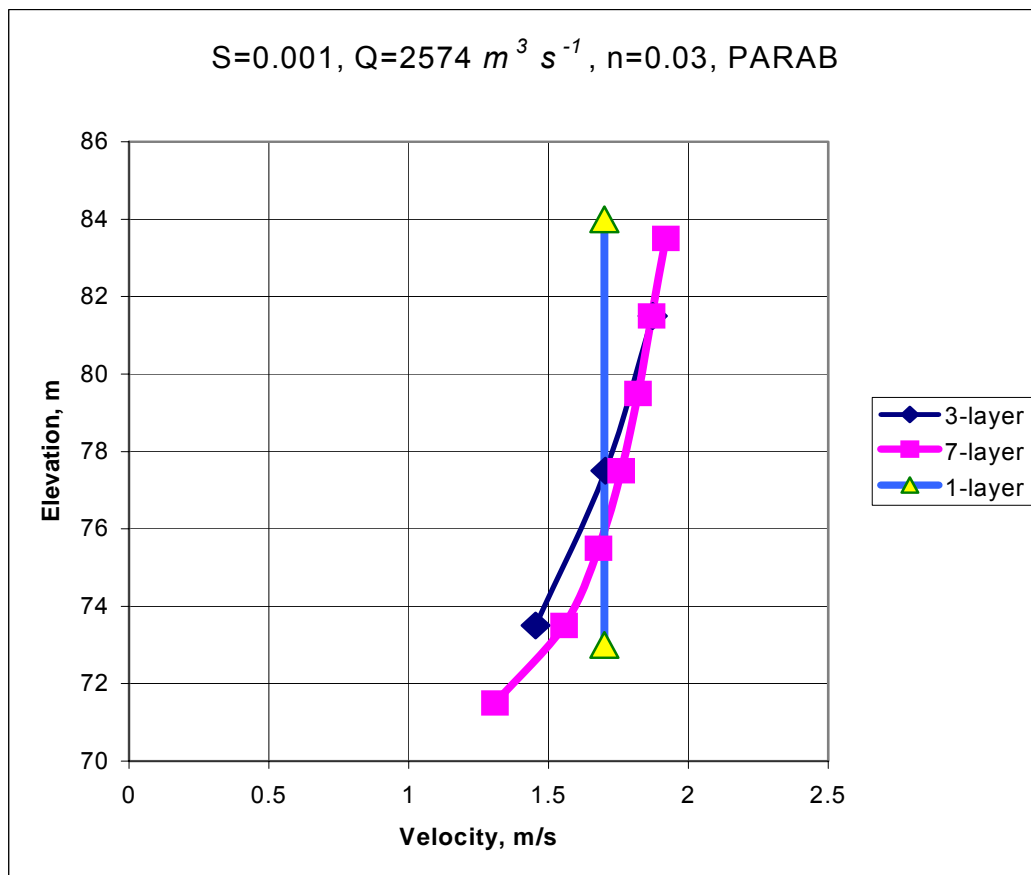


Figure A-37. Comparison of vertical velocity predictions with one, three, and seven vertical layers

[Figure A-38](#) shows how the change in the number of vertical layers affects the water surface slope over the domain length for a steady-state flow. In order to model the water surface slope of the 1-layer model with the 7-layer model, the apparent value of Manning’s friction factor would have to be reduced. Hence, the apparent friction decreases as the number of layers increase.

CE-QUAL-W2 V3 has also been compared to the 1D models DYNHYD (Ambrose et al., 1988) and CE-QUAL-RIV1 (Environmental Laboratory, 1995) by running W2 with only a single vertical layer.

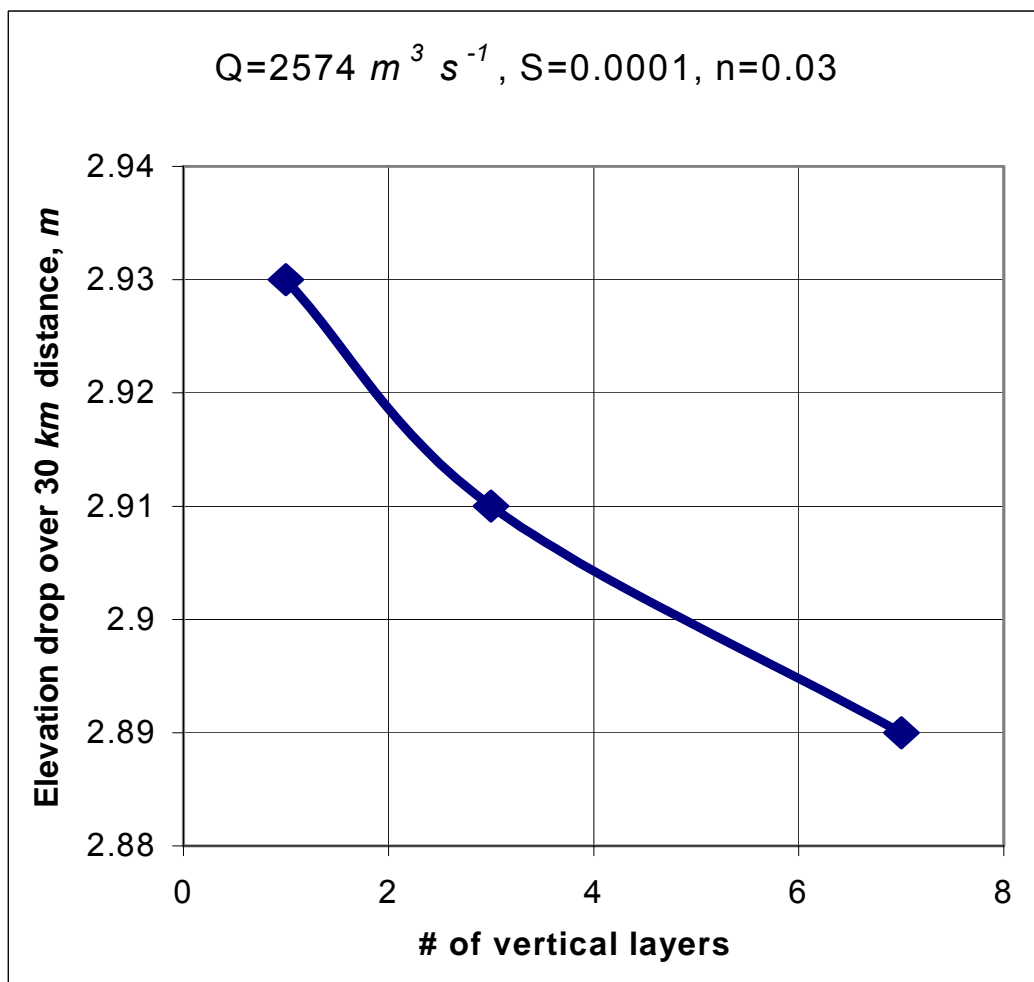


Figure A-38. Comparison of elevation drop of W2 model with one, three, and seven vertical layers with same Manning's friction factor.

The average velocities between the three models agreed well with theory but the water surface slopes are different. W2 predicts an elevation difference of 2.93 m, compared to 2.07 m for DYNHYD and 2.05 m for RIV1 over 30 km for a flow of 2574 m³ s⁻¹, a Manning's n of 0.03, a slope of 0.001, and a channel width of 100 m. Based on steady-state theory, the actual difference should be 2.9 m. Both the DYNHYD and RIV1 models require friction factors greater than expected to correspond to classical theory. This may be a result of these models not incorporating sidewall friction that was important during these test runs where the depth was 15 m and the width was 100 m.

Longitudinal Shear Stress

The longitudinal turbulent shear stress is defined as

$$\frac{\tau_{xx}}{\rho} = \nu_t \frac{\partial U}{\partial x} = A_x \frac{\partial U}{\partial x} \quad (\text{A-175})$$

where:

$A_x = \nu_t =$ longitudinal eddy viscosity

A_x is a user-defined constant in the model. This turbulence closure approximation is termed a zero-order closure model since no further equations are necessary to solve for the transmission of shear stress within the fluid.

This term is usually of very low magnitude except in areas near boundaries such as at a dam face where the longitudinal velocity goes to zero.

Hydraulic Structures

The model user can specify a pipe or culvert between model segments (Berger and Wells, 1999) and uses a 1D, unsteady hydraulic submodel that computes the flow between the two linked segments. The model computes the selective withdrawal outflow from the upstream segment with the model user specifying whether the inflow to the downstream segment is treated as mixed over the depth, inflow depth is determined from inflow density, or inflow depth is specified between an upper and lower elevation. The flow between an upstream segment and a downstream segment is shown in [Figure A-39](#).

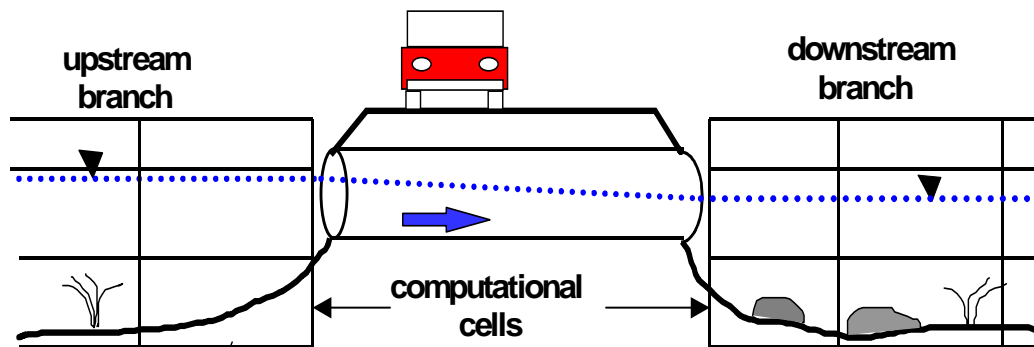


Figure A-39. Schematic of linkage of model segments with a culvert.

This model is only appropriate for simple piping systems that are not suddenly under a large hydraulic head. The governing equations for computing the flow and the numerical solution technique are shown below.

The governing equations used to predict flow through culverts are the 1D, time-dependent conservation of momentum and continuity equations (Yen, 1973).

$$\frac{\partial u}{\partial t} + u \frac{\partial u}{\partial x} + g \cos \phi \frac{\partial h}{\partial x} - g(S_o - S_f - S_m) = 0 \quad (\text{A-176})$$

$$\frac{\partial h}{\partial t} + u \frac{\partial h}{\partial x} + \frac{A}{T} \frac{\partial u}{\partial x} = 0 \quad (\text{A-177})$$

where:

u = velocity, $m \text{ s}^{-1}$

t = time, s

h = piezometric head, m

g = gravitational acceleration, $m^2 \text{ s}^{-2}$

x = distance along axis of culvert, m

A = cross-sectional area of culvert filled with water, m^2

T = width of water level surface, m

ϕ = angle between culvert axis and horizontal

S_o = culvert slope

S_f = friction slope.

S_m = minor loss slope

The friction slope S_f is estimated using the Manning formula:

$$S_f = \frac{n^2}{R^{4/3}} u |u| \quad (\text{A-178})$$

where:

n = Mannings roughness factor

R = hydraulic radius.

Minor losses due to entrance configuration, gates, valves, and corners are accounted for in the minor loss term S_m :

$$S_m = k \frac{u |u|}{2g} \frac{1}{L} \quad (\text{A-179})$$

where:

k = sum of minor loss coefficients

L = length

Pressurized or full culvert flow is modeled assuming a fictitious water surface width called a Preissmann slot (Yen, 1986). If the culvert is full, the surface width T is zero and the governing equations become singular. Using a Preissmann slot avoids having to switch between the open channel and pressurized flow equations. The slot must be narrow enough to minimize error in the mass and mo-

mentum balance but large enough to maintain numerical stability when solving the open channel St. Venant equations. A top width of 0.5% of the diameter is assumed for culverts flowing full.

The advantages of using a Preissmann slot are (Yen, 1986):

1. uses only Saint-Venant equations and avoids switching between the surcharge equation and open-channel flow equations and avoids the associated separate treatment of the boundary conditions
2. no need to define surcharge criteria
3. not necessary to keep inventory of the pipes that are surcharged at different times
4. permits the flow transition to progress computationally reach by reach in a sewer, as in the open-channel case, and hence it can account for the situation when only part of the length of the pipe is full
5. requires few additional assumptions than the standard approach to achieve numerical stability
6. simpler to program

The disadvantages are:

1. introduces a potential accuracy problem in the mass and momentum balance of the flow if the slot is too wide, and stability problems if it is too narrow
2. requires computation of two equations (continuity and momentum) for each of the reaches of the sewer when the sewer is full surcharged, whereas in the standard surcharge computation only one equation is applied to the entire length of the sewer
3. hypothetical rather than real

The Preissmann slot concept has been applied to other models for surcharged flow including the model described by Abbot (1982) and SWMM EXTRAN (Roesner et al. 1988).

The boundary condition used for solving the governing equations is the head or water level at each end of the culvert. However, if the water level at the downstream end of the culvert is less than the critical depth, the critical depth is used. Momentum is not transferred between model segments and the culverts. Initial conditions are the calculated velocities and heads at the previous time step.

The governing equations cannot be solved analytically and an implicit finite difference scheme is used to approximate the solution. The solution method employs the “leap-frog scheme” which calculates the head and velocity at alternating computational nodes (Anderson, et. al., 1984). The finite difference forms of the continuity and momentum equations are:

$$0 = \frac{h_i^{n+1} - h_i^n}{\Delta t} + \theta u_i^n \frac{h_{i+2}^{n+1} - h_{i-2}^{n+1}}{2\Delta x} + (1-\theta)u_i^n \frac{h_{i+2}^n - h_{i-2}^n}{2\Delta x} + \theta \frac{A_i^n}{T_i^n} \frac{u_{i+1}^{n+1} - u_{i-1}^{n+1}}{\Delta x} + (1-\theta) \frac{A_i^n}{T_i^n} \frac{u_{i+1}^n - u_{i-1}^n}{\Delta x} \tag{A-180}$$

$$\begin{aligned}
 0 = & \frac{u_i^{n+1} - u_i^n}{\Delta t} + \theta u_{i+1}^n \frac{u_{i+1}^{n+1} - u_{i-1}^{n+1}}{\Delta x} + (1 - \theta) u_{i+1}^n \frac{u_{i+1}^n - u_{i-1}^n}{\Delta x} + \theta g \frac{h_{i+2}^{n+1} - h_i^{n+1}}{\Delta x} \\
 & + (1 - \theta) g \frac{h_{i+2}^n - h_i^n}{\Delta x} + \theta g \frac{n^2}{R^{4/3}} u_{i+1}^{n+1} |u_{i+1}^n| + (1 - \theta) g \frac{n^2}{R^{4/3}} u_{i+1}^n |u_{i+1}^n| \\
 & + \theta \frac{k}{L} u_{i+1}^{n+1} |u_{i+1}^n| + (1 - \theta) \frac{k}{L} u_{i+1}^n |u_{i+1}^n|
 \end{aligned} \tag{A-181}$$

where n refers to the time level and i references the spatial node (Figure A-40).

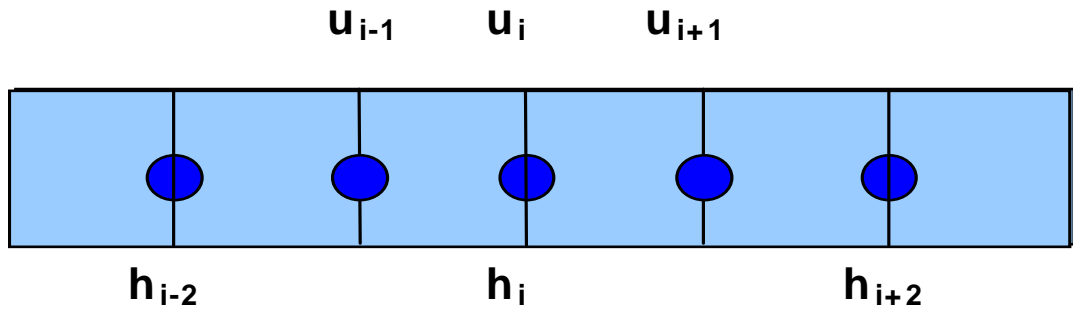


Figure A-40. Linkage schematic of model segments with a culvert.

Figure A-41 compares flow predictions using the dynamic culvert model with flow data taken within a culvert at NE 47th bridge in the Upper Columbia Slough, Portland, Oregon. Data was recorded using a flow meter placed directly in a culvert. The cyclical flows are the result of turning pumps on and off at a downstream pump station. The culvert was calibrated by adjusting the minor loss parameter.

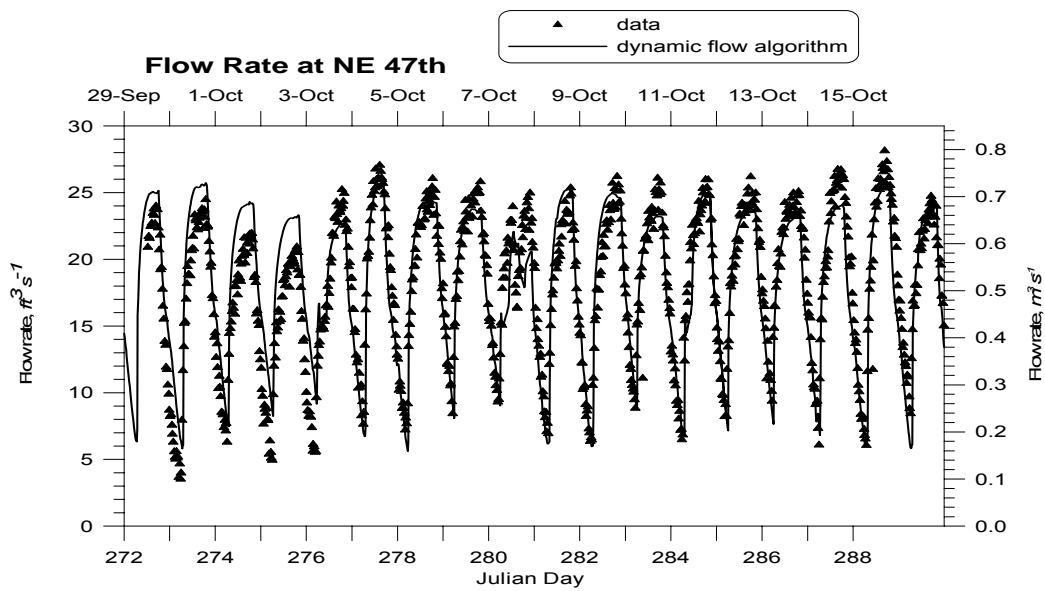


Figure A-41. Computed versus observed flow using dynamic culvert model.

Internal Weirs

The model can be used to set internal weirs at specified cell locations. The user specifies the location of the internal weir by providing a segment and layer number. The weir effectively acts as a barrier to flow and diffusion of mass/heat across the width of the waterbody as shown in [Figure A-42](#). This can be used to simulate submerged and curtain weirs within a waterbody.

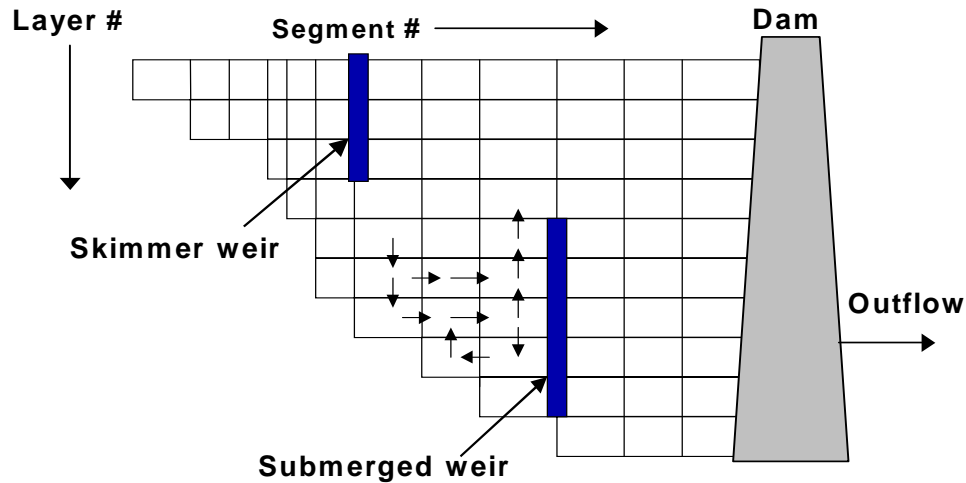


Figure A-42. Schematic representation of internal weirs.

Water Level Control

Many times, outflows in reservoirs are controlled by water levels. In order to facilitate management of the water body, a water level control algorithm was added to the code. Essentially, this is a pump based on a float controller.

The algorithm allows the user to specify the upstream and downstream segment for water to be transferred at a given flow rate based on the water level at the upstream segment. Reverse flow is not allowed. The withdrawal is treated as a lateral selective withdrawal and the segment that receives the inflow is treated as a tributary.

Outlet Structures

Outflows through hydraulic structures ([Figure A-43](#)) can either be specified or computed by the model based on user-supplied rating curves.

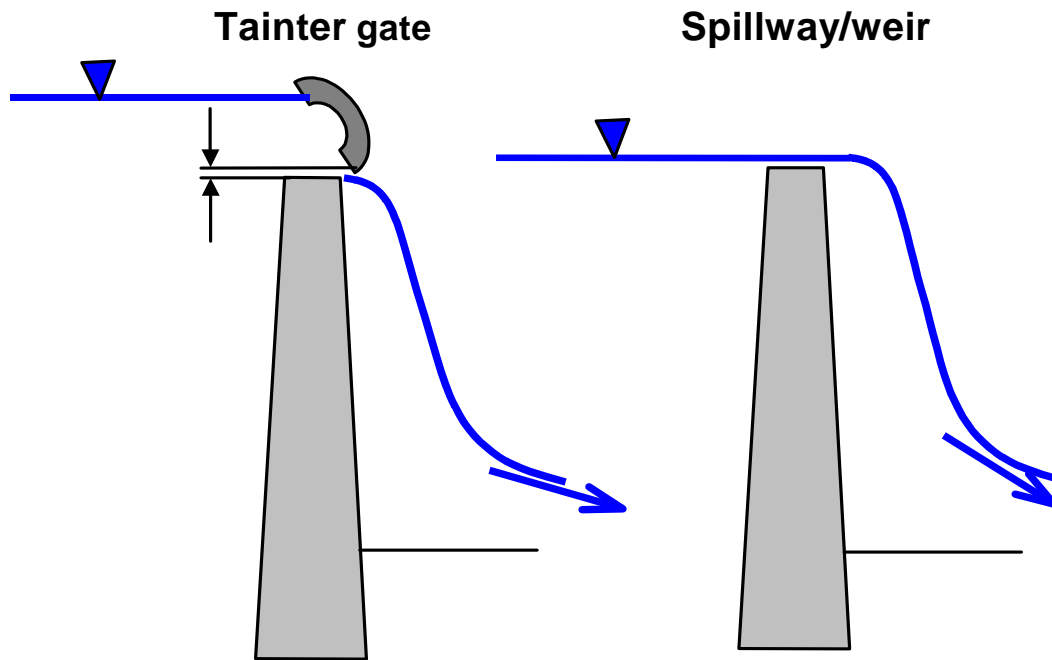


Figure A-43. Radial gates and spillway flow.

The UNET model (HEC, 1997a), a one-dimensional unsteady hydraulic model, formally accounts for spillway flow from weirs and spillways. For free or submerged flow from a spillway with a radial gate, UNET uses a general equation of the form:

$$Q_{sp} = CWA^\alpha B^\beta H^\eta \quad (\text{A-182})$$

where:

- α = empirical coefficient
- β = empirical coefficient
- η = empirical coefficient
- Q_{sp} = flow rate, $m^3 s^{-1}$
- A = trunnion height, m
- B = gate opening, m
- C = empirical coefficient
- W = gate width, m

and

$$H = Z_u - KZ_d - (1 - K)Z_{sp} \quad (\text{A-183})$$

where:

- Z_u = headwater elevation
- Z_d = tailwater elevation

$K = 1$ for submerged flow and 0 for free flow
 Z_{sp} = spillway elevation

This equation was developed based on rating curves for hydraulic control structures in Arizona. Submergence is defined as:

$$\frac{Z_d - Z_{sp}}{Z_u - Z_{sp}} > \frac{2}{3} \tag{A-184}$$

Note that weir flow is assumed to occur whenever $B = 0.8H$ and is computed as:

$$Q_{weir} = C_w F W \left((1 - K) Z_u + K Z_d - Z_{sp} \right) H^{1/2} \tag{A-185}$$

where:

C_w = weir coefficient

$$F = 3 \left(1 - \frac{Z_d - Z_{sp}}{Z_u - Z_{sp}} \right) \text{ when } K = 1$$

$F = 1$ when $K = 0$

For a concrete spillway, HEC (1997a) suggests using a weir coefficient value of 4. Note that the above two equations are considered equivalent whenever $B = 0.8H$.

HEC-RAS, a one-dimensional, steady-state hydraulic model, (HEC, 1997b), includes the ability to model flow over spillways including tainter and sluice gates, broad-crested weirs, and an ogee crest. Ineffective flow area, that area below the weir or gate opening, is used to block a part of the channel until it reaches the level of a spillway or weir.

A summary of the equations used by HEC-RAS (HEC, 1997b) as well as explanations are shown in [Table A-3](#).

Table A-3. HEC-RAS flow rates through weirs and sluice gates.

Condition	Equation	Description
Radial flow gate, flowing freely	$Q = C \sqrt{2g} W T^{T_E} B^{B_E} H^{H_E}$	When the upstream water surface is ≥ 1.25 times the gate opening height (above the spillway crest), Q = flow, <i>cfs</i> C = discharge coefficient (between 0.6 and 0.8) W = gated spillway width, <i>ft</i> T = trunnion height (from spillway crest to trunnion pivot point), <i>ft</i> B = gate opening height, <i>ft</i> H = upstream energy head above spillway crest, $Z_u - Z_{sp}$, <i>ft</i> Z_u = upstream energy grade line elevation, <i>ft</i> Z_d = downstream water surface elevation, <i>ft</i> Z_{sp} = spillway crest elevation, <i>ft</i> T_E = empirical trunnion height exponent, 0.16 B_E = gate opening coefficient, 0.72 H_E = head exponent, 0.62

Condition	Equation	Description
radial gate flowing under submerged conditions	$Q = 3C\sqrt{2g} WT^{T_E} B^{B_E} H^{H_E}$	When the upstream water surface is ≥ 1.25 times the gate opening height (above the spillway crest), whenever the tailwater depth divided by the energy depth above the spillway is greater than 0.67 $H = Z_u - Z_d$
freely flowing sluice gate	$Q = C\sqrt{2gH} WB$	When the upstream water surface is ≥ 1.25 times the gate opening height above the spillway crest $H =$ upstream energy head above the spillway, $Z_u - Z_{sp}$ $C =$ discharge coefficient, 0.5 to 0.7
submerged sluice gate	$Q = 3C\sqrt{2gH} WB$	When the upstream water surface is ≥ 1.25 times the gate opening height above the spillway crest, whenever the tailwater depth divided by the energy depth above the spillway is greater than 0.67 $H = Z_u - Z_d$
Low flow through gated structure	$Q = CLH^{\frac{3}{2}}$	When upstream water level is equal to or less than the top of the gate opening, weir flow equation is used $C =$ weir coefficient, 2.6-4.0 depending on broad crested or Ogee spillway and length of spillway crest $H =$ upstream energy head above spillway crest, for an Ogee spillway the value of C is adjusted according to a 1977 Bureau of Reclamation study on variability of C for Ogee spillways, suggested values of C are 2.6 for bridge decks and 3.0 for flow over elevated roadways

Spillways/Weirs

Analysis of flow over weirs has been studied extensively. Martin and McCutcheon (1999) show that a typical relationship between the pool depth and flow over a weir is:

$$Q = C_e W_c h_w^\eta \tag{A-186}$$

where C_e and η are empirical coefficients, W_c is the length of the weir crest, and h_w is the height of the pool above the weir crest. Theoretical calculations of steady-state flow over a weir can be complex depending on whether the weirs are sharp-crested, broad-crested, V-notched, rectangular, Cipolletti, parabolic, or some other type. [Table A-4](#) shows some examples from French (1985) and USBR (1999) on typical equations used for the different weir types. For many regular weir types, formulae exist for accurate estimation of the flow. However, in most cases a rating curve for a given installation is necessary because of the uncertainty of end effects, flow alignments, shallowness in the upstream pool, and other unique features of the installation (Martin and McCutcheon, 1999).

Table A-4. List of weir types (French, 1985; USBR, 1999)

Weir type	Weir Equation	Description
Rectangular broad crested weir	$Q = C_D C_v \frac{2}{3} \sqrt{\frac{2}{3}} g W H^{3/2}$	Valid when $0.08 < H/L < 0.5$ Q = flow rate C_D = discharge coefficient (0.84 to 1.06) C_v = velocity coefficient accounting for neglecting the velocity head in the approach channel (between 1.0 and 1.2) W = width at surface H = upstream head above spillway crest g = gravity acceleration
Rectangular, sharp crested weir	$Q = C_e \frac{2}{3} \sqrt{2g} B H^{3/2}$	Where B = width at bottom of weir crest Olson and Wright (1990) show that C_e depends on the approach velocity head, $V^2/2g$, and the contraction of streamlines just beyond the weir crest and show that $C_e = 0.611 + 0.075^*(H/Z)$ H = weir head, <i>ft</i> Z = weir crest head measured from the channel bottom, <i>ft</i> Clay (1995) suggests a simple equation of $Q=3.33BH^{3/2}$ of this form when approach velocities are less than 1 <i>fps</i> or $Q=3.33B[(H+h)^{3/2} - h_v^{3/2}]$ $h_v = V^2/2g$ V = approach velocity, <i>ft s⁻¹</i>
Parabolic, broad-crested	$Q = C_D C_v \sqrt{\frac{3}{4}} f g H^2$	f = distance from the bottom point of the weir to the weir focal point, <i>ft</i>
Parabolic, sharp-crested	$Q = C_e \frac{1}{2} \pi \sqrt{f g} H^2$	C_e = effective discharge coefficient
Triangular, broad-crested	$Q = C_D C_v \frac{16}{25} \sqrt{\frac{2}{5}} g \tan(0.5\Theta) H^{5/2}$	Θ = half angle of the triangular notch
Triangular, sharp-crested	$Q = C_e \frac{8}{25} \sqrt{2g} \tan(0.5\Theta) H^{5/2}$	C_e = function of notch angle and varies from 0.59 to 0.57 for angles between 20 and 100 degrees
Trapezoidal, broad-crested	$Q = C_D (W y_c + m y_c^2) [2g(H - y_c)]^{1/2}$	W = top width of trapezoidal weir m = slope of trapezoidal weir y_c = depth of water at the weir
Trapezoidal, sharp-crested	$Q = C_e \frac{2}{3} \sqrt{2g} (B + \frac{4}{5} H \tan 0.5\Theta) H^{1/2}$	B = bottom width of trapezoidal weir
Truncated triangular, broad-crested	$Q = C_D C_v \frac{2}{3} \sqrt{\frac{2}{3}} g W (H - 0.5H_b)^{3/2}$	Use when $H > 1.25H_b$, otherwise use equation for broad crested triangular weir H_b = depth from the bottom of the truncated triangular weir to the top of the triangle and the beginning of the rectangular section
Truncated triangular, sharp-crested	$Q = C_e \frac{4}{15} \sqrt{2g} \frac{W}{H_b} (H^{2.5} - (H - H_b)^{2.5})$	Use when $H > H_b$, otherwise use equation for sharp crested triangular weir
Cipoletti	$Q = C_D C_v \frac{2}{3} \sqrt{2g} W H^{3/2}$	A modification of the contracted, rectangular, sharp-crested weir with a trapezoidal control section and sides sloping outward with slopes of 4:1 W = top width of weir $C_D=0.63$ C_v varies from 1 to 1.2 and is a function of C_D and the ratio of area upstream of the control section and at the control section

Weir type	Weir Equation	Description
Proportional or sutro weir	$Q = C_D B \sqrt{2ga} \left(H - \frac{1}{3}a \right)$	B = bottom width of weir a = distance from weir bottom to top of the rectangular weir section

Since all weirs in practice are calibrated and a head discharge relationship is usually determined, the flow versus head relationship is used rather than an equation from [Table A-4](#). The user must then analyze the weir or spillway and input a relationship based on the weir or spillway geometry. The model accepts equations in the form of a power function for freely flowing conditions:

$$Q = \alpha_1 \Delta h^{\beta_1} \quad (\text{A-187})$$

where:

$$\begin{aligned} \alpha_1 &= \text{empirical parameter} \\ \beta_1 &= \text{empirical parameter} \\ \Delta h &= Z_u - Z_{sp} \\ Z_u &= \text{upstream head} \\ Z_{sp} &= \text{spillway crest elevation} \end{aligned}$$

and for submerged conditions

$$Q = \alpha_2 \Delta h^{\beta_2} \quad (\text{A-188})$$

where:

$$\begin{aligned} \alpha_2 &= \text{empirical parameter} \\ \beta_2 &= \text{empirical parameter} \\ \Delta h &= Z_u - Z_d \\ Z_u &= \text{upstream head} \\ Z_d &= \text{downstream head} \end{aligned}$$

Submerged conditions are defined when the tailwater depth over the upstream energy head (static head and velocity head) is greater than 0.67 (HEC, 1997b). Even though negative flow rates are possible using the second equation whenever $Z_d > Z_u$, these results should be used with caution since rarely are rating curves done for reverse flow over a spillway. The user needs to ensure there is a smooth transition between submerged flow conditions and free flowing conditions by proper choice of model coefficients. The following discussion shows how to generate a smooth flow transition from free flowing to submerged flow conditions ([Figure A-44](#)).

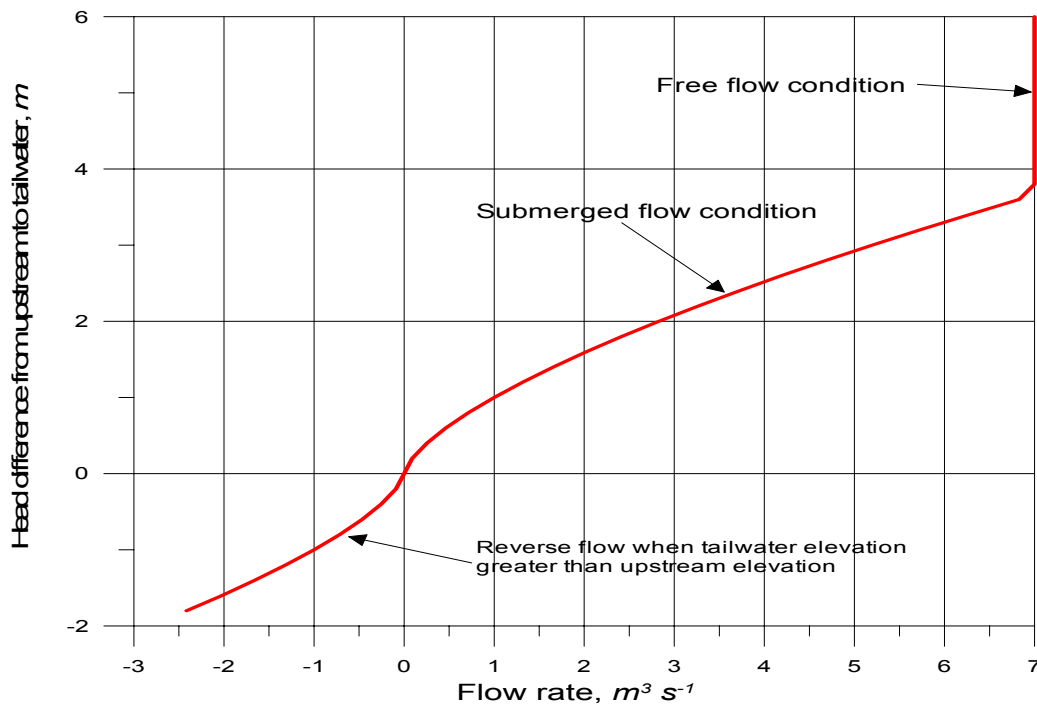


Figure A-44. Flow rate over a spillway or weir for submerged and free flowing conditions.

Consider the following weir flow condition in [Figure A-45](#).

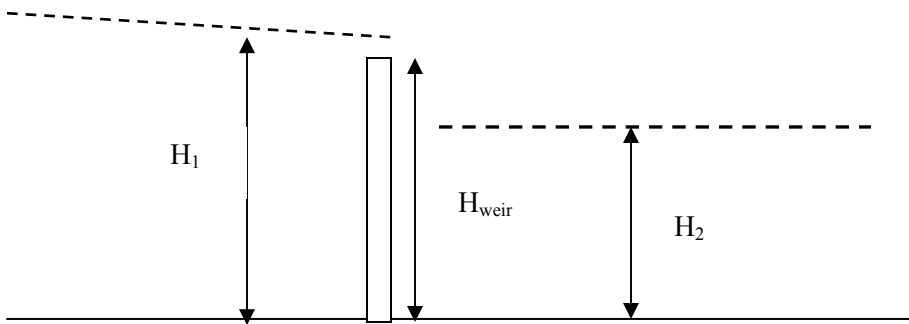


Figure A-45. Flow at a submerged weir.

In order to have a smooth transition, the two flows must be equal at the transition point. Using:

$$\begin{aligned} \Delta h_1 &= H_1 - H_{weir} \\ \Delta h_2 &= H_1 - 0.67H_1 = 0.33H_1 \end{aligned} \tag{A-189}$$

and setting the two equations equal and solving for α_2 :

$$\alpha_2 = \frac{\alpha_1 (H_1 - H_{weir})^{\beta_1}}{(0.33H_1)^{\beta_2}} \quad (\text{A-190})$$

In many cases a weir can be set as the downstream boundary condition of a river. In CE-QUAL-W2, the user can specify the weir crest as the channel bottom elevation, such that the weir equation is of the form:

$$Q = \alpha_1 H^{\beta_1} \quad (\text{A-191})$$

where H is the depth of the water at the weir. Setting this in the form of a stage-discharge relationship:

$$H = \left(\frac{Q}{\alpha_1} \right)^{\frac{1}{\beta_1}} \quad (\text{A-192})$$

or written in a form compatible with the stage discharge relationship:

$$H = \left(\frac{1}{\alpha_1} \right)^{\frac{1}{\beta_1}} Q^{\frac{1}{\beta_1}} \quad (\text{A-193})$$

Equating the coefficients used in the two approaches:

$$a = \left(\frac{1}{\alpha_1} \right)^{\frac{1}{\beta_1}} \quad (\text{A-194})$$

$$b = \frac{1}{\beta_1} \quad (\text{A-195})$$

and vice versa:

$$\alpha_1 = a^{-\beta_1} \quad (\text{A-196})$$

$$\beta_1 = \frac{1}{b} \quad (\text{A-197})$$

allows the user to set a weir-rating curve that reproduces the stage discharge relationship at a downstream boundary.

Gates

For a gated structure or sluice gate, a more complex rating curve is required based on the opening and the head difference between the upstream and downstream condition (the spillway crest if free flow and the tailwater elevation if submerged flow).

The following equation is used for freely flowing conditions:

$$Q = \alpha_1 \Delta h^{\beta_1} B^{\gamma_1} \quad (\text{A-198})$$

where:

- α_1 = empirical coefficient
- β_1 = empirical coefficient
- γ_1 = empirical coefficient
- $\Delta h = Z_u - Z_{sp}$
- Z_u = upstream head
- Z_{sp} = spillway crest elevation

and the following equation is used for submerged flow:

$$Q = \alpha_2 \Delta h^{\beta_2} B^{\gamma_2} \quad (\text{A-199})$$

where:

- α_2 = empirical coefficient
- β_2 = empirical coefficient
- γ_2 = empirical coefficient
- $\Delta h = Z_u - Z_d$
- Z_d = downstream head
- B = gate opening, m

In defining these parameters, the user also has to generate a time series file with the gate opening in m where a gate opening of $0 m$ is closed. Whenever the gate opening is equal to or greater than $0.8\Delta h$, a weir equation is used with no functional dependency on the gate opening. In this case, a rating curve must be supplied when the gate acts like a weir. [Figure A-46](#) shows the flow rate dependence on the gate opening.

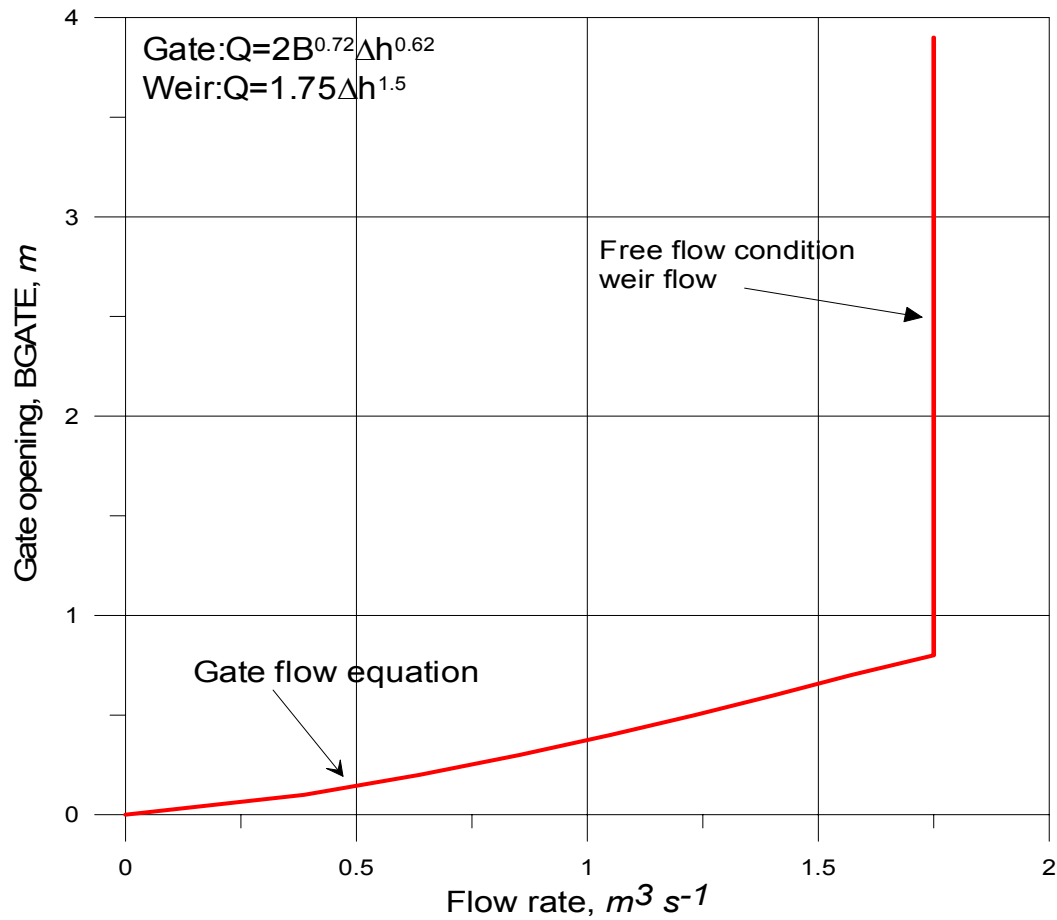


Figure A-46. Flow rate variation with gate opening.

In some reservoir systems, an outlet valve is connected to the reservoir and a head-discharge relationship is used based on the gate opening or number of gate turns. In this case, the outlet level is usually at a different elevation than the withdrawal elevation. The above gate formulation can still be used if no reverse flow occurs through the needle valve. This situation is illustrated in [Figure A-47](#). In this case, the elevation of the outflow is required in addition to the elevation at which the outflow is taken if a rating curve is used in the model. This use is described in the section on changes to the control file.

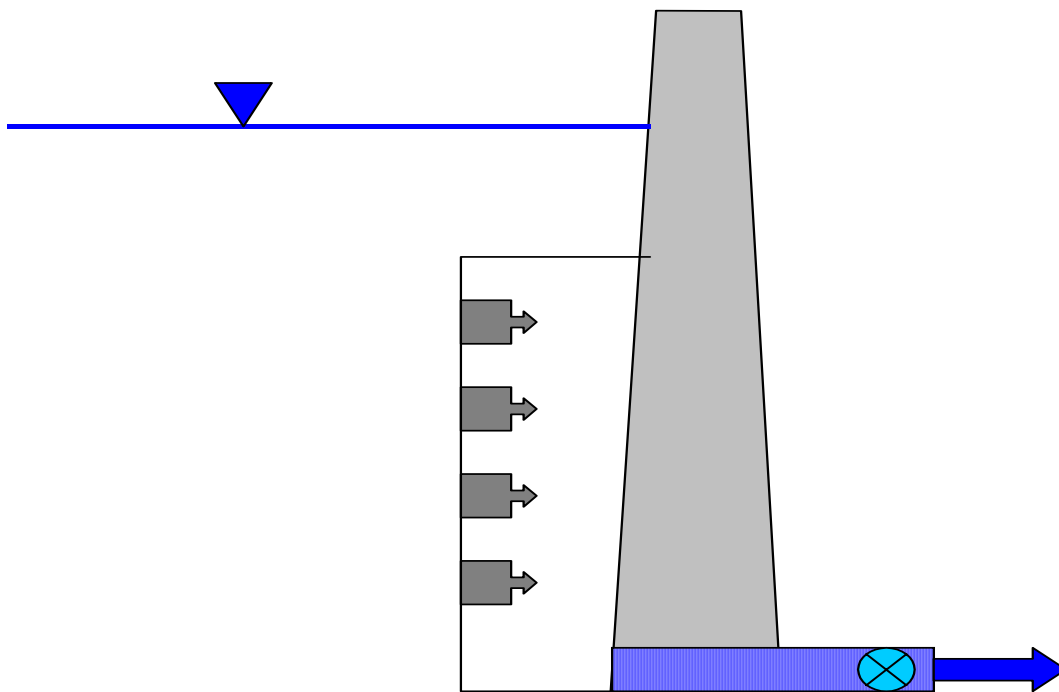


Figure A-47. Selective withdrawal with outflow connected to a valve with a gate.

The user can insert weirs and/or spillways, specify connectivity to other model segments, and insert the ratings curve parameters for each weir/spillway. The model treats each spillway, weir, or gate as a selective withdrawal outflow and uses the selective withdrawal algorithm for determining water flow from each vertical layer adjacent to the structure. Inflows from hydraulic control structures are treated as tributary inflows where the user must specify whether the inflow is placed according to density, equally distributed between all vertical layers, or distributed between a given elevation range.

Weir equations are used when gates are open and the open gate does not interfere with the flow (when $B \geq 0.8\Delta h$).

Branch Momentum Exchange

Version 3 conserves longitudinal momentum at branch intersections ([Figure A-48](#)). The vector component of velocity in the x-direction of the main channel, U_x , can be computed from the channel orientations. The x-direction component is $U_x = U \cos \beta$ where U is the longitudinal velocity of the tributary at the downstream segment that intersects the main branch and β is the difference in the angle between the main stem and tributary segments.

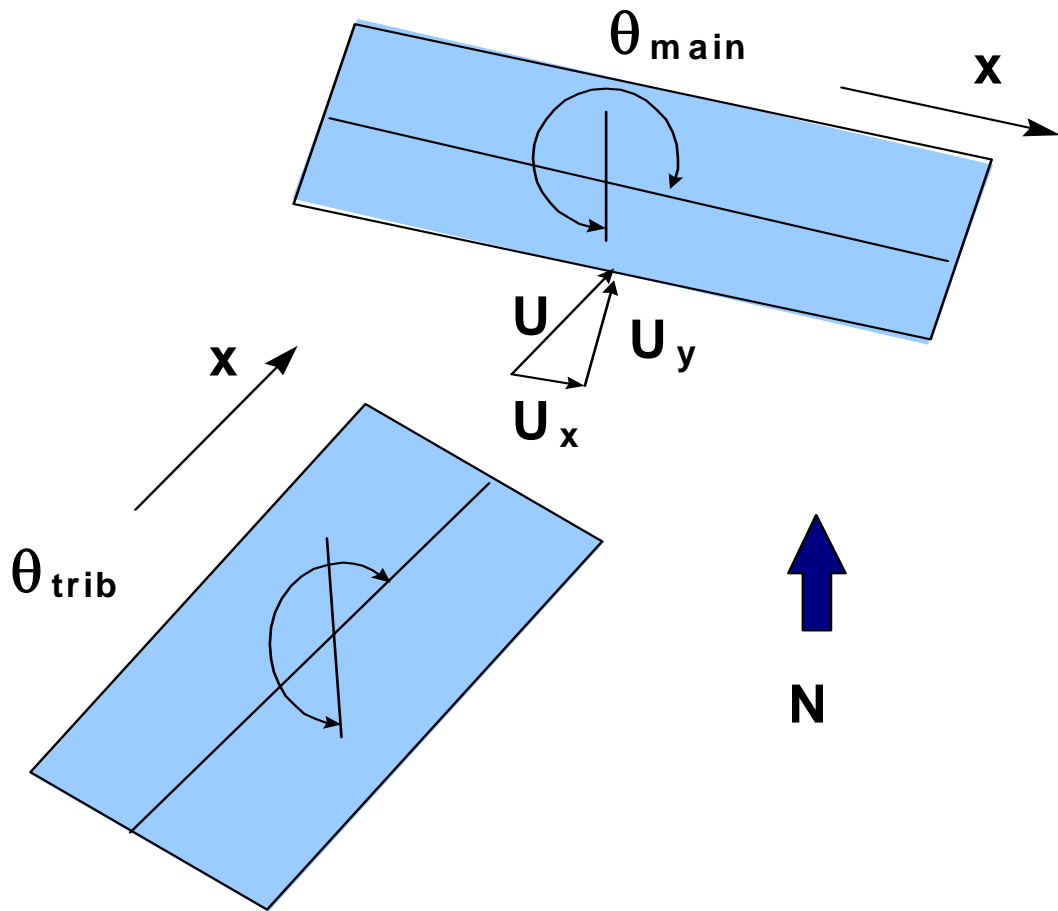


Figure A-48. Schematic of branch connection.

The conservation of momentum about a control volume, the main stem segment, would result in an additional source of momentum. Lai (1986) shows that the correction to the x-momentum equation would be:

$$qBU_x \tag{A-200}$$

where:

q = lateral inflow per unit length

This arises from re-deriving the momentum equations and assuming that all the fluid entering the segment is moving at the velocity U_x . The correction to the x-momentum equation is:

$$\begin{aligned} \frac{\partial UB}{\partial t} + \frac{\partial UUB}{\partial x} + \frac{\partial WUB}{\partial z} = gB \sin \alpha + g \cos \alpha B \frac{\partial \eta}{\partial x} - \frac{g \cos \alpha B}{\rho} \int_{\eta}^z \frac{\partial \rho}{\partial x} dz \\ + \frac{l}{\rho} \frac{\partial B \tau_{xx}}{\partial x} + \frac{l}{\rho} \frac{\partial B \tau_{xz}}{\partial z} + \underbrace{qBU_x}_{\text{side tributary momentum}} \end{aligned} \quad (\text{A-201})$$

Lateral Inflows

Wells (1997) proposed accounting for the cross-shear as a result of the y component of the velocity of a side branch in the computation of the vertical eddy viscosity. This was implemented by increasing the cross-shear velocity gradient. In Version 2, wind shear across the lateral axis of a segment also increased the vertical mixing by affecting the computation of A_z . Analogous to wind shear, an additional side shear is included in the calculation of the vertical eddy viscosity:

$$A_z = \kappa \left(\frac{l^2}{2} \right) \sqrt{\left(\frac{\partial U}{\partial z} \right)^2 + \left(\frac{\tau_{vy} e^{-2kz} + \tau_{trib}}{\rho A_z} \right)^2} e^{(-CR_t)} \quad (\text{A-202})$$

where:

$$\tau_{trib} \cong \rho \frac{f_i}{8} U_y^2$$

f_i = is an interfacial friction factor, ≈ 0.01

$$U_y = \frac{\sum Q_{in_y}}{\Delta z \Delta x}$$

$$\sum Q_{in_y} = [U_{br} \Delta z B] + [\sum Q_{trib}]$$

$$U_{br} = U_{br} \sin(\Theta_{main} - \Theta_{branch})$$

Δz = inflow cell layer height

B = inflow cell width

Δx = inflow cell segment length

Q_{trib} = tributary flow rate assumed to be at right angles to the main channel

This side shear effect is only computed when the vertical mixing algorithm chosen by the user is W2 or W2N.

Heat Exchange

Surface Heat Exchange

Surface heat exchange can be formulated as a term by-term process using the explicit adjacent cell transport computation as long as the integration timestep is shorter than or equal to the frequency of the meteorological data. Surface heat exchange processes depending on water surface temperatures

are computed using previous timestep data and are therefore lagged from transport processes by the integration timestep.

Term-by-term surface heat exchange is computed as:

$$H_n = H_s + H_a + H_e + H_c - (H_{sr} + H_{ar} + H_{br}) \quad (\text{A-203})$$

where:

- H_n = the net rate of heat exchange across the water surface, $W m^{-2}$
- H_s = incident short wave solar radiation, $W m^{-2}$
- H_a = incident long wave radiation, $W m^{-2}$
- H_{sr} = reflected short wave solar radiation, $W m^{-2}$
- H_{ar} = reflected long wave radiation, $W m^{-2}$
- H_{br} = back radiation from the water surface, $W m^{-2}$
- H_e = evaporative heat loss, $W m^{-2}$
- H_c = heat conduction, $W m^{-2}$

The short wave solar radiation is either measured directly or computed from sun angle relationships and cloud cover. The long wave atmospheric radiation is computed from air temperature and cloud cover or air vapor pressure using Brunt's formula. The right-hand terms are all water surface temperature dependent.

Water surface back radiation is computed as:

$$H_{br} = \varepsilon \sigma^* (T_s + 273.15)^4 \quad (\text{A-204})$$

where:

- ε = emissivity of water, 0.97
- σ^* = Stephan-Boltzman constant, $5.67 \times 10^{-8} W m^{-2} \circ K^{-4}$
- T_s = water surface temperature, $\circ C$

Like the remaining terms, it is computed for each surface layer cell on each iteration timestep.

Evaporative heat loss is computed as:

$$H_e = f(W) (e_s - e_a) \quad (\text{A-205})$$

where:

- $f(W)$ = evaporative wind speed function, $W m^{-2} mm Hg^{-1}$
- e_s = saturation vapor pressure at the water surface, $mm Hg$
- e_a = atmospheric vapor pressure, $mm Hg$

Evaporative heat loss depends on air temperature and dew point temperature or relative humidity. Surface vapor pressure is computed from the surface temperature for each surface cell on each iteration.

Surface heat conduction is computed as:

$$H_c = C_c f(W) (T_s - T_a) \quad (\text{A-206})$$

where:

C_c = Bowen's coefficient, $0.47 \text{ mm Hg } ^\circ\text{C}^{-1}$
 T_a = air temperature, $^\circ\text{C}$

Short wave solar radiation penetrates the surface and decays exponentially with depth according to Bears Law:

$$H_s(z) = (1 - \beta) H_s e^{-\eta z} \quad (\text{A-207})$$

where:

$H_s(z)$ = short wave radiation at depth z , $W \text{ m}^{-2}$
 β = fraction absorbed at the water surface
 η = extinction coefficient, m^{-1}
 H_s = short wave radiation reaching the surface, $W \text{ m}^{-2}$

Aside from the problems of measuring meteorological data relative to a large waterbody and translating data from oftentimes distant weather stations, the most uncertain parameter in the surface heat exchange computations is the evaporative wind speed function, $f(W)$. Various formulations of $f(W)$ have been catalogued and examined in Edinger, et al. (1974). The different formulations result from the empirical determination of $f(W)$ for waterbodies of different size and shape with data from different locations and averaged over different periods of time.

Evaporation

The model allows the user the freedom to include different evaporation formulations via a user defined evaporation wind speed formula of the form

$$f(W) = a + b W^c \quad (\text{A-208})$$

where:

$f(W)$ = wind speed function, $W \text{ m}^{-2} \text{ mm Hg}^{-1}$
 a = empirical coefficient, 9.2 default
 b = empirical coefficient, 0.46 default
 c = empirical coefficient, 2 default
 W = wind speed measure at 2 m above the ground, m s^{-1}

HEAT EXCHANGE

AUXILIARY FUNCTIONS

The function is used in computing both evaporative water and heat loss. The default values for a, b, and c are the ones suggested in Edinger, et. al. (1974). The model assumes that the wind is measured at a 2m height. The following equation converts b from any measurement height to 2 m:

$$b_{2m} = \alpha^c b_z \quad (\text{A-209})$$

where b_z is b measured at z m and α is the conversion factor between the wind at z and the wind at 2m using

$$\frac{W_{2m}}{W_z} = \frac{\ln\left(\frac{2}{z_0}\right)}{\ln\left(\frac{z}{z_0}\right)} = \frac{1}{\alpha} \quad (\text{A-210})$$

where:

W_{2m} = wind speed at elevation 2 m, $m\ s^{-1}$

W_z = wind speed at height z , $m\ s^{-1}$

z_0 = wind roughness height (assume 0.003 ft for wind < 5 mph and 0.015 for wind > 5 mph, range 0.0005 to 0.03 ft)

The Ryan-Harleman (1974) formulation has also been included :

$$f(W_z) = a + bW_z \quad (\text{A-211})$$

where:

$$b = 4.1\ W\ m^{-2}\ mm\ Hg^{-1}\ m^{-1}\ s^{-1}$$

$$a = \lambda(T_{sv} - T_{av})^{1/3}$$

$$\lambda = 3.59\ W\ m^2\ mm\ Hg\ ^\circ C^{-1/3}$$

$$T_v = T^* \left(1 - 0.378 \left[\frac{e}{p} \right] \right)^{-1},\ ^\circ K$$

$$p = 760\ mm\ Hg$$

For the Lake Hefner model, $a = 0$ and $b = 4.99\ W\ m^{-2}\ mm\ Hg^{-1}\ m^{-1}\ s^{-1}$.

If the virtual temperature difference, T_v , is negative or less than that computed using the Lake Hefner model, $f(W)$ reverts to the Lake Hefner evaporation model. [Figure A-49](#) shows a comparison of the Ryan-Harleman model with the model's default formulation.

Adams et al. (1981) recommended that the Lake Hefner model be used for natural lakes ([Table A-5](#)).

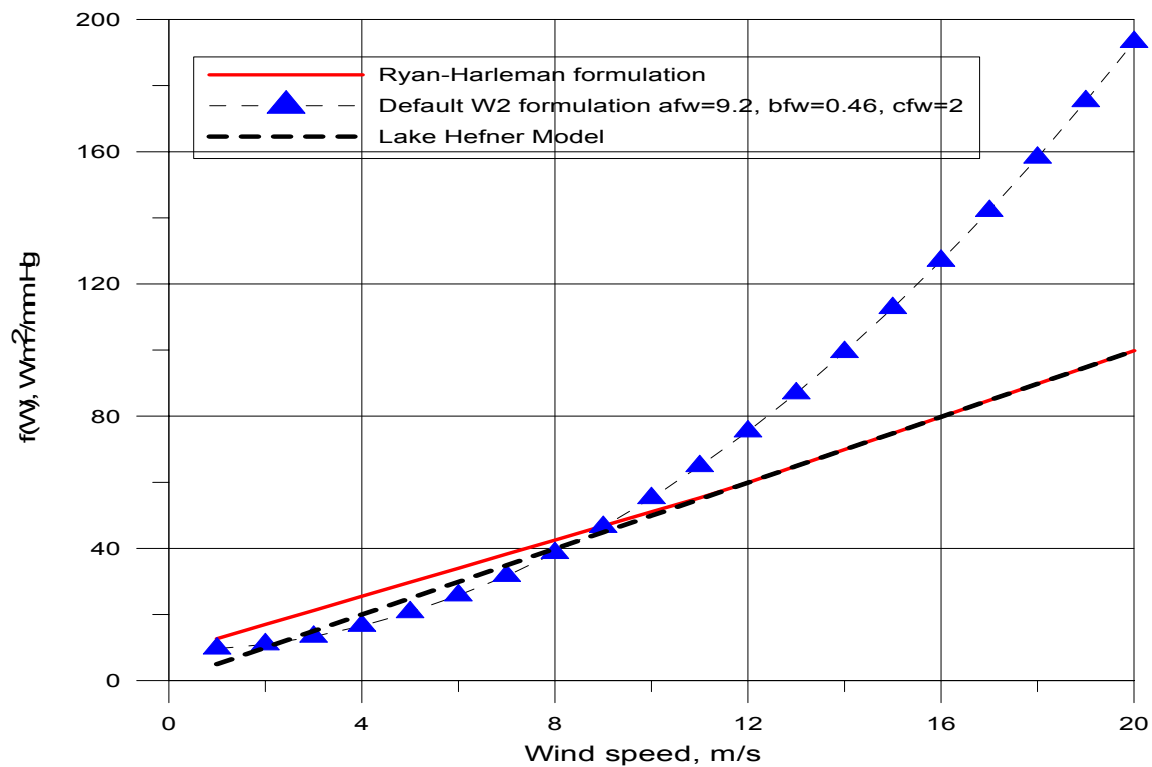


Figure A-49. Comparison of the wind speed formulation for Ryan-Harleman and W2 default (for $T_{air}=15^{\circ}C$, $T_{dew}=-5^{\circ}C$, $T_{surface}=25^{\circ}C$).

Summaries of several evaporation formulations are shown below in [Table A-5](#) as adapted from Adams, et al. (1981).

Table A-5. Typical Evaporation Formulae for Lakes and Reservoirs

Name	Time	Waterbody	ϕ_e	$f(W)$	Remarks
Lake Hefner	3 hrs and day	Lake Hefner, OK, 2587 acres	$17.2W_2(e_s-e_2)$	$5.06W_2$	good agreement with lake data from several lakes in US and Russia
Kohler	day	Lake Hefner OK, 2587 acres	$17.5W_2(e_s-e_2)$	$5.14W_2$	essentially the same as Lake Hefner formula
Zaykov	-	ponds and small reservoirs	$(1.3+14W_2)(e_s-e_2)$	$0.1708+4.11W_2$	based on Russian work
Meyer	month	small lakes and reservoirs	$(80+10W_2)(e_s-e_2)$	$10.512+2.94W_2$	e_a obtained daily from mean morning and evening measurements of air temperature and relative humidity
Morton	month	Class A pan	$(73.5+14.7W_2)(e_s-e_2)$	$9.658+4.32W_2$	data from meteorological stations, measurement heights assumed
Rohwer	day	pans, 85 ft dia tank, 1300 acre reservoir	$(67+10W_2)(e_s-e_2)$	$8.8+2.94W_2$	extensive pan measurements using different pans, correlated with tank and reservoir data
ϕ_e = evaporation at sea-level with wind corrected to 2 m, $BTU\ ft^2\ day^{-1}$ W = wind, mph e = vapor pressure, $mm\ Hg$ $W\ m^{-2} = 0.1314*BTU\ ft^2\ day^{-1}$ $10\ mb = 7.5006151\ mm\ Hg$					

Equilibrium Temperature

Since some of the terms in the term-by-term heat balance equation are surface temperature dependent and others are measurable or computable input variables, the most direct route is to define an equilibrium temperature, T_e , as the temperature at which the net rate of surface heat exchange is zero.

Linearization of the term-by-term heat balance along with the definition of equilibrium temperature allows expressing the net rate of surface heat exchange, H_n , as:

$$H_{aw} = -K_{aw}(T_w - T_e) \quad (\text{A-212})$$

where:

$$\begin{aligned} H_{aw} &= \text{rate of surface heat exchange, } W m^{-2} \\ K_{aw} &= \text{coefficient of surface heat exchange, } W m^{-2} \text{ } ^\circ C^{-1} \\ T_w &= \text{water surface temperature, } ^\circ C \\ T_e &= \text{equilibrium temperature, } ^\circ C \end{aligned}$$

Seven separate heat exchange processes are summarized in the coefficient of surface heat exchange and equilibrium temperature. The linearization is examined in detail by Brady, et al. (1968), and Edinger et al. (1974).

The definition of the coefficient of surface heat exchange can be shown to be the first term of a Taylor series expansion by considering the above equation as:

$$H_{aw} = -\frac{dH_{an}}{dT_s}(T_s - T_e) \quad (\text{A-213})$$

where the derivative of H_{aw} with respect to surface temperature is evaluated from equation A-191 to give K_{aw} , the coefficient of surface heat exchange. All approximations of the individual surface heat exchange terms enter into the evaluation of the coefficient of surface heat exchange and the equilibrium temperature.

The mass evaporation rate is computed by dividing evaporative heat loss by the latent heat of evaporation of water. Surface heat exchange always includes evaporative heat loss in the heat budget, but the user may choose to exclude it in the water budget. For many reservoirs, inflow rates are determined from storage estimates that implicitly include evaporation.

Sediment Heat Exchange

Sediment heat exchange with water is generally small compared to surface heat exchange and many previous modelers have neglected it. Investigations on several reservoirs have shown the process must be included to accurately reproduce hypolimnetic temperatures primarily because of the reduction in numerical diffusion that previously swamped the numerical solution. The formulation is similar to surface heat exchange:

$$H_{sw} = -K_{sw}(T_w - T_s) \quad (\text{A-214})$$

where:

$$\begin{aligned}
 H_{sw} &= \text{rate of sediment/water heat exchange, } W m^{-2} \\
 K_{sw} &= \text{coefficient of sediment/water heat exchange, } W m^{-2} \text{ } ^\circ C^{-1} \\
 T_w &= \text{water temperature, } ^\circ C \\
 T_s &= \text{sediment temperature, } ^\circ C
 \end{aligned}$$

Previous applications used a value of $0.3 W m^{-2} \text{ } ^\circ C^{-1}$ for K_{sw} that is approximately two orders of magnitude smaller than the surface heat exchange coefficient. Average yearly air temperature is a good estimate of T_s .

Dynamic Shading

Solar Altitude and Azimuth

The declination angle, δ , is computed from Spencer (1971):

$$\begin{aligned}
 \delta = & 0.006918 - 0.399912 \cos(\tau_d) + 0.070257 \sin(\tau_d) - 0.006758 \cos(2\tau_d) \\
 & + 0.000907 \sin(2\tau_d) - 0.0022697 \cos(3\tau_d) + 0.001480 \sin(3\tau_d)
 \end{aligned} \quad (\text{A-215})$$

where:

$$\tau_d = \frac{2\pi(JD_i - 1)}{365}$$

JD_i = Julian date integer value

The local hour is calculated as:

$$HOUR = 24(JD_r - JD_i) \quad (\text{A-216})$$

where:

JD_i = Julian date integer value

JD_r = Julian date floating-point value

An equation of time, EQT , correction is needed to calculate the local hour angle. The equation of time represents the difference between true and mean solar time due to seasonal variations in the earth's orbital velocity (DiLaura, D.L 1984) and is given as:

$$EQT = 0.17 \sin \frac{4\pi(JD_i - 80)}{373} - 0.129 \sin \frac{2\pi(JD_i - 8)}{355} \quad (\text{A-217})$$

where:

JD_i = Julian date integer value

The local hour angle, H , is calculated as:

$$H = \frac{2\pi}{24} \left[HOUR + (Long - \phi) \frac{24}{360} + EQT - 12 \right] \quad (\text{A-218})$$

The solar altitude, A_o , is the angle of inclination of the sun relative to the horizon from an observer's perspective as shown in [Figure A-50](#).

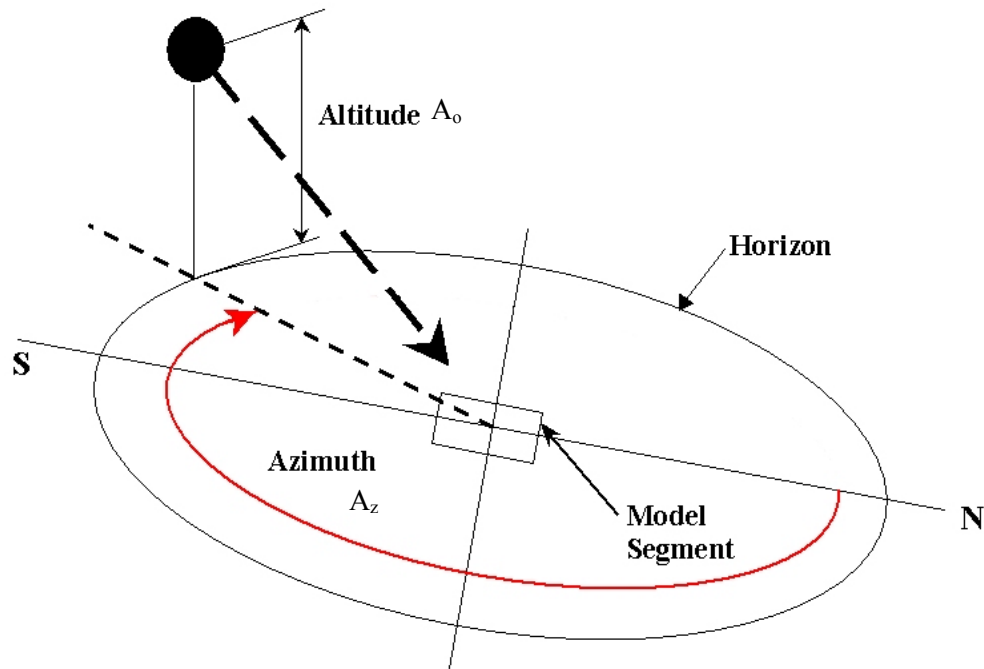


Figure A-50. Schematic of solar altitude, A_o , and azimuth, AZ

A_o is calculated from Wunderlich (1972):

$$A_o = A \sin \left[\sin \left(lat * \frac{\pi}{180} \right) \sin(\delta) + \cos \left(lat * \frac{\pi}{180} \right) \cos(\delta) \cos(H) \right] \quad (\text{A-219})$$

The solar azimuth is the direction of the sun with respect to a North-South axis measured clockwise from the North as shown in [Figure A-51](#). The solar azimuth is computed as (Annual Nautical Almanac, 2001):

$$X = \frac{\sin(\delta) \cos \left(\frac{Lat * \pi}{180} \right) - \cos(\delta) \cos(H) \sin \left(\frac{Lat * \pi}{180} \right)}{\cos A_o} \quad (\text{A-220})$$

$$\begin{aligned} \text{If } X > 1, \quad X &= 1 \\ \text{If } X < -1, \quad X &= -1 \end{aligned} \tag{A-221}$$

$$A = A \cos X \tag{A-222}$$

$$\begin{aligned} AZ &= 2\pi - A \\ \text{If } H < 0, \quad AZ &= A \end{aligned} \tag{A-223}$$

After computing the solar altitude and azimuth, the impact of shading ([Figure A-51](#)) on short-wave solar radiation is computed as follows.

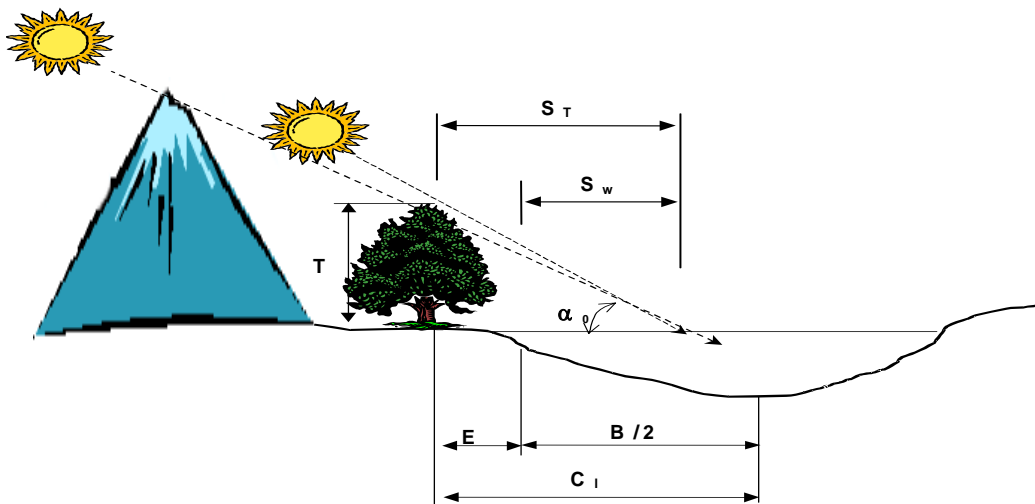


Figure A-51. Schematic of topographic and vegetative shading, solar altitude (α_0), and vegetation height (T) and their affect on shadow length.

Topographic Shading

The algorithm uses the position of the sun to determine which topographic inclination angle coincides with the direction of incoming solar radiation. The algorithm determines the closest two inclination angles in the direction of the incoming solar radiation and uses them to linearly interpolate an inclination angle for the specific direction of the incoming solar radiation. The calculated inclination angle is then used to determine if vegetative or topographic shading dominates at that time. If the solar altitude is below the calculated topographic inclination angle, then topographic shading dominates and the short wave solar radiation is reduced by 90% for complete shade. This allows for 10% of the incoming solar radiation as a result of diffuse radiation even when in the shade. If the solar altitude is above the calculated inclination angle, then vegetative shading dominates.

Vegetative Shading

If the topographic angle is less than the solar altitude, vegetative shade dominates and the algorithm calculates the shading influence by determining how far the shadow extends over the water. [Figure A-52](#) and [Figure A-53](#) show schematics of the azimuth angle, segment orientation and computed shadow lengths. The tree shadow length, S_T , is calculated using the tree height, T , and solar altitude,

A_0 , using Equation A-206. Then the length of the shadow cast over the water is calculated using Equation A-207 where E is the distance between the tree and the edge of water and $\tilde{\Theta}$ is the segment orientation. The shadow length, S_N , perpendicular to the edge of the water is then calculated using Equation A-208. Refer to [Figure A-52](#) and [Figure A-53](#) for diagrams showing the distance calculated in Equations A-206 to A-208.

$$S_T = \frac{T}{\tan A_0} \quad (\text{A-224})$$

$$S_w = S_T - \frac{E}{\sin(\Theta_0 - \alpha_A)} \quad (\text{A-225})$$

$$S_N = S_w \sin(\Theta_0 - \alpha_A) \quad (\text{A-226})$$

Simplifying Equations A-206 to A-208:

$$S_N = \frac{T * \sin(\Theta_0 - \alpha_A)}{\tan A_0} - E \quad (\text{A-227})$$

A shading reduction factor is applied in cases where a model segment has potential shading along only part of its segment length or the vegetation density is low. For example, if shade-producing vegetation exists along only half the length of a segment and is 100% opaque, a shade reduction factor of 0.5 is used. If shading is due to vegetation along only half of a segment with 80% opaqueness, a value of 0.4 is used.

The shade factor, $sfact$, is the shadow length perpendicular to the edge of the water, S_N , multiplied by the shade reduction factor, SRF , and divided by the segment width:

$$sfact = SRF \frac{S_N}{B} \quad (\text{A-228})$$

The amount of shade that should be applied to the incoming short wave solar radiation is calculated as:

$$Shade = (1 - sfact) \quad (\text{A-229})$$

The short wave solar radiation [SRO] computed by the model is reduced by the shade variable:

$$SRO_{net} = SRO * Shade \quad (\text{A-230})$$

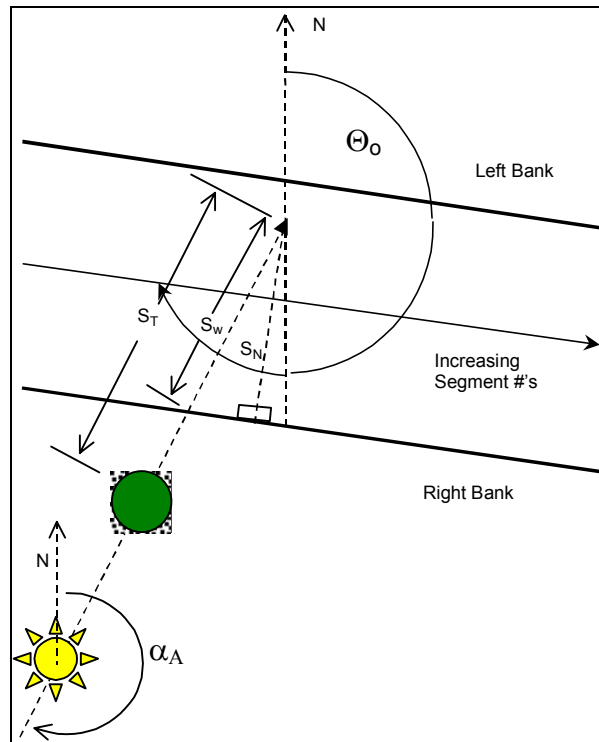


Figure A-52. Azimuth angle, α_{AZ} , and stream orientation, Θ_0 .

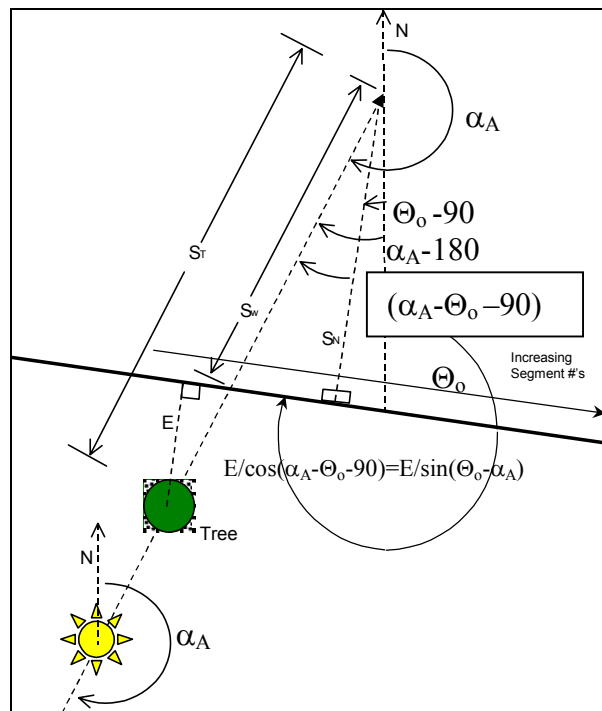


Figure A-53. Relationship between azimuth, stream orientation, and shadow length.

Data Requirements

Topography and vegetation data are stored in a user-defined input file. An example input file is shown in Appendix C. The file includes tree top elevations for both stream banks. The file also includes the distance from the centerline of the river to the controlling vegetation and the shade reduction factor (explained below) for both stream banks. The shade file has vegetation characteristics recorded by the left and right banks of the stream. The convention used for defining left or right bank is dependent on looking downstream in the system, the 'Left Bank' is on the left and the 'Right Bank' is to the right.

The shade algorithm reads in 18 topographic inclination angles surrounding each segment center-point. The inclination angles can be determined using topographical maps, Digital Elevation Models (DEM), or contour plots. The steepest inclination angle for each of the 18 locations surrounding a segment should be selected since this angle will control the topographic shading. The first inclination angle is taken from directly North of a segment (orientation angle 0.0) and moves clockwise to the East with increasing orientation angles around the segment in 20° increments.

How far away from the centerline of the river the topography should be analyzed will depend on the system. Wide flat river systems will utilize longer distances for identifying influencing topography than a narrow river canyon. In addition, rather than restricting the code to orientation angles only toward the south appropriate for the Northern hemisphere, using orientation angles that surround a segment allows the algorithm to be used in both the northern and southern hemispheres.

In addition, the user can specify dynamic shading reduction factors as a function of time. Usually, these would correspond to the times for leaf growth and fall for deciduous trees.

The topography and vegetation information is first read in from the input file. Then, using the segment orientation angle, Θ_0 , and the solar azimuth, α_A , the bank that has the sun behind it is computed. The criteria used for determining the bank with the sun behind it was modified from Chen (1996) because the segment orientation angle is determined differently in CE-QUAL-W2. [Table A-6](#) shows the criteria used in the model.

Table A-6. Criteria for determining sunward bank

Sunward Bank	$0^\circ < \Theta_0 \leq 180^\circ$	$180^\circ < \Theta_0 \leq 360^\circ$
Left	$\alpha_A < \Theta_0$ or $\alpha_A > \Theta_0 + 180^\circ$	$\Theta_0 - 180^\circ < \alpha_A < \Theta_0$
Right	$\Theta_0 < \alpha_A < \Theta_0 + 180^\circ$	$\alpha_A > \Theta_0$ or $\alpha_A < \Theta_0 - 180^\circ$

Ice Cover

Ice thickness, onset, and loss of ice cover play an important role in the heat budget of northern water-bodies. At high latitudes, ice cover may remain until late spring or early summer and prevent warming due to absorption of short wave solar radiation.

The ice model is based on an ice cover with ice-to-air heat exchange, conduction through the ice, conduction between underlying water, and a "melt temperature" layer on the ice bottom (Ashton, 1979). The overall heat balance for the water-to-ice-to-air system is:

$$\rho_i L_f \frac{\Delta h}{\Delta t} = h_{ai} (T_i - T_e) - h_{wi} (T_w - T_m) \quad (\text{A-231})$$

where:

- ρ_i = density of ice, $kg\ m^{-3}$
- L_f = latent heat of fusion of ice, $J\ kg^{-1}$
- $\Delta h/\Delta t$ = change in ice thickness (h) with time (t), $m\ sec^{-1}$
- h_{ai} = coefficient of ice-to-air heat exchange, $W\ m^{-2}\ ^\circ C^{-1}$
- h_{wi} = coefficient of water-to-ice heat exchange through the melt layer, $W\ m^{-2}\ C$
- T_i = ice temperature, $^\circ C$
- T_{ei} = equilibrium temperature of ice-to-air heat exchange, $^\circ C$
- T_w = water temperature below ice, $^\circ C$
- T_m = melt temperature, $0^\circ C$

The ice-to-air coefficient of surface heat exchange, h_{ai} , and its equilibrium temperature, T_{ei} , are computed the same as for surface heat exchange in Edinger, et al. (1974) because heat balance of the thin, ice surface water layer is the same as the net rate of surface heat exchange presented previously. The coefficient of water-to-ice exchange, h_{wi} , depends on turbulence and water movement under ice and their effect on melt layer thickness. It is a function of water velocity for rivers but must be empirically adjusted for reservoirs.

Ice temperature in the ice-heat balance is computed by equating the rate of surface heat transfer between ice and air to the rate of heat conduction through ice:

$$h_{ai} (T_i - T_{ei}) = \frac{-k_i(T_i - T_m)}{h} \quad (\text{A-232})$$

where:

- k_i = molecular heat conductivity of ice, $W\ m^{-1}\ ^\circ C^{-1}$

When solved for ice temperature, T_i , and inserted in the overall ice-heat balance, the ice thickness relationship becomes:

$$\frac{\rho_i L_f \Delta h}{\Delta t} = \frac{(T_m - T_{ei})}{\frac{h}{k_i} + \frac{1}{h_{ia}}} - h_{wi} (T_w - T_m) \quad (\text{A-233})$$

from which ice thickness can be computed for each longitudinal segment. Heat from water to ice transferred by the last term is removed in the water temperature transport computations.

Variations in the onset of ice cover and seasonal growth and melt over the waterbody depend on locations and temperatures of inflows and outflows, evaporative wind variations over the ice surface, and effects of water movement on the ice-to-water exchange coefficient. Ice will often form in reservoir branches before forming in the main pool and remain longer due to these effects.

A second, more detailed algorithm for computing ice growth and decay has been developed for the model. The algorithm consists of a series of one-dimensional, quasi steady-state, thermodynamic calculations for each timestep. It is similar to those of Maykut and Untersteiner (1971), Wake (1977) and Patterson and Hamblin (1988). The detailed algorithm provides a more accurate representation of the upper part of the ice temperature profile resulting in a more accurate calculation of ice surface temperature and rate of ice freezing and melting.

The ice surface temperature, T_s , is iteratively computed at each timestep using the upper boundary condition as follows. Assuming linear thermal gradients and using finite difference approximations, heat fluxes through the ice, q_i , and at the ice-water interface, q_{iw} , are computed. Ice thickness at time t , $\theta(t)$, is determined by ice melt at the air-ice interface, $\Delta\theta_{ai}$, and ice growth and melt at the ice-water interface, $\Delta\theta_{iw}$. The computational sequence of ice cover is presented below.

Initial Ice Formation

Formation of ice requires lowering the surface water temperature to the freezing point by normal surface heat exchange processes. With further heat removal, ice begins to form on the water surface. This is indicated by a negative water surface temperature. The negative water surface temperature is then converted to equivalent ice thickness and equivalent heat is added to the heat source and sink term for water. The computation is done once for each segment beginning with the ice-free period:

$$\theta_0 = \frac{-T_{wn} \rho_w C_{pw} h}{\rho_i L_f} \quad (\text{A-234})$$

where:

- θ_0 = thickness of initial ice formation during a timestep, m
- T_{wn} = local temporary negative water temperature, $^{\circ}C$
- h = layer thickness, m
- ρ_w = density of water, $kg\ m^{-3}$
- C_{pw} = specific heat of water, $J\ kg^{-1}\ ^{\circ}C^{-1}$
- ρ_i = density of ice, $kg\ m^{-3}$
- L_f = latent heat of fusion, $J\ kg^{-1}$

Air-Ice Flux Boundary Condition and Ice Surface Temperature Approximation

The ice surface temperature, T_s , must be known to calculate the heat components, H_{br} , H_e , H_c , and the thermal gradient in the ice since the components and gradient all are either explicitly or implicitly a function of T_s . Except during the active thawing season when ice surface temperature is constant at $0^{\circ}C$, T_s must be computed at each timestep using the upper boundary condition. The approximate value for T_s is obtained by linearizing the ice thickness across the timestep and solving for T_s .

$$T_s^n \approx \frac{\theta^{n-1}}{K_i} \left[H_{sn}^n + H_{an}^n - H_{br} T_s^n - H_e T_s^n - H_c T_s^n \right] \quad (\text{A-235})$$

$$H_{sn} + H_{an} - H_{br} - H_e - H_c + q_i = \rho_i L_f \frac{d\theta_{ai}}{dt}, \text{ for } T_s = 0^\circ \text{C} \quad (\text{A-236})$$

$$q_i = K_i \frac{T_f - T_s(t)}{\theta(t)} \quad (\text{A-237})$$

where:

K_i = thermal conductivity of ice, $W m^{-1} \text{ } ^\circ C^{-1}$

T_f = freezing point temperature, $^\circ C$

n = time level

Absorbed Solar Radiation by Water Under Ice

Although the amount of penetrated solar radiation is relatively small, it is an important component of the heat budget since it is the only heat source to the water column when ice is present and may contribute significantly to ice melting at the ice-water interface. The amount of solar radiation absorbed by water under the ice cover may be expressed as:

$$H_{ps} = H_s (1 - ALB_i) (1 - \beta_i) e^{-\gamma_i \theta(t)} \quad (\text{A-238})$$

where:

H_{ps} = solar radiation absorbed by water under ice cover, $W m^{-2}$

H_s = incident solar radiation, $W m^{-2}$

ALB_i = ice albedo

β_i = fraction of the incoming solar radiation absorbed in the ice surface

γ_i = ice extinction coefficient, m^{-1}

Ice Melt at Air-Ice Interface

The solution for T_s holds as long as net surface heat exchange, $H_n(T_s)$, remains negative corresponding to surface cooling, and surface melting cannot occur. If $H_n(T_s)$ becomes positive corresponding to a net gain of heat at the surface, q_i must become negative and an equilibrium solution can only exist if $T_s > T_f$. This situation is not possible as melting will occur at the surface before equilibrium is reached (Patterson and Hamblin, 1988). Because of a quasi-steady approximation, heat, which in reality is used to melt ice at the surface, is stored internally producing an unrealistic temperature profile. Stored energy is used for melting at each timestep and since total energy input is the same, net error is small. Stored energy used for melting ice is expressed as:

$$\rho_i C_{pi} \frac{T_s(t)}{2} \theta(t) = \rho_i L_f \Delta \theta_{ai} \quad (\text{A-239})$$

where:

$$C_{pi} = \text{specific heat of ice, } J \text{ kg}^{-1} \text{ } ^\circ\text{C}^{-1}$$

$$\theta_{ai} = \text{ice melt at the air-ice interface, } m^{-1}$$

Ice-Water Flux Boundary Condition Formulation

Both ice growth and melt may occur at the ice-water interface. The interface temperature, T_f , is fixed by the water properties. Flux of heat in the ice at the interface therefore depends on T_f and the surface temperature T_s through the heat flux q_i . Independently, heat flux from the water to ice, q_{iw} , depends only on conditions beneath the ice. An imbalance between these fluxes provides a mechanism for freezing or melting. Thus,

$$q_i - q_{iw} = \rho_i L_f \frac{d\theta_{iw}}{dt} \quad (\text{A-240})$$

where:

$$\theta_{iw} = \text{ice growth/melt at the ice-water interface}$$

The coefficient of water-to-ice exchange, K_{wi} , depends on turbulence and water movement under the ice and their effect on melt layer thickness. It is known to be a function of water velocity for rivers and streams but must be empirically adjusted for reservoirs. The heat flux at the ice-water interface is:

$$q_{iw} = h_{wi} (T_w(t) - T_f) \quad (\text{A-241})$$

where:

$$T_w = \text{water temperature in the uppermost layer under the ice, } ^\circ\text{C}$$

Finally, ice growth or melt at the ice-water interface is:

$$\Delta\theta_{iw}^n = \frac{I}{\rho_i L_f} \left[K_i \frac{T_f - T_s^n}{\theta^{n-1}} - h_{wi} (T_w^n - T_f) \right] \quad (\text{A-242})$$

Density

Accurate hydrodynamic calculations require accurate water densities. Water densities are affected by variations in temperature and solids concentrations given by :

$$\rho = \rho_T + \Delta \rho_S \quad (\text{A-243})$$

where:

$$\begin{aligned} \rho &= \text{density, } kg\ m^{-3} \\ \rho_T &= \text{water density as a function of temperature, } kg\ m^{-3} \\ \Delta \rho_S &= \text{density increment due to solids, } kg\ m^{-3} \end{aligned}$$

A variety of formulations has been proposed to describe water density variations due to temperatures. The following relationship is used in the model (Gill, 1982):

$$\begin{aligned} \rho_{T_w} = & 999.845259 - 4 + 6.793952 \times 10^{-2} T_w \\ & - 9.095290 \times 10^{-3} T_w^2 + 1.001685 \times 10^{-4} T_w^3 \\ & - 1.120083 \times 10^{-6} T_w^4 + 6.536332 \times 10^{-9} T_w^5 \end{aligned} \quad (\text{A-244})$$

Suspended and dissolved solids also affect density. For most applications, dissolved solids will be in the form of total dissolved solids. For estuarine applications, salinity should be specified. The effect of dissolved solids on density is calculated using either of these variables with the choice specified by the variable [WTYPE]. Density effects due to total dissolved solids are given by Ford and Johnson (1983):

$$\Delta \rho_{TDS} = (8.221 \times 10^{-4} - 3.87 \times 10^{-6} T_w + 4.99 \times 10^{-8} T_w^2) \Phi_{TDS} \quad (\text{A-245})$$

where:

$$\Phi_{TDS} = \text{TDS concentration, } g\ m^{-3}$$

and for salinity (Gill, 1982):

$$\begin{aligned} \Delta \rho_{sal} = & (0.824493 - 4.0899 \times 10^{-3} T_w + 7.6438 \times 10^{-5} T_w^2 \\ & - 8.2467 \times 10^{-7} T_w^3 + 5.3875 \times 10^{-9} T_w^4) \Phi_{sal} \\ & + (-5.72466 \times 10^{-3} + 1.0227 \times 10^{-4} T_w \\ & - 1.6546 \times 10^{-6} T_w^2) \Phi_{sal}^{1.5} + 4.8314 \times 10^{-4} \Phi_{sal}^2 \end{aligned} \quad (\text{A-246})$$

where:

$$\Phi_{sal} = \text{salinity, } kg\ m^{-3}$$

The suspended solids effects are given by Ford and Johnson (1983):

$$\Delta \rho_{ss} = \Phi_{ss} \left(1 - \frac{1}{SG} \right) \times 10^{-3} \quad (\text{A-247})$$

where:

$$\begin{aligned} \Phi_{ss} &= \text{suspended solids concentration, } g \, m^{-3} \\ SG &= \text{specific gravity of suspended solids} \end{aligned}$$

Assuming a specific gravity of 2.65, the above relationship is simplified to:

$$\Delta \rho_{ss} = 0.00062 \, \Phi_{ss} \quad (\text{A-248})$$

The total effect of solids is then:

$$\Delta \rho_s = (\Delta \rho_{sal} \text{ or } \Delta \rho_{tds}) + \Delta \rho_{ss} \quad (\text{A-249})$$

Selective Withdrawal

The latest version includes selective withdrawal for all outflows where layer locations and outflows at each layer are calculated based on the total outflow [\[QOUT\]](#), structure type [\[SINKC\]](#), elevation [\[ESTRI\]](#), and computed upstream density gradients. The selective withdrawal computation uses these values to compute vertical withdrawal zone limits and outflows. It also sums the outflows for multiple structures.

Outflow distribution is calculated in the subroutine SELECTIVE_WITHDRAWAL. This routine first calculates limits of withdrawal based on either a user specified point or line sink approximation for outlet geometry [\[SINKC\]](#). The empirical expression for point sink withdrawal limits is:

$$d = (c_{bi} Q/N)^{0.3333} \quad (\text{A-250})$$

and for a line sink:

$$d = (c_{bi} 2q/N)^{0.5} \quad (\text{A-251})$$

where:

$$\begin{aligned} d &= \text{withdrawal zone half height, } m \\ Q &= \text{total outflow, } m^3 \, s^{-1} \\ N &= \text{internal buoyancy frequency, } Hz \\ q &= \text{outflow per unit width, } m^2 \, s^{-1} \\ c_{bi} &= \text{boundary interference coefficient} \end{aligned}$$

The width is the outlet width. The point sink approximation assumes approach flow is radial both longitudinally and vertically while the line sink approximation assumes flow approaches the outlet radially in the vertical. The boundary interference coefficient is two near a physical boundary and one elsewhere.

Velocities are determined using a quadratic shape function:

$$V_k = I - \left[\frac{(\rho_k - \rho_o)}{(\rho_l - \rho_o)} \right]^2 \quad (\text{A-252})$$

where:

- V_k = normalized velocity in layer k
- ρ_k = density in layer k, $kg\ m^{-3}$
- ρ_o = density in the outlet layer, $kg\ m^{-3}$
- ρ_l = density of the withdrawal limit layer, $kg\ m^{-3}$

The shape function generates a maximum velocity at the outlet level with velocities approaching zero at withdrawal limits. During non-stratified periods, outflow from top to bottom is uniform. Uniform flows also result from large outflows during periods of mild stratification. As stratification develops, withdrawal limits decrease and outflow is weighted towards the outlet elevation.

Withdrawal limits can be varied by specifying a line sink and changing the effective width. Small outlet widths result in nearly uniform outflows, while large widths limit outflows to the outlet layer.

Sediment Resuspension

This algorithm is based on work from Kang et al. (1982) where the bottom shear stress is computed based on wind speed, wind fetch and depth. The wind blowing across a water surface creates wind waves that have orbital motion that decays with depth. The model user inputs a critical shear stress for detachment of the particles. If the critical shear stress is exceeded, then particles are resuspended. The approach of Kang et al. (1982) consists of the following steps:

1. Computation of the wave height, H_s in m,

$$H_s = \frac{W^2}{g} 0.283 \tanh \left[0.53 \left(\frac{gH}{W^2} \right)^{0.75} \right] \tanh \left[\frac{0.0125 \left(\frac{gF}{W^2} \right)^{0.42}}{\tanh \left[0.53 \left(\frac{gH}{W^2} \right)^{0.75} \right]} \right] \quad (\text{A-253})$$

where W is the wind velocity (m/s), F is the fetch (m), H is the mean depth (m)

2. Computation of wave period, T_s in s,

$$T_s = \frac{2\pi W}{g} 1.2 \tanh \left[0.833 \left(\frac{gH}{W^2} \right)^{0.375} \right] \tanh \left[\frac{0.077 \left(\frac{gF}{W^2} \right)^{0.25}}{\tanh \left[0.833 \left(\frac{gH}{W^2} \right)^{0.375} \right]} \right] \quad (\text{A-254})$$

3. Computation of the wavelength, L in m, iteratively from the following equation:

$$L = \frac{gT_s^2}{2\pi} \tanh \left[\frac{2\pi H}{L} \right] \quad (\text{A-255})$$

4. Computation of the orbital velocity, \bar{U} in cm/s,

$$\bar{U} = \frac{\pi H_s}{T_s} \frac{100}{\sinh(2\pi H / L)} \quad (\text{A-256})$$

5. Computation of bottom shear stress, τ in dynes/cm²,

$$\tau = 0.003 \bar{U}^2 \quad (\text{A-257})$$

6. Computation of actual bottom scour rate of suspended solids, ε in mass of sediments scoured per area or g/m²,

$$\varepsilon = 0 \quad \tau \leq \tau_c \quad (\text{A-258})$$

$$\varepsilon = \frac{\alpha_o}{t_d^2} (\tau - \tau_c)^3 \quad \tau > \tau_c \quad (\text{A-259})$$

where α_o is an empirical constant=0.008, $t_d=7$, and τ_c is the user-defined critical shear stress. Re-suspension supposedly only occurs during the first hour of the wind shear greater than the critical shear stress. Hence, the rate of resuspension per time, E in g/m²/hour, would be

$E = \frac{\varepsilon}{1hr}$ for the first hour and nothing after that. The resulting concentration of suspended solids

in the entire water column, c in mg/l, if distributed evenly over the entire volume would then be

$$c = \frac{10000\varepsilon A_{bottom}}{V} = \frac{10000\varepsilon}{H}$$

where A_{bottom} is the surface area of the bottom and V is the volume of the water column above the bottom (=HA_{bottom}). Chapra (1997) also uses this approach and provides an example calculation.

Appendix B Water Quality

The constituent transport relationships described in Appendix A compute the transport of constituents with their kinetic reaction rates expressed in source and sink terms. All sources/sinks (both internal and external) for water temperature are contained in the array [TSS]. The sources/sinks for constituents are separated into two arrays, [CSSB] and [CSSK]. [CSSB] contains boundary sources/sinks. [CSSK] contains internal sources/sinks due to kinetic interactions. The division of terms allows kinetic sources/sinks to be updated at different frequencies than boundary sources/sinks - consistent with coarser time scales associated with biological and chemical processes as opposed to hydrodynamics. Computational time is also reduced. The frequency at which kinetic sources/sinks [CSSK] are updated is specified by the parameter [\[CUF\]](#).

The source/sink term [CSSK] represents a mass rate of change ($grams\ sec^{-1}$) of a constituent due to kinetic reactions where concentrations are expressed as $grams\ meter^{-3}$. The kinetic reactions can be depicted graphically by considering each constituent as a compartment. Arrows represent mass transfer rates between compartments, with a source represented by a blue arrow leading to the compartment and a sink by a red arrow leading away. All of the rate terms in the following discussion are in units of sec^{-1} and these are the units used in the code. However, all rate units input into the model from the control file are in units of day^{-1} and are then converted to sec^{-1} before being used in the code. Both graphical and mathematical descriptions of the rate equation for each constituent are provided.

Overview of Kinetic Source/Sink Term

In order to solve the 2D advection-diffusion equation, the source/sink term, S_{ϕ} , must be specified. The model solves for temperature and a user specified number of water quality variables. Water Quality state variables along with their kinetic source/sink terms are shown in [Table B-1](#). The user can specify any number of generic constituents [\[NGC\]](#), suspended solids groups [\[NSS\]](#), CBOD groups [\[NBOD\]](#), algal groups [\[NAL\]](#), and epiphyton groups [\[NEP\]](#).

Table B-1. CE-QUAL-W2 V3.1 Water Quality State Variables

Constituent	Internal Source	Internal Sink
Total dissolved solids		
generic constituent, no interactions with other state variables bacteria tracer water age contaminants	0 order decay	settling 0 and 1 st order decay
Inorganic suspended solids		sedimentation
bioavailable P measured as one of the following ortho-P dissolved P SRP	algal/epiphyton respiration labile/refractory particulate/dissolved organic matter sediment release CBOD decay	algal/epiphyton growth adsorption onto inorganic suspended solids
ammonium	sediment release algal/epiphyton excretion labile/refractory dissolved/ particulate organic matter decay CBOD decay	algal/epiphyton growth nitrification
nitrate-nitrite	nitrification	denitrification algal/epiphyton growth
dissolved silica	anoxic sediment release particulate biogenic silica decay	algal/epiphyton growth adsorption onto suspended solids
particulate biogenic silica	algal/epiphyton mortality	settling decay
iron	anoxic sediment release	oxic water column settling
labile dissolved organic matter	algal/epiphyton mortality excretion	decay
refractory dissolved organic matter	labile dissolved organic matter decay	decay
labile particulate organic matter	algal/epiphyton mortality	settling decay
refractory particulate organic matter	labile particulate organic matter decay	settling decay
CBOD		decay
algae	algal growth	respiration excretion mortality settling
epiphyton	epiphyton growth	respiration excretion mortality settling
dissolved oxygen	surface exchange algal/epiphyton growth	surface exchange algal/epiphyton respiration nitrification CBOD decay 0 and 1 st order SOD labile/refractory dissolved/ particulate organic matter decay
total inorganic carbon	labile/refractory dissolved/ particulate organic matter decay sediment release surface exchange algal respiration	surface exchange algal/epiphyton growth CBOD decay
alkalinity		

In addition to these water quality state variables that are advected and diffused, the model also solves for pH and the carbonate cycle (CO₂, HCO₃, H₂CO₃), epiphyton, and sediment organic matter.

Generic Constituent

Any number of generic constituents [NGC] can be defined that can settle and decay. The user supplies a zero and/or 1st order decay coefficient with or without an Arrhenius temperature dependence function, and/or a settling velocity. Generic constituents do not interact with the hydrodynamics nor any other water quality state variables.

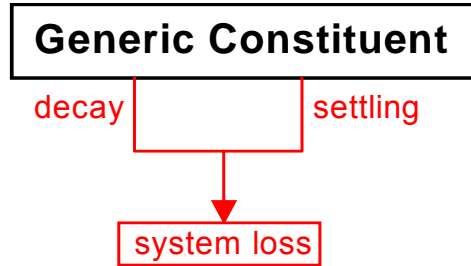


Figure B-1. Internal flux for generic constituent compartment.

Referring to [Figure B-1](#), the source/sink term for a generic constituent is:

$$S_g = \underbrace{-K_0 \theta_g^{(T-20)}}_{\text{0-order decay}} - \underbrace{K_1 \theta_g^{(T-20)} \Phi_g}_{\text{1st-order decay}} - \underbrace{\omega_g \frac{\partial \Phi_g}{\partial z}}_{\text{settling}} \quad (\text{B-1})$$

where:

- Y_g = temperature rate multiplier
- T = water temperature, °C
- ω_g = settling velocity, $m s^{-1}$
- K_0 = zero order decay coefficient, $g m^{-3} s^{-1}$ at $20^\circ C$
- K_1 = first order decay coefficient, s^{-1} at $20^\circ C$
- Φ_g = generic constituent concentration, $g m^{-3}$

A conservative tracer, coliform bacteria, and water age are some of the state variables that can be modeled using the generic constituent and are described further below.

Conservative Tracer

A conservative constituent is included to allow dye study simulations, movements of conservative materials through the waterbody, and as an aid in calibrating and testing flow regimes. As a conservative material, this constituent has no internal sources or sinks and the rate term [CSSK] is set to zero.

$$S_{tracer} = 0 \quad (\text{B-2})$$

Coliform Bacteria

Coliform bacteria is commonly used as an indicator of pathogen contamination. Safety standards and criteria for drinking and recreational purposes are based upon coliform concentrations. Predictions of coliform bacteria are important because of their impact on recreation and water supply.

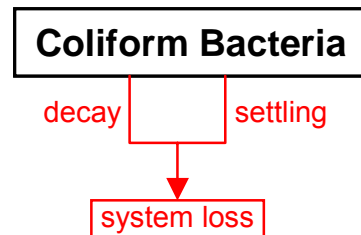


Figure B-2. Internal flux for coliform bacteria.

Total coliform, fecal coliform, fecal streptococci, and/or any other type of bacteria that do not interact with other state variables can be simulated with this generic constituent formulation. Referring to [Figure B-2](#), the rate equation for coliform bacteria is:

$$S_{col} = - \underbrace{K_{col} \theta^{(T-20)} \Phi_{col}}_{\text{1st-order decay}} - \underbrace{\omega_{col} \frac{\partial \Phi_{col}}{\partial z}}_{\text{settling}} \quad (\text{B-3})$$

where:

- θ = temperature factor (Q10)
- T = water temperature, °C
- K_{col} = coliform mortality rate, sec^{-1} at 20°C
- Φ_{col} = coliform concentration, $g m^{-3}$

The Q_{10} formulation arises from a doubling of the reaction rate with each 10°C increase in temperature. This doubling rate has not been found at lower temperatures (Hargrave 1972b) and is quite variable for various reactions (Giese 1968). Modeling coliform bacteria is discussed in detail in Zison, et al. (1978).

Water Age or Residence time

Setting the zero-order decay rate to -1 day^{-1} and zeroing out all other generic constituent kinetic parameters results in a state variable that increases by 1 day^{-1} , which is an exact representation of water age or hydraulic residence time. This is a very useful state variable when looking at hydrodynamics.

$$S_{age} = -1 \quad (\text{B-4})$$

Inorganic Suspended Solids

Inorganic suspended solids [ISS] are important in water quality simulations because of their influence on density, light penetration, and nutrient availability. Increased solids concentrations reduce light penetration in the water column thus affecting temperature that in turn affects biological and chemical reaction rates. Dissolved phosphorus and silica concentrations can also be affected by solids through sorption and settling. Light and nutrient availability largely control algal production.

The settling velocity of each inorganic suspended solids compartment is a user-defined parameter. Usually this is determined from Stoke's settling velocity for a particular sediment diameter and specific gravity. Any number of inorganic suspended solids groups can now be modeled.

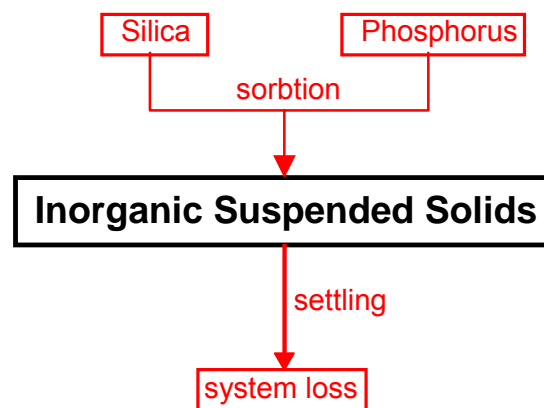


Figure B-3. Internal flux for inorganic suspended solids.

Referring to [Figure B-3](#), the rate equation for inorganic suspended solids is:

$$S_{ISS} = \omega_{ISS} \frac{\partial \Phi_{ISS}}{\partial z} \quad (\text{B-5})$$

where:

z = layer thickness, m

ω_{ISS} = settling velocity, $m \text{ sec}^{-1}$

Φ_{ISS} = inorganic suspended solids concentration, $g \text{ m}^{-3}$

In the finite difference representation of suspended solids concentrations, solids settling from layer [K]-1 serve as a source for the layer below it [K]. No provision is made to accumulate inorganic solids or allow resuspension in the sediments. A later version of the model will include these processes in a sediment transport compartment. Lateral averaging results in homogeneous solids concentrations laterally. In reality, concentrations generally decrease with distance away from the dominant flow path. This effect is not included. The rate term for inorganic suspended solids is evaluated in the subroutine SUSPENDED_SOLIDS.

Total Dissolved Solids or Salinity

Total dissolved solids (TDS) affect water density and ionic strength, thereby affecting water movements, pH, and the distribution of carbonate species. Dissolved solids are normally expressed as TDS in freshwater applications. Estuarine applications normally use salinity. Either TDS or salinity can be used with the choice indicated by the parameter `[WTYPEC]` specified in the control file. The choice is then reflected in the computation of density and ionic strength. If TDS is used, the units are $g\ m^{-3}$, while salinity is $kg\ m^{-3}$. It is important to keep in mind TDS and salinity are not equivalent - salinity is conservative while TDS is not. In the model, however, both are treated conservatively with the rate term set to zero.

Labile DOM

Because of the importance of dissolved oxygen in aquatic systems, all constituents exerting an oxygen demand must be included in kinetic formulations. This demand is often measured in rivers as the biochemical oxygen demand (BOD), which includes microbial respiration and metabolism of various organic and inorganic compounds. However, production of these materials occurs as well as decomposition, requiring the major components of BOD be modeled individually. One of these constituents is dissolved organic matter (DOM), which is composed of labile and refractory components. DOM is modeled as two separate compartments because of the different decomposition rates of the two groups.

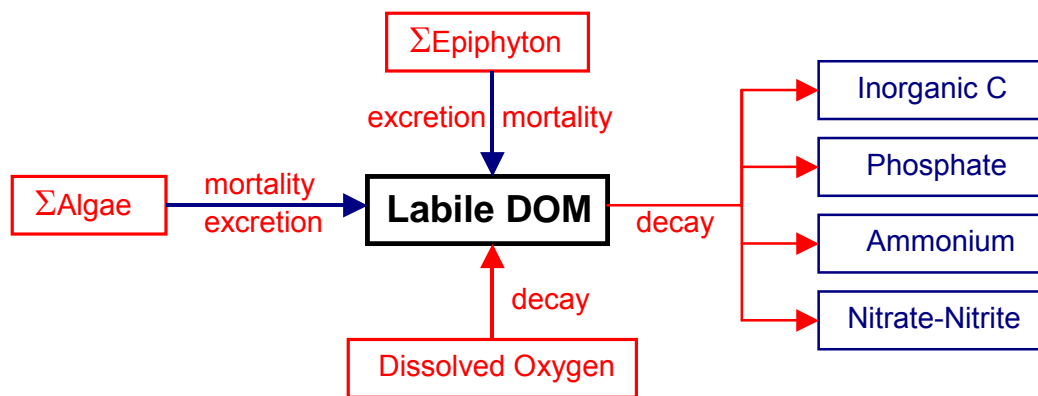


Figure B-4. Internal flux between labile DOM and other compartments

Referring to [Figure B-4](#), the rate equation for labile DOM is:

$$\begin{aligned}
 S_{L\text{DOM}} = & \underbrace{\sum K_{ae} \Phi_a}_{\text{algal excretion}} + \underbrace{\sum (1 - P_{am}) K_{am} \Phi_a}_{\text{algal mortality}} + \underbrace{\sum K_{ee} \Phi_e}_{\text{epiphyton excretion}} \\
 & + \underbrace{\sum (1 - P_{em}) K_{em} \Phi_e}_{\text{epiphyton mortality}} - \underbrace{\gamma_{OM} K_{L\text{DOM}} \Phi_{L\text{DOM}}}_{\text{labile DOM decay}} - \underbrace{K_{L \rightarrow R} \Phi_{L\text{DOM}}}_{\text{labile to refractory DOM decay}}
 \end{aligned}
 \tag{B-6}$$

where:

- P_{am} = pattern coefficient for algal mortality
- P_{em} = pattern coefficient for epiphyton mortality
- γ_{OM} = temperature rate multiplier for organic matter decay
- K_{ae} = algal excretion rate, sec^{-1}
- K_{am} = algal mortality rate, sec^{-1}
- K_{ee} = epiphyton excretion rate, sec^{-1}
- K_{em} = epiphyton mortality rate, sec^{-1}
- K_{LDOM} = labile DOM decay rate, sec^{-1}
- $K_{L \rightarrow R}$ = labile to refractory DOM transfer rate, sec^{-1}
- Φ_a = algal concentration, $g\ m^{-3}$
- Φ_e = epiphyton concentration, $g\ m^{-3}$
- Φ_{LDOM} = labile DOM concentration, $g\ m^{-3}$

Refractory DOM

Refractory DOM is composed of compounds in the aquatic environment that slowly decompose exerting oxygen demand over long periods. Internally, refractory DOM is produced from the decomposition of labile DOM.

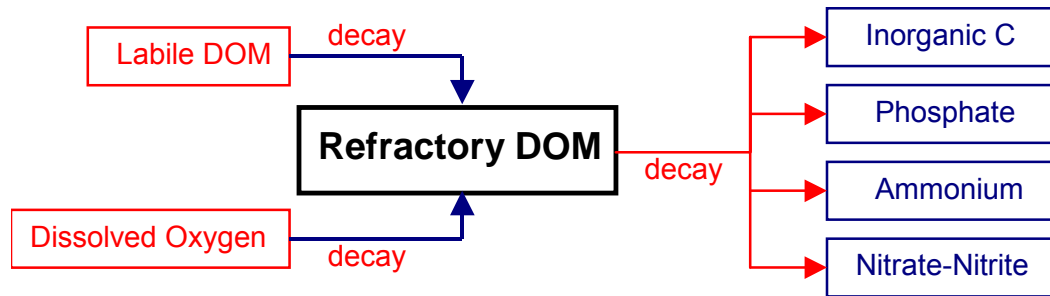


Figure B-5. Internal flux between refractory DOM and other compartments.

Referring to [Figure B-5](#), the rate equation for refractory DOM is:

$$S_{RDOM} = \underbrace{K_{L \rightarrow R} \Phi_{LDOM}}_{\text{labile to refractory DOM decay}} - \underbrace{\gamma_{OM} K_{RDOM} \Phi_{RDOM}}_{\text{decay}} \tag{B-7}$$

where:

- γ_{OM} = temperature rate multiplier
- K_{RDOM} = refractory DOM decay rate, sec^{-1}

$K_{L \rightarrow R}$ = transfer rate from labile DOM, sec^{-1}
 Φ_{LDOM} = labile DOM concentration, $g\ m^{-3}$
 Φ_{RDOM} = refractory DOM concentration, $g\ m^{-3}$

and the rate terms are evaluated in subroutine REFRACTORY_DOM.

Labile Particulate Organic Matter

Labile particulate organic matter (LPOM) represents particulate organic material in the water column. When decaying, particulate organic matter is a source of refractory particulate organic matter, nitrogen, phosphorus, and inorganic carbon. A stoichiometric relationship is used for mineralization of ammonium, phosphorus, and inorganic carbon, and an oxygen demand is exerted as LPOM decomposes. When LPOM settles to the bottom, it accumulates and decays in the sediment compartment if the 1st order sediment compartment is included in the simulation.

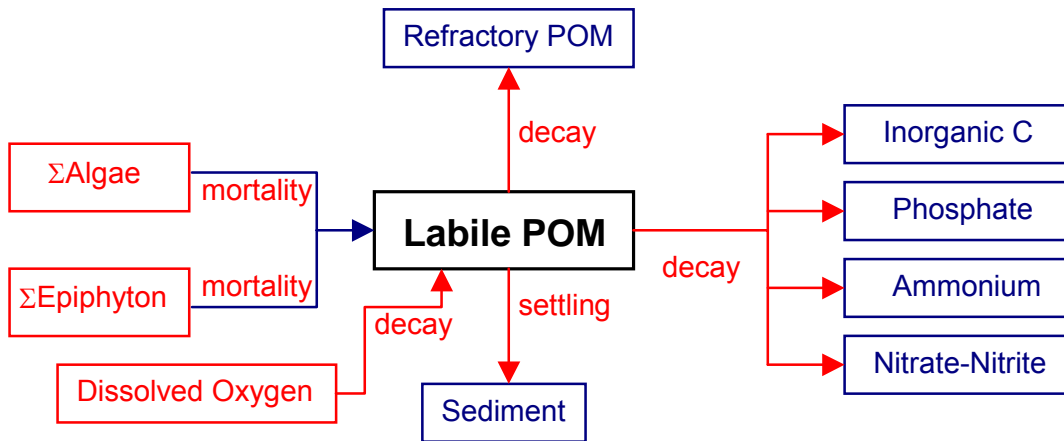


Figure B-6. Internal flux between Labile POM and other compartments.

Referring to [Figure B-6](#), the rate equation for LPOM is:

$$\begin{aligned}
 S_{LPOM} = & \underbrace{\sum P_{am} K_{am} \Phi_a}_{\text{algal mortality}} + \underbrace{\sum P_{em} K_{em} \Phi_e}_{\text{epiphyton mortality}} - \underbrace{K_{LPOM} \gamma_{OM} \Phi_{LPOM}}_{\text{decay}} \\
 & - \underbrace{K_{L \rightarrow R} \Phi_{LPOM}}_{\text{labile to refractory POM decay}} - \underbrace{\omega_{POM} \frac{\partial \Phi_{LPOM}}{\partial z}}_{\text{settling}}
 \end{aligned}
 \tag{B-8}$$

where:

P_{am} = partition coefficient for algal mortality
 P_{em} = partition coefficient for epiphyton mortality
 γ_{OM} = temperature rate multiplier for organic matter

- ω_{POM} = POM settling rate, $m\ sec^{-1}$
- K_{am} = algal mortality rate, sec^{-1}
- K_{em} = epiphyton mortality rate, sec^{-1}
- K_{LPOM} = labile POM decay rate, sec^{-1}
- $K_{L \rightarrow R}$ = transfer rate from labile POM to refractory POM, sec^{-1}
- Φ_a = algal concentration, $g\ m^{-3}$
- Φ_e = epiphyton concentration, $g\ m^{-3}$
- Φ_{LPOM} = detritus concentration, $g\ m^{-3}$

and the rate terms are evaluated in subroutine POM. POM settling and accumulation in the sediment compartment is handled identically to the algal compartment.

Refractory Particulate Organic Matter

Refractory POM is slowly decaying non-living, organic matter that settles. The source/sink terms are first order decay, the conversion of LPOM to RPOM, and sedimentation:

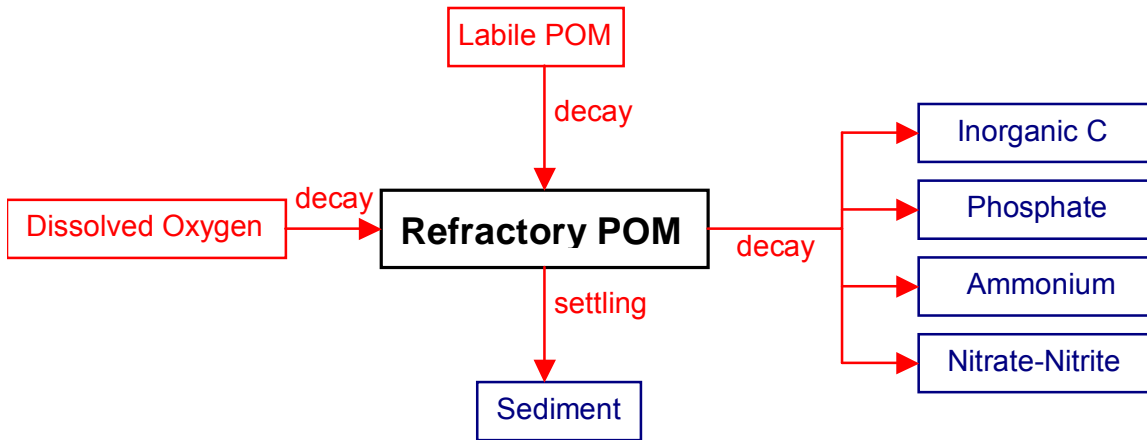


Figure B-7. Internal flux between refractory POM and other compartments.

Referring to [Figure B-7](#), the rate equation for labile POM is:

$$S_{RPOM} = \underbrace{K_{L \rightarrow R} \Phi_{LPOM}}_{\text{labile to refractory POM decay}} - \underbrace{\gamma_{OM} K_{RPOM} \Phi_{RPOM}}_{\text{decay}} - \underbrace{\omega_{RPOM} \frac{\partial \Phi_{RPOM}}{\partial z}}_{\text{settling}} \quad (\text{B-9})$$

where:

- γ_{OM} = temperature rate multiplier
- $K_{L \rightarrow R}$ = transfer rate from labile POM to refractory POM, sec^{-1}
- K_{RPOM} = refractory POM decay rate, sec^{-1}

ω_{POM} = POM settling velocity, m/sec^{-1}
 Φ_{LPOM} = labile POM concentration, $g\ m^{-3}$
 Φ_{RPOM} = refractory POM concentration, $g\ m^{-3}$

Carbonaceous Biochemical Oxygen Demand (CBOD)

Any number of CBOD groups with varying decay rates can be modeled allowing the user to more accurately characterize various CBOD sources to the prototype. Additionally, different CBOD sources can be tracked separately in the model to determine what affect they have at different locations in the system.

Care must be taken when including CBOD in the simulation to ensure that CBOD, DOM, POM, and algal biomass are properly accounted for. CBOD is typically specified as allochthonous inputs and the forms of autochthonous organic matter are kept track of in the various organic matter compartments. This ensures that no “double dipping” occurs.

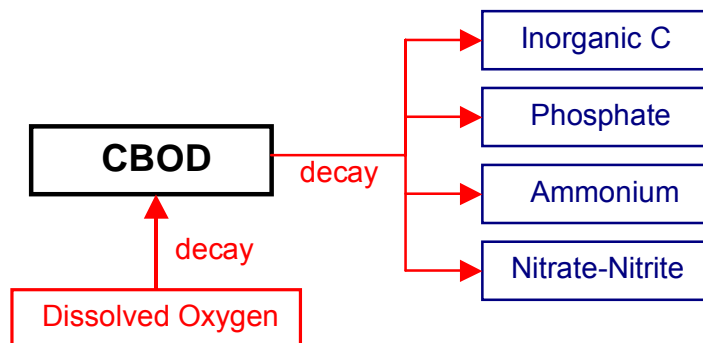


Figure B-8. Internal flux between CBOD and other compartments.

Referring to [Figure B-8](#), the rate equation for CBOD is:

$$S_{CBOD} = - \underbrace{\Theta^{T-20} K_{BOD} \Phi_{CBOD}}_{\text{decay}} \quad (\text{B-10})$$

where:

Θ = BOD temperature rate multiplier
 T = temperature, $^{\circ}C$
 K_{BOD} = CBOD decay rate, sec^{-1}
 Φ_{BOD} = CBOD concentration, $g\ m^{-3}$

Algae

Typically, the algal community is represented as a single assemblage or is broken down into diatoms, greens, and blue-greens. However, the current formulation now gives the user complete freedom in how many and what kinds of algal groups can be included in the simulation through careful specification of the kinetic rate parameters that define the characteristics of each algal group.

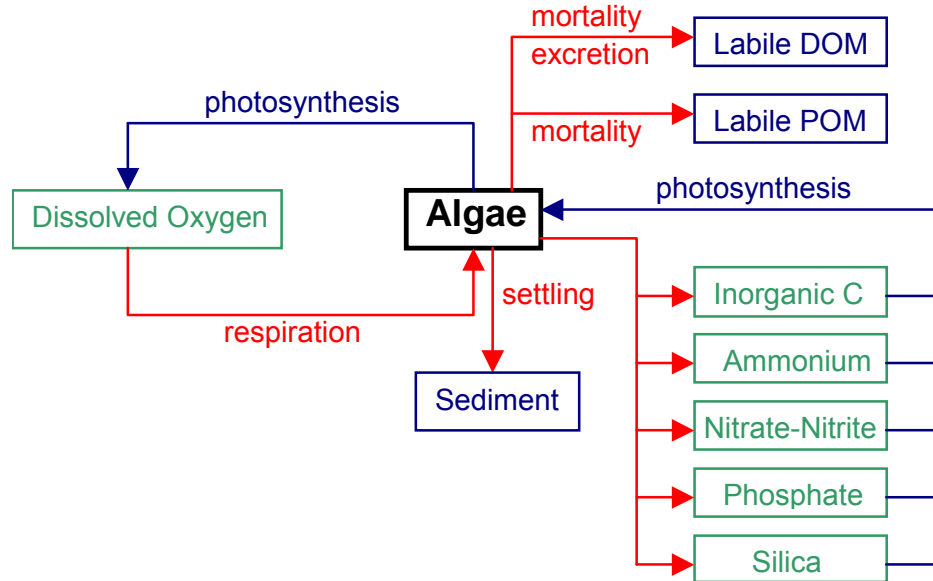


Figure B-9. Internal flux between algae and other compartments.

Referring to [Figure B-9](#), the rate equation for each algal group is:

$$S_a = \underbrace{K_{ag} \Phi_a}_{\text{growth}} - \underbrace{K_{ar} \Phi_a}_{\text{respiration}} - \underbrace{K_{ae} \Phi_a}_{\text{excretion}} - \underbrace{K_{am} \Phi_a}_{\text{mortality}} - \underbrace{\omega_a \frac{\partial \Phi_a}{\partial z}}_{\text{settling}} \quad (\text{B-11})$$

where:

- z = cell height
- K_{ag} = algal growth rate, sec^{-1}
- K_{ar} = algal dark respiration rate, sec^{-1}
- K_{ae} = algal excretion rate, sec^{-1}
- K_{am} = algal mortality rate, sec^{-1}
- ω_a = algal settling rate, $m sec^{-1}$
- Φ_a = algal concentration, $g m^{-3}$

Chlorophyll *a* (chl *a*) is most commonly available as an estimate of algal biomass. To convert chl *a* to algal biomass, chl *a* is typically multiplied by the given algae (as $g\ m^{-3}$ dry weight OM)/chl *a* ratio. This value can vary widely depending on the makeup of the algal population. Some previous studies determined the conversion factor by regressing particulate organic matter with chl *a*.

Algal growth rate is computed by modifying a maximum growth rate affected by temperature, light, and nutrient availability:

$$K_{ag} = \gamma_{ar} \gamma_{af} \lambda_{min} K_{agmax} \quad (\text{B-12})$$

where:

γ_{ar} = temperature rate multiplier for rising limb of curve

γ_{af} = temperature rate multiplier for falling limb of curve

λ_{min} = multiplier for limiting growth factor (minimum of light, phosphorus, silica, and nitrogen)

K_{ag} = algal growth rate, sec^{-1}

K_{agmax} = maximum algal growth rate, sec^{-1}

Rate multipliers for algal growth are computed based upon available light, phosphorus, nitrogen, and silica. The rate multiplier for light is based upon the Steele (1962) function:

$$\lambda_l = \frac{I}{I_s} e^{\left(-\frac{I}{I_s} + I\right)} \quad (\text{B-13})$$

where:

I = available light, $W\ m^{-2}$

I_s = saturating light intensity at maximum photosynthetic rate, $W\ m^{-2}$

λ_l = light limiting factor

The above expression allows for simulation of photoinhibition at light intensities greater than the saturation value. However, light penetration decreases with depth:

$$I = (1 - \beta) I_0 e^{-\alpha z} \quad (\text{B-14})$$

where:

I_0 = solar radiation at the water surface, $W\ m^{-2}$

α = attenuation coefficient, m^{-2}

z = depth, m

β = fraction of solar radiation absorbed at the water surface

The average effect of light on algal growth in a particular model cell can be obtained by combining the above two expressions and integrating over the cell depth to obtain (Chapra and Reckhow, 1983):

$$\lambda_l = \frac{e}{\alpha \Delta z} \left[e^{-\gamma_2} - e^{-\gamma_1} \right] \quad (\text{B-15})$$

where:

$$\gamma_1 = \frac{(1 - \beta) I_0}{I_s} e^{-\alpha d}$$

$$\gamma_2 = \frac{(1 - \beta) I_0}{I_s} e^{\alpha(d + \Delta z)}$$

d = depth at top of model cell, m

The fraction of solar radiation, β_{10} , is added directly to the surface layer. The attenuation coefficient, α , consists of a baseline value [EXH2O] to which the effects of inorganic [EXINOR] and organic [EXORG] suspended solids, and algae [EXA] are added.

Rate multipliers limiting maximum algal growth due to nutrient limitations are computed using the Monod relationship:

$$\lambda_i = \frac{\Phi_i}{P_i + \Phi_i} \quad (\text{B-16})$$

where:

Φ_i = phosphorus or nitrate + ammonium concentration, $g\ m^{-3}$

P_i = half-saturation coefficient for phosphorus or nitrate + ammonium, $g\ m^{-3}$

The algal nitrogen preference for ammonium is based upon the following (Thomann and Fitzpatrick, 1982).

$$P_{NH4} = \Phi_{NH4} \frac{\Phi_{NOx}}{(K_{NH4} + \Phi_{NH4})(K_{NH4} + \Phi_{NOx})} + \Phi_{NH4} \frac{K_{NH4}}{(\Phi_{NH4} + \Phi_{NOx})(K_{NH4} + \Phi_{NOx})} \quad (\text{B-17})$$

where:

P_{NH4} = ammonium preference factor

K_{NH4} = ammonia preference half-saturation coefficient, $g\ m^{-3}$

Φ_{NH4} = ammonium concentration, $g\ m^{-3}$

Φ_{NOx} = nitrate-nitrite concentration, $g\ m^{-3}$

This allows algae to use primarily ammonium and gradually switch to nitrate as ammonium concentrations decrease.

Algal dark respiration is computed using the rising limb of the temperature function:

$$K_{ar} = \gamma_{ar} \gamma_{af} K_{armax} \quad (\text{B-18})$$

where:

γ_{ar} = temperature rate multiplier for rising limb of curve

γ_{af} = temperature rate multiplier for falling limb of curve

K_{armax} = maximum dark respiration rate, sec^{-1}

Algal photorespiration (excretion) is evaluated using an inverse relation to the light rate multiplier:

$$K_{ae} = (1 - \lambda_l) \gamma_{ar} \gamma_{af} K_{aemax} \quad (\text{B-19})$$

where:

γ_{ar} = temperature rate multiplier for rising limb of curve

γ_{af} = temperature rate multiplier for falling limb of curve

K_{aemax} = maximum excretion rate constant, sec^{-1}

λ_l = light limiting factor

Excretion rates increase at both low and high light intensities, with excretion products contributing to labile DOM.

Algal mortality is defined as:

$$K_{am} = \gamma_{ar} \gamma_{af} K_{amax} \quad (\text{B-20})$$

where:

γ_{ar} = temperature rate multiplier for rising limb of curve

γ_{af} = temperature rate multiplier for falling limb of curve

K_{amax} = maximum mortality rate, sec^{-1}

This mortality rate represents both natural and predator mortality. Algal growth does not occur in the absence of light. Algal growth is not allowed to exceed the limit imposed by nutrient supply over a given timestep. Algal excretion is not allowed to exceed algal growth rates.

Similar to inorganic solids, settling algae serve as a source for the layer below. Unlike inorganic solids, algae passing to the sediments accumulate within the sediment compartment. POM is also accumulated in this sediment compartment.

Epiphyton

Any number of user defined epiphyton groups can be modeled. Similar to the 1st order sediment compartment, epiphyton are not transported in the water column and are thus not state variables.

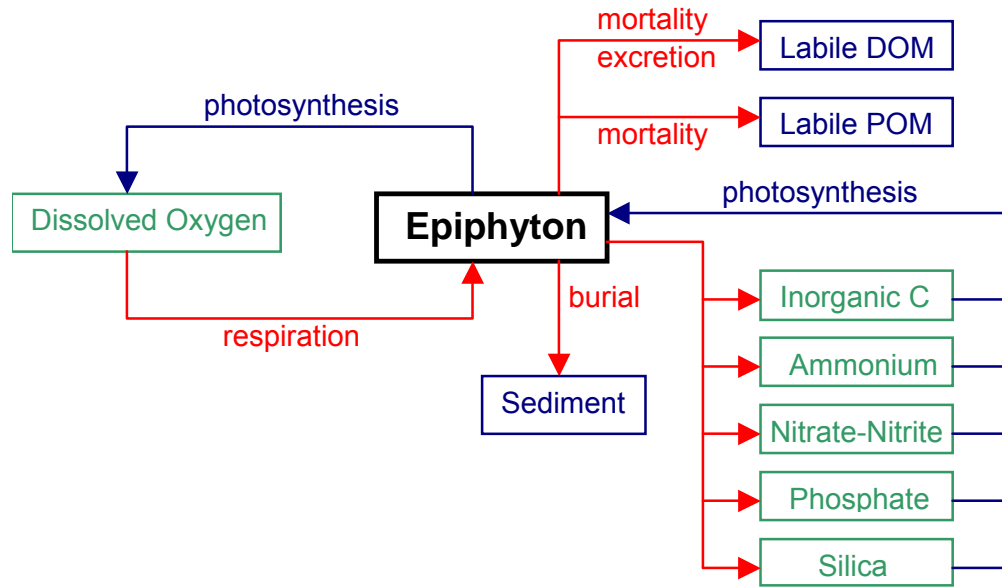


Figure B-10. Internal flux between epiphyton and other compartments.

Referring to [Figure B-10](#), the rate equation for each epiphyton group is:

$$S_e = \underbrace{K_{eg} \Phi_e}_{\text{growth}} - \underbrace{K_{er} \Phi_e}_{\text{respiration}} - \underbrace{K_{ee} \Phi_e}_{\text{excretion}} - \underbrace{K_{em} \Phi_e}_{\text{mortality}} - \underbrace{K_{eb} \Phi_e}_{\text{burial}} \quad (\text{B-21})$$

where:

- K_{eg} = epiphyton growth rate, sec^{-1}
- K_{er} = epiphyton dark respiration rate, sec^{-1}
- K_{ee} = epiphyton excretion rate, sec^{-1}
- K_{em} = epiphyton mortality rate, sec^{-1}
- K_{eb} = epiphyton burial rate, $m sec^{-1}$
- Φ_e = epiphyton concentration, $g m^{-3}$

Epiphyton growth rate is computed by modifying a maximum growth rate affected by epiphyton biomass, temperature, and nutrient availability:

$$K_{eg} = \gamma_{er} \gamma_{ef} \lambda_{min} K_{eg max} \quad (\text{B-22})$$

where:

γ_{er} = temperature rate multiplier for rising limb of curve

γ_{ef} = temperature rate multiplier for falling limb of curve

λ_{min} = multiplier for limiting growth factor (minimum of phosphorus, silica, nitrogen, and epiphyton biomass)

K_{eg} = epiphyton growth rate, sec^{-1}

K_{egmax} = maximum epiphyton growth rate, sec^{-1}

Rate multipliers for epiphyton growth are computed based upon available light, phosphorus, nitrogen, silica, and epiphyton biomass. Epiphyton biomass is included as a surrogate for light limited epiphyton self-shading and will be discussed in greater detail below.

The rate multiplier for light is based upon the Steele (1962) function:

$$\lambda_l = \frac{I}{I_s} e^{\left(-\frac{I}{I_s} + 1\right)} \quad (\text{B-23})$$

where:

I = available light, $W m^{-2}$

I_s = saturating light intensity at maximum photosynthetic rate, $W m^{-2}$

λ_l = light limiting factor

The above expression allows for simulation of photoinhibition at light intensities greater than the saturation value. However, light penetration decreases with depth:

$$I = (1 - \beta) I_0 e^{-\alpha z} \quad (\text{B-24})$$

where:

I_0 = solar radiation at the water surface, $W m^{-2}$

α = attenuation coefficient, m^{-1}

z = depth, m

β = fraction of solar radiation absorbed at the water surface

The average effect of light on epiphyton growth in a particular model cell can be obtained by combining the above two expressions and integrating over the cell depth to obtain (Chapra and Reckhow, 1983):

$$\lambda_l = \frac{e}{\alpha \Delta z} \left[e^{-\gamma_2} - e^{-\gamma_1} \right] \quad (\text{B-25})$$

where:

$$\gamma_1 = \frac{(1 - \beta) I_0}{I_s} e^{-\alpha d}$$

$$\gamma_2 = \frac{(1 - \beta) I_0}{I_s} e^{\alpha(d + \Delta z)}$$

d = depth at the top of computational cell, m

The attenuation coefficient, λ , is computed from a baseline value [\[EXH2O\]](#) to which the effects of inorganic [\[EXINOR\]](#) and organic [\[EXORG\]](#) suspended solids, as well as the extinction of each algal group, are added. Epiphyton self-shading are accounted for in the biomass limitation formulation.

Rate multipliers limiting epiphyton growth due to nutrient limitations are computed using the Monod relationship:

$$\lambda_i = \frac{\Phi_i}{P_i + \Phi_i} \quad (\text{B-26})$$

where:

Φ_i = phosphorus or nitrate + ammonium concentration, $g\ m^{-3}$

P_i = half-saturation coefficient for phosphorus or nitrate + ammonium, $g\ m^{-3}$

The epiphyton preference for ammonium is modeled using the following (Thomann and Fitzpatrick, 1982).

$$P_{NH4} = \Phi_{NH4} \frac{\Phi_{NOx}}{(K_{NH4} + \Phi_{NH4})(K_{NH4} + \Phi_{NOx})} + \Phi_{NH4} \frac{K_{NH4}}{(\Phi_{NH4} + \Phi_{NOx})(K_{NH4} + \Phi_{NOx})} \quad (\text{B-27})$$

P_{NH4} = ammonium preference factor

K_{NH4} = ammonia preference half-saturation coefficient, $g\ m^{-3}$

Φ_{NH4} = ammonium concentration, $g\ m^{-3}$

Φ_{NOx} = nitrate-nitrite concentration, $g\ m^{-3}$

Epiphyton dark respiration is computed using the rising limb of the temperature function:

$$K_{er} = \gamma_{er} \gamma_{ef} K_{ermax} \quad (\text{B-28})$$

where:

γ_{er} = temperature rate multiplier for rising limb of the curve
 γ_{ef} = temperature rate multiplier for falling limb of the curve
 K_{armax} = maximum dark respiration rate, sec^{-1}

Epiphyton excretion is evaluated using an inverse relation to the light rate multiplier:

$$K_{ee} = (1 - \lambda_l) \gamma_{er} \gamma_{ef} K_{ee\ max} \quad (\text{B-29})$$

where:

λ_l = light limiting factor
 γ_{er} = temperature rate multiplier for rising limb of the curve
 γ_{ef} = temperature rate multiplier for falling limb of the curve
 K_{eemax} = maximum excretion rate constant, sec^{-1}

Excretion rates increase at both low and high light intensities, with excretion products contributing to labile DOM.

Epiphyton mortality is defined as:

$$K_{em} = \gamma_{er} \gamma_{ef} K_{em\ max} \quad (\text{B-30})$$

where:

γ_{er} = temperature rate multiplier for rising limb of the curve
 γ_{ef} = temperature rate multiplier for falling limb of the curve
 K_{emmax} = maximum mortality rate, sec^{-1}

This mortality rate represents both natural and predator mortality. Epiphyton growth does not occur in the absence of light. Epiphyton growth is not allowed to exceed the limit imposed by nutrient supply over a given timestep. Epiphyton excretion is not allowed to exceed epiphyton growth rates.

The epiphyton burial rate represents the burial of dead epiphyton to the organic sediment compartment. Currently, there is no link between buried epiphyton and the 1st-order sediment compartment. Also, there is no sloughing of epiphyton into the water column as a function of velocity shear. These will limitations will be addressed in a later model release.

The epiphyton biomass is controlled by a biomass limitation equation based on Monod kinetics. The biomass limitation function, f , varies from 0 to 1 and is multiplied with the growth rate. This function is defined as

$$f = \left[1 - \frac{B}{B + K_B} \right] \quad (\text{B-31})$$

where:

$$B = \text{epiphyton areal biomass, } g/m^2$$

$$K_b = \text{epiphyton areal biomass half-saturation coefficient, } g/m^2$$

The areal biomass is calculated as follows:

$$B = \Phi_e \frac{V}{A} \quad (\text{B-32})$$

where:

$$A = \text{computational cell surface area, } m^2$$

$$V = \text{computational cell volume, } m^3$$

$$\Phi_e = \text{epiphyton concentration, } g \ m^{-3}$$

The biomass limitation is a surrogate calibration parameter for light limitation due to self-shading.

Phosphorus

Phosphorus is an important element in aquatic ecosystems since it serves as one of the primary nutrients for phytoplankton growth. In many fresh waters, phosphorus is considered to be the nutrient limiting maximum production of phytoplankton biomass (Schindler, 1971; Schindler et al., 1973; Vollenweider, 1968, 1976).

Phosphorus is assumed to be completely available as ortho-phosphate (PO_4) for uptake by phytoplankton. Measurements of soluble reactive phosphorus are closest to the form used in the model.

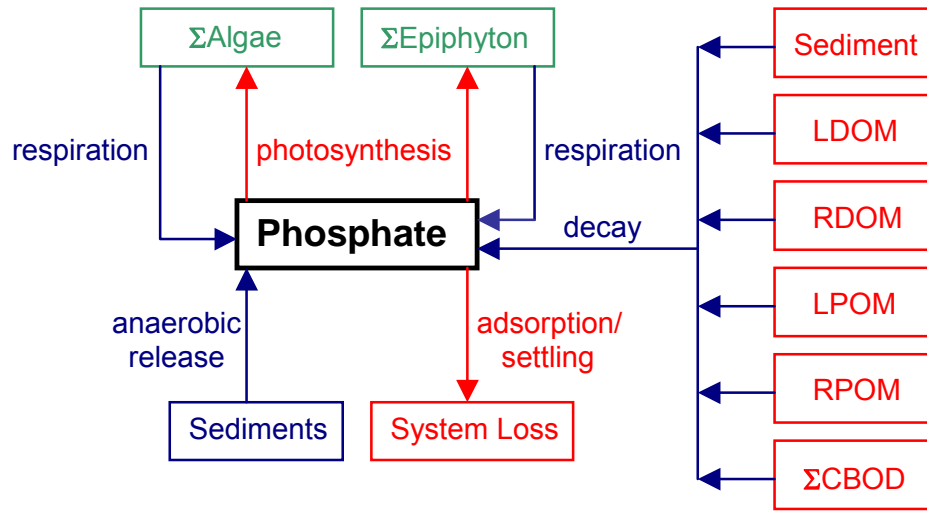


Figure B-11. Internal flux between phosphorus and other compartments.

Referring to [Figure B-11](#), the rate equation for phosphorus is:

$$\begin{aligned}
 S_p = & \underbrace{\sum (K_{ar} - K_{ag}) \delta_{Pa} \Phi_a}_{\text{algalnetgrowth}} + \underbrace{\sum (K_{er} - K_{eg}) \delta_{Pe} \Phi_e}_{\text{epiphytometgrowth}} + \underbrace{K_{LDOM} \delta_{POM} \gamma_{OM} \Phi_{LDOM}}_{\text{labileDOMdecay}} \\
 & + \underbrace{K_{RDOM} \delta_{POM} \gamma_{OM} \Phi_{RDOM}}_{\text{refractoryDOM decay}} + \underbrace{K_{LPOM} \delta_{POM} \gamma_{OM} \Phi_{LPOM}}_{\text{labilePOMdecay}} + \underbrace{K_{RPOM} \delta_{POM} \gamma_{OM} \Phi_{RPOM}}_{\text{refractoryPOMdecay}} \\
 & + \underbrace{\sum K_{CBOD} R_{CBOD} \delta_{P-CBOD} \Theta^{T-20} \Phi_{CBOD}}_{\text{CBOD decay}} + \underbrace{K_s \delta_{POM} \gamma_{OM} \Phi_s}_{\text{1st-ordersedimentrelease}} + \underbrace{SOD \gamma_{OM} \frac{A_{sed}}{V}}_{\text{0-ordersedimentrelease}} \\
 & - \underbrace{\left(\sum \omega_{ISS} \Phi_{ISS} + \omega_{Fe} \Phi_{Fe} \right) P_P}_{\text{inorganisolidsadsorption}} \Phi_P
 \end{aligned} \tag{B-33}$$

where:

- Δz = model cell thickness, m
- A_{sed} = sediment surface area, m^2
- V = cell volume, m^3
- P_P = adsorption coefficient, $m^3 g^{-1}$
- δ_{Pe} = epiphyton stoichiometric coefficient for phosphorus
- δ_{Pa} = algal stoichiometric coefficient for phosphorus
- δ_{POM} = organic matter stoichiometric coefficient for phosphorus
- δ_{P-CBOD} = phosphorus/CBOD stoichiometric ratio
- γ_{OM} = temperature rate multiplier for organic matter decay
- Θ = temperature rate multiplier for CBOD decay
- R_{BOD} = conversion ratio for 5-day CBOD to CBOD ultimate

$$\begin{aligned}
\omega_{ISS} &= \text{inorganic suspended solids settling velocity, } m \text{ sec}^{-1} \\
\omega_{Fe} &= \text{particulate organic matter settling velocity, } m \text{ sec}^{-1} \\
K_{ag} &= \text{algal growth rate, } sec^{-1} \\
K_{ar} &= \text{algal dark respiration rate, } sec^{-1} \\
K_{eg} &= \text{epiphyton growth rate, } sec^{-1} \\
K_{er} &= \text{epiphyton dark respiration rate, } sec^{-1} \\
K_{LDOM} &= \text{labile DOM decay rate, } sec^{-1} \\
K_{RDOM} &= \text{refractory DOM decay rate, } sec^{-1} \\
K_{LPOM} &= \text{labile POM decay rate, } sec^{-1} \\
K_{RPOM} &= \text{refractory POM decay rate, } sec^{-1} \\
K_{CBOD} &= \text{CBOD decay rate, } sec^{-1} \\
K_{sed} &= \text{sediment decay rate, } sec^{-1} \\
SOD &= \text{anaerobic sediment release rate, } g \text{ m}^{-2} \text{ s}^{-1} \\
\Phi_P &= \text{phosphorus concentration, } g \text{ m}^{-3} \\
\Phi_{Fe} &= \text{total iron concentration, } g \text{ m}^{-3} \\
\Phi_{ISS} &= \text{inorganic suspended solids concentration, } g \text{ m}^{-3} \\
\Phi_a &= \text{algal concentration, } g \text{ m}^{-3} \\
\Phi_e &= \text{epiphyton concentration, } g \text{ m}^{-3} \\
\Phi_{LDOM} &= \text{labile DOM concentration, } g \text{ m}^{-3} \\
\Phi_{LPOM} &= \text{labile POM concentration, } g \text{ m}^{-3} \\
\Phi_{RDOM} &= \text{refractory DOM concentration, } g \text{ m}^{-3} \\
\Phi_{RPOM} &= \text{refractory POM concentration, } g \text{ m}^{-3} \\
\Phi_{CBOD} &= \text{CBOD concentration, } g \text{ m}^{-3} \\
\Phi_{sed} &= \text{organic sediment concentration, } g \text{ m}^{-3}
\end{aligned}$$

and the rate terms are evaluated in subroutine PHOSPHORUS.

The contribution of algae, POM, and DOM to phosphorus is given in the rate equations and [Figure B-7](#). However, effects due to settling and contribution from sediments require some additional explanation.

Dissolved inorganic phosphorus adsorbs onto inorganic particulates under oxic conditions and is lost when these materials settle. Loss may be rapid in the upper end of reservoirs in the riverine and transition zones due to greater concentrations of allochthonous particulates. A Langmuir isotherm describes this process. Since phosphorus concentrations are generally small, only the isotherm's linear region is utilized and is represented by the product $P_p\Phi_p$. The adsorbed solids settle at a rate equal to the solids' settling velocity. Adsorption is not allowed to occur if dissolved oxygen concentrations are less than a minimum value [\[O2LIM\]](#).

Phosphorus adsorption onto inorganic suspended solids should be used cautiously. In most systems, available phosphorus sites for adsorption onto inflowing inorganic suspended solids are generally already in use, so little adsorption takes place when inorganic suspended solids enter into a reservoir or estuary. The phosphorus formulation needs to be recast with inorganic phosphorus as the state variable that is then partitioned between dissolved and particulate forms. This will be done in a future version. However, phosphorus sorption onto iron hydroxides that form when anoxic waters

come into contact with oxygen can be an important mechanism of phosphorus removal from the water column for certain waterbodies and should be included.

Sediment contribution of phosphorus to overlying waters can be simulated in three ways. In the first, the sediment compartment accumulates particulate organic matter and algae, which then decay. This is modeled as a 1st-order process. However, sediment phosphorus release depends upon sediment age, chemistry, overlying phosphorus concentrations, and other factors not included in the sediment compartment. In the second, sediments can be assigned a release rate for phosphorus that is independent of sediment concentrations. Sediments are modeled as a "black box" using a zero-order rate. Phosphorus release is only allowed to occur if the overlying water dissolved oxygen concentration is less than a minimum value [O2LIM]. The third method is a combination of the first two where organic materials accumulate and decay in the sediments along with a background decay rate independent of organic matter accumulation in the sediments.

Ammonium

Algae use ammonium during photosynthesis to form proteins. In many estuarine applications, nitrogen is the limiting nutrient for algal growth.

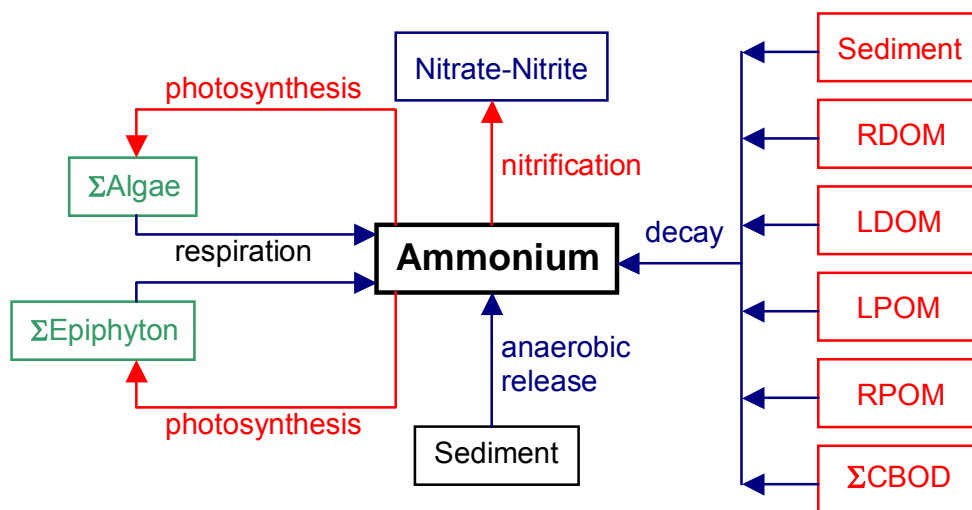


Figure B-12. Internal flux between ammonium and other compartments.

Referring to [Figure B-12](#), the rate equation for ammonium is:

$$\begin{aligned}
 S_{NH4} = & \underbrace{\sum K_{ar} \delta_{Na} \Phi_s}_{\text{algalrespiratin}} - \underbrace{\sum K_{ag} \delta_{Na} \Phi_a P_{NH4}}_{\text{algalgrowth}} + \underbrace{\sum K_{er} \delta_{Ne} \Phi_e}_{\text{epiphytorrespiratin}} - \underbrace{\sum K_{eg} \delta_{Ne} \Phi_e P_{NH4}}_{\text{epiphytorgrowth}} \\
 & + \underbrace{K_{LDOM} \delta_{NOM} \gamma_{OM} \Phi_{LDOM}}_{\text{labileDOMdecay}} + \underbrace{K_{RDOM} \delta_{NOM} \gamma_{OM} \Phi_{RDOM}}_{\text{refractoryDOMdecay}} + \underbrace{K_{LPOM} \delta_{NOM} \gamma_{OM} \Phi_{LPOM}}_{\text{labilePOMdecay}} \\
 & + \underbrace{K_{RPOM} \delta_{NOM} \gamma_{OM} \Phi_{RPOM}}_{\text{refractoryPOMdecay}} + \underbrace{K_s \delta_{NOM} \gamma_{OM} \Phi_s}_{\text{1st-ordersedimentrelease}} + \underbrace{SOD_{NH4} \gamma_{OM} \frac{A_{sed}}{V}}_{\text{0-ordersedimentrelease}} \\
 & + \underbrace{\sum K_{CBOD} R_{CBOD} \delta_{N-CBOD} \Theta^{T-20} \Phi_{CBOD}}_{\text{CBODdecay}} + \underbrace{K_{NOx} \gamma_{NOx} \Phi_{NOx}}_{\text{denitrification}} - \underbrace{K_{NH4} \gamma_{NH4} \Phi_{NH4}}_{\text{nitrificabn}}
 \end{aligned} \tag{B-34}$$

where:

- A_{sed} = sediment area, m^2
- V = volume of cell, m^3
- δ_{Na} = algal stoichiometric coefficient for nitrogen
- δ_{Ne} = epiphyton stoichiometric coefficient for nitrogen
- δ_{NOM} = organic matter stoichiometric coefficient for nitrogen
- δ_{N-CBOD} = CBOD stoichiometric coefficient for nitrogen
- γ_{NH4} = temperature rate multiplier for nitrification
- γ_{NOx} = temperature rate multiplier for denitrification
- γ_{OM} = temperature rate multiplier for organic matter decay
- Θ = temperature rate multiplier for CBOD decay
- R_{CBOD} = ratio of 5-day CBOD to ultimate CBOD
- P_{NH4} = ammonium preference factor
- K_{NOx} = nitrate-nitrogen decay rate, sec^{-1}
- K_{NH4} = ammonium decay rate, sec^{-1}
- K_{ar} = algal dark respiration rate, sec^{-1}
- K_{ag} = algal growth rate, sec^{-1}
- K_{LDOM} = labile DOM decay rate, sec^{-1}
- K_{RDOM} = refractory DOM decay rate, sec^{-1}
- K_{LPOM} = labile POM decay rate, sec^{-1}
- K_{RPOM} = refractory POM decay rate, sec^{-1}
- K_{CBOD} = CBOD decay rate, sec^{-1}
- K_{sed} = sediment decay rate, sec^{-1}
- SOD_{NH4} = sediment ammonium release rate, $g m^{-2} sec^{-1}$
- Φ_{ISS} = inorganic suspended solids concentration, $g m^{-3}$
- Φ_{NH4} = ammonium concentration, $g m^{-3}$
- Φ_{NOx} = nitrate-nitrogen concentration, $g m^{-3}$
- Φ_a = algal concentration, $g m^{-3}$

- Φ_{LDOM} = labile DOM concentration, $g\ m^{-3}$
- Φ_{RDOM} = refractory DOM concentration, $g\ m^{-3}$
- Φ_{LPOM} = labile POM concentration, $g\ m^{-3}$
- Φ_{RPOM} = refractory POM concentration, $g\ m^{-3}$
- Φ_{CBOD} = CBOD concentration, $g\ m^{-3}$
- Φ_{sed} = organic sediment concentration, $g\ m^{-3}$

and the rate terms are evaluated in subroutine AMMONIUM. As with phosphorus, 0-order sediment release only occurs when dissolved oxygen is less than a minimum value [O2LIM]. Either a 0- or 1st-order process or a combination of both may be used for sediment ammonium release.

Nitrate-Nitrite

This compartment represents nitrate plus nitrite. Nitrite is an intermediate product in nitrification between ammonium and nitrate. Nitrate is used as a source of nitrogen for algae and epiphyton during photosynthesis. Preferential uptake of ammonium over nitrate by algae and periphyton is now included.

Nitrogen may be the limiting nutrient for algae in systems with high phosphorus loadings or in estuaries. Some species of blue-green algae are capable of fixing atmospheric nitrogen for use in photosynthesis. This process can be included by setting the nitrogen half-saturation concentration for algal growth to zero.

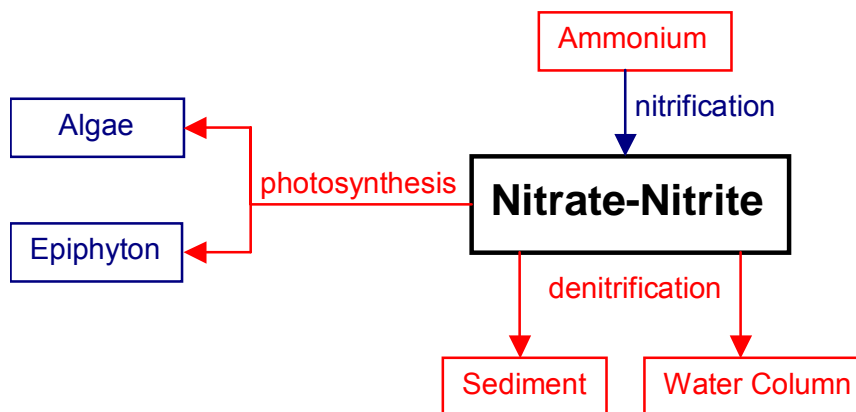


Figure B-13. Internal flux between nitrate + nitrite and other compartments.

Referring to [Figure B-13](#), the rate equation for nitrate-nitrite is:

$$\begin{aligned}
 S_{NOx} = & \underbrace{K_{NH4} \gamma_{NH4} \Phi_{NH4}}_{\text{nitrification}} - \underbrace{K_{NOx} \gamma_{NOx} \Phi_{NOx}}_{\text{water column denitrification}} - \underbrace{\omega_{NOx} \frac{\partial \Phi_{NOx}}{\partial z}}_{\text{sediment denitrification}} \\
 & - \underbrace{\sum K_{ag} \delta_{Na} \Phi_a (1 - P_{NH4})}_{\text{algal uptake}} - \underbrace{\sum K_{eg} \delta_{Ne} \Phi_e (1 - P_{NH4})}_{\text{epiphyton uptake}}
 \end{aligned}
 \tag{B-35}$$

where:

- γ_{NH4} = temperature rate multiplier for nitrification
- γ_{NOx} = temperature rate multiplier for denitrification
- δ_{Ne} = epiphyton stoichiometric coefficient for nitrogen
- δ_{Na} = algal stoichiometric coefficient for nitrogen
- P_{NH4} = ammonium preference factor
- K_{NH4} = nitrification rate, sec^{-1}
- K_{NOx} = denitrification rate, sec^{-1}
- K_{ag} = algal growth rate, sec^{-1}
- ω_{NOx} = sediment transfer velocity, $m sec^{-1}$
- Φ_{NH4} = ammonia-nitrogen concentration, $g m^{-3}$
- Φ_{NOx} = nitrate-nitrogen concentration, $g m^{-3}$
- Φ_a = algal concentration, $g m^{-3}$

and the rate terms are evaluated in subroutine NITRATE. Nitrification is only allowed to occur if oxygen is present, and denitrification is allowed only if dissolved oxygen is less than a specified minimum value [\[O2LIM\]](#).

Dissolved Silica

Dissolved silica is an important component of diatoms, providing the structural skeleton. In many cases diatoms can be silica limited. Dissolved silica is taken up by algae based on stoichiometric relationships and is produced by the decay of organic matter containing particulate biogenic silica. Also, dissolved silica is adsorbed onto inorganic suspended solids based on a partitioning coefficient.

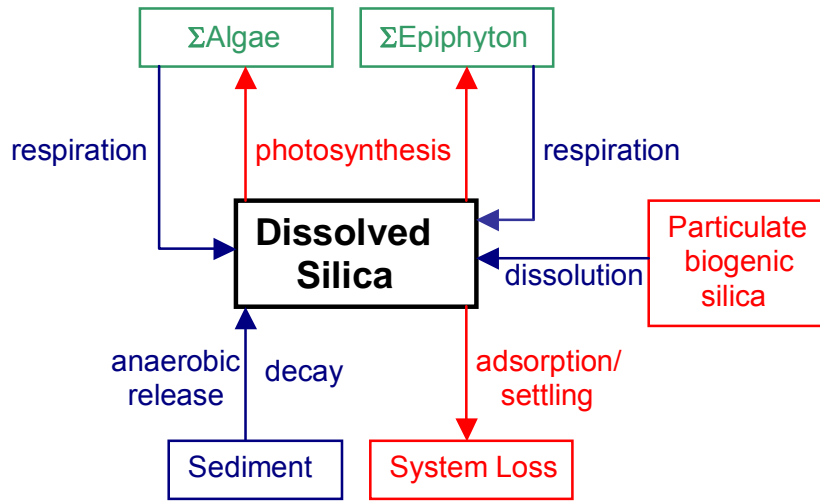


Figure B-14. Internal flux between dissolved silica and other compartments.

Referring to [Figure B-14](#), the rate equation for dissolved silica is:

$$\begin{aligned}
 S_{DSi} = & - \underbrace{\sum (K_{ag} - K_{ar}) \delta_{Sia} \Phi_a}_{\text{algal uptake}} - \underbrace{\sum (K_{eg} - K_{er}) \delta_{Sie} \Phi_e}_{\text{epiphyton uptake}} \\
 & + \underbrace{K_{sed} \delta_{SiOM} \gamma_{OM} \Phi_{sed}}_{\text{1st order sediment release}} + \underbrace{SOD \varphi_{Si} \gamma_{OM} \frac{A_{sed}}{V}}_{\text{0-order sediment release}} + \underbrace{K_{PSi} \gamma_{OM} \Phi_{PSi}}_{\text{particulate biogenic decay}} \\
 & - \underbrace{\frac{P_{Si} (\sum \omega_{ss} \Phi_{ss} + \omega_{POM} \Phi_{POML} + \omega_{POM} \Phi_{POMR} + \omega_{Fe} \Phi_{Fe})}{\Delta z}}_{\text{inorganic solids adsorption and settling}} \Phi_{DSi}
 \end{aligned} \tag{B-36}$$

where:

- θ = temperature rate factor for BOD decay
- γ_{OM} = temperature rate multiplier for organic matter decay
- φ_{Si} = fraction of SOD for silica release
- Δz = computational cell height, m
- δ_{Sie} = epiphyton stoichiometric ratio for silica
- δ_{Sia} = algal stoichiometric ratio for silica
- δ_{SiOM} = sediment organic matter stoichiometric ratio for silica
- A_{sed} = sediment area, m^2
- V = computational cell volume, m^3
- P_{Si} = silica adsorption coefficient, $m^3 g^{-1}$
- SOD = sediment oxygen demand, $g m^{-2} sec^{-1}$
- ω_{ISS} = inorganic suspended solids settling velocity, $m sec^{-1}$
- K_{ag} = algal growth rate, sec^{-1}
- K_{eg} = epiphyton growth rate, sec^{-1}
- K_{sed} = sediment decay rate, sec^{-1}

- Φ_a = algal concentration, $g\ m^{-3}$
- Φ_e = epiphyton concentration, $g\ m^{-3}$
- Φ_{sed} = organic sediment mass, g
- Φ_{ISS} = inorganic suspended solids concentration, $g\ m^{-3}$
- Φ_{DSi} = dissolved silica concentration, $g\ m^{-3}$
- Φ_{Fe} = total iron concentration, $g\ m^{-3}$

Particulate Biogenic Silica

Particulate biogenic silica results from diatom mortality and settles and also dissolves to form dissolved silica.

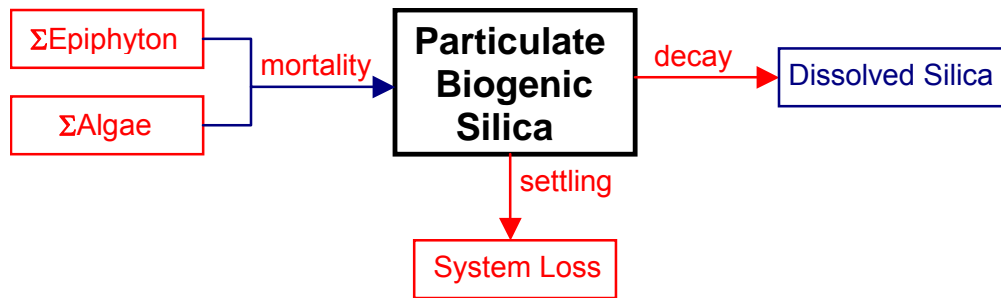


Figure B-15. Internal flux between particulate biogenic silica and other compartments

Referring to [Figure B-15](#), the rate equation for particulate biogenic silica is:

$$S_{PSi} = \underbrace{P_{am}\delta_{Sia}K_{am}\Phi_a}_{\text{algae mortality}} + \underbrace{P_{em}\delta_{Sie}K_{em}\Phi_e}_{\text{epiphyton mortality}} - \underbrace{K_{PSi}\gamma_{OM}\Phi_{PSi}}_{\text{decay}} - \underbrace{\frac{\omega_{PSi}\partial_z\Phi_{PSi}}{\partial z}}_{\text{settling}} \quad (\text{B-37})$$

where:

- P_{am} = partition coefficient for algal mortality
- δ_{Sie} = epiphyton stoichiometric coefficient for silica
- δ_{Sia} = algal stoichiometric coefficient for silica
- γ_{OM} = temperature rate multiplier for organic matter
- P_{em} = partition coefficient for epiphyton mortality
- K_{am} = algal mortality rate, sec^{-1}
- K_{em} = epiphyton mortality rate, sec^{-1}
- K_{PSi} = particulate biogenic silica decay rate, sec^{-1}
- ω_{PSi} = particulate biogenic silica settling rate, $m\ sec^{-1}$
- Φ_e = epiphyton concentration, $g\ m^{-3}$

$$\Phi_a = \text{algal concentration, } g\ m^{-3}$$

$$\Phi_{PSi} = \text{particulate biogenic silica concentration, } g\ m^{-3}$$

Total Iron

Total iron is included in the model primarily because of its effect on nutrient concentrations through adsorption and settling. Iron is commonly released from anoxic sediments and may influence nutrient dynamics in many reservoirs. Iron may also contribute to dissolved oxygen depletions, but the model does not presently include these effects. Iron sediment release is modeled as a zero-order process.

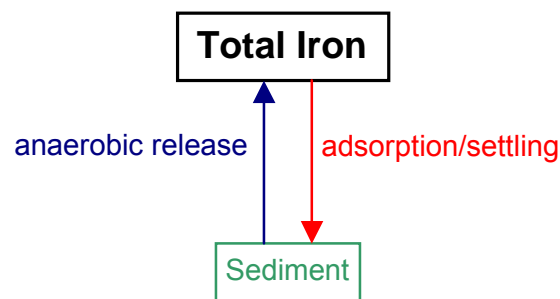


Figure B-16. Internal flux between total iron and other compartments.

Referring to [Figure B-16](#), the rate equation for total iron is:

$$S_{Fe} = \underbrace{SOD \gamma_{om} A_s}_{\text{0-order sediment release}} - \underbrace{\frac{\omega_{Fe} \partial \Phi_{Fe}}{\partial z}}_{\text{oxic water column settling}} \quad (\text{B-38})$$

where:

$$A_s = \text{sediment area, } m^2$$

$$\gamma_{OM} = \text{temperature rate multiplier}$$

$$\omega_{Fe} = \text{settling velocity, } m\ sec^{-1}$$

$$\Phi_{Fe} = \text{total iron concentration, } g\ m^{-3}$$

$$SOD = \text{sediment oxygen demand, } g\ m^{-2}\ sec^{-1}.$$

Dissolved Oxygen

Oxygen is one of the most important elements in aquatic ecosystems. It is essential for higher forms of life, controls many chemical reactions through oxidation, and is a surrogate variable indicating the general health of aquatic systems.

CE-QUAL-W2 includes both aerobic and anaerobic processes. The ability to model anaerobic periods is important since it provides information on potential problems with water quality. Simulations can be used to identify possibilities for both metalimnetic and hypolimnetic oxygen depletion and its impact on various water control management alternatives. If a single variable were to be measured in aquatic systems that would provide maximum information about the system state, it would be dissolved oxygen.

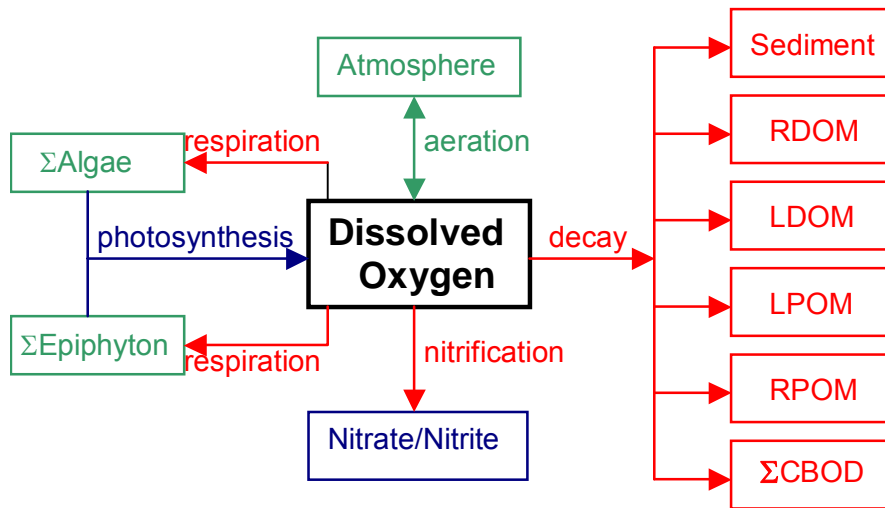


Figure B-17. Internal flux between dissolved oxygen and other compartments.

Referring to [Figure B-17](#), the rate equation for dissolved oxygen is:

$$\begin{aligned}
 S_{DO} = & \underbrace{\sum (K_{ag} - K_{ar}) \delta_{OM} \Phi_a}_{\text{algalnetproduction}} + \underbrace{\sum (K_{eg} - K_{er}) \delta_{OM} \Phi_e}_{\text{epiphytonnetproduction}} + \underbrace{A_{sur} K_L (\Phi'_{DO} - \Phi_{DO})}_{\text{aeration}} \\
 & - \underbrace{K_{RPOM} \delta_{OM} \gamma_{OM} \Phi_{RPOM}}_{\text{refractoryPOMdecay}} - \underbrace{K_{LPOM} \delta_{OM} \gamma_{OM} \Phi_{LPOM}}_{\text{labilePOMdecay}} - \underbrace{K_{LDOM} \gamma_{OM} \delta_{OM} \Phi_{LDOM}}_{\text{labileDOMdecay}} \\
 & - \underbrace{K_{RDOM} \delta_{OM} \gamma_{OM} \Phi_{RDOM}}_{\text{refractoryDOMdecay}} - \underbrace{K_s \delta_{OM} \gamma_{OM} \Phi_{sed}}_{\text{1st-ordersedimentdecay}} - \underbrace{SOD \gamma_{OM} \frac{A_{sed}}{V}}_{\text{0-orderSOD}} \\
 & - \underbrace{\sum K_{CBOD} R_{CBOD} \Theta^{T-20} \Phi_{CBOD}}_{\text{CBODdecay}} - \underbrace{K_{NH4} \delta_{NH4} \gamma_{NH4} \Phi_{NH4}}_{\text{nitrification}}
 \end{aligned}
 \tag{B-39}$$

where:

- δ_{OM} = oxygen stoichiometric coefficient for organic matter
- δ_{NH4} = oxygen stoichiometric coefficient for nitrification
- γ_{NH4} = temperature rate multiplier for nitrification
- γ_{OM} = temperature rate multiplier for organic matter decay
- R_{BOD} = conversion from CBOD in the model to CBOD ultimate
- Θ = BOD temperature rate multiplier
- V = volume of computational cell, m^3
- T = temperature, $^{\circ}C$
- A_{sed} = sediment surface area, m^2
- A_{sur} = water surface area, m^2
- K_{ag} = algal growth rate, sec^{-1}
- K_{ar} = algal dark respiration rate, sec^{-1}
- K_{eg} = epiphyton growth rate, sec^{-1}
- K_{er} = epiphyton dark respiration rate, sec^{-1}
- K_{NH4} = ammonia decay (nitrification) rate, sec^{-1}
- K_{LDOM} = labile DOM decay rate, sec^{-1}
- K_{RDOM} = refractory DOM decay rate, sec^{-1}
- K_{LPOM} = labile POM decay rate, sec^{-1}
- K_{RPOM} = refractory POM decay rate, sec^{-1}
- K_{BOD} = CBOD decay rate, sec^{-1}
- K_{sed} = sediment decay rate, sec^{-1}
- SOD = sediment oxygen demand, $g\ m^{-2}\ sec^{-1}$
- K_L = interfacial exchange rate for oxygen, $m\ sec^{-1}$
- Φ_{NH4} = ammonia-nitrogen concentration, $g\ m^{-3}$
- Φ_a = algal concentration, $g\ m^{-3}$
- Φ_e = epiphyton concentration, $g\ m^{-3}$
- Φ_{LDOM} = labile DOM concentration, $g\ m^{-3}$
- Φ_{RDOM} = refractory DOM concentration, $g\ m^{-3}$
- Φ_{LPOM} = labile POM concentration, $g\ m^{-3}$
- Φ_{RPOM} = refractory POM concentration, $g\ m^{-3}$
- Φ_{BOD} = CBOD concentration, $g\ m^{-3}$
- Φ_{sed} = organic sediment concentration, $g\ m^{-3}$
- Φ_{DO} = dissolved oxygen concentration, $g\ m^{-3}$
- Φ'_{DO} = saturation DO concentration, $g\ m^{-3}$

and the rate terms are evaluated in subroutine DISSOLVED_OXYGEN. Decay is not allowed to occur when dissolved oxygen concentrations are zero. This is accomplished by setting temperature rate multipliers equal to zero.

Since the river basin model will encompass waterbodies that are dependent on boundary shear in river segments and wind stress for lake or reservoir segments for turbulence, the reaeration formulae for these systems must be different. In the following sections, formulae for reaeration as a function of wind speed and boundary shear are presented. The user has the ability to select a different formu-

lation for each waterbody type selected. The reason for selecting a waterbody type is to force the user to select a system that best approximates the theory being used. The possible water body types are RIVER, LAKE, or ESTUARY.

River Reaeration Equations

Reaeration equations for rivers are given in [Table B-2](#). Most of these equations are based on field studies of selected streams or laboratory channels. Equations 7 and 8 were developed from Melting and Flores (1999) for a large data set of reaeration coefficients. These may be the best choice for rivers even though other equations have been used extensively.

Recently, Moog and Jirka (1998) suggested that formulations that do not account for channel slope should not be used. Therefore, equations 7 and 8 may again be the best selection of equations for river sections.

Thomann and Mueller (1987) suggested using Equation 1 except for small streams where Equation 3 for flow less than 10 cfs should be used. They also suggested a minimum value of K_L of 0.6 m day^{-1} . This value has been implemented as a lower limit in the code.

Mills et al. (1985) in a review of water quality reaeration coefficients used a different formulation than equation 3 in [Table B-2](#) based on a 1978 reference at 25°C :

$$\begin{aligned}
 K_a &= 7776 US \quad \text{for } Q < 10 \text{ cfs} \\
 K_a &= 4665.6 US \quad \text{for } 10 < Q < 3000 \text{ cfs} \\
 K_a &= 2592 US \quad \text{for } Q > 3000 \text{ cfs}
 \end{aligned}
 \tag{B-40}$$

However, Mills et al. (1985) only recommend its use for shallow low-flow streams. Therefore, equation 3 in [Table B-2](#) is exactly the same as the above formulation in the low flow regime.

Covar (1976) used an approach where the equations of O'Connor-Dobbins, Churchill, and Owens were used together based on the applicability of each equation. The applicability of each equation was based on the velocity of the stream and its depth. This is equation 0 in the following table.

Table B-2. River reaeration equations.

#	Equation	Comments	Applicability	Reference
0	Either Eq 1, 2 or 4	K_a – evaluated based on applicability criteria of these equations		Covar (1976)
1	$K_a = \frac{K_L}{H} = \frac{(D_{O_2} U)^{1/2}}{H^{3/2}}$	D_{O_2} = H_2O molecular diffusion, $\text{m}^2 \text{ s}^{-1}$ U = average velocity, m s^{-1} H = average channel depth, m	depths between 1-30 ft and velocities between 0.5-1.6 fps	O'Connor and Dobbins (1958)
2	$K_a = \frac{K_L}{H} = \frac{11.6U}{H^{1.67}}$	U , ft s^{-1} H , ft K_a , day^{-1}	depths between 2-11 ft and velocities between 1.8-5 fps	Churchill, Elmore and Buckingham (1962)

#	Equation	Comments	Applicability	Reference
3	$K_a = 0.88US$ for $10 < Q < 300$ cfs $K_a = 1.8US$ for $1 < Q < 10$ cfs	S , ft mile ⁻¹ U , ft s ⁻¹ K_a , day ⁻¹	suggested for use when $Q < 10$ cfs	Tsivoglou and Wallace (1972)
4	$K_a = \frac{K_L}{H} = \frac{21.6U^{0.67}}{H^{1.85}}$	U , ft s ⁻¹ H , ft	depths between 0.4-2.4 ft and velocities between 0.1-1.8 fps	Owens et al. (1964)
5	$K_a = \frac{K_L}{H} = \frac{25u^*}{H} (1 + F^{0.5})$	u^* = shear velocity, (HSg) ^{0.5} S = slope of energy grade line F = Froude number, $U/(gH)^{0.5}$		Thackston and Krenkel (1966)
6	$K_a = \frac{K_L}{H} = \frac{7.62U}{H^{1.33}}$	U , ft s ⁻¹ H , ft		Langbien and Durum (1967)
7	$K_a = 517(US)^{0.524} Q^{-0.242}$ for $Q < 0.556$ $K_a = 596(US)^{0.528} Q^{-0.136}$ for $Q > 0.556$	U , m s ⁻¹ S , m m ⁻¹ Q , m ³ s ⁻¹ K_a , day ⁻¹	for pool and riffle streams	Melching and Flores (1999)
8	$K_a = 88(US)^{0.313} D^{-0.353}$ for $Q < 0.556$ $K_a = 142(US)^{0.333} D^{-0.66} W^{-0.243}$ for $Q > 0.556$	U , m s ⁻¹ S , m m ⁻¹ W = stream top width, m D = average depth, m K_a , day ⁻¹	for channel-control streams	Melching and Flores (1999)
9	w/ channel slope - $K_a = C_1 U^{C_2} H^{C_3} S^{C_4}$ w/o channel slope - $K_a = C_1 U^{C_2} H^{C_3}$	U , m s ⁻¹ H , m S , non-dimensional K_a , day ⁻¹ C_1, C_2, C_3, C_4 = user defined parameters	user defined relationship	

Figure B-18 shows the functional dependence of these formulae assuming the following relationship between flow (Q), velocity (U) and depth (St. John et al., 1984):

$$V = 0.033 Q^{0.5}$$

$$H = 0.475 Q^{0.4}$$

$$S = 5.2 \text{ ft/mile}$$

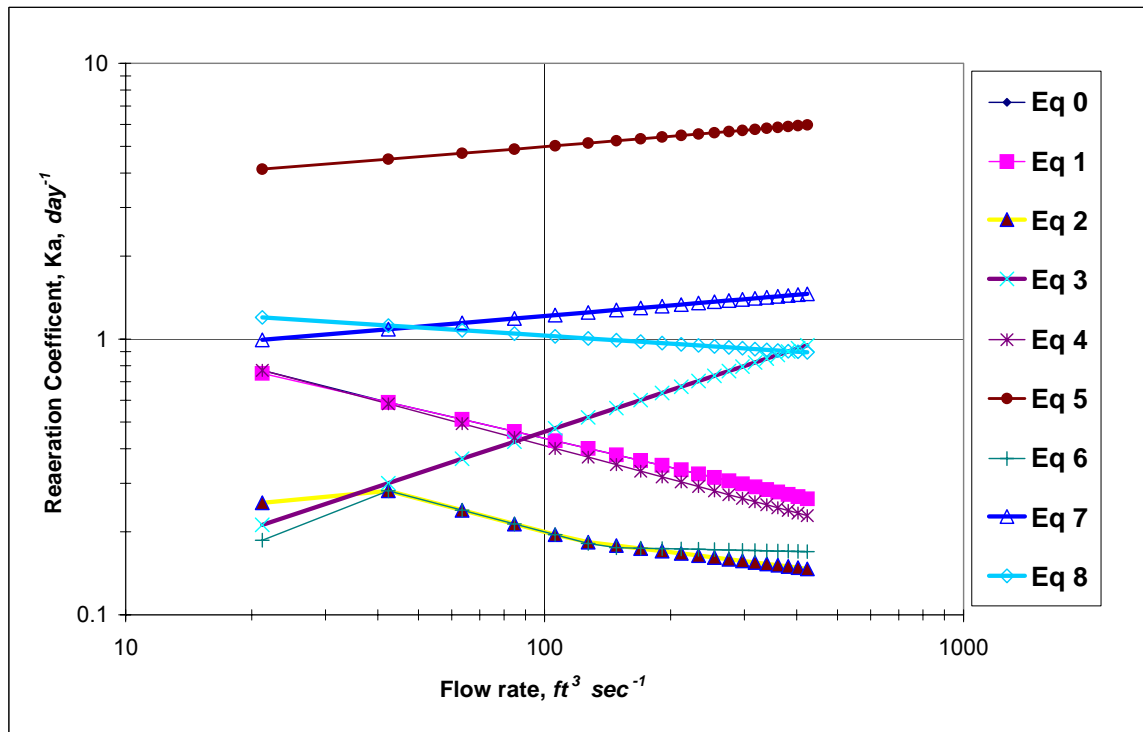


Figure B-18. Reaeration coefficient as a function of flow rate.

Lake Reaeration Equations

Wind effects rather than boundary shear more often control reaeration in lakes, reservoirs, and estuarine systems. There have been many wind studies for lakes (e.g., O'Connor, 1983) and open ocean systems. A summary of wind speed formulae for predicting reaeration is shown in [Table B-3](#) based on a 10 m wind measuring height.

Table B-3. Lake reaeration equations as a function of wind speed at 20°C.

#	Equation	Comments	Reference
1	$K_a = \frac{K_L}{H} = \frac{0.864W}{H}$	W, $m s^{-1}$ at 10 m H, m $K_L, m day^{-1}$	Broecker et al (1978)
2	$K_a = \frac{K_L}{H} = \frac{\alpha W^\beta}{H}$	$\alpha = 0.2, \beta = 1$ for $W < 3.5 m s^{-1}$ $\alpha = 0.057, \beta = 2$ for $W > 3.5 m s^{-1}$ where W is a daily average wind speed	Gelda et al (1996)
3	$K_a = \frac{K_L}{H} = \frac{0.728W^{0.5} - 0.317W + 0.1}{H}$	W, $m s^{-1}$ at 10 m $K_L, m day^{-1}$	Banks and Herrera (1977)
4	$K_a = \frac{K_L}{H} = \frac{0.0986W^{1.64}}{H}$ or $K_a = \frac{K_L}{H} = \frac{0.0986W^{1.64}}{H} \left(\frac{600}{Sc} \right)^{0.5}$	The latter equation was the original equation used where W is measured at 10 m and Sc is the Schmidt number (v/D)= $13750[0.10656\exp(-0.0627T)+0.00495]$ T = temperature, °C the former equation is at 20°C	Wanninkhof et al. (1991)

#	Equation	Comments	Reference
5	$K_a = \frac{K_L}{H} = \frac{D_{O_2}}{(200 - 60W^{0.5})10^{-6}H}$	D_{O_2} = oxygen molecular diffusivity, $m^2 s^{-1}$ W , $m s^{-1}$ K_L , $m s^{-1}$	Chen, Kanwisher (1963)
6	$K_a = \frac{K_L}{H} = \frac{0.5 + 0.05W^2}{H}$		Cole and Buchak (1993)
7	$K_a = \frac{K_L}{H} = \frac{0.362\sqrt{W}}{H} \quad W < 5.5 m/s$ $K_a = \frac{K_L}{H} = \frac{0.0277W^2}{H} \quad W > 5.5 m/s$		Banks (1975)
8	$K_a = \frac{K_L}{H} = \frac{0.64 + 0.128W^2}{H}$	Recommended form for WQRSS reservoir model	Smith (1978)
9	$K_a = \frac{K_L}{H} = \frac{0.156W^{0.63}}{H} \quad W \leq 4.1 m/s$ $K_a = \frac{K_L}{H} = \frac{0.0269W^{1.9}}{H} \quad W > 4.1 m/s$		Liss (1973)
10	$K_a = \frac{K_L}{H} = \frac{0.0276W^2}{H}$		Downing and Truesdale (1955)
11	$K_a = \frac{K_L}{H} = \frac{0.0432W^2}{H}$		Kanwisher (1963)
12	$K_a = \frac{K_L}{H} = \frac{0.319W}{H}$		Yu et al (1977)
13	$K_a = \frac{K_L}{H} = \frac{0.398}{H} \quad W < 1.6$ $K_a = \frac{K_L}{H} = \frac{0.155W^2}{H} \quad W \geq 1.6$	W = wind speed, $m s^{-1}$	Weiler (1974)
14	$K_a = \frac{K_L}{H} = \frac{C_1 + C_2W^{C_3}}{H}$	User defined relationship where: W , $m s^{-1}$ at 10 m K_a , day^{-1} C_1, C_2, C_3 are user defined	

Figure B-19 shows how these formulations vary with wind speed.

The definition of wind speed was usually taken at an elevation of 10 m for these formulations. The wind speed at 10 m elevation in the middle of a lake or reservoir, W_{10m} , can be computed from that measured at 10 m on land by using an approach from Fang and Stefan (1994).

$$W_{10m} = W_z f(fetch) \quad (\text{B-41})$$

where:

W_z = wind speed measured at 10 m height on land, m/s

$$f(fetch) = \frac{\ln \frac{10}{z_{o2}} \ln \frac{\delta}{z_{o1}}}{\ln \frac{10}{z_{o1}} \ln \frac{\delta}{z_{o2}}} \cong \frac{5ZB + 4.6052}{3ZB + 9.2103} \tag{B-42}$$

where:

z_{o1} = roughness of land (assume 0.01 m) (Kraus, 1972)

z_{o2} = roughness of water surface (assume 0.0001 m) (Ford and Stefan, 1980)

δ = thickness of wind boundary layer over smooth surface that is a function of the fetch length (Elliot, 1958), m

$$ZB = 0.8 \ln \frac{fetch}{2} - 1.0718$$

The function $f(fetch)$ varies from 1.056 for small lakes to 1.123 for large lakes. The fetch is the length in m of the wind over the water surface from one bank to the other.

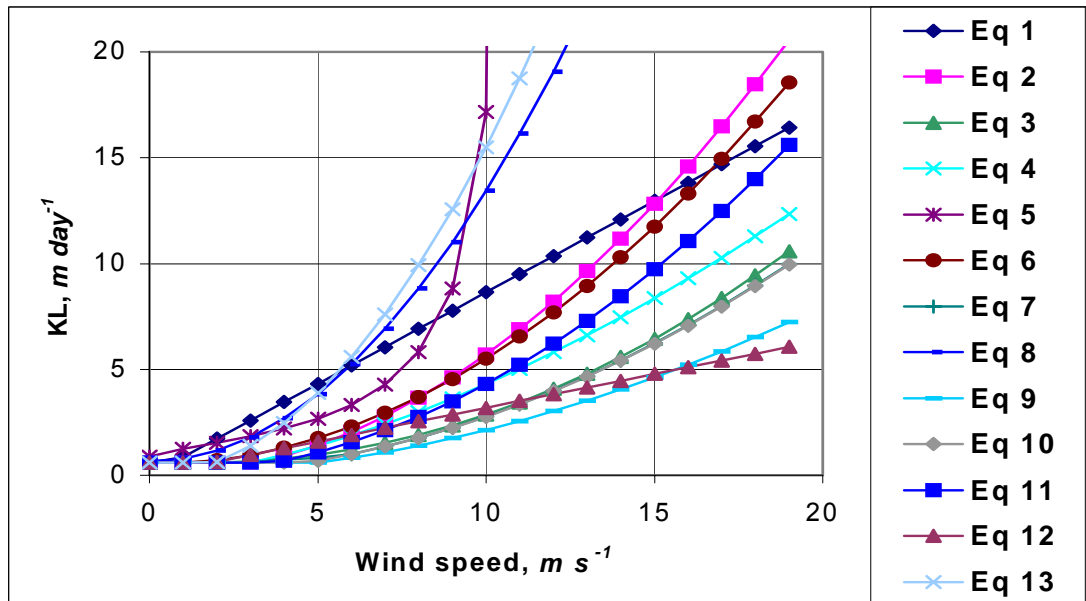


Figure B-19. Variation of wind speed and KL for lake/reservoir equations.

Equations for correcting the wind speed to 10 m and accounting for fetch dependence are included in the model. This dependence on measuring height, fetch, and wind speed is shown in [Figure B-20](#) and [Figure B-21](#).

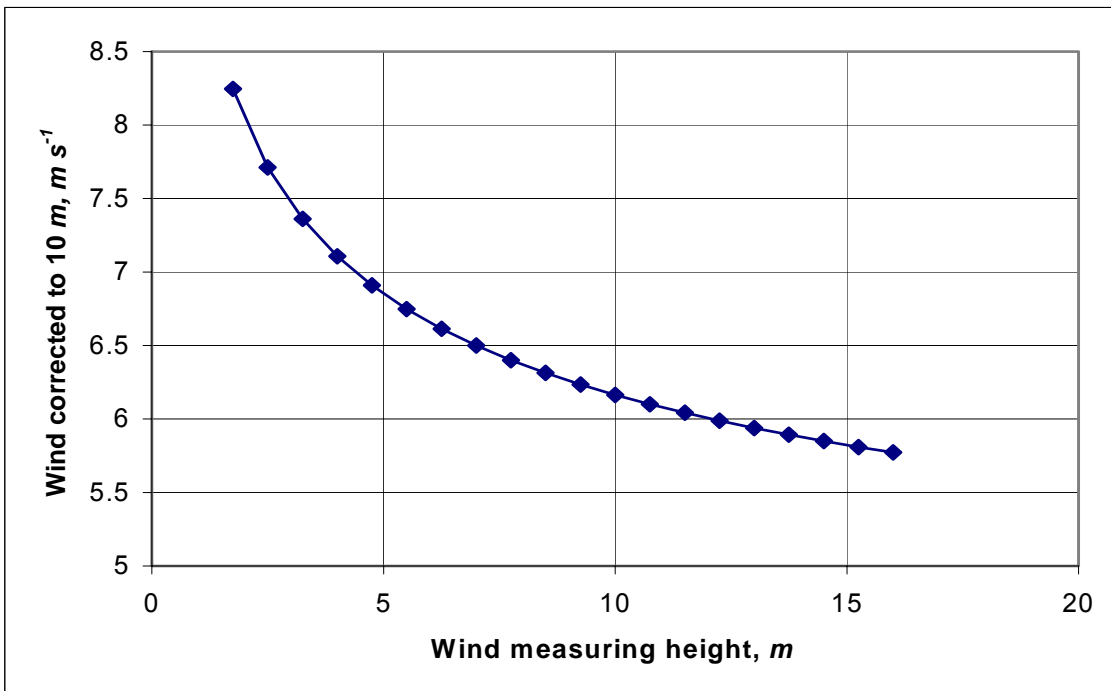


Figure B-20. Wind speed of 5 m s^{-1} and a fetch of 5 km corrected to 10 m as a function of measuring height on land.

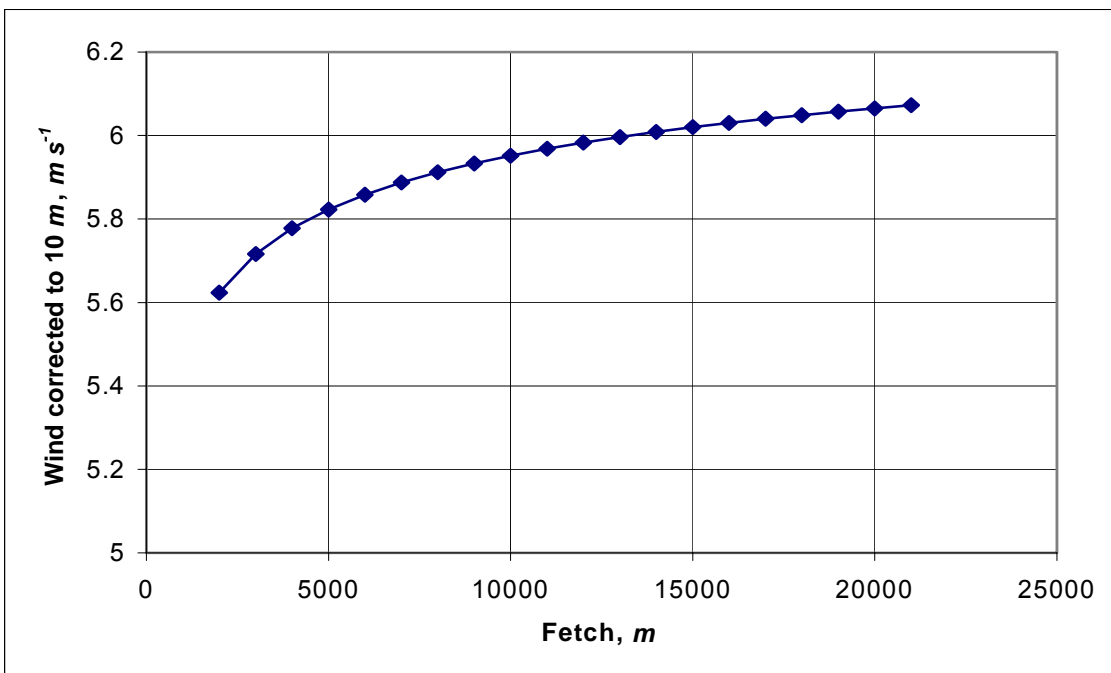


Figure B-21. Wind speed of 5 m s^{-1} corrected to 10 m as a function of fetch.

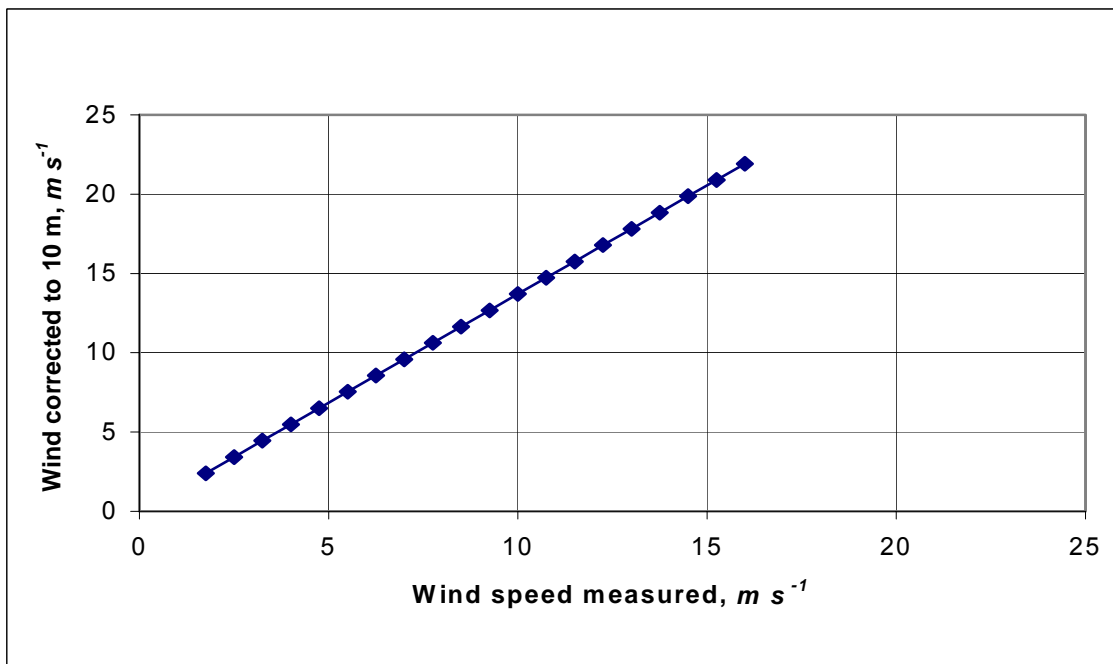


Figure B-22. Wind corrected to 10 m based on wind measured on land.

Estuarine Equations

For estuarine systems, Thomann and Mueller (1987) and Chapra (1997) suggest using any of the wind formulations in [Table B-4](#) or Equation 1 in [Table B-2](#) using the mean tidal velocity over a tidal cycle for the horizontal velocity. Table B-4 shows an additional formulation from Thomann and Fitzpatrick (1982) for estuaries, as well as the approach of Covar (1976) for rivers. Since many texts suggest using the mean tidal velocity, caution should be exercised in using these equations since they are based on the instantaneous velocity in the model.

Table B-4. Reaeration equations for estuarine waterbody at 20°C.

#	Equation	Comments	Reference
0	Either Eq 1, 2 or 4 from Table B-2	K_a is determined based on applicability criteria of each of these 3 formulations	Covar (1976)
1	$K_a = \frac{K_L}{H} = \frac{0.728W^{0.5} - 0.317W + 0.0372W^2}{H} + 3.93 \frac{\sqrt{U}}{H^{1.5}}$	$U, m s^{-1}$ this formula combines the effect of wind from Banks and Herrera (1977) and estuary tidal flow	Thomann and Fitzpatrick (1982)
2	$K_a = C_1 U^{C_2} H^{C_3} + \frac{0.5 + C_4 W^2}{H}$	$U, m s^{-1}$ H, m $W, m s^{-1}$ at 10 m K_a, day^{-1} $C_1, C_2, C_3,$ and C_4 - user defined parameters	User defined relationship

A computation can be performed to evaluate whether wind shear or boundary shear controls the turbulence intensity at the surface in an estuary. An algorithm will be added to the model in the future to include this computation.

Reaeration Temperature Dependence

Reaeration temperature dependence is based upon an Arrhenius formulation:

$$K_T = K_{20} \Theta^{T-20} \quad (\text{B-43})$$

where Θ is 1.024. The following relationship is used for reaeration formulae that use the molecular diffusivity of oxygen:

$$D_{O_2} = 4.58E - 11T + 1.2E - 9 \quad (\text{B-44})$$

where:

$$D_{O_2} = \text{molecular diffusivity of oxygen, } m^2 \text{ sec}^{-1}$$

$$T = \text{temperature, } ^\circ\text{C}$$

These two relationships yield similar results ([Figure B-23](#)).

No temperature correction was made to the calculated value of K_L in earlier versions of the model. The latest version includes the correction with theta set to 1.024.

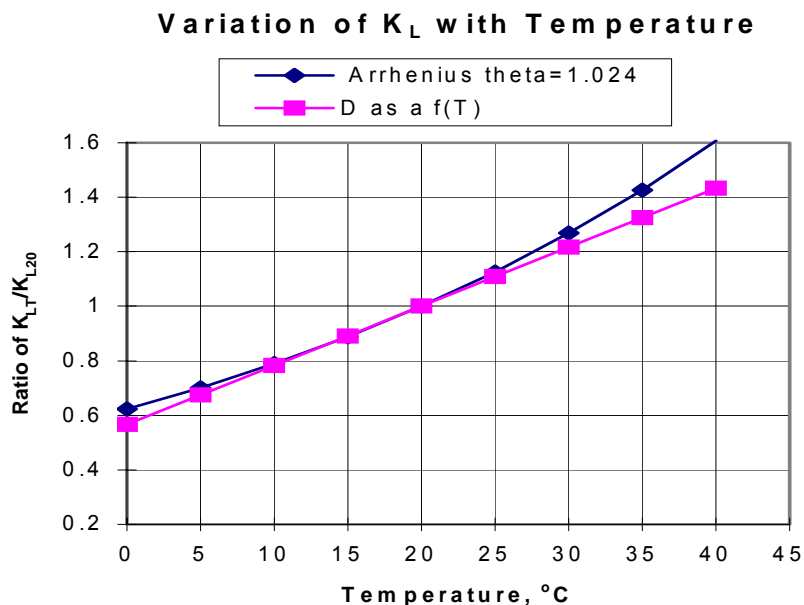


Figure B-23. Variation of K_{LT}/K_{L20} as a function of temperature.

Dam Reaeration

Many rivers and reservoirs have spillways or weirs over which water entrains oxygen into a pool below the dam. This section outlines the approach for including oxygen entrainment at dams and weirs.

Small Dams or Weirs

Many rivers have small spillways or weirs over which water flows that entrains oxygen. [Table B-5](#) lists formulae for predicting the entrainment of dissolved oxygen based on empirical data.

Table B-5. Formulae for small dam or weir reaeration effects.

Equation	Comments	Reference
$D_a - D_b = \left[1 - \frac{I}{1 + 0.11ab(1 + 0.046T)H} \right] D_a$ <p style="text-align: center;">or</p> $\frac{D_a}{D_b} = 1 + 0.11ab(1 + 0.046T)H$	D_a = DO deficit above dam, $g\ m^{-3}$ D_b = DO deficit below dam, $g\ m^{-3}$ T = temperature, °C H = height of water fall, ft a = 1.25 in clear to slightly polluted water to 1.00 in polluted water b = 1.00 for weir with free flow b = 1.3 for step weirs or cascades	Barrett et al. (1960)
$D_a - D_b = 0.037HD_a$	D_a = DO deficit above dam, $g\ m^{-3}$ D_b = DO deficit below dam, $g\ m^{-3}$ H = height of water fall, ft only valid for dams less than 15 ft and T between 20 and 25°C	Mastropietro (1968)
$\frac{D_a}{D_b} = 1 + 0.38ab(1 - 0.11H)(1 + 0.046T)H$	D_a = DO deficit above dam, $g\ m^{-3}$ D_b = DO deficit below dam, $g\ m^{-3}$ T = temperature, °C H = height of water fall, m a = 1.8 for clean water to 0.65 for gross polluted water b = 0.05 for sluice gates b = 1.0 for sharp crested straight faced weir b = 0.45 for flat broad crested curved face weir b = 0.7 for flat broad crested weir with regular step b = 0.8 for sharp crested vertical face weir b = 0.6 for flat broad crested weir vertical face	Butts and Evans (1983)

Most of these equations have been used for dams or weirs with heights of fall between 3 and 10 m. These equations do not generally predict supersaturation.

Large Dam Spillways/Gates

The USACE has been involved in gas abatement studies on the Columbia and Snake River system for many years (WES, 1996, 1997). Some of their research efforts have been focused on development of models of gas generation from spillways. These empirical models have been called CriSP 1.6 (Columbia Basin Research, 1998). The gas production equations used in CriSP are empirical correlations between total dissolved gas (TDG), usually measured a mile downstream of the dam after turbulence from the spillway had subsided, and discharge, usually measured in kcfs. The form of these equations is shown in [Table B-6](#).

Table B-6. Equations used in CRiSP model for gas production.

Equation type	Equation	Description of empirical coefficients
Linear function of total spill	$\%TDG = mQ_s + b$	Q_s = total spill, <i>kcf</i> s m = empirical coefficient b = empirical coefficient
Bounded exponential of total spill	$\%TDG = a + be^{cQ_s}$	Q_s = total spill, <i>kcf</i> s a = empirical coefficient b = empirical coefficient c = empirical coefficient
Bounded exponential of the spill on a per spillway basis	$\%TDG = a + be^{cq_s}$	q_s = spill through an individual spillway, <i>kcf</i> s a = empirical coefficient b = empirical coefficient c = empirical coefficient

Examples of some of these correlations are shown in [Table B-7](#). In many cases, the %TDG in these correlations was constrained to a maximum of 145% and when the flow reached only a few *kcf*s, there was assumed to be no change in TDG from the forebay to the tailrace. Also, the correlations in [Table B-7](#) sometimes changed from year to year based on changes in operating conditions or structural changes in the spillway or deflectors.

Table B-7. Equations used in CRiSP model for gas production.

Dam	Equation	Coefficients
Bonneville	$\%TDG = mQ_s + b$	$m = 0.12, b = 105.61$
Lower Granite	$\%TDG = a + be^{cq_s}$	$a = 138.0; b = -35.8; c = -0.10$
Dworshak	$\%TDG = a + be^{cQ_s}$	$a = 135.9; b = -71.1; c = -0.4787$
Ice Harbor	$\%TDG = a + be^{cQ_s}$	$a = 136.8; b = -42.0; c = -0.0340$ 1995 $a = 138.7; b = -79.0; c = -0.0591$ 1996 $a = 130.9; b = -26.5; c = -0.0220$ 1997 $a = 120.9; b = -20.5; c = -0.0230$ 1998
Hell's Canyon	$\%TDG = a + be^{cQ_s}$	$a = 138; b = -36; c = -0.02$ [Assumed relationship - no data]

DO Impacts of Spillways

For each spillway, weir, or gate, the user now has the choice of equation to use for computing the effects of hydraulic structures on downstream dissolved oxygen. The equations chosen are shown in [Table B-8](#). These equations are based on equations from [Table B-5](#) and [Table B-6](#).

Table B-8. Spillways and weirs reaeration

#	Equation type	Equation	Description of empirical coefficients
1	Linear function of spill on a per spillway basis	$\%TDG = aq_s + b$ DO concentration, Φ_{O_2} , is determined from $\Phi_{O_2} = \%TDG \Phi_s$	$\%TDG$ = % total dissolved gas saturation q_s = spill through an individual spillway, kcfs a = empirical coefficient Φ_s = dissolved oxygen saturation
2	empirical coefficients a and b	$\%TDG = a + be^{q_s}$ Φ_{O_2} , is then determined from $\Phi_{O_2} = \%TDG \Phi_{sat}$	q_s = spill through an individual spillway, kcfs a = empirical coefficient b = empirical coefficient c = empirical coefficient Φ_{sat} = dissolved oxygen saturation
3	Reaeration effect for a small height weir or dam (<10 m) empirical coefficients a, b, and c	$\frac{D_a}{D_b} = 1 + 0.38ab(1 - 0.11c)(1 + 0.046T)c$ Φ_{O_2} below the dam is then computed from: $\Phi_{O_2} = \Phi_{sat} - D_b$	D_a = DO deficit above dam, $g\ m^{-3}$ D_b = DO deficit below dam T = temperature in °C H = height of water fall, m a = 1.8 for clean water to 0.65 for gross polluted water b = 0.05 for sluice gates 1.0 for sharp crested, straight faced weir 0.45 for flat, broad crested, curved face weir 0.7 for flat, broad crested weir with regular step 0.8 for sharp crested, vertical face weir 0.6 for flat, broad crested weir with vertical face Φ_{sat} = dissolved oxygen saturation, $g\ m^{-3}$

Note that for equations 1 and 2, the maximum TDG allowed is 145%. If TDG is computed to be less than 100%, there is no effect of the spillway or gate on reaeration. For each spillway or gate defined in the model, there is a section to define whether gas effects for dissolved oxygen are computed and, if so, by which formula.

For each spillway or weir, the user turns on the computations and then selects an equation number from [Table B-8](#). This algorithm only computes gas effects for flow from upstream to downstream. There is no adjustment of dissolved oxygen for reverse flow.

Dissolved Oxygen Saturation Computations

The dissolved oxygen saturation is computed from Mortimer’s (1981) formulation:

$$\Phi_{O_2sat} = P_{at} e^{(7.7117 - 1.31403[\ln\{T + 45.93\}])} \tag{B-45}$$

where:

$$\begin{aligned} T &= \text{water temperature, } ^\circ\text{C} \\ P_{alt} &= \text{altitude correction factor,} \\ H &= \text{elevation of the waterbody, km above sea level} \end{aligned}$$

The saturation value is also a function of the chlorinity in saline environments. The following equation is used to compute DO saturation for a saltwater waterbody type that includes salinity effects (APHA, 1985; EPA 1985; Thomann and Mueller, 1987).

$$\Phi^*_{O2sat} = e^{\left(\ln(\Phi_{O2sat}) - S \left[1.7674 \times 10^{-2} - \frac{1.0754 \times 10^1}{T} + \frac{2.1407 \times 10^3}{T^2} \right] \right)} \quad (\text{B-46})$$

where:

$$\begin{aligned} S &= \text{salinity, kg m}^{-3} \\ T &= \text{temperature, } ^\circ\text{K} \end{aligned}$$

Sediments

Organic sediment contributions to nutrients and dissolved oxygen demand are simulated using two methods. The first method uses a constant, or zero-order, release and demand. This method has been frequently used to model sediment demands and nutrient release rates. It does not depend on sediment concentrations or require a separate sediment compartment. However, the formulation is not predictive as the rates do not vary over time except as a result of temperature dependence of the decay rate. As a consequence, results should be interpreted cautiously when evaluating effects of different nutrient loadings on dissolved oxygen in a waterbody.

The second method uses a sediment compartment to accumulate organic sediments and allow their decay. Nutrient releases and oxygen demand are thus dependent upon sediment accumulation – a 1st-order process. However, there is no release of phosphorus or other diagenesis products when overlying water is anoxic since this sediment compartment is labile, oxic decay of organics on the sediment surface. A later version will include a fully predictive sediment diagenesis model. Either of these methods, or a combination, may be used to simulate effects of organic sediments upon water quality. However, caution must be exercised to avoid errors if both methods are used.

The 0-order process uses a specified sediment oxygen demand and anoxic release rates for phosphorus, ammonium, inorganic carbon, and iron that are temperature dependent. Nutrient releases do not occur when dissolved oxygen concentrations are above a minimum value [\[O2LIM\]](#) nor do they occur if the SOD is set to zero. The sediment contribution to inorganic carbon is computed as a fraction of the sediment oxygen demand.

KINETICS

TOTAL INORGANIC CARBON

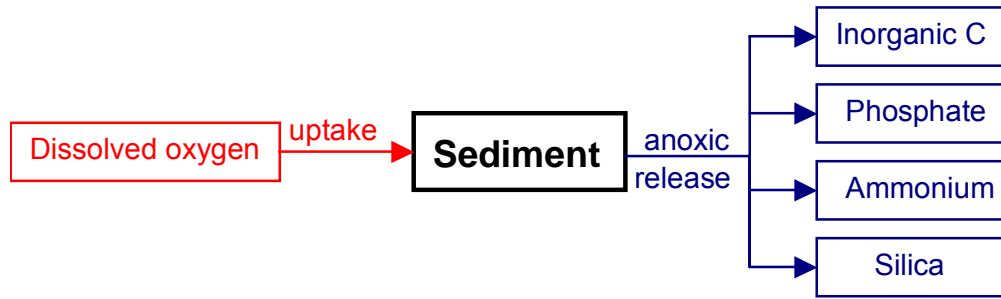


Figure B-24. Internal flux between 0-order sediment compartment and other compartments.

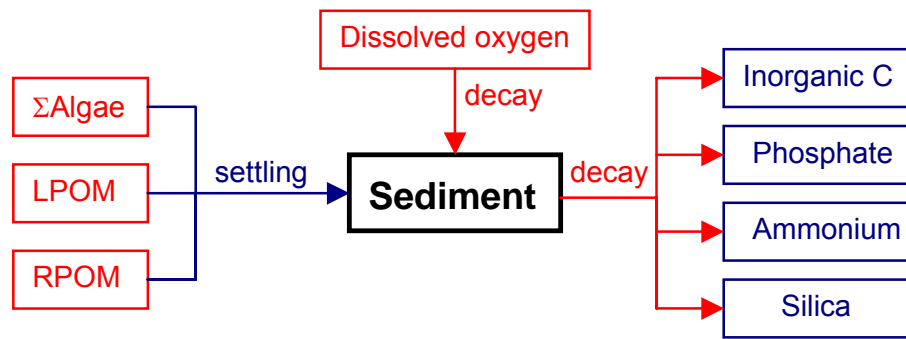


Figure B-25. Internal flux between 1st-order sediment compartment and other compartments.

The 1st-order sediment compartment requires specifying inclusion of this compartment in the simulation, a decay rate, and initial conditions. The sediment compartment is not transported. Instead, a compartmental equation is written for the sediment compartment that is solved in the subroutine SEDIMENT.

Referring to [Figure B-25](#), the equation for the 1st-order sediment compartment is:

$$S_{sed} = \underbrace{\frac{\omega_{POM}}{\Delta z} \Phi_{LPOM}}_{\text{labile POM settling}} + \underbrace{\frac{\omega_{POM}}{\Delta z} \Phi_{RPOM}}_{\text{refractory POM settling}} + \underbrace{\sum \frac{\omega_a}{\Delta z} \Phi_a}_{\text{algae settling}} - \underbrace{\gamma_{OM} K_{sed} \Phi_{sed}}_{\text{sediment decay}} \quad (\text{B-47})$$

where:

- γ_{OM} = rate multiplier for organic matter
- Δz = model cell thickness, m
- ω_{POM} = POM settling velocity, $m \text{ sec}^{-1}$
- ω_a = algal settling velocity, $m \text{ sec}^{-1}$
- K_{sed} = sediment decay rate, sec^{-1}
- Φ_a = algal concentration, $g \text{ m}^{-3}$
- Φ_{LPOM} = POM labile concentration, $g \text{ m}^{-3}$

Φ_{RPOM} = POM refractory concentration, $g\ m^{-3}$
 Φ_{sed} = organic sediment concentration, $g\ m^{-3}$

Total Inorganic Carbon

Carbon, hydrogen, and oxygen are the most abundant elements in living matter and form the essential backbone of organic material. Inorganic carbon directly influences pH.

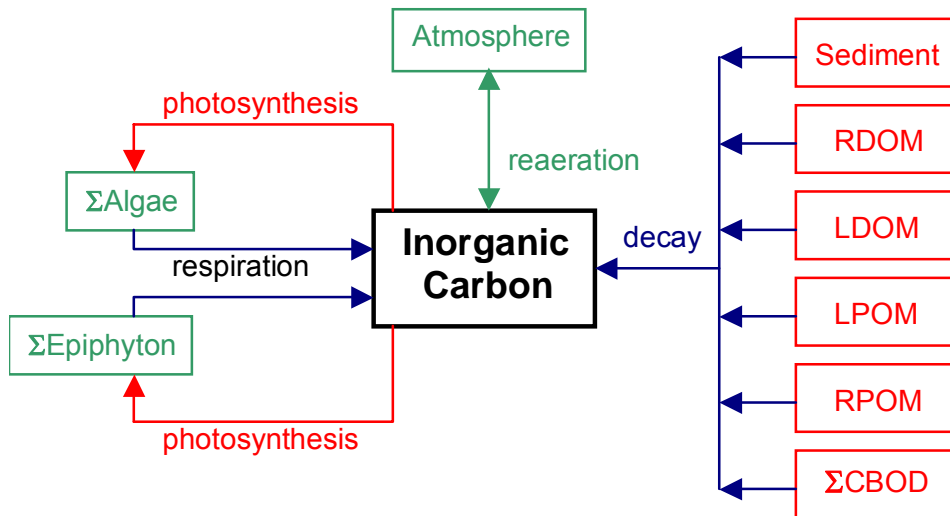


Figure B-26. Internal flux between inorganic carbon and other compartments.

Referring to [Figure B-26](#), the rate equation for total inorganic carbon is:

$$\begin{aligned}
 S_{TIC} = & \underbrace{\sum (K_{ar} - K_{ag}) \delta_{Ca} \Phi_a}_{\text{netalgalproduction}} + \underbrace{\sum (K_{er} - K_{eg}) \delta_{Ce} \Phi_e}_{\text{netepiphytoproduction}} + \underbrace{K_{LPOM} \delta_{COM} \gamma_{OM} \Phi_{LPOM}}_{\text{labilePOMdecay}} \\
 & + \underbrace{K_{LDOM} \gamma_{OM} \delta_{COM} \Phi_{LCOM}}_{\text{labileDOMdecay}} + \underbrace{K_{RDOM} \gamma_{OM} \delta_{COM} \Phi_{RDOM}}_{\text{refractoryDOMdecay}} + \underbrace{K_{RPOM} \delta_{COM} \gamma_{OM} \Phi_{RPOM}}_{\text{refractoryPOMdecay}} \\
 & + \underbrace{K_{sed} \gamma_{OM} \delta_{COM} \Phi_{sed}}_{\text{1st-ordersedimentrelease}} + \underbrace{SOD \gamma_{OM} \delta_{COM} \frac{A_{sed}}{V}}_{\text{0-ordersedimentrelease}} + \underbrace{A_{sur} K_{Lc} (\Phi'_{CO_2} - \Phi_{CO_2})}_{\text{reaeration}} \\
 & + \underbrace{\sum K_{CBOD} R_{CBOD} \delta_{C-CBOD} \Theta^{T-20} \Phi_{CBOD}}_{\text{CBODdecay}}
 \end{aligned} \tag{B-48}$$

where:

θ = temperature rate multiplier for BOD decay
 γ_{OM} = organic matter temperature rate multiplier

KINETICS

TOTAL INORGANIC CARBON

- δ_{Ce} = epiphyton stoichiometric coefficient for carbon
 δ_{Ca} = algal stoichiometric coefficient for carbon
 δ_{COM} = organic matter stoichiometric coefficient for carbon
 δ_{C-CBOD} = CBOD stoichiometric coefficient for carbon
 R_{BOD} = 5-day CBOD to ultimate CBOD ratio
 A_{sed} = sediment surface area, m^2
 A_{sur} = surface area of surface computational cell, m^2
 SOD = sediment oxygen demand, $g\ m^{-2}\ sec^{-1}$
 K_{Lc} = inorganic carbon interfacial exchange rate, $m\ sec^{-1}$
 K_{ar} = algal dark respiration rate, sec^{-1}
 K_{ag} = algal growth rate, sec^{-1}
 K_{er} = epiphyton dark respiration rate, sec^{-1}
 K_{eg} = epiphyton growth rate, sec^{-1}
 K_{LDOM} = labile DOM decay rate, sec^{-1}
 K_{RDOM} = refractory DOM decay rate, sec^{-1}
 K_{LPOM} = labile POM decay rate, sec^{-1}
 K_{RPOM} = refractory POM decay rate, sec^{-1}
 K_{CBOD} = CBOD decay rate, sec^{-1}
 K_{sed} = sediment decay rate, sec^{-1}
 Φ_a = algal concentration, $g\ m^{-3}$
 Φ_e = epiphyton concentration, $g\ m^{-3}$
 Φ_{LDOM} = labile DOM concentration, $g\ m^{-3}$
 Φ_{RDOM} = refractory DOM concentration, $g\ m^{-3}$
 Φ_{LPOM} = labile POM concentration, $g\ m^{-3}$
 Φ_{RPOM} = refractory POM concentration, $g\ m^{-3}$
 Φ_{CBOD} = CBOD concentration, $g\ m^{-3}$
 Φ_{sed} = organic sediment concentration, $g\ m^{-3}$
 Φ_{TIC} = inorganic carbon concentration, $g\ m^{-3}$
 Φ_{CO_2} = carbon dioxide concentration, $g\ m^{-3}$
 Φ'_{CO_2} = carbon dioxide saturation concentration, $g\ m^{-3}$

and the rate terms are evaluated in subroutine INORGANIC_CARBON.

The basic physics of gas transfer are the same for CO_2 and O_2 . Using Higbie penetration theory, the gas transfer coefficient for CO_2 is related to that of oxygen by:

$$KL_{CO_2} = KL_{O_2} \sqrt{\frac{D_{CO_2}}{D_{O_2}}} \quad (\text{B-49})$$

where:

- KL_{CO_2} = reaeration coefficient for CO_2
 KL_{O_2} = reaeration coefficient for oxygen
 D_{CO_2} = molecular diffusion coefficient for CO_2

D_{O_2} = molecular diffusion coefficient for oxygen

Using the fact that the ratio of molecular diffusion coefficients of two gases A and B are related to their molecular weights, MW (Thibedoux, 1996)

$$\frac{D_A}{D_B} = \sqrt{\frac{MW_B}{MW_A}} \quad \text{(B-50)}$$

then

$$KL_{CO_2} = KL_{O_2} \left(\frac{MW_{O_2}}{MW_{CO_2}} \right)^{0.25} = 0.923KL_{O_2} \quad \text{(B-51)}$$

Hence, the reaeration rate equations presented for oxygen transfer are applicable to CO₂ transfer using a factor of 0.923.

Carbon dioxide concentration for the interfacial exchange rate is determined from total inorganic carbon and alkalinity in subroutine PH_CO2. The saturation concentration of carbon dioxide is determined from:

$$\Phi'_{CO_2} = 0.286 e^{(-0.0314T_s)} P_a \quad \text{(B-52)}$$

where:

- Φ'_{CO_2} = carbon dioxide saturation concentration, $g\ m^{-3}$
- P_a = altitude correction factor
- T_s = surface cell water temperature, °C

Altitude correction is from Mortimer, 1981:

$$P_a = \left(1 - \frac{H}{44.3} \right)^{5.25} \quad \text{(B-53)}$$

where:

H = reservoir elevation from sea level, km

Alkalinity

Alkalinity provides an indication of the buffering capacity of aquatic systems and their resistance to pH changes from acidic or alkaline loadings. Alkalinity is treated as conservative in the model and

its internal rate term is set to zero. Alkalinity, along with total inorganic carbon, is used to determine pH and concentrations of carbonate species in subroutine PH_CO2.

In reality, alkalinity variations are common in most aquatic systems. Whittings, or large precipitations of carbonates, may occur. Sediment release of carbonates may increase alkalinity in the anoxic zones of many reservoirs. If these effects are important, a non-conservative model of alkalinity should be added.

pH and Carbonate Species

The pH and carbonate species are computed using water temperature, TDS or salinity, alkalinity, and total inorganic carbon concentrations using basic carbonate relationships. Computed carbonate species are carbon dioxide, bicarbonates, and carbonates. The pH and carbonate species are computed in subroutine PH_CO2. These materials are not subject to transport and are computed at each water quality update interval.

Calculations performed by subroutine PH_CO2 are based on the carbonate-bicarbonate equilibrium reaction (Stumm and Morgan 1981):



These equilibria express the source of bicarbonate and carbonate ions, alkaline constituents, and dissolution of atmospheric CO₂ in water. Contribution of calcium and magnesium carbonate to alkalinity is not included. The equilibrium state in terms of the equilibrium constants K_i is:

$$K_1 = \frac{[\text{H}^+][\text{HCO}_3^-]}{[\text{H}_2\text{CO}_3]} \quad (\text{B-56})$$

$$K_2 = \frac{[\text{H}^+][\text{CO}_3^{2-}]}{[\text{HCO}_3^-]} \quad (\text{B-57})$$

$$K_w = \frac{[\text{H}^+][\text{OH}^-]}{[\text{H}_2\text{O}]} \quad (\text{B-58})$$

where:

[X] = molar concentration, *moles liter*⁻¹
 [H₂O] = unity (by definition)

Alkalinity is defined as:

$$[\text{ALK}] = [\text{HCO}_3^-] + 2[\text{CO}_3^{2-}] + [\text{OH}^-] - [\text{H}^+] \quad (\text{B-59})$$

The following condition prevails for the dissolution of carbonic acid:

$$[\text{H}_2\text{CO}_3] + [\text{HCO}_3^-] + [\text{CO}_3^{2-}] = \text{CONSTANT} = C_T \quad (\text{B-60})$$

By combining equations B-53, B-54, and B-57, the quantities $[\text{HCO}_3^-]$ and $[\text{CO}_3^{2-}]$ can be expressed in terms of $[\text{H}^+]$ and the constant C_T . In addition, equation B-55 allows for $[\text{OH}^-]$ to be expressed in terms of $[\text{H}^+]$. When these expressions are included in equation B-56, the result is:

$$[\text{ALK}] = \frac{C_T [\text{H}^+] K_1}{[\text{H}^+] K_1 + K_1 K_2 + [\text{H}^+]^2} \frac{[\text{H}^+] + 2 K_2}{[\text{H}^+]} + \frac{K_w}{[\text{H}^+]} - [\text{H}^+] \quad (\text{B-61})$$

The model interprets the constant C_T as moles per liter of total inorganic carbon and assumes $[\text{ALK}]$ is known. Equation B-58 is iteratively solved in subroutine PH_CO2 until the value of $[\text{H}^+]$ converges. The negative logarithm of $[\text{H}^+]$ is, by definition, pH.

Once equation B-58 has been solved for $[\text{H}^+]$, then $[\text{H}_2\text{CO}_3]$ is given by:

$$[\text{H}_2\text{CO}_3] = \frac{C_T}{1 + \frac{K_1}{[\text{H}^+]} + \frac{K_1 K_2}{[\text{H}^+]^2}} \quad (\text{B-62})$$

and is the same as $[\text{CO}_2]$. Bicarbonate concentration is computed from:

$$[\text{HCO}_3^-] = \frac{C_T}{1 + \frac{[\text{H}^+]}{K_1} + \frac{K_2}{[\text{H}^+]}} \quad (\text{B-63})$$

and carbonate from:

$$[\text{CO}_3^{2-}] = \frac{C_T}{1 + \frac{[\text{H}^+]^2}{K_1 K_2} + \frac{[\text{H}^+]}{K_2}} \quad (\text{B-64})$$

which are then converted to grams per cubic meter.

Equilibrium constants in the preceding equations are obtained by first expressing a thermodynamic temperature dependence for a related constant, K_i^* :

$$\log K_i^* = a + \frac{b}{T} + cT + d \log T \quad (\text{B-65})$$

The constants a, b, c, and d are:

	a	b	c	d
K_w^*	35.3944	-5242.39	-0.00835	11.8261
K_1^*	14.8435	-3404.71	-0.03278	0
K_2^*	6.4980	-2902.39	-0.02379	0

The relation between K_i and K_i^* is obtained from the definition of the activity of a chemical species:

$$\{X\} = \gamma [X] \quad (\text{B-66})$$

where:

$\{X\}$ = activity of species X, *moles liter⁻¹*

γ = dimensionless activity coefficient

$[X]$ = concentration, *moles liter⁻¹*

For the reaction:



the equilibrium constant K^* is:

$$K^* = \frac{\{C\} \{D\}}{\{A\} \{B\}} \quad (\text{B-68})$$

thus:

$$K^* = \frac{\gamma_C [C] \gamma_D [D]}{\gamma_A [A] \gamma_B [B]} = \frac{\gamma_C \gamma_D}{\gamma_A \gamma_B} K \quad (\text{B-69})$$

$$K = \frac{\gamma_A \gamma_B}{\gamma_C \gamma_D} K^* \quad (\text{B-70})$$

Activity coefficients are obtained from an extension of Debye-Huckel theory as:

$$\text{Log } \gamma = \frac{-AZ^2 \sqrt{I}}{1 + 0.33a \sqrt{I}} + k_1 + k_2 I + k_3 I^2 \quad (\text{B-71})$$

where:

- I = ionic strength
- Z = ionic charge
- A = approximately 0.5 for water at 25°C
- a = ionic size parameter
- k_i = empirical coefficients

Ionic strength is approximated as (Sawyer and McCarty 1967):

$$I = 2.5 \times 10^{-5} \Phi_{TDS} \tag{B-72}$$

or for salinity:

$$I = 0.00147 + 0.019885 \Phi_{sal} + 0.000038 \Phi_{sal}^2 \tag{B-73}$$

where:

- Φ_{TDS} = total dissolved solids, $g\ m^{-3}$
- Φ_{sal} = salinity, $kg\ m^{-3}$

Values of the other parameters are:

	Z	a	k ₁	k ₂	k ₃
HCO ₃ ⁻	1	4	0.0047	0.042	-0.0093
CO ₃ ⁼	2	4.5	0.0121	0.0972	-0.0207

Activity coefficients for [H⁺], [OH⁻], [H₂CO₃], and [H₂O] are treated as special cases:

$$[H^+] \gamma = [H_2O] \gamma = 1 \tag{B-74}$$

$$[H_2CO_3] \gamma = [OH^-] \gamma = 0.07551 \tag{B-75}$$

Temperature Rate Multipliers

Most biological and chemical rates are temperature dependent. Subroutine RATE_MULTIPLIERS calculates the temperature dependence for all rates. It is called after the temperature solution so the temperature of the current computational interval is used.

A representative rate multiplier function is shown in [Figure B-27](#) with its K and T parameters. The curve represents how biological process rates exhibit an optimum range and diminish asymmetrically at higher and lower temperatures (Thornton and Lessem, 1978).

$$\lambda_T = 0 \quad \text{where } T \leq T_1$$

$$\lambda_T = \frac{K_1 e^{\gamma_1(T-T_1)}}{\underbrace{1 + K_1 e^{\gamma_1(T-T_1)} - K_1}_{\gamma_{ar}}} \frac{K_4 e^{\gamma_2(T_4-T)}}{\underbrace{1 + K_4 e^{\gamma_2(T_4-T)} - K_4}_{\gamma_{af}}} \quad \text{where } T_1 < T < T_4 \quad \text{(B-76)}$$

$$\lambda_T = 0 \quad \text{where } T \geq T_4$$

where:

$$\gamma_{ar} = \frac{1}{T_2 - T_1} \ln \frac{K_2(1 - K_1)}{K_1(1 - K_2)}$$

$$\gamma_{af} = \frac{1}{T_4 - T_3} \ln \frac{K_3(1 - K_4)}{K_4(1 - K_3)}$$

γ_{ar} and γ_{af} are the rising and falling limb temperature multipliers.

The user supplies temperatures T_1 to T_4 and multiplier factors K_1 to K_4 . Temperatures T_1 and T_4 represent mortality limits, and T_2 and T_3 are used to define the optimum range. Maximum reaction rates supplied by the user are multiplied by λT to determine rates corresponding to the water temperature of a model cell. For non-algae temperature rate multipliers, only the K_1 and K_2 corresponding to T_1 and T_2 are used.

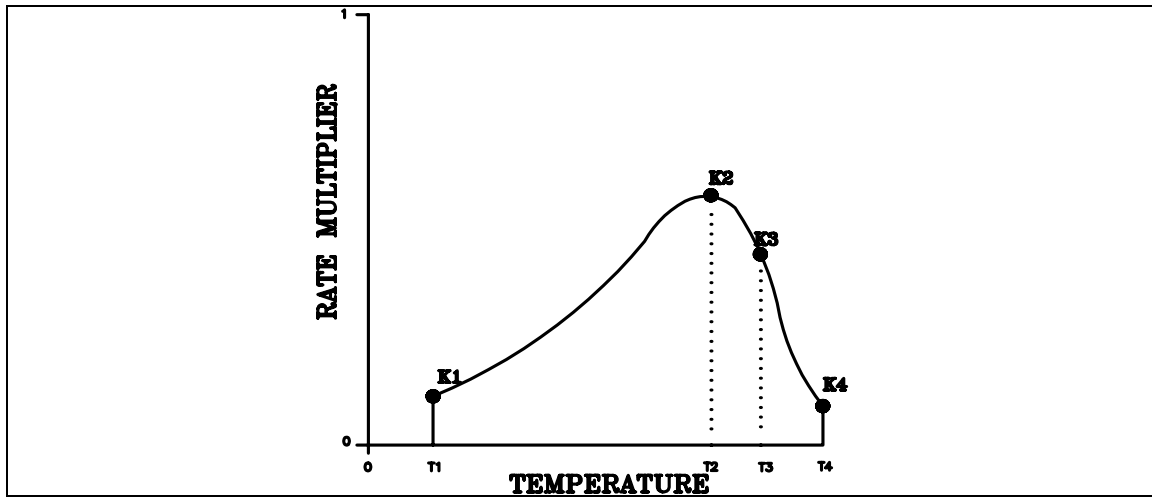


Figure B-27. Temperature rate multiplier function.

Appendix C Input/Output Data Description

Input file format has been developed for a full-screen text editor. Each input file begins with two lines used for file identification that are ignored by the program. The rest of the input file consists of groups of three lines - the first line is blank serving as a separator, the second line contains the card identification and the FORTRAN variable names associated with the input card, and the third line contains the input values. The identifier card is only checked by the pre-processor code. FORTRAN names are right justified according to the field widths associated with the input variable. There are 10 input fields associated with each card although the first field is not used in several of the input files. Each field has a length of eight characters.

Input Files

Control File

The control file [CONFN] contains the variables used to run the model. There are no optional cards in the control file - each card is *required* although there may be either zero or no values associated with the card. The following pages contain a description of each card. *All character inputs must be capitalized except the TITLE cards and input/output filenames* or the variable will take on the default value. An example of a portion of a control file is given with each card description and a complete control file is given at the end of the control file description. Hyperlinks to related input cards are included at the bottom of each card description.

Title (TITLE C)

FIELD	NAME	VALUE	DESCRIPTION
1			(Ignored by code)
2-10	TITLE	Character	Text for identification of simulation

There are 10 title cards for each a simulation that can be used to identify various types of output. Each line may contain up to 72 characters of text. Title cards appear in every output file except for the restart file. Uses for the title cards include identifying the simulation, the simulation time frame, the date the simulation was run, and other information specific to the simulation. A few words of wisdom - the user should be conscientious in updating the title cards for each simulation.

Example

```

TITLE C .....TITLE.....
Card 1 Version 3 Example Model
Card 2 PSU CE-QUAL-W2 Workshop Problem 7
Card 3 River with 2 branches
Card 4 Reservoir
Card 5 Estuary
Card 6 River Sloping Channels 2 Branches
Card 7 Temperature Mitigation Problem
Card 8 Temperature and residence time simulation
Card 9 Scott Wells - PSU
Card 10 Tom Cole - WES
    
```

Grid Dimensions (GRID)

FIELD	NAME	VALUE	DESCRIPTION
1			(Ignored by code)
2	NWB	Integer	Number of waterbodies in the computational grid
3	NBR	Integer	Number of branches in the computational grid
4	IMX	Integer	Number of segments in the computational grid
5	KMX	Integer	Number of layers in the computational grid

This card defines the computational grid including the total number of waterbodies [NWB], branches [NBR], segments [IMX], and layers [KMX]. These values are used to define the array dimensions in the code since the code has been converted over to FORTRAN 90 and now takes advantage of dynamic array allocation. This eliminates the need to recompile the code for each application.

Example

GRID	NWB	NBR	IMX	KMX
	3	4	43	24

Related Cards and Files

[Inflow/Outflow Dimensions](#)

[Constituent Dimensions](#)

[Miscellaneous Dimensions](#)

Inflow/Outflow Dimensions (IN/OUTFLOW)

FIELD	NAME	VALUE	DESCRIPTION
1			(Ignored by code)
2	NTR	Integer	Number of tributaries
3	NST	Integer	Number of structures
4	NIW	Integer	Number of internal weirs
5	NWD	Integer	Number of withdrawals
6	NGT	Integer	Number of gates
7	NSP	Integer	Number of spillways
8	NPI	Integer	Number of pipes
9	NPU	Integer	Number of pumps

This card defines the variables used to dimension the arrays for tributaries, internal weirs, and inflow/outflow hydraulic structures including lateral withdrawals, outlet gates, spillways, pipes, and pumps. All variables should be set to zero if they are not used.

Example

IN/OUTFLOW	NTR	NST	NIW	NWD	NGT	NSP	NPI	NPU
	1	3	1	0	1	2	1	0

Related Cards and Files

[Grid Dimensions](#)

[Constituent Dimensions](#)

[Miscellaneous Dimensions](#)

[Tributaries](#)

[Structures](#)

[Weirs](#)

[Withdrawals](#)

[Gates](#)

[Spillways](#)

[Pipes](#)

[Pumps](#)

Constituent Dimensions (CONSTITUENTS)

FIELD	NAME	VALUE	DESCRIPTION
1			(Ignored by code)
2	NCG	Integer	Number of generic constituents
3	NSS	Integer	Number of inorganic suspended solids
4	NAL	Integer	Number of algal groups
5	NEP	Integer	Number of epiphyton groups
5	NBOD	Integer	Number of CBOD groups

This card defines the array dimensions for the number of generic constituents, inorganic suspended solids groups, algal groups, and CBOD groups. The user has complete freedom to include as many of these groups as data are available for and the application warrants.

The generic constituent allows the user the freedom to model any number of constituents that can be defined using a 0-order decay rate and/or a 1st- order decay rate and/or a settling velocity and/or an Arrhenius temperature rate multiplier. Version 2 state variables that fall into the generic category include tracer and coliform. Thus, any number of tracers or coliform groups can be modeled. Additionally, residence time can be modeled in this group by setting the 0-order decay rate to -1.0 and setting all other kinetic parameters to zero.

The ability to model any number of CBOD groups now allows the model to characterize and track any number of point sources of CBOD. This should prove useful in determining which point source(s) is/are contributing to depressed dissolved oxygen levels or violations in a system and allow better management of resources to improve dissolved oxygen.

Care should be taken when including multiple algal and/or epiphyton groups to ensure that the data are sufficient to describe their variation in the system. As a general rule, it is better to start with as simple a description of the kinetics in a system that still allows the model to capture the important temporal and spatial changes in water quality.

Example

CONSTITUENTS	NCG	NSS	NAL	NEP	NBOD
	4	3	3	1	3

Related Cards and Files

[Grid Dimensions](#)
[Inflow/Outflow Dimensions](#)
[Miscellaneous Dimensions](#)

Miscellaneous Dimensions (MISCELL)

FIELD	NAME	VALUE	DESCRIPTION
1			(Ignored by code)
2	NDAY	Integer	Maximum number of output dates or timestep related changes

This card defines the maximum number of output dates that will be used in the simulation. This should be the maximum of timestep, snapshot, screen, profile, vector, contour, time series, withdrawal, and restart number of dates that are used to define when output frequencies, or, in the case of the timestep related cards, when the maximum timestep or the fraction of the timestep change. This can easily be set to a value greater than any anticipated number of dates without any impact as the memory used by these variables is trivial.

Example

```
MISCELL      NDAY
              100
```

Related Cards and Files

[Grid Dimensions](#)

[Inflow/Outflow Dimensions](#)

[Constituent Dimensions](#)

Time Control (TIME CON)

FIELD	NAME	VALUE	DESCRIPTION
1			(Ignored by code)
2	TMSTRT	Real	Starting time, <i>Julian day</i>
3	TMEND	Real	Ending time, <i>Julian day</i>
4	YEAR	Real	Starting year

The simulation starting and ending times are specified with this card. When making a simulation extending into another year, the ending time is calculated as 365 (or 366 for a leap year) + Julian date of ending time. Midnight, January 1 starts at Julian day 1.0 in the model.

Example

TIME CON	TMSTRT	TMEND	YEAR
	63.5	64.5	1980

Timestep Control (DLT CON)

FIELD	NAME	VALUE	DESCRIPTION
1			(Ignored by code)
2	NDT	Integer	Number of timestep intervals
3	DLTMIN	Real	Minimum timestep, sec

The number of timestep intervals and minimum timestep are specified on this card.

The autosteping algorithm calculates a maximum timestep based on an estimate of hydrodynamic numerical stability requirements and then uses a fraction of this value for the actual timestep. The user can specify any number of intervals up to the value specified for **[NDAY]** on the [Miscellaneous Dimensions](#) card in which the maximum timestep and fraction of the timestep can vary. The values are specified on the next three cards.

This option is useful during periods of very low flow where the timestep is very large. Under these conditions, small changes in flow will result in large timestep changes that can lead to an excessive number of timestep violations detected by the autosteping algorithm. The model automatically adjusts the timestep to ensure that it is never greater than the next time varying update, so the maximum timestep can be set to a value greater than the minimum time varying data update frequency.

The minimum timestep is useful during periods of extremely high flows. In these instances, the timestep could become too small to economically run the model. Care should be taken when using this variable as the model may become numerically unstable if the minimum value is set too high. The default value of 1 sec should not be increased unless the user is absolutely certain that this will not affect numerical stability.

Example

```
DLT CON      NDT  MINDLT
              2    1.0
```

Related Cards and Files

[Timestep Date](#)
[Maximum Timestep](#)
[Timestep Fraction](#)
[Timestep Limitation](#)

Timestep Date (DLT DATE)

FIELD	NAME	VALUE	DESCRIPTION
1			(Ignored by code)
2-10	DLTD	Real	Beginning of timestep interval, <i>Julian day</i>

The intervals for the maximum timestep are specified on this card. Any number of intervals up to the value of [NDAY] on the [Miscellaneous Dimensions](#) card can be specified. If there are more intervals than can be specified on one line, then they are continued on the next line without another **DLT DATE** card being specified.

Example

```
DLT DATE      DLTD      DLTD      DLTD      DLTD      DLTD      DLTD      DLTD      DLTD      DLTD
              63.5      63.52

```

Related Cards and Files

[Timestep Control](#)
[Maximum Timestep](#)
[Timestep Fraction](#)
[Timestep Limitation](#)

Maximum Timestep (DLT MAX)

FIELD	NAME	VALUE	DESCRIPTION
1			(Ignored by code)
2-10	DLTMAX	Real	Maximum timestep, sec

The maximum timestep for intervals provided on the timestep interval card are specified with this card. If there are more intervals than can be specified on one line, then they are continued on the next line without another **DLT MAX** card being specified.

Example

```
DLT MAX   DLTMAX  DLTMAX  DLTMAX  DLTMAX  DLTMAX  DLTMAX  DLTMAX  DLTMAX
          30.0   100.0
```

Related Cards and Files

[Timestep Control](#)

[Timestep Date](#)

[Timestep Fraction](#)

[Timestep Limitation](#)

Timestep Fraction (DLT FRN)

FIELD	NAME	VALUE	DESCRIPTION
1			(Ignored by code)
2-10	DLTF	Real	Fraction of calculated maximum timestep necessary for numerical stability

The fraction of the calculated maximum timestep for intervals given on the timestep interval card is specified here. If there are more intervals than can be specified on one line, then they are continued on the next line without another **DLT FRN** card being specified. If the number of timestep violations exceeds 5%, either [[DLTMAX](#)] on the [Maximum Timestep](#) card or [[DLTF](#)] should be decreased.

Decreasing [[DLTF](#)] usually decreases the number of timestep violations without affecting the maximum timestep that the model can use. Thus, during times of low velocities, the model can still use the maximum timestep, but during periods of high velocities, the model will use a smaller timestep than if [[DLTF](#)] were set to a higher value.

Example

```
DLT FRN      DLTF      DLTF      DLTFR      DLTFR      DLTFR      DLTFR      DLTFR      DLTFR      DLTFR
              0.9        0.9
```

Related Cards and Files

[Timestep Control](#)
[Timestep Date](#)
[Maximum Timestep](#)
[Timestep Limitation](#)

Timestep Limitations (DLT LIMIT)

FIELD	NAME	VALUE	DESCRIPTION
1			(Ignored by code)
2	VISC	Character	Turns ON/OFF vertical eddy viscosity limitation on timestep calculated in autostepping algorithm
3	CELC	Character	Turns ON/OFF internal gravity wave limitation on timestep calculated in autostepping algorithm

This card specifies whether the effects of the vertical eddy viscosity and/or the internal gravity wave are included in the autostepping algorithm. Separate values are specified on a separate card for each waterbody.

If the average timestep is very small, these can be turned OFF to decrease runtimes. However, care should be taken when using this option as experience has shown that, in certain applications, turning these OFF can affect the results. If either of these variables are turned OFF, the user should also make a run with them turned ON to see if this option affects the results. Results should never be a function of the timestep or grid spacing.

Example

DLT LIMIT	VISC	CELC
Wb 1	ON	ON
Wb 2	ON	ON
Wb 3	ON	ON

Related Cards and Files

[Timestep Control](#)

[Timestep Date](#)

[Maximum Timestep](#)

[Timestep Fraction](#)

Branch Geometry (BRANCH G)

FIELD	NAME	VALUE	DESCRIPTION
1			(Ignored by code)
2	US	Integer	Branch upstream segment
3	DS	Integer	Branch downstream segment
4	UHS	Integer	Upstream boundary condition
5	DHS	Integer	Downstream boundary condition
6	UQB	Integer	Upstream internal flow boundary condition
7	DQB	Integer	Downstream internal flow boundary condition
6	NLMIN	Integer	Minimum number of layers for a segment to be active
7	SLOPE	Real	Waterbody bottom slope

This card specifies the branch location in the grid and branch boundary conditions. No distinction is made between waterbodies. The mainstem of the first waterbody is always branch 1 and the mainstem of subsequent waterbodies is always the next branch after all branches have been numbered for the previous waterbody. Side branches for a given waterbody can be ordered in any fashion, but it is good practice to order the remaining branches starting with the most upstream branch and continuing downstream.

The branch upstream segment number **[US]** is the most upstream potentially active segment. For branch 1, this would always be segment 2. The branch downstream segment number **[DS]** is the most downstream *active* segment. The boundary segment is *never* included for either the upstream or downstream segment.

Four upstream and downstream boundary conditions can be specified. Boundary conditions along with the upstream head segment **[UHS]** and downstream head segment **[DHS]** values that specify these conditions are:

Boundary type	[UHS] and/or [DHS]
External head	-1
External/internal flow	0
Internal head	>0
Dam flow	<-1

For internal head boundary conditions between branches or dam flow boundary conditions between waterbodies, **[UHS]** and/or **[DHS]** correspond to the branch segment the branch attaches to. In the following example, branch 1 consists of segments 2 through 6 and attaches to branch 2 at segment 9. Branch 2 consists of segments 9 through 14 and attaches at segment 6 in branch 1 and segment 17 at branch 3. See [Chapter 3](#) for additional information on the computational grid setup. The current version does not use the **[UQB]** and **[DQB]** variables. A later version will use these to define internal flow boundary conditions, as this is a more straightforward way to define internal and external flow branch linkages. Instead, any internal flow such as flow over a spillway will have a 0 value for **[DHS]**. For the receiving branch, a negative number corresponding to the spillway segment number is specified for **[UHS]**.

The following example is taken from the example [control file](#) of the Spokane River/Long Lake application of V3.1. Branches one through four represent sloping river sections that are linked in series

GRID DEFINITION

CONTROL FILE

since the downstream head segment number [DHS=13 for branch one] is the upstream segment number [US=13 for branch 2] of the next branch and the upstream head segment number [UHS=10 for branch 2] is the downstream segment number [DS=10 for branch 1] of the preceding branch. Similar linkage occurs for branches two to three and three to four. Branch four, however, has a downstream head [DHS] set to 0, indicating either an internal (spillway or gate) or external (outlet structure) flow boundary condition.

In this example, branch four is connected to branch 5 via an internal flow from a spillway and the linkage is specified on the spillway card in the sample control file.

Example

BRANCH	G	US	DS	UHS	DHS	UQB	DQB	NL	SLOPE
Br 1		2	10	0	13	0	0	1	0.00181
Br 2		13	24	10	27	0	0	1	0.00152
Br 3		27	36	24	39	0	0	1	0.00328
Br 4		39	48	36	0	0	0	1	0.00142
Br 5		51	64	0	0	0	0	1	0.00000
Br 6		67	73	-64	76	0	0	1	0.00000
Br 7		76	86	73	0	0	0	1	0.00000
Br 8		89	94	-86	97	0	0	1	0.00256
Br 9		97	128	94	0	0	0	1	0.00208
Br 10		131	135	0	138	0	0	1	0.00000
Br 11		138	151	135	0	0	0	1	0.00000
Br 12		154	188	-151	0	0	0	1	0.00000

Related Cards and Files

[Bathymetry File](#)

[Branch Inflow File](#)

[Branch Inflow Temperature File](#)

[Branch Inflow Concentration File](#)

[Branch Outflow File](#)

[Branch External Upstream Head Elevation File](#)

[Branch External Upstream Head Temperature File](#)

[Branch External Upstream Head Concentration File](#)

[Branch External Downstream Head Elevation File](#)

[Branch External Downstream Head Temperature File](#)

[Branch External Downstream Head Concentration File](#)

Waterbody Definition (LOCATION)

FIELD	NAME	VALUE	DESCRIPTION
1			(Ignored by code)
2	LAT	Real	Latitude, <i>degrees</i>
3	LONG	Real	Longitude, <i>degrees</i>
4	EBOT	Real	Bottom elevation of waterbody, <i>m</i>
5	BS	Integer	Starting branch of waterbody
6	BE	Integer	Ending branch of waterbody
7	JBDN	Integer	Downstream branch of waterbody

This card specifies the waterbody latitude and longitude, bottom reference elevation, starting and ending branches of the waterbody, and the downstream most branch of the waterbody that connects to the next waterbody. The bottom elevation is used to tie computed water surface elevations to an external benchmark (e.g., *m* above sea level) and represents the elevation at the bottom of the bottommost active cell.

[JBDN] specifies the downstream branch from which [EBOT] is referenced. In the case of a complicated grid, this is the starting elevation for tying the rest of the elevation of the grid together. [EBOT] is the elevation of the bottom of the bottommost active layer in the computational grid [KMX]. Figure C-28 and Figure C-29 show [EBOT] for a sloping river and a reservoir, respectively. For a sloping river, [EBOT] would generally be located at the most downstream segment in the section. [EBOT] is defined as the elevation of KMX-1 of DS(JBDN).

Example

LOCATION	LAT	LONG	EBOT	BS	BE	JBDN
WB 1	45.44	122.18	36.00	1	2	2
WB 2	45.44	122.18	0.00	3	3	3
WB 3	45.44	122.18	-8.00	4	4	4

GRID DEFINITION

CONTROL FILE

Segment	4	5	6	7	8	9	10
DLX	33.49	149.18	108.37	196.35	306.19	87.04	87.04
ELWS	271	271	271	271	271	271	271
PHIO	3.5	3.5	4.71	4.71	3.14	3.14	3.14
Friction	0.04	0.05	0.05	0.05	0.05	0.05	0.05

Layer	Width	Elev-top	Width										
1	.00	276.83	.00	276.71	.00	276.55	.00	276.35	.00	276.02	.00	275.77	.00
2	90.00	276.23	90.00	276.11	90.00	275.95	90.00	275.75	90.00	275.42	90.00	275.17	.00
3	90.00	275.63	90.00	275.51	90.00	275.35	90.00	275.15	90.00	274.82	90.00	274.57	.00
4	90.00	275.03	90.00	274.91	90.00	274.75	90.00	274.55	90.00	274.22	90.00	273.97	.00
5	90.00	274.43	90.00	274.31	90.00	274.15	90.00	273.95	90.00	273.62	90.00	273.37	.00
6	90.00	273.83	90.00	273.71	90.00	273.55	90.00	273.35	90.00	273.02	90.00	272.77	.00
7	90.00	273.23	90.00	273.11	90.00	272.95	90.00	272.75	90.00	272.42	90.00	272.17	.00
8	60.00	272.63	60.00	272.51	60.00	272.35	60.00	272.15	60.00	271.82	60.00	271.57	.00
9	45.00	272.03	45.00	271.91	45.00	271.75	45.00	271.55	45.00	271.22	45.00	270.97	.00
10	30.00	271.43	30.00	271.31	30.00	271.15	30.00	270.95	30.00	270.62	30.00	270.37	.00
11	17.50	270.83	17.50	270.71	17.50	270.55	17.50	270.35	17.50	270.02	17.50	269.77	.00
12	10.00	270.23	10.00	270.11	10.00	269.95	10.00	269.75	10.00	269.42	10.00	269.17	.00
13	7.00	269.63	7.00	269.51	7.00	269.35	7.00	269.15	7.00	268.82	7.00	268.57	.00
14	.00	269.03	.00	268.91	.00	268.75	.00	268.55	.00	268.22	.00	267.97	.00

Figure C-28. Layer numbers and segments for a sloping waterbody where segment 9 is the last active segment of the waterbody. EBOT is 268.82 m, which is the lowest elevation in the waterbody and is the bottom elevation of layer KMX-1 (KMX=14).

Segment	29	30	31	32	33	34	35	36	37	38
DLX	117.988	28.3495	136.98	146.072	157.852	109.728	99.06	91.44	147.549	147.549
ELWS	264.5	264.5	264.5	264.5	264.5	264.5	264.5	264.5	264.5	264.5
PHIO	3.6	3.6	3.6	3.6	3.6	3.6	3.6	3.6	4.3	4.3
Friction	0.04	0.04	0.04	0.04	0.04	0.04	0.04	0.05	0.05	0.05

Layer	Elev-top	Width	Elev-top	Width	Elev-top	Width	Elev-top	Width	Elev-top	Width	Elev-top	Width								
1	264.41	.00	264.41	.00	264.41	.00	264.41	.00	264.41	.00	264.41	.00	264.41	.00	264.41	.00	264.41	.00	264.41	.00
2	264.16	33.00	264.16	32.00	264.16	25.00	264.16	38.00	264.16	161.00	264.16	211.00	264.16	52.00	264.16	51.00	264.16	30.00	264.16	.00
3	263.91	20.00	263.91	30.00	263.91	20.00	263.91	20.00	263.91	90.00	263.91	120.00	263.91	40.00	263.91	40.00	263.91	20.00	263.91	.00
4	263.66	20.00	263.66	20.00	263.66	12.00	263.66	12.00	263.66	70.00	263.66	80.00	263.66	30.00	263.66	30.00	263.66	15.00	263.66	.00
5	263.41	.00	263.41	15.00	263.41	10.00	263.41	10.00	263.41	50.00	263.41	50.00	263.41	20.00	263.41	20.00	263.41	9.00	263.41	.00
6	263.16	.00	263.16	.00	263.16	10.00	263.16	10.00	263.16	30.00	263.16	30.00	263.16	18.00	263.16	13.00	263.16	8.00	263.16	.00
7	262.91	.00	262.91	.00	262.91	.00	262.91	10.00	262.91	20.00	262.91	20.00	262.91	15.00	262.91	12.00	262.91	7.00	262.91	.00
8	262.66	.00	262.66	.00	262.66	.00	262.66	.00	262.66	15.00	262.66	10.00	262.66	10.00	262.66	11.00	262.66	6.00	262.66	.00
9	262.41	.00	262.41	.00	262.41	.00	262.41	.00	262.41	10.00	262.41	10.00	262.41	10.00	262.41	10.00	262.41	.00	262.41	.00
10	262.16	.00	262.16	.00	262.16	.00	262.16	.00	262.16	.00	262.16	10.00	262.16	10.00	262.16	10.00	262.16	.00	262.16	.00
11	261.91	.00	261.91	.00	261.91	.00	261.91	.00	261.91	.00	261.91	.00	261.91	10.00	261.91	8.00	261.91	.00	261.91	.00
12	261.66	.00	261.66	.00	261.66	.00	261.66	.00	261.66	.00	261.66	.00	261.66	.00	261.66	7.00	261.66	.00	261.66	.00
13	261.41	.00	261.41	.00	261.41	.00	261.41	.00	261.41	.00	261.41	.00	261.41	.00	261.41	6.00	261.41	.00	261.41	.00
14	261.21	.00	261.21	.00	261.21	.00	261.21	.00	261.21	.00	261.21	.00	261.21	.00	261.21	.00	261.21	.00	261.21	.00

Figure C-29. Layer numbers and segments for a branch with a zero slope where segment 37 is the last active segment of the branch. EBOT for this waterbody is 261.21 m and is the bottom elevation of layer KMX-1 (KMX=14).

Initial Conditions (INIT CND)

FIELD	NAME	VALUE	DEFAULT	DESCRIPTION
1				(Ignored by code)
2	T2I	Real		Initial temperature, °C
3	ICETHI	Real		Initial ice thickness, <i>m</i>
4	WTYPEC	Character	FRESH	Waterbody type

This card specifies the initial temperature and ice thickness, and waterbody type. Initial temperature can be specified as either a single value, a single vertical profile used to initialize every segment, or a vertical profile for each segment.

Initial condition	[T2I]
1. Isothermal	>0
2. Single vertical profile	-1.0
3. Vertical profile at each segment	-2.0

If option 2 or 3 is chosen, then the user must specify input files [\[VPRFN\]](#) or [\[LPRFN\]](#) containing the profile(s).

Initial ice thickness [\[ICETHI\]](#) is ignored if ice computations are turned off.

The waterbody type [\[WTYPEC\]](#) is either FRESH or SALT. If [\[WTYPEC\]](#) is set to SALT, then constituent computations [\[CCC\]](#) should be turned on and [salinity](#) should be included in the computations.

Example

INIT CND	T2I	ICETHI	WTYPEC
Wb 1	-1.0	0.0	FRESH
Wb 2	-1.0	0.0	FRESH
Wb 3	-1.0	0.0	FRESH

Related Cards and Files

[Constituent Computations](#)
[Constituent Initial Concentration](#)
[Vertical Profile File](#)
[Longitudinal Profile File](#)
[Ice Cover](#)

Calculations (CALCULAT)

FIELD	NAME	VALUE	DEFAULT	DESCRIPTION
1				(Ignored by code)
2	VBC	Character	OFF	Volume balance calculation, ON or OFF
3	EBC	Character	OFF	Thermal energy balance calculation, ON or OFF
3	MBC	Character	OFF	Mass balance calculation, ON or OFF
4	PQC	Character	OFF	Density placed inflows, ON or OFF
5	EVC	Character	OFF	Evaporation included in water budget, ON or OFF
6	PRC	Character	OFF	Precipitation included, ON or OFF

This card specifies whether the model performs certain optional calculations. Calculations are turned on or off by right justifying ON or OFF in the input field.

Volume balance calculations are useful during initial runs as a check to ensure the model is preserving continuity and should always be used as a check if the user modifies the code. In order to reduce roundoff errors, the volume balance algorithm accumulates spatial and temporal changes in volume over time and uses these for comparison. Once the user is satisfied the model is running correctly, volume balance calculations should be turned off to reduce computational time.

Thermal energy and mass balance calculations are similar in use to volume balance calculations. They should be used initially to ensure the model is running properly and turned off for further calculations. When this option is used, mass balances are performed for each constituent if constituent computations are turned on. Mass balances are not computed if only temperature is modeled.

There are two options for distributing mainstem and branch inflows. The default is inflows distributed evenly into each layer from top to bottom. If [PQC] is turned ON, then inflows are matched up with the layer(s) whose density most closely corresponds to inflow density.

If precipitation is specified, then the user must supply input files for precipitation and precipitation temperature. If constituents are being modeled, then the user must supply an input file for constituent concentrations included in the simulation. The [Precipitation Active Constituent Control](#) card specifies which concentrations are included. If all precipitation constituents are turned OFF, then the precipitation constituent concentration input file is not required.

Evaporation rates are sometimes accounted for in estimating the inflow record, such as when net inflows are computed from outflows and water surface elevations. If so, then [EVC] should be set to OFF. Evaporation is always considered in the surface heat exchange calculations.

CONTROL FILE

INITIAL CONDITIONS

Example

CALCULAT	VBC	EBC	MBC	PQC	EVC	PRC
Wb 1	ON	ON	ON	OFF	OFF	OFF
Wb 2	ON	ON	ON	OFF	OFF	OFF
Wb 3	ON	ON	ON	OFF	OFF	OFF

Related Cards and Files

[Precipitation Active Constituent Control](#)

[Branch Inflow File](#)

[Tributary Inflow File](#)

[Precipitation File](#)

Dead Sea (DEAD SEA)

FIELD	NAME	VALUE	DEFAULT	DESCRIPTION
1				(Ignored by code)
2	WINDC	Character	ON	Turn ON/OFF wind
3	QINC	Character	ON	Turn ON/OFF all sources of water
4	QOUTC	Character	ON	Turn ON/OFF all sinks of water
5	HEATC	Character	ON	Turn ON/OFF heat exchange

This card has been used primarily during model development debugging. It is in the release version because it can be useful in evaluating relative effects of the hydrodynamic forcing functions and also as a debugging tool if the user decides to modify the code. Occasionally in estuarine applications, temperature is treated conservatively with the initial and boundary conditions set at a constant temperature with bottom and surface heat exchange turned off, although it is not recommended.

Example

DEAD SEA	WINDC	QINC	QOUTC	HEATC
Wb 1	ON	ON	ON	ON
Wb 2	ON	ON	ON	ON
Wb 3	ON	ON	ON	ON

Interpolation (INTERPOL)

FIELD	NAME	VALUE	DEFAULT	DESCRIPTION
1				(Ignored by code)
2	QINIC	Character	OFF	Interpolate inflows, inflow temperatures, and inflow constituent concentrations, ON or OFF
3	DTRIC	Character	OFF	Interpolate distributed tributary inflows and inflow temperatures and constituent concentrations, ON or OFF
4	HDIC	Character	OFF	Interpolate head boundary elevations and boundary temperatures and constituent concentrations, ON or OFF

These options control whether time-varying data are input as a step function or linearly interpolated between data points. The latest version now gives the user control over inflow, distributed tributary inflow, and external head boundary elevations for each branch. If interpolation is used, then the user must ensure it is appropriate and the input data supply correct information. Many reservoirs have periods of no releases. If outflow interpolation is turned on, then input data must be set up so no outflow occurs during these periods. This is accomplished by including extra dates in the outflow file with zero outflows to ensure the interpolation routine yields zero outflows. For example, given the following outflow time-series in the branch [outflow file \[QOTFN\]](#):

```

      JDAY      QOT
    100.00     50.0
    110.00      0.0
    120.00     50.0

```

If interpolation is not used, then outflow from Julian day 100 to 110 is $50 \text{ m}^3 \text{ sec}^{-1}$, from Julian day 110 to 120 is $0.0 \text{ m}^3 \text{ sec}^{-1}$, and $50 \text{ m}^3 \text{ sec}^{-1}$ thereafter. If interpolation is turned on, then outflow linearly decreases from Julian day 100 to 110 and then increases from Julian day 110 to 120. To ensure no outflow occurs between day 110 and 120 with interpolation on, the outflow file should be setup as follows:

```

      JDAY      QOT
    100.0000     50.0
    109.9999     50.0
    110.0000      0.0
    119.9999      0.0
    120.0000     50.0

```

Example

INTERPOL	QINIC	DTRIC	HDIC
Br 1	ON	OFF	ON
Br 2	ON	OFF	ON
Br 3	ON	OFF	ON
Br 4	ON	OFF	ON

INITIAL CONDITIONS

CONTROL FILE

Related Cards and Files

[Branch Inflow File](#)

[Branch Distributed Tributary Inflow File](#)

[Branch Distributed Tributary Inflow Temperature File](#)

[Branch Distributed Tributary Inflow Concentration File](#)

[Branch External Upstream Head Elevation File](#)

[Branch External Upstream Head Temperature File](#)

[Branch External Upstream Head Concentration File](#)

[Branch External Downstream Head Elevation File](#)

[Branch External Downstream Head Temperature File](#)

[Branch External Downstream Head Concentration File](#)

Heat Exchange (HEAT EXCH)

FIELD	NAME	VALUE	DEFAULT	DESCRIPTION
1				(Ignored by code)
2	SLHTC	Character	ET	Specify either term-by-term (TERM) or equilibrium temperature computations (ET) for surface heat exchange
3	SROC	Character	OFF	Read in observed short wave solar radiation, ON or OFF
4	RHEVC	Character	OFF	Turns ON/OFF Ryan-Harleman evaporation formula
5	METIC	Character	OFF	Turns ON/OFF meteorological data interpolation
6	FETCHC	Character	OFF	Turns ON/OFF fetch calculation
7	AFW	Real	9.2	a coefficient in the wind speed formulation
8	BFW	Real	0.46	b coefficient in the wind speed formulation
9	CFW	Real	2.0	c coefficient in the wind speed formulation
10	WINDH	Real		Wind speed measurement height, m

This card specifies various parameters affecting surface heat exchange. [SLHTC] allows the user to specify whether a term-by-term accounting or the equilibrium temperature approach is used in the computation of surface heat exchange. Although the term-by-term approach is more theoretically sound, equilibrium temperatures have consistently given better results for the systems presented in Chapter 3. Predictions for a number of reservoirs in the Northeast underpredicted epilimnetic temperatures during the fall overturn period using the term-by-term method. The reasons for this are still being investigated.

The [METIC] variable turns ON/OFF linear interpolation of meteorological input data. The [SROC] variable allows the user to specify whether or not short wave solar radiation data are computed from cloud cover (the default), or whether the user specifies observed short wave solar radiation in the meteorological input file [METFN]. In the [meteorological data file](#), short wave solar radiation data are in units of W/m^2 and include only incident short-wave solar radiation on the water surface.

The [FETCHC] variable turns ON/OFF a technique of Fang and Stefan (1994) to compute fetch effects on wind. This should not be used for river sections and should be used with caution for reservoir/lake systems. A description is outlined in Appendix B under Dissolved Oxygen and reaeration coefficients.

The variables [AFW], [BFW], and [CFW] specify the coefficients to be used in the wind function used in computing surface heat exchange and evaporation. The function has been generalized in the model to the following:

$$f(W_z) = afw + bfw W_z^{cfw}$$

The default formulation is the recommended form of the function taken from Edinger, et. al. (1974), although there are several other forms that can be used. For systems that are thermally loaded such as cooling lakes, the Ryan-Harleman formulation that takes into account forced convection should be used with [RHEVC] set to ON. All of the wind speed formulations are referenced to a height at

INITIAL CONDITIONS

CONTROL FILE

which wind speeds were measured. The variable [WINDH] allows the user to specify the height at which wind speed measurements were taken, and the model converts them to the appropriate wind speed at the height the wind speed formulation is based on.

Example

HEAT EXCH	SLHTC	SROC	RHEVC	METIC	FETCHC	AFW	BFW	CFW	WINDH
Wb 1	TERM	OFF	OFF	ON	OFF	9.2	0.46	2.0	2.0
Wb 2	TERM	OFF	OFF	ON	OFF	9.2	0.46	2.0	2.0
Wb 3	TERM	OFF	OFF	ON	OFF	9.2	0.46	2.0	2.0

Related Cards and Files

[Meteorology file](#)

Ice Cover (ICE COVER)

FIELD	NAME	VALUE	DEFAULT	DESCRIPTION
1				(Ignored by code)
2	ICEC	Character	OFF	Allow ice calculations
3	SLICEC	Character	SIMPLE	Specifies the method of ice cover calculations - either SIMPLE or DETAIL
4	ALBEDO	Real	-	Ratio of reflection to incident radiation (albedo of ice)
5	HWI	Real	-	Coefficient of water-ice heat exchange
6	BETAI	Real	-	Fraction of solar radiation absorbed in the ice surface
7	GAMMAI	Real	-	Solar radiation extinction coefficient, m^{-1}
8	ICEMIN	Real	-	Minimum ice thickness before ice formation is allowed, m
9	ICET2	Real	3.0	Temperature above which ice formation is not allowed, $^{\circ}C$

Ice calculations are controlled with this card. The variable [ICEC] turns ON/OFF ice calculations. Two different methods for computing ice cover are available. The first method ([SLICEC] = SIMPLE) was included in version 1.0 and is available for backwards compatibility. The second method, DETAIL, is the preferred method.

The coefficient of water-ice heat exchange [HWI] is a user specified calibration parameter that determines the rate of heat exchange between water and ice. [BETAI] is the fraction of solar radiation absorbed at the ice surface and is similar to [BETA] in the surface heat exchange computations. [GAMMAI] is the solar radiation extinction coefficient through ice and is also similar to [GAMMA] in the surface heat exchange computations.

Albedo is the ratio of reflection to incident radiation. It is normally expressed by the albedo of a surface and varies widely depending on the solar altitude and the waterbody surface properties.

For free water surfaces, Anderson (1954), in his Lake Hefner studies, derived the following empirical formula for the water surface albedo, ALB_w , as a function of average solar altitude:

$$ALB_w = 1.18 A_s^{-0.77}$$

where A_s is average solar altitude in degrees. Anderson found the coefficient 1.18 and the exponent -0.77 to vary only slightly with cloud height and coverage.

For ice surface, a functional representation of albedo has not been established. Reported values for ice surface albedo vary greatly from about 10% for clear lake ice (Bolsenga, 1969) to almost 70% for snow free Arctic sea ice (Krutskih, et al., 1970). Krutskih, et al. suggest ice albedo is more dependent on air temperature than on solar altitude. Based on their extensive Arctic sea observations, ice surface albedo for solar radiation was determined as:

INITIAL CONDITIONS

CONTROL FILE

$$ALB_i = \varepsilon \quad \text{for } T_a \leq 0^\circ\text{C}$$

$$ALB_i = \xi + \omega e^{\Psi T_a} \quad \text{for } T_a > 0^\circ\text{C}$$

where ε , ξ , ω , and Ψ are empirical constants, and T_a is air temperature, °C. Equation [\(A-53\)](#) is an empirical fit to the observed data given by Krutskih, et al. for Arctic ice.

Note that the ice cover algorithm does not take into account snow accumulation on the ice surface.

Example

ICE COVER	ICEC	SLICEC	ALBEDO	HWI	BETAI	GAMMAI	ICEMIN	ICET2
Wb 1	OFF	DETAIL	0.25	10.0	0.6	0.07	0.05	3.0
Wb 2	OFF	DETAIL	0.25	10.0	0.6	0.07	0.05	3.0
Wb 3	OFF	DETAIL	0.25	10.0	0.6	0.07	0.05	3.0

Related Cards and Files

[Initial Conditions](#)

Transport Scheme (TRANSPORT)

FIELD	NAME	VALUE	DEFAULT	DESCRIPTION
1				(Ignored by code)
2	SLTRC	Character	ULTIMATE	Transport solution scheme, ULTIMATE, QUICKEST, or UPWIND
3	THETA	Real	0.55	Time-weighting for vertical advection scheme

This card specifies the transport solution scheme used by the model. There are three options for [SLTRC] – UPWIND, QUICKEST, or ULTIMATE with the latter being the recommended option. The older solution schemes are retained in this version of the model mainly as a means of comparing the different solution schemes. The QUICKEST option employs a higher-order solution scheme to reduce numerical diffusion present in the original UPWIND differencing scheme. The ULTIMATE option eliminates the physically unrealistic over/undershoots that QUICKEST generates near regions of sharp concentration gradients.

[THETA] specifies the amount of time weighting in the vertical advection scheme. A value of 0 specifies fully explicit vertical advection, 1 specifies fully implicit vertical advection, and 0.5 specifies a Crank-Nicholson scheme. The recommended value for [THETA] is 0.55. This ensures unconditional numerical stability for vertical transport. Vertical diffusion is always fully implicit.

It should be pointed out that while the addition of the ULTIMATE algorithm eliminates physically unrealistic over/undershoots due to longitudinal transport, the model could still generate over/undershoots when using implicit weighting for vertical transport. This is a result of phase errors generated when trying to resolve sharp vertical gradients over a few computational cells and can be eliminated completely by setting [THETA] to zero.

Example

```
TRANSPORT  SLTRC  THETA
Wb 1      ULTIMATE  0.55
Wb 2      ULTIMATE  0.55
Wb 3      ULTIMATE  0.55
```

Hydraulic Coefficients (HYD COEF)

FIELD	NAME	VALUE	DEFAULT	DESCRIPTION
1				(Ignored by code)
2	AX	Real	1.0	Longitudinal eddy viscosity, $m^2 sec^{-1}$
3	DX	Real	1.0	Longitudinal eddy diffusivity, $m^2 sec^{-1}$
4	CBHE	Real	0.3	Coefficient of bottom heat exchange, $W m^{-2} sec^{-1}$
5	TSED	Real	-	Sediment temperature, °C
6	FI	Real	0.01	Interfacial friction factor
7	TSEDF	Real	-	Heat lost to sediments that is added back to water column
8	FRICC	Character	CHEZY	Bottom friction solution, MANN or CHEZY

This card specifies hydraulic and bottom heat exchange coefficients that can be varied during model calibration. The horizontal eddy viscosity [AX] specifies dispersion of momentum in the X-direction. The horizontal eddy diffusivity [DX] specifies dispersion of heat and constituents in the X-direction. Both values are presently time and space invariant. The Chezy coefficient is used in calculating effects of bottom friction. The coefficient of bottom heat exchange [CBHE] and the sediment temperature [TSED] are used to compute heat exchange at the ground-water interface. Sediment temperature can be estimated from average annual temperature at the site. Recommended values are given in the example.

[TSEDF] is a coefficient that varies from 0 to 1. This regulates how short-wave solar radiation that penetrates to the bottom of the grid is handled in the code. A value of 1 specifies that 100% of the incident short wave solar impinging on the channel bottom is re-radiated as heat to the water column. A value of 0 means that 0% of the shortwave solar radiation is reradiated into the water column resulting in a loss of the solar radiation from the system.

Previous experience has shown recommended values produce remarkably accurate temperature predictions for a wide variety of systems. The horizontal eddy viscosities and diffusivities and Chezy or Manning's n coefficient may need additional tuning when calibrating for water quality since longitudinal temperature gradients in most applications are negligible. The Chezy or Manning's n coefficient is important in estuarine applications for calibrating tidal range and phase.

Typical values for the Chezy coefficient and Manning's friction factors have been 70 and 0.035, respectively. In estuaries and rivers, these values can vary widely, especially since often this friction factor incorporates errors in the bathymetry of the model. For Manning's friction factors, a range of values have been used in rivers and estuaries from 0.01 to 0.1 or higher. These are usually determined by calibrating the model to water surface elevation data.

Example

HYD COEF	AX	DX	CBHE	TSED	FI	TSEDF	FRICC
Wb 1	1.0	1.0	0.3	11.5	0.01	1.00	MANN
Wb 2	1.0	1.0	0.3	11.5	0.01	1.00	MANN
Wb 3	1.0	1.0	0.3	11.5	0.01	1.00	MANN

Vertical Eddy Viscosity (EDDY VISC)

FIELD	NAME	VALUE	DEFAULT	DESCRIPTION
1				(Ignored by code)
2	AZC	Character	W2	Form of vertical turbulence closure algorithm, NICK, PARAB, RNG, W2, W2N, or TKE
3	AZSLC	Character	EXP	Specifies either implicit, IMP, or explicit, EXP, treatment of the vertical eddy viscosity in the longitudinal momentum equation.
4	AZMAX	Real	1.0E-3	Maximum value for vertical eddy viscosity, $m^2 s^{-1}$

[AZC] specifies the vertical turbulence algorithm used in the horizontal momentum equation. The following table lists the options available in Version 3. For more information see Appendix A.

Table C-1. Vertical Eddy Viscosity Formulations

Formulation	Formula	Reference
Nickuradse [NICK]	$v_t = \ell_m^2 \left \frac{\partial u}{\partial z} \right e^{-CR_i}$ $\ell_m = H \left[0.14 - 0.08 \left(1 - \frac{z}{H} \right)^2 - 0.06 \left(1 - \frac{z}{H} \right)^4 \right]$	Rodi (1993)
Parabolic [PARAB]	$v_t = \kappa u_* z \left(1 - \frac{z}{H} \right) e^{-CR_i}$	Engelund (1976)
[W2] (used in V2)	$v_t = \kappa \left(\frac{l_m^2}{2} \right) \sqrt{\left(\frac{\partial U}{\partial z} \right)^2 + \left(\frac{\tau_{wy} e^{-2kz} + \tau_{y trib}}{\rho v_t} \right)^2} e^{-(CR_i)}$ $\ell_m = \Delta z_{max}$	Cole and Buchak (1995)
W2 with mixing length of Nickuradse [W2N]	$v_t = \kappa \left(\frac{l_m^2}{2} \right) \sqrt{\left(\frac{\partial U}{\partial z} \right)^2 + \left(\frac{\tau_{wy} e^{-2kz} + \tau_{y trib}}{\rho v_t} \right)^2} e^{-(CR_i)}$ $\ell_m = H \left[0.14 - 0.08 \left(1 - \frac{z}{H} \right)^2 - 0.06 \left(1 - \frac{z}{H} \right)^4 \right]$	Cole and Buchak (1995) and Rodi (1993)
[RNG] (renormalization group)	$v_t = \nu \left[1 + \psi \left(3\kappa \left(\frac{z u_*}{\nu} \right)^3 \left(1 - \frac{z}{H} \right)^3 - C_1 \right) \right]^{1/3} e^{-CR_i}$	Simoes (1998)

<p>TKE (Turbulent kinetic energy)</p>	$v_t = C_\mu \frac{k^2}{\varepsilon}$ <p>where k and ε are defined from</p> $\frac{\partial k B}{\partial t} + \frac{\partial k B U}{\partial x} + \frac{\partial k B W}{\partial z} - \frac{\partial}{\partial z} \left(B \frac{v_t}{\sigma_k} \frac{\partial k}{\partial z} \right) - \frac{\partial}{\partial x} \left(B \frac{v_t}{\sigma_k} \frac{\partial k}{\partial x} \right) = B(P + G - \varepsilon + P_k)$ $\frac{\partial \varepsilon B}{\partial t} + \frac{\partial \varepsilon B U}{\partial x} + \frac{\partial \varepsilon B W}{\partial z} - \frac{\partial}{\partial z} \left(B \frac{v_t}{\sigma_\varepsilon} \frac{\partial \varepsilon}{\partial z} \right) - \frac{\partial}{\partial x} \left(B \frac{v_t}{\sigma_\varepsilon} \frac{\partial \varepsilon}{\partial x} \right) = B \left(C_{\varepsilon 1} \frac{\varepsilon}{k} P + C_{\varepsilon 2} \frac{\varepsilon^2}{k} + P_\varepsilon \right)$	<p>Wells (2003)</p>
<p>ℓ_m = mixing length z = vertical coordiante H = depth, u: horizontal velocity Ri = Richardson number C = constant (assumed 0.15) u_* = shear velocity κ = von Karman constant</p>	<p>τ_{wy} = cross-shear from wind k = wave number ρ = liquid density Δz_{max} = maximum vertical grid spacing $\Psi(x) = \max(0, x)$ ν = molecular viscosity C_1 = empirical constant (assumed 100) τ_{ytrib} = cross-shear from lateral tributaries</p>	

Any of the first three formulations are appropriate for riverine sections in which shear due to friction is dominant. The last two formulations are appropriate for reservoirs where wind shear is dominant. There currently is no widely accepted algebraic formulation for estuaries. A later release of Version 3 will include an option for using a k-ε turbulence formulation that should eliminate specifying a turbulence scheme. This has been implemented in a research version of the code and is currently under-going testing.

To be backwards compatible with Version 2, set [AZC] to W2, [AZSLC] to EXP, and [AZMAX] to 1.0E-4 even though a value of 1.0E-3 is recommended as a minimum value of the maximum vertical eddy viscosity [AZ]. Note that for river and estuary applications it is recommended to set [AZSLC] to IMP and AZMAX to 1 m²s⁻¹. Setting [AZSLC] to EXP and [AZMAX] greater than 1.0E-2 will result in very low model time steps. In this case, setting [AZSLC] to IMP will remove the time step limitation allowing for much larger timesteps.

Example

EDDY VISC	AZC	AZSLC	AZMAX
Wb 1	NICK	IMP	1.0
Wb 2	W2	IMP	1.0E-3
Wb 3	NICK	IMP	1.0

Related Cards and Files

[Timestep Limitations](#)

Number of Structures (N STRUC)

FIELD	NAME	VALUE	DESCRIPTION
1			(Ignored by code)
2	NSTR	Integer	Number of branch outlet structures

This card specifies the number of outlet structures for each branch. Outflows are computed based on a selective withdrawal algorithm.

Example

N STRUC	NSTR
Br 1	0
Br 2	0
Br 3	3
Br 4	0

Related Cards and Files

[Inflow/Outflow Dimensions](#)

[Sink Type](#)

[Structure Elevation](#)

[Structure Width](#)

[Structure Interpolation](#)

[Structure Top Selective Withdrawal Limit](#)

[Structure Bottom Selective Withdrawal Limit](#)

[Outflow file](#)

Structure Interpolation (STR INT)

FIELD	NAME	VALUE	DEFAULT	DESCRIPTION
1				(Ignored by code)
2-10	STRIC	Character	OFF	Turns ON/OFF interpolation of structure outflows

The outflows specified by the outflow file can either be assumed to be step functions with [STRIC] set to OFF, or can be linearly interpolated between values with [STRIC] set to ON.

Example

```

STR INT      STRIC  STRIC  STRIC  STRIC  STRIC  STRIC  STRIC  STRIC  STRIC
Br 1
Br 2
Br 3         ON    ON    ON
Br 4
    
```

Related Cards and Files

- [Inflow/Outflow Dimensions](#)
- [Number of Structures](#)
- [Sink Type](#)
- [Structure Elevation](#)
- [Structure Width](#)
- [Structure Top Selective Withdrawal Limit](#)
- [Structure Bottom Selective Withdrawal Limit](#)
- [Outflow file](#)

Structure Top Selective Withdrawal Limit (STR TOP)

FIELD	NAME	VALUE	DESCRIPTION
1			(Ignored by code)
2-10	KTSTR	Integer	Top layer above which selective withdrawal will not occur

The selective withdrawal algorithm calculates vertical withdrawal zone limits based on outlet geometry, outflows, and in-pool densities. The algorithm then assigns flows for each layer within the withdrawal zone. This card specifies the top elevation for which outflows are calculated in the selective withdrawal algorithm. This option can be used to mimic the effects of a curtain weir that limits the upper extent of the withdrawal zone. In the absence of any structure or topographic feature that limits the top of the selective withdrawal zone, the elevation should be set to the top elevation of the computational grid.

Example

STR TOP	KTSTR								
Br 1									
Br 2									
Br 3	2	2	2						
Br 4									

Related Cards and Files

[Inflow/Outflow Dimensions](#)

[Number of Structures](#)

[Sink Type](#)

[Structure Elevation](#)

[Structure Width](#)

[Structure Interpolation](#)

[Structure Bottom Selective Withdrawal Limit](#)

[Outflow file](#)

Structure Bottom Selective Withdrawal Limit (STR BOT)

FIELD	NAME	VALUE	DESCRIPTION
1			(Ignored by code)
2-10	KBSTR	Integer	Bottom layer below which selective withdrawal will not occur

The selective withdrawal algorithm calculates vertical withdrawal zone limits based on outlet geometry, outflows, and in-pool densities. The algorithm then assigns flows for each layer within the withdrawal zone. This card specifies the bottom elevation for which outflows are calculated in the selective withdrawal algorithm. This option can be used to simulate the effects of an upstream submerged weir, accumulation of debris at the trash racks, an upstream cofferdam, etc. In the absence of any structure or topographic feature limiting the bottom withdrawal layer, the value should be set to the bottommost active layer at the downstream segment.

Example

STR BOT	KBSTR								
Br 1									
Br 2									
Br 3	22	22	22						
Br 4									

Related Cards and Files

- [Inflow/Outflow Dimensions](#)
- [Number of Structures](#)
- [Sink Type](#)
- [Structure Elevation](#)
- [Structure Width](#)
- [Structure Interpolation](#)
- [Structure Top Selective Withdrawal Limit](#)
- [Outflow file](#)

Sink Type (SINK TYPE)

FIELD	NAME	VALUE	DEFAULT	DESCRIPTION
1				(Ignored by code)
2-10	SINKC	Character	POINT	Sink type used in the selective withdrawal algorithm, LINE or POINT

This card specifies the sink type for each withdrawal. The options are LINE or POINT each of which has different selective withdrawal characteristics.

Line sinks are usually structures wide in relation to dam width ($> 1/10$). Point sinks are usually structures narrow in relation to dam width ($< 1/10$).

Example

```

SINK TYPE  SINKC  SINKC  SINKC  SINKC  SINKC  SINKC  SINKC  SINKC  SINKC
Br 1
Br 2
Br 3      POINT  POINT  POINT
Br 4

```

Related Cards and Files

[Inflow/Outflow Dimensions](#)

[Number of Structures](#)

[Structure Elevation](#)

[Structure Width](#)

[Structure Interpolation](#)

[Structure Top Selective Withdrawal Limit](#)

[Structure Bottom Selective Withdrawal Limit](#)

[Outflow file](#)

Structure Elevation (E STRUC)

FIELD	NAME	VALUE	DESCRIPTION
1			(Ignored by code)
2-10	ESTR	Real	Centerline elevation of structure, <i>m</i>

This card specifies the centerline elevation for each withdrawal structure by branch.

Example

```

E STRUC      ESTR      ESTR      ESTR      ESTR      ESTR      ESTR      ESTR      ESTR      WSTR
Br 1
Br 2
Br 3          45.0    25.00    15.00
Br 4
    
```

Related Cards and Files

- [Inflow/Outflow Dimensions](#)
- [Number of Structures](#)
- [Sink Type](#)
- [Structure Width](#)
- [Structure Interpolation](#)
- [Structure Top Selective Withdrawal Limit](#)
- [Structure Bottom Selective Withdrawal Limit](#)
- [Outflow file](#)

Structure Width (W STRUC)

FIELD	NAME	VALUE	DESCRIPTION
1			(Ignored by code)
2-10	WSTR	Real	Width of structure (line sink), <i>m</i>

This card specifies the width of the structures by branch if a link sink is specified as the sink type [[SINKC](#)]. The values are ignored if a point sink is specified. If there are more outlet structures than will fit on a line, then the widths are continued on the next line starting in field 2.

Example

W STRUC	WSTR								
Br 1									
Br 2									
Br 3	10.0	10.0	10.0						
Br 4									

Related Cards and Files

[Inflow/Outflow Dimensions](#)

[Number of Structures](#)

[Sink Type](#)

[Structure Elevation](#)

[Structure Interpolation](#)

[Structure Top Selective Withdrawal Limit](#)

[Structure Bottom Selective Withdrawal Limit](#)

[Outflow file](#)

Pipes (PIPES)

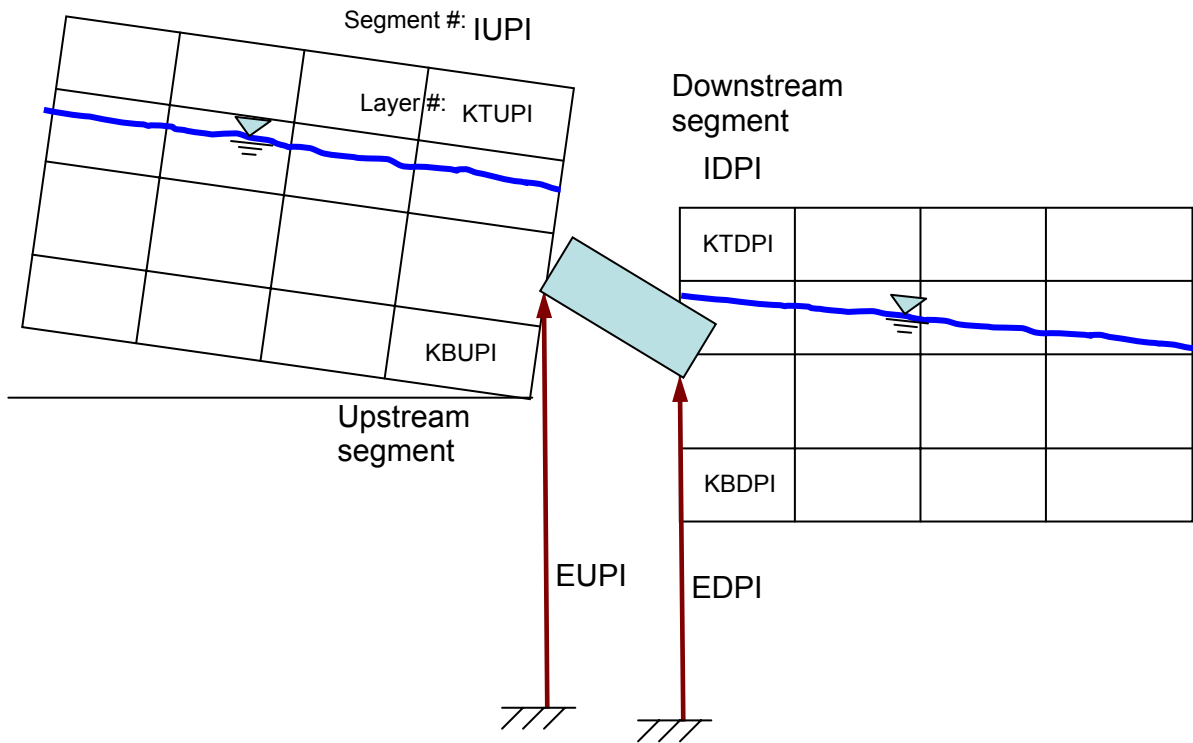
FIELD	NAME	VALUE	DEFAULT	DESCRIPTION
1				(Ignored by code)
2	IUPI	Integer		Pipe upstream segment number
3	IDPI	Integer		Pipe downstream segment number
4	EUPI	Real		Upstream invert elevation, <i>m</i>
5	EDPI	Real		Downstream invert elevation, <i>m</i>
6	WPI	Real		Pipe diameter, <i>m</i>
7	DLXPI	Real		Pipe length, <i>m</i>
8	FPI	Real		Bottom roughness
9	FMINPI	Real		Minor friction losses
10	LATPIC	Character	DOWN	Downstream or lateral pipe withdrawal, DOWN or LAT

This card specifies the characteristics for each pipe included in the simulation. [IUSPI] and [IDPI] specify the upstream segment location and downstream segment location of the pipe, respectively. The user must also set an upstream [EUPI] and downstream [EDPI] invert elevation, diameter [WPI], and length [DLXPI] for each pipe. [FPI] sets the bottom roughness value and [FMINPI] specifies the minor friction losses.

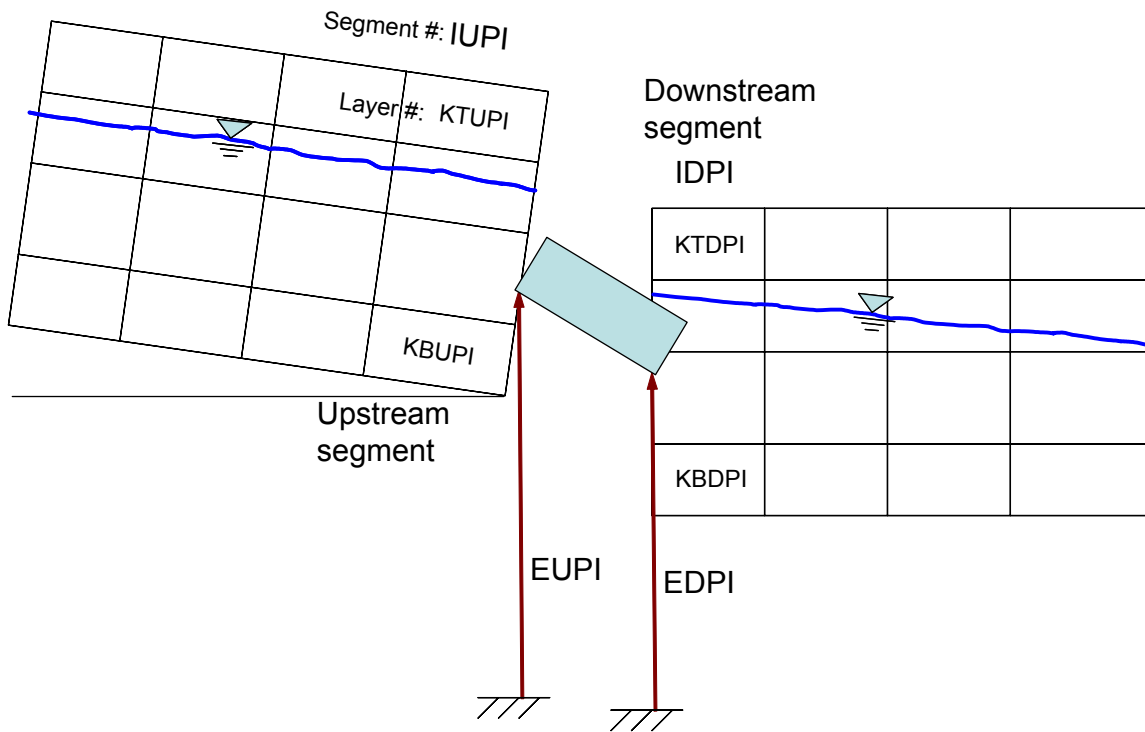
Setting the pipe location [LATPIC] to DOWN specifies that the pipe is at the downstream end of the segment. In this case the water surface elevations are computed based on the downstream segment location. Also, momentum from the outflow is preserved as in a downstream structure withdrawal. If the pipe location [LATPIC] is set to LAT, it is assumed that the outflow is treated as a lateral withdrawal at the segment center elevation. In both cases selective withdrawal is used in the computations.

Figure ?? and ?? show the layout of pipes set as a downstream [DOWN] and a lateral [LAT] withdrawal from the upstream segment, respectively.

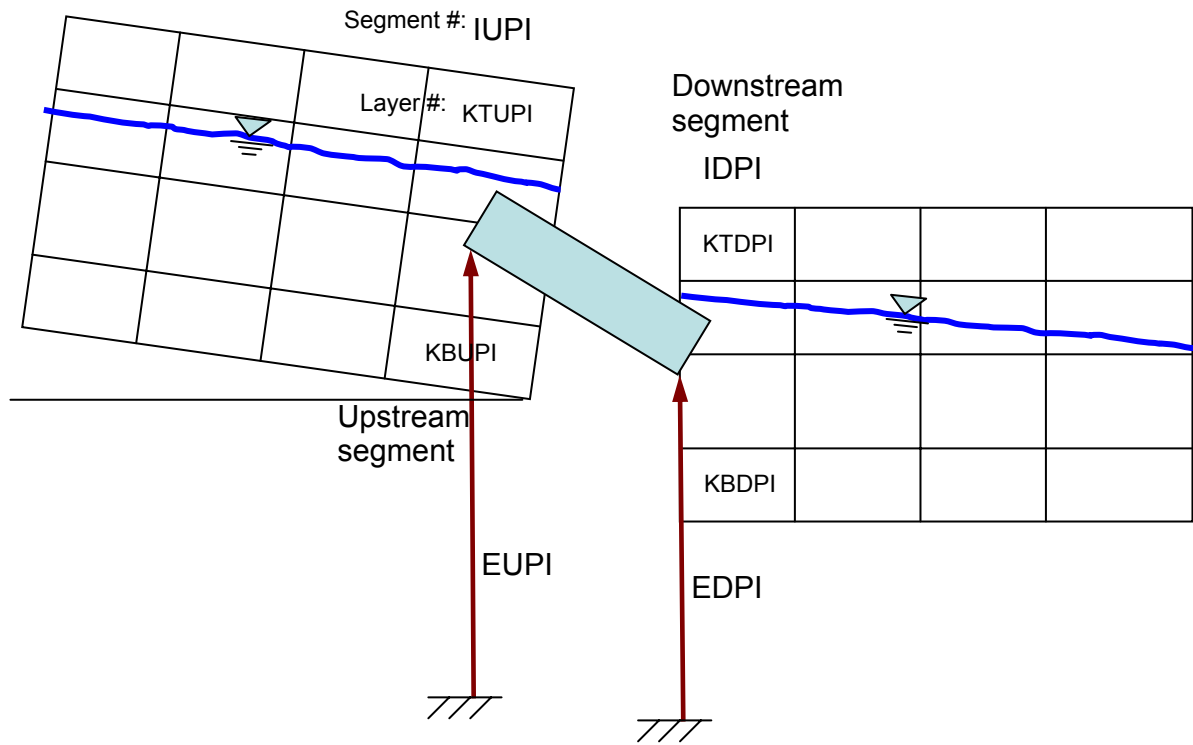
Downstream Pipe (DOWN)



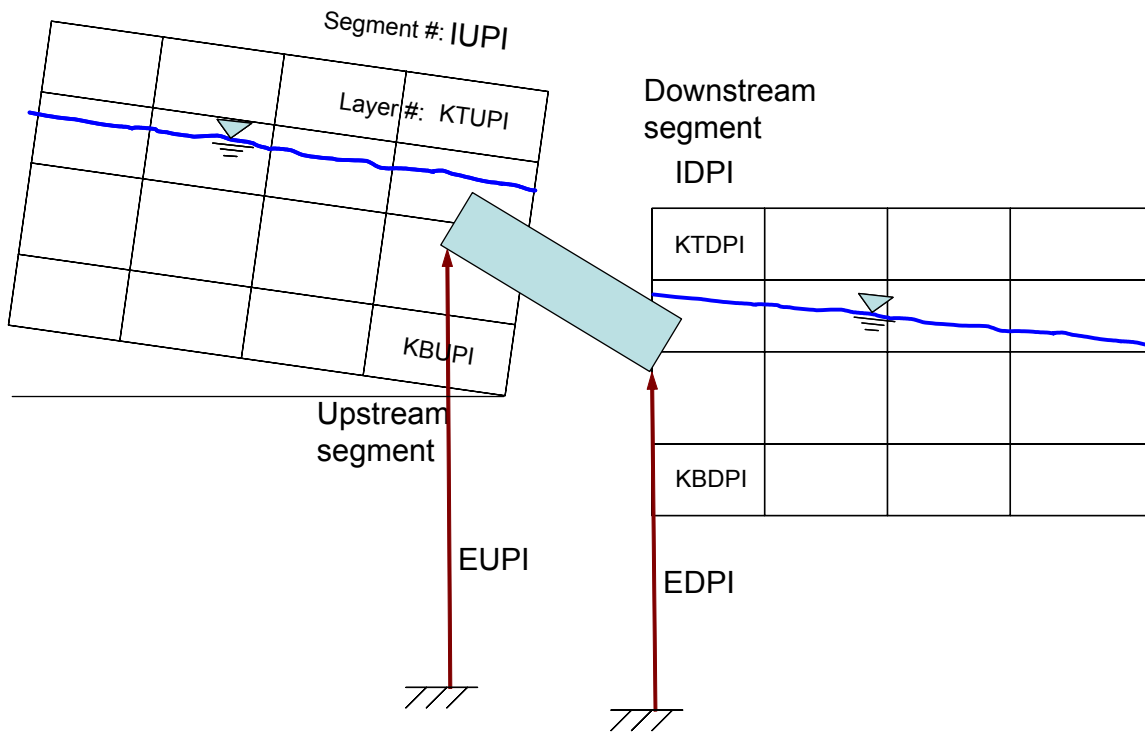
Downstream Pipe (DOWN)



Lateral Pipe (LAT)



Lateral Pipe (LAT)



Example

PIPE	IUPI	IDPI	EUPI	EDPI	WPI	DLXPI	FPI	FMINPI	LATPIC
Pi 1	24	28	28.0	27.0	0.5	230.0	0.065	0.10	DOWN

Related Cards and Files

- [Inflow/Outflow Dimensions](#)
- [Upstream Pipe](#)
- [Downstream Pipe](#)

Upstream Pipe (PIPE UP)

FIELD	NAME	VALUE	DEFAULT	DESCRIPTION
1				(Ignored by code)
2	PUPIC	Character	DISTR	Specifies how inflows enter into the upstream pipe segment, DISTR, DENSITY, or SPECIFY
3	ETUPI	Real		Top elevation pipe inflows enter when using SPECIFY option, <i>m</i>
3	EBUPI	Real		Bottom elevation pipe inflows enter when using SPECIFY option, <i>m</i>
5	KTUPI	Integer		Top layer above which selective withdrawal will not occur
5	KBUPI	Integer		Bottom layer below which selective withdrawal will not occur

This card specifies how inflows/outflows for the upstream pipe location are handled. Setting [TRIBPL] to DISTR distributes the inflows evenly from the water surface to the bottom active layer, setting it to DENSITY places the inflows into a layer with similar density, and setting it to SPECIFY allows the user to specify a top and bottom elevation into which inflows enter. If the SPECIFY option is used, then [TRIBTOP] and [TRIBBOT] are used to specify the top and bottom elevations that the inflows are distributed over.

[KWTOP] and [KWBOT] are used to set the upper and lower layers above and below which outflow does not occur in the selective withdrawal algorithm.

Example

```
PIPE UP      PUPIC  ETUPI  EBUPI  KTUPI  KBUPI
Pi 1        DISTR                2      19
```

Related Cards and Files

[Inflow/Outflow Dimensions](#)
[Pipes](#)
[Downstream Pipe](#)

Downstream Pipe (PIPE DOWN)

FIELD	NAME	VALUE	DEFAULT	DESCRIPTION
1				(Ignored by code)
2	PDPIC	Character	DISTR	How inflows enter into the downstream pipe segment, DISTR, DENSITY, or SPECIFY
3	ETDPI	Real		Top elevation pipe inflows enter using SPECIFY option, <i>m</i>
4	EBDPI	Real		Bottom elevation pipe inflows enter using SPECIFY option, <i>m</i>
5	KTDPI	Integer		Top layer above which selective withdrawal will not occur
6	KBDPI	Integer		Bottom layer below which selective withdrawal will not occur

This card specifies how inflows/outflows for the downstream pipe location are handled. Setting [PDPIC] to DISTR distributes the inflows evenly from the water surface to the bottom active layer, setting it to DENSITY places the inflows into a layer with similar density, and setting it to SPECIFY allows the user to specify a top and bottom elevation into which inflows enter. If the SPECIFY option is used, then [ETDPI] and [EBDPI] are used to specify the top and bottom elevations that the inflows are distributed over.

[KTDPI] and [KBDPI] are used to set the upper and lower layers above and below which outflow does not occur in the selective withdrawal algorithm.

Example

```
PIPE DOWN  PDPIC  ETDPI  EBDPI  KTDPI  KBDPI
Pi 1      DISTR                2      23
```

Related Cards and Files

- [Inflow/Outflow Dimensions](#)
- [Pipes](#)
- [Upstream Pipe](#)

Spillways (SPILLWAYS)

FIELD	NAME	VALUE	DEFAULT	DESCRIPTION
1				(Ignored by code)
2	IUSP	Integer		Spillway segment location
3	IDSP	Integer		Downstream segment spillway outflow enters
4	ESP	Real		Spillway elevation, <i>m</i>
5	A1SP	Real		Empirical coefficient
6	B1SP	Real		Empirical coefficient
7	A2SP	Real		Empirical coefficient
8	B2SP	Real		Empirical coefficient
9	LATSPC	Character	LAT	Downstream or lateral withdrawal, DOWN or LAT

This card specifies the spillway (or weir) characteristics. [IUSP] and [IDSP] specify the upstream and downstream segments for the spillway. Setting [IDSP] to 0 allows the user to spill water and have that water lost from the system. The model requires the user to specify a head (*h*) versus flow (*Q*) relationship in the following form for freely flowing conditions:

$$Q = \alpha_1 \Delta h^{\beta_1}$$

where:

- α_1 = empirical parameter
- β_1 = empirical parameter
- $\Delta h = Z_u - Z_{sp}$, *m*
- Z_u = upstream head, *m*
- Z_{sp} = the spillway crest elevation, *m*

And for submerged conditions:

$$Q = \alpha_2 \Delta h^{\beta_2}$$

where:

- α_2 = empirical parameter
- β_2 = empirical parameter
- $\Delta h = Z_u - Z_d$, *m*
- Z_u = upstream head, *m*
- Z_d = downstream head, *m*

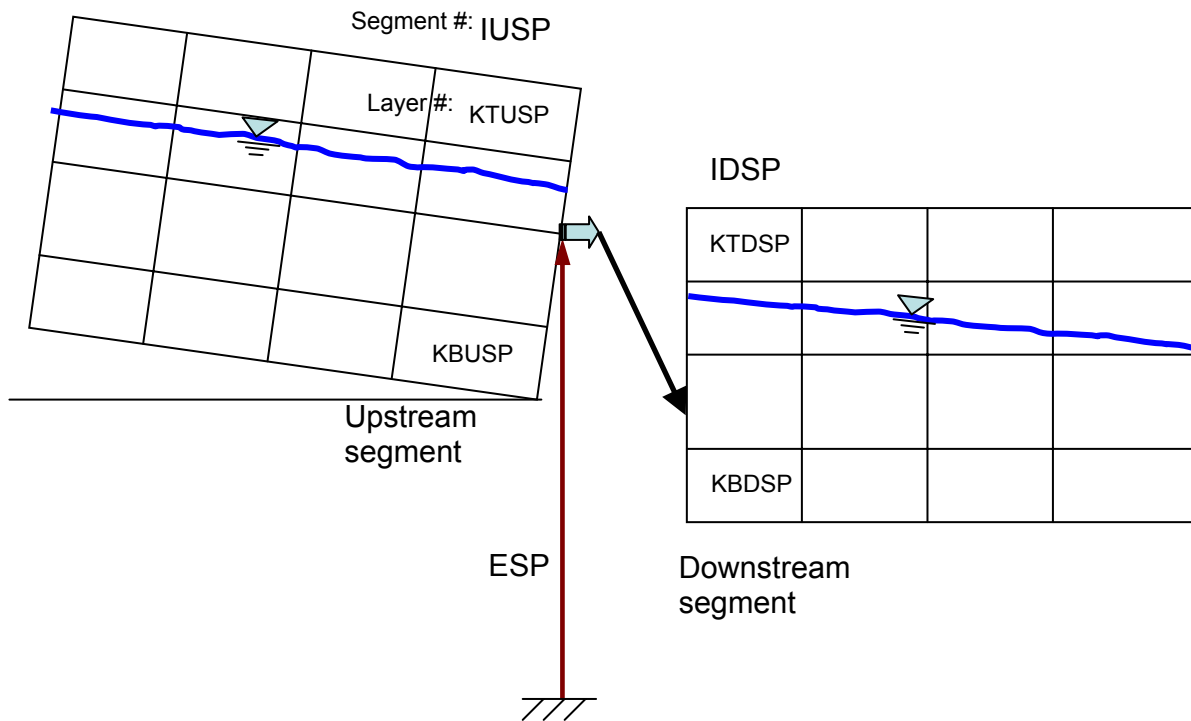
Submerged conditions are defined when the tailwater depth over the upstream energy head (static head and velocity head) is greater than 0.67. Even though negative flow rates are possible using the second equation when the downstream head is greater than the upstream head, these results should be used with caution since rarely are rating curves done for reverse flow. The user should ensure a

smooth transition between submerged and free flowing conditions by proper choice of model coefficients. See [Appendix A](#) for further information.

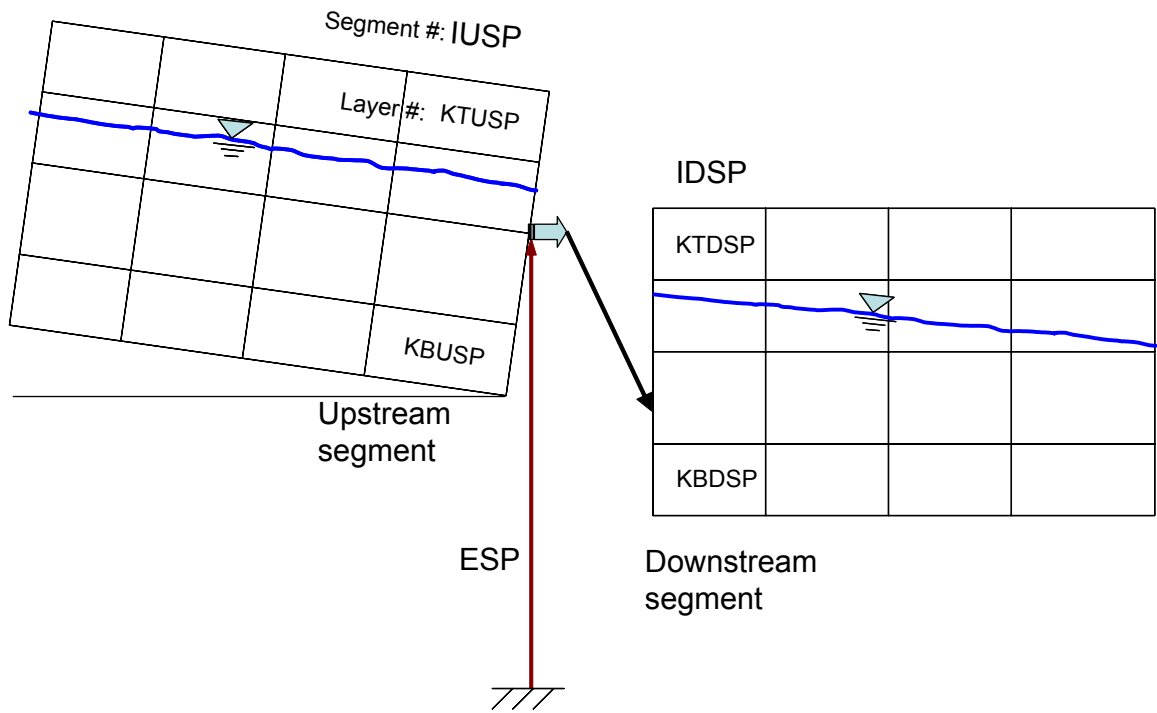
Setting the spillway location [LATSPC] to DOWN specifies that the spillway is at the downstream end of the segment. In this case the water surface elevations are computed based on the downstream segment location. Also, momentum from the outflow is preserved as in a downstream struture withdrawal. If the spillway location [LATPIC] is set to LAT, it is assumed that the outflow is treated as a lateral withdrawal at the segment center elevation. In both cases selective withdrawal is used in the computations.

Figure ?? and ?? show the layout of spillways set as a downstream [DOWN] and a lateral [LAT] withdrawal from the upstream segment, respectively.

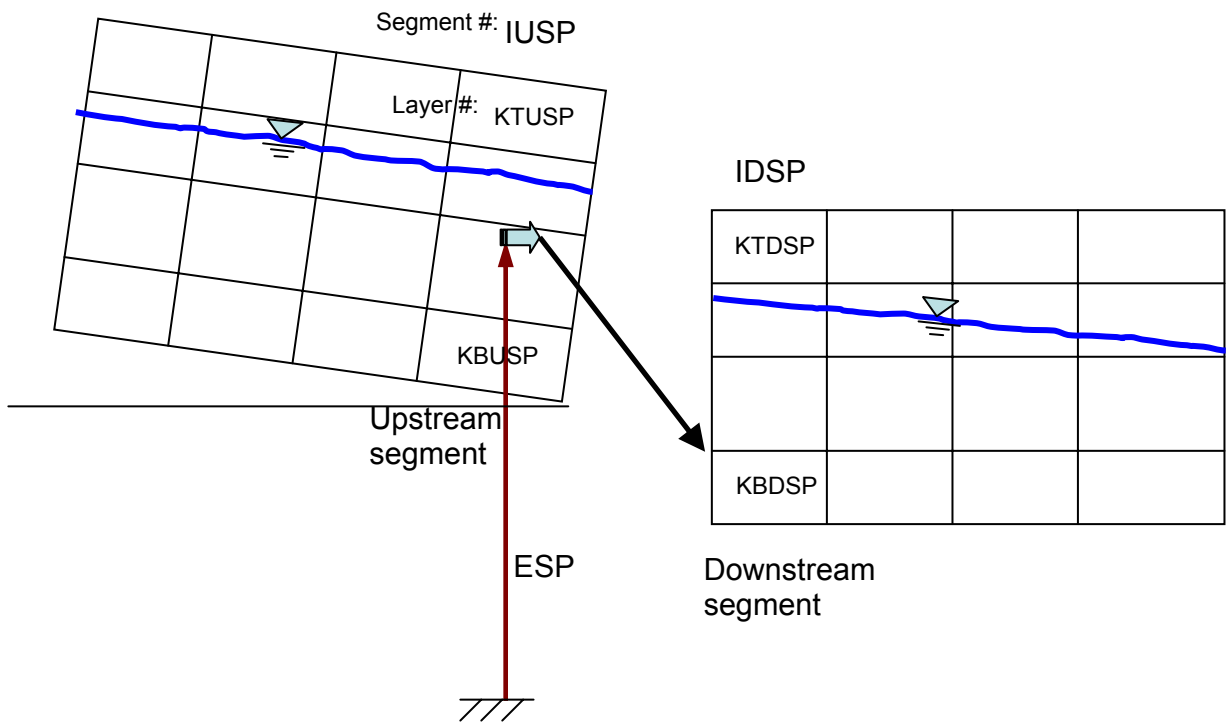
Downstream Spillway (DOWN)



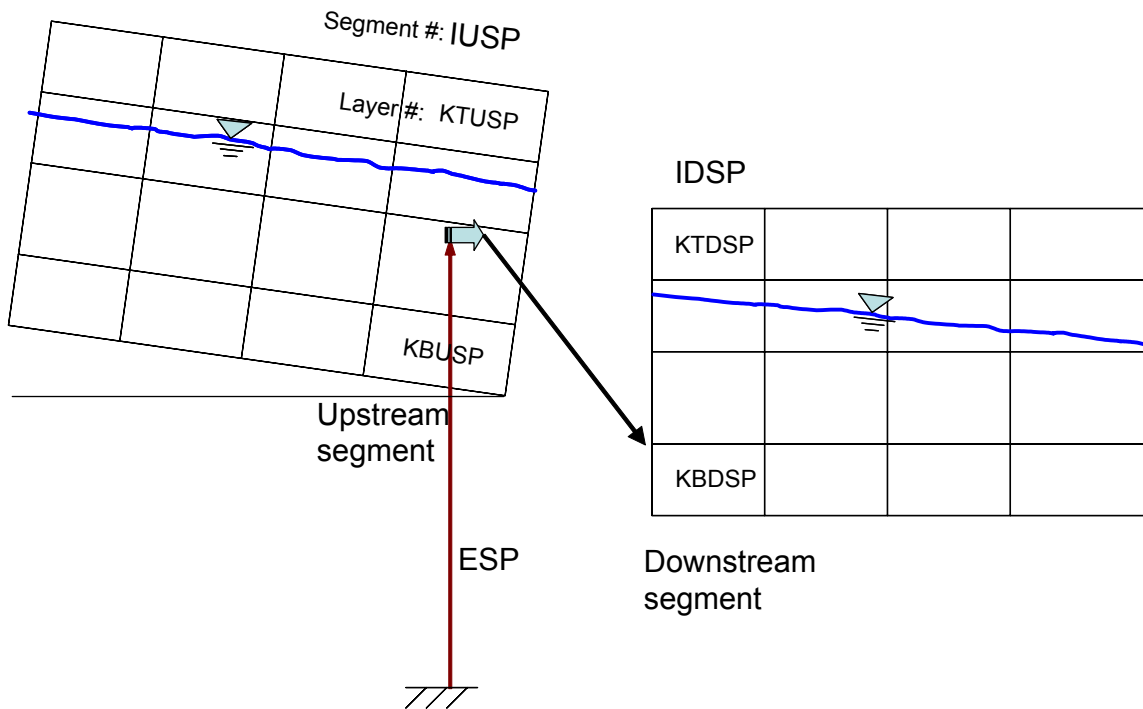
Downstream Spillway (DOWN)



Lateral Spillway (LAT)



Lateral Spillway (LAT)



Example

SPILLWAYS	IUSP	IDSP	ESP	A1SP	B1SP	A2SP	B2SP	LATSPC
Sp 1	30	33	45.5	45.33	1.5	34.45	1.0	DOWN
Sp 2	28	33	40.0	10.00	1.5	20.00	1.0	LAT

Related Cards and Files

- [Inflow/Outflow Dimensions](#)
- [Upstream Spillways](#)
- [Downstream Spillways](#)
- [Spillway Dissolved Gas](#)

Upstream Spillways (SPILL UP)

FIELD	NAME	VALUE	DEFAULT	DESCRIPTION
1				(Ignored by code)
2	PUSPC	Character	DISTR	How inflows enter into the upstream spillway segment, DISTR, DENSITY, or SPECIFY
3	ETUSP	Real		Top elevation spillway inflows enter using SPECIFY option, <i>m</i>
4	EBUSP	Real		Bottom elevation spillway inflows enter using SPECIFY option, <i>m</i>
5	KTUSP	Integer		Top layer above which selective withdrawal will not occur
6	KBUSP	Integer		Bottom layer below which selective withdrawal will not occur

This card specifies how inflows/outflows for the upstream spillway location are handled. Setting [PUSPC] to DISTR distributes the inflows evenly from the water surface to the bottom active layer, setting it to DENSITY places the inflows into a layer with similar density, and setting it to SPECIFY allows the user to specify a top and bottom elevation into which inflows enter. If the SPECIFY option is used, then [KTUSP] and [KBUSP] are used to specify the top and bottom elevations that the inflows are distributed over.

[KTUSP] and [KBUSP] are used to set the upper and lower layers above and below which outflow does not occur in the selective withdrawal algorithm.

Example

SPILL UP	PUSPC	ETUSP	EBUSP	KTUSP	KBUSP
Sp 1	DISTR			2	23
Sp 2	DISTR			2	23

Related Cards and Files

[Spillways](#)

[Downstream Spillways](#)

[Spillway Dissolved Gas](#)

Downstream Spillways (SPILL DOWN)

FIELD	NAME	VALUE	DEFAULT	DESCRIPTION
1				(Ignored by code)
2	PDSPC	Character	DISTR	How inflows enter into the downstream spillway segment, DISTR, DENSITY, or SPECIFY
3	ETDSP	Real		Top elevation spillway inflows enter using SPECIFY option, <i>m</i>
3	EBDSP	Real		Bottom elevation spillway inflows enter using SPECIFY option, <i>m</i>
5	KTDSP	Integer		Top layer above which selective withdrawal will not occur
5	KBDSP	Integer		Bottom layer below which selective withdrawal will not occur

This card specifies how inflows/outflows for the downstream spillway location are handled. Setting [PDSPC] to DISTR distributes the inflows evenly from the water surface to the bottom active layer, setting it to DENSITY places the inflows into a layer with similar density, and setting it to SPECIFY allows the user to specify a top and bottom elevation into which inflows enter. If the SPECIFY option is used, then [ETDSP] and [EBDSP] are used to specify the top and bottom elevations that the inflows are distributed over.

[KTDSP] and [KBDSP] are used to set the upper and lower layers above and below which outflow does not occur in the selective withdrawal algorithm.

Example

SPILL DOWN	PDSPC	ETDSP	EBDSP	KTDSP	KBDSP
Sp 1	DISTR			2	23
Sp 2	DISTR			2	23

Related Cards and Files

- [Inflow/Outflow Dimensions](#)
- [Spillways](#)
- [Upstream Spillways](#)
- [Spillway Dissolved Gas](#)

Spillway Dissolved Gas (SPILL GAS)

FIELD	NAME	VALUE	DEFAULT	DESCRIPTION
1				(Ignored by code)
2	GASSPC	Character	OFF	Dissolved gas computations, ON or OFF
3	EQSP	Integer		Equation number for computing dissolved gas
3	ASP	Real		a coefficient in dissolved gas equation
5	BSP	Real		b coefficient in dissolved gas equation
5	CSP	Real		c coefficient in dissolved gas equation

This card turns ON/OFF spillway gas computations [GASSPC] and specifies the parameters that define the dissolved gas relationship. If dissolved gas computations are turned ON, then an equation number must be supplied (1 to 3). Based on the equation number, two or three coefficients are required. These coefficients are *a*, *b*, and *c* as shown in [Table C-2](#). Note that if [IDSP] is 0, even if [GASSPC] is ON, the model will not compute any effects of gas transfer since the water exiting the spillway or weir is not accounted for in the system. This algorithm computes gas effects for flow from upstream to downstream and there is no adjustment of dissolved oxygen for reverse flow.

The Corps of Engineers has been involved in gas abatement studies on the Columbia and Snake River system for many years (WES, 1996, 1997). Some of their research efforts have been focused on development of models of spillway gas generations. These empirical models have been called CriSP 1.6 (Columbia Basin Research, 1998). The gas production equations used in CriSP are empirical correlations between total dissolved gas (TDG), usually measured a mile downstream of the dam after turbulence from the spillway had subsided, and discharge, usually measured in kcfs. The form of these equations is shown in [Table C-2](#).

Table C-2. Equations used in CRiSP model for gas production

Equation type	Equation	Coefficient description
Linear function of total spill	$\%TDG = mQ_s + b$	%TDG = % total dissolved gas saturation Q _s = total spill, kcfs m = empirical coefficient b = empirical coefficient
Bounded exponential of total spill	$\%TDG = a + b^{cQ_s}$	Q _s = total spill, kcfs a = empirical coefficient b = empirical coefficient c = empirical coefficient
Bounded exponential of the spill on a per spillway basis	$\%TDG = a + b^{cq_s}$	q _s = individual spillway spill, kcfs a = empirical coefficient b = empirical coefficient c = empirical coefficient

Examples of some of these correlations are shown in [Table C-3](#). In many cases the %TDG in these correlations was constrained to a maximum of 145% and when the flow reached only a few kcfs, there was assumed to be no change in TDG from the forebay to the tailrace. Also, the correlations in [Table C-2](#) sometimes changed from year to year based on changes in operating conditions or structural changes in the spillway or deflectors.

Table C-3. Equations used in CRiSP model for gas production at Columbia basin dams

Dam	Equation	Coefficients
Bonneville	$%TDG = mQ_s + b$	$m = 0.12$ $b = 105.61$
Lower Granite	$%TDG = a + b^{cQ_s}$	$a = 138.0$ $b = -35.8$ $c = -0.10$
Dworshak	$%TDG = a + b^{cQ_s}$	$a = 135.9$ $b = -71.1$ $c = -0.4787$
Ice Harbor	$%TDG = a + b^{cQ_s}$	$a = 136.8; b = -42.0; c = -0.0340 - 1995$ $a = 138.7; b = -79.0; c = -0.0591 - 1996$ $a = 130.9; b = -26.5; c = -0.0220 - 1997$ $a = 120.9; b = -20.5; c = -0.0230 - 1998$
Hell's Canyon	$%TDG = a + b^{cQ_s}$	$a = 138$ $b = -36$ $c = -0.02$ [Assumed relationship - no data]

For each spillway, the user now has a choice of equations to use for computing the effects of each hydraulic structure on downstream dissolved oxygen. The equations chosen are shown in [Table C-4](#). These equations are based on equations from [Table C-2](#) and [Table C-3](#).

Table C-4. Reaeration Effects of Spillways, Weirs, and Gates

#	Equation	Coefficient description
1. Linear function of spill on a per spillway basis; 2 empirical coefficients a and b	$%TDG = aq_s + b$ Once TDG is known below the spillway, the dissolved oxygen concentration, C_{O_2} , is determined from $C_{O_2} = \%TDG * C_{sO_2}$	$%TDG =$ % total dissolved gas saturation $q_s =$ individual spillway spill, $kcfs$ $a =$ empirical coefficient $b =$ empirical coefficient $C_{sO_2} =$ dissolved oxygen saturation, $g\ m^{-3}$
2. Bounded exponential of the spill on a per spillway basis; 3 empirical coefficients a , b , and c	$%TDG = a + be^{cq_s}$ Once TDG is known below the spillway, the dissolved oxygen concentration, C_{O_2} , is determined from $C_{O_2} = \%TDG * C_{sO_2}$	$q_s =$ individual spillway spill, $kcfs$ $a =$ empirical coefficient $b =$ empirical coefficient $c =$ empirical coefficient $C_{sO_2} =$ dissolved oxygen saturation, $g\ m^{-3}$

#	Equation	Coefficient description
3. Reaeration effect for a small height weir or dam (<10 m); 3 empirical coefficients <i>a</i> , <i>b</i> , and <i>c</i>	$\frac{D_a}{D_b} = 1 + 0.38ab(1 - 0.11c)$ $(1 + 0.046T)c$ <p><i>C</i>_{O₂} below the dam is computed from:</p> $C_{O_2} = C_{sO_2} - D_b$	<p><i>D</i>_a = DO deficit above dam, <i>g m</i>⁻³ <i>D</i>_b = DO deficit below dam, <i>g m</i>⁻³ <i>T</i> = temperature, °C <i>a</i> = 1.8 for clean water to 0.65 for gross polluted water <i>b</i> = 0.05 for sluice gates <i>b</i> = 1.0 for sharp crested straight faced weir <i>b</i> = 0.45 for flat broad crested curved face weir <i>b</i> = 0.7 for flat broad crested weir with regular step <i>b</i> = 0.8 for sharp crested vertical face weir <i>b</i> = 0.6 for flat broad crested weir vertical face <i>c</i> = water fall height, <i>m</i> <i>C</i>_{sO₂} = dissolved oxygen saturation, <i>g m</i>⁻³</p>

Note that for equations 1 and 2, the maximum *TDG* allowed is 145%, and if *TDG* is computed to be less than 100%, there is no effect of the spillway or gate on reaeration.

Example

SPILL	GAS	GASSPC	EQSP	ASP	BSP	CSP
Sp 1		ON	2	110.0	-0.1	-0.1
Sp 2		ON	1	10.0	110.0	10.0

Related Cards and Files

- [Inflow/Outflow Dimensions](#)
- [Spillways](#)
- [Upstream Spillways](#)
- [Downstream Spillways](#)
- [Spillway Dissolved Gas](#)

Gates (GATES)

FIELD	NAME	VALUE	DEFAULT	DESCRIPTION
1				(Ignored by code)
2	IUGT	Integer		Gate segment location
3	IDGT	Integer		Downstream segment gate outflow enters
4	EGT	Real		Gate elevation, m
5	A1GT	Real		α_1 coefficient in gate equation for free flowing conditions
6	B1GT	Real		β_1 coefficient in gate equation for free flowing conditions
7	G1GT	Real		γ_1 coefficient in gate equation for free flowing conditions
8	A2GT	Real		α_2 coefficient in gate equation for submerged conditions
9	B2GT	Real		β_2 coefficient in gate equation for submerged conditions
10	G2GT	Real		γ_2 coefficient in gate equation for submerged conditions
11	LATGTC	Character	LAT	Downstream or lateral withdrawal, DOWN or LAT

This card specifies the gate characteristics. [IUGT] and [IDGT] specify the upstream and downstream segments for the spillway. Setting the downstream spillway segment [IDSP] to 0 allows the user to spill water that is lost from the system. The following equation is used for freely flowing conditions:

$$Q = \alpha_1 \Delta h^{\beta_1} B^{\gamma_1}$$

where:

$$\begin{aligned} \beta_1 &= \text{empirical coefficient} \\ \gamma_1 &= \text{empirical coefficient} \\ \Delta h &= Z_u - Z_{sp}, m \\ Z_u &= \text{upstream head, } m \\ Z_{sp} &= \text{spillway crest elevation, } m \end{aligned}$$

and the following equation is used for submerged flow:

$$Q = \alpha_2 \Delta h^{\beta_2} B^{\gamma_2}$$

where

$$\begin{aligned} \alpha_2 &= \text{empirical coefficient} \\ \beta_2 &= \text{empirical coefficient} \\ \gamma_2 &= \text{empirical coefficient} \\ \Delta h &= Z_u - Z_d, m \end{aligned}$$

Z_d = downstream head, m

B = gate opening, m

In defining these parameters, the model user also has to generate a time series file of the gate openings **[GATEFN]**. Whenever the gate opening, B , is equal to or greater than $0.8(Z_u - Z_{sp})$, a weir equation is used with no functional dependency on the gate width. In this case, the user must also supply a rating curve when the gate acts like a weir.

If a valve-rating curve is used as a “gate” and the outlet elevation to compute the head difference is not the same as the withdrawal elevation, the following changes need to be included in the input variables:

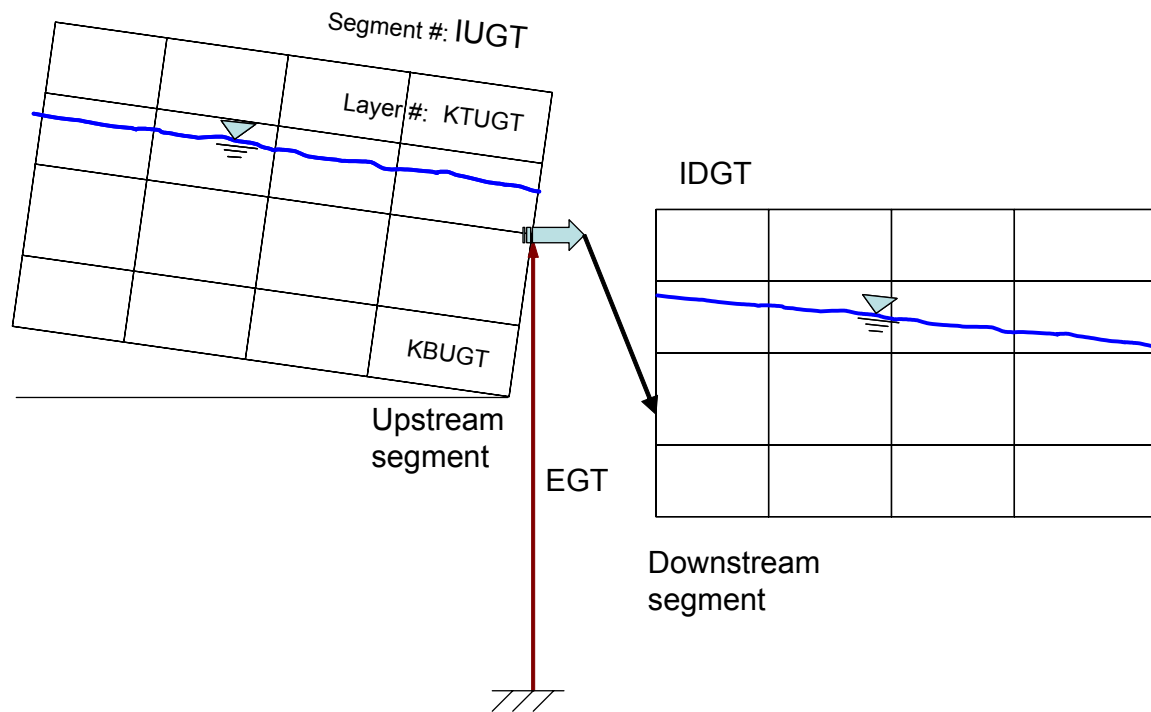
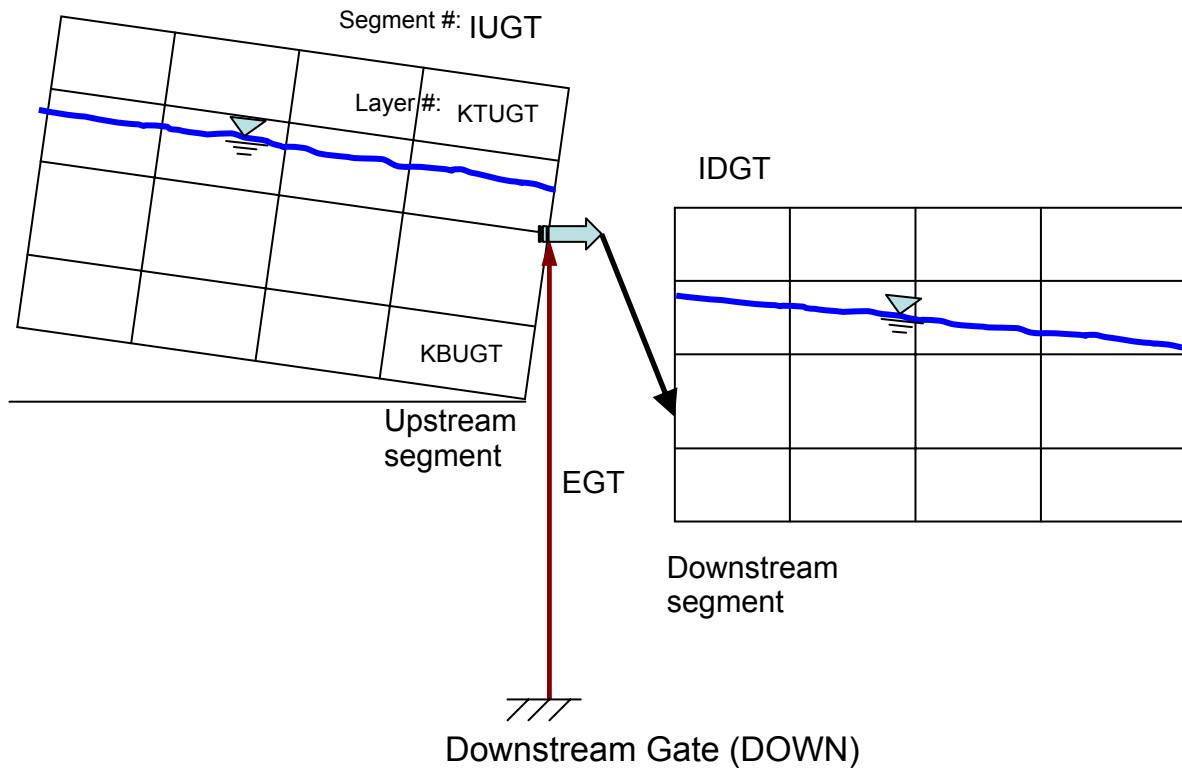
1. **[EGT]** is interpreted as the outlet level for the water being withdrawn
2. **[A2GT]** must be set to zero (no reverse flow equation is used)
3. **[G2GT]** is interpreted as the elevation used to compute the head on the outlet valve - whenever **[A2GT]** is set to zero and **[G2GT]** is non-zero, **[G2GT]** will be used to compute the head difference between the water level and the outlet rather than **[EGT]**, but **[EGT]** will still determine the location of the withdrawal.

In some reservoirs, an outlet valve is connected to the reservoir and a head-discharge relationship is used based on the gate opening or number of turns of the gate. In this case, the outlet level is usually at a different elevation than the withdrawal elevation. The gate formulation can still be used if there is no reverse flow through the needle valve.

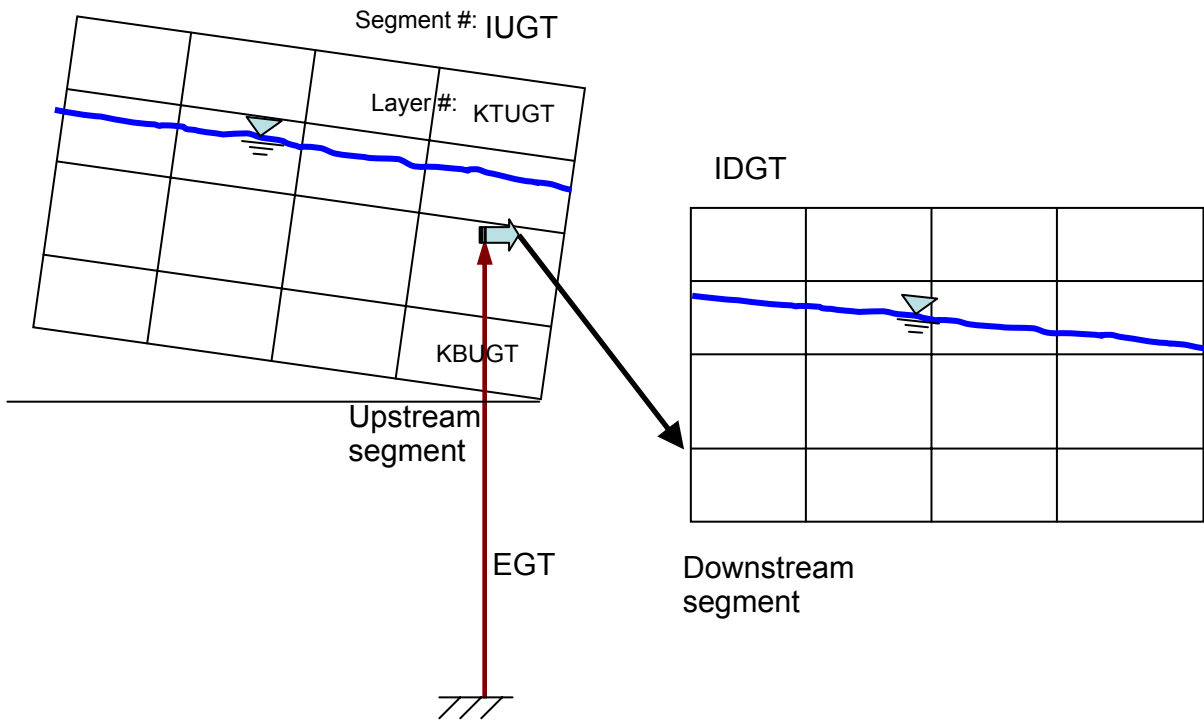
Setting the gate location **[LATGTC]** to **DOWN** specifies that the gate is located at the downstream end of the segment. In this case the water surface elevations are computed based on the downstream segment location. Also, momentum from the outflow is preserved as in a downstream structure withdrawal. If **[LATGTC]** is set to **LAT**, it is assumed that the outflow is treated as a lateral withdrawal at the segment center elevation. In both cases selective withdrawal is used in the computations.

Figure ?? and ?? show the layout of gates set as a downstream **[DOWN]** and a lateral **[LAT]** withdrawal from the upstream segment, respectively.

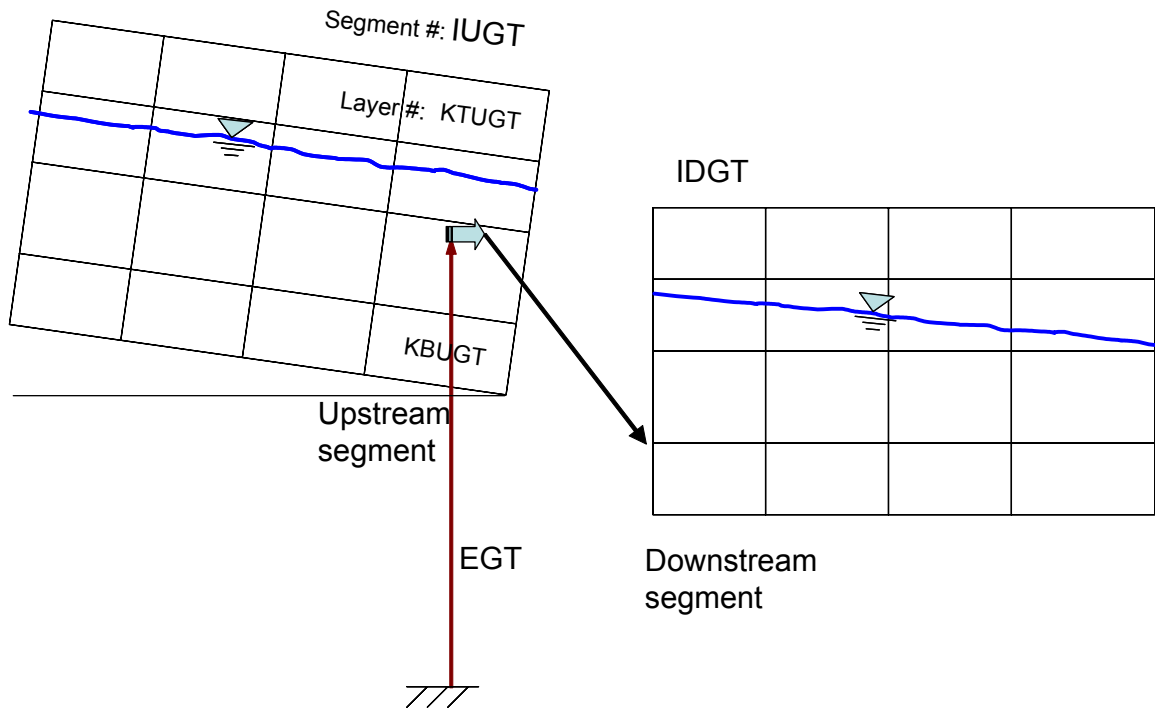
Downstream Gate (DOWN)



Lateral Gate (LAT)



Lateral Gate (LAT)



INFLOW/OUTFLOW

CONTROL FILE

Example

GATES	IUGT	IDGT	EGT	A1GT	B1GT	G1GT	A2GT	B2GT	G2GT	LATGTC
Gt 1	27	33	44.0	10.00	1.00	1.00	10.0	2.50	0.00	DOWN

Related Cards and Files

[Inflow/Outflow Dimensions](#)

[Gate Weir](#)

[Upstream Gate](#)

[Downstream Gate](#)

[Gate Dissolved Gas](#)

[Gate Filename](#)

Gate Weir (GATE WEIR)

FIELD	NAME	VALUE	DESCRIPTION
1			(Ignored by code)
2	GA1	Real	a_1 in gate equation for free flowing conditions
3	GB1	Real	b_1 in gate equation for free flowing conditions
4	GA2	Real	a_2 in gate equation for submerged conditions
5	GB2	Real	b_2 in gate equation for submerged conditions
6	DYNGTC	Character	

This card specifies the weir coefficients used when the gates are open and the open gate does not interfere with the flow (the gate width, $B \geq 0.8\Delta h$). For [GA1] equal to zero, only the gated equations on the preceding card are used. For [GA2] equal to zero, only the freely flowing equation will be used even if submerged or reverse flow occurs.

[DYNGC] is used to determine whether outflow from the gate is specified by a gate opening height or if the elevation of the gate is specified in the gate input file. If [DYNGC] is set to "B", then the gate opening height is used, and an elevation is used if [DYNGC] is set to "ZGT".

Example

GATE WEIR	GA1	GB1	GA2	GB2	DYNGC
Gt 1	10.0	1.5	10.0	1.5	B

Related Cards and Files

[Inflow/Outflow Dimensions](#)

[Gates](#)

[Upstream Gate](#)

[Downstream Gate](#)

[Gate Dissolved Gas](#)

[Gate Filename](#)

Upstream Gate (GATE UP)

FIELD	NAME	VALUE	DEFAULT	DESCRIPTION
1				(Ignored by code)
2	PUGTC	Character	DISTR	Specifies how inflows enter the upstream gate segment, DISTR, DENSITY, or SPECIFY
3	ETUGT	Real		Top elevation gate inflows enter using the SPECIFY option, <i>m</i>
4	EBUGT	Real		Bottom elevation gate inflows using the SPECIFY option, <i>m</i>
5	KTUGT	Integer		Top layer above which selective withdrawal will not occur
6	KBUGT	Integer		Bottom layer below which selective withdrawal will not occur

This card specifies how inflows/outflows for the upstream gate location are handled. Setting [PUGTC] to DISTR distributes the inflows evenly from the water surface to the bottom active layer, setting it to DENSITY places the inflows into a layer with similar density, and setting it to SPECIFY allows the user to specify a top and bottom elevation into which inflows enter. If the SPECIFY option is used, then [KTUGT] and [KBUGT] are used to specify the top and bottom elevations that the inflows are distributed over.

[KTUGT] and [KBUGT] are used to set the upper and lower layers above and below which outflow does not occur in the selective withdrawal algorithm.

Example

```
GATE UP      PUGTC  ETUGT  EBUGT  KTUGT  KBUGT
Gt 1        DISTR                2      23
```

Related Cards and Files

[Inflow/Outflow Dimensions](#)

[Gates](#)

[Gate Weir](#)

[Downstream Gate](#)

[Gate Dissolved Gas](#)

[Gate Filename](#)

Downstream Gate (GATE DOWN)

FIELD	NAME	VALUE	DEFAULT	DESCRIPTION
1				(Ignored by code)
2	PDGTC	Character	DISTR	Specifies how inflows enter the downstream gate segment, DISTR, DENSITY, or SPECIFY
3	ETDGT	Real		Top elevation gate inflows enter using the SPECIFY option, <i>m</i>
4	EBDGT	Real		Bottom elevation gate inflows enter using the SPECIFY option, <i>m</i>
5	KTDGT	Integer		Top layer above which selective withdrawal will not occur
6	KBDGT	Integer		Bottom layer below which selective withdrawal will not occur

This card specifies how inflows/outflows for the downstream gate location are handled. Setting [PDGTC] to DISTR distributes the inflows evenly from the water surface to the bottom active layer, setting it to DENSITY places the inflows into a layer with similar density, and setting it to SPECIFY allows the user to specify a top and bottom elevation into which inflows enter. If the SPECIFY option is used, then [ETDGT] and [EBDGT] are used to specify the top and bottom elevations that the inflows are distributed over.

[KTDGT] and [KBDGT] are used to set the upper and lower layers above and below which outflow does not occur in the selective withdrawal algorithm.

Example

```
GATE DOWN PDGTC ETDGT EBDGT KTDGT KBDGT
Gt 1      DISTR          2      23
```

Related Cards and Files

[Inflow/Outflow Dimensions](#)

[Gates](#)

[Gate Weir](#)

[Upstream Gate](#)

[Gate Dissolved Gas](#)

[Gate Filename](#)

Gate Dissolved Gas (GATE GAS)

FIELD	NAME	VALUE	DEFAULT	DESCRIPTION
1				(Ignored by code)
2	GASGTC	Character	OFF	Dissolved gas computations, ON or OFF
3	EQGT	Integer		Equation number for computing dissolved gas
3	AGASGT	Real		a coefficient in dissolved gas equation
5	BGASGT	Real		b coefficient in dissolved gas equation
5	CGASGT	Real		c coefficient in dissolved gas equation

For each gate, the model user activates or deactivates the computation by selecting ON or OFF for [GASGTC]. If the user activates this computation by choosing ON, then an equation number must be supplied (1 to 3). Based on the equation number, two or three coefficients are required. These coefficients are *a*, *b*, and *c* as shown in Table C-5. Note that if [IDGT] is 0, even if [GASGTC] is ON, the model will not compute any effects of gas transfer since the water exiting the spillway or weir is not accounted for in the system. This algorithm only computes gas effects for upstream to downstream flow and there is no adjustment of dissolved oxygen for reverse flow.

The Corps of Engineers has been involved in Gas Abatement Studies on the Columbia and Snake River system for many years (WES, 1996, 1997). Some of their research efforts have been focused on development of models of gas generation from spillways. These empirical models have been called CriSP 1.6 (Columbia Basin Research, 1998). The gas production equations used in CriSP are empirical correlations between total dissolved gas (TDG), usually measured a mile downstream of the dam after turbulence from the spillway had subsided, and discharge, usually measured in kcfs. The form of these equations is shown in Table C-5.

Table C-5. Equations used in CRiSP model for gas production

Equation type	Equation	Coefficient Description
Linear function of total spill	$%TDG = mQ_s + b$	%TDG = % total dissolved gas saturation <i>Q_s</i> = total spill, kcfs <i>m, b</i> = empirical coefficients
Bounded exponential of total spill	$%TDG = a + b^{cQ_s}$	<i>Q_s</i> = total spill, kcfs <i>a, b, c</i> = empirical coefficients
Bounded exponential of the spill on a per spillway basis	$%TDG = a + b^{cq_s}$	<i>q_s</i> = spill through individual spillway, kcfs <i>a, b, c</i> = empirical coefficients

Examples of some of these correlations are shown in Table C-6. In many cases the %TDG in these correlations was constrained to a maximum of 145% and when the flow reached only a few thousand cfs, no change in TDG was assumed from the forebay to the tailrace. Also, the correlations in Table C-6 sometimes changed from year to year based on changes in operating conditions or structural changes in the spillway or deflectors.

Table C-6. Equations used in CRiSP model for gas production at Columbia basin dams

Dam	Equation	Coefficients
Bonneville	$%TDG = mQ_s + b$	<i>m</i> = 0.12 <i>b</i> = 105.61
Lower Granite	$%TDG = a + b^{cQ_s}$	<i>a</i> = 138.0

		$b = -35.8$ $c = -0.10$
Dworshak	$\%TDG = a + b^{cQ_s}$	$a = 135.9$ $b = -71.1$ $c = -0.4787$
Ice Harbor	$\%TDG = a + b^{cQ_s}$	$a = 136.8; b = -42.0; c = -0.0340$ 1995; $a = 138.7; b = -79.0; c = -0.0591$ 1996; $a = 130.9; b = -26.5; c = -0.0220$ 1997; $a = 120.9; b = -20.5; c = -0.0230$ 1998
Hell's Canyon	$\%TDG = a + b^{cQ_s}$	$a = 138; b = -36; c = -0.02$ [Assumed relationship - no data]

For each gate, the user now has the choice of equation to use for computing the effects of each hydraulic structure on downstream dissolved oxygen. The equations chosen are shown in [Table C-7](#). These equations are based on equations from [Table C-5](#) and [Table C-6](#).

Table C-7. Reaeration effects of gates

#	Equation	Empirical Coefficient Description
1. Linear function of spill on a per spillway basis; 2 empirical coefficients: a and b	$\%TDG = aq_s + b$ Once %TDG is known below the spillway, the dissolved oxygen concentration, C_{O_2} , is determined from $C_{O_2} = \%TDG * C_{sO_2}$	$\%TDG$ = total dissolved gas saturation, % q_s = spill through an individual spillway, $kcfs$ a = empirical coefficient b = empirical coefficient C_{sO_2} = dissolved oxygen saturation, $g\ m^{-3}$
2. Bounded exponential of the spill on a per spillway basis; 3 empirical coefficients: a, b, c	$\%TDG = a + be^{cq_s}$ Once %TDG is known below the spillway, the dissolved oxygen concentration, C_{O_2} , is determined from $C_{O_2} = \%TDG * C_{sO_2}$	q_s = spill through an individual spillway, $kcfs$ a = empirical coefficient b = empirical coefficient c = empirical coefficient C_{sO_2} = dissolved oxygen saturation $g\ m^{-3}$
3. Reaeration effect for a small height weir or dam (<10 m); 3 empirical coefficients: a, b, c	$\frac{D_a}{D_b} = 1 + 0.38ab(1 - 0.11c)$ $(1 + 0.046T)c$ C_{O_2} below the dam is computed from: $C_{O_2} = C_{sO_2} - D_b$	D_a = DO deficit above dam, $g\ m^{-3}$ D_b = DO deficit below dam, $g\ m^{-3}$ T = temperature, $^{\circ}C$ c = height of water fall, m $a = 1.8$ for clean water to 0.65 for gross polluted water $b = 0.05$ for sluice gates $b = 1.00$ for sharp crested straight faced weir $b = 0.45$ for flat broad crested curved face weir $b = 0.70$ for flat broad crested weir with regular step $b = 0.8$ for sharp crested vertical face weir $b = 0.60$ for flat broad crested weir vertical face C_{sO_2} = dissolved oxygen saturation, $g\ m^{-3}$

Note that for equations 1 and 2, the maximum TDG allowed is 145%, and if TDG is computed to be less than 100%, there is no effect of the gate on reaeration.

INFLOW/OUTFLOW

CONTROL FILE

Example

GATE	GAS	GASGTC	EQGT	AGASGT	BGASGT	CGASGT
Gt	1	ON	1	10.0	120.0	1.0

Related Cards and Files

[Inflow/Outflow Dimensions](#)

[Gates](#)

[Gate Weir](#)

[Upstream Gate](#)

[Downstream Gate](#)

[Gate Filename](#)

Pumps 1 (PUMPS 1)

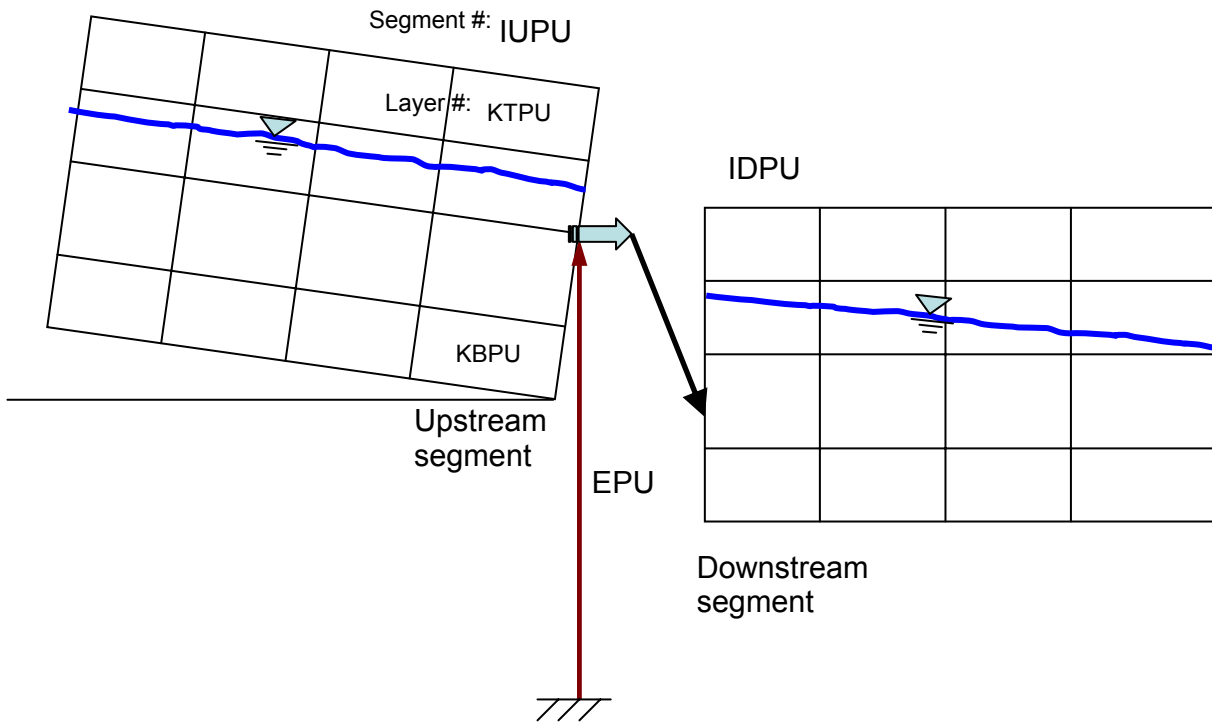
FIELD	NAME	VALUE	DEFAULT	DESCRIPTION
1				(Ignored by code)
2	IUPU	Integer		Upstream segment of pump where water is withdrawn
3	IDPU	Integer		Downstream segment of pump where water enters
4	EPU	Real		Elevation of pump, <i>m</i>
5	STRTPU	Real		Starting day of pumping, <i>Julian day</i>
6	ENDPU	Real		Ending day of pumping, <i>Julian day</i>
7	EONPU	Real		Pump starting elevation, <i>m</i>
8	EOFFPU	Real		Pump stopping elevations, <i>m</i>
9	QPU	Real		Pump flow rate, $m^3 \text{ sec}^{-1}$
10	LATPUC	Character	DOWN	Downstream or lateral withdrawal, DOWN or LAT

This card specifies the characteristics of the pumps in the system. [IUPU] and [IDPU] specify the segments from which water is withdrawn and added back to the system, respectively. IF [IDPU] is zero water is only withdrawn from the system. The elevation of the pump [EPU] is used to specify the vertical location of the pump for the selective withdrawal algorithm. [STRTPU] and [ENDPU] specify the starting and ending times during which pumping occurs, [EONPU] and [EOFFPU] specify the elevations at which pumping is activated/deactivated, and [QPU] specifies the pumping rate.

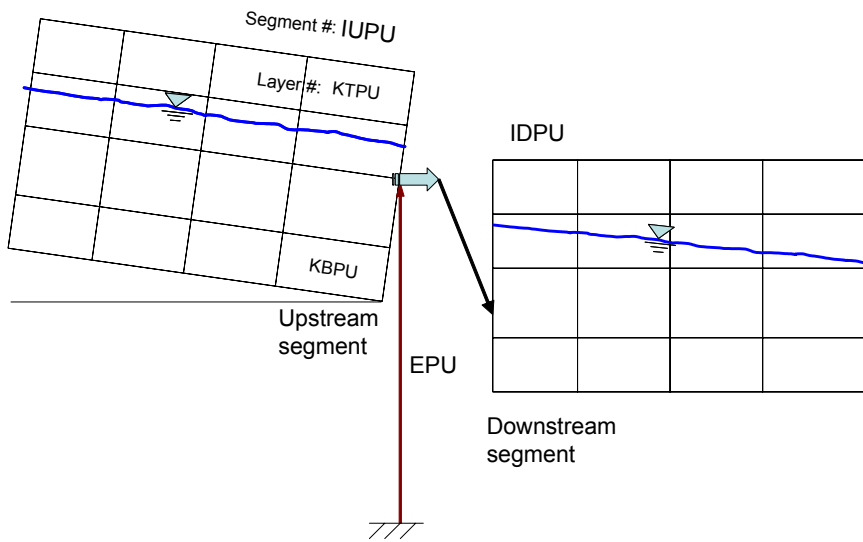
Setting the pump location [LATPUC] to DOWN specifies that the pump is at the downstream end of the segment. In this case the water surface elevations are computed based on the downstream segment location. Also, momentum from the outflow is preserved as in a downstream structure withdrawal. If [LATPUC] is set to LAT, it is assumed that the outflow is treated as a lateral withdrawal at the segment center elevation. In both cases selective withdrawal is used in the computations.

Figure ?? and ?? show the layout of pumps set as a downstream [DOWN] and a lateral [LAT] withdrawal from the upstream segment, respectively.

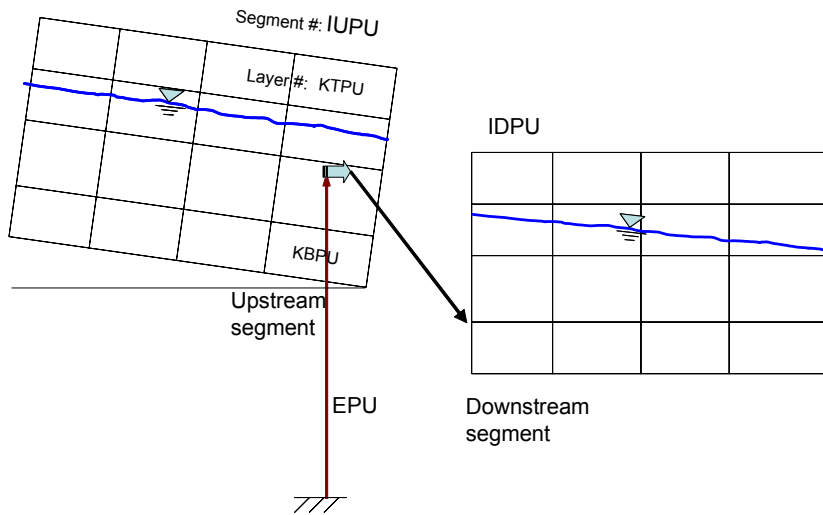
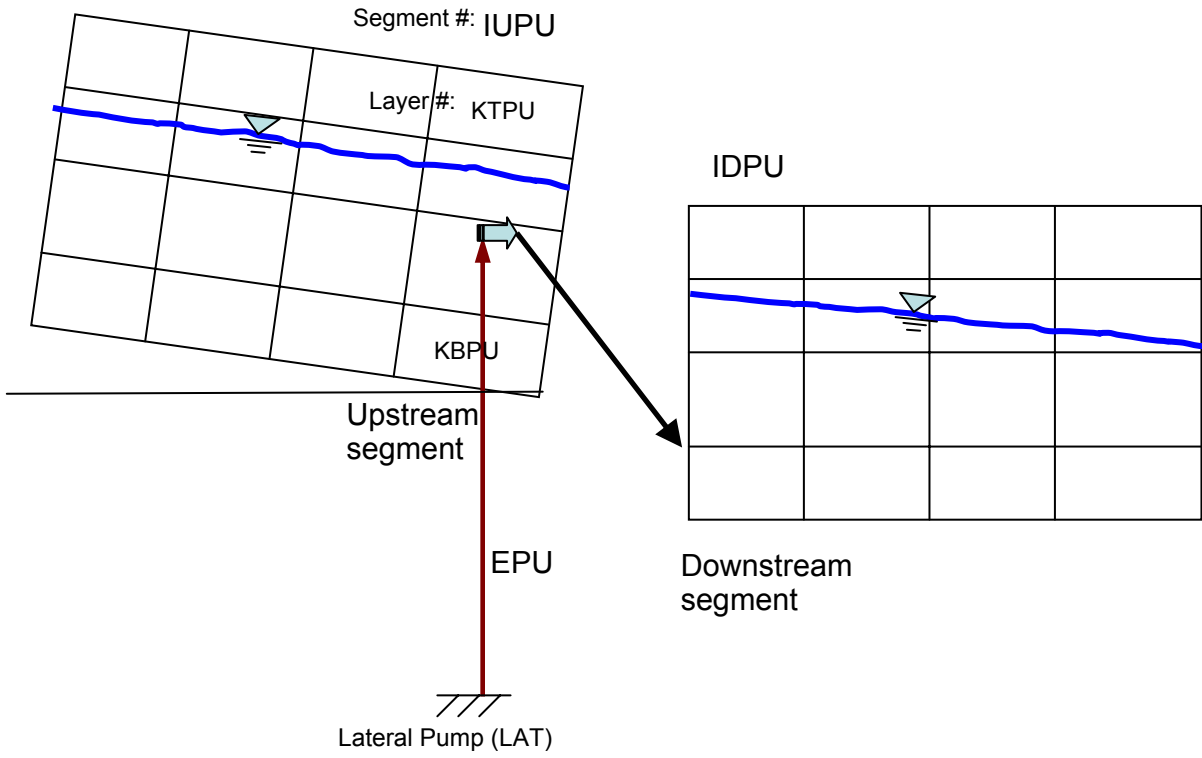
Downstream Pump (DOWN)



Downstream Pump (DOWN)



Lateral Pump (LAT)



Example

PUMPS 1	IUPU	IDPU	EPU	STRTPU	ENDPU	EONPU	EOFFPU	QPU	LATPUC
Pu 1	30	33	2.4	1.0	900.0	3.0	2.4	3.0	DOWN

INFLOW/OUTFLOW

CONTROL FILE

Related Cards and Files

[Inflow/Outflow Dimensions
Pumps 2](#)

Pumps 2 (PUMPS 2)

FIELD	NAME	VALUE	DEFAULT	DESCRIPTION
1				(Ignored by code)
2	PPUC	Character	DISTR	How inflows enter into the downstream water level control segment, DISTR, DENSITY, or SPECIFY
3	ETPU	Real		Top elevation water level control inflows enter using SPECIFY option, <i>m</i>
3	EBPU	Real		Bottom elevation water level control inflows enter using SPECIFY option, <i>m</i>
5	KTPU	Integer		Top layer above which selective withdrawal does not occur
5	KBPU	Integer		Bottom layer below which selective withdrawal will not occur

This card specifies how inflows/outflows for the water level controls are handled. Setting [PPUC] to DISTR distributes the inflows evenly from the water surface to the bottom active layer, setting it to DENSITY places the inflows into a layer with similar density, and setting it to SPECIFY allows the user to specify a top and bottom elevation into which inflows enter. If the SPECIFY option is used, then [ETPU] and [EBPU] are used to specify the top and bottom elevations that the inflows are distributed over.

[KTPU] and [KBPU] are used to set the upper and lower layers above and below which outflow does not occur in the selective withdrawal algorithm. For the pumps algorithm, in contrast to gates, spillways (weirs), and pipes, flow is only in 1-direction, i.e., only outflow is allowed from the upstream segment.

Example

```
PUMPS 2      PPUC      ETPU      EBPU      KTPU      KBPU
Pu 1         DISTR
```

Related Cards and Files

[Inflow/Outflow Dimensions Pumps 1](#)

Internal Weir Segment Location (WEIR SEG)

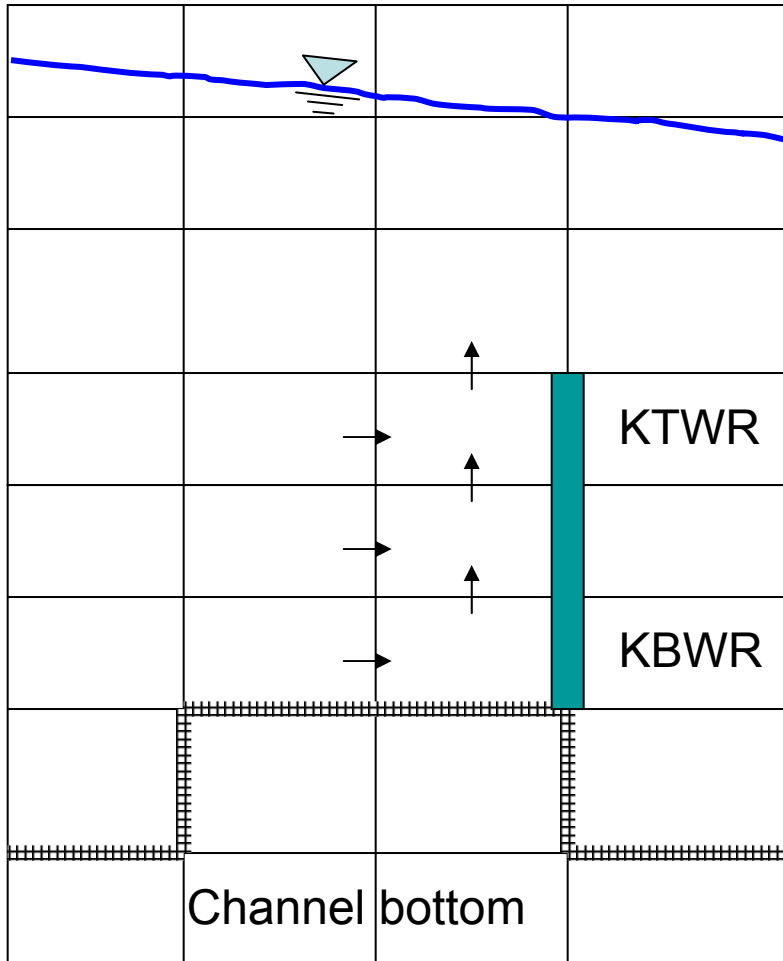
FIELD	NAME	VALUE	DESCRIPTION
1			(Ignored by code)
2-10	IWR	Integer	Weir segment location

This card specifies the segment location of the internal weir in the grid. If there are more internal weirs than can be specified on one line, then the segment locations are continued on the next line without another WEIR SEG card being specified.

Figure X illustrates the location of the internal weir. Note that the internal weir is always on the right side of a segment.

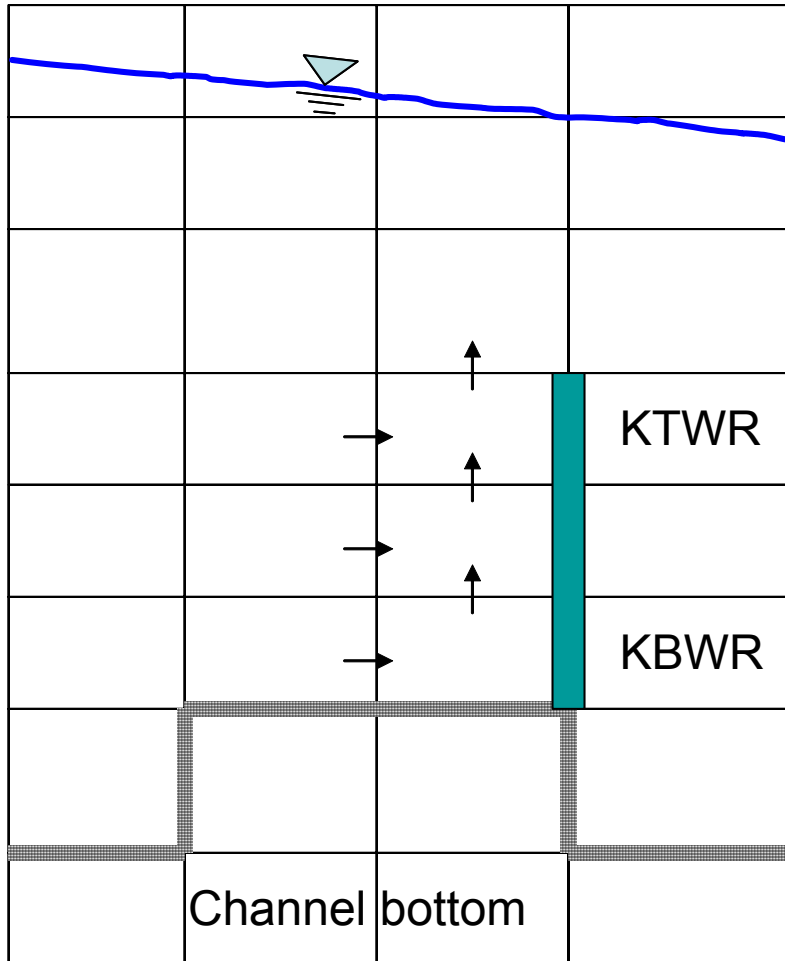
Internal Weir

IWR



Internal Weir

IWR



Example

WEIR SEG IWR IWR IWR IWR IWR IWR IWR IWR IWR
 25

Related Cards and Files

- [Inflow/Outflow Dimensions](#)
- [Weir Top Layer](#)
- [Weir Bottom Layer](#)

Internal Weir Top Layer (WEIR TOP)

FIELD	NAME	VALUE	DESCRIPTION
1			(Ignored by code)
2-10	KTWR	Integer	Weir top layer

This card specifies the top layer location of the internal weir. For a submerged weir, this should be set to the layer above which flow is allowed to occur between segments. If there are more internal weirs than can be specified on one line, then the top layer locations are continued on the next line without another WEIR TOP card being specified.

Example

```
WEIR TOP      KTWR      KTWR      KTWR      KTWR      KTWR      KTWR      KTWR      KTWR
              25
```

Related Cards and Files

[Inflow/Outflow Dimensions](#)

[Weir Segment Location](#)

[Weir Bottom Layer](#)

Internal Weir Bottom Layer (WEIR BOT)

FIELD	NAME	VALUE	DESCRIPTION
1			(Ignored by code)
2-10	KBWR	Integer	Weir bottom layer

This card specifies the bottom layer location of the internal weir. For a curtain weir, [KBWR] should be set to the bottommost layer above which flow between segments will not occur. For a submerged weir, [KBWR] should be set to the bottommost active layer for the segment specified in the [WEIR SEG](#) card. If there are more internal weirs than can be specified on one line, then the top layer locations are continued on the next line without another WEIR BOT card being specified.

Example

```
WEIR BOT      KBWR      KBWR      KBWR      KBWR      KBWR      KBWR      KBWR      KBWR
              25
```

Related Cards and Files

- [Inflow/Outflow Dimensions](#)
- [Weir Segment Location](#)
- [Weir Top Layer](#)

Withdrawal Interpolation (WD INT)

FIELD	NAME	VALUE	DEFAULT	DESCRIPTION
1				(Ignored by code)
2-10	WDIC		OFF	Withdrawal outflow interpolation, ON or OFF

This card specifies whether interpolation is turned on for lateral withdrawal outflow. If there are *more* withdrawal interpolations than can be specified on one line, then they are continued on the next line without another WD INT card being specified.

If [WDIC] is turned ON, then flows are linearly interpolated between updates. If interpolation is used, then the user must ensure it is appropriate and the input data supply correct information. Withdrawals can have periods of no releases. If withdrawal interpolation is turned on, then input data must be set up so no outflow occurs during these periods. This is accomplished by including extra dates in the withdrawal file with zero outflows to ensure the interpolation routine yields zero outflows. For example, given the following withdrawal time-series in the withdrawal file [QWDFN]:

```

JDAY      QWD
100.00    50.0
110.00    0.0
120.00    50.0

```

If interpolation is not used, then outflow from Julian day 100 to 110 is $50 \text{ m}^3 \text{ sec}^{-1}$, from Julian day 110 to 120 is $0.0 \text{ m}^3 \text{ sec}^{-1}$, and $50 \text{ m}^3 \text{ sec}^{-1}$ thereafter. If interpolation is turned on, then outflow linearly decreases from Julian day 100 to 110 and then increases from Julian day 110 to 120. To ensure no outflow occurs between day 110 and 120 with interpolation on, the withdrawal file should be setup as follows:

```

JDAY      QWD
109.9999  50.0
110.0000  0.0
119.9999  0.0
120.0000  50.0

```

Example

```

WD INT      WDIC      WDIC      WDIC      WDIC      WDIC      WDIC      WDIC      WDIC
              ON

```

Related Cards and Files

[Inflow/Outflow Dimensions](#)
[Withdrawal Segment](#)
[Withdrawal Elevation](#)
[Withdrawal Top Layer](#)
[Withdrawal Bottom Layer](#)
[Withdrawal File](#)
[Withdrawal Filename](#)

Withdrawal Segment (WD SEG)

FIELD	NAME	VALUE	DESCRIPTION
1			(Ignored by code)
2-10	IWD	Integer	Withdrawal segment number

This card specifies the withdrawal segment location. If there are more withdrawal segments than can be specified on one line, then they are continued on the next line without another WD SEG card being specified.

Example

```

W  SEGMENT      IWD      IWD      IWD      IWD      IWD      IWD      IWD      IWD
                4
    
```

Related Cards and Files

- [Inflow/Outflow Dimensions](#)
- [Withdrawal Interpolation](#)
- [Withdrawal Elevation](#)
- [Withdrawal Top Layer](#)
- [Withdrawal Bottom Layer](#)
- [Withdrawal File](#)
- [Withdrawal Filename](#)

Withdrawal Elevation (WD ELEV)

FIELD	NAME	VALUE	DESCRIPTION
1			(Ignored by code)
2-10	EWD	Real	Withdrawal centerline elevation, <i>m</i>

This card specifies the centerline elevation of the withdrawal. If there are more withdrawal elevations than can be specified on one line, then they are continued on the next line without another WD ELEV card being specified.

Example

```

W EL      EWD      EWD      EWD      EWD      EWD      EWD      EWD      EWD
          40.0

```

Related Cards and Files

[Inflow/Outflow Dimensions](#)

[Withdrawal Interpolation](#)

[Withdrawal Segment](#)

[Withdrawal Top Layer](#)

[Withdrawal Bottom Layer](#)

[Withdrawal File](#)

[Withdrawal Filename](#)

Withdrawal Top Layer (WD TOP)

FIELD	NAME	VALUE	DESCRIPTION
1			(Ignored by code)
2-10	KTWD	Integer	Top layer above which selective withdrawal will not occur

This card specifies the layer above which no flows will be computed in the selective withdrawal algorithm. For most situations, this should be set to layer 2, which ensures that water can be withdrawn all the way to the surface layer. It should be set to something greater than 2 if a structure is somehow limiting the withdrawal of water, such as a curtain weir. If there are more withdrawal elevations than can be specified on one line, then they are continued on the next line without another WD TOP card being specified.

Example

```
WD TOP      KTWD      KTWD      KTWD      KTWD      KTWD      KTWD      KTWD      KTWD      KTWD
           2
```

Related Cards and Files

- [Inflow/Outflow Dimensions](#)
- [Withdrawal Interpolation](#)
- [Withdrawal Segment](#)
- [Withdrawal Elevation](#)
- [Withdrawal Bottom Layer](#)
- [Withdrawal File](#)
- [Withdrawal Filename](#)

Withdrawal Bottom Layer (WD BOT)

FIELD	NAME	VALUE	DESCRIPTION
1			(Ignored by code)
2-10	KBWD	Integer	Bottom layer below which selective withdrawal will not occur

This card specifies the layer below which no flows will be computed in the selective withdrawal algorithm. For most situations, this should be set to the bottommost active layer of the withdrawal segment, which ensures that water can be withdrawn all the way to the bottom layer. It should be set to something other than the bottommost active layer if a structure is somehow limiting the withdrawal of water, such as a submerged weir. If there are more bottom withdrawal layers than can be specified on one line, then they are continued on the next line without another WD BOT card being specified.

Example

```
WD BOT      KBWD      KBWD      KBWD      KBWD      KBWD      KBWD      KBWD      KBWD
           10
```

Related Cards and Files

[Inflow/Outflow Dimensions](#)

[Withdrawal Interpolation](#)

[Withdrawal Segment](#)

[Withdrawal Elevation](#)

[Withdrawal Top Layer](#)

[Withdrawal File](#)

[Withdrawal Filename](#)

Tributary Inflow Placement (TRIB PLACE)

FIELD	NAME	VALUE	DESCRIPTION
1			(Ignored by code)
2-10	TRC	Character	Tributary inflow placement, DISTR, DENSITY, SPECIFY

This card specifies how tributary inflows are distributed into the model layers. There are three options. Inflows can be distributed evenly from top to bottom ([PTRC] = DISTR), placed according to density ([PTRC] = DENSITY), or the user may specify a range of layer elevations in which the tributary inflows are distributed evenly ([PTRC] = SPECIFY). This is similar to the branch inflows, but with the additional option allowing the user to specify the range of layer elevations in which to distribute the inflows. This option is particularly useful when trying to model discharges from a pipe such as wastewater treatment effluent.

If there are more tributaries than can be specified on one line, then they are continued on the next line without another TRIB PLACE card being specified.

Example

```

TRIB PLACE PTRC PTRC PTRC PTRC PTRC PTRC PTRC PTRC PTRC
          DENSITY DISTR SPECIFY DENSITY DENSITY DENSITY DENSITY DENSITY
    
```

Related Cards and Files

- [Inflow/Outflow Dimensions](#)
- [Tributary Interpolation](#)
- [Tributary Segment](#)
- [Tributary Inflow Top Elevation](#)
- [Tributary Inflow Bottom Elevation](#)
- [Tributary Active Constituent Control](#)
- [Tributary Inflow File](#)
- [Tributary Temperature File](#)
- [Tributary Concentration File](#)
- [Tributary Inflow Filename](#)
- [Tributary Inflow Temperature Filename](#)
- [Tributary Inflow Concentration Filename](#)

Tributary Interpolation (TRIB INT)

FIELD	NAME	VALUE	DEFAULT	DESCRIPTION
1				(Ignored by code)
2-10	TRIC	Character	OFF	Turns ON/OFF interpolation of tributary inflows

The tributary inflow specified by the tributary files for flow, temperature, and concentration can either be assumed to be step functions, [TRIC] set to OFF, or can be linearly interpolated between values, [TRIC] set to ON.

Example

```

TRIB INT      TRIC      TRIC      TRIC      TRIC      TRIC      TRIC      TRIC      TRIC      TRIC
              ON        ON        ON
  
```

Related Cards and Files

[Inflow/Outflow Dimensions](#)
[Tributary Inflow Placement](#)
[Tributary Segment](#)
[Tributary Inflow Top Elevation](#)
[Tributary Inflow Bottom Elevation](#)
[Tributary Active Constituent Control](#)
[Tributary Inflow File](#)
[Tributary Temperature File](#)
[Tributary Concentration File](#)
[Tributary Inflow Filename](#)
[Tributary Inflow Temperature Filename](#)
[Tributary Inflow Concentration Filename](#)

Tributary Segment (TRIB SEG)

FIELD	NAME	VALUE	DESCRIPTION
1			(Ignored by code)
2-10	ITR	Integer	Segment tributary enters

This card specifies the segment that the tributary enters. Tributary flows are either placed into a layer whose density most closely corresponds to that of the tributary flows, are evenly distributed from top to bottom, or are specified to enter over a range of elevations (see [\[TRC\]](#)). Flows that enter segments upstream of the current upstream segment [\[CUS\]](#) for a branch are combined with the branch inflow.

If there are more tributary segments than can be specified on one line, then they are continued on the next line without another TRIB SEG card being specified.

Example

```

TRIB SEG      ITR      ITR      ITR      ITR      ITR      ITR      ITR      ITR      ITR
              2        3        4        3        4        5        6        7
    
```

Related Cards and Files

- [Inflow/Outflow Dimensions](#)
- [Tributary Inflow Placement](#)
- [Tributary Interpolation](#)
- [Tributary Inflow Top Elevation](#)
- [Tributary Inflow Bottom Elevation](#)
- [Tributary Active Constituent Control](#)
- [Tributary Inflow File](#)
- [Tributary Temperature File](#)
- [Tributary Concentration File](#)
- [Tributary Inflow Filename](#)
- [Tributary Inflow Temperature Filename](#)
- [Tributary Inflow Concentration Filename](#)

Tributary Inflow Top Elevation (TRIB TOP)

FIELD	NAME	VALUE	DESCRIPTION
1			(Ignored by code)
2-10	ETRT	Real	Tributary inflow top elevation, <i>m</i>

This card specifies the upper elevation for each tributary inflow in which the user has specified that inflows will be placed over a range of elevations. Only tributaries that are specified as SPECIFY on the [Tributary Inflow Placement](#) card need top elevations specified on this card.

If there are more tributary top elevations than can be specified on one line, then they are continued on the next line without another TRIB TOP card being specified.

Example

```

TRIB TOP      ETRT      ETRT      ETRT      ETRT      ETRT      ETRT      ETRT      ETRT      ETRT
              116.0

```

Related Cards and Files

[Inflow/Outflow Dimensions](#)
[Tributary Inflow Placement](#)
[Tributary Interpolation](#)
[Tributary Segment](#)
[Tributary Inflow Top Elevation](#)
[Tributary Inflow Bottom Elevation](#)
[Tributary Active Constituent Control](#)
[Tributary Inflow File](#)
[Tributary Temperature File](#)
[Tributary Concentration File](#)
[Tributary Inflow Filename](#)
[Tributary Inflow Temperature Filename](#)
[Tributary Inflow Concentration Filename](#)

Tributary Inflow Bottom Elevation (ELEV BOT)

FIELD	NAME	VALUE	DESCRIPTION
1			(Ignored by code)
2-10	ETRB	Real	Tributary inflow bottom elevation, <i>m</i>

This card specifies the bottom elevation for each tributary inflow in which the user has specified that inflows will be placed over a range of elevations. Only tributaries that are specified as SPECIFY on the [Tributary Inflow Placement](#) card need bottom elevations specified on this card.

If there are more tributary bottom elevations than can be specified on one line, then they are continued on the next line without another TRIB BOT card being specified.

Example

```

TRIB BOT      ETRB      ETRB      ETRB      ETRB      ETRB      ETRB      ETRB      ETRB      ETRB
              114.0
    
```

Related Cards and Files

- [Inflow/Outflow Dimensions](#)
- [Tributary Inflow Placement](#)
- [Tributary Interpolation](#)
- [Tributary Segment](#)
- [Tributary Inflow Top Elevation](#)
- [Tributary Inflow Bottom Elevation](#)
- [Tributary Active Constituent Control](#)
- [Tributary Inflow File](#)
- [Tributary Temperature File](#)
- [Tributary Concentration File](#)
- [Tributary Inflow Filename](#)
- [Tributary Inflow Temperature Filename](#)
- [Tributary Inflow Concentration Filename](#)

Distributed Tributaries (DST TRIB)

FIELD	NAME	VALUE	DEFAULT	DESCRIPTION
1				(Ignored by code)
2	DTRC	Character	OFF	Distributed tributary option, ON or OFF

This card specifies whether or not a branch contains a distributed tributary inflow and whether or not the inflows, inflow temperatures, and inflow concentrations are linearly interpolated between input dates. A distributed tributary is equivalent to a non-point source loading. This option may be turned ON or OFF for each branch and is useful in accounting for unaged flows for the water budget. The flow is distributed among the segments in each branch proportional to their surface areas. There is one value of [DTRC] for each branch. See the INTERPOL card for turning ON/OFF interpolation for distributed tributaries.

For each distributed tributary specified, the user must supply an inflow file [[QDTFN](#)], an inflow temperature file [[TDTFN](#)], and, if constituents are modeled, an inflow constituent concentration file [[CDTFN](#)].

If constituents are modeled, the user can select which constituents are included in the distributed tributary concentrations input file (see [Distributed Tributary Active Constituent Control](#) card).

Example

```
DST TRIB      DTRC
Br 1          ON
Br 2          ON
Br 3          OFF
Br 4          OFF
```

Related Cards and Files

[Distributed Tributary Active Constituent Control](#)
[Distributed Tributary Inflow File](#)
[Distributed Tributary Temperature File](#)
[Distributed Tributary Concentration File](#)
[Distributed Tributary Inflow Filename](#)
[Distributed Tributary Inflow Temperature Filename](#)
[Distributed Tributary Inflow Concentration Filename](#)

Pump Storage Operations (PUMPBACK)

FIELD	NAME	VALUE	DESCRIPTION
1			(Ignored by code)
2	JBG	Integer	Upstream branch location for outflows during power generation or inflows during pumpback
3	KTG	Integer	Top layer for flows entering the upstream branch location during pumpback
4	KBG	Integer	Bottom layer for flows entering the upstream branch location during pumpback
5	JBP	Integer	Downstream branch location for inflows during power generation or outflows during pumpback
6	KTP	Integer	Top layer for flows entering the downstream branch location during generation
7	KBP	Integer	Bottom layer for flows entering the downstream branch location during generation

This card allows the user to dynamically link branches for simulating pump storage operations. The upstream branch [JBG] and downstream branch [JBP] specify the branch locations where outflows occur due to generation and pumpback, respectively. The variables [KTG], [KBG], [KTP], and [KBP] allow the user to specify the layers that inflows enter the downstream branch during generation, and the layers that inflows enter the upstream branch during pumpback operations.

The actual flows are specified in the [branch outflow file \[QOTFN\]](#). Power generation flows are specified as positive and pumpback flows are specified as negative. The selective withdrawal algorithm is used to compute outflow/inflow temperatures during generation and pumpback.

Example

PUMPBACK	JBG	KTG	KBG	JBP	KTP	KBP
	1	12	16	3	6	10

Printer Control (PRINTER)

FIELD	NAME	VALUE	DEFAULT	DESCRIPTION
1				(Ignored by code)
2	LJC	Character	OFF	Output format for the preprocessor and snapshot file

This card specifies the LaserJet equivalent model used for the snapshot file [SNPFN]. [LJPC] can be specified as either OFF, II, III, or IV. The model will output the appropriate codes so that the preprocessor output and snapshot will print on a laserjet compatible hardcopy device. If [LJPC] is set to OFF, then no codes are output and the user must then have an output device, such as a line printer, that supports 132 column output.

Example

```
PRINTER      LJC
              IV
```

Hydrodynamic Output Control (HYD PRINT)

FIELD	NAME	VALUE	DEFAULT	DESCRIPTION
1				(Ignored by code)
2-10	HPRWBC	Character	OFF	Output hydrodynamic terms to the snapshot file, ON or OFF

This card specifies whether or not certain hydrodynamic terms are included as output in the snapshot file. The hydrodynamic terms include timestep violations, horizontal and vertical velocities, temperatures, and all the terms that comprise the horizontal momentum equation. The latest version allows the user to turn ON/OFF hydrodynamic output for each waterbody as shown in the example. Values for each waterbody continue across the line. If there are more than nine waterbodies, then additional values continue on the next line starting in field two. Output formatting and animation of these variables can be specified in the graph.npt file.

Table C-8. Hydraulic Print Parameters

Term	Explanation
[NLIM]	Location and number of limiting time steps in the model grid
[U]	Longitudinal velocity
[W]	Vertical velocity
[T]	Temperature
[RHO]	Density
[AZ]	Vertical turbulent eddy viscosity
[SHEAR]	Velocity shear stress
[ST]	Shear stress at top of model layer
[SB]	Shear stress at bottom of model layer
[ADMX]	Longitudinal advection of momentum
[DM]	Longitudinal momentum transport by eddy viscosity
[HDG]	Horizontal density gradient
[ADMZ]	Vertical advection of momentum
[HPG]	Horizontal pressure gradient
[GRAV]	Gravity force term

Example

HYD PRINT	HPRWBC								
NLIM	ON	ON	ON						
U	ON	ON	ON						
W	ON	ON	ON						
T	ON	ON	ON						
RHO	ON	ON	ON						
AZ	ON	ON	ON						
SHEAR	ON	ON	ON						
ST	ON	ON	ON						
SB	ON	ON	ON						
ADMX	ON	ON	ON						
DM	ON	ON	ON						
HDG	ON	ON	ON						
ADMZ	ON	ON	ON						
HPG	ON	ON	ON						
GRAV	ON	ON	ON						

Snapshot Print (SNP PRINT)

FIELD	NAME	VALUE	DEFAULT	DESCRIPTION
1				(Ignored by code)
2	SNPC	Character	OFF	Specifies if information is written to snapshot file, ON or OFF
3	NSNP	Integer		Number of snapshot dates
4	NISNP	Integer		Number of segments output

This card specifies if information is output to the snapshot file [SNPFN], number of snapshot intervals for specifying output dates and frequencies, and the number of segments that will be output to each snapshot file. Each water body has separate controls so that the user can include/suppress snapshot output for each waterbody.

Snapshot file output provides the user with a hard copy of computed values for hydrodynamic and constituent variables for user assigned segments. Output from this file can take up a tremendous amount of disk space and when printed can use up large quantities of computer paper in a short time. This option is generally used during initial runs and then turned off before the user becomes buried in computer output.

The number of snapshot dates [NSNP] refers to the option of writing information to the snapshot file for different dates and frequencies. For example, the user may specify output is to begin on Julian day 224.4 and output every 0.1 days until day 225.5. Information is then output every day until the end of the simulation. In this case, [NSNP] would be set to 2. Values for each waterbody start on a new line.

Example

SNP PRINT	SNPC	NSNP	NISNP
Wb 1	ON	3	11
Wb 2	ON	1	14
Wb 3	ON	1	10

Related Cards and Files

- [Snapshot Dates](#)
- [Snapshot Frequency](#)
- [Snapshot Segments](#)
- [Snapshot Filename](#)
- [Constituent Output](#)

Snapshot Dates (SNP DATE)

FIELD	NAME	VALUE	DESCRIPTION
1			(Ignored by code)
2-10	SNPD	Real	Output dates, <i>Julian day</i>

This card specifies the dates that information is output to the snapshot file [SNPFN]. The total number of dates specified on this card must match [NSNP] on the [Snapshot Print](#) card.

If there are more dates than can be specified on one line, then the values for [SNPD] are continued on the next line without another SNP DATE card being specified. Values for each waterbody start on a new line.

Example

SNP DATE	SNPD	SNPD	SNPD	SNPD	SNPD	SNPD	SNPD	SNPD	SNPD
Wb 1	63.50	100.5	200.5						
Wb 2	63.50								
Wb 3	63.50								

Related Cards and Files

- [Snapshot Print](#)
- [Snapshot Frequency](#)
- [Snapshot Segments](#)
- [Snapshot Filename](#)
- [Constituent Output](#)

Snapshot Frequency (SNP FREQ)

FIELD	NAME	VALUE	DESCRIPTION
1			(Ignored by code)
2-10	SNPF	Real	Output frequency, <i>days</i>

This card specifies the frequency information is output to the snapshot file [SNPFN]. Frequency can be changed at any time during the simulation by specifying appropriate dates on the [Snapshot Date](#) card and frequencies on the **Snapshot Frequency** card. If output is needed only for the date specified on the [Snapshot Date](#) card, then set the frequency to be greater than the number of days before the next output date.

If there are more frequencies than can be specified on one line, then they are continued on the next line without another SNP FREQ card being specified. Values for each waterbody start on a new line.

Example

SNP FREQ	SNPF	SNPF	SNPF	SNPF	SNPF	SNPF	SNPF	SNPF	SNPF	SNPF
Wb 1	0.1	500.0	7.0							
Wb 2	0.1									
Wb 3	0.1									

Related Cards and Files

[Snapshot Print](#)
[Snapshot Dates](#)
[Snapshot Segments](#)
[Snapshot Filename](#)
[Constituent Output](#)

Snapshot Segments (SNP SEG)

FIELD	NAME	VALUE	DESCRIPTION
1			(Ignored by code)
2-10	ISNP	Integer	Output segments

This card specifies the segments to be included in the snapshot file for each waterbody. The user can include all segments in the computational grid. However, if the user wants to create a hardcopy that can be printed out, he should not specify more than 21 values for each waterbody. The user should also omit boundary segments that are not part of the computational grid.

If there are more dates than can be specified on one line, then the values for [ISNP] are continued on the next line without another SNP SEG card being specified. Values for each waterbody start on a new line.

Example

SNP SEG	ISNP									
Wb 1	2	3	4	5	6	9	10	11	12	
	13	14								
Wb 2	17	18	19	20	21	22	23	24	25	
	26	27	28	29	30					
Wb 3	33	34	35	36	37	38	39	40	41	
	42									

Related Cards and Files

- [Snapshot Print](#)
- [Snapshot Dates](#)
- [Snapshot Frequency](#)
- [Snapshot Filename](#)
- [Constituent Output](#)

Screen Print (SCR PRNT)

FIELD	NAME	VALUE	DEFAULT	DESCRIPTION
1				(Ignored by code)
2	SCRC	Character	OFF	Specifies if information is written to the screen, ON or OFF
3	NSCR	Integer		Number of screen update intervals

This card specifies if information is output to the screen during the run and the number of intervals during which the frequency of updating the screen can change. The frequency at which the screen is updated should be large (at least 0.1 days). Experience has shown that updating the screen every timestep can easily *double* the runtime. Values for each waterbody start on a new line.

Example

SCR PRINT	SCRC	NSCR
Wb 1	ON	1
Wb 2	ON	1
Wb 3	ON	1

Related Cards and Files

[Screen Dates](#)

[Screen Frequency](#)

Screen Dates (SCR DATE)

FIELD	NAME	VALUE	DESCRIPTION
1			(Ignored by code)
2-10	SCRD	Real	Output dates, <i>Julian day</i>

This card specifies the dates information is output to the screen. The total number of dates specified on this card must match [NSCR] on the [Screen Print](#) card.

If there are more dates than can be specified on one line, then the values for [SCRD] are continued on the next line without another SCR DATE card being specified. Values for each waterbody start on a new line.

Example

SCR DATE	SCRD								
Wb 1	63.5								
Wb 2	63.5								
Wb 3	63.5								

Related Cards and Files

- [Screen Print](#)
- [Screen Frequency](#)

Screen Frequency (SCR_FREQ)

FIELD	NAME	VALUE	DESCRIPTION
1			(Ignored by code)
2-10	SCR_F	Real	Output frequency, <i>days</i>

This card specifies the frequency information is output to the screen. Frequency can be changed at any time during the simulation by specifying appropriate dates on the [Screen Date](#) card and frequencies on the **Screen Frequency** card. The frequency at which the screen is updated should be large (at least 0.1 days and more often 1.0 days). Experience has shown that updating the screen every timestep can easily double the runtime. If output is needed only for the date specified on the [Screen Date](#) card, then set the frequency to be greater than the number of days before the next output date.

If there are more frequencies than can be specified on one line, then they are continued on the next line without another **Screen Frequency** card being specified. Values for each waterbody start on a new line.

Example

```
SCR_FREQ  SCR_F  SCR_F  SCR_F  SCR_F  SCR_F  SCR_F  SCR_F  SCR_F  SCR_F
Wb 1      0.15
Wb 2      0.15
Wb 3      0.15
```

Related Cards and Files

[Screen Print](#)
[Screen Dates](#)

Profile Plot (PRF PLOT)

FIELD	NAME	VALUE	DEFAULT	DESCRIPTION
1				(Ignored by code)
2	PRFC	Character	OFF	Specifies if information is written to the profile file, ON or OFF
3	NPRF	Integer		Number of profile dates
4	NIPRF	Integer		Number of segments output

This card specifies if information is output to the [profile output file \[PRFFN\]](#), the number of profile intervals for specifying output dates and frequencies, and the number of segments included in the output.

The [profile output file \[PRFFN\]](#) is used to plot vertical profiles of temperature and constituents at a specified model segment. This option is normally turned off during initial runs while the user is verifying the model is performing correctly. It is turned on to compare observed data with simulated data during calibration runs.

This file is in a form suitable for FORTRAN postprocessing. The [spreadsheet output file \[SPRFN\]](#) can be used for processing output data in a spreadsheet.

The [Constituent Output](#) card controls which constituents are output to the profile file. Temperature is always output to the profile file. Values for each waterbody start on a new line.

Example

PRF PLOT	PRFC	NPRF	NIPRF
Wb 1	ON	1	1
Wb 2	OFF	0	0
Wb 3	ON	1	1

Related Cards and Files

[Profile Date](#)
[Profile Frequency](#)
[Profile Segment](#)
[Profile Filename](#)
[Constituent Output](#)

Profile Date (PRF DATE)

FIELD	NAME	VALUE	DESCRIPTION
1			(Ignored by code)
2-10	PRFD	Real	Output dates, <i>Julian day</i>

This card specifies the dates that information is output to the [profile output file \[PRFFN\]](#). If there are more dates than can be specified on one line, then they are continued on the next line without another PRF DATE card being specified. Values for each waterbody start on a new line.

Example

PRF DATE	PRFD								
Wb 1	63.5								
Wb 2									
Wb 3	63.5								

Related Cards and Files

[Profile Plot](#)

[Profile Frequency](#)

[Profile Segment](#)

[Profile Filename](#)

[Constituent Output](#)

Profile Frequency (PRF FREQ)

FIELD	NAME	VALUE	DESCRIPTION
1			(Ignored by code)
2-10	PRFF	Real	Output frequency, <i>days</i>

This card specifies the frequency information is output to the [profile output file \[PRFFN\]](#). Frequency can be changed at any time during the simulation by specifying appropriate dates on the [Profile Date](#) card and frequencies on the **Profile Frequency** card. If output is needed only for the date specified on the [Profile Date](#) card, then set the frequency to be greater than the number of days before the next output date.

If there are more frequencies than can be specified on one line, then they are continued on the next line without another **PRF FREQ** card being specified. Values for each waterbody start on a new line.

Example

```
PRF FREQ  PRFF  PRFF  PRFF  PRFF  PRFF  PRFF  PRFF  PRFF  PRFF
Wb 1      1.0
Wb 2
Wb 3      1.0
```

Related Cards and Files

- [Profile Plot](#)
- [Profile Date](#)
- [Profile Segment](#)
- [Profile Filename](#)
- [Constituent Output](#)

Profile Segment (PRF SEG)

FIELD	NAME	VALUE	DESCRIPTION
1			(Ignored by code)
2-10	IPRF	Integer	Output segments

This card specifies model segments for which information is output to the [profile output file PRFFN](#). If there are more segments than can be specified on one line, then they are continued on the next line without another **PRF SEG** card being specified. Values for each waterbody start on a new line.

Example

PRF SEG	IPRF								
Wb 1	14								
Wb 2									
Wb 3	42								

Related Cards and Files

[Profile Plot](#)

[Profile Date](#)

[Profile Frequency](#)

[Profile Filename](#)

[Constituent Output](#)

Spreadsheet Plot (SPR PLOT)

FIELD	NAME	VALUE	DEFAULT	DESCRIPTION
1				(Ignored by code)
2	SPRC	Character	OFF	Specifies if information is written to the spreadsheet file
3	NSPR	Integer		Number of spreadsheet dates
4	NISPR	Integer		Number of segments in output

This card specifies if information is output to the [spreadsheet output file \[SPRFN\]](#), the number of intervals for specifying output dates and frequencies, and the number of segments included in the output.

The [spreadsheet output file \[SPRFN\]](#) is used to plot vertical profiles of temperature and constituents at a specified model segment and is suitable as ASCII input into a spreadsheet type database. This option is normally turned off during initial runs while the user is verifying the model is performing correctly. It is turned on to compare observed data with simulated data during calibration.

The [Constituent Output](#) card controls which constituents are output to the spreadsheet file. Temperature is always output to the spreadsheet file. Values for each waterbody start on a new line.

Example

SPR PLOT	SPRC	NSPR	NISPR
Wb 1	OFF	0	0
Wb 2	OFF	1	1
Wb 3	OFF	1	1

Related Cards and Files

[Spreadsheet Date](#)
[Spreadsheet Frequency](#)
[Spreadsheet Segment](#)
[Spreadsheet Filename](#)
[Constituent Output](#)

Spreadsheet Date (SPR DATE)

FIELD	NAME	VALUE	DESCRIPTION
1			(Ignored by code)
2-10	SPRD	Real	Output dates, <i>Julian Day</i>

This card specifies the dates that information is output to the [spreadsheet output file \[SPRFN\]](#). If there are more dates than can be specified on one line, then they are continued on the next line without another **SPR DATE** card being specified. Values for each waterbody start on a new line.

Example

SPR DATE	SPRD								
Wb 1									
Wb 2	63.5								
Wb 3	63.5								

Related Cards and Files

[Spreadsheet Plot](#)
[Spreadsheet Frequency](#)
[Spreadsheet Segment](#)
[Spreadsheet Filename](#)
[Constituent Output](#)

Spreadsheet Frequency (SPR FREQ)

FIELD	NAME	VALUE	DESCRIPTION
1			(Ignored by code)
2-10	SPRF	Real	Output frequency, <i>days</i>

This card specifies the frequency information is output to the [spreadsheet output file \[SPRFN\]](#). Frequency can be changed at any time during the simulation by specifying appropriate dates on the [Spreadsheet Date](#) card and frequencies on the **Spreadsheet Frequency** card. If output is needed only for the date specified on the [Spreadsheet Date](#) card, then set the frequency to be greater than the number of days before the next output date.

If there are more frequencies than can be specified on one line, then they are continued on the next line without another **SPR FREQ** card being specified. Values for each waterbody start on a new line.

Example

```
SPR FREQ  SPRF  SPRF  SPRF  SPRF  SPRF  SPRF  SPRF  SPRF  SPRF
Wb 1
Wb 2      7.0
Wb 3      7.0
```

Related Cards and Files

- [Spreadsheet Plot](#)
- [Spreadsheet Date](#)
- [Spreadsheet Segment](#)
- [Spreadsheet Filename](#)
- [Constituent Output](#)

Spreadsheet Segment (SPR SEG)

FIELD	NAME	VALUE	DESCRIPTION
1			(Ignored by code)
2-10	ISPR	Integer	Output segments

This card specifies model segments for which information is output to the [spreadsheet output file \[SPRFN\]](#). If there are more segments than can be specified on one line, then they are continued on the next line without another **SPR SEG** card being specified.

Example

```

SPR SEG      ISPR      ISPR      ISPR      ISPR      ISPR      ISPR      ISPR      ISPR      ISPR
Wb 1
Wb 2          14
Wb 3          42

```

Related Cards and Files

[Spreadsheet Plot](#)
[Spreadsheet Date](#)
[Spreadsheet Frequency](#)
[Spreadsheet Filename](#)
[Constituent Output](#)

Vector Plot (VPL PLOT)

FIELD	NAME	VALUE	DEFAULT	DESCRIPTION
1				(Ignored by code)
2	VPLC	Character	OFF	Specifies if information is written to the vector file, ON or OFF
3	NVPL	Integer		Number of vector plot dates

This card specifies if information is output to the [vector plot file \[VPLFN\]](#) and the number of vector plot intervals for specifying output dates and frequencies. The current version still requires the user to develop their own means of postprocessing data for vector plots.

Example

```
VPL PLOT      VPLC      NVPL
Wb 1          ON        7
Wb 2          ON        7
Wb 3          ON        7
```

Related Cards and Files

- [Vector Plot Date](#)
- [Vector Plot Frequency](#)
- [Vector Plot Filename](#)

Vector Plot Date (VPL DATE)

FIELD	NAME	VALUE	DESCRIPTION
1			(Ignored by code)
2-10	VPLD	Real	Output dates, <i>Julian day</i>

This card specifies the dates that information is output to the [vector plot file \[VPLFN\]](#). If there are more dates than can be specified on one line, then they are continued on the next line without another **VPL DATE** card being specified.

Example

VPL DATE	VPLD	VPLD	VPLD						
Wb 1	224.5	225.5	226.5	227.5	228.5	229.5	230.5		
Wb 2	224.5	225.5	226.5	227.5	228.5	229.5	230.5		
Wb 3	224.5	225.5	226.5	227.5	228.5	229.5	230.5		

Related Cards and Files

[Vector Plot](#)

[Vector Plot Frequency](#)

[Vector Plot Filename](#)

Vector Plot Frequency (VPL FREQ)

FIELD	NAME	VALUE	DESCRIPTION
1			(Ignored by code)
2-10	VPLF	Real	Output frequency, <i>days</i>

This card specifies the frequency information is output to the [vector plot file \[VPLFN\]](#). Frequency can be changed at any time during the simulation by specifying the dates on the [Vector Plot Date](#) card and the frequencies on the **Vector Plot Frequency** card. If output is needed only for the date specified on the [Vector Plot Date](#) card, then set the frequency to be greater than the number of days before the next output date.

If there are more frequencies than can be specified on one line, then they are continued on the next line without another **VPL FREQ** card being specified.

Example

VPL FREQ	VPLF	VPLF	VPLF						
Wb 1	100.0	100.0	100.0	100.0	100.0	100.0	100.0		
Wb 2	100.0	100.0	100.0	100.0	100.0	100.0	100.0		
Wb 3	100.0	100.0	100.0	100.0	100.0	100.0	100.0		

Related Cards and Files

- [Vector Plot](#)
- [Vector Plot Date](#)
- [Vector Plot Filename](#)

Contour Plot (CPL PLOT)

FIELD	NAME	VALUE	DEFAULT	DESCRIPTION
1				(Ignored by code)
2	CPLC	Character	OFF	Specifies if information is output to the contour file, ON or OFF
3	NCPL	Integer		Number of contour plot dates

This card specifies if information is output to the [contour plot file \[CPLFN\]](#) and the number of contour plot intervals for specifying output dates and frequencies. The current version still requires the user to develop their own means of postprocessing data for contour plots. This also requires the user to “get under the hood” of the code in order to determine the data output and the format of the output to generate their own contour plots.

Example

CPL PLOT	CPLC	NCPL
Wb 1	ON	7
Wb 2	ON	7
Wb 3	ON	7

Related Cards and Files

[Contour Plot Date](#)
[Contour Plot Frequency](#)
[Contour Plot Filename](#)
[Constituent Output](#)

Contour Plot Dates (CPL DATE)

FIELD	NAME	VALUE	DESCRIPTION
1			(Ignored by code)
2-10	CPLD	Real	Output dates, <i>Julian day</i>

This card specifies the dates that information is output to the [contour plot file \[CPLFN\]](#). If there are more dates than can be specified on one line, then they are continued on the next line without another **CPL DATE** card being specified.

Example

CPL DATE	CPLD	CPLD	CPLD						
Wb 1	224.5	225.5	226.5	227.5	228.5	229.5	230.5		
Wb 2	224.5	225.5	226.5	227.5	228.5	229.5	230.5		
Wb 3	224.5	225.5	226.5	227.5	228.5	229.5	230.5		

Related Cards and Files

- [Contour Plot](#)
- [Contour Plot Frequency](#)
- [Contour Plot Filename](#)
- [Constituent Output](#)

Contour Plot Frequency (CPL FREQ)

FIELD	NAME	VALUE	DESCRIPTION
1			(Ignored by code)
2-10	CPLF	Real	Output frequency, <i>days</i>

This card specifies the frequency information is output to the [contour plot file \[CPLFN\]](#). Frequency can be changed at any time during the simulation by specifying appropriate dates on the [Contour Plot Date](#) card and frequencies on the **Contour Plot Frequency** card. If output is needed only for the date specified on the [Contour Plot Date](#) card, then set the frequency to be greater than the number of days before the next output date.

If there are more frequencies than can be specified on one line, then they are continued on the next line without another **CPL FREQ** card being specified.

Example

CPL FREQ	CPLF								
Wb 1	10.0	10.0	10.0	10.0	10.0	10.0	10.0		
Wb 2	10.0	10.0	10.0	10.0	10.0	10.0	10.0		
Wb 3	10.0	10.0	10.0	10.0	10.0	10.0	10.0		

Related Cards and Files

[Contour Plot](#)
[Contour Plot Date](#)
[Contour Plot Filename](#)
[Constituent Output](#)

Kinetic Flux Output (FLUXES)

FIELD	NAME	VALUE	DEFAULT	DESCRIPTION
1				(Ignored by code)
2	FLXC	Character	OFF	Specifies if information is sent to the kinetic flux output file, ON or OFF
3	NFLX	Integer		Number of kinetic flux dates

This card specifies if information is output to the [kinetic flux file \[KFLFN\]](#) and the number of kinetic flux intervals for specifying output dates and frequencies. This file contains advective, diffusive, and kinetic fluxes that allow the user to determine the dominant forcing function responsible for a given constituents increase/decrease in concentrations and is particularly useful during water quality calibration as the user can identify which kinetic processes are most responsible for the model behavior of a given constituent and adjust the rate coefficients correspondingly. Advective and diffusive fluxes are currently not implemented.

Example

FLUXES	FLXC	NFLX
Wb 1	OFF	0
Wb 2	OFF	0
Wb 3	OFF	0

Related Cards and Files

[Kinetic Flux Date](#)

[Kinetic Flux Frequency](#)

[Kinetic Flux Filename](#)

Kinetic Flux Date (KFL DATE)

FIELD	NAME	VALUE	DESCRIPTION
1			(Ignored by code)
2-10	KFLD	Real	Output dates, <i>Julian day</i>

This card specifies the dates that information is output to the [kinetic flux file \[KFLFN\]](#). If there are more dates than can be specified on one line, then they are continued on the next line without another **KFL DATE** card being specified.

Example

```

FLX DATE      FLXD      FLXD      FLXD      FLXD      FLXD      FLXD      FLXD      FLXD
Wb 1
Wb 2
Wb 3

```

Related Cards and Files

[Kinetic Flux Output](#)
[Kinetic Flux Frequency](#)
[Kinetic Flux Filename](#)

Kinetic Flux Frequency (FLX FREQ)

FIELD	NAME	VALUE	DESCRIPTION
1			(Ignored by code)
2-10	FLXF	Real	Output frequency, <i>days</i>

This card specifies the frequency information is output to the [kinetic flux file \[KFLFN\]](#). If there are more dates than can be specified on one line, then they are continued on the next line without another **KFL FREQ** card being specified. If output is needed only for the date specified on the [Kinetic Flux Date](#) card, then set the frequency to be greater than the number of days before the next output date.

Example

```

FLX FREQ   FLXF   FLXF   FLXF   FLXF   FLXF   FLXF   FLXF   FLXF
Wb 1
Wb 2
Wb 3
    
```

Related Cards and Files

- [Kinetic Flux Output](#)
- [Kinetic Flux Date](#)
- [Kinetic Flux Filename](#)

Time Series Plot (TSR PLOT)

FIELD	NAME	VALUE	DEFAULT	DESCRIPTION
1				(Ignored by code)
2	TSRC	Character	OFF	Specifies if information is written to time series file, ON or OFF
3	NTSR	Integer		Number of time series dates
4	NIKTSR	Integer		Number of time series computational cells

This card specifies if information is output to the [times series file](#) [[TSRFN](#)] the number of time series intervals for specifying output dates and frequencies, and the number of time series computational cells for which information will be output.

Time series output consists of the Julian date, timestep, water surface elevation, temperature, flow rate (for the entire segment), shortwave solar radiation (net) incident on the surface (i.e., it does not include the reflected solar), equilibrium temperature, depth to bottom of channel (m), surface width (m), shade fraction (1.0 is no shade, 0.0 is 100% reduction in solar radiation), active constituents and derived constituents, and vertically integrated segment flow rate at the specified model segment and layer. The constituent concentrations output are the constituents specified for output on the [Constituent Output](#) card. The derived constituent concentrations output are the constituents specified on the [Derived Constituent](#) card.

Example

TSR PLOT	TSRC	NTSR	NIKTSR
Wb 1	OFF	0	0
Wb 2	ON	1	5
Wb 3	OFF	0	0

Related Cards and Files

[Time Series Date](#)
[Time Series Frequency](#)
[Time Series Segment](#)
[Time Series Elevation](#)
[Constituent Output](#)

Time Series Date (TSR DATE)

FIELD	NAME	VALUE	DESCRIPTION
1			(Ignored by code)
2-10	TSRD	Real	Output dates, <i>Julian day</i>

This card specifies the dates that information is output to the [times series file \[TSRFN\]](#). If there are more dates than can be specified on one line, then they are continued on the next line without another **TSR DATE** card being specified.

Example

TSR DATE	TSRD								
Wb 1	63.5								
Wb 2	63.5								
Wb 3	63.5								

Related Cards and Files

- [Time Series Plot](#)
- [Time Series Frequency](#)
- [Time Series Segment](#)
- [Time Series Elevation](#)
- [Constituent Output](#)

Time Series Frequency (TSR FREQ)

FIELD	NAME	VALUE	DESCRIPTION
1			(Ignored by code)
2-10	TSRF	Real	Output frequency, <i>days</i>

This card specifies the frequency information is output to the [times series file \[TSRFN\]](#). Frequency can be changed at any time during the simulation by specifying the dates on the [Time Series Date](#) card and the frequencies on the **Time Series Frequency** card. If output is needed only for the date specified on the [Time Series Date](#) card, then set the frequency to be greater than the number of days before the next output date.

If there are more frequencies than can be specified on one line, then they are continued on the next line without another **TSR FREQ** card being specified.

Example

```

TSR FREQ   TSRF   TSRF   TSRF   TSRF   TSRF   TSRF   TSRF   TSRF   TSRF
Wb 1
Wb 2       0.2
Wb 3

```

Related Cards and Files

[Time Series Plot](#)
[Time Series Date](#)
[Time Series Segment](#)
[Time Series Elevation](#)
[Constituent Output](#)

Time Series Segment (TSR SEG)

FIELD	NAME	VALUE	DESCRIPTION
1			(Ignored by code)
2-10	ITSR	Integer	Output segments

This card, along with the [Time Series Elevation](#) card, defines which computational cells are output to the [times series file \[TSRFN\]](#). To specify multiple cells in a segment, the segment number must be duplicated for each computational cell to be output.

Example

TSR SEG	ITSR								
Wb 1	20	23	26	30	30				
Wb 2	33	35	36	40	40				
Wb 3	43	45	47	49	50				

Related Cards and Files

[Time Series Plot](#)

[Time Series Date](#)

[Time Series Frequency](#)

[Time Series Elevation](#)

[Constituent Output](#)

Time Series Elevation (TSR ELEV)

FIELD	NAME	VALUE	DESCRIPTION
1			(Ignored by code)
2-10	ETSR	Real	Layer corresponding to time series segment

This card specifies the elevation from the water surface that corresponds to the segment [[ITSR](#)] specified on the [Time Series Segment](#) card. Specifying a negative number results in the layer number being used for the vertical location. For example, setting [ETSR] to -5.0 results in output from layer 5.

Example

TSR ELEV	ETSR								
Wb 1	1.0	5.0	10.0	-1.0	-8.0				
Wb 2	1.0	5.0	10.0	-1.0	-8.0				
Wb 3	1.0	5.0	10.0	-1.0	-8.0				

Related Cards and Files

[Time Series Plot](#)
[Time Series Date](#)
[Time Series Frequency](#)
[Time Series Segment](#)
[Constituent Output](#)

Withdrawal Output (WITH OUT)

FIELD	NAME	VALUE	DEFAULT	DESCRIPTION
1				(Ignored by code)
2	WDOC	Character	OFF	Specifies if information is written to withdrawal output file, ON or OFF
3	NWDO	Integer		Number of withdrawal output dates
4	NIWDO	Integer		Number of withdrawal output segments

This card specifies if information is output to a separate [withdrawal outflow file \[WDOFN\]](#) for outflow, outflow temperature, outflow constituent concentrations, and outflow derived constituent concentrations. This option is useful for comparing time series results of these variables. The names of the outflow files are appended with the segment number to differentiate each of the files.

The information can also be used to link output from one waterbody to a downstream waterbody. Currently, the model uses the minimum timestep necessary to maintain numerical stability throughout the entire system. In many cases, the riverine sections linking reservoirs and/or estuaries together in the system determine this. This option is provided to allow the user to break up the waterbasin so that each waterbody can be run separately. As a consequence, the separate waterbodies can now run at a timestep necessary to maintain numerical stability based on the limiting timestep criteria for the individual waterbody rather than the limiting criteria for the entire system.

When using this option, the user should investigate how the frequency of output affects the results by first running the model with the frequency set to 0.0 and then increasing the frequency until the results change substantially. Model results should not be a function of the input frequency of boundary conditions.

Example

```
WITH OUT      WDOC      NWDO      NIWDO
              ON        1          2
```

Related Cards and Files

- [Withdrawal Output Date](#)
- [Withdrawal Output Frequency](#)
- [Withdrawal Output Segment](#)

Withdrawal Output Date (WDO DATE)

FIELD	NAME	VALUE	DESCRIPTION
1			(Ignored by code)
2	WDOD	Real	Output dates, <i>Julian day</i>

This card specifies the dates information is output to the [withdrawal outflow file \[WDOFN\]](#). If there are more dates than can be specified on one line, then they are continued on the next line without another **WDO DATE** card being specified.

Example

```
WDO DATE      WDOD      WDOD      WDOD      WDOD      WDOD      WDOD      WDOD      WDOD
              63.5
```

Related Cards and Files

[Withdrawal Output](#)
[Withdrawal Output Frequency](#)
[Withdrawal Output Segment](#)

Withdrawal Output Frequency (WDO FREQ)

FIELD	NAME	VALUE	DESCRIPTION
1			(Ignored by code)
2-10	WDOF	Real	Output frequency, <i>days</i>

This card specifies the frequency information is output to the [withdrawal outflow file \[WDOFN\]](#). Frequency can be changed at any time during the simulation by specifying the dates on the [Withdrawal Output Date](#) card and the frequencies on the [Withdrawal Output Frequency](#) card. If output is needed only for the date specified on the [Withdrawal Output Date](#) card, then set the frequency to be greater than the number of days before the next output date.

If there are more frequencies than can be specified on one line, then they are continued on the next line without another **WDO FREQ** card being specified.

Example

```
WDO FREQ      WDOF      WDOF      WDOF      WDOF      WDOF      WDOF      WDOF      WDOF      WDOF
              0.2
```

Related Cards and Files

- [Withdrawal Output](#)
- [Withdrawal Output Date](#)
- [Withdrawal Output Segment](#)

Withdrawal Output Segment (WITH SEG)

FIELD	NAME	VALUE	DESCRIPTION
1			(Ignored by code)
2-10	IWDO	Integer	Output segments

This card specifies model segments for which information is output to the withdrawal output file [[WDOFN](#)]. If a downstream segment of a reservoir is specified, then information is output at the frequency specified in the [Withdrawal Output Frequency](#) card that can be used as input files to a waterbody downstream of the reservoir.

If there are more segments than can be specified on one line, then they are continued on the next line without another **WITH SEG** card being specified.

Example

```
WITH SEG  IWDO  IWDO  IWDO  IWDO  IWDO  IWDO  IWDO  IWDO  IWDO
          30    32
```

Related Cards and Files

[Withdrawal Output](#)
[Withdrawal Output Date](#)
[Withdrawal Output Frequency](#)

Restart (RESTART)

FIELD	NAME	VALUE	DEFAULT	DESCRIPTION
1				(Ignored by code)
2	RSOC	Character	OFF	Specifies if information is output to the restart file, ON or OFF
3	NRSO	Integer		Number of restart dates
4	RSIC	Character	OFF	Specifies if information is input from the restart file, ON or OFF

This card specifies if information is output to the restart output file [[RSOFN](#)] or read into the model from a previously output restart file [[RSIFN](#)] and the number of restart dates. This option is currently not working in the current release, but will be made functional in the next release.

Example

```

RESTART      RSOC      NRSO      RSIC
              ON        2          OFF
    
```

Related Cards and Files

- [Restart Date](#)
- [Restart Frequency](#)

Restart Date (RSO DATE)

FIELD	NAME	VALUE	DESCRIPTION
1			(Ignored by code)
2-10	RSOD	Real	Output dates, Julian day

This card specifies dates information is output to the restart file [\[RSOFN\]](#). If there are more dates than can be specified on one line, then they are continued on the next line without another **RSO DATE** card being specified.

Example

```
RSO DATE      RSOD      RSOD      RSOD      RSOD      RSOD      RSOD      RSOD      RSOD      RSOD
              224.5    230.5
```

Related Cards and Files

[Restart](#)
[Restart Frequency](#)

Restart Frequency (RSO FREQ)

FIELD	NAME	VALUE	DESCRIPTION
1			(Ignored by code)
2-10	RSOF	Real	Output frequency, <i>days</i>

This card specifies the frequency information is output to the restart plot file [[RSOFN](#)]. Frequencies can be changed at any time during the simulation by specifying the appropriate dates on the [Restart Date](#) card and frequencies on the Restart Frequency card. If output is needed only for the date specified on the [Restart Date](#) card, then set the frequency to be greater than the number of days before the next output date.

If there are more frequencies than can be specified on one line, then they are continued on the next line without another **RSO FREQ** card being specified.

Example

```
RSO FREQ      RSOF      RSOF      RSOF      RSOF      RSOF      RSOF      RSOF      RSOF      RSOF
              100.0     100.0
```

Related Cards and Files

- [Restart](#)
- [Restart Date](#)

Constituent Computations (CST COMP)

FIELD	NAME	VALUE	DEFAULT	DESCRIPTION
1				(Ignored by code)
2	CCC	Character	OFF	Specifies if constituents are computed, ON or OFF
3	LIMC	Character	OFF	Output algal growth limiting factor, ON or OFF
4	CUF	Integer	1	Frequency which constituent kinetics are updated

This card starts the specification of constituent computations. [CCC] determines if constituent computations are performed. If this variable is turned off, then constituent computations are not performed and all information specified on the remaining constituent control cards is ignored. Individual constituent computations are controlled on the [Active Constituents](#) card. During the initial calibration runs for freshwater systems, constituent computations are usually turned off until temperature, water surface elevations, and velocities are calibrated.

The [LIMC] variable specifies whether the factor limiting algal growth is output to the [snapshot file \[SNPFN\]](#).

The model allows the user to update constituent kinetics at a different frequency than constituent transport. The constituent update frequency [CUF] specifies how many transport iterations are performed before constituent kinetics are updated. This option is included primarily to reduce computation time. This variable should be set to one during initial calibration. If computation time is of concern, [CUF] can be increased until water quality results begin to deviate. Model results should not be a function of the timestep used during the simulation.

Example

```
CST COMP      CCC      LIMC      CUF
              ON       OFF       1
```

Related Cards and Files

[Active Constituents](#)
[Constituent Initial Concentration](#)
[Constituent Output](#)
[Inflow Active Constituent Control](#)
[Tributary Active Constituent Control](#)
[Distributed Tributary Active Constituent Control](#)
[Precipitation Active Constituent Control](#)

Active Constituents (CST ACTIVE)

FIELD	NAME	VALUE	DEFAULT	DESCRIPTION
1				(Ignored by code)
2-10	CAC	Character	OFF	Specifies if calculations are to be performed for this constituent, ON or OFF

This card specifies which constituents are included in water quality calculations. The current version now allows the user the flexibility to include any number of generic, inorganic suspended solids, algal and/or epiphyton groups, and CBOD groups. The number of these groups is specified on the [Constituent Dimension](#) card. The generic constituent can be used to simulate any number of constituents that can be defined with a zero-order decay rate and/or a first order decay rate, and/or a settling velocity, and/or an Arrhenius temperature rate multiplier. This includes a conservative tracer with all kinetic coefficients set to zero, residence time with the zero-order decay rate set to -1.0 day^{-1} , and coliform bacteria where a temperature rate multiplier, first-order decay rate, and/or a settling velocity are defined.

The user has the flexibility of including/excluding any of the constituent state variables. The constituent kinetics are strongly coupled and failure to include one or more constituents can have far reaching effects that are hard to determine beforehand, so use this option carefully. Some previous applications have modeled only dissolved oxygen with the zero-order sediment oxygen demand used for calibration. This was deemed acceptable as the applications were looking only at how different reservoir operations and their impacts on hydrodynamics would affect temperature and dissolved oxygen.

CONTROL FILE

CONSTITUENT CONTROL

Example

CST ACTIVE	CAC	
TDS	OFF	Total dissolved solids or salinity
TRACER	OFF	Generic constituent 1 - conservative tracer
AGE	OFF	Generic constituent 1 - residence time
COL1	ON	Generic constituent 1 - coliform group 1
COL2	ON	Generic constituent 1 - coliform group 2
ISS1	ON	Inorganic suspended solids group 1
ISS2	ON	Inorganic suspended solids group 1
ISS3	ON	Inorganic suspended solids group 1
PO4	ON	Dissolved inorganic phosphorus
NH4	ON	Ammonium
NO3	ON	Nitrate-nitrite
DSI	ON	Dissolved silica
PSI	ON	Particulate biogenic silica
FE	ON	Dissolved iron
LDOM	ON	Labile dissolved organic matter
RDOM	ON	Refractory dissolved organic matter
LPOM	ON	Labile particulate organic matter
RPOM	ON	Refractory particulate organic matter
CBOD1	ON	CBOD group 1
CBOD2	ON	CBOD group 2
CBOD3	ON	CBOD group 3
ALG1	ON	Algal group 1
ALG2	ON	Algal group 2
ALG3	ON	Algal group 3
DO	ON	Dissolved oxygen
TIC	ON	Total inorganic carbon
ALK	ON	Alkalinity

Related Cards and Files

[Constituent Computations](#)

[Constituent Initial Concentration](#)

[Constituent Output](#)

[Inflow Active Constituent Control](#)

[Tributary Active Constituent Control](#)

[Distributed Tributary Active Constituent Control](#)

[Precipitation Active Constituent Control](#)

Derived Constituents (CST DERIVE)

FIELD	NAME	VALUE	DEFAULT	DESCRIPTION
1				(Ignored by code)
2-10	CDWBC	Character	OFF	Specifies if derived variables are output for each waterbody, ON or OFF

This card allows the user to specify whether certain derived constituents are computed and output in order to compare with observed data. Derived constituents are constituents that are not state variables, but are useful for gaining a better understanding of how the water quality formulations are simulating the prototype. They are also useful for comparing computed versus observed data for water quality parameters that are not state variables, but that are routinely monitored, such as total Kjeldahl nitrogen.

In Version 2, pH computations were incorrectly included as a state variable. The current version now includes pH computations as a derived variable as pH is computed from the total inorganic carbon and alkalinity state variables.

Example

CST	DERIVE	CDWBC								
DOC		OFF	OFF	OFF						Dissolved organic carbon
POC		OFF	OFF	OFF						Particulate organic carbon
TOC		OFF	OFF	OFF						Total organic carbon
DON		OFF	OFF	OFF						Dissolved organic nitrogen
PON		OFF	OFF	OFF						Particulate organic nitrogen
TON		OFF	OFF	OFF						Total organic nitrogen
TKN		OFF	OFF	OFF						Total Kjeldahl nitrogen
TN		OFF	OFF	OFF						Total nitrogen
DOP		OFF	OFF	OFF						Dissolved organic phosphorus
POP		OFF	OFF	OFF						Particulate organic phosphorus
TOP		OFF	OFF	OFF						Total organic phosphorus
TP		OFF	OFF	OFF						Total phosphorus
APR		OFF	OFF	OFF						Algal production
CHLA		OFF	OFF	OFF						Chlorophyll a
ATOT		OFF	OFF	OFF						Total algal biomass
%DO		OFF	OFF	OFF						Dissolved oxygen saturation
TSS		OFF	OFF	OFF						Total suspended solids
TISS		OFF	OFF	OFF						Total inorganic suspended solids
CBODU		OFF	OFF	OFF						Total carbonaceous BOD (ultimate)
Ph		ON	OFF	OFF						pH
CO2		OFF	OFF	OFF						Carbon dioxide
HCO3		OFF	OFF	OFF						Bicarbonate
CO3		OFF	OFF	OFF						Carbonate

Related Cards and Files

- [Constituent Computations](#)
- [Active Constituents](#)

Constituent Fluxes (CST FLUX)

FIELD	NAME	VALUE	DEFAULT	DESCRIPTION
1				(Ignored by code)
2-10	CFWBC	Character	OFF	Specifies which kinetic fluxes are output for each waterbody, ON or OFF

This card allows the user to specify whether constituent advective, diffusive, and kinetic fluxes are computed and output in order to evaluate their importance on the resulting constituent state variable computed concentrations. For example, if all the fluxes associated with dissolved oxygen in the model are output, then the user can determine the most important fluxes affecting DO and adjust the kinetic rate coefficients accordingly during calibration. This should greatly reduce the time required for water quality calibration and provide a greater understanding of kinetic behavior in the model and the prototype. Only the kinetic fluxes are computed in the current release. Advective and diffusive fluxes will be included in the next release.

Example

CST FLUX	CFWBC	CFWBC	CFWBC	CFWBC	CFWBC	CFWBC	CFWBC	CFWBC	CFWBC
TISSIN	OFF	OFF	OFF	Total inorganic suspended solids settling, source					
TISSOUT	OFF	OFF	OFF	Total inorganic suspended solids settling, sink					
PO4AR	OFF	OFF	OFF	PO4 from algal respiration, source					
PO4AG	OFF	OFF	OFF	PO4 from algal growth, sink					
PO4AP	OFF	OFF	OFF	Net PO4 algal uptake, source/sink					
PO4ER	OFF	OFF	OFF	PO4 from epiphyton respiration, source					
PO4EG	OFF	OFF	OFF	PO4 from epiphyton growth, sink					
PO4EP	OFF	OFF	OFF	Net PO4 epiphyton uptake, source/sink					
PO4POM	OFF	OFF	OFF	PO4 from particulate organic matter, source					
PO4DOM	OFF	OFF	OFF	PO4 from dissolved organic matter, source					
PO4OM	OFF	OFF	OFF	PO4 from organic matter, source					
PO4SED	OFF	OFF	OFF	PO4 from sediment compartment, source					
PO4SOD	OFF	OFF	OFF	PO4 from 0-order sediment release, source					
PO4SET	OFF	OFF	OFF	Sorbed PO4 from settling, source/sink					
NH4NITR	OFF	OFF	OFF	NH4 from nitrification, sink					
NH4AR	OFF	OFF	OFF	NH4 from algal respiration, source					
NH4AG	OFF	OFF	OFF	NH4 from algal growth, sink					
NH4AP	OFF	OFF	OFF	Net NH4 from algal growth, sink					
NH4ER	OFF	OFF	OFF	NH4 from epiphyton respiration, source					
NH4EG	OFF	OFF	OFF	NH4 from epiphyton growth, sink					
NH4EP	OFF	OFF	OFF	Net NH4 from epiphyton growth, sink					
NH4ANET	OFF	OFF	OFF	Net NH4 algal uptake, source/sink					
NH4POM	OFF	OFF	OFF	NH4 from particulate organic matter, source					
NH4DOM	OFF	OFF	OFF	NH4 from dissolved organic matter, source					
NH4OM	OFF	OFF	OFF	NH4 from organic matter decay					
NH4SED	OFF	OFF	OFF	NH4 from sediment compartment, source					
NH4SOD	OFF	OFF	OFF	NH4 from 0-order sediment release, source					
NO3DEN	OFF	OFF	OFF	NO3 from denitrification, sink					
NO3AG	OFF	OFF	OFF	NO3 from algal growth, sink					
NO3EG	OFF	OFF	OFF	NO3 from epiphyton growth, sink					
NO3SED	OFF	OFF	OFF	NO3 from sediment compartment, source					
DSIAG	OFF	OFF	OFF	Dissolved Si from algal growth, sink					
DSIEG	OFF	OFF	OFF	Dissolved Si from epiphyton growth, sink					
DSIPBSI	OFF	OFF	OFF	Dissolved Si from particulate biogenic Si, source					
DSISED	OFF	OFF	OFF	Dissolved Si from sediment compartment, source					
DSISOD	OFF	OFF	OFF	Dissolved Si from 0-order sediment release, source					
DSISET	OFF	OFF	OFF	Dissolved Si from sorbed Si settling, source/sink					
PBSIAM	OFF	OFF	OFF	Particulate biogenic Si from algal mortality, source					
PBSINET	OFF	OFF	OFF	Particulate biogenic Si from settling, source/sink					
PBSIDK	OFF	OFF	OFF	Particulate biogenic Si decay, sink					
FESET	OFF	OFF	OFF	Fe from settling, source/sink					

CONSTITUENT CONTROL

CONTROL FILE

FESED	OFF	OFF	OFF Fe from sediment release, source
LDOMDK	OFF	OFF	OFF Labile DOM decay, sink
LRDOM	OFF	OFF	OFF Labile to refractory DOM decay, sink
RDOMDK	OFF	OFF	OFF Refractory DOM decay, sink
LDOMAP	OFF	OFF	OFF Labile DOM from algal mortality, source
LDOMEPI	OFF	OFF	OFF Labile DOM from epiphyton mortality, source
LPOMDK	OFF	OFF	OFF Labile POM decay, sink
LRPOM	OFF	OFF	OFF Refractory to refractory POM decay, sink
RPOMDK	OFF	OFF	OFF Refractory POM decay, sink
LPOMAP	OFF	OFF	OFF Labile POM from algal mortality, source
LPOMSET	OFF	OFF	OFF Labile POM from settling, source/sink
RPOMSET	OFF	OFF	OFF Refractory POM from settling, source/sink
CBODDK	OFF	OFF	OFF CBOD decay, sink
DOAP	OFF	OFF	OFF DO from algal production, source
DOAR	OFF	OFF	OFF DO from algal respiration, sink
DOEP	OFF	OFF	OFF DO from epiphyton production, source
DOER	OFF	OFF	OFF DO from epiphyton respiration, sink
DOPOM	OFF	OFF	OFF DO from POM decay, sink
DODOM	OFF	OFF	OFF DO from DOM decay, sink
DOOM	OFF	OFF	OFF DO from OM decay, sink
DONITR	OFF	OFF	OFF DO from nitrification, sink
DOCBOD	OFF	OFF	OFF DO from CBOD decay, sink
DOREAR	OFF	OFF	OFF DO from reaeration, source
DOSED	OFF	OFF	OFF DO from sediment compartment decay, sink
DOSOD	OFF	OFF	OFF DO from 0-order sediment compartment, sink
TICAG	OFF	OFF	OFF Total inorganic carbon from algal growth, sink
TICEG	OFF	OFF	OFF Total inorganic carbon from epiphyton growth, sink
SEDDK	OFF	OFF	OFF Sediment compartment decay, sink
SEDAS	OFF	OFF	OFF Sediment compartment from algal settling, source
SEDLPOM	OFF	OFF	OFF Sediment compartment from LPOM settling, source
SEDSET	OFF	OFF	OFF Sediment compartment from net settling, source/sink
SODDK	OFF	OFF	OFF Sediment compartment from decay, sink

Related Cards and Files

[Constituent Computations](#)
[Active Constituents](#)

Constituent Initial Concentration (CST ICON)

FIELD	NAME	VALUE	DESCRIPTION
1			(Ignored by code)
2-10	C2IWB	Real	Initializes entire grid to this concentration, or specifies a vertical and/or longitudinal profile be used to initialize grid, $g\ m^{-3}$

This card allows the user to specify an initial concentration for each constituent. The user has three options. Initial concentrations can be specified as a single value, a single vertical profile which is used to initialize every segment, or a vertical profile for each segment.

Initial condition	[IC2]
Isoconcentration	>0.0
Single vertical profile	-1.0
Vertical profile at each segment	-2.0

Example

CST ICON	C2IWB	C2IWB	C2IWB	C2IWB	C2IWB	C2IWB	C2IWB	C2IWB	C2IWB
TDS	200.0	200.0	200.0	200.0	Total dissolved solids or salinity				
TRACER	1000.0	1000.0	1000.0	1000.0	Generic constituent 1 - conservative tracer				
AGE	0.0	0.0	0.0	0.0	Generic constituent 2 - residence time				
COL1	1.0	1.0	1.0	1.0	Generic constituent 3 - coliform group 1				
COL2	1.0	1.0	1.0	1.0	Generic constituent 4 - coliform group 1				
ISS1	5.0	5.0	5.0	5.0	Inorganic suspended solids group 1				
ISS2	3.5	3.5	3.5	3.5	Inorganic suspended solids group 2				
ISS3	4.5	4.5	4.5	4.5	Inorganic suspended solids group 3				
PO4	0.1	0.1	0.1	0.1	Dissolved inorganic phosphorus				
NH4	0.1	0.1	0.1	0.1	Ammonium				
NO3	0.1	0.1	0.1	0.1	Nitrate-nitrite				
DSI	5.0	5.0	5.0	5.0	Dissolved silica				
PSI	1.0	1.0	1.0	1.0	Particulate biogenic silica				
FE	1.0	1.0	1.0	1.0	Iron				
LDOM	1.0	1.0	1.0	1.0	Labile dissolved organic matter				
RDOM	1.0	1.0	1.0	1.0	Refractory dissolved organic matter				
LPOM	2.0	2.0	2.0	2.0	Labile particulate organic matter				
RPOM	1.0	1.0	1.0	1.0	Refractory particulate organic matter				
CBOD1	1.0	1.0	1.0	1.0	Carbonaceous biochemical oxygen demand group 1				
CBOD2	1.0	1.0	1.0	1.0	Carbonaceous biochemical oxygen demand group 2				
CBOD3	1.0	1.0	1.0	1.0	Carbonaceous biochemical oxygen demand group 3				
ALG1	1.0	1.0	1.0	1.0	Algal group 1				
ALG2	1.0	1.0	1.0	1.0	Algal group 2				
ALG3	1.0	1.0	1.0	1.0	Algal group 3				
DO	8.0	8.0	7.0	7.0	Dissolved oxygen				
TIC	3.5	3.5	3.5	3.5	Total inorganic carbon				
ALK	80.0	50.0	30.0	30.0	Alkalinity				

Related Cards and Files

[Constituent Computations](#)
[Active Constituents](#)
[Vertical Profile File](#)
[Longitudinal Profile File](#)

Constituent Output (CST PRINT)

FIELD	NAME	VALUE	DEFAULT	DESCRIPTION
1				(Ignored by code)
2-10	CPRWBC	Character	OFF	Specifies which constituents are printed to output files, ON or OFF

This card specifies which constituents are printed to the [snapshot file \[SNPFN\]](#), [time series file \[TSRFN\]](#), [profile plot file \[PRFFN\]](#), and [contour plot file \[CPLFN\]](#). The user does not have control over which constituents will be sent to an individual file.

Example

CST PRINT	CPRWBC	CPRWBC	CPRWBC	CPRWBC	CPRWBC	CPRWBC	CPRWBC	CPRWBC	CPRWBC
TDS	ON	ON	ON	Total dissolved solids or salinity					
TRACER	ON	ON	ON	Generic constituent 1 - tracer					
AGE	ON	ON	ON	Generic constituent 2 - residence time					
COL1	ON	ON	ON	Generic constituent 3 - coliform group 1					
COL2	ON	ON	ON	Generic constituent 4 - coliform group 2					
ISS1	ON	ON	ON	Inorganic suspended solids group 1					
ISS2	ON	ON	ON	Inorganic suspended solids group 2					
ISS3	ON	ON	ON	Inorganic suspended solids group 3					
PO4	ON	ON	ON	Inorganic dissolved phosphorus					
NH4	ON	ON	ON	Ammonium					
NO3	ON	ON	ON	Nitrate-nitrite					
DSI	ON	ON	ON	Dissolved silica					
PSI	ON	ON	ON	Particulate biogenic silica					
FEe	ON	ON	ON	Iron					
LDOM	ON	ON	ON	Labile dissolved organic matter					
RDOM	ON	ON	ON	Refractory dissolved organic matter					
LPOM	ON	ON	ON	Labile particulate organic matter					
RPOM	ON	ON	ON	Refractory particulate organic matter					
CBOD1	ON	ON	ON	Carbonaceous BOD group 1					
CBOD2	ON	ON	ON	Carbonaceous BOD group 2					
CBOD3	ON	ON	ON	Carbonaceous BOD group 3					
ALG1	ON	ON	ON	Algal group 1					
ALG2	ON	ON	ON	Algal group 2					
ALG3	ON	ON	ON	Algal group 3					
DO	ON	ON	ON	Dissolved oxygen					
TIC	ON	ON	ON	Total inorganic carbon					
ALK	ON	ON	ON	Alkalinity					

Related Cards and Files

- [Snapshot Print](#)
- [Profile Plot](#)
- [Time Series Plot](#)
- [Spreadsheet Plot](#)
- [Contour Plot](#)

Inflow Active Constituent Control (CIN CON)

FIELD	NAME	VALUE	DEFAULT	DESCRIPTION
1				(Ignored by code)
2-10	CINBRC	Character	OFF	Specifies which constituents are included in inflow constituent file, ON or OFF

For some applications, inflow concentrations for a particular constituent may not be available. This card allows the user to include in the [inflow concentration file \[CINFN\]](#) only those constituents for which there is a concentration. For those excluded, the model uses a zero concentration for the inflow. As shown in the example, descriptions can be included after the input fields to aid in identifying a given constituent.

Example

CIN CON	CINBRC	CINBRC	CINBRC	CINBRC	CINBRC	CINBRC	CINBRC	CINBRC	CINBRC
TDS	ON	ON	ON	ON	ON	Total dissolved solids or salinity			
TRACER	ON	ON	ON	ON	ON	Generic constituent 1 - tracer			
AGE	OFF	OFF	OFF	OFF	OFF	Generic constituent 2 - residence time			
COL1	ON	ON	ON	ON	ON	Generic constituent 3 - coliform group 1			
COL2	ON	ON	ON	ON	ON	Generic constituent 4 - coliform group 2			
ISS1	ON	ON	ON	ON	ON	Inorganic suspended solids group 1			
ISS2	ON	ON	ON	ON	ON	Inorganic suspended solids group 2			
ISS3	ON	ON	ON	ON	ON	Inorganic suspended solids group 3			
PO4	ON	ON	ON	ON	ON	Inorganic dissolved phosphorus			
NH4	ON	ON	ON	ON	ON	Ammonium			
NO3	ON	ON	ON	ON	ON	Nitrate-nitrite			
DSI	ON	ON	ON	ON	ON	Dissolved silica			
PSI	ON	ON	ON	ON	ON	Particulate biogenic silica			
FE	ON	ON	ON	ON	ON	Iron			
LDOM	ON	ON	ON	ON	ON	Labile dissolved organic matter			
RDOM	ON	ON	ON	ON	ON	Refractory dissolved organic matter			
LPOM	ON	ON	ON	ON	ON	Labile particulate organic matter			
RPOM	ON	ON	ON	ON	ON	Refractory particulate organic matter			
CBOD1	ON	ON	ON	ON	ON	Carbonaceous BOD group 1			
CBOD2	ON	ON	ON	ON	ON	Carbonaceous BOD group 2			
CBOD3	ON	ON	ON	ON	ON	Carbonaceous BOD group 3			
ALG1	ON	ON	ON	ON	ON	Algal group 1			
ALG2	ON	ON	ON	ON	ON	Algal group 2			
ALG3	ON	ON	ON	ON	ON	Algal group 3			
DO	ON	ON	ON	ON	ON	Dissolved oxygen			
TIC	ON	ON	ON	ON	ON	Total inorganic carbon			
ALK	ON	ON	ON	ON	ON	Alkalinity			

Related Cards and Files

[Branch Inflow Constituent File](#)
[Branch Inflow Constituent Filename](#)

Tributary Active Constituent Control (CTR CON)

FIELD	NAME	VALUE	DEFAULT	DESCRIPTION
1				(Ignored by code)
2-10	CTRTRC	Character	OFF	Specifies which constituents are included in tributary inflow constituent file for each tributary, ON or OFF

For some applications, tributary inflow concentrations for a particular constituent may not be available. This card allows the user to include in the [tributary inflow concentration file \[CTR FN\]](#) only those constituents for which there is a concentration.

Example

CTR CON	CTRTRC	CTRTRC	CTRTRC	CTRTRC	CTRTRC	CTRTRC	CTRTRC	CTRTRC	CTRTRC
TDS	ON	Total dissolved solids or salinity							
TRACER	ON	Generic constituent 1 - tracer							
AGE	OFF	Generic constituent 2 - residence time							
COL1	ON	Generic constituent 3 - coliform group 1							
COL2	ON	Generic constituent 4 - coliform group 2							
ISS1	ON	Inorganic suspended solids group 1							
ISS2	ON	Inorganic suspended solids group 2							
ISS3	ON	Inorganic suspended solids group 3							
PO4	ON	Inorganic dissolved phosphorus							
NH4	ON	Ammonium							
NO3	ON	Nitrate-nitrite							
DSI	ON	Dissolved silica							
PSI	ON	Particulate biogenic silica							
FE	ON	Iron							
LDOM	ON	Labile dissolved organic matter							
RDOM	ON	Refractory dissolved organic matter							
LPOM	ON	Labile particulate organic matter							
RPOM	ON	Refractory particulate organic matter							
CBOD1	ON	Carbonaceous BOD group 1							
CBOD2	ON	Carbonaceous BOD group 2							
CBOD3	ON	Carbonaceous BOD group 3							
ALG1	ON	Algal group 1							
ALG2	ON	Algal group 2							
ALG3	ON	Algal group 3							
DO	ON	Dissolved oxygen							
TIC	ON	Total inorganic carbon							
ALK	ON	Alkalinity							

Related Cards and Files

- [Tributary Inflow Concentration File](#)
- [Tributary Inflow Concentration Filename](#)

Distributed Trib Active Constituent (CDT CON)

FIELD	NAME	VALUE	DEFAULT	DESCRIPTION
1				(Ignored by code)
2-10	CDTBRC	Character	OFF	Specifies which constituents are included in distributed tributary inflow constituent file for each branch, ON or OFF

For some applications, distributed tributary inflow concentrations for a particular constituent may not be available. This card allows the user to include in the [distributed tributary inflow concentration file \[CDTFN\]](#) only those constituents for which there is a concentration.

Example

CDT CON	CDTBRC	CDTBRC	CDTBRC	CDTBRC	CDTBRC	CDTBRC	CDTBRC	CDTBRC	CDTBRC
TDS	OFF	OFF	OFF	OFF	OFF	Total dissolved solids or salinity			
TRACER	OFF	OFF	OFF	OFF	OFF	Generic constituent 1 - tracer			
AGE	OFF	OFF	OFF	OFF	OFF	Generic constituent 2 - residence time			
COL1	OFF	OFF	OFF	OFF	OFF	Generic constituent 3 - coliform group 1			
COL2	OFF	OFF	OFF	OFF	OFF	Generic constituent 4 - coliform group 2			
ISS1	OFF	OFF	OFF	OFF	OFF	Inorganic suspended solids group 1			
ISS2	OFF	OFF	OFF	OFF	OFF	Inorganic suspended solids group 2			
ISS3	OFF	OFF	OFF	OFF	OFF	Inorganic suspended solids group 3			
PO4	OFF	OFF	OFF	OFF	OFF	Inorganic dissolved phosphorus			
NH4	OFF	OFF	OFF	OFF	OFF	Ammonium			
NO3	OFF	OFF	OFF	OFF	OFF	Nitrate-nitrite			
DSI	OFF	OFF	OFF	OFF	OFF	Dissolved silica			
PSI	OFF	OFF	OFF	OFF	OFF	Particulate biogenic silica			
FE	OFF	OFF	OFF	OFF	OFF	Iron			
LDOM	OFF	OFF	OFF	OFF	OFF	Labile dissolved organic matter			
RDOM	OFF	OFF	OFF	OFF	OFF	Refractory dissolved organic matter			
LPOM	OFF	OFF	OFF	OFF	OFF	Labile particulate organic matter			
RPOM	OFF	OFF	OFF	OFF	OFF	Refractory particulate organic matter			
CBOD1	OFF	OFF	OFF	OFF	OFF	Carbonaceous BOD group 1			
CBOD2	OFF	OFF	OFF	OFF	OFF	Carbonaceous BOD group 2			
CBOD3	OFF	OFF	OFF	OFF	OFF	Carbonaceous BOD group 3			
ALG1	OFF	OFF	OFF	OFF	OFF	Algal group 1			
ALG2	OFF	OFF	OFF	OFF	OFF	Algal group 2			
ALG3	OFF	OFF	OFF	OFF	OFF	Algal group 3			
DO	OFF	OFF	OFF	OFF	OFF	Dissolved oxygen			
TIC	OFF	OFF	OFF	OFF	OFF	Total inorganic carbon			
ALK	OFF	OFF	OFF	OFF	OFF	Alkalinity			

Related Cards and Files

[Distributed Tributary Inflow Concentration File](#)
[Distributed Tributary Inflow Concentration Filename](#)

Precipitation Active Constituent Control (CPR CON)

FIELD	NAME	VALUE	DEFAULT	DESCRIPTION
1				(Ignored by code)
2-10	CPRBRC	Character	OFF	Specifies which constituents are included in the precipitation inflow constituent file for each branch, ON or OFF

For some applications, precipitation concentrations for a particular constituent may not be available. This card allows the user to include in the [precipitation concentration file \[CPRFN\]](#) only those constituents for which there is a concentration.

Example

CPR CON	CPRBRC	CPRBRC	CPRBRC	CPRBRC	CPRBRC	CPRBRC	CPRBRC	CPRBRC	CPRBRC
TDS	OFF	OFF	OFF	OFF	OFF	Total dissolved solids or salinity			
TRACER	OFF	OFF	OFF	OFF	OFF	Generic constituent 1 - tracer			
AGE	OFF	OFF	OFF	OFF	OFF	Generic constituent 2 - residence time			
COL1	OFF	OFF	OFF	OFF	OFF	Generic constituent 3 - coliform group 1			
COL2	OFF	OFF	OFF	OFF	OFF	Generic constituent 4 - coliform group 2			
ISS1	OFF	OFF	OFF	OFF	OFF	Inorganic suspended solids group 1			
ISS2	OFF	OFF	OFF	OFF	OFF	Inorganic suspended solids group 2			
ISS3	OFF	OFF	OFF	OFF	OFF	Inorganic suspended solids group 3			
PO4	OFF	OFF	OFF	OFF	OFF	Inorganic dissolved phosphorus			
NH4	OFF	OFF	OFF	OFF	OFF	Ammonium			
NO3	OFF	OFF	OFF	OFF	OFF	Nitrate-nitrite			
DSI	OFF	OFF	OFF	OFF	OFF	Dissolved silica			
PSI	OFF	OFF	OFF	OFF	OFF	Particulate biogenic silica			
FE	OFF	OFF	OFF	OFF	OFF	Iron			
LDOM	OFF	OFF	OFF	OFF	OFF	Labile dissolved organic matter			
RDOM	OFF	OFF	OFF	OFF	OFF	Refractory dissolved organic matter			
LPOM	OFF	OFF	OFF	OFF	OFF	Labile particulate organic matter			
RPOM	OFF	OFF	OFF	OFF	OFF	Refractory particulate organic matter			
CBOD1	OFF	OFF	OFF	OFF	OFF	Carbonaceous BOD group 1			
CBOD2	OFF	OFF	OFF	OFF	OFF	Carbonaceous BOD group 2			
CBOD3	OFF	OFF	OFF	OFF	OFF	Carbonaceous BOD group 3			
ALG1	OFF	OFF	OFF	OFF	OFF	Algal group 1			
ALG2	OFF	OFF	OFF	OFF	OFF	Algal group 2			
ALG3	OFF	OFF	OFF	OFF	OFF	Algal group 3			
DO	OFF	OFF	OFF	OFF	OFF	Dissolved oxygen			
TIC	OFF	OFF	OFF	OFF	OFF	Total inorganic carbon			
ALK	OFF	OFF	OFF	OFF	OFF	Alkalinity			

Related Cards and Files

[Calculations](#)

[Precipitation Concentration File](#)

[Precipitation Concentration Filename](#)

Extinction Coefficient (EX COEF)

FIELD	NAME	VALUE	DEFAULT	DESCRIPTION
1				(Ignored by code)
2	EXH2O	Real	0.25 or 0.45	Extinction for pure water, m^{-1}
3	EXSS	Real	0.1	Extinction due to inorganic suspended solids, m^{-1}
4	EXOM	Real	0.1	Extinction due to organic suspended solids, m^{-1}
5	BETA	Real	0.45	Fraction of incident solar radiation absorbed at the water surface
6	EXC	Character	OFF	Read extinction coefficients, ON or OFF
7	EXIC	Character	OFF	Interpolate extinction coefficients, ON or OFF

This card specifies the short wave solar radiation extinction coefficients and amount of solar radiation, β , absorbed in the surface layer. Extinction coefficients are used to calculate a net extinction coefficient, λ , which is determined from the following equation:

$$\lambda = \lambda_{H2O} + \lambda_{ISS} + \lambda_{POM} + \lambda_a$$

where:

$$\lambda_{ISS} = \varepsilon_{ISS} \sum_{\#ISS} \Phi_{ISS}$$

ε_{ISS} = extinction parameter for inorganic suspended solids, $m^{-1}/(g\ m^{-3})$ - user supplied parameter

Φ_{ISS} = inorganic suspended solids concentration for each size fraction (up to 9)

$$\lambda_{POM} = \varepsilon_{POM} \sum \Phi_{POM}$$

ε_{POM} = extinction parameter for particulate organic matter, $m^{-1}/g\ m^{-3}$ - user supplied parameter

Φ_{POM} = particulate organic matter concentration = particulate labile + particulate refractory organic matter concentration

$$\lambda_a = \sum \varepsilon_a \Phi_a$$

ε_a = extinction coefficient for each algal group, $m^{-1}/g\ m^{-3}$ - user supplied parameter

Φ_a = algal concentration for each algal group, $g\ m^{-3}$

λ_{H2O} = extinction coefficient for water (for a wavelength of between 0.5 and 0.6 μm , the absorption coefficient for *pure water* is about 0.1 m^{-1}).

λ_{H2O} varies greatly depending upon the dissolved substances in the water. [Table C-9](#) gives values reported in the literature that can be used as rudimentary guidelines for selecting a value of λ_{H2O} .

Table C-9. Extinction Coefficient Literature Values

Location	Description	λ, m^{-1}	Reference
Lake Tahoe, CA	Oligotrophic	0.2	Wetzel, 1975
Crystal Lake, WI	Oligotrophic	0.2	Wetzel, 1975
Crater Lake, OR	Oligotrophic	0.18	Spence, 1981
Lake Borrallie, Scotland	Calcareous water	0.34	Spence, 1981
Wintergreen Lake, MI	Eutrophic	0.46-1.68	Wetzel, 1975
Lake Paajarvi, Finland	Brown-stained	0.7	Verduin, 1982
Loch Unagan, Scotland	Brown-stained	1.53	Spence, 1981

Location	Description	λ, m^{-1}	Reference
Loch Leven, Scotland	Turbid, eutrophic	2.58	Spence, 1981
Neusiedlersee, Austria	Turbid	3.31	Spence, 1981
Highly stained lakes	Average	4.0	Wetzel, 1975

Megard et al. (1980) and Smith and Baker (1978) determined each gram per cubic meter of chlorophyll increased ϵ_{POM} by 22 and 16 m^{-1} , respectively. Averaging the two values and assuming a carbon to algal biomass ratio of 0.45 and a carbon to chlorophyll ratio of 50, then each gram per cubic meter of algal biomass should increase ϵ_{POM} by about 0.17 m^{-1} . However, the carbon to chlorophyll ratios vary from 25 to 150. Values for ϵ_{ISS} should be of the same order of magnitude as ϵ_{POM} .

If any constituents included in the above equation are not included in the simulation, then the value for λ_{H2O} should be increased to account for the constituent left out. The following equation can be used to estimate the extinction coefficient (Williams et al. 1980)

$$\lambda = 1.11Z_s^{-0.73}$$

where:

λ = net extinction coefficient
 Z_s = secchi disk depth, m

The above equation includes the effects of ϵ_{ISS} and ϵ_{OSS} and should be used only when inorganic and organic suspended solids are not included in the simulation.

The fraction of incident solar radiation absorbed at the water surface, β , represents solar radiation absorbed in a 0.6 m surface layer. Once λ has been determined, the equation below can be used to determine β :

$$\beta = 0.27 \ln(\lambda) + 0.61$$

The model user can input a file of extinction coefficients as a function of time for each water body if [EXC] is ON. Interpolation of this input file is performed when [EXIC] is ON. The extinction coefficients can be derived from secchi disk or light photometer data. The input file is specified under the Extinction Coefficient file name. When the extinction coefficient is read in, all other calculations of light extinction are ignored.

Example

EX COEF	EXH2O	EXSS	EXOM	BETA	EXC	EXIC
WB 1	0.25	0.01	0.01	0.45	OFF	OFF
WB 2	0.25	0.01	0.01	0.45	OFF	OFF
WB 3	0.25	0.01	0.01	0.45	OFF	OFF

Related Cards and Files

[Algal Extinction](#)
[Light Extinction File](#)
[Light Extinction Filename](#)

Algal Extinction (ALG EX)

FIELD	NAME	VALUE	DEFAULT	DESCRIPTION
1				(Ignored by code)
2-10	EXA	Real	0.2	Algal light extinction, m^{-1}

This card specifies the effect of algae on short wave solar radiation extinction in the water column. See the [Extinction Coefficient](#) card for a more complete description.

Example

ALG EX	EXA								
	0.2	0.2	0.2						

Related Cards and Files

[Extinction Coefficient](#)

Generic Constituent (GENERIC)

FIELD	NAME	VALUE	DEFAULT	DESCRIPTION
1				(Ignored by code)
2	CGQ10	Real		Arrhenius temperature rate multiplier
3	CG0DK	Real		0-order decay rate, day^{-1}
4	CG1DK	Real		1st -order decay rate, day^{-1}
5	CGS	Real		Settling rate, $m\ day^{-1}$

This card specifies the Arrhenius temperature rate multiplier, 0-order decay rate, 1st-order decay rate, and settling rate for a generic constituent. New to Version 3.1 is the ability to model any number of generic constituents whose kinetics can be described by these parameters. This includes tracers, residence time or water age, coliform bacteria, etc. For a tracer, all of the kinetic parameters should be set to zero. For residence time, the 0-order decay rate should be set to -1.0. Since this is a decay rate, setting it to -1.0 specifies a growth rate of 1 day^{-1} .

Unlike other state variables, the generic constituent uses an Arrhenius temperature rate multiplier (or Q_{10}) formulation to modify the generic constituent decay rate as a function of temperature as this is what is most likely to be encountered in the literature, particularly for coliform bacteria. Care must be taken when using this formulation at low ($< 6^{\circ}C$) temperatures. For coliform bacteria, the Q_{10} coefficient is usually 1.04. A range of values for coliform can be found in Zison et al. (1978).

Coliform decay rate is a function of sedimentation, solar radiation, nutrient availability, predation, algae, bacterial toxins, and physicochemical factors. For studies in which bacterial contamination is of important concern, efforts should be made to obtain *in situ* decay rate measurements. Methods for obtaining decay rates can be found in Frost and Streeter (1924), Marais (1974), and Zison et al. (1978). [Table C-10](#) gives reported literature values for coliform decay rates.

Table C-10. *In Situ* Coliform Decay Rates

Location	Season/ Temperature	Rate, day^{-1}	Reference
Ohio River	Summer, 20°C	1.18	Frost and Streeter, 1924
Ohio River	Winter, 5°C	1.08	Frost and Streeter, 1924
Upper Illinois River	June-September	2.04	Hoskins, et al, 1927
Upper Illinois River	October-May	2.52, 0.89	Hoskins, et al, 1927
Upper Illinois River	December-March	0.57, 0.62	Hoskins, et al, 1927
Upper Illinois River	April-November	1.03, 0.70	Hoskins, et al, 1927
Missouri River	Winter	0.48	Kittrell and Furfari, 1963
Tennessee River	Summer	1.03, 1.32	Kittrell and Furfari, 1963
Tennessee River	Summer	1.32	Kittrell and Furfari, 1963
Sacramento River	Summer	1.75	Kittrell and Furfari, 1963
Cumberland River	Summer	5.52	Kittrell and Furfari, 1963
Leaf River, MS		0.41	Mahloch, 1974
Wastewater lagoon	7.0-25.5°C	0.20-0.70	Klock, 1971
Maturation ponds	19°C	1.68	Marais, 1974
Oxidation ponds	20 °C	2.59	Marais, 1974

Example

GENERIC	CGQ10	CG0DK	CG1DK	CGS
CG 1	0.00	0.0	0.0	0.0
CG 2	0.00	-1.0	0.0	0.0
CG 4	1.04	0.0	0.2	1.0

Suspended Solids (S SOLIDS)

FIELD	NAME	VALUE	DEFAULT	DESCRIPTION
1				(Ignored by code)
2-10	SSS	Real	1.0	Suspended solids settling rate, $m\ day^{-1}$
3	SEDRC	Real	1.0	Turns ON or OFF sediment resuspension
4	TAUCR	Real	1.0E-5	Critical shear velocity for sediment resuspension, $m\ sec^{-1}$

This card specifies the suspended solids settling rates for each inorganic suspended solids state variable specified in the [Constituent Dimensions](#) card. Currently, phosphorus partitioning as specified on the [Inorganic Phosphorus](#) card is the same for all inorganic suspended solids. New to V3.2 is the ability to resuspend inorganic suspended solids due to wind shear and the resulting wind waves that cause sediment resuspension (Chapra, 1997). The computations are included by turning [[SEDRC](#)] to ON. The critical shear velocity is specified by [[TAUCR](#)]. Details of this computation for resuspension are found in Appendix A.

Example

S SOLIDS	SSS	SEDRC	TAUCR
SSS 1	1.5	ON	1.E-5
SSS 2	1.5	ON	1.E-4

Algal Rates (ALGAL RATE)

FIELD	NAME	VALUE	DEFAULT	DESCRIPTION
1				(Ignored by code)
2	AG	Real	2.0	Maximum algal growth rate, day^{-1}
3	AR	Real	0.04	Maximum algal respiration rate, day^{-1}
4	AE	Real	0.04	Maximum algal excretion rate, day^{-1}
5	AM	Real	0.1	Maximum algal mortality rate, day^{-1}
6	AS	Real	0.1	Algal settling rate, $m day^{-1}$
7	AHSP	Real	0.003	Algal half-saturation for phosphorus limited growth, $g m^{-3}$
8	AHSN	Real	0.014	Algal half-saturation for nitrogen limited growth, $g m^{-3}$
9	AHSSI	Real	0.0	Algal half-saturation for silica limited growth, $g m^{-3}$
10	ASAT	Real	75.0	Light saturation intensity at maximum photosynthetic rate, $W m^{-2}$

This card specifies rates for algal growth, mortality, excretion, respiration, and settling. Additionally, values that affect the maximum algal growth rate including light and nutrient limited growth are also specified here.

[AG] is the maximum gross production rate that is not corrected for respiration, mortality, excretion, or sinking. Most literature values report net production rates that take into account respiration so care must be taken when using reported literature values. The user must evaluate the experimental design to determine if reported values represent gross or net production rates. Also, [AG] is temperature dependent. If the expected temperature in the photic zone is 25 °C, then the user should select rates measured near this temperature. The default value of 2 day^{-1} has given excellent results on previous studies.

Table C-11. Gross Production Rates of Phytoplankton.

Species	[AG], day^{-1}	Temperature, °C	Reference
<i>Diatoms</i>			
<i>Asterionella formosa</i>	0.81	20	Holm and Armstrong, 1981
<i>Asterionella Formosa</i>	0.69	10	Hutchinson, 1957
<i>Asterionella Formosa</i>	1.38	20	Hutchinson, 1957
<i>Asterionella Formosa</i>	1.66	25	Hutchinson, 1957
<i>Asterionella Formosa</i>	1.71	20	Fogg, 1969
<i>Asterionella Formosa</i>	0.28	4	Talling 1955
<i>Asterionella Formosa</i>	0.69	10	Talling 1955
<i>Asterionella Formosa</i>	1.38	20	Talling 1955
<i>Asterionella Formosa</i>	2.2	20	Hoogenhout and Amesz, 1965
<i>Asterionella formosa</i>	1.9	18.5	Hoogenhout and Amesz, 1965
<i>Asterionella japonica</i>	1.19	22	Fogg, 1969
<i>Asterionella japonica</i>	1.3	18	Hoogenhout and Amesz, 1965
<i>Asterionella japonica</i>	1.7	25	Hoogenhout and Amesz, 1965
<i>Biddulphia</i> sp.	1.5	11	Castenholz, 1964
<i>Coscinodiscus</i> sp.	0.55	18	Fogg, 1969
<i>Cyclotella meneghiniana</i>	0.34	16	Hoogenhout and Amesz, 1965
<i>Cyclotell nana</i>	3.4	20	Hoogenhout and Amesz, 1965
<i>Detonula confervacea</i>	0.62	2	Smayda, 1969
<i>Detonula confervacea</i>	1.4	10	Hoogenhout and Amesz, 1965
<i>Ditylum brightwellii</i>	2.1	20	Paasche, 1968
<i>Fragilaria</i> sp.	0.85	20	Rhee and Gotham, 1981b

CONTROL FILE

KINETIC COEFFICIENTS

<i>Fragilaria</i> sp.	1.7	11	Castenholz, 1964
<i>Melosira</i> sp.	0.7	11	Castenholz, 1964
<i>Navicula minima</i>	1.4	25	Hoogenhout and Amesz, 1965
<i>Navicula pelliculosa</i>	2.0	20	Hoogenhout and Amesz, 1965
<i>Nitzschia palea</i>	2.1	25	Hoogenhout and Amesz, 1965
<i>Nitzschia turgidula</i>	2.5	20	Paasche, 1968
<i>Phaeoactylum tricornutum</i>	1.66	25	Fogg, 1969
<i>Phaeoactylum tricornutum</i>	2.7	19	Hoogenhout and Amesz, 1965
<i>Rhizosolenia fragillissima</i>	1.2	21	Ignatiades and Smayda, 1970
<i>Skeletonema costatum</i>	1.26	18	Fogg, 1969
<i>Skeletonema costatum</i>	2.30	20	Jorgensen, 1968
<i>Skeletonema costatum</i>	1.52	20	Stemann-Nielsen and Jorgensen, 1968
<i>Skeletonema costatum</i>	1.23	20	Jitts, et al., 1964
<i>Synedra</i> sp.	1.2	11	Castenholz, 1964
<i>Thalassiosira nordenskioldii</i>	0.77	12	Jitts, et al., 1964
Natural diatom community	3.1	20	Verduin, 1952
Greens			
<i>Ankistrodesmus braunii</i>	2.33	25	Hoogenhout and Amesz, 1965
<i>Chlorella pyrenoidosa</i>	2.22	28	Shelef, 1968
<i>Chlorella ellipsoidea</i>	3.6	25	Hoogenhout and Amesz, 1965
<i>Chlorella luteoviridis</i>	0.56	22.4	Hoogenhout and Amesz, 1965
<i>Chlorella miniata</i>	0.87	25	Hoogenhout and Amesz, 1965
<i>Chlorella pyrenoidosa</i>	2.14	25	Fogg, 1969
<i>Chlorella pyrenoidosa</i>	1.95	25.5	Sorokin and Meyers, 1953
<i>Chlorella pyrenoidosa</i>	9.00	39	Castenholz, 1969
<i>Chlorella pyrenoidosa</i>	9.2	39	Hoogenhout and Amesz, 1965
<i>Chlorella seccharophila</i>	1.2	25	Hoogenhout and Amesz, 1965
<i>Chlorella variegata</i>	0.86	25	Hoogenhout and Amesz, 1965
<i>Chlorella vulgaris</i>	2.9	25	Hoogenhout and Amesz, 1965
<i>Chlorella vulgaris</i>	1.59	20	Goldman and Graham, 1981
<i>Dunaliella tertiolecta</i>	1.0	16	Hoogenhout and Amesz, 1965
<i>Dunaliella tertiolecta</i>	0.77	36	Jitts, et al., 1964
<i>Haematococcus pluvialis</i>	1.2	23	Hoogenhout and Amesz, 1965
<i>Nanochloris atomus</i>	1.0	20	Hoogenhout and Amesz, 1965
<i>Platymonas subcordiformia</i>	1.5	16	Hoogenhout and Amesz, 1965
<i>Scenedesmus</i> sp.	1.34	20	Rhee and Gotham, 1981b
<i>Scenedesmus costulatus</i>	2.0	24.5	Hoogenhout and Amesz, 1965
<i>Scenedesmus obliquus</i>	2.11	20	Goldman and Graham, 1981
<i>Scenedesmus obliquus</i>	2.2	25	Hoogenhout and Amesz, 1965
<i>Scenedesmus quadricauda</i>	4.1	25	Hoogenhout and Amesz, 1965
<i>Scenedesmus quadricauda</i>	2.29	27	Goldman, et al., 1972
<i>Selenastrum capricornutum</i>	2.45	27	Goldman, et al., 1972
<i>Selenastrum westii</i>	1.0	25	Hoogenhout and Amesz, 1965
<i>Stichococcus</i> sp.	0.7	20	Hoogenhout and Amesz, 1965
Golden-Brown			
<i>Botrydiopsis intercedens</i>	1.5	25	Hoogenhout and Amesz, 1965
<i>Bumilleriopsis brevis</i>	2.9	25	Hoogenhout and Amesz, 1965
<i>Cricosphaera carterae</i>	0.82	18	Fogg, 1969
<i>Isochrysis galbana</i>	0.55	20	Fogg, 1969
<i>Isochrysis galbana</i>	0.8	25	Hoogenhout and Amesz, 1965
<i>Monochrysis lutheri</i>	1.5	15	Hoogenhout and Amesz, 1965
<i>Monochrysis lutheri</i>	0.39	24	Jitts, et al., 1964
<i>Monodus subterraneus</i>	0.93	25	Hoogenhout and Amesz, 1965
<i>Monodus subterraneus</i>	0.39	30	Fogg, 1969
<i>Tribonema aequale</i>	0.7	25	Hoogenhout and Amesz, 1965
<i>Tribonema minus</i>	1.0	25	Hoogenhout and Amesz, 1965
<i>Vischera stellata</i>	0.7	25	Hoogenhout and Amesz, 1965
<i>Euglena gracilis</i>	2.2	25	Hoogenhout and Amesz, 1965
Dinoflagellate			
<i>Amphidinium carteri</i>	1.88	18	Fogg, 1969
<i>Amphidinium carteri</i>	0.32	32	Jitts, et al., 1964
<i>Ceratium tropes</i>	0.20	20	Fogg, 1969
<i>Gonyaulax polyedra</i>	2.1	21.5	Hoogenhout and Amesz, 1965

<i>Gymnodinium splendens</i>	0.92	20	Hoogenhout and Amesz, 1965
<i>Peridinium</i> sp.	0.9	18	Hoogenhout and Amesz, 1965
<i>Prorocentrum gracile</i>	0.83	18	Hoogenhout and Amesz, 1965
<i>Prorocentrum micans</i>	0.71	25	Hoogenhout and Amesz, 1965
<i>Prorocentrum micans</i>	0.3	20	Fogg, 1969
Cyanobacteria			
<i>Agmenellum quadriplaticum</i>	8.0	39	Hoogenhout and Amesz, 1965
<i>Anabaena cylindrical</i>	0.96	25	Hoogenhout and Amesz, 1965
<i>Anabaena variabilis</i>	3.9	34.5	Hoogenhout and Amesz, 1965
<i>Anacystis nidulans</i>	2.9	25	Hoogenhout and Amesz, 1965
<i>Anacystis nidulans</i>	11.0	40	Castenholz, 1969
<i>Chloropseudomonas ethylicum</i>	3.3	30	Hoogenhout and Amesz, 1965
<i>Cyanidium caldarium</i>	2.4	40	Hoogenhout and Amesz, 1965
<i>Cylindrospermum sphaerica</i>	0.17	25	Hoogenhout and Amesz, 1965
<i>Gloeotrichia echinulata</i>	0.2	26.5	Hoogenhout and Amesz, 1965
<i>Microcystis aeruginosa</i>	0.25	20	Holm and Armstrong, 1981
<i>Microcystis aeruginosa</i>	1.6	23	Hoogenhout and Amesz, 1965
<i>Microcystis luminmosis</i>	1.5	40	Castenholz, 1969
<i>Nostoc muscorum</i>	2.9	32.5	Hoogenhout and Amesz, 1965
<i>Oscillatoria prinsips</i>	0.5	40	Castenholz, 1969
<i>Oscillatoria terebriformis</i>	3.36	40	Castenholz, 1969
<i>Oscillatoria rubescens</i>	5.04	30	Zimmerman, 1969
<i>Rhodopseudomonas sphaeroides</i>	10.8	34	Hoogenhout and Amesz, 1965
<i>Rhodospirillum rubrum</i>	4.85	25	Hoogenhout and Amesz, 1965
<i>Schizothrix calcicola</i>	3.4	30	Hoogenhout and Amesz, 1965
<i>Synechococcus lividus</i>	4.98	40	Castenholz, 1969
<i>Synechococcus</i> sp.	8.0	37	Hoogenhout and Amesz, 1965
<i>Tolypothrix tenuis</i>	4.0	38	Hoogenhout and Amesz, 1965
<i>Leotocylindroc danicus</i>	0.67-2.0	10-20	Verity, 1981
<i>Anabaena variabilis</i>	0.07-2.0	10-35	Collins and Boylen, 1982a

Maximum algal mortality rate [AM] is also temperature dependent. A general rule of thumb is the maximum algal mortality rate [AM] should be less than 10% of the maximum algal growth rate [AG]. Values ranging from 0.03 to 0.3 have been used in previous modeling studies, with the default value of 0.1 day^{-1} providing excellent results on a large number of systems.

[AE] is the maximum algal excretion (or photorespiration) rate that goes directly to the labile DOM compartment. The default value is 0.04 day^{-1} . [AR] is the maximum dark algal respiration rate. Respiration rates are often expressed as millilitres of oxygen consumed per milligram of organism dry weight per hour. To convert to model units ($\text{mg O}_2 \text{ mg}^{-1} \text{ organism dry weight day}^{-1}$), multiply dark respiration rates by $0.74 \text{ mg dry weight/1 ml O}_2$. Literature values are reported in [Table C-12](#) and [Table C-13](#). The default value is 0.04 day^{-1} .

Table C-12. Maximum Algal Excretion Rate Literature Values

Species	Excretion Rate, day^{-1}	Reference
<i>Actinastrum hantzschii</i>	0.044	Nalewajko, 1966
<i>Ankistrodesmus falcatus</i>	0.031	Nalewajko, 1966
<i>Asterococcus superbus</i>	0.036	Nalewajko, 1966
<i>Chlorella pyrenoidosa</i>	0.032	Nalewajko, 1966
<i>Eudorina elegans</i>	0.023	Nalewajko, 1966
<i>Micractinium pusillum</i>	0.014	Nalewajko, 1966

Table C-13. Algal Dark Respiration Rate Literature Values

Species	Respiration Rate, day^{-1}	Reference
<i>Anabaena variabilis</i>	0.10-0.92	Collins and Boylen, 1978
<i>Chlorella pyrenoidosa</i>	0.01-0.03	Myers and Graham, 1961
<i>Coscinodiscus excentricus</i>	0.07-0.11	Riley and von Aux, 1949

Dunaliella teriolecta	0.12-0.16	Laws and Wong, 1978
Mesodinium rubrum	0.05	Smith, 1979
Monochrysis lutheri	0.15-0.32	Laws and Wong, 1978
Thalassiosira allenii	0.05-0.59	Laws and Wong, 1978

Literature value for algal settling velocities [AS] are given in [Table C-14](#), but care must be taken in their use. Laboratory and *in situ* methods for determining settling velocities each have their drawbacks when attempting to measure net settling velocities. The settling velocity is very dependent upon the type of algae present, so a single default value is not recommended. Previous studies have used a settling velocity of 0.2 m day^{-1} for diatoms, 0.1 m day^{-1} for greens, and $0.0-0.05 \text{ m day}^{-1}$ for cyanobacteria.

Table C-14. Algal settling Velocity Literature Values

Species	Settling velocity, m day^{-1}	Reference
Diatoms		
Asterionella formosa	0.26-0.76	Smayda, 1974
Bacteriastrum hyalinum	0.39-1.27	Smayda & Boleyn, 1966
Chaetoceros didymus	0.85	Eppley Holmes, & Strickland, 1967b
Chaetoceros lauderi	0.46-1.54	Smayda & Boleyn, 1966
Chaetoceros spp.	0.85	Margalef, 1961
Chaetoceros spp.	4.00	Allen, 1932
Coscinodiscus wailesii	7.00-30.2	Eppley Holmes, & Strickland, 1967b
Coscinodiscus sp.	1.95-6.83	Eppley Holmes, & Strickland, 1967b
Cyclotella meneghiniana	0.08-0.24	Titman & Kilham, 1976
Cyclotella nana	0.16-0.76	Eppley Holmes, & Strickland, 1967b
Ditylum brightwellii	0.60-3.09	Eppley Holmes, & Strickland, 1967b
Fragilaria crotonensis	0.27	Burns & Rosa, 1980
Leptocylindrum danicus	0.08-0.42	Margalef, 1961
Melosira agassizii	0.67-1.87	Titman & Kilham, 1976
Nitzschia closterium	0.52	Margalef, 1961
Nitzschia seriata	0.35-0.50	Smayda & Boleyn, 1965
Phaeodactylum tricornutum	0.02-0.06	Riley, 1943
Rhizosolenia hebetata	0.22	Eppley, Holmes, & Strickland, 1967b
Rhizosolenia setigera	0.10-6.30	Smayda & Boleyn, 1974
Rhizosolenia stouterfothii	1.00-1.9	Eppley, Holmes, & Strickland, 1967b
Rhizosoleni sp.	0.00-0.72	Margalef, 1961
Skeletonema costatum	0.30-1.35	Smayda & Boleyn, 1974
Stephanopyxis turris	1.10	Eppley, Holmes, & Strickland, 1967b
Thalassionema nitzsoides	0.35-0.78	Smayda (unpublished)
Thalassiosira fluviatilis	0.60-1.10	Eppley, Holmes, & Strickland, 1967b
Thalassiosira nana	0.10-0.28	Smayda & Boleyn, 1966
Thalassiosira rotula	0.39-2.10	Smayda & Boleyn, 1966
Dinoflagellates		
Gonyaulax polyedra	2.80-6.10	Bramlette, 1961
Coccolithophorids		
Coccolithus huxleyi	0.28, 1.2	Eppley, Holmes, & Strickland, 1967b
Cricosphaera carterae	1.7	Eppley, Holmes, & Strickland, 1967b
Cricosphaera elongata	0.25	Eppley, Holmes, & Strickland, 1967b
Cyccoccolithus fragilis	10.3-13.2	Bernard, 1963
Microflagellates		
Cryptomonas reosa	0.31	Burns & Rosa, 1980

[AHSP] is the algal half-saturation constant for phosphorous and is defined as the phosphorous concentration at which the uptake rate is one-half the maximum rate. This represents the upper concentration at which algal growth is directly proportional to phosphorous concentrations

Table C-15. Phosphorus Half-Saturation Constant Literature Values

Species	Half-Saturation Constant, $mg\ l^{-1}$	Reference
<i>Asterionella formosa</i>	0.002	Holm & Armstrong, 1981
<i>Asterionella japonica</i>	0.014	Thomas & Dodson, 1968
<i>Biddulphia sinensis</i>	0.016	Quasim, et al., 1973
<i>Cerataulina bergonii</i>	0.003	Finenko & Krupatkina, 1974
<i>Chaetoceros curvistus</i>	0.074-0.105	Finenko & Krupatkina, 1974
<i>Chaetoceros socialis</i>	0.001	Finenko & Krupatkina, 1974
<i>Chlorella pyrenoidosa</i>	0.380-0.475	Jeanjean, 1969
<i>Cyclotella nana</i>	0.055	Fuhs, et al., 1972
<i>Cyclotella nana</i>	0.001	Fogg, 1973
<i>Dinobryon cylindrium</i>	0.076	Lehman (unpublished)
<i>Dinobryon sociale</i>	0.047	Lehman (unpublished)
<i>Euglena gracilis</i>	1.520	Dlum, 1966
<i>Microcystis aeruginosa</i>	0.006	Holm & Armstrong, 1981
<i>Nitzschia actinastreoides</i>	0.095	Von Muller, 1972
<i>Pediastrum duplex</i>	0.105	Lehman (unpublished)
<i>Pithophora oedogonia</i>	0.980	Spencer & Lembi, 1981
<i>Scenedesmus obliquus</i>	0.002	Fogg, 1973
<i>Scenedesmus sp.</i>	0.002-0.050	Rhee, 1973
<i>Thalossiosira fluviatilis</i>	0.163	Fogg, 1973

[AHSN] is the algal half-saturation constant for nitrogen and is defined as the nitrogen concentration (ammonium + nitrate/nitrite) at which the uptake rate is one-half the maximum rate. This represents the upper concentration at which algal growth is proportional to nitrogen. [Table C-16](#) gives literature values for the nitrogen half-saturation constant.

Table C-16. Nitrogen Half-Saturation Constant Literature Values

Species	Half saturation constant	N source	Reference
Diatoms			
<i>Biddulphia aurita</i>	0.056-0.197	NO ₃	Underhill, 1977
<i>Chaetoceros gracilis</i>	0.012	NO ₃	Eppley, Rogers, & McCarthy, 1969
	0.012	NH ₄	Eppley, Rogers, & McCarthy, 1969
<i>Coscinodiscus lineatus</i>	0.012	NO ₃	Eppley, Rogers, & McCarthy, 1969
	0.012	NH ₄	Eppley, Rogers, & McCarthy, 1969
<i>Cyclotella nana</i>	0.025-0.117	NO ₃	Carpenter & Guillard, 1971
	0.111		Maclsaac & Dugdale, 1969
	0.027		Caperon & Meyer, 1972
	0.031		Eppley, Rogers, & McCarthy, 1969
<i>Ditylum brightwellii</i>	0.037	NO ₃	Eppley, Rogers, & McCarthy, 1969
	0.020	NO ₃	Eppley, Rogers, & McCarthy, 1969
<i>Dunaliella teriolecta</i>	0.013	NO ₃	Caperon & Meyer, 1972
	0.013	NH ₄	Caperon & Meyer, 1972
	0.087	NO ₃	Eppley, Rogers, & McCarthy, 1969
<i>Fragilaria pinnata</i>	0.037-0.100	NO ₃	Carpenter & Guillard, 1971
<i>Leptocylindrous danicus</i>	0.078	NO ₃	Eppley, Rogers, & McCarthy, 1969
	0.013	NH ₄	Eppley, Rogers, & McCarthy, 1969
<i>Navicula pelliculosa</i>	0.923	NO ₃	Wallen & Cartier, 1975
<i>Phaeodactylum tricornutum</i>	0.161	NO ₃	Ketchum, 1939
<i>Rhizosolenia robusta</i>	0.186	NO ₃	Eppley, Rogers, & McCarthy, 1969
	0.135	NH ₄	Eppley, Rogers, & McCarthy, 1969
<i>Rhizosolenia stolterfothii</i>	0.105	NO ₃	Eppley, Rogers, & McCarthy, 1969
	0.009	NH ₄	Eppley, Rogers, & McCarthy, 1969
<i>Skeletonema costatum</i>	0.027	NO ₃	Eppley, Rogers, & McCarthy, 1969
	0.014	NH ₄	Eppley, Rogers, & McCarthy, 1969
Bluegreens			

Species	Half saturation constant	N source	Reference
Anabaena cylindrica	4.34	NO3	Hattori, 1962
	2.48	NO3	Hattori, 1962
Asterionella formosa	0.074-0.093	NO3	Eppley & Thomas, 1969
	0.062	NH4	Eppley & Thomas, 1969
Oscillatoria agardhii	0.22	NO3	van Lierre, 1977
Microflagellates			
Bellochia sp.	0.001-0.16	NO3	Carpenter & Guillard, 1971
Monochrysis lutheri	0.026	NO3	Caperon & Meyer, 1972
	0.052	NH4	Caperon & Meyer, 1972
	0.037	NO3	Eppley, Rogers, & McCarthy, 1969
	0.007	NH4	Eppley, Rogers, & McCarthy, 1969
Coccolithophorids			
Coccolithus huxleyi	0.006	NO3	Eppley, Rogers, & McCarthy, 1969
	0.002	NH4	Eppley, Rogers, & McCarthy, 1969
Greens			
Chlorella pyrenoidosa	0.006-0.14		Pickett, 1975
	1.15	NO3	Knudsen, 1965
Pithophora cedogonia	1.236	NO3	Spencer & Lembi, 1981
Dinoflagellates			
Gonyaulax polyedra	0.589	NO3	Eppley, Rogers, & McCarthy, 1969
	0.099	NH4	Eppley, Rogers, & McCarthy, 1969
Gymnodinium splendens	0.235	NO3	Eppley, Rogers, & McCarthy, 1969
	0.099	NH4	Eppley, Rogers, & McCarthy, 1969
Gymnodinium walesii	0.223	NO3	Eppley, Rogers, & McCarthy, 1969
	0.088	NH4	Eppley, Rogers, & McCarthy, 1969
Chrysophytes			
Isochrysis galbana	0.006	NO3	Eppley, Rogers, & McCarthy, 1969

[ASAT] is the saturating light intensity at the maximum photosynthetic rate. Since phytoplankton adapt to low light regimes, saturation coefficients may be lower than those measured in the laboratory. [Table C-17](#) gives literature values for [ASAT]. To simulate algal nitrogen fixation, set AHSN equal to 0.0.

Table C-17. Literature values for saturating light intensity

Species	Saturation, $W m^{-2}$	Reference
<i>Cryptomonas ovata</i>	12-36	Cloern, 1977
<i>Oscillatoria agardhii</i>	10	van Lierre, et al., 1978
<i>Oscillatoria rubescens</i>	36-61	Konopka, 1983
<i>Scenedesmus protuberans</i>	24	van Lierre, et al., 1978
Mixed diatoms	86	Belay, 1981
Mixed phytoplankton	36	Belay, 1981
Shade-adapted phytoplankton	18-29	Belay, 1981

Example

ALGAL RATE	AG	AR	AE	AM	AS	AHSP	AHSN	AHSSI	ASAT
Alg 1	1.5	0.04	0.04	0.15	0.20	0.003	0.014	0.003	75.0
Alg 2	2.5	0.04	0.04	0.10	0.10	0.003	0.014	0.000	75.0
Alg 3	0.5	0.04	0.04	0.05	0.02	0.003	0.010	0.000	75.0

Related Cards and Files

[Algal Extinction](#)

KINETIC COEFFICIENTS

CONTROL FILE

[Algal Temperature Rate Coefficients](#)
[Algal Stoichiometry](#)

Algal Temperature Rate Coefficients (ALG TEMP)

FIELD	NAME	VALUE	DEFAULT	DESCRIPTION
1				(Ignored by code)
2	AT1	Real	5.0	Lower temperature for algal growth, °C
3	AT2	Real	25.0	Lower temperature for maximum algal growth, °C
4	AT3	Real	35.0	Upper temperature for maximum algal growth, °C
5	AT4	Real	40.0	Upper temperature for algal growth, °C
6	AK1	Real	0.1	Fraction of algal growth rate at AT1
7	AK2	Real	0.99	Fraction of maximum algal growth rate at AT2
8	AK3	Real	0.99	Fraction of maximum algal growth rate at AT3
9	AK4	Real	0.1	Fraction of algal growth rate at AT4

This card specifies the lower, maximum lower, upper, and maximum upper temperatures used in defining the curve that determines effects of temperature on algal rates. Also specified is the fraction of maximum algal rates that occurs at the specified temperature. The default values are ones for a single algal assemblage used in Version 2. When including multiple algal groups, the temperature rate coefficients are one of the most important parameters determining algal succession. Diatoms would have much lower temperatures for AT1-AT4 and cyanobacteria would have higher values.

Example

ALGAL TEMP	AT1	AT2	AT3	AT4	AK1	AK2	AK3	AK4
Alg 1	5.0	18.0	20.0	24.0	0.1	0.99	0.99	0.01
Alg 2	10.0	30.0	35.0	40.0	0.1	0.99	0.99	0.01
Alg 3	10.0	35.0	40.0	50.0	0.1	0.99	0.99	0.01

Related Cards and Files

[Algal Rates](#)

[Algal Extinction](#)

[Algal Stoichiometry](#)

Algal Stoichiometry (ALG STOICH)

FIELD	NAME	VALUE	DEFAULT	DESCRIPTION
1				(Ignored by code)
2	AP	Real	0.005	Stoichiometric equivalent between algal biomass and phosphorus
3	AN	Real	0.08	Stoichiometric equivalent between algal biomass and nitrogen
4	AC	Real	0.45	Stoichiometric equivalent between algal biomass and carbon
5	ASI	Real	0.18	Stoichiometric equivalent between algal biomass and silica
6	ACHLA	Real	145.0	Ratio between algal biomass and chlorophyll a
7	APOM	Real	0.8	Fraction of algal biomass that is converted to particulate organic matter when algae die
8	ANEQN	Integer	2	Equation number for algal ammonium preference (either 1 or 2)
9	ANPR	Real	0.001	Algal half saturation constant for ammonium preference

This card specifies the stoichiometric equivalences used for determining the amount of nutrients in algal biomass. Numerous researchers have noted that these ratios are not constant over time and vary by algal species. In addition, the algal to chlorophyll *a* ratio [ACHLA] is known to be different for different algal species and is known to vary over time for a given algal species. Currently, the model does not include variable stoichiometry or biomass to chlorophyll *a*. This is an area that will be improved upon in the future. [APOM] is the fraction of algal biomass lost by mortality going into the detritus compartment with the remainder going to labile DOM. Otsuki and Hayna (1972) have reported a value of 0.8 for *Scenedesmus* sp. and this is the default value.

Certain algal groups are known to preferentially uptake ammonium over nitrate. If the equation number [ANEQN] for algal nitrogen uptake is set to 1, then the algal nitrogen preference factor for ammonium is computed using:

$$P_{NH_4} = \frac{C_{NH_4}}{(C_{NO_3} + C_{NH_4})}$$

and the preference for nitrate is:

$$P_{NO_3} = \frac{C_{NO_3}}{(C_{NO_3} + C_{NH_4})}$$

If the equation number [ANEQN] is set to 2, then the phytoplankton nitrogen preference for ammonium is computed using the following equation (Thomann and Fitzpatrick, 1982):

$$P_{NH_4} = C_{NH_4} \frac{C_{NO_3}}{(K_{mN} + C_{NH_4})(K_{mN} + C_{NO_3})} + C_{NH_4} \frac{K_{mN}}{(C_{NH_4} + C_{NO_3})(K_{mN} + C_{NO_3})}$$

P_{NH_4} = ammonium preference factor

CONTROL FILE

KINETIC COEFFICIENTS

K_{mN} = N half-saturation coefficient, $mg\ l^{-1}$

C_{NH4} = ammonium nitrogen concentration, $mg\ l^{-1}$

C_{NOx} = nitrate-nitrite nitrogen concentration, $mg\ l^{-1}$

The nitrite-nitrate nitrogen preference factor is then calculated from:

$$P_{NOx} = 1 - P_{NH4}$$

Example

ALG	STOICH	ALGP	ALGN	ALGC	ALGSI	ACHLA	APOM	ANEQN	ANPR
Alg 1		0.005	0.08	0.45	0.18	145.00	0.8	2	0.001
Alg 2		0.005	0.08	0.45	0.00	145.00	0.8	2	0.001
Alg 3		0.005	0.08	0.45	0.00	145.00	0.8	2	0.001

Related Cards and Files

[Algal Rates](#)

[Algal Extinction](#)

[Algal Temperature Rate Coefficients](#)

Epiphyte Control (EPIPHYTE)

FIELD	NAME	VALUE	DEFAULT	DESCRIPTION
1				(Ignored by code)
2-10	EPIWBC	Character	OFF	Waterbody epiphyte computations, ON or OFF

This card allows the user to turn ON/OFF epiphyton computations and their effects on water quality for a given waterbody. This flexibility allows the user to decrease model complexity and computation time for waterbodies where epiphyton impacts are not considered important.

Example

```
EPIPHYTE  EPIWBC  EPIWBC  EPIWBC  EPIWBC  EPIWBC  EPIWBC  EPIWBC  EPIWBC
Epi 1      ON      ON      ON      ON      ON      ON      ON      ON
```

Related Cards and Files

[Epiphyte Print](#)
[Epiphyte Initial Density](#)
[Epiphyte Rate](#)
[Epiphyte Half-Saturation](#)
[Epiphyte Temperature Rate Coefficients](#)
[Epiphyte Stoichiometry](#)

Epiphyte Print (EPI PRINT)

FIELD	NAME	VALUE	DEFAULT	DESCRIPTION
1				(Ignored by code)
2-10	EPRWBC	Character	OFF	epiphyte areal density output, ON or OFF

This card allows the user to turn ON/OFF epiphyton biomass output in terms of areal density to the various output files for each waterbody.

Example

```
EPI PRINT EPRWBC  EPRWBC  EPRWBC  EPRWBC  EPRWBC  EPRWBC  EPRWBC  EPRWBC
Epi 1          ON      ON      ON      ON      ON      ON      ON      ON
```

Related Cards and Files

[Epiphyte Control](#)
[Epiphyte Initial Density](#)
[Epiphyte Rate](#)
[Epiphyte Half-Saturation](#)
[Epiphyte Temperature Rate Coefficients](#)
[Epiphyte Stoichiometry](#)

Epiphyte Initial Density (EPI INI)

FIELD	NAME	VALUE	DESCRIPTION
1			(Ignored by code)
2-10	EPIWBCI	Real	Initial areal density for each epiphyton group, $g\ m^{-2}$

This card specifies the initial epiphyton areal density for each waterbody.

Example

```
EPI INIT EPIWBCI EPIWBCI EPIWBCI EPIWBCI EPIWBCI EPIWBCI EPIWBCI EPIWBCI
Epi 1      10.0    10.0    10.0    10.0
```

Related Cards and Files

[Epiphyte Control](#)

[Epiphyte Print](#)

[Epiphyte Rate](#)

[Epiphyte Half-Saturation](#)

[Epiphyte Temperature Rate Coefficients](#)

[Epiphyte Stoichiometry](#)

Epiphyte Rate (EPI RATE)

FIELD	NAME	VALUE	DEFAULT	DESCRIPTION
1				(Ignored by code)
2	EG	Real	2.0	maximum epiphyton growth rate, day^{-1}
3	ER	Real	0.04	maximum epiphyton respiration rate, day^{-1}
4	EE	Real	0.04	maximum epiphyton excretion rate, day^{-1}
5	EM	Real	0.1	maximum epiphyton mortality rate, day^{-1}
6	EB	Real	0.001	epiphyton burial rate, $m day^{-1}$
7	EHSP	Real	0.003	epiphyton half-saturation for phosphorus limited growth, $g m^{-3}$
8	EHSN	Real	0.014	epiphyton half-saturation for nitrogen limited growth, $g m^{-3}$
9	EHSSI	Real	-	epiphyton half-saturation for silica limited growth, $g m^{-3}$

This card specifies rates for epiphyton growth, mortality, excretion, respiration, and burial. Additionally, values that affect the maximum epiphyton growth rate including nutrient limited growth are also specified here. See the [Algal Rate](#) card for more detailed information, as the kinetic formulations are similar. The burial rate causes epiphyton to be lost from the system. A future upgrade will have epiphyton contribution to the sediment compartment when they are buried.

Example

EPI RATE	EG	ER	EE	EM	EB	EHSP	EHSN	EHSSI
Epi 1	2.0	0.04	0.04	0.1	0.001	0.002	0.002	0.0

Related Cards and Files

- [Epiphyte Control](#)
- [Epiphyte Print](#)
- [Epiphyte Initial Density](#)
- [Epiphyte Half-Saturation](#)
- [Epiphyte Temperature Rate Coefficients](#)
- [Epiphyte Stoichiometry](#)

Epiphyte Half-Saturation (EPI HALF)

FIELD	NAME	VALUE	DEFAULT	DESCRIPTION
1				(Ignored by code)
2	ESAT	Real	75.0	light saturation intensity at maximum photosynthetic rate, $W m^{-2}$
3	EHS	Real	15.0	biomass limitation factor, $g m^{-2}$
4	ENEQN	Integer	2	ammonia preference factor equation for epiphyton (1 or 2)
4	ENPR	Real	0.001	nitrogen half-saturation preference constant, mg/l - only used if ENEQN=2

This card specifies the light saturation intensity at maximum photosynthetic rate [ESAT], the half-saturation coefficient for epiphyton biomass limitation [EHS], and the nitrogen preference during epiphyton growth [ENPR]. The ratio of nitrate-nitrite to ammonium taken up during epiphyton growth increases as [ENPR] increases.

Certain epiphyton groups are known to preferentially uptake ammonium over nitrate. If the equation number [ANEQN] for algal nitrogen uptake is set to 1, then the epiphyton nitrogen preference factor for ammonium is computed using:

$$P_{NH_4} = \frac{C_{NH_4}}{(C_{NO_3} + C_{NH_4})}$$

and the preference for nitrate is:

$$P_{NO_3} = \frac{C_{NO_3}}{(C_{NO_3} + C_{NH_4})}$$

If the equation number [ANEQN] is set to 2, then the epiphyton preference for ammonium is computed using the following equation (Thomann and Fitzpatrick, 1982):

$$P_{NH_4} = C_{NH_4} \frac{C_{NO_x}}{(K_{mN} + C_{NH_4})(K_{mN} + C_{NO_x})} + C_{NH_4} \frac{K_{mN}}{(C_{NH_4} + C_{NO_x})(K_{mN} + C_{NO_x})}$$

P_{NH_4} = ammonium preference factor

K_{mN} = N half-saturation coefficient, $mg l^{-1}$

C_{NH_4} = ammonium nitrogen concentration, $mg l^{-1}$

C_{NO_x} = nitrate-nitrite nitrogen concentration, $mg l^{-1}$

The nitrite-nitrate preference factor is then calculated from:

$$P_{NO_x} = 1 - P_{NH_4}$$

CONTROL FILE

KINETIC COEFFICIENTS

Example

EPI HALF	ESAT	EHS	ENEQN	ENPR
Epi 1	150.00	15.0	2	0.001

Related Cards and Files

[Epiphyte Control](#)

[Epiphyte Print](#)

[Epiphyte Initial Density](#)

[Epiphyte Rate](#)

[Epiphyte Temperature Rate Coefficients](#)

[Epiphyte Stoichiometry](#)

Epiphyte Temperature Rate Coefficients (EPI TEMP)

FIELD	NAME	VALUE	DEFAULT	DESCRIPTION
1				(Ignored by code)
2	ET1	Real	5.0	Lower temperature for epiphyton growth, °C
3	ET2	Real	25.0	Lower temperature for maximum epiphyton growth, °C
4	ET3	Real	35.0	Upper temperature for maximum epiphyton growth, °C
5	ET4	Real	40.0	Upper temperature for epiphyton growth, °C
6	EK1	Real	0.1	Fraction of epiphyton growth rate at ET1
7	EK2	Real	0.99	Fraction of maximum epiphyton growth rate at ET2
8	EK3	Real	0.99	Fraction of maximum epiphyton growth rate at ET3
9	EK4	Real	0.1	Fraction of epiphyton growth rate at ET4

This card specifies the lower, maximum lower, upper, and maximum upper temperatures used in defining the curve that determines effects of temperature on epiphyton rates. Also specified is the fraction of maximum epiphyton rates that occurs at the specified temperature. Since the epiphyton compartment is new to V3.1, the default values have no basis other than these are the same default values used for algae in V2, so there is little experience in the use of these values.

Example

EPI TEMP	ET1	ET2	ET3	ET4	EK1	EK2	EK3	EK4
Epi 1	5.0	18.0	20.0	24.0	0.1	0.99	0.99	0.01
Epi 2	10.0	30.0	35.0	40.0	0.1	0.99	0.99	0.01
Epi 3	10.0	35.0	40.0	50.0	0.1	0.99	0.99	0.01

Related Cards and Files

[Epiphyte Control](#)

[Epiphyte Print](#)

[Epiphyte Initial Density](#)

[Epiphyte Rate](#)

[Epiphyte Half-Saturation](#)

[Epiphyte Stoichiometry](#)

Epiphyte Stoichiometry (EPI STOICH)

FIELD	NAME	VALUE	DEFAULT	DESCRIPTION
1				(Ignored by code)
2	EP	Real	0.005	Stoichiometric equivalent between epiphyton biomass and phosphorus
3	EN	Real	0.08	Stoichiometric equivalent between epiphyton biomass and nitrogen
4	EC	Real	0.45	Stoichiometric equivalent between epiphyton biomass and carbon
5	ESI	Real	0.18	Stoichiometric equivalent between epiphyton biomass and silica
6	ECHLA	Real	145.0	Ratio between epiphyton biomass and chlorophyll <i>a</i>
7	EPOM	Real	0.8	Fraction of epiphyton biomass that is converted to particulate organic matter when epiphyton die

This card specifies the stoichiometric equivalences used for determining the amount of nutrients in epiphyton biomass. These ratios are not constant over time and vary by epiphyton species. In addition, the epiphyton to chlorophyll *a* ratio [ECHLA] is known to be different for different epiphyton species and is known to vary over time for a given epiphyton species. Currently, the model does not include variable stoichiometry or biomass to chlorophyll *a* ratios. This is an area that will be improved upon in the future. [EPOM] is the fraction of epiphyton biomass lost by mortality going into the detritus compartment with the remainder going to labile DOM.

Example

EPI STOICH	EP	EN	EC	ESI	ECHLA	EPOM
Epi 1	0.005	0.08	0.45	0.18	65.0	0.8
Epi 2	0.005	0.08	0.45	0.00	65.0	0.8
Epi 3	0.005	0.08	0.45	0.00	65.0	0.8

Related Cards and Files

[Epiphyte Control](#)

[Epiphyte Print](#)

[Epiphyte Initial Density](#)

[Epiphyte Rate](#)

[Epiphyte Half-Saturation](#)

[Epiphyte Temperature Rate Coefficients](#)

Dissolved Organic Matter (DOM)

FIELD	NAME	VALUE	DEFAULT	DESCRIPTION
1				(Ignored by code)
2	LDOMDK	Real	0.1	Labile DOM decay rate, <i>day</i> ⁻¹
3	RDOMDK	Real	0.001	Refractory DOM decay rate, <i>day</i> ⁻¹
4	LRDDK	Real	0.01	Labile to refractory DOM decay rate, <i>day</i> ⁻¹

This card specifies decay rates associated with dissolved organic matter. Dissolved organic matter in the model is divided into labile and refractory partitions. The labile partition has a higher decay rate and generally consists of autochthonous inputs such as early products of algal decay. The refractory decay rate, [RDOMDK], is generally two orders of magnitude smaller than the labile decay rate [LDOMDK]. If BOD decay rates are available, then they should be used as a starting point for [LDOMDK].

Table C-18. Labile DOM Decay Rate Literature Values.

Compound	Decay Rate, <i>day</i> ⁻¹	Reference
Acetate	0.20	Wright, 1975
Amino acids	0.64	Williams et al., 1976
Glucose	0.24	Williams et al., 1976
Glucose	0.32-0.50	Toerien and Cavari, 1982
Glucose	0.11	Wright, 1975
Glutamate	0.11-0.63	Carney and Colwell, 1976
Glycine	0.31-0.45	Vaccaro, 1969
Glycolate	0.01-0.43	Wright, 1975

Example

DOM	LDOMDK	RDOMDK	LRDDK
Wb 1	0.12	0.001	0.001
Wb 2	0.12	0.001	0.001
Wb 3	0.12	0.001	0.001

Related Cards and Files

[Particulate Organic Matter](#)
[Organic Matter Stoichiometry](#)
[Organic Matter Temperature Rate Multipliers](#)
[Carbonaceous Biochemical Oxygen Demand](#)

Particulate Organic Matter (POM)

FIELD	NAME	VALUE	DEFAULT	DESCRIPTION
1				(Ignored by code)
2	LPOMDK	Real	0.08	Labile POM decay rate, day^{-1}
3	RPOMDK	Real	0.001	Refractory POM decay rate, day^{-1}
4	LRPDK	Real	0.01	Labile to refractory POM decay rate, day^{-1}
5	POMS	Real	0.1	POM settling rate, $m\ day^{-1}$

Detritus in the model consists of autochthonous and allochthonous particulate organic matter (POM). The model uses a single decay rate [LPOMDK], but in reality, detritus is a heterogeneous mixture in various stages of decay. Allochthonous inputs are usually dominated by the refractory component while autochthonous inputs are initially labile becoming refractory over time. Literature values are given in the following tables.

Table C-19. Detritus Decay Rate Literature Values

Detritus Source	Detritus Decay Rate, day^{-1}	Reference
Cladophera glomerata	0.007	Piecznska, 1972
Gloeotrichia echinulata	0.001-0.007	Piecznska, 1972
Isoetes lancustris	0.003-0.015	Hanlon, 1982
Potamogeton crispus	0.002-0.004	Rogers & Breen, 1982
Potamogeton perfoliatus	0.002-0.007	Hanlon, 1982
Beech litter	0.001-0.004	Hanlon, 1982
Green algae	0.016-0.076	Otsuki & Hayna, 1972
Mixed algae	0.007-0.111	Jewell & McCarty, 1971
Mixed algae	0.007-0.060	Fitzgerald, 1964
Leaf packs	0.005-0.017	Sedell, Triska, and Triska, 1975

Detrital settling velocities [POMS] vary over a large range (0.001 to $> 20\ m\ day^{-1}$) depending upon the detritus. Again, the model allows for only a single value. Literature values are given in [Table C-20](#).

Table C-20. Detritus Settling Velocity Literature Values

Detritus Source	Settling Velocity, $m\ day^{-1}$	Reference
Ceratium balticum	9.0	Apstein, 1910
Chaetoceros borealis	9.0	Apstein, 1910
Chaetoceros didymus	0.85	Eppley, Holmes, & Strickland, 1967
Cricosphaera carterae	1.70	Eppley, Holmes, & Strickland, 1967
Ditylum brightwellii	2.0	Apstein, 1910
Phaeodactylum tricornutum	0.02-0.04	Riley, 1943
Rhizosolenia herbetata	0.22	Eppley, Holmes, & Strickland, 1967b
Stephanopyxis tunis	2.1	Eppley, Holmes, & Strickland, 1976b
Tabellaria flocculosa	0.46-1.5	Smayda, 1971
Thalassiosira pseudonana	0.85	Hecky & Kilham, 1974

Example

POM	LPOMDK	RPOMDK	LRPDK	POMS
WB 1	0.08	0.001	0.001	0.5
WB 2	0.08	0.001	0.001	0.5
WB 3	0.08	0.001	0.001	0.5

KINETIC COEFFICIENTS

CONTROL FILE

Related Cards and Files

[Dissolved Organic Matter](#)

[Organic Matter Stoichiometry](#)

[Organic Matter Temperature Rate Multipliers](#)

[Carbonaceous Biochemical Oxygen Demand](#)

Organic Matter Stoichiometry (OM STOICH)

FIELD	NAME	VALUE	DEFAULT	DESCRIPTION
1				(Ignored by code)
2	ORGP	Real	0.005	Stoichiometric equivalent between organic matter and phosphorus
3	ORGN	Real	0.08	Stoichiometric equivalent between organic matter and nitrogen
4	ORGC	Real	0.45	Stoichiometric equivalent between organic matter and carbon
5	ORGSi	Real	0.18	Stoichiometric equivalent between organic matter and silica

This card specifies the stoichiometric relationship between organic matter and inorganic nutrients. The user has the ability to change the relationship between waterbodies, although this option is not recommended. The values should not be changed from the defaults unless the user has the data to support the changes.

Example

OM STOICH	ORGP	ORGN	ORGC	ORGSi
Wb 1	0.005	0.08	0.45	0.18
Wb 2	0.005	0.08	0.45	0.18
Wb 3	0.005	0.08	0.45	0.18

Related Cards and Files

[Dissolved Organic Matter](#)

[Particulate Organic Matter](#)

[Organic Matter Temperature Rate Multipliers](#)

[Carbonaceous Biochemical Oxygen Demand](#)

Organic Matter Temperature Rate Multipliers (OM RATE)

FIELD	NAME	VALUE	DEFAULT	DESCRIPTION
1				(Ignored by code)
2	OMT1	Real	4.0	Lower temperature for organic matter decay, °C
3	OMT2	Real	25.0	Upper temperature for organic matter decay, °C
4	OMK1	Real	0.1	Fraction of organic matter decay rate at OMT1
5	OMK2	Real	0.99	Fraction of organic matter decay rate at OMT2

This card specifies the lower and maximum temperatures used in defining the curve that determines effects of temperature on organic matter decay. Recommended values are given in the example.

Example

OM RATE	OMT1	OMT2	OMK1	OMK2
Wb 1	4.0	25.0	0.1	0.99
Wb 2	4.0	25.0	0.1	0.99
Wb 3	4.0	25.0	0.1	0.99

Related Cards and Files

[Dissolved Organic Matter](#)

[Particulate Organic Matter](#)

[Organic Matter Stoichiometry](#)

[Carbonaceous Biochemical Oxygen Demand](#)

Carbonaceous Biochemical Oxygen Demand (CBOD)

FIELD	NAME	VALUE	DEFAULT	DESCRIPTION
1				(Ignored by code)
2	KBOD	Real		5-day decay rate @ 20°C, day^{-1}
3	TBOD	Real		Temperature coefficient
4	RBOD	Real		Ratio of CBOD5 to ultimate CBOD

The model allows the user to include any number of CBOD groups (see [Constituent Dimensions](#) card). This allows the user to specify multiple point source loadings of CBOD with different rates associated with them and track them in the model over space and time.

[KBOD] is the first-order reaction rate for CBOD decay. [TBOD] is used to adjust the decay rate for temperature effects according to the following equation:

$$KBOD = KBOD_{20} * TBOD^{T-20}$$

where:

T = temperature, °C

$KBOD_{20}$ = decay rate at 20 °C

[RBOD] is used to convert 5-day CBOD values to ultimate CBOD. This formulation is included for applications that involve determining the effects of waste effluents on dissolved oxygen in which loadings are typically expressed in terms of CBOD.

Example

CBOD	KBOD	TBOD	RBOD
CBOD 1	0.25	1.0147	1.85
CBOD 2	0.25	1.0147	1.85
CBOD 3	0.25	1.0147	1.85

Related Cards and Files

[CBOD Stoichiometry](#)

CBOD Stoichiometry (CBOD STOICH)

FIELD	NAME	VALUE	DEFAULT	DESCRIPTION
1				(Ignored by code)
2	CBODP	Real		P stoichiometry for CBOD decay
3	CBODN	Real		N stoichiometry for CBOD decay
4	CBODC	Real		C stoichiometry for CBOD decay

The stoichiometric coefficients define the stoichiometry of BOD in terms of N, P, and C. Each coefficient expresses the fraction of N, P or C in terms of BOD. These are not the same as the organic matter stoichiometric coefficients defined in terms of N, P, or C in terms of organic matter. A typical conversion from organic matter to oxygen is about 1.4 (see [Oxygen Stoichiometry 1](#)).

Example

CBOD STOIC	CBODP	CBODN	CBODC
CBOD 1	0.004	0.06	0.32
CBOD 2	0.004	0.06	0.32
CBOD 3	0.004	0.06	0.32

Related Cards and Files

[Carbenaceous Biochemichal Oxygen Demand](#)

Inorganic Phosphorus (PHOSPHOR)

FIELD	NAME	VALUE	DEFAULT	DESCRIPTION
1				(Ignored by code)
2	PO4R	Real	0.001	Sediment release rate of phosphorus, fraction of SOD
3	PARTP	Real	0.0	Phosphorus partitioning coefficient for suspended solids

[PO4REL] is the sediment release rate of phosphorous under anaerobic conditions specified as a fraction of the sediment oxygen demand. Values up to 0.03 have been used in previous studies. [PARTP] is the phosphorous partitioning coefficient for sorption onto suspended solids. In the current model formulations, it is not recommended to allow phosphorus to sorb onto inorganic suspended solids, so [PARTP] should be set to zero.

Example

PHOSPHOR	PO4R	PARTP
wb 1	0.015	0.0
wb 2	0.015	0.0
wb 3	0.015	0.0

Ammonium (AMMONIUM)

FIELD	NAME	VALUE	DEFAULT	DESCRIPTION
1				(Ignored by code)
2	NH4REL	Real	0.001	Sediment release rate of ammonium, fraction of SOD
3	NH4DK	Real	0.12	Ammonium decay rate, day^{-1}

[NH4REL] is the sediment release rate of ammonium anaerobic conditions specified as a fraction of the sediment oxygen demand. Values up to 0.4 have been used in previous studies.

[NH4DK] is the rate at which ammonium is oxidized to nitrate-nitrite. Since the model considers nitrate-nitrite as one compartment, the rate specified should be the rate for conversion of ammonium to nitrate. Literature values are given in the following table.

Table C-21. Ammonium Decay Rate Literature Values

Site	Ammonium decay rate, day^{-1}	Reference
Grand River, IL	0.80	Bansal, 1976
Grasmerer Lake, UK	0.001-0.013	Hall, 1982
Truckee River, NV	0.09-1.30	Bansal, 1976
Mohawk River, NY	0.23-0.40	Bansal, 1976
Ohio River	0.25	Bansal, 1976
Big Blue River, NB	0.17-0.25	Bansal, 1976
Flint River, MI	0.76-0.95	Bansal, 1976

Example

AMMONIUM	NH4R	NH4DK
wb 1	0.08	0.12
wb 2	0.08	0.12
wb 3	0.08	0.12

Related Cards and Files

[Ammonium Temperature Rate Multipliers](#)

Ammonium Temperature Rate Multipliers (NH4 RATE)

FIELD	NAME	VALUE	DEFAULT	DESCRIPTION
1				(Ignored by code)
2	NH4T1	Real	5.0	Lower temperature for ammonia decay, °C
3	NH4T2	Real	25.0	Lower temperature for maximum ammonia decay, °C
4	NH4K1	Real	0.1	Fraction of nitrification rate at NH4T1
5	NH4K2	Real	0.99	Fraction of nitrification rate at NH4T2

This card specifies the lower and maximum lower temperatures used in defining the curve that determines the effect of temperature on ammonia nitrification. See Appendix B for more details on the mathematical formulation for the temperature coefficients. Recommended values are given in the example.

Example

NH4 RATE	NH4T1	NH4T2	NH4K1	NH4K2
Wb 1	5.0	25.0	0.1	0.99
Wb 2	5.0	25.0	0.1	0.99
Wb 3	5.0	25.0	0.1	0.99

Related Cards and Files

[Ammonium](#)

Nitrate (NITRATE)

FIELD	NAME	VALUE	DEFAULT	DESCRIPTION
1				(Ignored by code)
2	NO3DK	Real	0.03	Nitrate decay rate, day^{-1}
3	NO3S	Real	1.0	Denitrification rate from sediments, $m\ day^{-1}$

This card specifies the denitrification rates in the water column and from the water column to the sediments. Values use in previous modeling studies for the nitrate decay rate [NO3DK] have ranged from 0.05-0.15 day^{-1} . [NO3S] is analogous to a settling velocity and represents how fast nitrate is diffused into the sediments where it undergoes denitrification.

Example

NITRATE	NO3DK	NO3S
Wb 1	0.05	1.0
Wb 2	0.05	1.0
Wb 3	0.05	1.0

Related Cards and Files

[Nitrate Temperature Rate Multipliers](#)

Nitrate Temperature Rate Multipliers (NO3 RATE)

FIELD	NAME	VALUE	DEFAULT	DESCRIPTION
1				(Ignored by code)
2	NO3T1	Real	5.0	Lower temperature for nitrate decay, °C
3	NO3T2	Real	25.0	Lower temperature for maximum nitrate decay, °C
4	NO3K1	Real	0.1	Fraction of denitrification rate at NO3T1
5	NO3K2	Real	0.99	Fraction of denitrification rate at NO3T2

This card specifies the lower and maximum lower temperatures used in defining the curve that determines the effect of temperature on denitrification. See [Appendix B](#) for more details on the mathematical formulation for the temperature coefficients. Recommended values are given in the example.

Example

NO3 RATE	NO3T1	NO3T2	NO3K1	NO3K2
Wb 1	5.0	25.0	0.1	0.99
Wb 2	5.0	25.0	0.1	0.99
Wb 3	5.0	25.0	0.1	0.99

Related Cards and Files

[Nitrate](#)

Silica (SILICA)

FIELD	NAME	VALUE	DEFAULT	DESCRIPTION
1				(Ignored by code)
2	DSIR	Real	0.1	Dissolved silica sediment release rate, fraction of SOD
3	PSIS	Real	1.0	Particulate biogenic settling rate, $m\ sec^{-1}$
4	PSIDK	Real	0.3	Particulate biogenic silica decay rate, day^{-1}
5	PARTSI	Real	0.0	Dissolved silica partitioning coefficient

This card specifies the relevant kinetic coefficient for silica kinetics. [DSIR] is the sediment release rate of dissolved silica from the zero-order sediment compartment. [PSIS] is the particulate biogenic settling rate and [PSIDK] is the particulate biogenic decay rate. Particulate biogenic silica represents the skeletal remains of diatoms. Dissolved silica is allowed to partition onto suspended solids and [PARTSI] is the value of the partitioning coefficient.

Example

SILICA	DSIR	PSIS	PSIDK	PARTSI
Wb 1	0.1	0.0	0.3	0.2
Wb 2	0.1	0.0	0.3	0.2
Wb 3	0.1	0.0	0.3	0.2

Related Cards and Files

[Algal Stoichiometry](#)

[Epiphyte Stoichiometry](#)

[Zero-Order Sediment Oxygen Demand](#)

Iron (IRON)

FIELD	NAME	VALUE	DEFAULT	DESCRIPTION
1				(Ignored by code)
2	FEREL	Real	0.5	Iron sediment release rate, fraction of sediment oxygen demand
3	FESETL	Real	2.0	Iron settling velocity, $m\ day^{-1}$

[FER] specifies the iron release rate from the sediments as a fraction of the sediment oxygen demand. Values between 0.3 and 0.5 have been used in previous modeling studies, but this is a function of the 0-order SOD calibration values that should change from system to system.

[FES] is the particulate iron settling rate in the water column under oxic conditions. Values between 0.5 and 2.0 have been used in previous modeling studies.

Example

```
IRON          FER      FES
              0.5      2.0
```

Related Cards and Files

[Zero-Order Sediment Oxygen Demand](#)

Sediment Carbon Dioxide Release (SED CO2)

FIELD	NAME	VALUE	DEFAULT	DESCRIPTION
1				(Ignored by code)
2	CO2REL	Real	0.1	Sediment carbon dioxide release rate, fraction of sediment oxygen demand

This card specifies the carbon dioxide release rate from the sediments as a fraction of the 0-order sediment oxygen demand.

Example

```
SED CO2  CO2REL  
          0.1
```

Related Cards and Files

[Zero-Order Sediment Oxygen Demand](#)

Oxygen Stoichiometry 1 (STOICH 1)

FIELD	NAME	VALUE	DEFAULT	DESCRIPTION
1				(Ignored by code)
2	O2NH4	Real	4.57	Oxygen stoichiometry for nitrification
3	O2OM	Real		Oxygen stoichiometry for organic matter decay

This card specifies the stoichiometric equivalents of oxygen for nitrification, organic matter decay. The default values should not be changed unless the user has data to support the change.

Example

```

STOICH 1  O2NH4  O2OM
Wb 1      4.57   1.4
Wb 2      4.57   1.4
Wb 3      4.57   1.4

```

Related Cards and Files

[Oxygen Stoichiometry 2](#)
[Oxygen Stoichiometry 3](#)

Oxygen Stoichiometry 2 (STOICH 2)

FIELD	NAME	VALUE	DEFAULT	DESCRIPTION
1				(Ignored by code)
2	O2AR	Real	1.1	Oxygen stoichiometry for algal respiration
3	O2AG	Real	1.4	Oxygen stoichiometry for algal primary production

This card specifies the stoichiometric equivalents of oxygen for algal respiration and algal primary production. The default values should not be changed unless the user has data to support the change.

Example

```
STOICH 2   O2AR   O2AG
Alg 1      1.1    1.4
Alg 2      1.1    1.4
Alg 3      1.1    1.4
```

Related Cards and Files

[Oxygen Stoichiometry 1](#)
[Oxygen Stoichiometry 3](#)

Oxygen Stoichiometry 3 (STOICH 3)

FIELD	NAME	VALUE	DEFAULT	DESCRIPTION
1				(Ignored by code)
2	O2ER	Real	1.1	Oxygen stoichiometry for epiphyton respiration
3	O2EG	Real	1.4	Oxygen stoichiometry for epiphyton primary production

This card specifies the stoichiometric equivalents of oxygen for epiphyton respiration and epiphyton primary production. The default values should not be changed unless the user has data to support the change.

Example

```

STOICH 3   O2ER   O2EG
Ep 1      1.1    1.4
Ep 2      1.1    1.4
Ep 3      1.1    1.4

```

Related Cards and Files

[Oxygen Stoichiometry 1](#)
[Oxygen Stoichiometry 2](#)

Oxygen Limit (O2 LIMIT)

FIELD	NAME	VALUE	DEFAULT	DESCRIPTION
1				(Ignored by code)
2	O2LIM	Real	0.1	Dissolved oxygen concentration at which anaerobic processes begin, $g\ m^{-3}$

This card specifies the dissolved oxygen concentration below which anaerobic processes such as nitrification and sediment nutrient releases take place.

Example

```
O2 LIMIT  O2LIM  
          0.1
```

Sediment Compartment (SEDIMENT)

FIELD	NAME	VALUE	DEFAULT	DESCRIPTION
1				(Ignored by code)
2	SEDC	Character	OFF	Turns ON/OFF the first-order sediment compartment
3	PRNSC	Character	OFF	Turns ON/OFF printing sediment organic matter concentrations to the snapshot file
4	SEDCI	Real		Initial sediment concentration, $g\ m^{-2}$
5	SEDK	Real		Sediment decay rate, day^{-1}
6	FSOD	Real		Fraction of the zero-order SOD rate used
7	FSED	Real		Fraction of the first-order sediment rate used

This card controls the behavior of the 0- and 1st-order sediment compartment. [SEDC] turns ON/OFF the 1st-order sediment compartment. The 1st-order sediment compartment is not a true sediment diagenesis compartment as it does not keep track of organic nutrient delivery to the sediments, their decay, and subsequent release back into the water column during hypoxic/anoxic conditions. However, it does keep track of organic matter delivery to the sediments via particulate organic matter and dead algal cells, and the subsequent water column oxygen demand that is exerted. The inclusion of the 1st-order sediment compartment makes the model more predictive in that any increase of organic matter delivery to the sediments will have an affect on the SOD.

[PRNSC] controls whether or not sediment organic matter concentrations that accumulate in the first-order SOD algorithm are output to the snapshot file. [SEDCI] specifies the initial “concentration(s)” for the 1st-order sediment compartment and its behavior is exactly the same as for setting the initial concentrations of any of the water column state variables. [SEDDK] specifies the sediment decay rate and should be somewhat less than the labile POM decay rate. [FSOD] multiplies the values specified for the zero-order sediment compartment and can be used to rapidly adjust the SOD values during calibration. [FSED] is similar to [FSOD] in that it multiplies the value of the 1st-order decay rate.

Example

EDIMENT	SEDC	PRNSC	SEDCI	SEDK	FSOD	FSED
Wb 1	ON	ON	0.0	0.1	1.0	1.0
Wb 2	ON	ON	0.0	0.1	1.0	1.0
Wb 3	ON	ON	0.0	0.1	1.0	1.0

Related Cards and Files

[Zero-Order Sediment Oxygen Demand
SOD Temperature Rate Multipliers](#)

SOD Temperature Rate Multipliers (SOD RATE)

FIELD	NAME	VALUE	DEFAULT	DESCRIPTION
1				(Ignored by code)
2	SODT1	Real	4.0	Lower temperature for zero-order SOD or first-order sediment decay, °C
3	SODT2	Real	25.0	Upper temperature for zero-order SOD or first-order sediment decay, °C
4	SODK1	Real	0.1	Fraction of SOD or sediment decay rate at lower temperature
5	SODK2	Real	0.99	Fraction of SOD or sediment decay rate at upper temperature

This card specifies the temperature rate multipliers that adjust the 0-order SOD or 1st-order decay rate. The model is very sensitive to these values and they are an important calibration parameter for accurately reproducing the timing of water column oxygen decreases early during stratified periods.

Example

SOD RATE	SODT1	SODT2	SODK1	SODK2
Wb 1	4.0	30.0	0.1	0.99
Wb 2	4.0	30.0	0.1	0.99
Wb 3	4.0	30.0	0.1	0.99

Related Cards and Files

[Sediment Compartment](#)

Zero-Order Sediment Oxygen Demand (S DEMAND)

FIELD	NAME	VALUE	DESCRIPTION
1			(Ignored by code)
2-10	SOD	Real	Zero-order sediment oxygen demand for each segment, $g O_2 m^{-2} day^{-1}$

This card specifies the 0-order sediment oxygen demand for each segment (including boundary segments) in the computational grid. If there are *more* values than can be specified on one line, then they are continued on the next line without another **S DEMAND** card being specified.

Sediment oxygen demand is known to vary spatially in reservoirs due to differences in sedimentation patterns and algal production (Cole & Hannan, 1989). In the model, the user can specify a separate value of sediment oxygen demand [SOD] for each model segment. Sediment oxygen demand typically ranges from 0.1 to 1.0 $gO_2 m^{-2} day^{-1}$, but can be higher (Newbold and Liggett, 1974). Additional information can be found in Gunnison, Chen, and Brannon (1983) and Chen, Brannon, and Gunnison (1984). Additional values are given in the following table.

Table C-22. Sediment Oxygen Demand Literature Values

Site	SOD, $g O_2 m^{-2} day^{-1}$	Reference
Cayuga Lake, NY	0.3-1.0	Newbold & Liggett, 1974
Lake Sammamish, WA	1.0	Bella, 1970
Lake Lyndon B. Johnson, TX	1.7-5.8	Schnoor & Fruh, 1979
Saginaw River, MI	0.1-5.3	Chiaro & Burke, 1980

Example

S DEMAND	SOD								
	0.3	0.3	0.3	0.3	0.3	0.3	0.3	0.3	0.3
	0.3	0.3	0.3	0.3	0.3	0.3	0.3	0.3	0.3
	0.3	0.3	0.3	0.3	0.3	0.3	0.3	0.3	0.3
	0.3	0.3	0.3	0.3	0.3	0.3	0.3	0.3	0.3
	0.3	0.3	0.3	0.3	0.3	0.3	0.3	0.3	0.3

Related Cards and Files

[Sediment Compartment](#)
[SOD Temperature Rate Multipliers](#)

Reaeration (REAERAT)

FIELD	NAME	VALUE	DEFAULT	DESCRIPTION
1				(Ignored by code)
2	REARC	Character	LAKE	Type of waterbody, RIVER, LAKE, or ESTUARY
3	EQN#	Integer	6	Equation number used for determining reaeration
4	COEF1	Real		User defined parameter
5	COEF2	Real		User defined parameter
6	COEF3	Real		User defined parameter
7	COEF4	Real		User defined parameter

This card allows the user to specify the appropriate reaeration formulation for the specific type of waterbody being simulated. [REARC] is used to specify the type of waterbody. [EQN#] is then used to specify the reaeration equation appropriate for the type of waterbody. The following table lists the equations for the RIVER waterbody type.

Table C-23. River Reaeration Equations

#	Equation	Comments	Applicability	Reference
0	Either Eq 1, 2 or 4	K_a is determined based on applicability criteria of each of these 3 formulations		Covar (1976)
1	$K_a = \frac{K_L}{H} = \frac{(D_{O_2} U)^{1/2}}{H^{3/2}}$	D_{O_2} = water molecular diffusion coefficient at 20°C, $8.1 E^{-5} \text{ ft}^2 \text{ hr}^{-1}$ or $2.09E-5 \text{ cm}^2 \text{ s}^{-1}$ $D_{O_2} = 1.91E-3(1.037)^{T-20}$, $\text{ft}^2 \text{ day}^{-1}$ U = velocity, ft/day H = depth, ft	Depths between 1-30 ft and velocities between 0.5-1.6 fps	O'Connor and Dobbins (1958)
2	$K_a = \frac{K_L}{H} = \frac{11.6U}{H^{1.67}}$	U = velocity, ft s^{-1} H = depth, ft K_a = reaeration rate, day^{-1}	Depths between 2-11 ft and velocities between 1.8-5 fps	Churchill, Elmore and Buckingham (1962)
3	$K_a = 0.88US \text{ for } 10 < Q < 300 \text{ cfs}$ $K_a = 1.8US \text{ for } 1 < Q < 10 \text{ cfs}$	S = slope, ft mile^{-1} U = velocity, ft s^{-1} K_a = reaeration rate, day^{-1}	Suggested for use when $Q < 10 \text{ cfs}$	Tsvoglou and Wallace (1972)
4	$K_a = \frac{K_L}{H} = \frac{21.6U^{0.67}}{H^{1.85}}$	U = velocity, ft s^{-1} H = depth, ft	Depths between 0.4-2.4 ft and velocities between 0.1-1.8 fps	Owens et al. (1964)
5	$K_a = \frac{K_L}{H} = \frac{25u^*}{H} (1 + F^{0.5})$	u^* = shear velocity, $(\text{HSG})^{0.5}$ S = energy grade line slope F = Froude number, $U/(gH)^{0.5}$		Thackston and Krenkel (1966)
6	$K_a = \frac{K_L}{H} = \frac{7.62U}{H^{1.33}}$	U = velocity, ft s^{-1} H = depth, ft		Langbien and Durum (1967)

#	Equation	Comments	Applicability	Reference
7	$K_a = 517(US)^{0.524}Q^{-0.242} \text{ for } Q < 0.556 \text{ m}^3\text{s}^{-1}$ $K_a = 596(US)^{0.528}Q^{-0.136} \text{ for } Q > 0.556 \text{ m}^3\text{s}^{-1}$	U = velocity, m s^{-1} S = slope, m m^{-1} Q = flow, $\text{m}^3 \text{s}^{-1}$ K _a = reaeration rate, day^{-1}	For pool and riffle streams	Melching and Flores (1999)
8	$K_a = 88(US)^{0.313}D^{0.353} \text{ for } Q < 0.556 \text{ m}^3\text{s}^{-1}$ $K_a = 142(US)^{0.333}D^{0.66}W^{0.243} \text{ for } Q > 0.556 \text{ m}^3\text{s}^{-1}$	U = velocity, m s^{-1} S = slope, m m^{-1} W = stream top width, m D = average depth, m K _a = reaeration rate, day^{-1}	For channel-control streams	Melching and Flores (1999)
9	$K_a = C_1 U^{C_2} H^{C_3} S^{C_4}$ <p>and if no channel slope:</p> $K_a = C_1 U^{C_2} H^{C_3}$	U = velocity, m s^{-1} H = depth, m S = slope [m/m or ft/ft], K _a = reaeration rate, day^{-1} C ₁ = user defined C ₂ = user defined C ₃ = user defined C ₄ = user defined	User defined relationship	

Table C-24 lists the reaeration equations available for lakes, reservoirs, and estuaries in which it is assumed that wind is the dominant forcing function for reaeration.

Table C-24. Lake Reaeration Equations

#	Equation	Comments	Reference
1	$K_a = \frac{K_L}{H} = \frac{0.864W}{H}$	W = wind speed at 10 m, m s^{-1} H = depth, m K _L = reaeration velocity, m day^{-1}	Broecker et al (1978)
2	$K_a = \frac{K_L}{H} = \frac{\alpha W^\beta}{H}$	$\alpha=0.2, \beta=1.0$ for $W < 3.5 \text{ m s}^{-1}$ $\alpha=0.057, \beta=2.0$ for $W > 3.5 \text{ m s}^{-1}$ W = daily average wind speed, m s^{-1}	Gelda et al (1996)
3	$K_a = \frac{K_L}{H} = \frac{0.728W^{0.5} - 0.317W + 0.0372W^2}{H}$	W = wind speed at 10 m, m s^{-1} K _L = reaeration velocity, m day^{-1}	Banks and Herrera (1977)
4	$K_a = \frac{K_L}{H} = \frac{0.0986W^{1.64}}{H} \text{ at } T=20^\circ\text{C or}$ $K_a = \frac{K_L}{H} = \frac{0.0986W^{1.64}}{H} \left(\frac{600}{Sc} \right)^{0.5}$	W = wind speed at 10 m, m s^{-1} Sc = Schmidt number, $(\nu/D)=13750[0.10656 \exp(-0.0627T)+0.00495]$ T = temperature, $^\circ\text{C}$	Wanninkhof et al. (1991)
5	$K_a = \frac{K_L}{H} = \frac{D_{O_2}}{(200 - 60W^{0.5})10^{-6}H}$	D _{O₂} = molecular diffusivity of oxygen, $\text{m}^2 \text{s}^{-1}$, $2.1\text{E-}9 \text{ m}^2 \text{s}^{-1}$ at 20°C W = wind speed, m s^{-1} K _L = reaeration velocity, m s^{-1}	Chen, Kanwisher (1963)
6	$K_a = \frac{K_L}{H} = \frac{0.5 + 0.05W^2}{H}$		Cole and Buchak (1993)
7	$K_a = \frac{K_L}{H} = \frac{0.362\sqrt{W}}{H} \text{ } W < 5.5 \text{ m/s}$ $K_a = \frac{K_L}{H} = \frac{0.0277W^2}{H} \text{ } W > 5.5 \text{ m/s}$		Banks (1975)

#	Equation	Comments	Reference
8	$K_a = \frac{K_L}{H} = \frac{0.64 + 0.128W^2}{H}$	Recommended form for WQRSS reservoir model	Smith (1978)
9	$K_a = \frac{K_L}{H} = \frac{0.156W^{0.63}}{H} \quad W \leq 4.1 \text{ m s}^{-1}$ $K_a = \frac{K_L}{H} = \frac{0.0269W^{1.9}}{H} \quad W > 4.1 \text{ m s}^{-1}$		Liss (1973)
10	$K_a = \frac{K_L}{H} = \frac{0.0276W^2}{H}$		Downing and Truesdale (1955)
11	$K_a = \frac{K_L}{H} = \frac{0.0432W^2}{H}$		Kanwisher (1963)
12	$K_a = \frac{K_L}{H} = \frac{0.319W}{H}$		Yu et al (1977)
13	$K_a = \frac{K_L}{H} = \frac{0.398}{H} \quad W < 1.6 \text{ m s}^{-1}$ $K_a = \frac{K_L}{H} = \frac{0.155W^2}{H} \quad W \geq 1.6 \text{ m s}^{-1}$		Weiler (1974)
14	$K_a = \frac{K_L}{H} = \frac{C_1 + C_2W^{C_3}}{H}$	W = wind speed, m s^{-1} at 10 m K_a = reaeration rate, day^{-1} C_1 = user defined C_2 = user defined C_3 = user defined	

For estuary systems, Thomann and Mueller (1987) and Chapra (1997) suggest using any of the wind formulations in [Table C-24](#) or Equation 1 in [Table C-23](#) (O'Connor-Dobbins formula) using the mean tidal velocity over a tidal cycle. [Table C-25](#) shows an additional formulation from Thomann and Fitzpatrick (1982) for estuaries, as well as the approach of Covar (1976) for rivers. Since many texts suggest using the mean tidal velocity, caution should be used in using these equations since they are based on the instantaneous velocity.

Table C-25. Estuarine Reaeration Equations

#	Equation	Comments	Reference
0	Either Eq 1, 2 or 4 from Table C-23	K_a is determined based on applicability criteria of each of these 3 formulations	Covar (1976)
1	$K_a = \frac{K_L}{H} = \frac{0.728W^{0.5} - 0.317W + 0.0372W^2}{H}$ $+ 3.93 \frac{\sqrt{U}}{H^{1.5}}$	U = mean tidal velocity, m s^{-1} W = wind speed, m s^{-1} H = depth, m Kl = reaeration velocity, $m \text{ s}^{-1}$ This formula combines the effect of wind from Banks and Herrera (1977) and estuary tidal flow	Thomann and Fitzpatrick (1982)
2	$K_a = C_1 U^{C_2} H^{C_3} + \frac{0.5 + C_4 W^2}{H}$	U = velocity, m s^{-1} H = depth, m W = wind speed at 10 m K_a = reaeration rate, day^{-1} C_1 = user defined C_2 = user defined C_3 = user defined C_4 = user defined	User defined relationship

CONTROL FILE

KINETIC COEFFICIENTS

In an estuary situation, a computation can be performed to evaluate whether wind shear or boundary shear controls the turbulence intensity at the surface. This algorithm will be added to the code in a future release version. For further information, see Appendix B.

Example

REAERAT	REARC	EQN#	COEF1	COEF2	COEF3	COEF4
Wb 1	RIVER	7				
Wb 2	LAKE	5				
Wb 3	ESTUARY	1				

Restart Input Filename (RSI FILE)

FIELD	NAME	VALUE	DESCRIPTION
1			(Ignored by code)
2-10	RSIFN	Character	Restart input data filename

This card specifies the filename used as input for restarts.

Example

```
RSI FILE.....RSIFN.....  
      rsi.npt
```

Withdrawal Filename (QWD FILE)

FIELD	NAME	VALUE	DESCRIPTION
1			(Ignored by code)
2-10	QWDFN	Character	Withdrawal filename

This card specifies the filename for withdrawal outflows. See a description of the [withdrawal file](#) for more information on data setup.

Example

```
QWD FILE.....QWDFN.....  
      qwd.npt
```

Gate Outflow Filename (QGT FILE)

FIELD	NAME	VALUE	DESCRIPTION
1			(Ignored by code)
2-10	QGTFN	Character	Gated outflow filename

This card specifies the filename(s) for branch outflows. See a description of the [gate outflow file](#) for more information on data setup.

Example

```
QGT FILE..... QGTFN.....
      qgt.npt
```

Wind Sheltering Filename (WSC FILE)

FIELD	NAME	VALUE	DESCRIPTION
1			(Ignored by code)
2-10	WSCFN	Character	Wind sheltering Coefficient sheltering filename

This card specifies the filename containing the wind sheltering coefficients as a function of segment number and Julian date. One file contains all the wind sheltering coefficients for all waterbodies. See a description of the [wind-sheltering file](#) for more information on data setup.

Example

```
WSC FILE.....WSCFN.....
      wsc_wb1.npt
```

Dynamic Shading Filename (SHD FILE)

FIELD	NAME	VALUE	DESCRIPTION
1			(Ignored by code)
2-10	SHDFN	Character	Dynamic shading filename

This card specifies the filename containing the wind sheltering coefficients as a function of segment number and Julian date. One file contains all the dynamic shading coefficients for all waterbodies. See a description of the [dynamic shading file](#) for more information on data setup.

Example

```
SHD FILE.....SHDFN.....
      shd.npt
```

Bathymetry Filename (BTH FILE)

FIELD	NAME	VALUE	DESCRIPTION
1			(Ignored by code)
2-10	BTHFN	Character	Bathymetry filename

This card specifies the filename(s) containing the waterbody bathymetry. See a description of the [bathymetry file](#) for more information on the data setup.

Example

```

BTH FILE.....BTHFN.....
Wb 1    bth_wb1.npt
Wb 2    bth_wb2.npt
Wb 3    bth_wb3.npt

```

Meteorology Filename (MET FILE)

FIELD	NAME	VALUE	DESCRIPTION
1			(Ignored by code)
2-10	METFN	Character	Meteorologic input data filename

This card specifies the filename(s) for time-varying meteorologic data. More information on data setup can be found in the description of the [meteorology input file](#).

Example

```

MET FILE.....METFN.....
Wb 1    met_wb1.npt
Wb 2    met_wb2.npt
Wb 3    met_wb3.npt

```

Light Extinction Filename (EXT FILE)

FIELD	NAME	VALUE	DESCRIPTION
1			(Ignored by code)
2-10	EXTFN	Character	Light extinction input data filename

This card specifies the filename(s) for time-varying light extinction data in Julian day versus light extinction coefficient in m^{-1} . More information on data setup can be found in the description of the [light extinction file](#).

Example

```
EXT FILE.....EXTFN.....
Wb 1   ext_wb1.npt - not used
Wb 2   ext_wb2.npt - not used
Wb 3   ext_wb3.npt - not used
```

Vertical Profile Filename (VPR FILE)

FIELD	NAME	VALUE	DESCRIPTION
1			(Ignored by code)
2-10	VPRFN	Character	Temperature and constituent vertical profile filename used for specifying initial conditions for the grid

This card specifies the filename(s) used to specify vertically varying initial temperatures and concentrations for the grid. More information on data setup can be found at the description of the [vertical profile file](#).

Example

```
VPR FILE.....VPRFN.....  
Wb 1    vpr_wb1.npt  
Wb 2    vpr_wb2.npt  
Wb 3    vpr_wb3.npt
```

Longitudinal Profile Filename (LPR FILE)

FIELD	NAME	VALUE	DESCRIPTION
1			(Ignored by code)
2-10	LPRFN	Character	Temperature and constituent longitudinal profile filename used for specifying initial conditions for the grid

This card specifies the filename(s) used to specify vertically and longitudinally varying initial temperatures and concentrations for the grid. More information on data setup can be found at the description of the [longitudinal profile file](#).

Example

```
LPR FILE.....LPRFN.....
Wb 1    lpr_wb1.npt
Wb 2    lpr_wb2.npt
Wb 3    lpr_wb3.npt
```

Branch Inflow Filename (QIN FILE)

FIELD	NAME	VALUE	DESCRIPTION
1			(Ignored by code)
2-10	QINFN	Character	Inflow filename

This card specifies the filename(s) for branch inflows. More information on data setup can be found at the description of the [branch inflow file](#).

Example

```

QIN FILE.....QINFN.....
Br 1    qin_br1.npt
Br 2    qin_br2.npt
Br 3    qin_br3.npt
Br 4    qin_br4.npt

```

Branch Inflow Temperature Filename (TIN FILE)

FIELD	NAME	VALUE	DESCRIPTION
1			(Ignored by code)
2-10	TINFN	Character	Inflow temperature filename

This card specifies the filename(s) for branch inflow temperatures. More information on data setup can be found at the description of the [branch inflow temperature file](#).

Example

```
TIN FILE.....TINFN.....
Br 1   tin_br1.npt
Br 2   tin_br2.npt
Br 3   tin_br3.npt
Br 4   tin_br4.npt
```

Branch Inflow Constituent Filename (CIN FILE)

FIELD	NAME	VALUE	DESCRIPTION
1			(Ignored by code)
2-10	CINFN	Character	Inflow constituent filename

This card specifies the filename(s) for branch inflow concentrations. More information on data setup can be found at the description of the [branch inflow concentration file](#).

Example

```
CIN FILE.....CINFN.....  
Br 1   cin_br1.npt  
Br 2   cin_br2.npt  
Br 3   cin_br3.npt  
Br 4   cin_br4.npt
```

Branch Outflow Filename (QOT FILE)

FIELD	NAME	VALUE	DESCRIPTION
1			(Ignored by code)
2-10	QOTFN	Character	Outflow filename

This card specifies the filename(s) for branch outflows. More information on data setup can be found at the description of the [branch outflow file](#).

Example

```
QOT FILE.....QOTFN.....  
Br 1    qot_br1.npt  
Br 2    qot_br2.npt  
Br 3    qot_br3.npt  
Br 4    qot_br4.npt
```

Tributary Inflow Filename (QTR FILE)

FIELD	NAME	VALUE	DESCRIPTION
1			(Ignored by code)
2-10	QTRFN	Character	Tributary inflow filename

This card specifies the filename(s) for tributary inflows. There must be a separate file for each tributary. More information on data setup can be found at the description of the [tributary inflow file](#).

Example

```
QTR FILE.....QTRFN.....
Tr 1      qtr_tr1.npt
```

Tributary Inflow Temperature Filename (TTR FILE)

FIELD	NAME	VALUE	DESCRIPTION
1			(Ignored by code)
2-10	TTRFN	Character	Tributary temperature filename

This card specifies the filename(s) for tributary inflow temperatures. There must be a separate file for each tributary. More information on data setup can be found at the description of the [tributary inflow temperature file](#).

Example

```
TTR FILE.....TTRFN.....
Tr 1    ttr_tr1.npt
```

Tributary Inflow Concentration Filename (CTR FILE)

FIELD	NAME	VALUE	DESCRIPTION
1			(Ignored by code)
2-10	CTRFN	Character	Tributary inflow concentration filename

This card specifies the filename(s) for tributary inflow concentrations. There must be a separate file for each tributary. More information on data setup can be found at the description of the [tributary inflow concentration file](#).

Example

```
CTR FILE.....CTRFN.....
Tr 1      ctr_tr1.npt
```

Distributed Tributary Inflow Filename (QDT FILE)

FIELD	NAME	VALUE	DESCRIPTION
1			(Ignored by code)
2-10	QDTFN	Character	Distributed tributary inflow filename

This card specifies the filename(s) for distributed tributary inflow. There must be a separate file for each branch. More information on data setup can be found at the description of the [distributed tributary inflow file](#).

Example

```

QDT FILE.....QDTFN.....
Br 1    qdt_tr1.npt
Br 2    qdt_tr2.npt
Br 3    qdt_tr3.npt
Br 4    qdt_tr4.npt

```

Distributed Tributary Inflow Temperature Filename (TDT FILE)

FIELD	NAME	VALUE	DESCRIPTION
1			(Ignored by code)
2-10	TDTFN	Character	Distributed tributary temperature filename

This card specifies the filename(s) for distributed tributary inflow temperatures. There must be a separate file for each branch. More information on data setup can be found at the description of the [distributed tributary inflow temperature file](#).

Example

```
TDT FILE.....TDTFN.....
Br 1    tdt_tr1.npt
Br 2    tdt_tr2.npt
Br 3    tdt_tr3.npt
Br 4    tdt_tr4.npt
```

Distributed Tributary Inflow Concentration Filename (CDT FILE)

FIELD	NAME	VALUE	DESCRIPTION
1			(Ignored by code)
2-10	CDTFN	Character	Distributed tributary inflow concentration filename

This card specifies the filename(s) for distributed tributary inflow concentrations. There must be a separate file for each branch. More information on data setup can be found at the description of the [distributed tributary inflow concentration file](#).

Example

```

CDT FILE.....CDTFN.....
Br 1    cdt_tr1.npt
Br 2    cdt_tr2.npt
Br 3    cdt_tr3.npt
Br 4    cdt_tr4.npt

```

Precipitation Filename (PRE FILE)

FIELD	NAME	VALUE	DESCRIPTION
1			(Ignored by code)
2-10	PREFN	Character	Precipitation filename

This card specifies the filename(s) for each branch precipitation. There must be a separate file for each branch. More information on data setup can be found at the description of the [precipitation file](#). The “ - not used” tag at the end of the filename is useful when looking at the echoing of input filenames in the [preprocessor output](#) and can alert the user to an input option that is or is not being used. If precipitation is turned ON for a branch, then the “ - not used” tag should be removed.

Example

```
PRE FILE.....PREFN.....
Br 1   pre_br1.npt - not used
Br 2   pre_br2.npt - not used
Br 3   pre_br3.npt - not used
Br 4   pre_br4.npt - not used
```

Precipitation Temperature Filename (TPR FILE)

FIELD	NAME	VALUE	DESCRIPTION
1			(Ignored by code)
2-10	TPRFN	Character	Precipitation temperature filename

This card specifies the filename(s) for branch precipitation temperatures. There must be a separate file for each branch. More information on data setup can be found at the description of the [precipitation temperature file](#). The “ - not used” tag at the end of the filename is useful when looking at the echoing of input filenames in the [preprocessor output](#) and can alert the user to an input option that is or is not being used. If precipitation is turned ON for a branch, then the “ - not used” tag should be removed.

Example

```
TPR FILE.....TPRFN.....
Br 1    tpr_br1.npt - not used
Br 2    tpr_br2.npt - not used
Br 3    tpr_br3.npt - not used
Br 4    tpr_br4.npt - not used
```

Precipitation Concentration Filename (CPR FILE)

FIELD	NAME	VALUE	DESCRIPTION
1			(Ignored by code)
2-10	CPRFN	Character	Precipitation concentration filename

This card specifies the filename(s) for branch precipitation constituent concentrations. There must be a separate file for each branch. More information on data setup can be found at the description of the [precipitation concentration file](#). The “ - not used” tag at the end of the filename is useful when looking at the echoing of input filenames in the [preprocessor output](#) and can alert the user to an input option that is or is not being used. If precipitation is turned ON for a branch, then the “ - not used” tag should be removed.

Example

```
CPR FILE.....CPRFN.....
Br 1    cpr_br1.npt - not used
Br 2    cpr_br2.npt - not used
Br 3    cpr_br3.npt - not used
Br 4    cpr_br4.npt - not used
```

External Upstream Head Filename (EUH FILE)

FIELD	NAME	VALUE	DESCRIPTION
1			(Ignored by code)
2-10	EUHFN	Character	External upstream head filename

This card specifies the filename(s) for branch external upstream heads. There must be a separate file for each branch. More information on data setup can be found at the description of the [upstream head file](#). The “ - not used” tag at the end of the filename is useful when looking at the echoing of input filenames in the [preprocessor output](#) and can alert the user to an input option that is or is not being used. If precipitation is turned ON for a branch, then the “ - not used” tag should be removed.

Example

```

EUH FILE.....EUHFN.....
Br 1   euh_br1.npt - not used
Br 2   euh_br2.npt - not used
Br 3   euh_br3.npt - not used
Br 4   euh_br4.npt - not used

```

External Upstream Head Temperature Filename (TUH FILE)

FIELD	NAME	VALUE	DESCRIPTION
1			(Ignored by code)
2-10	TUHFN	Character	External upstream head temperature filename

This card specifies the filename(s) for branch external upstream head vertical temperatures. There must be a separate file for each branch. More information on data setup can be found at the description of the [upstream head temperature file](#). The “ - not used” tag at the end of the filename is useful when looking at the echoing of input filenames in the [preprocessor output](#) and can alert the user to an input option that is or is not being used. If precipitation is turned ON for a branch, then the “ - not used” tag should be removed.

Example

```
TUH FILE.....TUHFN.....
Br 1    tuh_br1.npt - not used
Br 2    tuh_br2.npt - not used
Br 3    tuh_br3.npt - not used
Br 4    tuh_br4.npt - not used
```

External Upstream Head Concentration Filename (CUH FILE)

FIELD	NAME	VALUE	DESCRIPTION
1			(Ignored by code)
2-10	CUHFN	Character	External upstream head concentration filename

This card specifies the filename(s) for branch external upstream head constituent concentrations. There must be a separate file for each branch. More information on data setup can be found at the description of the [upstream head concentration file](#). The “ - not used” tag at the end of the filename is useful when looking at the echoing of input filenames in the [preprocessor output](#) and can alert the user to an input option that is or is not being used. If precipitation is turned ON for a branch, then the “ - not used” tag should be removed.

Example

```
CUH FILE.....CUHFN.....
Br 1    cuh_br1.npt - not used
Br 2    cuh_br2.npt - not used
Br 3    cuh_br3.npt - not used
Br 4    cuh_br4.npt - not used
```

External Downstream Head Filename (EDH FILE)

FIELD	NAME	VALUE	DESCRIPTION
1			(Ignored by code)
2-10	EDHFN	Character	External downstream head filename

This card specifies the filename(s) for branch external downstream heads. There must be a separate file for each branch. More information on data setup can be found at the description of the [downstream head file](#). The “ - not used” tag at the end of the filename is useful when looking at the echoing of input filenames in the [preprocessor output](#) and can alert the user to an input option that is or is not being used. If precipitation is turned ON for a branch, then the “ - not used” tag should be removed.

Example

```
EDH FILE.....EDHFN.....
Br 1    edh_br1.npt - not used
Br 2    edh_br2.npt - not used
Br 3    edh_br3.npt - not used
Br 4    edh_br4.npt
```

External Downstream Head Temperature Filename (TDH FILE)

FIELD	NAME	VALUE	DESCRIPTION
1			(Ignored by code)
2-10	TDHFN	Character	External downstream head temperature filename

This card specifies the filename(s) for branch external downstream head vertical temperatures. There must be a separate file for each branch. More information on data setup can be found at the description of the [downstream head temperature file](#). The “ - not used” tag at the end of the filename is useful when looking at the echoing of input filenames in the [preprocessor output](#) and can alert the user to an input option that is or is not being used. If precipitation is turned ON for a branch, then the “ - not used” tag should be removed.

Example

```
TDH FILE.....TDHFN.....
Br 1    tdh_br1.npt - not used
Br 2    tdh_br2.npt - not used
Br 3    tdh_br3.npt - not used
Br 4    tdh_br4.npt
```

External Downstream Head Concentration Filename (CDH FILE)

FIELD	NAME	VALUE	DESCRIPTION
1			(Ignored by code)
2-10	CDHFN	Character	External downstream had concentration filename

This card specifies the filename(s) for branch external downstream head constituent concentrations. There must be a separate file for each branch. More information on data setup can be found at the description of the [downstream head concentration file](#). The “ - not used” tag at the end of the filename is useful when looking at the echoing of input filenames in the [preprocessor output](#) and can alert the user to an input option that is or is not being used. If precipitation is turned ON for a branch, then the “ - not used” tag should be removed.

Example

```

CDH FILE.....CDHFN.....
Br 1    cdh_br1.npt - not used
Br 2    cdh_br2.npt - not used
Br 3    cdh_br3.npt - not used
Br 4    cdh_br4.npt

```

Snapshot Filename (SNP FILE)

FIELD	NAME	VALUE	DESCRIPTION
1			(Ignored by code)
2-10	SNPFN	Character	Snapshot filename

This card specifies the snapshot filename(s).

Example

```
SNP FILE.....SNPFN.....  
Wb 1    snp_wb1.opt  
Wb 2    snp_wb2.opt  
Wb 3    snp_wb3.opt
```

Profile Plot Filename (PRF FILE)

FIELD	NAME	VALUE	DESCRIPTION
1			(Ignored by code)
2-10	PRFFN	Character	Profile plot filename

This card specifies the vertical profile plot filename(s).

Example

```
PRF FILE.....PRFFN.....
Wb 1    prf_wb1.opt
Wb 2    prf_wb2.opt
Wb 3    prf_wb3.opt
```

Vector Plot Filename (VPL FILE)

FIELD	NAME	VALUE	DESCRIPTION
1			(Ignored by code)
2-10	VPLFN	Character	Vector plot filename

This card specifies the velocity vector plot filename(s).

Example

```
VPL FILE.....VPLFN.....
Wb 1    vpl_wb1.opt
Wb 2    vpl_wb2.opt
Wb 3    vpl_wb3.opt
```

Contour Plot Filename (CPL FILE)

FIELD	NAME	VALUE	DESCRIPTION
1			(Ignored by code)
2-10	CPLFN	Character	Contour plot filename

This card specifies the contour plot filename(s).

Example

```

CPL FILE.....CPLFN.....
Wb 1    cpl_wb1.opt
Wb 2    cpl_wb2.opt
Wb 3    cpl_wb3.opt
    
```

Spreadsheet Plot Filename (SPR FILE)

FIELD	NAME	VALUE	DESCRIPTION
1			(Ignored by code)
2-10	SPRFN	Character	Spreadsheet plot filename

This card specifies the spreadsheet output filename(s). Output from this file is suitable for import into a spreadsheet or graphics package that uses a spreadsheet format for data management.

Example

```
SPR FILE.....SPRFN.....
Wb 1    spr_wb1.opt
Wb 2    spr_wb2.opt
Wb 3    spr_wb3.opt
```

Flux Filename (FLX FILE)

FIELD	NAME	VALUE	DESCRIPTION
1			(Ignored by code)
2-10	FLXFN	Character	Flux filename

This card specifies the kinetic fluxes filename(s). Output from this file is suitable for import into a spreadsheet or graphics package that uses a spreadsheet format for data management.

Example

```

FLX FILE.....FLXFN.....
Wb 1      flx_wb1.opt
Wb 2      flx_wb2.opt
Wb 3      flx_wb3.opt
    
```

Time Series Plot Filename (TSR FILE)

FIELD	NAME	VALUE	DESCRIPTION
1			(Ignored by code)
2-10	TSRFN	Character	Time series plot filename

This card specifies the time series plot filename(s).

Example

```
TSR FILE.....TSRFN.....  
      tsr.opt
```

Withdrawal Output Filename (WDO FILE)

FIELD	NAME	VALUE	DESCRIPTION
1			(Ignored by code)
2-10	WDOFN	Character	Withdrawal output filename

This card specifies the withdrawal output filename(s).

Example

```
WDO FILE.....WDOFN.....  
      wdo.opt
```

Sample Control Input File

Spokane River/Long Lake Model Version 3.1

TITLE CTITLE.....

Card 1 Version 3.1 Spokane River/Long Lake application
 Card 2 WB 1 - Sloping branches between State line and Upriver Pool
 Card 3 WB 2 - Pool of Upriver DAm
 Card 4 Wb 3 - Pool of Upper Falls Dam
 Card 5 WB 4 - 2 sloping branches above 9-mile dam pool
 Card 6 WB 5 - Nine Mile dam pool
 Card 7 WB 6 - Long Lake
 Card 8 Scott Wells, PSU
 Card 9 Rob Annear, PSU; Chris Berger, PSU
 Card 10 Tom Cole, WES

GRID	NWB	NBR	IMX	KMX					
	6	12	189	47					
IN/OUTFLOW	NTR	NST	NIW	NWD	NGT	NSP	NPI	NPU	
	7	7	0	0	0	6	0	0	
CONSTITUENTS	NCG	NSS	NAL	NEP	NBOD				
	5	1	1	1	5				
MISCELL	NDAY								
	100								
TIME CON	TMSTRT	TMEND	YEAR						
	1.0402	303.89	2000						
DLT CON	NDLT	DLTMIN							
	6	0.1							
DLT DATE	DLTD	DLTD							
	1.00	1.2	172.0	225.0	231.0	251.0			
DLT MAX	DLTMAX	DLTMAX							
	5.0	65.0	10.0	10.0	5.0	10.0			
DLT FRN	DLTF	DLTF							
	0.90	0.90	0.90	0.90	0.90	0.90			
DLT LIMIT	VISC	CELC							
Wb 1	ON	ON							
Wb 2	ON	ON							
Wb 3	ON	ON							
Wb 4	ON	ON							
Wb 5	ON	ON							
Wb 6	ON	ON							
BRANCH G	US	DS	UHS	DHS	UQB	DQB	NL	SLOPE	
Br 1	2	10	0	13	0	0	1	0.00181	
Br 2	13	24	10	27	0	0	1	0.00152	
Br 3	27	36	24	39	0	0	1	0.00328	
Br 4	39	48	36	0	0	0	1	0.00142	
Br 5	51	64	0	0	0	0	1	0.00000	
Br 6	67	73	-64	76	0	0	1	0.00000	
Br 7	76	86	73	0	0	0	1	0.00000	
Br 8	89	94	-86	97	0	0	1	0.00256	
Br 9	97	128	94	0	0	0	1	0.00208	
Br 10	131	135	0	138	0	0	1	0.00000	
Br 11	138	151	135	0	0	0	1	0.00000	
Br 12	154	188	-151	0	0	0	1	0.00000	

SAMPLE CONTROL FILE

CONTROL FILE

LOCATION	LAT	LONG	EBOT	BS	BE	JBDN
WB 1	47.8	117.8	578.72	1	4	4
WB 2	47.8	117.8	571.00	5	5	5
WB 3	47.8	117.8	560.00	6	7	7
WB 4	47.8	117.8	485.51	8	9	9
WB 5	47.8	117.8	481.00	10	11	11
WB 6	47.8	117.8	422.10	12	12	12

INIT CND	T2I	ICEI	WTYPEC
Wb 1	4.0	0.0	FRESH
Wb 2	4.0	0.0	FRESH
Wb 3	4.0	0.0	FRESH
Wb 4	4.0	0.0	FRESH
Wb 5	4.0	0.0	FRESH
Wb 6	4.0	0.0	FRESH

CALCULAT	VBC	EBC	MBC	PQC	EVC	PRC
Wb 1	ON	ON	ON	OFF	OFF	OFF
Wb 2	ON	ON	ON	OFF	OFF	OFF
Wb 3	ON	ON	ON	OFF	OFF	OFF
Wb 4	ON	ON	ON	OFF	OFF	OFF
Wb 5	ON	ON	ON	OFF	OFF	OFF
Wb 6	ON	ON	ON	OFF	OFF	OFF

DEAD SEA	WINDC	QINC	QOUTC	HEATC
Wb 1	ON	ON	ON	ON
Wb 2	ON	ON	ON	ON
Wb 3	ON	ON	ON	ON
Wb 4	ON	ON	ON	ON
Wb 5	ON	ON	ON	ON
Wb 6	ON	ON	ON	ON

INTERPOL	QINIC	DTRIC	HDIC
Br 1	ON	OFF	ON
Br 2	ON	OFF	ON
Br 3	ON	OFF	ON
Br 4	ON	OFF	ON
Br 5	ON	OFF	ON
Br 6	ON	OFF	ON
Br 7	ON	OFF	ON
Br 8	ON	OFF	ON
Br 9	ON	OFF	ON
Br 10	ON	OFF	ON
Br 11	ON	OFF	ON
Br 12	ON	OFF	ON

HEAT EXCH	SLHTC	SROC	RHEVAP	METIC	FETCHC	AFW	BFW	CFW	WINDH
Wb 1	TERM	OFF	OFF	ON	OFF	9.2	0.46	2.0	2.0
Wb 2	TERM	OFF	OFF	ON	OFF	9.2	0.46	2.0	2.0
Wb 3	TERM	OFF	OFF	ON	OFF	9.2	0.46	2.0	2.0
Wb 4	TERM	OFF	OFF	ON	OFF	9.2	0.46	2.0	2.0
Wb 5	TERM	OFF	OFF	ON	OFF	9.2	0.46	2.0	2.0
Wb 6	TERM	OFF	OFF	ON	OFF	9.2	0.46	2.0	2.0

ICE COVER	ICEC	SLICEC	ALBEDO	HWICE	BICE	GICE	ICEMIN	ICET2
Wb 1	OFF	DETAIL	0.25	10.0	0.6	0.07	0.05	3.0
Wb 2	OFF	DETAIL	0.25	10.0	0.6	0.07	0.05	3.0
Wb 3	OFF	DETAIL	0.25	10.0	0.6	0.07	0.05	3.0
Wb 4	OFF	DETAIL	0.25	10.0	0.6	0.07	0.05	3.0
Wb 5	OFF	DETAIL	0.25	10.0	0.6	0.07	0.05	3.0
Wb 6	OFF	DETAIL	0.25	10.0	0.6	0.07	0.05	3.0

CONTROL FILE

SAMPLE CONTROL FILE

TRANSPORT	SLTRC	THETA
Wb 1	ULTIMATE	0.55
Wb 2	ULTIMATE	0.55
Wb 3	ULTIMATE	0.55
Wb 4	ULTIMATE	0.55
Wb 5	ULTIMATE	0.55
Wb 6	ULTIMATE	0.55

HYD COEF	AX	DX	CBHE	TSED	FI	TSEDF	FRICC
Wb 1	1.0	1.0	0.3	11.5	0.01	1.00	MANN
Wb 2	1.0	1.0	0.3	11.5	0.01	1.00	MANN
Wb 3	1.0	1.0	0.3	11.5	0.01	1.00	MANN
Wb 4	1.0	1.0	0.3	11.5	0.01	1.00	MANN
Wb 5	1.0	1.0	0.3	11.5	0.01	1.00	MANN
Wb 6	1.0	1.0	0.3	11.5	0.01	1.00	MANN

EDDY VISC	AZC	AZSLC	AZMAX
Wb 1	W2N	IMP	1.0
Wb 2	W2	IMP	1.0
Wb 3	W2	IMP	1.0
Wb 4	W2N	IMP	1.0
Wb 5	W2	IMP	1.0
Wb 6	W2	IMP	1.0

N STRUC	NSTR
Br 1	0
Br 2	0
Br 3	0
Br 4	0
Br 5	2
Br 6	0
Br 7	2
Br 8	0
Br 9	0
Br 10	0
Br 11	2
BRr 12	1

STR INT	STRIC								
Br 1									
Br 2									
Br 3									
Br 4									
Br 5	OFF	OFF							
Br 6									
Br 7	OFF	OFF							
Br 8									
Br 9									
Br 10									
Br 11	OFF	OFF							
Br 12	OFF								

STR TOP	KTSTR								
Br 1									
Br 2									
Br 3									
Br 4									
Br 5	2	2							
Br 6									
Br 7	2	2							
Br 8									
Br 9									
Br 10									
Br 11	2	2							
Br 12	2								

SAMPLE CONTROL FILE

CONTROL FILE

STR BOT	KBSTR									
Br 1										
Br 2										
Br 3										
Br 4										
Br 5	41	41								
Br 6										
Br 7	38	38								
Br 8										
Br 9										
Br 10										
Br 11	39	39								
Br 12	46									

STR SINK	SINKC									
Br 1										
Br 2										
Br 3										
Br 4										
Br 5	POINT	LINE								
Br 6										
Br 7	POINT	POINT								
Br 8										
Br 9										
Br 10										
Br 11	POINT	POINT								
Br 12	POINT									

STR ELEV	ESTR	ESTR	ESTR	ESTR	ESTR	ESTR	ESTR	ESTR	ESTR	WSTR
Br 1										
Br 2										
Br 3										
Br 4										
Br 5	579.5	577.1								
Br 6										
Br 7	565.15	567.25								
Br 8										
Br 9										
Br 10										
Br 11	485.0	489.0								
Br 12	456.9									

STR WIDTH	WSTR									
Br 1										
Br 2										
Br 3										
Br 4										
Br 5		70.0								
Br 6										
Br 7										
Br 8										
Br 9										
Br 10										
Br 11										
Br 12										

PIPES	IUPI	IDPI	EUPI	EDPI	WPI	DLXPI	FPI	FMINPI	LATPIC
Pi 1	24	28	28.0	27.0	0.5	230.0	0.065	0.1	DOWN

PIPE UP	PUPIC	ETUPI	EBUPI	KTUPI	KBUPI
Pi 1	DISTR			2	23

PIPE DOWN	PDPIC	ETDPI	EBDPI	KTDPI	KBDPI
Pi 1	DISTR			2	23

CONTROL FILE

SAMPLE CONTROL FILE

SPILLWAY	IUSP	IDSP	ESP	AISP	B1SP	A2SP	B2SP	LATSPC		
Spill 1	64	67	592.14	10000.0	1.5	20.00	1.5	DOWN		
Spill 2	86	89	580.14	7000.0	1.5	20.00	1.5	DOWN		
Spill 3	151	154	497.00	10000.0	1.5	20.00	1.5	DOWN		
Spill 4	188	0	469.00	20000.0	1.5	20.00	1.5	DOWN		
Spill 5	48	51	579.80	80.00	1.5	30.00	1.5	DOWN		
Spill 6	128	131	486.50	60.00	1.5	30.00	1.5	DOWN		
SPILL UP	PUSPC	ETUSP	EBUSP	KTUSP	KBUSP					
Spill1	DISTR			2	41					
Spill2	DISTR			2	38					
Spill3	DISTR			2	39					
Spill4	DISTR			2	46					
Spill5	DISTR			2	45					
Spill6	DISTR			2	46					
SPILL DOWN	PDSPC	ETDSP	EBDSP	KTDSP	KBDSB					
Spill1	DISTR			2	36					
Spill2	DISTR			2	45					
Spill3	DISTR			2	6					
Spill4	DISTR			2	46					
Spill5	DISTR			2	43					
Spill6	DISTR			2	39					
SPILL GAS	GASSP	EQSP	ASP	BSP	CSP					
Spill1	OFF									
Spill2	OFF									
Spill3	OFF									
Spill4	OFF									
Spill5	OFF									
Spill6	OFF									
GATES	IUGT	IDGT	EGT	A1GT	B1GT	G1GT	A2GT	B2GT	G2GT	LATGTC
Gt 1	27	33	44.0	10.00	1.0	1.0	10.0	2.5	0.0	DOWN
GATE WEIR	GA1	GB1	GA2	GB2	DYNGTC					
Gt 1	10.0	1.5	10.0	1.5	B					
GATE UP	PUGTC	ETUGT	EBUGT	KTUGT	KBUGT					
Gt 1	DISTR			3	23					
GATE DOWN	PDGTC	ETDGT	EBDGT	KT DGT	KBDGT					
Gt 1	DISTR			3	23					
GATE GAS	GASGT	EQGT	AGASG	BGASG	CGASG					
Gt 1	ON	1	10.0	120.00	1.0					
PUMPS 1	IUPU	IDPU	EPU	STRTPU	ENDPU	EONPU	EOPFPU	QPU	LATPUC	
Pu 1	30	33	2.4	1.0	900.0	3.0	2.4	3.0	DOWN	
PUMPS 2	PPUC	ETPU	EBPU	KTPU	KBPU					
Pu 1	DISTR			4	23					
WEIR SEG	IWR	IWR	IWR	IWR	IWR	IWR	IWR	IWR	IWR	
Wr 1	27									
WEIR TOP	KTWR	KTWR	KTWR	KTWR	KTWR	KTWR	KTWR	KTWR	KTWR	
Wr 1	9									
WEIR BOT	KBWR	KBWR	KBWR	KBWR	KBWR	KBWR	KBWR	KBWR	KBWR	
Wr 1	23									
WD INT	WDIC	WDIC	WDIC	WDIC	WDIC	WDIC	WDIC	WDIC	WDIC	
Wd 1										
WD SEG	IWD	IWD	IWD	IWD	IWD	IWD	IWD	IWD	IWD	
Wd 1										

SAMPLE CONTROL FILE

CONTROL FILE

WD ELEV	EWD								
Wd 1									
WD TOP	ETWD								
Wd 1									
WD BOT	EBWD								
Wd 1									
TRIB PLACE	PTRC								
	DISTR								
TRIB INT	TRIC								
	OFF								
TRIB SEG	ITR								
	15	43	56	98	114	147	155		
TRIB TOP	ETRT								
TRIB BOT	ETRB								
DST TRIB	DTRC								
Br 1	ON								
Br 2	ON								
Br 3	ON								
Br 4	ON								
Br 5	ON								
Br 6	ON								
Br 7	ON								
Br 8	ON								
Br 9	ON								
Br 10	ON								
Br 11	ON								
Br 12	ON								
PUMPBACK	JBG	KTG	KBG	JBP	KTP	KBP			
PRINTER	LJC								
	IV								
HYD PRINT	HPRWBC								
NVIOL	ON								
U	ON								
W	ON								
T	ON								
RHO	OFF								
AZ	OFF								
SHEAR	OFF								
ST	OFF								
SB	OFF								
ADMX	OFF								
DM	OFF								
HDG	OFF								
ADMZ	OFF								
HPG	OFF								
GRAV	OFF								
SNP PRINT	SNPC	NSNP	NISNP						
Wb 1	ON	2	16						
Wb 2	ON	2	8						
Wb 3	ON	2	3						
Wb 4	ON	2	6						
Wb 5	ON	2	5						
Wb 6	ON	2	6						

CONTROL FILE

SAMPLE CONTROL FILE

SNP DATE	SNPD								
Wb 1	1.0	1.6							
Wb 2	1.0	1.6							
Wb 3	1.0	1.6							
Wb 4	1.0	1.6							
Wb 5	1.0	1.6							
Wb 6	1.0	1.6							

SNP FREQ	SNPF								
Wb 1	0.1	7.0							
Wb 2	0.1	7.0							
Wb 3	0.1	7.0							
Wb 4	0.1	7.0							
Wb 5	0.1	7.0							
Wb 6	0.1	7.0							

SNP SEG	ISNP								
Wb 1	2	10	13	24	27	36	39	40	41
	42	43	44	45	46	47	48		
Wb 2	51	53	55	57	59	61	63	64	
Wb 3	84	85	86						
Wb 4	89	90	92	122	123	124			
Wb 5	131	138	139	148	151				
Wb 6	154	155	156	175	187	188			

SCR PRINT	SCRC	NSCR							
Wb 1	OFF	1							
Wb 2	OFF	1							
Wb 3	OFF	1							
Wb 4	OFF	1							
Wb 5	OFF	1							
Wb 6	ON	1							

SCR DATE	SCRD								
Wb 1	1.0								
Wb 2	1.0								
Wb 3	1.0								
Wb 4	1.0								
Wb 5	1.0								
Wb 6	1.0								

SCR FREQ	SCRFF								
Wb 1	0.05								
Wb 2	0.10								
Wb 3	0.10								
Wb 4	0.10								
Wb 5	0.10								
Wb 6	0.10								

PRF PLOT	PRFC	NPRF	NIPRF						
Wb 1	OFF	0	0						
Wb 2	ON	12	4						
Wb 3	OFF	0	0						
Wb 4	OFF	0	0						
Wb 5	ON	12	6						
Wb 6	ON	12	7						

PRF DATE	PRFD								
Wb 1									
Wb 2	158.5	179.5	200.5	228.5	229.5	242.5	244.5	245.5	249.5
	257.5	270.5	271.5						
Wb 3									
Wb 4									
Wb 5	158.5	179.5	200.5	228.5	229.5	242.5	244.5	245.5	249.5
	257.0	270.0	271.0						
Wb 6	158.67	179.67	200.67	228.67	229.67	242.67	244.67	245.67	249.67
	257.67	270.67	271.67						

SAMPLE CONTROL FILE

CONTROL FILE

PRF	FREQ	PRFF								
Wb 1										
Wb 2		500.0	500.0	500.0	500.0	500.0	500.0	500.0	500.0	500.0
		500.0	500.0	500.0						
Wb 3										
Wb 4										
Wb 5		500.0	500.0	500.0	500.0	500.0	500.0	500.0	500.0	500.0
		500.0	500.0	500.0						
Wb 6		500.0	500.0	500.0	500.0	500.0	500.0	500.0	500.0	500.0
		500.0	500.0	500.0						
PRF	SEG	IPRF								
Wb 1										
Wb 2		57	60	62	64					
Wb 3										
Wb 4										
Wb 5		135	139	141	143	147	150			
Wb 6		157	161	168	174	180	183	187		
SPR	PLOT	SPRC	NSPR	NISPR						
Wb 1		OFF	0	0						
Wb 2		OFF	0	0						
Wb 3		OFF	0	0						
Wb 4		OFF	0	0						
Wb 5		OFF	0	0						
Wb 6		OFF	0	0						
SPR	DATE	SPRD								
Wb 1										
Wb 2										
Wb 3										
Wb 4										
Wb 5										
Wb 6										
SPR	FREQ	SPRF								
Wb 1										
Wb 2										
Wb 3										
Wb 4										
Wb 5										
Wb 6										
SPR	SEG	ISPR								
Wb 1										
Wb 2										
Wb 3										
Wb 4										
Wb 5										
Wb 6										
VPL	PLOT	VPLC	NVPL							
Wb 1		OFF	1							
Wb 2		OFF	1							
Wb 3		OFF	1							
Wb 4		OFF	1							
Wb 5		OFF	1							
Wb 6		OFF	1							
VPL	DATE	VPLD								
Wb 1		63.5								
Wb 2		63.5								
Wb 3		63.5								
Wb 4		63.5								
Wb 5		63.5								
Wb 6		63.5								

CONTROL FILE

SAMPLE CONTROL FILE

VPL FREQ	VPLF								
Wb 1	1.0								
Wb 2	1.0								
Wb 3	1.0								
Wb 4	1.0								
Wb 5	1.0								
Wb 6	1.0								

CPL PLOT	CPLC	NCPL
Wb 1	ON	24
Wb 2	ON	24
Wb 3	ON	24
Wb 4	ON	24
Wb 5	ON	24
Wb 6	ON	24

CPL DATE	CPLD	CPLD	CPLD	CPLD	CPLD	CPLD	CPLD	CPLD	CPLD
Wb 1	9.67	37.67	72.75	100.6	128.67	163.75	187.6	191.6	208.4
	215.5	219.75	228.4	228.6	229.4	229.6	251.5	254.75	270.4
	270.6	271.4	271.6	284.4	319.35	347.35			
Wb 2	9.67	37.67	72.75	100.6	128.67	163.75	187.6	191.6	208.4
	215.5	219.75	228.4	228.6	229.4	229.6	251.5	254.75	270.4
	270.6	271.4	271.6	284.4	319.35	347.35			
Wb 3	9.67	37.67	72.75	100.6	128.67	163.75	187.6	191.6	208.4
	215.5	219.75	228.4	228.6	229.4	229.6	251.5	254.75	270.4
	270.6	271.4	271.6	284.4	319.35	347.35			
Wb 4	9.67	37.67	72.75	100.6	128.67	163.75	187.6	191.6	208.4
	215.5	219.75	228.4	228.6	229.4	229.6	251.5	254.75	270.4
	270.6	271.4	271.6	284.4	319.35	347.35			
Wb 5	9.67	37.67	72.75	100.6	128.67	163.75	187.6	191.6	208.4
	215.5	219.75	228.4	228.6	229.4	229.6	251.5	254.75	270.4
	270.6	271.4	271.6	284.4	319.35	347.35			
Wb 6	9.67	37.67	72.75	100.6	128.67	163.75	187.6	191.6	208.4
	215.5	219.75	228.4	228.6	229.4	229.6	251.5	254.75	270.4
	270.6	271.4	271.6	284.4	319.35	347.35			

CPL FREQ	CPLF								
Wb 1	500.0	500.0	500.0	500.0	500.0	500.0	500.0	500.0	500.0
	500.0	500.0	500.0	500.0	500.0	500.0	500.0	500.0	500.0
	500.0	500.0	500.0	500.0	500.0	500.0			
Wb 2	500.0	500.0	500.0	500.0	500.0	500.0	500.0	500.0	500.0
	500.0	500.0	500.0	500.0	500.0	500.0	500.0	500.0	500.0
	500.0	500.0	500.0	500.0	500.0	500.0			
Wb 3	500.0	500.0	500.0	500.0	500.0	500.0	500.0	500.0	500.0
	500.0	500.0	500.0	500.0	500.0	500.0	500.0	500.0	500.0
	500.0	500.0	500.0	500.0	500.0	500.0			
Wb 4	500.0	500.0	500.0	500.0	500.0	500.0	500.0	500.0	500.0
	500.0	500.0	500.0	500.0	500.0	500.0	500.0	500.0	500.0
	500.0	500.0	500.0	500.0	500.0	500.0			
Wb 5	500.0	500.0	500.0	500.0	500.0	500.0	500.0	500.0	500.0
	500.0	500.0	500.0	500.0	500.0	500.0	500.0	500.0	500.0
	500.0	500.0	500.0	500.0	500.0	500.0			
Wb 6	500.0	500.0	500.0	500.0	500.0	500.0	500.0	500.0	500.0
	500.0	500.0	500.0	500.0	500.0	500.0	500.0	500.0	500.0
	500.0	500.0	500.0	500.0	500.0	500.0			

FLUXES	FLXC	NFLX
Wb 1	OFF	0
Wb 2	OFF	0
Wb 3	OFF	0
Wb 4	OFF	0
Wb 5	OFF	0
Wb 6	OFF	0

SAMPLE CONTROL FILE

CONTROL FILE

FLX DATE	FLXD								
Wb 1									
Wb 2									
Wb 3									
Wb 4									
Wb 5									
Wb 6									
FLX FREQ	FLXF								
Wb 1									
Wb 2									
Wb 3									
Wb 4									
Wb 5									
Wb 6									
TSR PLOT	TSRC ON	NTSR 1	NIKTSR 30						
TSR DATE	TSRD 1.0	TSRD							
TSR FREQ	TSRF 0.1	TSRF							
TSR SEG	ITSR 2 86 150 188	ITSR 13 89 151 128	ITSR 17 94 154 131	ITSR 24 97 155	ITSR 36 106 161	ITSR 48 114 168	ITSR 64 119 174	ITSR 67 135 180	ITSR 73 141 181
TSR LAYER	ETSR 0.1 0.1 0.1 0.1								
WITH OUT	WDOC ON	NWDO 1	NIWDO 7						
WITH DATE	WDOD 1.0	WDOD							
WITH FREQ	WDOF 0.1	WDOF							
WITH SEG	IWDO 64	IWDO 86	IWDO 151	IWDO 188	IWDO 13	IWDO 24	IWDO 97	IWDO	IWDO
RESTART	RSOC OFF	NRSO 0	RSIC OFF						
RSO DATE	RSOD								
RSO FREQ	RSOF								
CST COMP	CCC ON	LIMC ON	CUF 10						

CONTROL FILE

SAMPLE CONTROL FILE

CST ACTIVE	CAC	
TDS	ON	!1
AGE	ON	!2
TRACER	ON	!3
COLIFORM	ON	!4
CONDUCT	ON	!5
CHLORIDE	ON	!6
ISS	ON	!7
PO4	ON	!8
NH4	ON	!9
NOX	ON	!10
DSI	OFF	!11
PSI	OFF	!12
TFE	OFF	!13
LDOM	ON	!14
RDOM	ON	!15
LPOM	ON	!16
RPOM	ON	!17
CBOD 1	ON	!18
CBOD 2	ON	!19
CBOD 3	ON	!20
CBOD 4	ON	!21
CBOD 5	ON	!22
ALGAE	ON	!23
DO	ON	!24
TIC	ON	!25
ALK	ON	!26

CST DERIV	CDWBC									
DOC	ON	!1								
POC	OFF	!2								
TOC	ON	!3								
DON	OFF	!4								
PON	OFF	!5								
TON	ON	!6								
TKN	ON	!7								
TN	ON	!8								
DOP	OFF	!9								
POP	OFF	!10								
TOP	ON	!11								
TP	ON	!12								
APR	OFF	!13								
CHLA	ON	!14								
ATOT	OFF	!15								
%DO	OFF	!16								
TSS	ON	!17								
TISS	OFF	!18								
CBODU	OFF	!19								
pH	ON	!20								
CO2	OFF	!21								
HCO3	OFF	!22								
CO3	OFF	!23								

CST FLUX	CFWBC									
TISSIN	OFF	!1								
TISSOUT	OFF	!2								
PO4AR	OFF	!3								
PO4AG	OFF	!4								
PO4AP	OFF	!5								
PO4ER	OFF	!6								
PO4EG	OFF	!7								
PO4EP	OFF	!8								
PO4POM	OFF	!9								
PO4DOM	OFF	!10								
PO4OM	OFF	!11								
PO4SED	OFF	!12								
PO4SOD	OFF	!13								
PO4SET	OFF	!14								

SAMPLE CONTROL FILE

CONTROL FILE

NH4NITR	OFF	OFF	OFF	OFF	OFF	OFF				!15
NH4AR	OFF	OFF	OFF	OFF	OFF	OFF				!16
NH4AG	OFF	OFF	OFF	OFF	OFF	OFF				!17
NH4AP	OFF	OFF	OFF	OFF	OFF	OFF				!18
NH4ER	OFF	OFF	OFF	OFF	OFF	OFF				!19
NH4EG	OFF	OFF	OFF	OFF	OFF	OFF				!20
NH4EP	OFF	OFF	OFF	OFF	OFF	OFF				!21
NH4POM	OFF	OFF	OFF	OFF	OFF	OFF				!22
NH4DOM	OFF	OFF	OFF	OFF	OFF	OFF				!23
NH4OM	OFF	OFF	OFF	OFF	OFF	OFF				!24
NH4SED	OFF	OFF	OFF	OFF	OFF	OFF				!25
NH4SOD	OFF	OFF	OFF	OFF	OFF	OFF				!26
NO3DEN	OFF	OFF	OFF	OFF	OFF	OFF				!27
NO3AG	OFF	OFF	OFF	OFF	OFF	OFF				!28
NO3EG	OFF	OFF	OFF	OFF	OFF	OFF				!29
NO3SED	OFF	OFF	OFF	OFF	OFF	OFF				!30
DSIAG	OFF	OFF	OFF	OFF	OFF	OFF				!31
DSIEG	OFF	OFF	OFF	OFF	OFF	OFF				!32
DSIPIS	OFF	OFF	OFF	OFF	OFF	OFF				!33
DSISED	OFF	OFF	OFF	OFF	OFF	OFF				!34
DSISOD	OFF	OFF	OFF	OFF	OFF	OFF				!35
DSISET	OFF	OFF	OFF	OFF	OFF	OFF				!36
PSIAM	OFF	OFF	OFF	OFF	OFF	OFF				!37
PSINET	OFF	OFF	OFF	OFF	OFF	OFF				!38
PSIDK	OFF	OFF	OFF	OFF	OFF	OFF				!39
FESET	OFF	OFF	OFF	OFF	OFF	OFF				!40
FESED	OFF	OFF	OFF	OFF	OFF	OFF				!41
LDOMDK	OFF	OFF	OFF	OFF	OFF	OFF				!42
LRDOM	OFF	OFF	OFF	OFF	OFF	OFF				!43
RDOMDK	OFF	OFF	OFF	OFF	OFF	OFF				!44
LDOMAP	OFF	OFF	OFF	OFF	OFF	OFF				!45
LDOMEAP	OFF	OFF	OFF	OFF	OFF	OFF				!46
LPOMDK	OFF	OFF	OFF	OFF	OFF	OFF				!47
LRPOM	OFF	OFF	OFF	OFF	OFF	OFF				!48
RPOMDK	OFF	OFF	OFF	OFF	OFF	OFF				!49
LPOMAP	OFF	OFF	OFF	OFF	OFF	OFF				!50
LPOMEAP	OFF	OFF	OFF	OFF	OFF	OFF				!51
LPOMSET	OFF	OFF	OFF	OFF	OFF	OFF				!52
RPOMSET	OFF	OFF	OFF	OFF	OFF	OFF				!53
CBODDK	OFF	OFF	OFF	OFF	OFF	OFF				!54
DOAP	OFF	OFF	OFF	OFF	OFF	OFF				!55
DOAR	OFF	OFF	OFF	OFF	OFF	OFF				!56
DOEP	OFF	OFF	OFF	OFF	OFF	OFF				!57
DOER	OFF	OFF	OFF	OFF	OFF	OFF				!58
DOPOM	OFF	OFF	OFF	OFF	OFF	OFF				!59
DODOM	OFF	OFF	OFF	OFF	OFF	OFF				!60
DOOM	OFF	OFF	OFF	OFF	OFF	OFF				!61
DONITR	OFF	OFF	OFF	OFF	OFF	OFF				!62
DOCBOD	OFF	OFF	OFF	OFF	OFF	OFF				!63
DOREAR	OFF	OFF	OFF	OFF	OFF	OFF				!64
DOSED	OFF	OFF	OFF	OFF	OFF	OFF				!65
DOSOD	OFF	OFF	OFF	OFF	OFF	OFF				!66
TICAG	OFF	OFF	OFF	OFF	OFF	OFF				!67
TICEG	OFF	OFF	OFF	OFF	OFF	OFF				!68
SEDDK	OFF	OFF	OFF	OFF	OFF	OFF				!69
SEDAS	OFF	OFF	OFF	OFF	OFF	OFF				!70
SEDLPOM	OFF	OFF	OFF	OFF	OFF	OFF				!71
SEDSET	OFF	OFF	OFF	OFF	OFF	OFF				!72
SODDK	OFF	OFF	OFF	OFF	OFF	OFF				!73

CST ICON	C2IWB									
TDS	0.0	0.0	0.0	0.0	0.0	0.0				!1
AGE	0.0	0.0	0.0	0.0	0.0	0.0				!2
TRACER	0.0	0.0	0.0	0.0	0.0	0.0				!3
COLI	0.0	0.0	0.0	0.0	0.0	0.0				!4
CONDUCT	0.0	0.0	0.0	0.0	0.0	0.0				!5
CHLORIDE	0.0	0.0	0.0	0.0	0.0	0.0				!6
ISS	0.0	0.0	0.0	0.0	0.0	0.0				!7

CONTROL FILE

SAMPLE CONTROL FILE

PO4	0.03	0.03	0.03	0.03	0.03	0.03					!8
NH4	0.01	0.01	0.01	0.01	0.01	0.01					!9
NOX	0.3	0.3	0.3	0.3	0.3	0.3					!10
DSI	0.0	0.0	0.0	0.0	0.0	0.0					!11
PSI	0.0	0.0	0.0	0.0	0.0	0.0					!12
TFE	0.0	0.0	0.0	0.0	0.0	0.0					!13
LDOM	0.1	0.1	0.1	0.1	0.1	0.1					!14
RDOM	0.1	0.1	0.1	0.1	0.1	0.1					!15
LPOM	0.1	0.1	0.1	0.1	0.1	0.1					!16
RPOM	0.1	0.1	0.1	0.1	0.1	0.1					!17
CBOD 1	0.0	0.0	0.0	0.0	0.0	0.0					!18
CBOD 2	0.0	0.0	0.0	0.0	0.0	0.0					!19
CBOD 3	0.0	0.0	0.0	0.0	0.0	0.0					!20
CBOD 4	0.0	0.0	0.0	0.0	0.0	0.0					!21
CBOD 5	0.0	0.0	0.0	0.0	0.0	0.0					!22
ALGAE	0.1	0.1	0.1	0.1	0.1	0.1					!23
DO	12.0	12.0	12.0	12.0	12.0	12.0					!24
TIC	5.0	5.0	5.0	5.0	5.0	5.0					!25
ALK	19.8	19.8	19.8	19.8	19.8	19.8					!26

| CST PRINT | CPRWBC | |
|-----------|--------|--------|--------|--------|--------|--------|--------|--------|--------|--------|-----|
| TDS | ON | !1 |
| AGE | ON | !2 |
| TRACER | ON | !3 |
| COLIFORM | ON | !4 |
| CONDUCT | ON | !5 |
| CHLORIDE | ON | !6 |
| ISS | ON | !7 |
| PO4 | ON | !8 |
| NH4 | ON | !9 |
| NOX | ON | !10 |
| DSI | OFF | !11 |
| PSI | OFF | !12 |
| TFE | OFF | !13 |
| LDOM | ON | !14 |
| RDOM | ON | !15 |
| LPOM | ON | !16 |
| RPOM | ON | !17 |
| CBOD 1 | ON | !18 |
| CBOD 2 | ON | !19 |
| CBOD 3 | ON | !20 |
| CBOD 4 | ON | !21 |
| CBOD 5 | ON | !22 |
| ALGAE | ON | !23 |
| DO | ON | !24 |
| TIC | ON | !25 |
| ALK | ON | !26 |

| CIN CON | CINBRC | |
|----------|--------|--------|--------|--------|--------|--------|--------|--------|--------|--------|-----|
| TDS | ON | !1 |
| AGE | OFF | !2 |
| TRACER | ON | !3 |
| COLIFORM | ON | !4 |
| CONDUCT | ON | !5 |
| CHLORIDE | ON | !6 |
| ISS | ON | !7 |
| PO4 | ON | !8 |
| NH4 | ON | !9 |
| NOX | ON | !10 |

SAMPLE CONTROL FILE

CONTROL FILE

DSI	ON	ON	ON	OFF	OFF	OFF	OFF	OFF	OFF	!11
	OFF	OFF	OFF							
PSI	OFF	!12								
	OFF	OFF	OFF							
TFE	OFF	!13								
	OFF	OFF	OFF							
LDOM	ON	!14								
	ON	ON	ON							
RDOM	ON	!15								
	ON	ON	ON							
LPOM	ON	!16								
	ON	ON	ON							
RPOM	ON	!17								
	ON	ON	ON							
CBOD 1	ON	!18								
	ON	ON	ON							
CBOD 2	ON	!19								
	ON	ON	ON							
CBOD 3	ON	!20								
	ON	ON	ON							
CBOD 4	ON	!21								
	ON	ON	ON							
CBOD 5	ON	!22								
	ON	ON	ON							
ALGAE	ON	!23								
	ON	ON	ON							
DO	ON	!24								
	ON	ON	ON							
TIC	ON	!25								
	ON	ON	ON							
ALK	ON	!26								
	ON	ON	ON							

CTR CON	CTRTRC									
TDS	ON	!1								
AGE	OFF	!2								
TRACER	ON	!3								
COLIFORM	ON	!4								
CONDUCT	ON	!5								
CHLORIDE	ON	!6								
ISS	ON	!7								
PO4	ON	!8								
NH4	ON	!9								
NOx	ON	!10								
DSi	OFF	!11								
PSi	OFF	!12								
TFe	OFF	!13								
LDOM	ON	!14								
RDOM	ON	!15								
LPOM	ON	!16								
RPOM	ON	!17								
CBOD 1	ON	!18								
CBOD 2	ON	!19								
CBOD 3	ON	!20								
CBOD 4	ON	!21								
CBOD 5	ON	!22								
ALGAE	ON	!23								
DO	ON	!24								
TIC	ON	!25								
ALK	ON	!26								

CDT CON	CDTBRC									
TDS	ON	!1								
	ON	ON	ON							
AGE	OFF	!2								
	OFF	OFF	OFF							
TRACER	ON	!3								

CONTROL FILE

SAMPLE CONTROL FILE

	ON	ON	ON							
COLIFORM	ON	! 4								
	ON	ON	ON							
CONDUCT	ON	! 5								
	ON	ON	ON							
CHLORIDE	ON	! 6								
	ON	ON	ON							
ISS	ON	! 7								
	ON	ON	ON							
PO4	ON	! 8								
	ON	ON	ON							
NH4	ON	! 9								
	ON	ON	ON							
NOX	ON	! 10								
	ON	ON	ON							
DSI	OFF	! 11								
	OFF	OFF	OFF							
PSI	OFF	! 12								
	OFF	OFF	OFF							
TFE	OFF	! 13								
	OFF	OFF	OFF							
LDOM	ON	! 14								
	ON	ON	ON							
RDOM	ON	! 15								
	ON	ON	ON							
LPOM	ON	! 16								
	ON	ON	ON							
RPOM	ON	! 17								
	ON	ON	ON							
CBOD 1	ON	! 18								
	ON	ON	ON							
CBOD 2	ON	! 19								
	ON	ON	ON							
CBOD 3	ON	! 20								
	ON	ON	ON							
CBOD 4	ON	! 21								
	ON	ON	ON							
CBOD 5	ON	! 22								
	ON	ON	ON							
ALGAE	ON	! 23								
	ON	ON	ON							
DO	ON	! 24								
	ON	ON	ON							
TIC	ON	! 25								
	ON	ON	ON							
ALK	ON	! 26								
	ON	ON	ON							

CPR CON	CPRBRC									
TDS	ON	! 1								
	ON	ON	ON							
AGE	OFF	! 2								
	OFF	OFF	OFF							
TRACER	ON	! 3								
	ON	ON	ON							
COLIFORM	ON	! 4								
	ON	ON	ON							
CONDUCT	ON	! 5								
	ON	ON	ON							
CHLORIDE	ON	! 6								
	ON	ON	ON							
ISS1	ON	! 7								
	ON	ON	ON							
PO4	ON	! 8								
	ON	ON	ON							
NH4	ON	! 9								
	ON	ON	ON							
NOx	ON	! 10								

SAMPLE CONTROL FILE

CONTROL FILE

DSI	ON	ON	ON	OFF	OFF	OFF	OFF	OFF	OFF	!11
	OFF	OFF	OFF	OFF	OFF	OFF	OFF	OFF	OFF	
PSI	OFF	OFF	OFF	OFF	OFF	OFF	OFF	OFF	OFF	!12
	OFF	OFF	OFF	OFF	OFF	OFF	OFF	OFF	OFF	
TFE	OFF	OFF	OFF	OFF	OFF	OFF	OFF	OFF	OFF	!13
	OFF	OFF	OFF	OFF	OFF	OFF	OFF	OFF	OFF	
LDOM	ON	ON	ON	ON	ON	ON	ON	ON	ON	!14
	ON	ON	ON	ON	ON	ON	ON	ON	ON	
RDOM	ON	ON	ON	ON	ON	ON	ON	ON	ON	!15
	ON	ON	ON	ON	ON	ON	ON	ON	ON	
LPOM	ON	ON	ON	ON	ON	ON	ON	ON	ON	!16
	ON	ON	ON	ON	ON	ON	ON	ON	ON	
RPOM	ON	ON	ON	ON	ON	ON	ON	ON	ON	!17
	ON	ON	ON	ON	ON	ON	ON	ON	ON	
CBOD 1	ON	ON	ON	ON	ON	ON	ON	ON	ON	!18
	ON	ON	ON	ON	ON	ON	ON	ON	ON	
CBOD 2	ON	ON	ON	ON	ON	ON	ON	ON	ON	!19
	ON	ON	ON	ON	ON	ON	ON	ON	ON	
CBOD 3	ON	ON	ON	ON	ON	ON	ON	ON	ON	!20
	ON	ON	ON	ON	ON	ON	ON	ON	ON	
CBOD 4	ON	ON	ON	ON	ON	ON	ON	ON	ON	!21
	ON	ON	ON	ON	ON	ON	ON	ON	ON	
CBOD 5	ON	ON	ON	ON	ON	ON	ON	ON	ON	!22
	ON	ON	ON	ON	ON	ON	ON	ON	ON	
ALGAE	ON	ON	ON	ON	ON	ON	ON	ON	ON	!23
	ON	ON	ON	ON	ON	ON	ON	ON	ON	
DO	ON	ON	ON	ON	ON	ON	ON	ON	ON	!24
	ON	ON	ON	ON	ON	ON	ON	ON	ON	
TIC	ON	ON	ON	ON	ON	ON	ON	ON	ON	!25
	ON	ON	ON	ON	ON	ON	ON	ON	ON	
ALK	ON	ON	ON	ON	ON	ON	ON	ON	ON	!26
	ON	ON	ON	ON	ON	ON	ON	ON	ON	
EX COEF	EXH2O	EXSS	EXOM	BETA	EXC	EXIC				
Wb 1	0.45	0.01	0.40	0.45	OFF	OFF				
Wb 2	0.45	0.01	0.40	0.45	OFF	OFF				
Wb 3	0.45	0.01	0.40	0.45	OFF	OFF				
Wb 4	0.45	0.01	0.40	0.45	OFF	OFF				
Wb 5	0.45	0.01	0.40	0.45	OFF	OFF				
Wb 6	0.45	0.01	0.40	0.45	OFF	OFF				
ALG EX	EXA	EXA	EXA	EXA	EXA	EXA				
	0.10	0.2	0.2	0.2	0.2	0.2				
GENERIC	CGQ10	CG0DK	CG1DK	CGS						
AGE	0.00	-1.0	0.0	0.0						
TRACER	0.00	0.0	0.0	0.0						
COLIFORM	1.04	0.0	0.5	0.0						
CONDUCT	0.00	0.0	0.0	0.0						
CHLORIDE	0.00	0.0	0.0	0.0						
S SOLIDS	SSS	SEDRC	TAUCR							
SSS 1	1.5	OFF	0.0							
ALGAL RATE	AG	AR	AE	AM	AS	AHSP	AHSN	AHSSI	ASAT	
Alg 1	2.0	0.12	0.02	0.05	0.04	0.005	0.005	0.0	50.0	
ALGAL TEMP	AT1	AT2	AT3	AT4	AK1	AK2	AK3	AK4		
Alg 1	5.0	12.0	20.0	30.0	0.1	0.99	0.99	0.1		
ALG STOICH	ALGP	ALGN	ALGC	ALGSI	ACHLA	APOM	ANEQN	ANPR		
Alg 1	0.005	0.08	0.45	0.00	130.00	0.8	2	0.001		
EPIPHYTE	EPIC	EPIC	EPIC	EPIC	EPIC	EPIC	EPIC	EPIC	EPIC	
Epi 1	ON	ON	ON	ON	ON	ON	ON	ON	ON	

CONTROL FILE

SAMPLE CONTROL FILE

EPI PRINT	EPRC	EPRC	EPRC	EPRC	EPRC	EPRC	EPRC	EPRC	EPRC
Epi 1	ON	ON	ON	ON	ON	ON			
EPI INIT	EPICI	EPICI	EPICI	EPICI	EPICI	EPICI	EPICI	EPICI	EPICI
Epi 1	20.0	-1.0	-1.0	20.0	-1.0	-1.0			
EPI RATE	EG	ER	EE	EM	EB	EHSP	EHSN	EHSSI	
Epi 1	1.7	0.05	0.02	0.05	0.05	0.002	0.004	0.0	
EPI HALF	ESAT	EHS	ENEQN	ENPR					
Epi 1	150.00	40.0	2	0.001					
EPI TEMP	ET1	ET2	ET3	ET4	EK1	EK2	EK3	EK4	
Epi 1	2.0	5.0	20.0	30.0	0.1	0.99	0.99	0.1	
EPI STOICH	EP	EN	EC	ESI	ECHLA	EPOM			
Epi 1	0.005	0.08	0.45	0.0	65.0	0.8			
DOM	LDOMDK	RDOMDK	LRDDK						
Wb 1	0.10	0.001	0.001						
Wb 2	0.10	0.001	0.001						
Wb 3	0.10	0.001	0.001						
Wb 4	0.10	0.001	0.001						
Wb 5	0.10	0.001	0.001						
Wb 6	0.10	0.001	0.001						
POM	LPOMDK	RPOMDK	LRPDK	POMS					
Wb 1	0.08	0.001	0.001	0.1					
Wb 2	0.08	0.001	0.001	0.1					
Wb 3	0.08	0.001	0.001	0.1					
Wb 4	0.08	0.001	0.001	0.1					
Wb 5	0.08	0.001	0.001	0.1					
Wb 6	0.08	0.001	0.001	0.1					
OM STOICH	ORGP	ORGN	ORGC	ORGS					
Wb 1	0.005	0.08	0.45	0.18					
Wb 2	0.005	0.08	0.45	0.18					
Wb 3	0.005	0.08	0.45	0.18					
Wb 4	0.005	0.08	0.45	0.18					
Wb 5	0.005	0.08	0.45	0.18					
Wb 6	0.005	0.08	0.45	0.18					
OM RATE	OMT1	OMT2	OMK1	OMK2					
Wb 1	4.0	30.0	0.1	0.99					
Wb 2	4.0	30.0	0.1	0.99					
Wb 3	4.0	30.0	0.1	0.99					
Wb 4	4.0	30.0	0.1	0.99					
Wb 5	4.0	30.0	0.1	0.99					
Wb 6	4.0	30.0	0.1	0.99					
CBOD STOIC	BODP	BODN	BODC	BODSI					
CBOD 1	0.005	0.08	0.45	0.18					
CBOD 2	0.005	0.08	0.45	0.18					
CBOD 3	0.005	0.08	0.45	0.18					
CBOD 4	0.005	0.08	0.45	0.18					
CBOD 5	0.005	0.08	0.45	0.18					
CBOD	KBOD	TBOD	RBOD						
CBOD 1	0.0418	1.0147	1.0						
CBOD 2	0.1302	1.0147	1.0						
CBOD 3	0.0469	1.0147	1.0						
CBOD 4	0.0880	1.0147	1.0						
CBOD 5	0.050	1.0147	1.0						

SAMPLE CONTROL FILE

CONTROL FILE

PHOSPHOR	PO4R	PARTP		
Wb 1	0.001	0.0		
Wb 2	0.001	0.0		
Wb 3	0.001	0.0		
Wb 4	0.001	0.0		
Wb 5	0.001	0.0		
Wb 6	0.001	0.0		
AMMONIUM	NH4R	NH4DK		
Wb 1	0.001	0.50		
Wb 2	0.001	0.50		
Wb 3	0.001	0.50		
Wb 4	0.001	0.50		
Wb 5	0.001	0.50		
Wb 6	0.001	0.50		
NH4 RATE	NH4T1	NH4T2	NH4K1	NH4K2
Wb 1	5.0	25.0	0.1	0.99
Wb 2	5.0	25.0	0.1	0.99
Wb 3	5.0	25.0	0.1	0.99
Wb 4	5.0	25.0	0.1	0.99
Wb 5	5.0	25.0	0.1	0.99
Wb 6	5.0	25.0	0.1	0.99
NITRATE	NO3DK	NO3S		
Wb 1	0.05	0.0		
Wb 2	0.05	0.0		
Wb 3	0.05	0.0		
Wb 4	0.05	0.0		
Wb 5	0.05	0.0		
Wb 6	0.05	0.0		
NO3 RATE	NO3T1	NO3T2	NO3K1	NO3K2
Wb 1	5.0	25.0	0.1	0.99
Wb 2	5.0	25.0	0.1	0.99
Wb 3	5.0	25.0	0.1	0.99
Wb 4	5.0	25.0	0.1	0.99
Wb 5	5.0	25.0	0.1	0.99
Wb 6	5.0	25.0	0.1	0.99
SILICA	DSIR	PSIS	PSIDK	PARTSI
Wb 1	0.1	0.0	0.3	0.2
Wb 2	0.1	0.0	0.3	0.2
Wb 3	0.1	0.0	0.3	0.2
Wb 4	0.1	0.0	0.3	0.2
Wb 5	0.1	0.0	0.3	0.2
Wb 6	0.1	0.0	0.3	0.2
IRON	FEREL	FESETL		
Wb 1	0.1	0.0		
Wb 2	0.1	0.0		
Wb 3	0.1	0.0		
Wb 4	0.1	0.0		
Wb 5	0.1	0.0		
Wb 6	0.1	0.0		
SED CO2	CO2R			
Wb 1	0.1			
Wb 2	0.1			
Wb 3	0.1			
Wb 4	0.1			
Wb 5	0.1			
Wb 6	0.1			

SAMPLE CONTROL FILE

CONTROL FILE

```
QWD FILE.....QWDFN.....
    qwd.npt

QGT FILE.....QGTFN.....
    qgt.npt

WSC FILE.....WSCFN.....
    wsc.npt

SHD FILE.....SHDFN.....
    shd.npt

BTH FILE.....BTHFN.....
Wb 1    bth_wb1.npt
Wb 2    bth_wb2.npt
Wb 3    bth_wb3.npt
Wb 4    bth_wb4.npt
Wb 5    bth_wb5.npt
Wb 6    bth_wb6.npt

MET FILE.....METFN.....
Wb 1    met_wb1.npt
Wb 2    met_wb2.npt
Wb 3    met_wb3.npt
Wb 4    met_wb4.npt
Wb 5    met_wb5.npt
Wb 6    met_wb6.npt

EXT FILE.....EXTFN.....
Wb 1    ext_wb1.npt - not used
Wb 2    ext_wb2.npt - not used
Wb 3    ext_wb3.npt - not used
Wb 4    ext_wb3.npt - not used
Wb 5    ext_wb3.npt - not used
Wb 6    ext_wb3.npt - not used

VPR FILE.....VPRFN.....
Wb 1    vpr_wb1.npt
Wb 2    vpr_wb2.npt
Wb 3    vpr_wb3.npt
Wb 4    vpr_wb4.npt
Wb 5    vpr_wb5.npt
Wb 6    vpr_wb6.npt

LPR FILE.....LPRFN.....
Wb 1    lpr_wb1.npt - not used
Wb 2    lpr_wb2.npt - not used
Wb 3    lpr_wb3.npt - not used
Wb 4    lpr_wb4.npt - not used
Wb 5    lpr_wb5.npt - not used
Wb 6    lpr_wb6.npt - not used

QIN FILE.....QINFN.....
Br 1    qin_br1.npt
Br 2    qin_br2.npt - not used
Br 3    qin_br3.npt - not used
Br 4    qin_br4.npt - not used
Br 5    qin_br5.npt
Br 6    qin_br6.npt
Br 7    qin_br7.npt - not used
Br 8    qin_br8.npt
Br 9    qin_br9.npt - not used
Br 10   qin_br10.npt
Br 11   qin_br11.npt - not used
Br 12   qin_br12.npt
```

CONTROL FILE

SAMPLE CONTROL FILE

```
TIN FILE.....TINFN.....
Br 1   tin_br1.npt
Br 2   tin_br2.npt - not used
Br 3   tin_br3.npt - not used
Br 4   tin_br4.npt - not used
Br 5   tin_br5.npt
Br 6   tin_br6.npt
Br 7   tin_br7.npt - not used
Br 8   tin_br8.npt
Br 9   tin_br9.npt - not used
Br 10  tin_br10.npt
Br 11  tin_br11.npt - not used
Br 12  tin_br12.npt

CIN FILE.....CINFN.....
Br 1   cin_br1.npt
Br 2   cin_br2.npt - not used
Br 3   cin_br3.npt - not used
Br 4   cin_br4.npt - not used
Br 5   cin_br5.npt
Br 6   cin_br6.npt
Br 7   cin_br7.npt - not used
Br 8   cin_br8.npt
Br 9   cin_br9.npt - not used
Br 10  cin_br10.npt
Br 11  cin_br11.npt - not used
Br 12  cin_br12.npt

QOT FILE.....QOTFN.....
Br 1   qot_br1.npt - not used
Br 2   qot_br2.npt - not used
Br 3   qot_br3.npt - not used
Br 4   qot_br4.npt - not used
Br 5   qot_br5.npt
Br 6   qot_br6.npt - not used
Br 7   qot_br7.npt
Br 8   qot_br8.npt - not used
Br 9   qot_br9.npt - not used
Br 10  qot_br10.npt - not used
Br 11  qot_br11.npt
Br 12  qot_br12.npt

QTR FILE.....QTRFN.....
Tr 1   qtr_tr1.npt
Tr 2   qtr_tr2.npt
Tr 3   qtr_tr3.npt
Tr 4   qtr_tr4.npt
Tr 5   qtr_tr5.npt
Tr 6   qtr_tr6.npt
Tr 7   qtr_tr7.npt

TTR FILE.....TTRFN.....
Tr 1   ttr_tr1.npt
Tr 2   ttr_tr2.npt
Tr 3   ttr_tr3.npt
Tr 4   ttr_tr4.npt
Tr 5   ttr_tr5.npt
Tr 6   ttr_tr6.npt
Tr 7   ttr_tr7.npt

CTR FILE.....CTRFN.....
Tr 1   ctr_tr1.npt
Tr 2   ctr_tr2.npt
Tr 3   ctr_tr3.npt
Tr 4   ctr_tr4.npt
Tr 5   ctr_tr5.npt
Tr 6   ctr_tr6.npt
Tr 7   ctr_tr7.npt
```

SAMPLE CONTROL FILE

CONTROL FILE

QDT FILE.....QDTFN.....

Br 1 qdt_br1.npt
Br 2 qdt_br2.npt
Br 3 qdt_br3.npt
Br 4 qdt_br4.npt
Br 5 qdt_br5.npt
Br 6 qdt_br6.npt
Br 7 qdt_br7.npt
Br 8 qdt_br8.npt
Br 9 qdt_br9.npt
Br 10 qdt_br10.npt
Br 11 qdt_br11.npt
Br 12 qdt_br12.npt

TDT FILE.....TDTFN.....

Br 1 tdt_br1.npt
Br 2 tdt_br2.npt
Br 3 tdt_br3.npt
Br 4 tdt_br4.npt
Br 5 tdt_br5.npt
Br 6 tdt_br6.npt
Br 7 tdt_br7.npt
Br 8 tdt_br8.npt
Br 9 tdt_br9.npt
Br 10 tdt_br10.npt
Br 11 tdt_br11.npt
Br 12 tdt_br12.npt

CDT FILE.....CDTFN.....

Br 1 cdt_br1.npt
Br 2 cdt_br2.npt
Br 3 cdt_br3.npt
Br 4 cdt_br4.npt
Br 5 cdt_br5.npt
Br 6 cdt_br6.npt
Br 7 cdt_br7.npt
Br 8 cdt_br8.npt
Br 9 cdt_br9.npt
Br 10 cdt_br10.npt
Br 11 cdt_br11.npt
Br 12 cdt_br12.npt

PRE FILE.....PREFN.....

Br 1 pre_br1.npt - not used
Br 2 pre_br2.npt - not used
Br 3 pre_br3.npt - not used
Br 4 pre_br4.npt - not used
Br 5 pre_br5.npt - not used
Br 6 pre_br6.npt - not used
Br 7 pre_br7.npt - not used
Br 8 pre_br8.npt - not used
Br 9 pre_br9.npt - not used
Br 10 pre_br10.npt - not used
Br 11 pre_br11.npt - not used
Br 12 pre_br12.npt - not used

CONTROL FILE

SAMPLE CONTROL FILE

```
TPR FILE.....TPRFN.....
Br 1   tpr_br1.npt - not used
Br 2   tpr_br2.npt - not used
Br 3   tpr_br3.npt - not used
Br 4   tpr_br4.npt - not used
Br 5   tpr_br5.npt - not used
Br 6   tpr_br6.npt - not used
Br 7   tpr_br7.npt - not used
Br 8   tpr_br8.npt - not used
Br 9   tpr_br9.npt - not used
Br 10  tpr_br10.npt - not used
Br 11  tpr_br11.npt - not used
Br 12  tpr_br12.npt - not used

CPR FILE.....CPRFN.....
Br 1   cpr_br1.npt - not used
Br 2   cpr_br2.npt - not used
Br 3   cpr_br3.npt - not used
Br 4   cpr_br4.npt - not used
Br 5   cpr_br5.npt - not used
Br 6   cpr_br6.npt - not used
Br 7   cpr_br7.npt - not used
Br 8   cpr_br8.npt - not used
Br 9   cpr_br9.npt - not used
Br 10  cpr_br10.npt - not used
Br 11  cpr_br11.npt - not used
Br 12  cpr_br12.npt - not used

EUH FILE.....EUHFN.....
Br 1   euh_br1.npt - not used
Br 2   euh_br2.npt - not used
Br 3   euh_br3.npt - not used
Br 4   euh_br4.npt - not used
Br 5   euh_br5.npt - not used
Br 6   euh_br6.npt - not used
Br 7   euh_br7.npt - not used
Br 8   euh_br8.npt - not used
Br 9   euh_br9.npt - not used
Br 10  euh_br10.npt - not used
Br 11  euh_br11.npt - not used
Br 12  euh_br12.npt - not used

TUH FILE.....TUHFN.....
Br 1   tuh_br1.npt - not used
Br 2   tuh_br2.npt - not used
Br 3   tuh_br3.npt - not used
Br 4   tuh_br4.npt - not used
Br 5   tuh_br5.npt - not used
Br 6   tuh_br6.npt - not used
Br 7   tuh_br7.npt - not used
Br 8   tuh_br8.npt - not used
Br 9   tuh_br9.npt - not used
Br 10  tuh_br10.npt - not used
Br 11  tuh_br11.npt - not used
Br 12  tuh_br12.npt - not used

CUH FILE.....CUHFN.....
Br 1   cuh_br1.npt - not used
Br 2   cuh_br2.npt - not used
Br 3   cuh_br3.npt - not used
Br 4   cuh_br4.npt - not used
Br 5   cuh_br5.npt - not used
Br 6   cuh_br6.npt - not used
Br 7   cuh_br7.npt - not used
Br 8   cuh_br8.npt - not used
Br 9   cuh_br9.npt - not used
Br 10  cuh_br10.npt - not used
Br 11  cuh_br11.npt - not used
Br 12  cuh_br12.npt - not used
```

SAMPLE CONTROL FILE

CONTROL FILE

```
EDH FILE.....EDHFN.....
Br 1    edh_br1.npt - not used
Br 2    edh_br2.npt - not used
Br 3    edh_br3.npt - not used
Br 4    edh_br4.npt - not used
Br 5    edh_br5.npt - not used
Br 6    edh_br6.npt - not used
Br 7    edh_br7.npt - not used
Br 8    edh_br8.npt - not used
Br 9    edh_br9.npt - not used
Br 10   edh_br10.npt - not used
Br 11   edh_br11.npt - not used
Br 12   edh_br12.npt - not used

TDH FILE.....TDHFN.....
Br 1    tdh_br1.npt - not used
Br 2    tdh_br2.npt - not used
Br 3    tdh_br3.npt - not used
Br 4    tdh_br4.npt - not used
Br 5    tdh_br5.npt - not used
Br 6    tdh_br6.npt - not used
Br 7    tdh_br7.npt - not used
Br 8    tdh_br8.npt - not used
Br 9    tdh_br9.npt - not used
Br 10   tdh_br10.npt - not used
Br 11   tdh_br11.npt - not used
Br 12   tdh_br12.npt - not used

CDH FILE.....CDHFN.....
Br 1    cdh_br1.npt - not used
Br 2    cdh_br2.npt - not used
Br 3    cdh_br3.npt - not used
Br 4    cdh_br4.npt - not used
Br 5    cdh_br5.npt - not used
Br 6    cdh_br6.npt - not used
Br 7    cdh_br7.npt - not used
Br 8    cdh_br8.npt - not used
Br 9    cdh_br9.npt - not used
Br 10   cdh_br10.npt - not used
Br 11   cdh_br11.npt - not used
Br 12   cdh_br12.npt - not used

SNP FILE.....SNPFN.....
WB 1    snp_wb1.opt
WB 2    snp_wb2.opt
WB 3    snp_wb3.opt
WB 4    snp_wb4.opt
WB 5    snp_wb5.opt
WB 6    snp_wb6.opt

PRF FILE.....PRFFN.....
WB 1    prf_wb1.opt
WB 2    prf_wb2.opt
WB 3    prf_wb3.opt
WB 4    prf_wb4.opt
WB 5    prf_wb5.opt
WB 6    prf_wb6.opt

VPL FILE.....VPLFN.....
WB 1    vpl_wb1.opt
WB 2    vpl_wb2.opt
WB 3    vpl_wb3.opt
WB 4    vpl_wb4.opt
WB 5    vpl_wb5.opt
WB 6    vpl_wb6.opt
```

CONTROL FILE

SAMPLE CONTROL FILE

```
CPL FILE.....CPLFN.....
WB 1    cpl_wb1.opt
WB 2    cpl_wb2.opt
WB 3    cpl_wb3.opt
WB 4    cpl_wb4.opt
WB 5    cpl_wb5.opt
WB 6    cpl_wb6.opt

SPR FILE.....SPRFN.....
WB 1    spr_wb1.opt
WB 2    spr_wb2.opt
WB 3    spr_wb3.opt
WB 4    spr_wb4.opt
WB 5    spr_wb5.opt
WB 6    spr_wb6.opt

FLX FILE.....KFLFN.....
WB 1    kfl_wb1.opt
WB 2    kfl_wb2.opt
WB 3    kfl_wb3.opt
WB 4    kfl_wb4.opt
WB 5    kfl_wb5.opt
WB 6    kfl_wb6.opt

TSR FILE.....TSRFN.....
      tsr.opt

WDO FILE.....WDOFN.....
      wdo.opt
```

Bathymetry File

The bathymetry file(s) contains information specifying the segment lengths, water surface elevations, segment orientations, bottom friction, and layer heights for each segment, and average widths for each grid cell. The following is a list of guidelines for file preparation.

1. The first three lines are ignored and can be used to comment the input file.
2. Segment lengths, water surface elevations, segment orientations, layer heights, and cell widths at each segment are preceded by two lines that are ignored. They can be used to comment each individual segment's bathymetry.
3. Input format for each cell width is F8.0 with 10 cell widths per line.
4. It is recommended the user number the branches starting with the mainstem as branch 1. The remaining branch numbers should be numbered consecutively starting with the most upstream branch followed by the remaining branches as one moves downstream.
5. Each branch is surrounded by a segment of boundary cells (cells with zero widths) on both the upstream and downstream ends. Note this requirement results in two segments of zero widths between each branch.
6. Boundary cells must also be included at the top and bottom of each segment.
7. If there are more cell widths than can fit on one line, then they are continued immediately on the next line.
8. Cell widths start at layer 1 and continue to the maximum number of layers [KMX]. The number of layers specified in this file must match the value of [KMX] in the control file.
9. Only cells that are potentially active have non-zero widths. The first layer, boundary segment cells, and cells below the reservoir bottom elevation at a given segment have zero widths.

The following bathymetry files illustrate an example for a three-waterbody system with four branches involving a two-branch river system where the branches are connected in series with different bottom slopes, a reservoir, and an estuary.

Example

Waterbody 1 bathymetry

```

Segment lengths [DLX]
1200.00 1200.00 1200.00 1200.00 1200.00 1200.00 1200.00 1200.00 1200.00 1200.00
1200.00 1200.00 1200.00 1200.00 1200.00

Water surface elevation [WSEL]
49.80 49.20 48.00 46.80 45.60 44.40 43.20 44.40 43.20 42.96
42.72 42.48 42.24 42.00 41.80

Segment orientation [PHI0]
0.00 0.00 0.00 0.00 0.00 0.00 0.00 0.00 0.00 0.00
0.00 0.00 0.00 0.00 0.00

Bottom friction [FRICTC]
0.04 0.04 0.04 0.04 0.04 0.04 0.04 0.04 0.04 0.04
0.04 0.04 0.04 0.04 0.04

Layer heights [H]
2.00 2.00 2.00 2.00 2.00 2.00 2.00 2.00 2.00 2.00
2.00 2.00 2.00 1.00 1.00 1.00 1.00 1.00 1.00 1.00
1.00 1.00 1.00 1.00

```

INPUT FILES

BATHYMETRY

Segment 1 - branch 1										
0.0	0.0	0.0	0.0	0.0	0.0	0.0	0.0	0.0	0.0	0.0
0.0	0.0	0.0	0.0	0.0	0.0	0.0	0.0	0.0	0.0	0.0
0.0	0.0	0.0	0.0							
Segment 2 - branch 1										
0.0	300.0	300.0	300.0	300.0	300.0	300.0	300.0	300.0	300.0	300.0
300.0	300.0	300.0	300.0	300.0	300.0	300.0	300.0	300.0	300.0	300.0
250.0	200.0	050.0	0.0							
Segment 3 - branch 1										
0.0	300.0	300.0	300.0	300.0	300.0	300.0	300.0	300.0	300.0	300.0
300.0	300.0	300.0	300.0	300.0	300.0	300.0	300.0	300.0	300.0	300.0
250.0	200.0	050.0	0.0							
Segment 4 - branch 1										
0.0	300.0	300.0	300.0	300.0	300.0	300.0	300.0	300.0	300.0	300.0
300.0	300.0	300.0	300.0	300.0	300.0	300.0	300.0	300.0	300.0	300.0
250.0	200.0	050.0	0.0							
Segment 5 - branch 1										
0.0	300.0	300.0	300.0	300.0	300.0	300.0	300.0	300.0	300.0	300.0
300.0	300.0	300.0	300.0	300.0	300.0	300.0	300.0	300.0	300.0	300.0
250.0	200.0	050.0	0.0							
Segment 6 - branch 1										
0.0	300.0	300.0	300.0	300.0	300.0	300.0	300.0	300.0	300.0	300.0
300.0	300.0	300.0	300.0	300.0	300.0	300.0	300.0	300.0	300.0	300.0
250.0	200.0	050.0	0.0							
Segment 7 - branch 1										
0.0	0.0	0.0	0.0	0.0	0.0	0.0	0.0	0.0	0.0	0.0
0.0	0.0	0.0	0.0	0.0	0.0	0.0	0.0	0.0	0.0	0.0
0.0	0.0	0.0	0.0							
Segment 8 - branch 2										
0.0	0.0	0.0	0.0	0.0	0.0	0.0	0.0	0.0	0.0	0.0
0.0	0.0	0.0	0.0	0.0	0.0	0.0	0.0	0.0	0.0	0.0
0.0	0.0	0.0	0.0							
Segment 9 - branch 2										
0.0	300.0	300.0	300.0	300.0	300.0	300.0	300.0	300.0	300.0	300.0
300.0	300.0	300.0	300.0	300.0	300.0	300.0	300.0	300.0	300.0	300.0
300.0	200.0	050.0	0.0							
Segment 10 - branch 2										
0.0	300.0	300.0	300.0	300.0	300.0	300.0	300.0	300.0	300.0	300.0
300.0	300.0	300.0	300.0	300.0	300.0	300.0	300.0	300.0	300.0	300.0
300.0	200.0	075.0	0.0							
Segment 11 - branch 2										
0.0	300.0	300.0	300.0	300.0	300.0	300.0	300.0	300.0	300.0	300.0
300.0	300.0	300.0	300.0	300.0	300.0	300.0	300.0	300.0	300.0	300.0
300.0	200.0	075.0	0.0							
Segment 12 - branch 2										
0.0	300.0	300.0	300.0	300.0	300.0	300.0	300.0	300.0	300.0	300.0
300.0	300.0	300.0	300.0	300.0	300.0	300.0	300.0	300.0	300.0	300.0
300.0	200.0	100.0	0.0							
Segment 13 - branch 2										
0.0	300.0	300.0	300.0	300.0	300.0	300.0	300.0	300.0	300.0	300.0
300.0	300.0	300.0	300.0	300.0	300.0	300.0	300.0	300.0	300.0	300.0
300.0	200.0	150.0	0.0							
Segment 14 - branch 2										
0.0	300.0	300.0	300.0	300.0	300.0	300.0	300.0	300.0	300.0	300.0

BATHYMETRY

INPUT FILES

300.0	300.0	300.0	300.0	300.0	300.0	300.0	300.0	300.0	300.0	300.0
300.0	250.0	200.0	0.0							

Segment 15 - branch 2

0.0	0.0	0.0	0.0	0.0	0.0	0.0	0.0	0.0	0.0	0.0
0.0	0.0	0.0	0.0	0.0	0.0	0.0	0.0	0.0	0.0	0.0
0.0	0.0	0.0	0.0							

Waterbody 2 bathymetry

Segment length [DLX]

1200.0	1200.0	1200.0	1200.0	1200.0	1200.0	1200.0	1200.0	1200.0	1200.0	1200.0
1200.0	1200.0	1200.0	1200.0	1200.0	1200.0					

Water surface elevation [ELWS]

42.00	42.00	42.00	42.00	42.00	42.00	42.00	42.00	42.00	42.00	42.00
42.00	42.00	42.00	42.00	42.00	42.00					

Segment orientation [PHI0]

0.00	0.00	0.00	0.00	0.00	0.00	0.00	0.00	0.00	0.00	0.00
0.00	0.00	0.00	0.00	0.00	0.00					

Bottom friction [MANN]

0.04	0.04	0.04	0.04	0.04	0.04	0.04	0.04	0.04	0.04	0.04
0.04	0.04	0.04	0.04	0.04	0.04					

Layer height [H]

2.00	2.00	2.00	2.00	2.00	2.00	2.00	2.00	2.00	2.00	2.00
2.00	2.00	2.00	2.00	2.00	2.00	2.00	2.00	2.00	2.00	2.00
2.00	2.00	2.00	2.00							

Width [B] - segment 16

0.0	0.0	0.0	0.0	0.0	0.0	0.0	0.0	0.0	0.0	0.0
0.0	0.0	0.0	0.0	0.0	0.0	0.0	0.0	0.0	0.0	0.0
0.0	0.0	0.0	0.0							

Width [B] - segment 17

0.0	300.0	300.0	300.0	300.0	300.0	300.0	300.0	300.0	300.0	300.0
300.0	300.0	300.0	0.0	0.0	0.0	0.0	0.0	0.0	0.0	0.0
0.0	0.0	0.0	0.0							

Width [B] - segment 18

0.0	350.0	350.0	350.0	350.0	350.0	350.0	350.0	350.0	350.0	350.0
350.0	350.0	350.0	350.0	0.0	0.0	0.0	0.0	0.0	0.0	0.0
0.0	0.0	0.0	0.0							

Width [B] - segment 19

0.0	500.0	500.0	500.0	500.0	500.0	500.0	500.0	500.0	500.0	500.0
500.0	500.0	500.0	500.0	500.0	0.0	0.0	0.0	0.0	0.0	0.0
0.0	0.0	0.0	0.0							

Width [B] - segment 20

0.0	500.0	500.0	500.0	500.0	500.0	500.0	500.0	500.0	500.0	500.0
500.0	500.0	500.0	500.0	500.0	500.0	500.0	0.0	0.0	0.0	0.0
0.0	0.0	0.0	0.0							

Width [B] - segment 21

0.0	500.0	500.0	500.0	500.0	500.0	500.0	500.0	500.0	500.0	500.0
500.0	500.0	500.0	500.0	500.0	500.0	500.0	500.0	500.0	0.0	0.0
0.0	0.0	0.0	0.0							

Width [B] - segment 22

0.0	500.0	500.0	500.0	500.0	500.0	500.0	500.0	500.0	500.0	500.0
500.0	500.0	500.0	500.0	500.0	500.0	500.0	500.0	500.0	0.0	0.0
0.0	0.0	0.0	0.0							

INPUT FILES

BATHYMETRY

```

Width [B] - segment 23
  0.0  500.0  500.0  500.0  500.0  500.0  500.0  500.0  500.0  500.0
  500.0  500.0  500.0  500.0  500.0  500.0  500.0  500.0  500.0  0.0
  0.0    0.0    0.0    0.0

Width [B] - segment 24
  0.0  500.0  500.0  500.0  500.0  500.0  500.0  500.0  500.0  500.0
  500.0  500.0  500.0  500.0  500.0  500.0  500.0  500.0  500.0  0.0
  0.0    0.0    0.0    0.0

Width [B] - segment 25
  0.0  600.0  600.0  600.0  600.0  600.0  600.0  600.0  600.0  600.0
  600.0  600.0  600.0  600.0  600.0  600.0  600.0  600.0  600.0  600.0
  0.0    0.0    0.0    0.0

Width [B] - segment 26
  0.0  600.0  600.0  600.0  600.0  600.0  600.0  600.0  600.0  600.0
  600.0  600.0  600.0  600.0  600.0  600.0  600.0  600.0  600.0  600.0
  0.0    0.0    0.0    0.0

Width [B] - segment 27
  0.0  700.0  700.0  700.0  700.0  700.0  700.0  700.0  700.0  700.0
  700.0  700.0  700.0  700.0  700.0  700.0  700.0  700.0  700.0  700.0
  700.0    0.0    0.0    0.0

Width [B] - segment 28
  0.0  800.0  800.0  800.0  800.0  800.0  800.0  800.0  800.0  800.0
  800.0  800.0  800.0  800.0  800.0  800.0  800.0  800.0  800.0  800.0
  800.0  800.0  800.0    0.0

Width [B] - segment 29
  0.0  800.0  800.0  800.0  800.0  800.0  800.0  800.0  800.0  800.0
  800.0  800.0  800.0  800.0  800.0  800.0  800.0  800.0  800.0  800.0
  800.0  800.0  800.0    0.0

Width [B] - segment 30
  0.0  800.0  800.0  800.0  800.0  800.0  800.0  800.0  800.0  800.0
  800.0  800.0  800.0  800.0  800.0  800.0  800.0  800.0  800.0  800.0
  800.0  800.0  800.0    0.0

Width [B] - segment 31
  0.0    0.0    0.0    0.0    0.0    0.0    0.0    0.0    0.0    0.0
  0.0    0.0    0.0    0.0    0.0    0.0    0.0    0.0    0.0    0.0
  0.0    0.0    0.0    0.0

```

Waterbody 3 bathymetry

```

Width [B] - segment length [DLX]
  1200.0  1200.0  1200.0  1200.0  1200.0  1200.0  1200.0  1200.0  1200.0  1200.0
  1200.0  1200.0

Water surface elevation [ELWS]
  8.00    8.00    8.00    8.00    8.00    8.00    8.00    8.00    8.00    8.00
  8.00    8.00

Width [B] - segment orientation [PHI0]
  0.00    0.00    0.00    0.00    0.00    0.00    0.00    0.00    0.00    0.00
  0.00    0.00

Bottom friction [MANN]
  0.035  0.040  0.045  0.040  0.035  0.030  0.030  0.035  0.035  0.035
  0.040  0.040

Layer height [H]
  2.00    2.00    2.00    2.00    2.00    2.00    2.00    2.00    2.00    2.00
  2.00    2.00    2.00    2.00    2.00    2.00    2.00    2.00    2.00    2.00
  2.00    2.00    2.00    2.00

```

BATHYMETRY

INPUT FILES

```
Width [B] - segment 32
  0.0  0.0  0.0  0.0  0.0  0.0  0.0  0.0  0.0  0.0
  0.0  0.0  0.0  0.0  0.0  0.0  0.0  0.0  0.0  0.0
  0.0  0.0  0.0  0.0

Width [B] - segment 33
  0.0  800.0  800.0  800.0  800.0  800.0  800.0  800.0  800.0  800.0
  800.0  800.0  800.0  800.0  800.0  800.0  800.0  800.0  800.0  800.0
  800.0  800.0  800.0  0.0

Width [B] - segment 34
  0.0  800.0  800.0  800.0  800.0  800.0  800.0  800.0  800.0  800.0
  800.0  800.0  800.0  800.0  800.0  800.0  800.0  800.0  800.0  800.0
  800.0  800.0  800.0  0.0

Width [B] - segment 35
  0.0  800.0  800.0  800.0  800.0  800.0  800.0  800.0  800.0  800.0
  800.0  800.0  800.0  800.0  800.0  800.0  800.0  800.0  800.0  800.0
  800.0  800.0  800.0  0.0

Width [B] - segment 36
  0.0  800.0  800.0  800.0  800.0  800.0  800.0  800.0  800.0  800.0
  800.0  800.0  800.0  800.0  800.0  800.0  800.0  800.0  800.0  800.0
  800.0  800.0  800.0  0.0

Width [B] - segment 37
  0.0  800.0  800.0  800.0  800.0  800.0  800.0  800.0  800.0  800.0
  800.0  800.0  800.0  800.0  800.0  800.0  800.0  800.0  800.0  800.0
  800.0  800.0  800.0  0.0

Width [B] - segment 38
  0.0  800.0  800.0  800.0  800.0  800.0  800.0  800.0  800.0  800.0
  800.0  800.0  800.0  800.0  800.0  800.0  800.0  800.0  800.0  800.0
  800.0  800.0  800.0  0.0

Width [B] - segment 39
  0.0  850.0  850.0  850.0  850.0  850.0  850.0  850.0  850.0  850.0
  850.0  850.0  850.0  850.0  850.0  850.0  850.0  850.0  850.0  850.0
  850.0  850.0  850.0  0.0

Width [B] - segment 40
  0.0  900.0  900.0  900.0  900.0  900.0  900.0  900.0  900.0  900.0
  900.0  900.0  900.0  900.0  900.0  900.0  900.0  900.0  900.0  900.0
  900.0  900.0  900.0  0.0

Width [B] - segment 41
  0.0  1000.0  1000.0  1000.0  1000.0  1000.0  1000.0  1000.0  1000.0  1000.0
  1000.0  1000.0  1000.0  1000.0  1000.0  1000.0  1000.0  1000.0  1000.0  1000.0
  1000.0  1000.0  1000.0  0.0

Width [B] - segment 42
  0.0  1100.0  1100.0  1100.0  1100.0  1100.0  1100.0  1100.0  1100.0  1100.0
  1100.0  1100.0  1100.0  1100.0  1100.0  1100.0  1100.0  1100.0  1100.0  1100.0
  1100.0  1100.0  1100.0  0.0

Width [B] - segment 43
  0.0  0.0  0.0  0.0  0.0  0.0  0.0  0.0  0.0  0.0
  0.0  0.0  0.0  0.0  0.0  0.0  0.0  0.0  0.0  0.0
  0.0  0.0  0.0  0.0
```

Meteorology File

The meteorologic input file contains the following data:

Variable Description	Name	Format
Julian date	[JDAY]	F8.0
Air temperature, °C	[TAIR]	F8.0
Dewpoint temperature, °C	[TDEW]	F8.0
Wind speed, $m\ sec^{-1}$	[WIND]	F8.0
Wind direction, rad	[PHI]	F8.0
Cloud cover	[CLOUD]	F8.0
Incident short wave solar radiation, $W\ m^{-2}$	[SRO]	F8.0

The following is a list of guidelines for file preparation:

1. Data is read in according to an F8.0 format which allows the user to override the decimal point location according to the location specified in the input file. The field widths must be the same as specified above.
2. The first two lines are ignored and can be used to comment the file.
3. The third line contains the variable names which are right justified according to the input field. This line is also ignored although the preprocessor checks to ensure the fields are aligned correctly.
4. Data can be input at any frequency and may vary during the simulation. The user need only specify the Julian date corresponding to the data.
5. Short wave solar radiation is required if the user has set [[SROC](#)] to ON in the [HEAT EXCH](#) card in the control file. Otherwise, this field is not required. This represents, not global radiation, but only the penetrating short-wave solar radiation component.

Example

Sample meteorologic input file

JDAY	TAIR	TDEW	WIND	PHI	CLOUD	SRO
1.0	7.8	-0.9	2.19	2.0	8.0	0.0
2.0	3.3	1.3	4.75	2.0	6.0	0.0
3.0	3.3	1.3	4.75	2.0	3.0	0.0
4.0	2.2	-3.5	3.33	2.0	4.0	0.0
5.0	6.4	-2.4	1.86	2.0	4.0	0.0
6.0	7.5	2.4	4.00	2.0	10.0	0.0
7.0	1.9	-4.9	4.83	2.0	2.0	0.0
8.0	1.7	-6.6	4.00	2.0	0.0	0.0

Gate File

This file contains the dynamic gate height for each gate based on the rating curve supplied in the gates section in the control file. A separate file is required for each gate specified in the control file and contains the following data.

Variable Description	Name	Format
Julian day	[JDAY]	F8.0
Gate opening, <i>m</i>	[GATEH]	F8.0

The following is a list of guidelines for file preparation:

1. Data is read in according to an F8.0 format which allows the user to override the decimal point location according to the location specified in the input file. The field widths must be the same as specified above.
2. The first two lines are ignored and can be used to comment the file.
3. The third line contains the variable names which are right justified according to the input field. This line is also ignored although the preprocessor checks to ensure the fields are aligned correctly.
4. Data can be input at any frequency and may vary during the simulation. The user need only specify the Julian date corresponding to the data.

Example

Tainter gate opening, m

```

      JDAY   GATEH
      1.00    1.2
     200.30    0
     204.65    1.25
     209.50    2.50
     368.00    0

```

In some cases, gate openings can be used to open or close a valve or gate dynamically. In the following example, the dynamic opening is either closed (0) or fully open (1). In either case, the model uses the rating curve for the gate as specified in the control file.

Example

```

QGATE
simulating Willamette Falls 1999
      Jday   Gate 1
      1.00    1
     200.30    0
     204.65    1
     209.50    0
     368.00    0

```

Also, if the gate is specified as a dynamic weir, then the bottom elevation is included in this file rather than the gate opening. For example, if flashboards are raised, the weir equations will be used but with the dynamic weir crest elevation. The example below shows a dynamic flashboard height.

INPUT FILES

GATE

Example

```
QGATE
Dynamic flashboards 1999
  Jday Gate 1
    1.00  23.5
  200.30  25.5
  204.65  25.5
  209.50  23.5
  368.00  23.5
```

This file has also been used to predict the flow through needle valves where a rating curve based on the number of turns of the gate valve was developed. In this case, the dynamic height was interpreted as “turns” of a valve and is dependent on the supplied rating curve.

Light Extinction File

The light extinction input file contains the following data:

Variable Description	Name	Format
Julian date	[JDAY]	F8.0
Light extinction, m^{-1}	[EXH2O]	F8.0

These data are usually obtained by Secchi disk measurements. Due to inaccuracies in these measurements, a more appropriate method is the measurement of light extinction directly using a photometer. If dynamic light extinction is read in, all other internal calculations of light extinction are ignored. The following is a list of guidelines for file preparation:

1. Input format for each field is F8.0 that allows the user to specify the decimal point location.
2. The first two lines are ignored and can be used to comment the file.
3. The third line contains the variable name which is right justified according to the input field. This line is also ignored although the preprocessor checks to ensure the fields are aligned correctly.
4. The first field is the Julian date [JDAY], which can be entered at any frequency. The frequency between updates may vary during the simulation.
5. The second field contains values for observed light extinction, m^{-1} .

Example

Observed light extinction

```

JDAY  EXH2O
1.00  0.20
110.0  0.25
140.0  0.34
157.0  0.41
158.0  0.44
165.0  0.45
200.0  0.38
220.0  0.25
240.0  0.20
250.0  0.24
260.0  0.20
275.0  0.24
280.0  0.27
320.0  0.35
340.0  0.40
365.00 0.20
410.00 0.22
479.00 0.24
525.00 0.30
540.00 0.41
575.00 0.30
650.00 0.25

```

Wind Sheltering Coefficient File

The wind sheltering input file contains the following data:

Variable Description	Name	Format
Julian date	[JDAY]	F8.0
Wind-sheltering coefficient	[WSC]	F8.0

This file contains the wind-sheltering as a function of segment and time. This is a representation of having segment-by-segment wind velocity data, which is preferable if the data exist based on only one meteorological station. The following is a list of guidelines for file preparation:

1. Input format for each field is F8.0 that allows the user to specify the decimal point location.
2. The first two lines are ignored and can be used to comment the file.
3. The third line contains the variable name which is right justified according to the input field. This line is also ignored although the preprocessor checks to ensure the fields are aligned correctly.
4. The first field is the Julian date, which can be entered at any frequency. The frequency between updates may vary during the simulation.
5. The next fields are the wind-sheltering coefficients for all model segments including the boundary segments at the given Julian date.
6. The Julian date [JDAY] and wind-sheltering coefficient [WSC] are repeated as required to provide for dynamic wind sheltering.

Example

Alum Creek wind sheltering coefficients

JDAY	WSC								
1.0	0.1	0.2	0.3	0.4	0.5	0.6	0.7	0.8	0.9
	1.0	1.0	1.0	1.0	1.0	1.0	1.0	1.0	1.0
	1.0	1.0	1.0	1.0	1.0	1.0	1.0	1.0	1.0
	1.0	1.0	1.0	1.0	1.0	1.0	1.0	1.0	1.0
1.1	0.2	0.3	0.4	0.5	0.6	0.7	0.8	0.9	1.0
	1.0	1.0	1.0	1.0	1.0	1.0	1.0	1.0	1.0
	1.0	1.0	1.0	1.0	1.0	1.0	1.0	1.0	1.0
	1.0	1.0	1.0	1.0	1.0	1.0	1.0	1.0	1.0
365.0	1.0	1.0	1.0	1.0	1.0	1.0	1.0	1.0	1.0
	1.0	1.0	1.0	1.0	1.0	1.0	1.0	1.0	1.0
	1.0	1.0	1.0	1.0	1.0	1.0	1.0	1.0	1.0
	1.0	1.0	1.0	1.0	1.0	1.0	1.0	1.0	1.0

Shade Input File

The shade input file contains the following data:

Variable Description	Name	Format
Segment Number	[SEG]	F8.0
Dynamic shading or static shading	[DYNSH]	F8.0
Vegetative elevation left bank, m	[VEL]	F8.0
Vegetative elevation right bank, m	[VER]	F8.0
Distance to vegetation left bank, m	[DL]	F8.0
Distance to vegetation right bank, m	[DR]	F8.0
Shade reduction factor #1, left bank	[SRFL1]	F8.0
Shade reduction factor #2, left bank	[SRFL2]	F8.0
Shade reduction factor #1, right bank	[SRFR1]	F8.0
Shade reduction factor #2, right bank	[SRFR2]	F8.0
Topographic angle #1 at 0°, radians	[TOPO1]	F8.0
Topographic angle #2 at 20°, radians	[TOPO2]	F8.0
Topographic angle #3 at 40°, radians	[TOPO3]	F8.0
Topographic angle #4 at 60°, radians	[TOPO4]	F8.0
Topographic angle #5 at 80°, radians	[TOPO5]	F8.0
Topographic angle #6 at 100°, radians	[TOPO6]	F8.0
Topographic angle #7 at 120°, radians	[TOPO7]	F8.0
Topographic angle #8 at 140°, radians	[TOPO8]	F8.0
Topographic angle #9 at 160°, radians	[TOPO9]	F8.0
Topographic angle #10 at 180°, radians	[TOPO10]	F8.0
Topographic angle #11 at 200°, radians	[TOPO11]	F8.0
Topographic angle #12 at 220°, radians	[TOPO12]	F8.0
Topographic angle #13 at 240°, radians	[TOPO13]	F8.0
Topographic angle #14 at 260°, radians	[TOPO14]	F8.0
Topographic angle #15 at 280°, radians	[TOPO15]	F8.0
Topographic angle #16 at 300°, radians	[TOPO16]	F8.0
Topographic angle #17 at 320°, radians	[TOPO17]	F8.0
Topographic angle #18 at 340°, radians	[TOPO18]	F8.0
Starting date for SRF#1, Julian day	[JDSRF1]	F8.0
Starting date for SRF#2, Julian day	[JDSRF2]	F8.0

This file contains the shade information for computing the vegetative and topographic shading dynamically for a model segment. If the dynamic shading value [DYNSH] is set from 0 to 1, then static shading is used and the shade factor takes on the specified value. This means that a dynamic shading value [DYNSH] of 0.8 allows 80% of the incoming short-wave solar to reach the water surface of that segment – or 20% fully shaded. This would apply for all times. If dynamic shading [DYNSH] is set to a negative value, then the remaining columns are read for dynamic shading information and the shade percentage is computed dynamically.

The shade file consists of four types of vegetative information for each bank of the river, topographic information, and the time for leaf growth and leaf fall if the trees are deciduous. More detailed information on the shading model and data preparation is given in Appendix A and Annear, et. al. (2001).

[Table C-26](#) provides a description of the input variables controlling dynamic shading.

Table C-26. Description of Dynamic Shading Input Variables

Heading	Description
SEG	Segment number in the model – include all segment numbers and leave blank those that are inactive.
DYNOSH	If between 0 and 1, this is a non-dynamic constant shade reduction similar to that used in Version 3.0 and the columns to the right are ignored. If this number is negative, this means that the rest of the columns to the right will be read and dynamic shading will be implemented.
VEL	Tree top elevation on the left bank (m). The elevation of the left bank plus the height of the tree/vegetation are used to provide the tree top elevation. This is the absolute elevation that the entire model is referenced to. In most cases this is m, NGVD, or m MSL. This is not the elevation above the top of the bank.
VER	Tree top elevation on the right bank (m).
CDL	Distance from the centerline of the river segment to the shade controlling line of vegetation on the left bank (m).
CDR	Distance from the centerline of the river segment to the shade controlling line of vegetation on the right bank (m).
SRFL1	Shade reduction factor, left bank. This applies from SRFJD1 to SRFJD2 (and over multiple years for the same time period of the simulation goes over 360 days). It is based on the extent of vegetation along the length of the segment and the density of the vegetation (0 to 1).
SRFL2	Shade reduction factor, left bank bank (0 to 1). This applies from SRFJD2 to SRFJD1 (and over multiple years for the same time period of the simulation goes over 360 days). It is based on the extent of vegetation along the length of the segment and the density of the vegetation (0 to 1).
SRFR1	Shade reduction factor, right bank. This applies from SRFJD1 to SRFJD2 (and over multiple years for the same time period of the simulation goes over 360 days). It is based on the extent of vegetation along the length of the segment and the density of the vegetation (0 to 1).
SRFR2	Shade reduction factor, right bank (0 to 1).). This applies from SRFJD2 to SRFJD1 (and over multiple years for the same time period if the simulation goes over 360 days). It is based on the extent of vegetation along the length of the segment and the density of the vegetation (0 to 1).
TOPO1 to TOPO18	Topographic inclination angle (radians) for every 20° around a segment starting with TOPO1 at 0° North and moving clockwise. The topographic angles are most easily computed using Digital Elevation Maps (DEMs) and using GIS or other programs to automatically compute controlling topographic angles from the DEM.
JDSRF1	Shading reduction factor Julian day for which SRF #1 starts to apply. This is typically thought of as “leaf-out” conditions for deciduous trees.
JDSRF2	Shading reduction factor Julian day for which SRF #2 starts to apply. This is typically thought of as when deciduous trees loose their leaves.

The following discussion provides an overview of data development for the dynamic shading file.

Vegetation Elevation

The algorithm uses elevations for the grid development so the vegetation’s elevation is used instead of height. If shading is due to brush along side a river, the top elevation of the brush would be used

in the model. The tree top elevation consists of the vegetation height and the bank surface elevation where the vegetation is standing as shown in [Figure C-1](#). The vegetation height can be obtained from field surveys or from a GIS vegetation coverage. The surface elevation of the banks can be obtained from field surveys or from the U.S. Geological Survey digital elevation model (DEM). The frequency of tree top elevation measurements along a river bank depends on the variability of the controlling vegetation. The more comprehensive the elevation information, the more accurately the model will simulate shade. Tree top elevations should be collected for both river banks.

Centerline Distance

The centerline distance is the distance between the river centerline and the controlling vegetation on each bank. As shown in [Figure C-1](#), the information will vary for each bank depending on the location of the river centerline and the offset of the vegetation from the wetted edge. The frequency of the distances should match the tree top elevation data and reflect the variability of the vegetation. Less frequent data may be acceptable if there is not much variability in the controlling vegetation and the stream width does not change much.

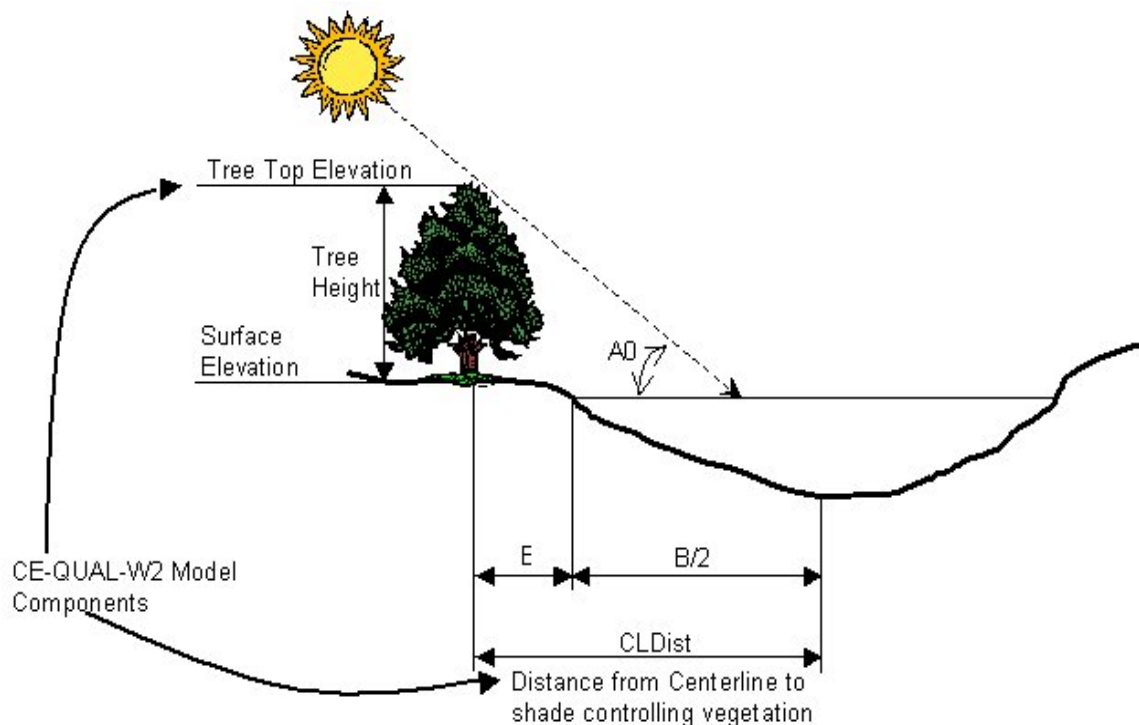


Figure C-1. Tree top elevation and vegetation offset from a river.

Shade reduction factor

The shade reduction factor is based on the density and extent of the vegetation along the length of each model segment. If shade producing vegetation exists along only half the length of a segment and was 100% opaque, a shade reduction factor of 0.50 would be used. If shade was due to vegetation along only half of the segment with 80% density, then a shade reduction factor of 0.40 would be

used. The shade reduction factors, [SRFR1] and [SRFR2], are expressed as a fraction from 0.0 to 1.0.

The extent of the vegetation along the segment length will depend on the grid discretization and the amount of vegetation. Vegetation density can be obtained from field surveys or from GIS vegetation information. The shade reduction factor is designed to attenuate the shade since some short-wave solar radiation penetrates the vegetation. The shade reduction factor should be developed for both banks and can be used as a calibration parameter if field data is uncertain or incomplete.

Topographic Shading

In addition to the vegetation near a river, the local topography can influence the amount of solar radiation reaching the water surface. [Figure C-2](#) illustrates the influence of topographic shading on the water surface of a river.

The local topography around a river can be developed using survey information of the river channel or from a digital elevation map (DEM). To characterize the influence of the topography, inclination angles can be obtained every 20 degrees around each model segment center point as shown in [Figure C-3](#). For each 20-degree increment around a model segment, an array of elevation points and their distances from the center point are obtained from the DEM. The elevations and distances are then used to calculate the highest inclination angle relative to the center point. The distance away from each segment center point that should be analyzed to obtain the controlling inclination angle will vary depending on the terrain surrounding the river. Wide open channels will require larger distances away from the channel to be analyzed than if the river channel is in a deep, narrow canyon. Inclination angles are then generated that control topographic shading for each of the 20-degree increments around a segment's center point. The inclination angles are converted to radians and specified in the dynamic shading input file [SHDFN]. The first column of the topographic inclination angles represents the inclination angle at 0° north with subsequent inclination angles obtained by moving clockwise to the east.

The shade algorithm can be used in both the northern and southern hemispheres, so inclination angles are provided for 360 degrees around each segment. If there is no topographic shading in a specific direction due to the latitude or the surrounding terrain, zero can be used as the inclination angle. The model uses all 18 topographic inclination angles. Based on the position of the sun, the algorithm will interpolate between the two nearest inclination angles to obtain the most appropriate inclination angle. The inclination angles are then used in the shading algorithm to determine if vegetative or topographic shading dominates at a specific time during the day.

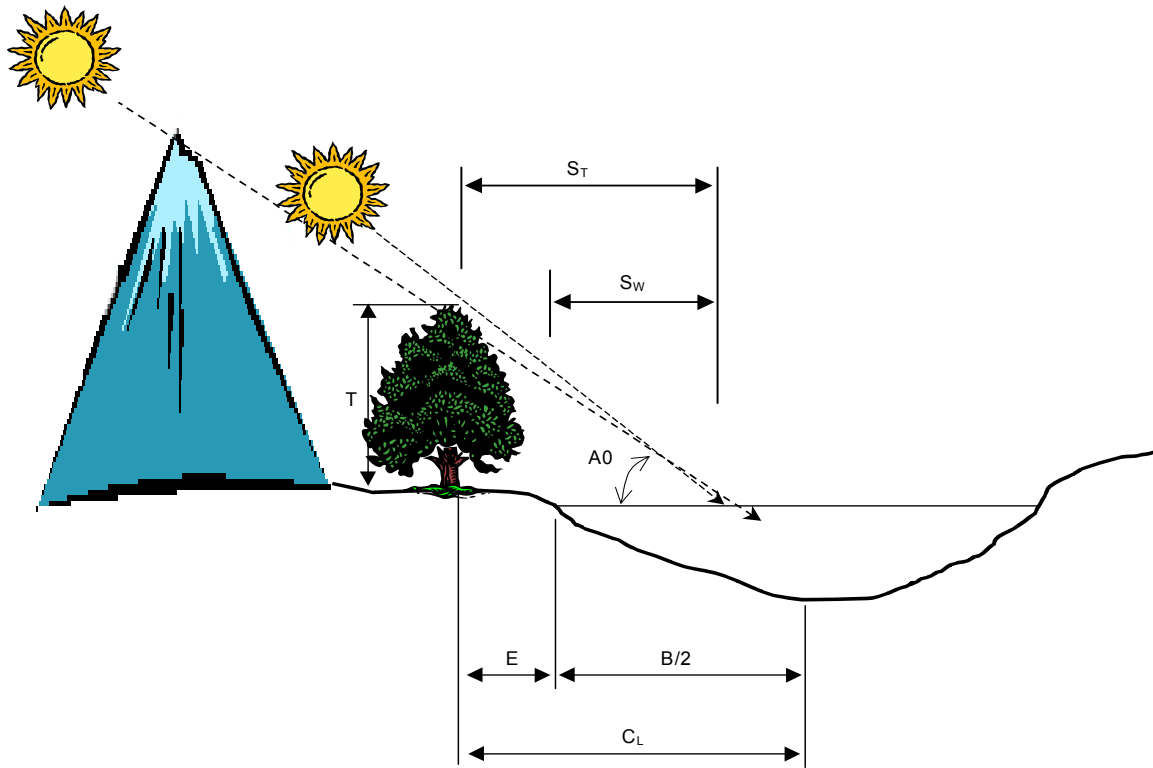


Figure C-2. The influence of topographic shading along a river.

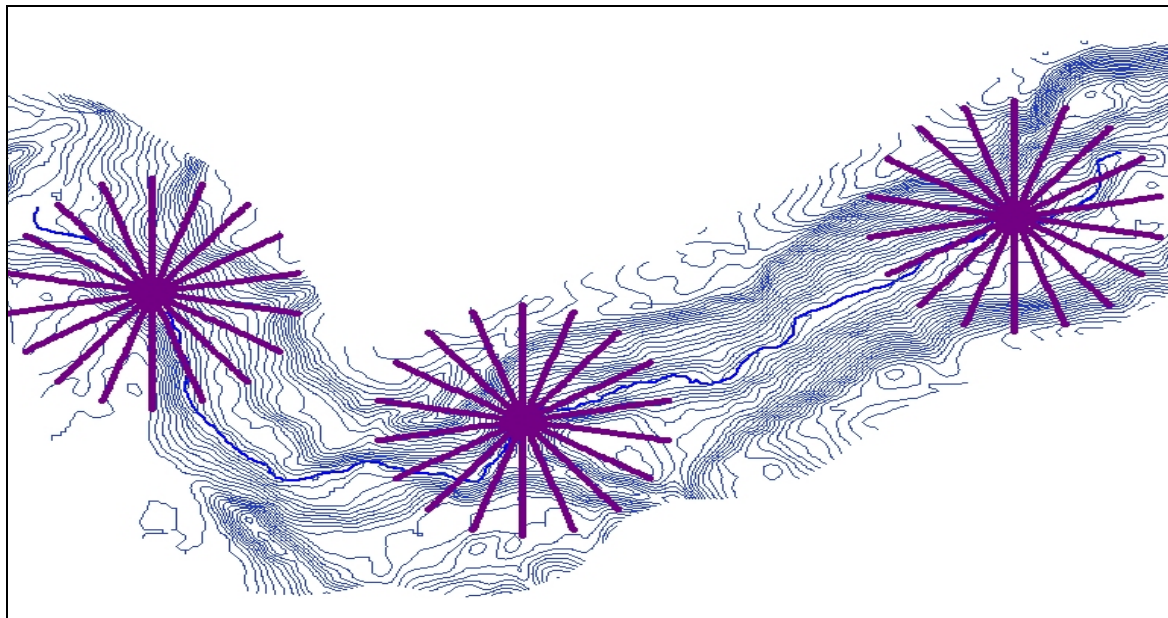


Figure C-3. Topographic slices at three segments along a river.

INPUT FILES

SHADE

Example

W2 Shading Input File, Vegetation and Topography, calibrated veg characteristics and corrected topography

SEGMENT	DYN5H	TTELELB	TTELERB	CLDISLB	CLDIRB	SRFLB1	SRFLB2	SRFRB1	SRFRB2	TOPO1	TOPO2	TOPO3	TOPO4	TOPO5	TOPO6	TOPO7	TOPO8	TOPO9	TOPO10	TOPO11	TOPO12	TOPO13	TOPO14	TOPO15	TOPO16	TOPO17	TOPO18	SRFJD1	SRFJD2
1																													
2	-1.0	233.37	224.39	33.22	12.50	0.00	0.57	0.00	0.50	0.486	0.490	0.414	0.295	0.191	0.149	0.134	0.296	0.353	0.359	0.329	0.250	0.120	0.123	0.242	0.298	0.310	0.414	80.00	288.00
3	-1.0	233.37	224.39	33.22	12.50	0.00	0.57	0.00	0.50	0.501	0.505	0.476	0.383	0.201	0.121	0.122	0.231	0.257	0.221	0.136	0.083	0.101	0.166	0.258	0.318	0.361	0.427	80.00	288.00
4	-1.0	233.37	224.39	33.22	12.50	0.00	0.57	0.00	0.50	0.599	0.583	0.566	0.458	0.478	0.469	0.409	0.296	0.246	0.221	0.180	0.077	0.137	0.289	0.350	0.433	0.530	0.588	80.00	288.00
5																													
6																													
7	-1.0	231.01	230.66	34.00	13.27	0.00	0.54	0.00	0.59	0.468	0.427	0.371	0.286	0.183	0.345	0.454	0.504	0.487	0.400	0.268	0.159	0.163	0.312	0.399	0.416	0.445	0.466	80.00	288.00
8	-1.0	227.30	240.49	35.22	14.49	0.00	0.55	0.00	0.53	0.468	0.418	0.332	0.251	0.127	0.185	0.230	0.255	0.247	0.197	0.102	0.134	0.253	0.427	0.522	0.536	0.534	0.500	80.00	288.00
9	-1.0	225.48	245.29	35.81	15.09	0.00	0.55	0.00	0.58	0.462	0.392	0.304	0.218	0.196	0.229	0.272	0.224	0.162	0.120	0.062	0.271	0.396	0.567	0.645	0.701	0.667	0.561	80.00	288.00
10																													
11																													
12	-1.0	225.00	237.01	28.08	15.14	0.00	0.51	0.00	0.58	0.393	0.310	0.236	0.216	0.228	0.228	0.250	0.222	0.169	0.119	0.283	0.558	0.736	0.809	0.770	0.699	0.668	0.564	80.00	288.00
13	-1.0	224.44	237.11	18.84	15.21	0.00	0.50	0.00	0.59	0.271	0.229	0.182	0.247	0.329	0.370	0.344	0.294	0.238	0.189	0.111	0.177	0.290	0.358	0.397	0.431	0.391	0.357	80.00	288.00
14	-1.0	225.46	222.71	16.11	16.02	0.00	0.59	0.00	0.58	0.243	0.190	0.215	0.346	0.394	0.425	0.428	0.405	0.372	0.287	0.162	0.068	0.210	0.288	0.297	0.308	0.324	0.302	80.00	288.00
15																													
16																													
17	-1.0	227.96	233.53	19.56	17.52	0.00	0.52	0.00	0.56	0.194	0.173	0.171	0.260	0.346	0.437	0.493	0.529	0.443	0.279	0.217	0.089	0.042	0.124	0.210	0.300	0.287	0.314	80.00	288.00
18	-1.0	230.47	224.35	23.00	19.02	0.00	0.55	0.00	0.54	0.184	0.162	0.103	0.187	0.280	0.392	0.365	0.271	0.299	0.311	0.246	0.128	0.051	0.155	0.197	0.300	0.281	0.285	80.00	288.00
19	-1.0	232.80	225.12	26.21	20.42	0.00	0.68	0.00	0.63	0.188	0.174	0.173	0.149	0.223	0.254	0.228	0.328	0.367	0.237	0.152	0.101	0.061	0.211	0.244	0.310	0.326	0.309	80.00	288.00
20																													
21																													

Branch Inflow File

This file contains the inflow for a branch with an [upstream flow boundary condition](#). The following is a list of guidelines for file preparation:

1. A separate file is required for each branch with an upstream flow boundary condition. This allows the user to update inflows for one branch independent of another branch.
2. Input format for each field is F8.0 that allows the user to specify the decimal point location.
3. The first two lines are ignored and can be used to comment the file.
4. The third line contains the variable names which are right justified according to the input field. This line is also ignored although the preprocessor checks to ensure the fields are aligned correctly.
5. The first field is the Julian date that can be entered at any frequency. The frequency between updates may vary during the simulation.
6. The second field is the inflow rate, $m^3 sec^{-1}$.

Note the following example takes advantage of the algorithm's capability to use data at varying frequencies.

Example

CE-QUAL-W2 sample inflow file

JDAY	QIN
182.0000	0.0
182.5416	283.0
182.6250	566.0
182.6666	1699.0
182.7916	566.0
182.8333	283.0
182.9166	0.0
185.5416	283.0
185.6250	566.0
185.6666	1699.0
185.7916	566.0
185.8333	283.0
185.9166	0.0
186.5416	283.0

Branch Inflow Temperature File

This file contains the inflow temperatures for a branch with an [upstream flow boundary condition](#). The following is a list of guidelines for file preparation:

1. A separate file is required for each branch with an upstream flow boundary condition. This allows the user to update temperatures for one branch independent of another branch.
2. Input format for each field is F8.0 that allows the user to specify the decimal point location.
3. The first two lines are ignored and can be used to comment the file.
4. The third line contains the variable names which are right justified according to the input field. This line is also ignored although the preprocessor checks to ensure the fields are aligned correctly.
5. The first field is the Julian date that can be entered at any frequency. The frequency between updates may vary during the simulation.
6. The second field is the inflow temperature, °C.

Example

CE-QUAL-W2 sample inflow temperature file

JDAY	TIN
1.00	6.80
2.00	6.70
3.00	7.00
4.00	6.30
5.00	6.40
6.00	6.10
7.00	6.60
8.00	5.70
9.00	5.20
10.00	5.40
11.00	7.10
12.00	6.60
13.00	5.50
14.00	5.60
15.00	7.30
16.00	9.50

Branch Inflow Constituent Concentration File

This file contains the inflow concentrations for a branch with an [upstream flow boundary condition](#). The following is a list of guidelines for file preparation:

1. *If* constituents are being modeled, a separate file is required for each branch with an upstream flow boundary condition. This allows the user to update constituent concentrations for one branch independent of another branch.
2. Input format for all fields is F8.0 that allows the user to specify the decimal point location. The number of fields is determined by (6) below and they are always located on one line.
3. The first two lines are ignored and can be used to comment the file.
4. The next line contains the abbreviations for the constituent names that are right justified according to the input field. This line is also ignored although the preprocessor checks to ensure the fields are aligned correctly.
5. The first field is the Julian date that can be entered at any frequency. The frequency between updates may vary during the simulation.
6. The remaining fields contain the concentration for each constituent specified on the [Inflow Active Constituent Control](#) card. Only those constituents specified as active on the [Inflow Active Constituent Control](#) card are included in the constituent inflow concentration file.

INPUT FILES

BRANCH INFLOW CONCENTRATION

Example

CE-QUAL-W2 constituent inflow concentration sample input file

JDAY	PO4	NH4	NOx	LDOM	RDOM	LPOM	RPOM	CBOD1	CBOD2	CBOD3	CBOD4	CBOD5	ALG1	DO
1.040	0.030	0.010	0.300	0.1000	0.1000	0.1000	0.1000	0.000	0.000	0.000	0.000	0.000	0.100	12.000
1.100	0.030	0.011	0.307	0.1040	0.0991	0.0989	0.0989	0.000	0.000	0.000	0.000	0.000	0.098	12.000
1.200	0.029	0.012	0.323	0.1100	0.0968	0.0963	0.0963	0.000	0.000	0.000	0.000	0.001	0.095	11.800
1.300	0.048	0.017	0.458	0.1250	0.0944	0.0935	0.0936	0.000	0.000	0.000	0.229	0.003	0.091	11.900
1.400	0.043	0.018	0.441	0.1360	0.0936	0.0924	0.0925	0.000	0.000	0.000	0.167	0.010	0.090	11.900
1.500	0.043	0.013	0.498	0.1430	0.0874	0.0861	0.0862	0.000	0.000	0.000	0.192	0.011	0.084	11.900
1.600	0.047	0.006	0.542	0.1530	0.0852	0.0837	0.0838	0.000	0.000	0.008	0.241	0.015	0.083	12.000
1.700	0.046	0.001	0.565	0.1690	0.0820	0.0804	0.0805	0.000	0.004	0.032	0.248	0.017	0.081	12.000
1.800	0.045	0.002	0.577	0.1730	0.0790	0.0773	0.0773	0.000	0.020	0.041	0.249	0.016	0.077	11.900
1.900	0.044	0.005	0.579	0.1790	0.0724	0.0705	0.0706	0.002	0.026	0.055	0.249	0.078	0.071	11.800
2.000	0.034	0.022	0.480	0.1230	0.0146	0.0142	0.0141	0.003	0.033	0.058	0.250	0.715	0.042	11.800

Branch Outflow File

This file contains the outflow for a branch with a [downstream flow boundary condition](#). The following is a list of guidelines for file preparation:

1. A separate file is required for each branch with a downstream flow boundary condition. This allows the user to update outflows for one branch independent of another branch.
2. Input format for each field is F8.0 that allows the user to specify the decimal point location. There are a maximum of 10 fields to a line. If there are more outflows than can be specified on one line, then they are continued on the next line with blanks inserted in the Julian date field.
3. The first two lines are ignored and can be used to comment the file.
4. The next line contains the variable names which are right justified according to the input field. This line is also ignored although the preprocessor checks to ensure the fields are aligned correctly.
5. The first field is the Julian date that can be entered at any frequency. The frequency between updates may vary during the simulation.
6. The remaining fields are the outflow rate, $m^3 sec^{-1}$.
7. A separate column of outflow values must be specified for each outlet structure.

Example

CE-QUAL-W2 sample outflow file

JDAY	QOUT	QOUT	QOUT	QOUT	QOUT	QOUT	QOUT	QOUT	QOUT
1.00	8.13	8.13	8.13						
2.00	6.77	6.77	6.77						
3.00	18.60	18.60	18.60						
4.00	0.60	0.60	0.60						
5.00	7.50	7.50	7.50						
6.00	2.87	2.87	2.87						

Withdrawal File

This contains the outflow for each withdrawal specified on the [Inflow/Outflow Dimensions](#) card. The following is a list of guidelines for file preparation:

1. The order in which withdrawal outflows appear in the file *must* correspond with the order specified on the Withdrawal Segment and the [Withdrawal Elevation](#) cards.
2. Input format for each field is F8.0 with 10 fields to a line. The F8.0 input field allows the user to specify the decimal point location.
3. The first two lines are ignored and can be used to comment the file.
4. The third line contains the variable names which are right justified according to the input field. This line is also ignored although the preprocessor checks to ensure the fields are aligned correctly.
5. The first field is the Julian date that can be entered at any frequency. The frequency between updates may vary during the simulation.
6. The remaining fields are the withdrawal outflow rate, $m^3 sec^{-1}$
7. Outflows from a single withdrawal structure spanning more than one layer in the computational grid can be divided up into several outflows and the total outflow apportioned among them.
8. If there are *more* withdrawals than can be specified on one line, then they are continued on the next line with blanks inserted under the JDAY field.

Example

CE-QUAL-W2 sample withdrawal outflow file

JDAY	QWD								
182.0000	51.	51.	51.	51.	51.	51.	51.	51.	51.
	51.								
182.2500	0.	0.	0.	0.	0.	0.	0.	0.	0.
	0.								
183.0000	51.	51.	51.	51.	51.	51.	51.	51.	0.
	51.								
183.2500	0.	0.	0.	0.	0.	0.	0.	0.	0.
	0.								

Tributary Inflow File

This file contains the inflows for a tributary specified on the [Tributary Segment](#) card. The following is a list of guidelines for file preparation:

1. A separate file is required for each tributary. This allows the user to update inflows for one tributary independent of another tributary.
2. Input format for each field is F8.0 that allows the user to specify the decimal point location.
3. The first two lines are ignored and can be used to comment the file.
4. The third line contains the variable names which are right justified according to the input field. This line is also ignored although the preprocessor checks to ensure the fields are aligned correctly.
5. The first field is the Julian date that can be entered at any frequency. The frequency between updates may vary during the simulation.
6. The second field is the inflow rate, $m^3 sec^{-1}$.

Example

CE-QUAL-W2 sample tributary inflow file

JDAY	QTR
1.0	22.8
5.0	44.5
12.0	31.2
23.0	80.4
35.0	50.6
74.5	103.0
74.7	185.6
75.0	212.3
75.5	178.6
80.0	123.4
80.5	78.3
90.0	46.5
112.0	35.9

Tributary Inflow Temperature File

This file contains the inflow temperatures for a tributary specified on the [Tributary Segment](#) card. The following is a list of guidelines for file preparation:

1. A separate file is required for each tributary. This allows the user to update inflow temperatures for one tributary independent of another tributary.
2. Input format for each field is F8.0 that allows the user to specify the decimal point location.
3. The first two lines are ignored and can be used to comment the file.
4. The third line contains the variable names which are right justified according to the input field. This line is also ignored although the preprocessor checks to ensure the fields are aligned correctly.
5. The first field is the Julian date that can be entered at any frequency. The frequency between updates may vary during the simulation.
6. The second field is the inflow temperature, °C.

Example

CE-QUAL-W2 sample tributary inflow temperature file

JDAY	TTR
1.0	10.3
5.0	9.5
12.0	10.1
23.0	8.6
35.0	11.2
74.5	13.9
74.7	13.1
75.0	12.8
75.5	12.5
80.0	12.6
80.5	12.7
90.0	15.4

Tributary Inflow Concentration File

This file contains the inflow constituent concentrations for each tributary specified on the [Tributary Segment](#) card. The following is a list of guidelines for file preparation:

1. *If* constituents are being modeled, a separate file is required for each tributary. This allows the user to update constituent inflow concentrations for one tributary independent of another tributary.
2. Input format for all fields is F8.0 that allows the user to specify the decimal point location. The number of fields is determined by (6) below and they are always located on one line.
3. The first two lines are ignored and can be used to comment the file.
4. The next line contains the abbreviations for the constituent names which are right justified according to the input field. This line is also ignored although the preprocessor checks to ensure the fields are aligned correctly.
5. The first field is the Julian date that can be entered at any frequency. The frequency between updates may vary during the simulation.
6. The remaining fields contain the concentration for each constituent specified on the [Tributary Active Constituent Control](#) card. Only those constituents specified as *active* on the [Tributary Active Constituent Control](#) card may be included in the tributary inflow concentration file.

Example

```
CE-QUAL-W2 sample tributary constituent inflow concentration file
JDAY CLFORM  SSOLID   LDOM   RDOM  ALGAE  LPOM   PO4   NH4   NO3   O2     Fe
 1.   17.    62.   7.333 17.111  0.0   0.9   0.02  0.10  0.42  13.9   0.4
 8.   13.    0.0   8.000 18.667  0.0   0.4   0.01  0.03  0.37  14.0   0.2
15.   11.    17.   9.333 21.778  0.0   0.0   0.00  0.01  0.17  10.0   0.3
22.   14.    34.  10.000 23.333  0.0   0.0   0.05  0.00  0.20  10.4   1.6
29.   17.    38.   4.467 10.422  0.0   0.4   0.01  0.11  0.26  11.6   0.4
36.  101.    24.   3.867  9.022  0.0   0.2   0.01  0.00  0.23  12.2   0.3
43.   10.    11.   4.133  9.644  0.0   0.2   0.02  0.07  0.20  12.2   0.1
```

Branch Distributed Tributary Inflow File

This file contains the inflows for a distributed tributary specified on the [Distributed Tributary](#) card. The following is a list of guidelines for file preparation:

1. A separate file is required for each distributed tributary. This approach allows the user to update inflows for one distributed tributary independent of another distributed tributary.
2. Input format for each field is F8.0 that allows the user to specify the decimal point location.
3. The first two lines are ignored and can be used to comment the file.
4. The third line contains the variable names which are right justified according to the input field. This line is also ignored although the preprocessor checks to ensure the fields are aligned correctly.
5. The first field is the Julian date that can be entered at any frequency. The frequency between updates may vary during the simulation.
6. The second field is the inflow rate, m³ sec⁻¹.

Example

CE-QUAL-W2 sample distributed tributary inflow file

JDAY	QDTR
1.0	22.8
5.0	44.5
12.0	31.2
23.0	80.4
35.0	50.6
74.5	103.0
74.7	185.6
75.0	212.3
75.5	178.6
80.0	123.4
80.5	78.3
90.0	46.5

Branch Distributed Tributary Inflow Temperature File

This file contains the inflow temperatures for a distributed tributary specified on the [Distributed Tributary](#) card. The following is a list of guidelines for file preparation:

1. A separate file is required for each distributed tributary. This allows the user to update inflow temperatures for one distributed tributary independent of another distributed tributary.
2. Input format for each field is F8.0 that allows the user to specify the decimal point location.
3. The first two lines are ignored and can be used to comment the file.
4. The third line contains the variable names which are right justified according to the input field. This line is also ignored although the preprocessor checks to ensure the fields are aligned correctly.
5. The first field is the Julian date that can be entered at any frequency. The frequency between updates may vary during the simulation.
6. The second field is the inflow temperature, °C.

Example

CE-QUAL-W2 sample tributary inflow temperature file

JDAY	TDTR
1.0	10.3
5.0	9.5
12.0	10.1
23.0	8.6
35.0	11.2
74.5	13.9
74.7	13.1
75.0	12.8
75.5	12.5
80.0	12.6
80.5	12.7

Branch Distributed Tributary Inflow Concentration File

This file contains the inflow concentrations for a distributed tributary specified on the [Distributed Tributary](#) card. The following is a list of guidelines for file preparation:

1. *If* constituents are being modeled, a separate file is required for each branch. This allows the user to update constituent inflow concentrations for one branch independent of another branch.
2. Input format for all fields is F8.0 that allows the user to specify the decimal point location. The number of fields is determined by (6) below and they are always located on one line.
3. The first two lines are ignored and can be used to comment the file.
4. The next line contains the abbreviations for the constituent names which are right justified according to the input field. This line is also ignored although the preprocessor checks to ensure the fields are aligned correctly.
5. The first field is the Julian date that can be entered at any frequency. The frequency between updates may vary during the simulation.
6. The remaining fields contain the concentration for each constituent specified on the [Distributed Tributary Active Constituent Control](#) card. Only those constituents specified as *active* on the [Distributed Tributary Active Constituent Control](#) card may be included in the distributed tributary inflow concentration file.

Example

```
CE-QUAL-W2 sample distributed tributary constituent inflow concentration file
JDAY CLFORM    ISS    LDOM    RDOM    ALGAE DETRIT    PO4    NH4    NO3    O2    Fe
 1.    17.    62.    7.333  17.111    0.0    0.9    0.02    0.10    0.42    13.9    0.4
 8.    13.    0.0    8.000  18.667    0.0    0.4    0.01    0.03    0.37    14.0    0.2
15.    11.    17.    9.333  21.778    0.0    0.0    0.00    0.01    0.17    10.0    0.3
22.    14.    34.   10.000  23.333    0.0    0.0    0.05    0.00    0.20    10.4    1.6
29.    17.    38.    4.467  10.422    0.0    0.4    0.01    0.11    0.26    11.6    0.4
```

Branch Precipitation File

This file contains the precipitation values for a branch and is needed only if the precipitation option [\[PRC\]](#) is turned on. The following is a list of guidelines for file preparation:

1. A separate file is required for each branch. This allows the user to update precipitation for one branch independent of another branch if needed.
2. Input format for each field is F8.0 that allows the user to specify the decimal point location.
3. The first two lines are ignored and can be used to comment the file.
4. The third line contains the variable names which are right justified according to the input field. This line is also ignored although the preprocessor checks to ensure the fields are aligned correctly.
5. The first field is the Julian date that can be entered at any frequency. The frequency between updates may vary during the simulation.
6. The second field is the precipitation rate, m sec-1.

Note the following example takes advantage of the algorithm's capability to use data at varying frequencies.

Example

CE-QUAL-W2 sample precipitation file

JDAY	PRE
182.0000	0.000
182.5416	0.001
182.6250	0.002
182.6666	0.000
188.475	0.002
189.500	0.000

Branch Precipitation Temperature File

This file contains the precipitation temperatures for a branch and is needed only if the precipitation option [[PRC](#)] is turned on. The following is a list of guidelines for file preparation:

1. A separate file is required for each branch. This allows the user to update temperatures for one branch independent of another branch.
2. Input format for each field is F8.0 that allows the user to specify the decimal point location.
3. The first two lines are ignored and can be used to comment the file.
4. The third line contains the variable names which are right justified according to the input field. This line is also ignored although the preprocessor checks to ensure the fields are aligned correctly.
5. The first field is the Julian date that can be entered at any frequency. The frequency between updates may vary during the simulation.
6. The second field is the precipitation temperature, °C.

Example

CE-QUAL-W2 sample precipitation temperature file

JDAY	TPR
1.00	6.80
2.00	6.70
3.00	7.00
4.00	6.30
5.00	6.40
6.00	6.10
7.00	6.60
8.00	5.70
9.00	5.20
10.00	5.40
11.00	7.10
12.00	6.60

Branch Precipitation Concentration File

This file contains the precipitation concentrations for a branch and is needed only if the precipitation option [[PRC](#)] is turned on. The following is a list of guidelines for file preparation:

1. *If* constituents are being modeled, a separate file is required for each branch. This allows the user to update constituent concentrations for one branch independent of another branch.
2. Input format for all fields is F8.0 that allows the user to specify the decimal point location. The number of fields is determined by (6) below and they are always located on one line.
3. The first two lines are ignored and can be used to comment the file.
4. The next line contains the abbreviations for the constituent names that are right justified according to the input field. This line is also ignored although the preprocessor checks to ensure the fields are aligned correctly.
5. The first field is the Julian date that can be entered at any frequency. The frequency between updates may vary during the simulation.
6. The remaining fields contain the concentration for each constituent specified on the [Precipitation Active Constituent Control](#) card. Only those constituents specified as *active* on the [Precipitation Active Constituent Control](#) card may be included in the constituent inflow concentration file. In the following example, only DO has been included.

Example

```
CE-QUAL-W2 constituent precipitation concentration sample input file
```

JDAY	DO
180.000	8.7
190.000	8.2
195.000	8.0
220.000	7.8

Branch External Upstream Head Elevation File

This file contains the elevations for a branch with an [external upstream head boundary condition](#). The following is a list of guidelines for file preparation:

1. A separate file is required for each branch with an external upstream head boundary condition. This allows the user to update elevations for one branch independent of another branch.
2. Input format for each field is F8.0 that allows the user to specify the decimal point location.
3. The first two lines are ignored and can be used to comment the file.
4. The next line contains the variable names which are right justified according to the input field. This line is also ignored although the preprocessor checks to ensure the fields are aligned correctly.
5. The first field is the Julian date that can be entered at any frequency. The frequency between updates may vary during the simulation.
6. The next field is the external head elevation (m above datum specified on the [LOCATION](#) card).

Example

CE-QUAL-W2 sample external head elevation file

JDAY	ELUH
180.000	431.12
180.050	431.15
180.100	431.20
180.150	431.25
180.200	431.30

Branch External Upstream Head Temperature File

This file contains the upstream temperature profiles for a branch with an [external upstream head boundary condition](#). The following is a list of guidelines for file preparation:

1. A separate file is required for each branch. This allows the user to update temperatures for one branch independent of another branch.
2. Input format for each field is F8.0 that allows the user to specify the decimal point location.
3. The first two lines are ignored and can be used to comment the file.
4. The third line contains the variable names which are right justified according to the input field. This line is also ignored although the preprocessor checks to ensure the fields are aligned correctly.
5. The first field is the Julian date that can be entered at any frequency. The frequency between updates may vary during the simulation.
6. The next fields are the upstream boundary temperatures, °C
7. Temperature values must be specified for each cell starting from layer two and extending to the bottom active layer at the upstream segment. If the values do not all fit on one line, then they are continued on the next line with the first field (corresponding to the Julian date field) left blank. The reason why the temperatures must start at layer two is the water surface may vary over many layers during the simulation and it is impossible to know beforehand exactly what time layers will be added or subtracted. When preparing the boundary temperature profiles, it is best to assign boundary temperatures starting from the bottom layer. Once the surface layer has been reached, then use this value to assign values up to layer two. In the following example, the surface layer [KT] starts out at layer six and the bottom is at layer 22. The first four values correspond to layers two through five and must be defined even if they are never used.

Example

CE-QUAL-W2 sample external upstream boundary temperature file

JDAY	TUH								
180.500	19.3	19.3	19.3	19.3	19.3	19.0	18.8	18.7	18.6
	18.4	18.0	17.0	15.0	14.0	13.5	13.2	13.0	12.8
	12.8	12.8	12.8						
187.500	20.3	20.3	20.3	20.3	20.3	20.0	19.8	19.7	19.6
	19.4	19.0	18.0	15.5	14.0	13.5	13.2	13.0	12.8
	12.8	12.8	12.8						

Branch External Upstream Head Constituent Concentration File

This file contains the upstream constituent concentration profiles for a branch with an [external upstream head boundary condition](#). The following is a list of guidelines for file preparation:

1. *If* constituents are being modeled, then a separate file is required for each branch. This allows the user to update temperatures for one branch independent of another branch.
2. Input format for each field is F8.0 that allows the user to specify the decimal point location.
3. The first two lines are ignored and can be used to comment the file.
4. The third line contains the variable names which are right justified according to the input field. This line is also ignored although the preprocessor checks to ensure the fields are aligned correctly.
5. The first field is the Julian date that can be entered at any frequency. The frequency between updates may vary during the simulation.
6. The next fields are the upstream boundary constituent concentrations.
7. Constituents must appear in the same order as they are turned on in the [Active Constituent](#) card. A boundary concentration is *required for each* active constituent.
8. Concentration values must be specified for each cell starting from layer two and extending to the bottom active layer at the upstream segment. If the values do not all fit on one line, then they are continued on the next line with the first field (corresponding to the Julian date field) left blank. The reason why the concentrations must start at layer two is the water surface may vary over many layers during the simulation and it is impossible to know beforehand exactly what time layers will be added or subtracted. When preparing the boundary concentration profiles, it is best to assign concentrations starting from the bottom layer. Once the surface layer has been reached, then use this value to assign values up to layer two. In the following example, the surface layer [KT] starts out at layer six and the bottom is at layer 22. The first four values correspond to layers two through five and must be defined even if they are never used. Salinity and dissolved oxygen are the only values specified as active.

Example

```

CE-QUAL-W2 sample external upstream boundary constituent concentration file
      JDAY      CUH      CUH      CUH      CUH      CUH      CUH      CUH      CUH      CUH
180.000    23.5    23.5    23.5    23.5    23.5    23.9    24.5    25.0    26.0
           27.0    28.0    29.0    29.5    30.0    30.2    30.4    30.6    30.6
           30.6    30.6    30.6    30.6
180.000     9.0     9.0     9.0     9.0     9.0     9.0     9.0     8.8     8.7
           8.6     8.4     8.0     7.5     7.0     6.0     5.5     5.5     5.5
           5.5     5.5     5.5     5.5
190.000    23.5    23.5    23.5    23.5    23.5    23.9    24.5    25.0    26.0
           27.0    28.0    29.0    29.5    30.0    30.2    30.4    30.6    30.6
           30.6    30.6    30.6    30.6
190.000     9.0     9.0     9.0     9.0     9.0     9.0     9.0     8.8     8.7
           8.6     8.4     8.0     7.0     6.0     5.0     5.0     5.0     5.0
           5.0     5.0     5.0     5.0

```

Branch External Downstream Head Elevation File

This file contains the elevations for a branch with an [external downstream head boundary condition](#). The following is a list of guidelines for file preparation:

1. A separate file is required for each branch with an external downstream head boundary condition. This allows the user to update elevations for one branch independent of another branch.
2. Input format for each field is F8.0 that allows the user to specify the decimal point location.
3. The first two lines are ignored and can be used to comment the file.
4. The next line contains the variable names which are right justified according to the input field. This line is also ignored although the preprocessor checks to ensure the fields are aligned correctly.
5. The first field is the Julian date that can be entered at any frequency. The frequency between updates may vary during the simulation.
6. The next field is the external head elevation (m above datum specified on the [Initial Condition](#) card).

Example

CE-QUAL-W2 sample external downstream head elevation file

JDAY	ELUH
180.000	431.12
180.050	431.15
180.100	431.20
180.150	431.25
180.200	431.30

Branch External Downstream Head Temperature File

This file contains the downstream temperature profiles for a branch with an [external downstream head boundary condition](#). The following is a list of guidelines for file preparation:

1. A separate file is required for each branch. This allows the user to update temperatures for one branch independent of another branch.
2. Input format for each field is F8.0 that allows the user to specify the decimal point location.
3. The first two lines are ignored and can be used to comment the file.
4. The third line contains the variable names which are right justified according to the input field. This line is also ignored although the preprocessor checks to ensure the fields are aligned correctly.
5. The first field is the Julian date that can be entered at any frequency. The frequency between updates may vary during the simulation.
6. The next fields are the downstream boundary temperatures, °C
7. Temperature values must be specified for each cell starting from layer two and extending to the bottom active layer at the downstream segment. If the values do not all fit on one line, then they are continued on the next line with the first field (corresponding to the Julian date field) left blank. The reason why the temperatures must start at layer two is the water surface may vary over many layers during the simulation and it is impossible to know beforehand exactly what time layers will be added or subtracted. When preparing the boundary temperature profiles, it is best to assign boundary temperatures starting from the bottom layer. Once the surface layer has been reached, then use this value to assign values up to layer two. In the following example, the surface layer [KT] starts out at layer six and the bottom is at layer 22. The first four values correspond to layers two through five and must be defined even if they are never used.

Example

CE-QUAL-W2 sample external downstream boundary temperature file

JDAY	TUH								
180.500	19.3	19.3	19.3	19.3	19.3	19.0	18.8	18.7	18.6
	18.4	18.0	17.0	15.0	14.0	13.5	13.2	13.0	12.8
	12.8	12.8	12.8						
187.500	20.3	20.3	20.3	20.3	20.3	20.0	19.8	19.7	19.6
	19.4	19.0	18.0	15.5	14.0	13.5	13.2	13.0	12.8
	12.8	12.8	12.8						

Branch External Downstream Head Concentration File

This file contains the downstream constituent concentration profiles for a branch with an [external downstream head boundary condition](#). The following is a list of guidelines for file preparation:

1. A separate file is required for each branch. This allows the user to update temperatures for one branch independent of another branch.
2. Input format for each field is F8.0 that allows the user to specify the decimal point location.
3. The first two lines are ignored and can be used to comment the file.
4. The third line contains the variable names which are right justified according to the input field. This line is also ignored although the preprocessor checks to ensure the fields are aligned correctly.
5. The first field is the Julian date that can be entered at any frequency. The frequency between updates may vary during the simulation.
6. The next fields are the downstream boundary constituent concentrations.
7. Constituents must appear in the same order as they are turned on in the [Active Constituent](#) card. A boundary concentration profile is *required for each* active constituent.
8. Concentration values must be specified for each cell starting from layer two and extending to the bottom active layer at the downstream segment. If the values do not all fit on one line, then they are continued on the next line with the first field (corresponding to the Julian date field) left blank. The reason why the concentrations must start at layer two is the water surface may vary over many layers during the simulation and it is impossible to know beforehand exactly what time layers will be added or subtracted. When preparing the boundary concentration profiles, it is best to assign concentrations starting from the bottom layer. Once the surface layer has been reached, then use this value to assign values up to layer two. In the following example, the surface layer [KT] starts out at layer six and the bottom is at layer 22. The first four values correspond to layers two through five and must be defined even if they are never used. Salinity and dissolved oxygen are the only values specified as active.

Example

```
CE-QUAL-W2 sample external downstream boundary constituent concentration file

      JDAY      CUH      CUH      CUH      CUH      CUH      CUH      CUH      CUH      CUH
180.000  23.5  23.5  23.5  23.5  23.5  23.9  24.5  25.0  26.0
Salinity  27.0  28.0  29.0  29.5  30.0  30.2  30.4  30.6  30.6
          30.6  30.6  30.6  30.6
180.000    9.0    9.0    9.0    9.0    9.0    9.0    9.0    8.8    8.7
Temp      8.6    8.4    8.0    7.5    7.0    6.0    5.5    5.5    5.5
          5.5    5.5    5.5    5.5
190.000  23.5  23.5  23.5  23.5  23.5  23.9  24.5  25.0  26.0
Salinity  27.0  28.0  29.0  29.5  30.0  30.2  30.4  30.6  30.6
          30.6  30.6  30.6  30.6
190.000    9.0    9.0    9.0    9.0    9.0    9.0    9.0    8.8    8.7
Temp      8.6    8.4    8.0    7.0    6.0    5.0    5.0    5.0    5.0
          5.0    5.0    5.0    5.0
```

Vertical Profile File

This file contains a single vertical profile used to specify initial conditions for temperatures and/or constituent concentrations. The vertically varying profile is then used to initialize all segments in the computational grid. This file is most commonly used for vertically stratified waterbodies with no longitudinal gradients. The following is a list of guidelines for file preparation:

1. An initial vertical profile is specified by inputting -1.0 for the initial temperature on the [Initial Conditions](#) card or a constituent's initial concentration on the [Initial Concentration](#) card. If temperature is included, then it *must* be the first profile in the file. Constituent profiles *must* be input in the same order as they are specified on the [Initial Concentration](#) card.
2. Input format for each field is F8.0 that allows the user to specify the decimal point location.
3. The first two lines are ignored and can be used to comment the file.
4. The third line contains in the first field a constituent identifier name to aid in creating and editing the file. The remaining fields contain the variable name which is right justified according to the input field. This line is also ignored although the preprocessor checks to ensure the fields are aligned correctly.
5. The first field is left blank or can be used for comments since it is ignored on input. The remaining fields are used for specifying the temperature or concentration at a given layer. If there are *more* values than can be specified on one line, then they are continued on the next line leaving the first field blank or using it for comments.
6. Values for the vertical profile start at the water surface layer [KT] and stop at the bottom layer. Boundary segments are *not* included in the file.

The following sample input file contains vertically varying initial temperature and dissolved oxygen profiles that correspond to the sample input bathymetry. The surface layer [KT] is located at layer five.

Example

```

CE-QUAL-W2 sample vertical profile initial conditions file

TEMP VPR      T1      T1      T1      T1      T1      T1      T1      T1      T1
15.2    15.0    14.7    14.5    14.3    14.2    11.7     8.5     6.7
6.2      6.0      6.0      6.0      6.0      6.0      6.0      6.0      6.0
6.0      6.0

DO VPR        C1      C1      C1      C1      C1      C1      C1      C1      C1
12.0    12.0    12.0    12.0    11.9    11.9    11.7     8.5     6.7
6.2      6.0      6.0      6.0      6.0      6.0      6.0      6.0      6.0
6.0      6.0
    
```

Longitudinal Profile File

This file contains vertical profiles for each segment used to initialize temperature and/or constituent concentrations for each computational grid cell. It is useful when temperature or a constituent is both vertically and longitudinally stratified where a single value or profile is not representative of the initial conditions. The following is a list of guidelines for file preparation:

1. An initial longitudinal profile input is specified by inputting -2.0 for the initial temperature on the [Initial Conditions](#) card or a constituent's initial concentration on the [Initial Concentration](#) card. If temperature is included, then it *must* be the first series of profiles in the file. Constituent profiles *must* be input in the same order as they are specified on the [Initial Concentration](#) card.
2. Input format for each field is F8.0 that allows the user to specify the decimal point location.
3. The first two lines are ignored and can be used to comment the file.
4. The third line contains in the first field a constituent identifier name to aid in creating and editing the file. The remaining fields contain the variable name which is right justified according to the input field. This line is also ignored although the preprocessor checks to ensure the fields are aligned correctly.
5. The first field is left blank or can be used for comments since it is ignored on input. The remaining fields are used for specifying the temperature or concentration at a given layer. If there are *more* values than can be specified on one line, then they are continued on the next line leaving the first field blank or using it for comments.
6. Values for the vertical profile at each segment start at the water surface layer [KT] and stop at the bottom layer. Boundary segments are *not* included in the file.

The following sample input file includes vertically and longitudinally varying initial conditions for temperature and dissolved oxygen that corresponds to the sample input bathymetry. The surface layer [KT] is located at layer five.

Example

```

CE-QUAL-W2 sample longitudinal profile file
Segment 2
Temperature T1 T1 T1 T1 T1 T1 T1 T1 T1
15.0 14.8 14.5 14.3 14.2 14.1 11.5 8.2 6.5
6.2 6.0 6.0
Segment 3
Temperature T1 T1 T1 T1 T1 T1 T1 T1 T1
15.0 14.8 14.5 14.3 14.2 14.1 11.5 8.2 6.5
6.2 6.0
Segment 4
Temperature T1 T1 T1 T1 T1 T1 T1 T1 T1
15.0 14.8 14.5 14.3 14.2 14.1 11.5 8.2 6.5
6.2
Segment 5
Temperature T1 T1 T1 T1 T1 T1 T1 T1 T1
15.0 14.8 14.5 14.3 14.2 14.1 11.5 8.2 6.5
Segment 6
Temperature T1 T1 T1 T1 T1 T1 T1 T1 T1
15.1 14.9 14.5 14.4 14.2 14.2 11.7 8.5 6.7
6.2 6.0 6.0
Segment 7
Temperature T1 T1 T1 T1 T1 T1 T1 T1 T1
15.1 14.9 14.6 14.4 14.2 14.2 11.7 8.5 6.7

```

LONGITUDINAL PROFILE

INPUT FILES

	6.2	6.0	6.0	6.0	6.0	6.0			
Segment 8									
Temperature	T1	T1	T1						
	15.2	15.0	14.7	14.5	14.3	14.2	11.7	8.5	6.7
	6.2	6.0	6.0	6.0	6.0	6.0	6.0	6.0	6.0
Segment 9									
Temperature	T1	T1	T1						
	15.2	15.0	14.7	14.5	14.3	14.2	11.7	8.5	6.7
	6.2	6.0	6.0	6.0	6.0	6.0	6.0	6.0	6.0
	6.0	6.0							
Segment 12									
Temperature	T1	T1	T1						
	15.5	15.3	14.8	14.5	14.3	14.2	10.6	7.2	
Segment 13									
Temperature	T1	T1	T1						
	15.4	15.2	14.8	14.5	14.3	14.2	10.6	7.2	6.8
	6.2	6.0							
Segment 14									
Temperature	T1	T1	T1						
	15.4	15.2	14.8	14.5	14.3	14.2	10.6	7.2	6.5
	6.2	6.0	6.0	6.0					
Segment 15									
Temperature	T1	T1	T1						
	15.5	15.3	14.8	14.5	14.3	14.2	10.6	7.2	6.4
	6.2	6.0	6.0	6.0	6.0				
Segment 18									
Temperature	T1	T1	T1						
	15.5	15.3	14.8	14.5	14.3	14.2	10.6	7.2	6.4
	6.2	6.0	6.0	6.0	6.0	6.0	6.0	6.0	
Segment 19									
Temperature	T1	T1	T1						
	15.5	15.3	14.8	14.5	14.3	14.2	10.6	7.2	6.4
	6.2	6.0	6.0	6.0	6.0	6.0	6.0	6.0	6.0
	6.0								
Segment 2									
DO	C1	C1	C1						
	12.0	12.0	12.0	12.0	11.9	11.9	11.5	8.2	6.5
	6.2	6.0	6.0						
Segment 3									
DO	C1	C1	C1						
	12.0	12.0	12.0	12.0	11.9	11.9	11.5	8.2	6.5
	6.2	6.0							
Segment 4									
DO	C1	C1	C1						
	12.0	12.0	12.0	12.0	11.9	11.9	11.5	8.2	6.5
	6.2								
Segment 5									
DO	C1	C1	C1						
	12.0	12.0	12.0	12.0	11.9	11.9	11.5	8.3	6.5
	6.2	6.0							
Segment 6									
DO	C1	C1	C1						
	12.0	12.0	12.0	12.0	11.9	11.9	11.6	8.4	6.7
	6.2	6.0	6.0						
Segment 7									
DO	C1	C1	C1						
	12.0	12.0	12.0	12.0	11.9	11.9	11.6	8.5	6.7
	6.2	6.0	6.0	6.0	6.0	6.0			
Segment 8									
DO	C1	C1	C1						
	12.0	12.0	12.0	12.0	11.9	11.9	11.6	8.5	6.7
	6.2	6.0	6.0	6.0	6.0	6.0	6.0	6.0	6.0
Segment 9									
DO	C1	C1	C1						
	12.0	12.0	12.0	12.0	11.9	11.9	11.7	8.5	6.7
	6.2	6.0	6.0	6.0	6.0	6.0	6.0	6.0	6.0
	6.0	6.0							
Segment 12									

INPUT FILES

LONGITUDINAL PROFILE

DO	C1	C1	C1						
	12.0	15.3	14.8	14.5	14.3	14.2	11.7	8.5	
Segment 13									
DO	C1	C1	C1						
	12.0	12.0	12.0	12.0	11.9	11.9	11.7	8.5	6.8
	6.2	6.0							
Segment 14									
DO	C1	C1	C1						
	12.0	12.0	12.0	12.0	11.9	11.9	11.7	8.5	6.5
	6.2	6.0	6.0	6.0					
Segment 15									
DO	C1	C1	C1						
	12.0	12.0	12.0	12.0	11.9	11.9	11.7	8.5	6.4
	6.2	6.0	6.0	6.0	6.0				
Segment 18									
DO	C1	C1	C1						
	12.0	12.0	12.0	12.0	11.9	11.9	11.7	8.5	6.4
	6.2	6.0	6.0	6.0	6.0	6.0	6.0	6.0	
Segment 19									
DO	C1	C1	C1						
	12.0	12.0	12.0	12.0	11.9	11.9	11.7	8.5	6.4
	6.2	6.0	6.0	6.0	6.0	6.0	6.0	6.0	6.0
	6.0								

Graph Input File

The file graph.npt is required for all model simulations of W2 on a PC using the downloadable executable. This file controls the animation using Compaq Visual FORTRAN's Array Viewer as well as output formats and numeric precision of output data.

The first section of the file contains a line for each active constituent defined in the control file. The concentration multiplier [CMULT] is a conversion factor and multiplies the output by the value specified. This is most useful when converting from $g\ m^{-3}$ to $mg\ m^{-3}$ for nutrient values. The concentration minimum [CMIN] and maximum [CMAX] define the limits of the Array Viewer animation scaling. If [CMAX] is set to a negative number, the plots are scaled dynamically. The constituent plot control [CPLTC] turns on the Array Viewer animation for each variable. Note that severe performance degradation can occur depending upon output frequency and number of output windows open.

The second section contains hydraulic variables. The hydrodynamic format [HFMT] specifies the output variable format for the snapshot output file. The hydrodynamic minimum [HMIN] and maximum [HMAX] specify the plotting limits when viewing the output using Array Viewer. The hydrodynamic plot control [HPLTC] specifies whether the animation is turned ON or OFF during the simulation.

The third section contains derived constituent variables. The derived constituent multiplier [CDMULT] can be used to convert the output to units other than $g\ m^{-3}$. The derived constituent minimum [CDMIN] and maximum [CDMAX] concentration specify the plotting limits when viewing the output using Array Viewer. A negative value for [CDMAX] results in automatic scaling of the plot output. The derived constituent plot control [CDPLTC] specifies whether the animation is turned ON or OFF during the simulation.

Example

Hydrodynamic, constituent, and derived constituent names, formats, multipliers, and array viewer controls

.....HNAME.....	FMTH	HMULT	HMIN	HMAX	HPLTC	#
Limiting fimestep [DLTLIM]	(F10.0)	1.0	-1.0	1.0	OFF	1
Horizontal velocity [U], m/s	(F10.3)	1.0	-.1E-6	0.01	OFF	2
Vertical velocity [W], m/s	(F10.3)	1.0	10.0	26.0	OFF	3
Temperature [T1], deg C	(F10.3)	1.0	-1.0	30.0	OFF	4
Density [RHO], g/m ³	(F10.3)	1.0	997.0	1001.0	OFF	5
Vertical eddy viscosity [AZ], m ² /s	(F10.3)	1.0	-1E-08	0.01	OFF	6
Velocity shear stress [SHEAR], 1/s ²	(F10.3)	1.0	-1E-08	0.01	OFF	7
Internal shear [ST], m ³ /s	(F10.3)	1.0	-1E-08	0.01	OFF	8
Bottom shear [SB], m ³ /s	(F10.3)	1.0	-1E-08	0.01	OFF	9
Longitudinal momentum [ADMX], m ³ /s	(F10.3)	1.0	-1E-08	0.01	OFF	10
Longitudinal momentum [DM], m ³ /s	(F10.3)	1.0	-1E-08	0.01	OFF	11
Horizontal density gradient [HDG], m ³ /s	(F10.3)	1.0	-1E-08	0.01	OFF	12
Vertical momentum [ADMZ], m ³ /s	(F10.3)	1.0	-1E-08	0.01	OFF	13
Horizontal pressure gradient [HPG], m ³ /s	(F10.3)	1.0	-1E-08	10.0	OFF	14
Gravity term channel slope [GRAV], m ³ /s	(F10.3)	1.0	0.0	0.0	OFF	15
.....CNAME.....	FMTC	CMULT	CMIN	CMAX	CPLTC	
TDS, g/m ³	(F10.3)	1.0	-1.0	200.0	OFF	1
Age, days	(F10.3)	1.0	-1.0	-1.0	OFF	2
Inorganic suspended solids, g/m ³	(F10.3)	1.0	-20.000	100.0	OFF	3
Phosphate, mg/m ³	(F10.3)	1000.0	-1.0	500.0	OFF	4
Ammonium, mg/m ³	(F10.3)	1000.0	-0.1000	300.0	OFF	5
Nitrate-Nitrite, g/m ³	(F10.3)	1.0	-0.1000	5.0	OFF	

INPUT FILES

GRAPH

Dissolved silica, g/m ³	(F10.3)	1.0	-1.0	10.0	OFF	7
Particulate silica, g/m ³	(F10.3)	1.0	-0.2000	15.0	OFF	8
Total iron, g/m ³	(F10.3)	1.0	-0.1000	2.0	OFF	9
Labile DOM, g/m ³	(F10.3)	1.0	-0.1000	-3.0	OFF	10
Refractory DOM, g/m ³	(F10.3)	1.0	-0.1000	-4.0	OFF	11
Labile POM, g/m ³	(F10.3)	1.0	-0.1000	-3.0	OFF	12
Refractory POM, g/m ³	(F10.3)	1.0	-0.1000	-4.0	OFF	13
CBOD, g/m ³	(F10.3)	1.0	-0.0100	3.0	OFF	14
Algae, g/m ³	(F10.3)	1.0	-0.0100	6.0	OFF	15
Dissolved oxygen, g/m ³	(F10.3)	1.0	-0.0100	-1.0	OFF	16
Inorganic carbon, g/m ³	(F10.3)	1.0	-0.0100	3.0	OFF	17
Alkalinity, g/m ³	(F10.3)	1.0	-0.0100	3.0	OFF	18
.....CDNAME.....	CDMULT	CDMULT	CDMIN	CDMAX	CDPLTC	#
Dissolved organic carbon, g/m ³	(F10.3)	1.0	-1.0	25.0	OFF	1
Particulate organic carbon, g/m ³	(F10.3)	1.0	-1.0	50.0	OFF	2
Total organic carbon, g/m ³	(F10.3)	1.0	-1.0	25.0	OFF	3
Dissolved organic nitrogen, g/m ³	(F10.3)	1.0	-1.0	25.0	OFF	4
Particulate organic nitrogen, g/m ³	(F10.3)	1.0	-1.0	25.0	OFF	5
Total organic nitrogen, g/m ³	(F10.3)	1.0	-1.0	50.0	OFF	6
Total Kheldahl Nitrogen, g/m ³	(F10.3)	1.0	-1.0	15.0	OFF	7
Total nitrogen, g/m ³	(F10.3)	1.0	-1.0	15.0	OFF	8
Dissolved organic phosphorus, mg/m ³	(F10.3)	1000.0	-1.0	25.0	OFF	9
Particulate organic phosphorus, mg/m ³	(F10.3)	1000.0	-1.0	-1.0	OFF	10
Total organic phosphorus, mg/m ³	(F10.3)	1000.0	-1.0	5.0	OFF	11
Total phosphorus, mg/m ³	(F10.3)	1000.0	-1.0	20.0	OFF	12
Algal production, g/m ² /day	(F10.3)	1.0	-1.0	5.0	OFF	13
Chlorophyll a, mg/m ³	(F10.3)	1.0	-5.0	145.0	OFF	14
Total algae, g/m ³	(F10.3)	1.0	-1.0	60.0	OFF	15
Oxygen % Gas Saturation	(F10.3)	1.0	-1.0	50.0	OFF	16
Total suspended Solids, g/m ³	(F10.3)	1.0	-1.0	5.0	OFF	17
Total Inorganic Suspended Solids, g/m ³	(F10.3)	1.0	-1.0	20.0	OFF	18
Carbonaceous Ultimate BOD, g/m ³	(F10.3)	1.0	5.0	9.0	OFF	19
pH	(F10.3)	1.0	-1.0	10.0	OFF	20
Carbon dioxide	(F10.3)	1.0	-1.0	10.0	OFF	21
Bicarbonate	(F10.3)	1.0	-1.0	10.0	OFF	22
Carbonate	(F10.3)	0.0	0.0	0.0	OFF	23

GRAPH

INPUT FILES

Output Files

Snapshot

The snapshot file was designed for output to a hard copy printer and contains useful information that can be utilized during model application. The file can also be pulled into a text editor such as Programmer's File Editor (available for free on the web) and quickly viewed and searched for specific information.

Title Cards

The first lines of output contain the information specified in the **Title Card** for identifying the run plus the date and time that the run occurred. This information will appear everytime output is updated to the file based on the update dates [SNPD] and frequency [SNPF] specified in the control file. Following the title cards is information related to the progress of the run including the output date and timestep information.

EXAMPLE

```

CE-QUAL-W2 V3.1
Burnsville Reservoir - March 15 through December 11, 1992
Density placed inflow, point sink outflows
Default hydraulic coefficients
Default light absorption/extinction coefficients
Default kinetic coefficients
Temperature and water quality simulation
Run 8
Testing sensitivity to wind
Wind sheltering set to 0.75
Jim Stiles and Vince Marchese, USACE Huntington District
Model run at 16:58:03 on 07/22/02

Time Parameters
Gregorian date      [GDAY] =          March 15, 1992
Julian date         [JDAY] =          75 days 12.00 hours
Elapsed time        [ELTMJD] =         0 days 12.00 hours
Timestep            [DLT] =           356 sec
  at location       [KLOC,ILOC] = (26,47)
Minimum timestep    [MINDLT] =         378 sec
  at Julian day     [JDMIN] =          75 days  7.31 hours
  at location       [KMIN,IMIN] = (27,19)
Average timestep    [DLTAV] =          600 sec
Number of iterations [NIT] =           72
Number of violations [NV] =            5

```

Time Parameters

The time parameter information includes the date at which the information was output, the elapsed time of the simulation, and useful information about the timestep and its behavior. This includes the current timestep and where the computational cell is located that was used to determine the current timestep based on numerical stability criterion. The current minimum timestep that has occurred, the date at which it occurred, and the location is also given. The average timestep for the simulation up

to this time, the total number of iterations, and the number of timestep violations that required restoring variables and recomputing the water surface elevations and velocities is also output.

The timestep information can be very useful in providing information that can be analyzed to see where violations are occurring and possibly altering inputs or the bathymetry to increase the average timestep without impacting the results. For example, the location of the minimum timestep can be checked to see if the width can be increased without impacting results. The number of violations provides information as to whether or not the fraction of the computed timestep used needs to be decreased. If the number of violations exceeds 5% of the number of iterations, the fraction of the timestep [DLTF] should be decreased 5-10%.

Meteorological Parameters

The next information includes meteorological parameters used at the current timestep. This can be useful when trying to better understand temperature simulations such as “why is the model overpredicting epilimnetic temperatures on August 14?”. If the equilibrium temperature is > 45 °C and there is no wind, then the model is behaving exactly as the user is telling it to behave. Running sensitivity analyses on meteorological forcing data during this time period can show that the model will reproduce observed data if the forcing data are more accurate.

EXAMPLE

```

Meteorological Parameters
Input
Air temperature      [TAIR] =    0.55 °C
Dewpoint temperature [TDEW] =   -8.59 °C
Wind direction      [PHI] =    4.65 rad
Cloud cover         [CLOUD] =    4.53
Calculated
Equilibrium temperature [ET] =    0.00 °C
Surface heat exchange [CSHE] = 0.00E+00 m/sec
Short wave radiation  [SRO] = 0.14E-03 °C m/sec
    
```

Inflow/Outflow Parameters

Inflows, inflow placement, and inflow temperatures are then output to provide information as to what the model is seeing at all inflow boundaries during the current timestep. This information can be very useful in determining if the model is seeing what the user thinks he has input into the model and should always be checked once at the beginning of the simulation and whenever inflow boundary files are changed during the course of the simulation.

All outflows are also printed out including individual structure outflows, the layer-by-layer outflow computed from the selective withdrawal algorithm, and the total outflow. Again, this is useful to ensure that the model is seeing what the user thinks the model is seeing.

EXAMPLE

```

Inflows
Upstream inflows
Branch 1
Layer      [KQIN] = 23-23
Inflow     [QIN] =   7.13 m^3/sec
Temperature [TIN] =   3.59 °C
Branch 2
    
```

OUTPUT FILES

SNAPSHOT

```
Layer      [KQIN] = 29-29
Inflow     [QIN] = 0.87 m^3/sec
Temperature [TIN] = 5.10 øC
Branch 3
Layer      [KQIN] = 35-35
Inflow     [QIN] = 0.18 m^3/sec
Temperature [TIN] = 5.10 øC
Branch 4
Layer      [KQIN] = 28-28
Inflow     [QIN] = 0.12 m^3/sec
Temperature [TIN] = 5.10 øC
Branch 5
Layer      [KQIN] = 28-28
Inflow     [QIN] = 0.06 m^3/sec
Temperature [TIN] = 5.10 øC
Branch 6
Layer      [KQIN] = 24-24
Inflow     [QIN] = 0.04 m^3/sec
Temperature [TIN] = 5.10 øC

Tributaries
Segment    [ITR] = 24
Layer      [KTWB] = 23-38
Inflow     [QTR] = 0.09
Temperature [TTR] = 5.10

Outflows

Structure outflows [QSTR]
Branch 1 = 12.56 0.00 0.00

Total outflow [QOUT] = 12.56 m^3/s
Outlets
Layer      [KOUT] = 23 24 25 26 27 28 29 30
31 32 33 34 35 36 37 38
Outflow (m^3/sec) [QOUT] = 1.77 1.26 1.18 1.15 1.14 1.12 0.96 0.86
0.79 0.70 0.61 0.51 0.16 0.16 0.14 0.07
```

The final information regarding boundary forcing functions is output next and includes inflow constituent concentrations for all boundary inflows. A great deal of grief can be saved by checking to ensure that the concentrations are correct as it is very easy to get the inflow concentrations out of order.

EXAMPLE

```
Constituent Inflow Concentrations
Branch 1 [CIN]
Dissolved solids = 43.004 g/m^3
Suspended solids1 = 2.000 g/m^3
Phosphate = 0.020 g/m^3
Ammonium = 0.100 g/m^3
Nitrate nitrite = 0.200 g/m^3
Labile DOM = 0.382 g/m^3
Refractory_DOM = 0.892 g/m^3
Labile POM = 0.425 g/m^3
Algae = 0.000 g/m^3
Dissolved oxygen = 12.000 g/m^3
Tributary 1 [CTR]
Dissolved solids = 161.196 g/m^3
Suspended solids1 = 2.000 g/m^3
Phosphate = 0.020 g/m^3
Ammonium = 0.100 g/m^3
Nitrate nitrite = 0.200 g/m^3
Labile DOM = 0.405 g/m^3
Refractory_DOM = 0.945 g/m^3
```

```

Labile POM          = 0.450 g/m^3
Algae               = 0.000 g/m^3
Dissolved oxygen   = 11.980 g/m^3
    
```

Balances

If volume, thermal, and/or constituent mass balances are turned on, then the balances are output next. They are computed for separately for each branch and summed for each waterbody. Information includes the spatially and temporally integrated change in volume since the start of the simulation, the total volume error between the two, and the percent error based on the total volume change. Using the change in volume rather than the total volume is important for preventing roundoff error from masking the results of the balance. The volume balance is computed as:

$$\underbrace{\Delta S}_{\text{spatially integrated volume}} = \underbrace{\sum Q_{in} - \sum Q_{out}}_{\text{temporally integrated volume}}$$

where:

```

ΔS = change in volume, m^3
ΣQin = sum of all inflows, m^3
ΣQout = sum of all outflows, m^3
    
```

Energy and mass balances are computed similarly. Errors should be on the order of 10⁻⁸ to 10⁻¹³ percent, which means that the model is essentially conserving water to machine accuracy. Any model that cannot show this adherence to the fundamental principle of mass balance involved in hydrodynamic and water quality modeling should immediately be suspect. This computation is routinely used to debug and find errors in the code.

EXAMPLE

Water Balance

```

Waterbody 1
  Spatial change [VOLSR] = -0.20089851E+06 m^3
  Temporal change [VOLTR] = -0.20089851E+06 m^3
  Volume error = 0.10186341E-08 m^3
  Percent error = -0.50703913E-12 %
Branch 1
  Spatial change [VOLSBR] = -0.13863158E+06 m^3
  Temporal change [VOLTBR] = -0.13863158E+06 m^3
  Volume error = 0.10768417E-08 m^3
  Percent error = -0.77676510E-12 %
Branch 2
  Spatial change [VOLSBR] = -0.28973777E+05 m^3
  Temporal change [VOLTBR] = -0.28973777E+05 m^3
  Volume error = -0.76397555E-10 m^3
  Percent error = 0.26367827E-12 %
    
```

Energy Balance

```

Waterbody 1
  Spatially integrated energy [ESR] = 0.29332063E+12 kJ
  Temporally integrated energy [ETR] = 0.29332063E+12 kJ
  Energy error = -0.28701192E+01 kJ
  Percent error = -0.97849211E-09 %
Branch 1
  Spatially integrated energy [ESBR] = 0.20810993E+12 kJ
    
```

OUTPUT FILES

SNAPSHOT

```
Temporally integrated energy [ETBR] = 0.20812486E+12 kJ
Energy error                        = 0.79701322E+01 kJ
Percent error                       = 0.38294956E-08 %
Branch 2
Spatially integrated energy [ESBR] = 0.46706347E+11 kJ
Temporally integrated energy [ETBR] = 0.46709696E+11 kJ
Energy error                        = -0.72348511E+01 kJ
Percent error                       = -0.15488971E-07 %
```

Mass Balance

```
Branch 1
Dissolved solids
  Spatially integrated mass [CMBRS] = 0.42683593E+09 g
  Temporally integrated mass [CMBRT] = 0.42683593E+09 g
  Mass error                    = -0.15495062E-01 g
  Percent error                 = -0.36302150E-08 %
Residence time
  Spatially integrated mass [CMBRS] = 0.46090907E+07
  Temporally integrated mass [CMBRT] = 0.46090907E+07
  Mass error                    = -0.14215708E-04
  Percent error                 = -0.30842760E-09 %
Suspended solids1
  Spatially integrated mass [CMBRS] = 0.10093689E+08 g
  Temporally integrated mass [CMBRT] = 0.10093689E+08 g
  Mass error                    = -0.31241588E-03 g
  Percent error                 = -0.30951605E-08 %
Phosphate
  Spatially integrated mass [CMBRS] = 0.17123908E+06 g
  Temporally integrated mass [CMBRT] = 0.17123908E+06 g
  Mass error                    = -0.72119292E-05 g
  Percent error                 = -0.42116142E-08 %
Ammonium
  Spatially integrated mass [CMBRS] = 0.48859061E+06 g
  Temporally integrated mass [CMBRT] = 0.48859061E+06 g
  Mass error                    = -0.20249572E-04 g
  Percent error                 = -0.41444865E-08 %
Nitrate nitrite
  Spatially integrated mass [CMBRS] = 0.18775938E+07 g
  Temporally integrated mass [CMBRT] = 0.18775938E+07 g
  Mass error                    = -0.75169839E-04 g
  Percent error                 = -0.40035198E-08 %
Labile DOM
  Spatially integrated mass [CMBRS] = 0.61793186E+07 g
  Temporally integrated mass [CMBRT] = 0.61793186E+07 g
  Mass error                    = -0.24503283E-03 g
  Percent error                 = -0.39653698E-08 %
Refractory_DOM
  Spatially integrated mass [CMBRS] = 0.14555086E+08 g
  Temporally integrated mass [CMBRT] = 0.14555086E+08 g
  Mass error                    = -0.57210773E-03 g
  Percent error                 = -0.39306379E-08 %
Labile POM
  Spatially integrated mass [CMBRS] = 0.65861106E+07 g
  Temporally integrated mass [CMBRT] = 0.65861106E+07 g
  Mass error                    = -0.26675593E-03 g
  Percent error                 = -0.40502802E-08 %
Algae
  Spatially integrated mass [CMBRS] = 0.57925594E+07 g
  Temporally integrated mass [CMBRT] = 0.57925594E+07 g
  Mass error                    = -0.22346061E-03 g
  Percent error                 = -0.38577180E-08 %
Dissolved oxygen
  Spatially integrated mass [CMBRS] = 0.10224093E+09 g
  Temporally integrated mass [CMBRT] = 0.10224093E+09 g
  Mass error                    = -0.40865839E-02 g
  Percent error                 = -0.39970136E-08 %
Branch 2
```

SNAPSHOT

OUTPUT FILES

```
Dissolved solids
  Spatially integrated mass [CMBRS] = 0.10016615E+09 g
  Temporally integrated mass [CMBRT] = 0.10016615E+09 g
  Mass error = 0.12986526E-01 g
  Percent error = 0.12964984E-07 %
Residence time
  Spatially integrated mass [CMBRS] = 0.10294782E+07
  Temporally integrated mass [CMBRT] = 0.10294782E+07
  Mass error = 0.98625082E-04
  Percent error = 0.95801035E-08 %
Suspended solids1
  Spatially integrated mass [CMBRS] = 0.21809107E+07 g
  Temporally integrated mass [CMBRT] = 0.21809107E+07 g
  Mass error = 0.29512448E-03 g
  Percent error = 0.13532167E-07 %
Phosphate
  Spatially integrated mass [CMBRS] = 0.38423775E+05 g
  Temporally integrated mass [CMBRT] = 0.38423775E+05 g
  Mass error = 0.63260450E-05 g
  Percent error = 0.16463882E-07 %
Ammonium
  Spatially integrated mass [CMBRS] = 0.10661579E+06 g
  Temporally integrated mass [CMBRT] = 0.10661579E+06 g
  Mass error = 0.16890146E-04 g
  Percent error = 0.15842068E-07 %
Nitrate nitrite
  Spatially integrated mass [CMBRS] = 0.41545882E+06 g
  Temporally integrated mass [CMBRT] = 0.41545882E+06 g
  Mass error = 0.67292654E-04 g
  Percent error = 0.16197190E-07 %
Labile DOM
  Spatially integrated mass [CMBRS] = 0.13767130E+07 g
  Temporally integrated mass [CMBRT] = 0.13767130E+07 g
  Mass error = 0.22568717E-03 g
  Percent error = 0.16393189E-07 %
Refractory_DOM
  Spatially integrated mass [CMBRS] = 0.32433662E+07 g
  Temporally integrated mass [CMBRT] = 0.32433662E+07 g
  Mass error = 0.52960077E-03 g
  Percent error = 0.16328738E-07 %
Labile POM
  Spatially integrated mass [CMBRS] = 0.14806668E+07 g
  Temporally integrated mass [CMBRT] = 0.14806668E+07 g
  Mass error = 0.24347263E-03 g
  Percent error = 0.16443445E-07 %
Algae
  Spatially integrated mass [CMBRS] = 0.13063015E+07 g
  Temporally integrated mass [CMBRT] = 0.13063015E+07 g
  Mass error = 0.21586171E-03 g
  Percent error = 0.16524647E-07 %
Dissolved oxygen
  Spatially integrated mass [CMBRS] = 0.22578360E+08 g
  Temporally integrated mass [CMBRT] = 0.22578360E+08 g
  Mass error = 0.36302954E-02 g
  Percent error = 0.16078649E-07 %
```

Geometry

The water surface layer number, elevation at the downstream segment, and the current upstream segment number for each branch are then output. Note that in the example, the current upstream segment is located at segment 8.

EXAMPLE

Geometry

Surface layer [KT] = 23
 Elevation [ELKT] = 238.575 m

Current upstream segment [CUS]
 Branch 1 =8
 Branch 2 =30
 Branch 3 =41
 Branch 4 =46
 Branch 5 =51
 Branch 6 =55

Water Surface

The water surface elevation and the water surface deviation from the top of the water surface layer number is output next. The water surface deviation uses the oceanographic convention in which the deviation downwards from the top of the surface layer is positive. The output includes information only for the segments specified on the [Snapshot Segments](#) card.

EXAMPLE

```

Water Surface, m
      8      9      10      11      12      13      14      15
238.574 238.573 238.574 238.573 238.574 238.574 238.574 238.574

Water Surface Deviation (positive downwards), m
      8      9      10      11      12      13      14      15
-0.2136 -0.2135 -0.2135 -0.2135 -0.2136 -0.2139 -0.2138 -0.2137
    
```

Temperature/Water Quality

The last information available from the snapshot file is information related to hydrodynamics and water quality. The user has complete control of how much information is output including which hydrodynamic and water quality variables are included in the output. The file can rapidly become quite large, so only variables of interest should be output. This information is useful for quickly looking at the results of a run to gain a feel for how the variables of concern are behaving over time. Title cards are printed on each new page for ease in identifying the simulation.

SNAPSHOT

OUTPUT FILES

EXAMPLE

Burnsville Reservoir - March 15 through December 11, 1992
Density placed inflow, point sink outflows
Default hydraulic coefficients
Default light absorption/extinction coefficients
Default kinetic coefficients
Temperature and water quality simulation
Run 8
Testing sensitivity to wind
Wind sheltering set to 0.75
Jim Stiles and Vince Marchese, USACE Huntington District
Model run at 08:25:31 on 07/23/02

March 15, 1992		Julian day = 75 days 12.00 hours											Temperature [T1], deg C
Layer	Depth	8	9	10	11	12	13	14	15	16	17	18	
23	0.41	3.74	3.77	4.19	5.02	5.53	5.62	5.49	5.51	5.50	5.55	5.58	
24	1.13	3.81	3.77	4.19	4.96	5.32	5.43	5.26	5.34	5.29	5.34	5.35	
25	1.74	3.83	3.76	4.19	5.03	5.27	5.31	5.17	5.30	5.23	5.28	5.29	
26	2.35	3.81	3.76	4.19	5.07	5.26	5.22	5.11	5.25	5.19	5.24	5.30	
27	2.96		3.76	4.19	5.08	5.27	5.14	5.05	5.27	5.17	5.24	5.33	
28	3.57		3.76	4.19	5.08	5.26	5.14	5.01	5.29	5.20	5.26	5.31	
29	4.18			4.19	5.11	5.23	5.14	5.01	5.32	5.36	5.31	5.33	
30	4.79			4.19	5.21	5.22	5.14	5.19	5.31	5.35	5.34	5.33	
31	5.40			4.63	5.21	5.22	5.14	5.23	5.31	5.33	5.33	5.32	
32	6.01			5.06	5.32	5.24	5.14	5.24	5.31	5.31	5.31	5.31	
33	6.62			5.31	5.34	5.26	5.14	5.26	5.31	5.30	5.31	5.31	
34	7.23					5.32	5.22	5.30	5.31	5.30	5.30	5.31	
35	7.84							5.33	5.32	5.30	5.29	5.31	
36	8.45									5.30	5.29	5.31	

Time Series

A time series history can be output for any number of cells in the computational grid with output for each cell written to a separate output file. Output is suitable for import into a spreadsheet program for analysis and plotting. The model takes the name of the time series file specified on the [TIME SERIES PLOT FILENAME](#) card and appends an “_x” to the filename where x is 1, 2, 3, etc., depending upon whether the cell is the first, second, third, etc. one specified on the [TIME SERIES SEGMENT](#) card. Title cards are included at the beginning of the output as an aid in identifying the particular model run. Information includes the Julian date, current time step, water surface elevation for the cell’s segment location, temperature, flow through the segment, net short wave solar radiation incident on the water surface (reflection is not included), equilibrium temperature, depth from water surface to channel bottom (m), surface width (m), shade (shade factor multiplied by SRON, if SHADE =1, no shade, if shade =0, no short wave solar reaches the water surface) and active constituent and derived constituent concentrations.

TIME SERIES

OUTPUT FILES

Example

Version 3.1 Spokane R. Model
WB 1 : Sloping branches between State line and Upriver Pool
WB 2 : Pool of Upriver DAM
WB 3 : Pool of Upper Falls Dam
WB 4 : 2 sloping branches above 9-mile dam pool
WB 5 : Nine Mile dam pool
WB 6 : Long Lake
Tom Cole, WES; Scott Wells, PSU; Rob Annear, PSU; Chris Berger, PSU
This one appears to reproduce the late bloom in the uppermost stations

Model run at 13:26:31 on 08/01/03

JDAY	DLT	ELWS	T2	Q	SRON	ET	DEPTH	SUR WIDTH	SHADE	TDS	AGE	TRACER
87.005	354.47	467.99	3.99	0.00	0.00	0.00	45.89	624.10	1.00	0.132E-01	0.485E-02	0.00
87.100	307.25	468.00	3.99	0.00	0.00	0.00	45.90	624.10	1.00	0.163E-01	0.100	0.00
87.200	306.77	468.02	3.98	0.00	0.00	0.00	45.92	624.10	1.00	0.328E-01	0.200	0.00
87.300	306.98	468.02	3.97	0.00	248.37	0.00	45.92	624.10	1.00	0.494E-01	0.300	0.00
87.400	303.82	468.02	4.01	0.00	545.47	0.00	45.92	624.10	1.00	0.675E-01	0.400	0.00
87.500	304.93	468.02	4.57	0.00	604.59	0.00	45.92	624.10	1.00	0.290	0.498	0.00
87.600	306.27	468.02	4.99	0.00	384.22	0.00	45.92	624.10	1.00	0.457	0.598	0.00
87.700	232.79	468.02	4.88	0.00	52.69	0.00	45.92	624.10	1.00	0.536	0.698	0.00
87.800	303.65	468.02	4.54	0.00	0.00	0.00	45.92	624.10	1.00	0.582	0.798	0.00
87.900	305.36	468.02	4.26	0.00	0.00	0.00	45.92	624.10	1.00	0.292	0.898	0.00
88.000	306.51	468.02	4.15	0.00	0.00	0.00	45.92	624.10	1.00	0.215	0.998	0.00
88.100	293.91	468.02	4.07	0.00	0.00	0.00	45.92	624.10	1.00	0.173	1.10	0.00
88.200	205.64	468.02	4.03	0.00	0.00	0.00	45.92	624.10	1.00	0.179	1.20	0.00
88.300	261.97	468.02	4.01	0.00	250.17	0.00	45.92	624.10	1.00	0.190	1.30	0.00
88.400	251.84	468.02	4.05	0.00	549.25	0.00	45.92	624.10	1.00	0.222	1.40	0.00
88.500	220.22	468.03	4.33	0.00	607.58	0.00	45.93	624.10	1.00	0.375	1.50	0.00
88.600	299.69	468.03	4.62	0.00	390.21	0.00	45.93	624.10	1.00	0.552	1.59	0.00
88.700	304.83	468.03	4.58	0.00	61.14	0.00	45.93	624.10	1.00	0.678	1.69	0.00
88.800	306.37	468.03	4.39	0.00	0.00	0.00	45.93	624.10	1.00	0.676	1.79	0.00
88.900	306.17	468.04	4.19	0.00	0.00	0.00	45.94	624.10	1.00	0.502	1.90	0.00
89.000	307.07	468.04	4.05	0.00	0.00	0.00	45.94	624.10	1.00	0.291	2.00	0.00
89.100	303.25	468.04	4.02	0.00	0.00	0.00	45.94	624.10	1.00	0.300	2.10	0.00
89.200	302.38	468.04	3.99	0.00	0.00	0.00	45.94	624.10	1.00	0.310	2.20	0.00
89.300	301.57	468.04	3.98	0.00	255.15	0.00	45.94	624.10	1.00	0.323	2.30	0.00
89.400	299.23	468.04	4.00	0.00	554.97	0.00	45.94	624.10	1.00	0.337	2.40	0.00
89.500	299.37	468.04	4.39	0.00	615.00	0.00	45.94	624.10	1.00	0.543	2.49	0.00
89.600	299.56	468.04	4.79	0.00	396.94	0.00	45.94	624.10	1.00	0.805	2.59	0.00
89.700	298.99	468.04	4.85	0.00	65.43	0.00	45.94	624.10	1.00	1.03	2.68	0.00
89.800	298.82	468.04	4.66	0.00	0.00	0.00	45.94	624.10	1.00	1.21	2.78	0.00
89.900	297.05	468.04	4.37	0.00	0.00	0.00	45.94	624.10	1.00	1.01	2.88	0.00
90.000	299.07	468.04	4.06	0.00	0.00	0.00	45.94	624.10	1.00	0.442	3.00	0.00
90.100	299.01	468.04	4.03	0.00	0.00	0.00	45.94	624.10	1.00	0.453	3.09	0.00
90.200	297.46	468.04	4.01	0.00	0.00	0.00	45.94	624.10	1.00	0.465	3.19	0.00
90.300	295.88	468.04	4.00	0.00	269.99	0.00	45.94	624.10	1.00	0.479	3.29	0.00
90.400	296.40	468.04	4.17	0.00	566.26	0.00	45.94	624.10	1.00	0.581	3.39	0.00
90.500	295.08	468.05	4.67	0.00	620.13	0.00	45.95	624.10	1.00	0.828	3.49	0.00
90.600	293.92	468.05	5.10	0.00	392.06	0.00	45.95	624.10	1.00	1.08	3.58	0.00
90.700	294.41	468.05	5.02	0.00	60.79	0.00	45.95	624.10	1.00	1.15	3.68	0.00

Preprocessor

The preprocessor produces several output files including a file that echoes all control file inputs along with additional information (pre.opt), a warning file that attempts to alert the user to potential problems with inputs (pre.wrn), and an error file that points out serious problems in the input data that will probably prevent the model from running or running correctly. It is important to run the preprocessor periodically to ensure that changes made to various inputs during the course of the project have not introduced problems in the simulation.

Output (pre.opt)

As in nearly all output, the title cards are echoed at the beginning of the output followed by a complete echoing of all control file input. A description of the input, the FORTRAN variable name used in the control file, and the value of the variable are then output. The sequence of output tries to closely follow the sequence of input in the control file, but in some cases is different as certain types of output are more logically grouped together.

The first information includes variables affecting the time of simulation and the timestep for the simulation. Next is information that is used to set initial conditions and variables that are used to control certain calculations in the model.

EXAMPLE

```
Burnsville Reservoir - March 15 through December 11, 1992
Density placed inflow, point sink outflows
Default hydraulic coefficients
Default light absorption/extinction coefficients
Default kinetic coefficients
Temperature and water quality simulation
Run 8
Testing sensitivity to wind
Wind sheltering set to 0.75
Jim Stiles and Vince Marchese, USACE Huntington District
```

```
Time Control
Starting time (Julian day) [TMSTRT] = 75.00
Ending time (Julian day) [TMEND] = 320.00
Year [YEAR] = 1992
# Timestep intervals [NDLT] = 1
Minimum timestep (sec) [DLTMIN] = 1.0
Timestep day (Julian day) [DLTD] = 1.0
Maximum timestep (sec) [DLTMAX] = 1800.0
Fraction of timestep [DLTF] = 0.85
Timestep limitation
Waterbody 1
Vertical eddy viscosity [VISC] = ON
Internal gravity wave [CELC] = ON
```

```
Initial Conditions
Waterbody 1
Temperature [T2I] = Downstream vertical profile
Water type [WTYPEC] = FRESH water
Ice thickness [ICEI] = 0.000 m
```

```
Calculations
Waterbody 1
```

PREPROCESSOR

OUTPUT FILES

```
Evaporation      [EVC] = OFF
Precipitation    [PRC] = OFF
Volume balance   [VBC] = ON
Energy balance   [EBC] = ON
Mass balance     [MBC] = ON
Place inflows    [PQC] = ON
Wind             [WINDC] = ON
Inflow          [QINC] = ON
Outflow         [QOUTC] = ON
Heat exchange    [HEATC] = ON
Heat exchange    [SLHTC] = TERM
Waterbody 1
  read radiation      [SROC] = OFF
  wind function coefficient a [AFW] = 9.20
  wind function coefficient b [BFW] = 0.46
  wind function coefficient c [CFW] = 2.00
  wind height        [WINDH] = 10.00
  Ryan-Harleman evaporation [RHEVC] = OFF
```

The next output includes controls for all input interpolation. These are located at various places in the control file, but are grouped together in the output. These are then followed by meteorological parameters that affect wind and surface heat exchange.

EXAMPLE

Input Interpolations

```
Branch 1
  Inflow          [QINIC] = ON
  Distributed tributary [DTRIC] = OFF
  Head boundary    [HDIC] = OFF
Branch 2
  Inflow          [QINIC] = ON
  Distributed tributary [DTRIC] = OFF
  Head boundary    [HDIC] = OFF
Branch 3
  Inflow          [QINIC] = ON
  Distributed tributary [DTRIC] = OFF
  Head boundary    [HDIC] = OFF
Branch 4
  Inflow          [QINIC] = ON
  Distributed tributary [DTRIC] = OFF
  Head boundary    [HDIC] = OFF
Branch 5
  Inflow          [QINIC] = ON
  Distributed tributary [DTRIC] = OFF
  Head boundary    [HDIC] = OFF
Branch 6
  Inflow          [QINIC] = ON
  Distributed tributary [DTRIC] = OFF
  Head boundary    [HDIC] = OFF
Waterbody 1
  Meteorology     [METIC] = ON
Tributary 1
  [TRIC] = ON
Branch 1
  Structure 1     [STRIC] = ON
  Structure 2     [STRIC] = ON
  Structure 3     [STRIC] = ON
```

Meteorological Parameters

```
Waterbody 1
  Latitude        [LAT] = 38.80
  Longitude       [LONG] = 80.60
Axis orientation
Segment #        2    3    4    5    6    7    8    9    10   11   12   13   14   15
[PHI0] (rads)   1.22 5.22 4.62 0.65 5.67 3.84 5.08 6.27 0.19 5.58 5.32 0.44 0.35 4.54
Segment #       21   22   23   24   25   26   27   28   29   30   31   32   33   34
```

OUTPUT FILES

TIME SERIES

```
[PHI0] (rads)  4.82 0.24 6.16 0.04 0.00 0.00 5.24 5.18 4.14 5.01 4.35 4.00 3.30 5.15
Segment #      40  41  42  43  44  45  46  47  48  49  50  51  52  53
[PHI0] (rads)  6.13 0.35 0.33 0.00 0.00 0.35 6.20 5.64 0.00 0.00 3.51 3.77 3.40 0.00
```

Variables affecting the transport solution and hydraulics are output next along with variables affecting ice cover.

EXAMPLE

Transport Solution

```
Waterbody 1
  Transport [SLTRC] = QUICKEST
  Theta    [THETA] = 0.55
```

Hydraulic coefficients

```
Waterbody 1
  Longitudinal eddy viscosity      [AX] = 1.00 m^2/sec
  Longitudinal eddy diffusivity   [DX] = 1.00 m^2/sec
  Sediment temperature            [TSED] = 11.80 øC
  Coefficient of bottom heat exchange [CBHE] = 0.3 W/m^2/sec
```

Ice cover

```
Waterbody 1
  Ice calculations                [ICEC] = OFF
  Solution                        [SLICEC] = DETAIL
  Albedo                          [ALBEDO] = 0.25
  Ice-water heat exchange         [HWI] = 10.00
  Light absorption                [BETAI] = 0.60
  Light decay                     [GAMMAI] = 0.07
```

Output controls excluding constituents are output next. As in the control file, all constituent related variables are grouped together.

EXAMPLE

Output Control

```
Waterbody 1
  Timestep violations [NVIOL] = OFF
  Horizontal velocity [U], m/s = OFF
  Vertical velocity [W], m/s = OFF
  Temperature [T1], deg C = ON
  Density [RHO], g/m^3 = OFF
  Vertical eddy viscosity [AZ], m^2/s = OFF
  Velocity shear stress [SHEAR], 1/s^2 = OFF
  Internal shear [ST], m^3/s = OFF
  Bottom shear [SB], m^3/s = OFF
  Longitudinal momentum [ADMX], m^3/s = OFF
  Longitudinal momentum [DM], m^3/s = OFF
  Horizontal density gradient [HDG], m^3/s = OFF
  Vertical momentum [ADMZ], m^3/s = OFF
  Horizontal pressure gradient [HPG], m^3/s = OFF
  Gravity term channel slope [GRAV], m^3/s = OFF
Waterbody 1
  Snapshot [SNPC] = ON
  Number of time intervals [NSNP] = 7
  Date (Julian day) [SNPD] = 75.50 139.50 153.50 167.50 195.50 223.60 252.60
  Frequency (days) [SNPF] = 100.00 100.00 100.00 100.00 100.00 100.00 100.00
  Screen [SCRC] = ON
  Number of time intervals [NSCR] = 1
  Date (Julian day) [SCRD] = 75.50
  Frequency (days) [SCRF] = 1.00
  Fluxes [FLXC] = ON
  Number of time intervals [NFLX] = 1
  Date (Julian day) [FLXD] = 77.70
```

PREPROCESSOR

OUTPUT FILES

```
Frequency (days)      [FLXF] = 100.00
Vector plot           [VPLC] = ON
Number of time intervals [NVPL] = 1
Date (Julian day)     [VPLD] = 75.70
Frequency (days)     [VPLF] = 100.00
Profile plot          [PRFC] = ON
Number of time intervals [NPRF] = 7
Number of stations    [NIPRF] = 1
Segment location      [IPRF] = 24
Date (Julian day)     [PRFD] = 75.70 139.50 153.50 167.50 195.50 223.60 252.60
Frequency (days)     [PRFF] = 100.00 100.00 100.00 100.00 100.00 100.00 100.00
Spreadsheet plot [SPRC] = ON
Number of time intervals [NSPR] = 7
Number of stations    [NISPR] = 1
Segment location      [ISPR] = 24
Date (Julian day)     [SPRD] = 75.70 139.50 153.50 167.50 195.50 223.60 252.60
Frequency (days)     [SPRF] = 100.00 100.00 100.00 100.00 100.00 100.00 100.00
Contour plot          [CPLC] = ON
Number of time intervals [NCPL] = 1
Date (Julian day)     [CPLD] = 75.70
Frequency (days)     [CPLF] = 15.00
Time series           [TSRC] = ON
Number of time intervals [NTSR] = 1
Date (Julian day)     [TSRD] = 75.70
Frequency (days)     [TSRF] = 1.00
Restart out           [RSOC] = OFF
Restart in            [RSIC] = OFF
```

Inflow/outflow information is output next.

EXAMPLE

Inflow/Outflow

Selective Withdrawal

Branch	# of structures [NSTR]
1	3
2	0
3	0
4	0
5	0
6	0

Branch 1

Structure	Type	Width (m)	Elevation (m)	Bottom Layer
1	POINT	0.0	237.7	38
2	POINT	0.0	234.7	38
3	LINE	6.1	231.9	38

Number of withdrawals [NWD] = 0

Number of tributaries [NTR] = 1

```
segment number [ITR] = 24
Inflow placement [PTRC] = DISTR
Top elevation [ETTR] = 2.00
Bottom elevation [EBTR] = 38.00
```

Distributed tributaries [DTRC]

```
Branch 1 = OFF
Branch 2 = OFF
Branch 3 = OFF
Branch 4 = OFF
Branch 5 = OFF
Branch 6 = OFF
```

Input and output filenames are then output.

EXAMPLE

Input Filenames

OUTPUT FILES

TIME SERIES

```
Control      = w2_con.npt
Restart     = rsi.npt - not used
Withdrawal  = qwd.npt - not used
Waterbody 1
  Bathymetry      = bth.npt
  Meteorology     = met.npt
  Vertical profile = vpr.npt
  Longitudinal profile = lpr.npt - not used
Branch 1
  Inflow              = qin_brl.npt
  Inflow temperature = tin_brl.npt
  Inflow concentrations = cin_brl.npt
  Outflow             = qot_brl.npt
  Distributed tributary inflows = qin_brl.npt - not used
  Distributed tributary temperatures = tdt_brl.npt - not used
  Distributed tributary concentrations = cdt_brl.npt - not used
  Precipitation       = pre_brl.npt - not used
  Precipitation temperatures = tpr_brl.npt - not used
  Precipitation concentrations = cpr_brl.npt - not used
  Upstream head       = euh_brl.npt - not used
  Upstream head temperatures = tuh_brl.npt - not used
  Upstream head concentrations = cuh_brl.npt - not used
  Downstream head     = edh_brl.npt - not used
  Downstream head temperatures = tdh_brl.npt - not used
  Downstream head concentrations = cdh_brl.npt - not used
Tributary 1
  Inflow              = qtr_tr1.npt
  Inflow temperature = ttr_tr1.npt
  Inflow concentration = ctr_tr1.npt

Output Filenames
Error      = pre.err
Warning    = pre.wrn
Time series = tsr.opt
Withdrawal = wdo.opt
Waterbody 1
  Snapshot   = snp.opt
  Fluxes     = flx.opt
  Profile    = prf.opt
  Vector plot = vpl.opt
  Contour plot = cpl.opt
```

The next section includes all variables affecting water quality simulations including input/output controls, initial concentrations, active constituents, derived variables, kinetic fluxes, and kinetic rates constants.

EXAMPLE

```
Constituents [CCC] = ON
Algal limiting nutrient [LIMC] = OFF
Kinetics update frequency [CUF] = 2
```

Waterbody 1

State Variables

Constituent [CNAME]	Computation [CAC]	Initial Conc [C2IWB,g/m ³]	Fluxes [CFWBC]	Printout [CPRWBC]
Dissolved solids	ON	-1.000	OFF	ON
Residence time	ON	0.000	OFF	OFF
Suspended solids1	ON	-1.000	OFF	ON
Phosphate	ON	0.020	OFF	ON
Ammonium	ON	0.050	OFF	ON
Nitrate nitrite	ON	0.200	OFF	ON
Dissolved silica	OFF	0.000	OFF	OFF
Particulate silica	OFF	0.000	OFF	OFF
Total Iron	OFF	10.000	OFF	OFF
Labile DOM	ON	0.675	OFF	ON

PREPROCESSOR

OUTPUT FILES

Refractory_DOM	ON	1.575	OFF	ON
Labile POM	ON	0.750	OFF	ON
Refractory POM	OFF	0.000	OFF	OFF
Algae	ON	0.650	OFF	ON
Dissolved oxygen	ON	-1.000	OFF	ON
Inorganic carbon	OFF	11.910	OFF	OFF
Alkalinity	OFF	40.000	OFF	OFF
Sediments	OFF	0.000	OFF	OFF

Branch 1

State Variables

Constituent [CNAME]	Inflow [CINBRC]	Distributed trib [CDTBRC]	Precipitation [CPRBRC]
Dissolved solids	ON	OFF	OFF
Residence time	OFF	OFF	OFF
Suspended solids1	ON	OFF	OFF
Phosphate	ON	OFF	OFF
Ammonium	ON	OFF	OFF
Nitrate nitrite	ON	OFF	OFF
Dissolved silica	OFF	OFF	OFF
Particulate silica	OFF	OFF	OFF
Total Iron	OFF	OFF	OFF
Labile DOM	ON	OFF	OFF
Refractory_DOM	ON	OFF	OFF
Labile POM	ON	OFF	OFF
Refractory POM	OFF	OFF	OFF
Algae	ON	OFF	OFF
Dissolved oxygen	ON	OFF	OFF
Inorganic carbon	OFF	OFF	OFF
Alkalinity	OFF	OFF	OFF

Branch 2

State Variables

Constituent [CNAME]	Inflow [CINBRC]	Distributed trib [CDTBRC]	Precipitation [CPRBRC]
Dissolved solids	ON	OFF	OFF
Residence time	OFF	OFF	OFF
Suspended solids1	ON	OFF	OFF
Phosphate	ON	OFF	OFF
Ammonium	ON	OFF	OFF
Nitrate nitrite	ON	OFF	OFF
Dissolved silica	OFF	OFF	OFF
Particulate silica	OFF	OFF	OFF
Total Iron	OFF	OFF	OFF
Labile DOM	ON	OFF	OFF
Refractory_DOM	ON	OFF	OFF
Labile POM	ON	OFF	OFF
Refractory POM	OFF	OFF	OFF
Algae	ON	OFF	OFF
Dissolved oxygen	ON	OFF	OFF
Inorganic carbon	OFF	OFF	OFF
Alkalinity	OFF	OFF	OFF

Branch 3

State Variables

Constituent [CNAME]	Inflow [CINBRC]	Distributed trib [CDTBRC]	Precipitation [CPRBRC]
Dissolved solids	ON	OFF	OFF
Residence time	OFF	OFF	OFF
Suspended solids1	ON	OFF	OFF
Phosphate	ON	OFF	OFF
Ammonium	ON	OFF	OFF
Nitrate nitrite	ON	OFF	OFF
Dissolved silica	OFF	OFF	OFF
Particulate silica	OFF	OFF	OFF
Total Iron	OFF	OFF	OFF
Labile DOM	ON	OFF	OFF
Refractory_DOM	ON	OFF	OFF

OUTPUT FILES

TIME SERIES

Labile POM	ON	OFF	OFF
Refractory POM	OFF	OFF	OFF
Algae	ON	OFF	OFF
Dissolved oxygen	ON	OFF	OFF
Inorganic carbon	OFF	OFF	OFF
Alkalinity	OFF	OFF	OFF

Branch 4

State Variables

Constituent [CNAME]	Inflow [CINBRC]	Distributed trib [CDTBRC]	Precipitation [CPRBRC]
Dissolved solids	ON	OFF	OFF
Residence time	OFF	OFF	OFF
Suspended solids1	ON	OFF	OFF
Phosphate	ON	OFF	OFF
Ammonium	ON	OFF	OFF
Nitrate nitrite	ON	OFF	OFF
Dissolved silica	OFF	OFF	OFF
Particulate silica	OFF	OFF	OFF
Total Iron	OFF	OFF	OFF
Labile DOM	ON	OFF	OFF
Refractory_DOM	ON	OFF	OFF
Labile POM	ON	OFF	OFF
Refractory POM	OFF	OFF	OFF
Algae	ON	OFF	OFF
Dissolved oxygen	ON	OFF	OFF
Inorganic carbon	OFF	OFF	OFF
Alkalinity	OFF	OFF	OFF

Branch 5

State Variables

Constituent [CNAME]	Inflow [CINBRC]	Distributed trib [CDTBRC]	Precipitation [CPRBRC]
Dissolved solids	ON	OFF	OFF
Residence time	OFF	OFF	OFF
Suspended solids1	ON	OFF	OFF
Phosphate	ON	OFF	OFF
Ammonium	ON	OFF	OFF
Nitrate nitrite	ON	OFF	OFF
Dissolved silica	OFF	OFF	OFF
Particulate silica	OFF	OFF	OFF
Total Iron	OFF	OFF	OFF
Labile DOM	ON	OFF	OFF
Refractory_DOM	ON	OFF	OFF
Labile POM	ON	OFF	OFF
Refractory POM	OFF	OFF	OFF
Algae	ON	OFF	OFF
Dissolved oxygen	ON	OFF	OFF
Inorganic carbon	OFF	OFF	OFF
Alkalinity	OFF	OFF	OFF

Branch 6

State Variables

Constituent [CNAME]	Inflow [CINBRC]	Distributed trib [CDTBRC]	Precipitation [CPRBRC]
Dissolved solids	ON	OFF	OFF
Residence time	OFF	OFF	OFF
Suspended solids1	ON	OFF	OFF
Phosphate	ON	OFF	OFF
Ammonium	ON	OFF	OFF
Nitrate nitrite	ON	OFF	OFF
Dissolved silica	OFF	OFF	OFF
Particulate silica	OFF	OFF	OFF
Total Iron	OFF	OFF	OFF
Labile DOM	ON	OFF	OFF
Refractory_DOM	ON	OFF	OFF
Labile POM	ON	OFF	OFF
Refractory POM	OFF	OFF	OFF

PREPROCESSOR

OUTPUT FILES

Algae	ON	OFF	OFF
Dissolved oxygen	ON	OFF	OFF
Inorganic carbon	OFF	OFF	OFF
Alkalinity	OFF	OFF	OFF

Derived Variables

Constituent [CDNAME]	Computation [CDWBC]
Dissolved organic carbon, g/m ³	OFF
Particulate organic carbon, g/m ³	OFF
Total organic carbon, g/m ³	OFF
Dissolved organic nitrogen, g/m ³	OFF
Particulate organic nitrogen, g/m ³	OFF
Total organic nitrogen, g/m ³	OFF
Total nitrogen, g/m ³	OFF
Dissolved organic phosphorus, mg/m ³	OFF
Particulate organic phosphorus, mg/m ³	OFF
Total organic phosphorus, mg/m ³	OFF
Total phosphorus, mg/m ³	OFF
Algal production, g/m ² /day	OFF
Chlorophyll a, mg/m ³	OFF
Total algae, g/m ³	OFF
Oxygen gas saturation, %	OFF
Total suspended solids, g/m ³	OFF
Total inorganic suspended solids, g/m ³	OFF
Total Kheldahl nitrogen, g/m ³	OFF
Carbonaceous ultimate BOD, g/m ³	OFF
pH	OFF
Carbon dioxide, g/m ³	OFF
Bicarbonate, g/m ³	OFF
Carbonate, g/m ³	OFF

Tributary 1

State Variables

Constituent [CNAME]	Inflow [CINTRC]
Dissolved solids	ON
Residence time	OFF
Suspended solids1	ON
Phosphate	ON
Ammonium	ON
Nitrate nitrite	ON
Dissolved silica	OFF
Particulate silica	OFF
Total Iron	OFF
Labile DOM	ON
Refractory_DOM	ON
Labile POM	ON
Refractory POM	OFF
Algae	ON
Dissolved oxygen	ON
Inorganic carbon	OFF
Alkalinity	OFF

Waterbody 1

Constituent Rates

Constituent	Rate/Coefficient
Residence time	Temperature mult [CGQ10] = 0.000
	0-Order Decay [CG0DK] = -1.000/day
	1-Order Decay [CG1DK] = 0.000/day
	Settling [CGS] = 0.000 m/day
Suspended solids	Settling [SSS] = 1.000 m/day
Labile DOM	Decay [LDOMDK] = 0.120 /day
	to refractory [LRDDK] = 0.001 /day
Refractory DOM	Decay [RDOMDK] = 0.001 /day
	to refractory [LRDDK] = 0.001 /day
Labile POM	Decay [LPOMDK] = 0.060 /day
	to refractory [LRPDK] = 0.001 /day
	Settling [POMS] = 0.350 m/day

OUTPUT FILES

TIME SERIES

```

Refractory POM      Decay      [RPOMDK] = 0.010 /day
Algal group 1      Growth      [AG] = 1.100 /day
                  Mortality   [AM] = 0.010 /day
                  Excretion   [AE] = 0.010 /day
                  Respiration [AR] = 0.020 /day
                  Settling    [AS] = 0.140 m/day
                  Org-P      [ALGP] = 0.011
                  Org-N      [ALGN] = 0.080
                  Org-C      [ALGC] = 0.450
                  Org-Si     [ALGSI] = 0.000
                  Chl a/algae ratio [ACHLA] = 65.000 ug/mg
                  Fraction algae to POM [APOM] = 0.80

Phosphorous        Release     [PO4R] = 0.015 g/m^2/day
Ammonium           Decay      [NH4DK] = 0.120 /day
                  Release     [NH4R] = 0.080 g/m^2/day
Nitrate-Nitrite    Decay      [NO3DK] = 0.102 /day
Silica             Decay      [PSIDK] = 0.100 /day
                  Release     [DSIR] = 0.300 g/m^2/day
                  Settling    [PSIS] = 0.100 m/day
Sediment           Decay      [SEDDK] = 0.080 /day
Iron               Settling   [FES] = 2.000 m/day
                  Release     [FER] = 0.500 g/m^2/day
Oxygen             Sediment demand [SOD] = 1.0 1.0 1.0 1.0 1.0 1.0 1.0
                  1.0 1.0 1.0 1.0 1.0 1.0 1.0
                  1.0 1.0 1.0 1.0 1.0 1.0 1.0
                  1.0 1.0 1.0 1.0 1.0 1.0 1.0
                  1.0 1.0 1.0 1.0
SOD fraction       [FSOD] = 1.0
Sediment fraction [FSED] = 1.0

Upper Temperature Bounds
Constituent Rate Upper Max Upper
Ammonium Decay [NH4T1] = 5.0 [NH4T2] = 25.0
Nitrate Decay [NO3T1] = 5.0 [NO3T2] = 25.0
Organic Decay [OMT1] = 4.0 [OMT2] = 20.0
Sediment Decay [SEDT1] = 4.0 [SEDT2] = 20.0
Algal group 1 Growth [AT1] = 10.0 [AT2] = 30.0

Lower Temperature Bounds
Constituent Rate Lower Max Lower
Algal group 1 Growth [AT3] = 35.0 [AT4] = 40.0

Stoichiometric Equivalence
Oxygen
Ammonium [O2NH4] = 4.57
Organic matter [O2OM] = 1.40
Respiration [O2AR] = 1.40
Algal growth [O2AG] = 1.40
Organic Matter
Carbon [BIOC] = 0.450
Phosphorous [BIOP] = 0.011
Nitrogen [BION] = 0.080
Silica [BIOSI] = 0.180

Half Saturation
Algal group 1
Phosphorous [AHSP] = 0.009 g/m^3
Nitrogen [AHSN] = 0.014 g/m^3
Silica [AHSSI] = 0.000 g/m^3

Light
Attenuation
Surface layer [BETA] = 0.45
Water [EXH2O] = 0.55 /m
Inorganic solids [EXSS] = 0.01 /m
Organic solids [EXOM] = 0.01 /m
Algal group 1 [EXA] = 0.20 /m
Saturation Intensity
Algal group 1 [ASAT] = 150.0 W/m^2

Diffusion
Oxygen [DMO2] = 2.040E-09 m^2/g
Carbon dioxide [DMCO2] = 1.630E-09 m^2/g

```

PREPROCESSOR

OUTPUT FILES

```
Partitioning Coefficients
  Phosphorous [PARTP] = 1.200 m^3/g
  Silica      [PARTSI] = 0.200 m^3/g
Miscellaneous Constants
  Aerobic oxygen limit      [O2LIM] = 0.20 g/m^3
  CO2 sediment release     [CO2R] = 0.10 g/m^2/day
```

The next section contains summary statistics regarding inflows and inflow constituent concentrations. This is useful for screening time-varying input files if the user has not already plotted up and screened them.

EXAMPLE

```
Water Balance Summary
Waterbody 1
  total inflows      total outflows
  average maximum   average maximum
  6.22  124.38      6.25  38.19

Branch 1
  Inflows
    total
    average maximum
    5.29  124.38
    upstream      tributaries      distributed tributaries      precipitation
    average maximum average maximum   average maximum   average maximum
    5.22  124.38   0.07  1.60           0.00  0.00           0.00  0.00
  Outflows
    outlets      withdrawals
    average maximum average maximum   average maximum
    6.25  38.19   0.00  0.00

Inflow Constituent Statistics
Branch 1
  Constituent name      Average      Maximum      Minimum
  Dissolved solids      49.576      99.000      10.000
  Suspended solids1     4.467      156.000     2.000
  Phosphate              0.020      0.020      0.020
  Ammonium               0.100      0.100      0.100
  Nitrate nitrite       0.200      0.200      0.200
  Labile DOM             0.382      0.382      0.382
  Refractory_DOM        0.892      0.892      0.892
  Labile POM             0.425      0.425      0.425
  Algae                  0.000      0.000      0.000
  Dissolved oxygen       9.851      14.000     0.000
```

Geometric information follows including all information in the control and bathymetry file along with a computed area-volume-elevation table that also includes average width and depth. Theoretical hydraulic residence at each elevation is also included if the waterbody is a reservoir. The location of the surface layer is indicated by a [KT] next to the layer number. The computational grid showing cell widths is then output.

EXAMPLE

```
Geometry
Overall Grid
  Total
  segments [IMX] = 58
  layers   [KMX] = 39
  branches [NBR] = 6

Waterbody 1
  Segments = 1-58
```

OUTPUT FILES

TIME SERIES

```

Branches = 1-6
Bottom elevation [ELBOT] = 228.60 m
Surface layer [KT] = 23
Vertical spacing [H]
  Layer      1    2    3    4    5    6    7    8    9   10  11  12  13  14
            15  16  17  18  19
  Height (m) 0.6 0.6 0.6 0.6 0.6 0.6 0.6 0.6 0.6 0.6 0.6 0.6 0.6 0.6
            0.6 0.6 0.6 0.6 0.6
  Layer      20   21   22   23   24   25   26   27   28   29   30   31   32   33
            34   35   36   37   38
  Height (m) 0.6 0.6 0.6 0.6 0.6 0.6 0.6 0.6 0.6 0.6 0.6 0.6 0.6 0.6
            0.6 0.6 0.6 0.6 0.6
  Layer      39
  Height (m) 0.6

Branch 1
  Upstream segment [US] = 2      Downstream segment [DS] = 24
  Upstream head segment [UHS] = 0  Downstream head segment [DHS] = 0

Branch 2
  Upstream segment [US] = 27     Downstream segment [DS] = 36
  Upstream head segment [UHS] = 0 Downstream head segment [DHS] = 19

Branch 3
  Upstream segment [US] = 39     Downstream segment [DS] = 42
  Upstream head segment [UHS] = 0 Downstream head segment [DHS] = 17

Branch 4
  Upstream segment [US] = 45     Downstream segment [DS] = 47
  Upstream head segment [UHS] = 0 Downstream head segment [DHS] = 21

Branch 5
  Upstream segment [US] = 50     Downstream segment [DS] = 52
  Upstream head segment [UHS] = 0 Downstream head segment [DHS] = 36

Branch 6
  Upstream segment [US] = 55     Downstream segment [DS] = 57
  Upstream head segment [UHS] = 0 Downstream head segment [DHS] = 32

```

Initial Branch Volume [VOLB] = 9495622.2 m³

Branch 1 Volume-Area-Elevation Table

Layer	Elevation (m)	Area (1.0E6 m ²)	Volume (1.0E6 m ³)	Active Cells	Average depth (m)	Average width (m)
2	251.17	5.171	58.316	630	11.3	262.48
3	250.56	5.002	55.162	607	11.0	253.90
4	249.95	4.923	52.111	584	10.6	249.88
5	249.34	4.828	49.108	563	10.2	245.09
6	248.73	4.706	46.163	542	9.8	238.89
7	248.12	4.624	43.292	521	9.4	234.74
8	247.51	4.522	40.471	500	9.0	229.52
9	246.90	4.350	37.713	479	8.7	220.84
10	246.29	4.191	35.059	458	8.4	212.73
11	245.68	4.059	32.503	437	8.0	206.02
12	245.07	3.835	30.027	417	7.8	194.70
13	244.46	3.661	27.688	397	7.6	185.86
14	243.85	3.570	25.454	378	7.1	181.21
15	243.24	3.476	23.277	359	6.7	176.45
16	242.63	3.363	21.156	341	6.3	170.73
17	242.02	3.083	19.104	323	6.2	156.48
18	241.41	2.972	17.224	305	5.8	150.88
19	240.80	2.878	15.411	287	5.4	146.07
20	240.19	2.777	13.655	269	4.9	140.96
21	239.58	2.626	11.962	251	4.6	133.29
22	238.97	2.485	10.360	233	4.2	126.14
23 KT	238.36	2.413	8.844	216	3.7	122.50
24	237.75	2.282	7.372	199	3.2	115.85
25	237.14	1.927	5.980	182	3.1	97.83
26	236.53	1.716	4.804	165	2.8	87.12
27	235.92	1.290	3.757	148	2.9	65.48
28	235.31	1.150	2.970	132	2.6	58.38
29	234.70	0.995	2.269	116	2.3	50.52

PREPROCESSOR

OUTPUT FILES

30	234.09	0.839	1.662	101	2.0	42.61
31	233.48	0.595	1.150	86	1.9	30.19
32	232.87	0.410	0.787	71	1.9	20.84
33	232.26	0.306	0.536	56	1.8	15.51
34	231.65	0.225	0.350	41	1.6	11.41
35	231.04	0.145	0.213	28	1.5	7.34
36	230.43	0.106	0.125	17	1.2	5.39
37	229.82	0.074	0.060	8	0.8	3.76
38	229.21	0.024	0.015	3	0.6	1.23

Initial Branch Volume [VOLB] = 2111233.1 m³

Branch 2 Volume-Area-Elevation Table

Layer	Elevation (m)	Area (1.0E6 m ²)	Volume (1.0E6 m ³)	Active Cells	Average depth (m)	Average width (m)
2	251.17	1.253	13.852	270	11.1	166.71
3	250.56	1.224	13.088	260	10.7	162.83
4	249.95	1.202	12.341	250	10.3	159.89
5	249.34	1.179	11.608	240	9.8	156.87
6	248.73	1.155	10.889	230	9.4	153.75
7	248.12	1.133	10.185	220	9.0	150.82
8	247.51	1.104	9.493	210	8.6	146.96
9	246.90	1.082	8.819	200	8.2	143.99
10	246.29	1.046	8.159	190	7.8	139.25
11	245.68	1.014	7.521	180	7.4	134.98
12	245.07	0.987	6.902	170	7.0	131.38
13	244.46	0.957	6.300	160	6.6	127.41
14	243.85	0.926	5.716	150	6.2	123.22
15	243.24	0.834	5.151	140	6.2	110.92
16	242.63	0.778	4.643	130	6.0	103.53
17	242.02	0.701	4.168	120	5.9	93.34
18	241.41	0.656	3.740	110	5.7	87.24
19	240.80	0.595	3.340	100	5.6	79.21
20	240.19	0.566	2.977	92	5.3	75.36
21	239.58	0.548	2.632	84	4.8	72.89
22	238.97	0.534	2.298	76	4.3	71.10
23 KT	238.36	0.517	1.972	68	3.8	68.81
24	237.75	0.488	1.656	60	3.4	64.89
25	237.14	0.471	1.359	53	2.9	62.69
26	236.53	0.447	1.071	46	2.4	59.53
27	235.92	0.370	0.798	39	2.2	49.26
28	235.31	0.339	0.573	32	1.7	45.10
29	234.70	0.216	0.366	25	1.7	28.68
30	234.09	0.153	0.234	18	1.5	20.31
31	233.48	0.094	0.141	14	1.5	12.52
32	232.87	0.074	0.084	10	1.1	9.82
33	232.26	0.035	0.039	7	1.1	4.61
34	231.65	0.024	0.018	4	0.7	3.18
35	231.04	0.005	0.003	1	0.6	0.69
36	230.43	0.000	0.000	0	0.0	0.00
37	229.82	0.000	0.000	0	0.0	0.00
38	229.21	0.000	0.000	0	0.0	0.00

OUTPUT FILES

PREPROCESSOR

Waterbody 1 Bathymetry [B], m

	2	3	4	5	6	7	8	9	10	11	12
	19162	18000	16925	15787	14762	13925	13100	12337	11400	10400	9410
1	0.	0.	0.	0.	0.	0.	0.	0.	0.	0.	0.
2	23.	23.	59.	169.	169.	169.	137.	136.	216.	216.	442.
3	10.	14.	58.	168.	168.	168.	134.	131.	213.	213.	402.
4	0.	0.	56.	166.	166.	166.	130.	130.	212.	212.	401.
5	0.	0.	55.	163.	163.	163.	126.	126.	204.	204.	393.
6	0.	0.	52.	148.	148.	148.	123.	123.	201.	201.	387.
7	0.	0.	50.	140.	143.	143.	122.	120.	198.	198.	381.
8	0.	0.	33.	133.	140.	140.	119.	116.	195.	195.	378.
9	0.	0.	28.	128.	133.	133.	116.	113.	192.	192.	332.
10	0.	0.	26.	93.	131.	131.	114.	110.	187.	187.	320.
11	0.	0.	0.	73.	128.	128.	111.	105.	183.	183.	314.
12	0.	0.	0.	36.	93.	123.	108.	102.	180.	180.	277.
13	0.	0.	0.	0.	73.	120.	98.	98.	175.	175.	259.
14	0.	0.	0.	0.	36.	119.	96.	96.	172.	172.	256.
15	0.	0.	0.	0.	0.	119.	94.	94.	171.	171.	250.
16	0.	0.	0.	0.	0.	116.	93.	93.	168.	168.	219.
17	0.	0.	0.	0.	0.	111.	91.	81.	98.	98.	189.
18	0.	0.	0.	0.	0.	101.	90.	78.	85.	85.	186.
19	0.	0.	0.	0.	0.	93.	88.	73.	75.	75.	180.
20	0.	0.	0.	0.	0.	73.	84.	69.	64.	64.	177.
21	0.	0.	0.	0.	0.	36.	40.	67.	53.	53.	174.
22	0.	0.	0.	0.	0.	0.	32.	62.	46.	46.	155.
23 KT	0.	0.	0.	0.	0.	0.	30.	52.	43.	43.	152.
24	0.	0.	0.	0.	0.	0.	27.	49.	41.	41.	131.
25	0.	0.	0.	0.	0.	0.	16.	43.	37.	37.	125.
26	0.	0.	0.	0.	0.	0.	6.	24.	34.	34.	122.
27	0.	0.	0.	0.	0.	0.	0.	23.	30.	30.	37.
28	0.	0.	0.	0.	0.	0.	0.	18.	26.	26.	27.
29	0.	0.	0.	0.	0.	0.	0.	0.	20.	20.	18.
30	0.	0.	0.	0.	0.	0.	0.	0.	17.	17.	15.
31	0.	0.	0.	0.	0.	0.	0.	0.	15.	15.	12.
32	0.	0.	0.	0.	0.	0.	0.	0.	13.	13.	11.
33	0.	0.	0.	0.	0.	0.	0.	0.	10.	10.	9.
34	0.	0.	0.	0.	0.	0.	0.	0.	0.	0.	6.
35	0.	0.	0.	0.	0.	0.	0.	0.	0.	0.	0.
36	0.	0.	0.	0.	0.	0.	0.	0.	0.	0.	0.
37	0.	0.	0.	0.	0.	0.	0.	0.	0.	0.	0.
38	0.	0.	0.	0.	0.	0.	0.	0.	0.	0.	0.
39	0.	0.	0.	0.	0.	0.	0.	0.	0.	0.	0.

PREPROCESSOR

OUTPUT FILES

Finally, initial conditions for the water surface deviation, temperature, and constituent concentrations are output. The user should check these to ensure that the initial concentrations are correct, particularly when using the vertical and/or longitudinal profile files to set initial conditions. Inactive segments are output to ensure the user realizes that the initial water surface has caused upstream segments to be subtracted. The example illustrates this.

OUTPUT FILES

PREPROCESSOR

EXAMPLE

```
Water Surface [Z],
      2      3      4      5      6      7      8      9      10     11     12     13
    -0.2700 -0.2700 -0.2700 -0.2700 -0.2700 -0.2700 -0.2700 -0.2700 -0.2700 -0.2700 -0.2700 -0.2700

Temperature [T1], deg C
      2      3      4      5      6      7      8      9      10     11     12     13
23      5.500  5.500  5.500  5.500  5.500  5.500  5.500  5.500  5.500  5.500  5.500
24      5.500  5.500  5.500  5.500  5.500  5.500  5.500  5.500  5.500  5.500  5.500
25      5.500  5.500  5.500  5.500  5.500  5.500  5.500  5.500  5.500  5.500  5.500
26      5.400  5.400  5.400  5.400  5.400  5.400  5.400  5.400  5.400  5.400  5.400
27      5.400  5.400  5.400  5.400  5.400  5.400  5.400  5.400  5.400  5.400  5.400
28      5.500  5.500  5.500  5.500  5.500  5.500  5.500  5.500  5.500  5.500  5.500
29      5.400  5.400  5.400  5.400  5.400  5.400  5.400  5.400  5.400  5.400  5.400
30      5.300  5.300  5.300  5.300  5.300  5.300  5.300  5.300  5.300  5.300  5.300
31      5.300  5.300  5.300  5.300  5.300  5.300  5.300  5.300  5.300  5.300  5.300
32      5.400  5.400  5.400  5.400  5.400  5.400  5.400  5.400  5.400  5.400  5.400
33      5.300  5.300  5.300  5.300  5.300  5.300  5.300  5.300  5.300  5.300  5.300
34      5.200  5.200
```

Warning Messages (pre.wrn)

The preprocessor does an extensive check of inputs in order to determine if inputs “make sense”. For many cases, it is easy to determine if the input is valid or not. For these cases, information is written to the error output file (pre.err) if the information is invalid. For instance, an algal growth rate that is less than the respiration rate. However, because the model is so flexible, certain inputs are not necessarily errors, but should be flagged so that the user can check to ensure that what they have input is indeed what they mean to be doing. Additionally, when kinetic rates differ from valid ranges or a specific value that should not normally be changed, a warning message is also generated.

For example, the preprocessor warns the user that certain active constituents are given a zero initial concentration, are not included in branch inflows, or a number of other things that are okay to do, but need to be checked to see if this is what the user really wants to do. This is entirely analogous to a FORTRAN compiler that will issue warning and error messages. Warning messages are meant to alert the user to potential problems. Error messages are meant to alert the user that they cannot continue until the problem is fixed.

All warning messages include a concise statement in English what the problem is. Also included is the FORTRAN variable name as it appears in the input file header along with its value where appropriate. This is illustrated in the following example.

EXAMPLE

```
Epiphyton excretion rate [EE=0.000] < 0.001 for epiphyton group 1
Oxygen to algal respiration stoichiometry [O2AR=1.400] /= 1.1 for waterbody 1
Phosphorus/organic matter stoichiometry [ORGP=0.011] /= 0.005 for waterbody 1
Water surface elevation is below bottom elevation at segment 1
Water surface elevation is below bottom elevation at segment 2
Water surface elevation is below bottom elevation at segment 3
Water surface elevation is below bottom elevation at segment 4
Water surface elevation is below bottom elevation at segment 5
Water surface elevation is below bottom elevation at segment 6
Water surface elevation is below bottom elevation at segment 7
Water surface elevation is below bottom elevation at segment 26
Water surface elevation is below bottom elevation at segment 27
Water surface elevation is below bottom elevation at segment 28
Water surface elevation is below bottom elevation at segment 44
Water surface elevation is below bottom elevation at segment 45
Water surface elevation is below bottom elevation at segment 49
Water surface elevation is below bottom elevation at segment 50
```

In the above example, the user is warned that the epiphyton excretion rate is less than the recommended minimum value. Likewise, the stoichiometric relationships are flagged as these should not be changed from their default values unless the user has data that indicates a different stoichiometry. The remaining warning messages inform the user that part of the system is dry based on the given initial water surface elevation.

A very important point – the user should not assume that because there are no warnings generated that there are no problems with inputs. It is not possible to check all possible combinations of inputs, so there may be problems that were not flagged.

OUTPUT FILES

PREPROCESSOR ERRORS

Error Messages (pre.err)

Input errors that will prevent the model from running correctly or running at all are extensively screened and, when found, are included in the preprocessor error output file. All error messages include a concise statement in English what the problem is along with the FORTRAN variable name as it appears in the input file header and its input value where appropriate. This is illustrated in the following example.

EXAMPLE

```
Starting time [TMSTRT=75.000] < ending time [TMEND=-320.000]
Timestep fraction [DLTF(1)=-0.850] <= 0.0
Internal gravity wave limitation control [CELC= on] /= " ON" or "OFF" for waterbody 1
Heat exchange solution control [SLHTC= term] /= " TERM" or " ET" for waterbody 1
Vertical advection time weighting [THETA=-0.550] < 0.0 for waterbody 1
Selective withdrawal elevation [ESTR=137.700] < the bottom active cell elevation
```

Spreadsheet Plot

The spreadsheet output was designed to be easily imported into a spreadsheet program for plotting vertical profiles of temperature, constituents, and derived constituents. Output consists of the variable name, Julian date, depth below water surface, elevation, and temperature and/or concentrations for the output segment. Additional segments each contain a depth, elevation, and temperature/concentration column and are continued to the right.

EXAMPLE

Constituent	Julian_day	Depth	Elevation	Seg_24
Temperature	75.703	-0.403	238.152	6.04
Temperature	75.703	-1.110	237.444	5.86
Temperature	75.703	-1.720	236.834	5.65
Temperature	75.703	-2.330	236.224	5.50
Temperature	75.703	-2.940	235.614	5.41
Temperature	75.703	-3.550	235.004	5.34
Temperature	75.703	-4.160	234.394	5.30
Temperature	75.703	-4.770	233.784	5.28
Temperature	75.703	-5.380	233.174	5.31
Temperature	75.703	-5.990	232.564	5.34
Temperature	75.703	-6.600	231.954	5.33
Temperature	75.703	-7.210	231.344	5.32
Temperature	75.703	-7.820	230.734	5.31
Temperature	75.703	-8.430	230.124	5.31
Temperature	75.703	-9.040	229.514	5.31
Temperature	75.703	-9.650	228.904	5.31
Dissolved solids, g/m ³	75.703	-0.403	238.152	0.42E+02
Dissolved solids, g/m ³	75.703	-1.110	237.444	0.42E+02
Dissolved solids, g/m ³	75.703	-1.720	236.834	0.42E+02
Dissolved solids, g/m ³	75.703	-2.330	236.224	0.42E+02
Dissolved solids, g/m ³	75.703	-2.940	235.614	0.42E+02
Dissolved solids, g/m ³	75.703	-3.550	235.004	0.42E+02
Dissolved solids, g/m ³	75.703	-4.160	234.394	0.42E+02
Dissolved solids, g/m ³	75.703	-4.770	233.784	0.42E+02
Dissolved solids, g/m ³	75.703	-5.380	233.174	0.47E+02
Dissolved solids, g/m ³	75.703	-5.990	232.564	0.56E+02
Dissolved solids, g/m ³	75.703	-6.600	231.954	0.61E+02
Dissolved solids, g/m ³	75.703	-7.210	231.344	0.62E+02
Dissolved solids, g/m ³	75.703	-7.820	230.734	0.62E+02
Dissolved solids, g/m ³	75.703	-8.430	230.124	0.62E+02
Dissolved solids, g/m ³	75.703	-9.040	229.514	0.62E+02
Dissolved solids, g/m ³	75.703	-9.650	228.904	0.62E+02
Suspended solids1, g/m ³	75.703	-0.403	238.152	0.60E+00
Suspended solids1, g/m ³	75.703	-1.110	237.444	0.76E+00
Suspended solids1, g/m ³	75.703	-1.720	236.834	0.83E+00
Suspended solids1, g/m ³	75.703	-2.330	236.224	0.86E+00
Suspended solids1, g/m ³	75.703	-2.940	235.614	0.87E+00
Suspended solids1, g/m ³	75.703	-3.550	235.004	0.88E+00
Suspended solids1, g/m ³	75.703	-4.160	234.394	0.88E+00
Suspended solids1, g/m ³	75.703	-4.770	233.784	0.86E+00
Suspended solids1, g/m ³	75.703	-5.380	233.174	0.90E+00
Suspended solids1, g/m ³	75.703	-5.990	232.564	0.14E+01
Suspended solids1, g/m ³	75.703	-6.600	231.954	0.22E+01
Suspended solids1, g/m ³	75.703	-7.210	231.344	0.28E+01
Suspended solids1, g/m ³	75.703	-7.820	230.734	0.29E+01
Suspended solids1, g/m ³	75.703	-8.430	230.124	0.30E+01
Suspended solids1, g/m ³	75.703	-9.040	229.514	0.30E+01
Suspended solids1, g/m ³	75.703	-9.650	228.904	0.30E+01

Profile Plot

The profile plot output file was originally developed to provide data for a plotting package from Computer Associates called DISSPLA. This was a popular set of FORTRAN callable subroutines developed back in the 1970's for visualizing scientific computing. The vertical temperature plots with statistics presented in Chapter 3 were produced using a DISSPLA compatible software package developed for the PC. If the user should decide to develop their own plotting program, then the following describes the information located in the [profile plot output file](#).

As in most other output files, the card titles are included for identifying the run prior to plotting and also for including information about the run on the plot.

```
Burnsville Reservoir - March 15 through December 11, 1992
Density placed inflow, point sink outflows
Default hydraulic coefficients
Default light absorption/extinction coefficients
Default kinetic coefficients
Temperature and water quality simulation
Run 8
Testing sensitivity to wind
Wind sheltering set to 0.75
Jim Stiles and Vince Marchese, USACE Huntington District
Model run at 13:18:39 on 07/23/02
```

The next line reports:

1. maximum number of layers [KMX]
2. number of segments for which information is output [NIPRF]
3. total number of output dates [NDSP]
4. total number of constituents regardless of whether they are included in the simulations [NCT]
5. total number of derived constituents regardless of whether they are included in the output [NDC]
6. pointer to the profile date currently in effect [\[PRFDP\]](#)
7. waterbody surface layer [KTWB]
8. logical variable that is T if constituents are simulated, otherwise F

```
39      1      3      17      23      12      1      23 T
```

The next line reports the segment(s) output [\[IPRF\]](#):

```
18      24
```

The next three lines report which constituents are active:

```
ON ON OFF ON ON ON ON OFF OFF OFF ON ON ON OFF ON ON OFF OFF OFF OFF
OFF OFF OFF OFF OFF OFF OFF OFF OFF OFF OFF OFF OFF OFF OFF OFF OFF
OFF
```

Constituent and derived constituent names are included in the next 21 lines:

```
Temperature, °C          Dissolved solids, g/m^3
Residence time, days    Suspended solids1, g/m^3
Phosphate, mg/m^3       Ammonium, mg/m^3
```

PROFILE PLOT

OUTPUT FILES

```

Nitrate nitrite, g/m^3      Dissolved silica, g/m^3
Particulate silica, g/m^3  Total Iron, g/m^3
Labile DOM, g/m^3          Refractory_DOM, g/m^3
Labile POM, g/m^3          Refractory POM, g/m^3
Algae, g/m^3               Dissolved oxygen, g/m^3
Inorganic carbon, g/m^3   Alkalinity, g/m^3
Dissolved organic carbon, g/m^3  Particulate organic carbon, g/m^3
Total organic carbon, g/m^3      Dissolved organic nitrogen, g/m^3
Particulate organic nitrogen, g/m^3  Total organic nitrogen, g/m^3
Total nitrogen, g/m^3           Dissolved organic phosphorus, mg/m^3
Particulate organic phosphorus, mg/m^3  Total organic phosphorus, mg/m^3
Total phosphorus, mg/m^3        Algal production, g/m^2/day
Chlorophyll a, mg/m^3           Total algae, g/m^3
Oxygen gas saturation, %        Total suspended solids, g/m^3
Total inorganic suspended solids, g/m^3  Total Kheldahl nitrogen, g/m^3
Carbonaceous ultimate BOD, g/m^3        pH
Carbon dioxide, g/m^3            Bicarbonate, g/m^3
Carbonate, g/m^3

```

The constituent and derived constituent numbers follow on the next line. Temperature is always considered constituent 1 and derived constituents continue increasing from the last constituent number.

```

1  2  3  4  5  6  7  11  12  13  15  16

```

The bottom active layer for each output segment is given on the next line.

```

36  38

```

Layer heights for layers 1 through the maximum [KMX] are output next.

```

0.61  0.61  0.61  0.61  0.61  0.61  0.61  0.61  0.61  0.61
0.61  0.61  0.61  0.61  0.61  0.61  0.61  0.61  0.61  0.61
0.61  0.61  0.61  0.61  0.61  0.61  0.61  0.61  0.61  0.61
0.61  0.61  0.61  0.61  0.61  0.61  0.61  0.61  0.61  0.61

```

Initial temperatures/constituent concentrations for each segment specified in the profile segment card are then output. Initial temperatures/constituent concentrations are always output in case the user wants to include these in their plot to show how much change has occurred over time. The first line contains the constituent abbreviation and the number of values corresponding to the number of active layers output. The next line(s) contain the temperatures/concentrations for a given segment.

```

TEMP      14
5.50      5.50      5.50      5.40      5.40      5.50      5.40      5.30
5.30      5.40      5.30      5.20      5.20      5.20
TEMP      16
5.50      5.50      5.50      5.40      5.40      5.50      5.40      5.30
5.30      5.40      5.30      5.20      5.20      5.20      5.20      5.20
TDS       14
0.400E+02 0.400E+02 0.400E+02 0.400E+02 0.450E+02 0.500E+02 0.550E+02 0.680E+02
0.700E+02 0.650E+02 0.600E+02 0.550E+02 0.500E+02 0.450E+02
TDS       16
0.400E+02 0.400E+02 0.400E+02 0.400E+02 0.450E+02 0.500E+02 0.550E+02 0.680E+02
0.700E+02 0.650E+02 0.600E+02 0.550E+02 0.500E+02 0.450E+02 0.400E+02 0.340E+02
ISS       14
0.100E+01 0.100E+01 0.100E+01 0.100E+01 0.100E+01 0.100E+01 0.100E+01 0.100E+01
0.100E+01 0.200E+01 0.200E+01 0.500E+01 0.500E+01 0.500E+01
ISS       16
0.100E+01 0.100E+01 0.100E+01 0.100E+01 0.100E+01 0.100E+01 0.100E+01 0.100E+01
0.100E+01 0.200E+01 0.200E+01 0.500E+01 0.500E+01 0.500E+01 0.150E+02 0.300E+02
PO4       14
0.200E-01 0.200E-01 0.200E-01 0.200E-01 0.200E-01 0.200E-01 0.200E-01 0.200E-01
0.200E-01 0.200E-01 0.200E-01 0.200E-01 0.200E-01 0.200E-01

```

OUTPUT FILES

PROFILE PLOT

```

PO4      16
 0.200E-01 0.200E-01 0.200E-01 0.200E-01 0.200E-01 0.200E-01 0.200E-01 0.200E-01
 0.200E-01 0.200E-01 0.200E-01 0.200E-01 0.200E-01 0.200E-01 0.200E-01 0.200E-01
NH4      14
 0.500E-01 0.500E-01 0.500E-01 0.500E-01 0.500E-01 0.500E-01 0.500E-01 0.500E-01
 0.500E-01 0.500E-01 0.500E-01 0.500E-01 0.500E-01 0.500E-01
NH4      16
 0.500E-01 0.500E-01 0.500E-01 0.500E-01 0.500E-01 0.500E-01 0.500E-01 0.500E-01
 0.500E-01 0.500E-01 0.500E-01 0.500E-01 0.500E-01 0.500E-01 0.500E-01 0.500E-01
NO3      14
 0.200E+00 0.200E+00 0.200E+00 0.200E+00 0.200E+00 0.200E+00 0.200E+00 0.200E+00
 0.200E+00 0.200E+00 0.200E+00 0.200E+00 0.200E+00 0.200E+00
NO3      16
 0.200E+00 0.200E+00 0.200E+00 0.200E+00 0.200E+00 0.200E+00 0.200E+00 0.200E+00
 0.200E+00 0.200E+00 0.200E+00 0.200E+00 0.200E+00 0.200E+00 0.200E+00 0.200E+00
LDOM     14
 0.675E+00 0.675E+00 0.675E+00 0.675E+00 0.675E+00 0.675E+00 0.675E+00 0.675E+00
 0.675E+00 0.675E+00 0.675E+00 0.675E+00 0.675E+00 0.675E+00
LDOM     16
 0.675E+00 0.675E+00 0.675E+00 0.675E+00 0.675E+00 0.675E+00 0.675E+00 0.675E+00
 0.675E+00 0.675E+00 0.675E+00 0.675E+00 0.675E+00 0.675E+00 0.675E+00 0.675E+00
RDOM     14
 0.157E+01 0.157E+01 0.157E+01 0.157E+01 0.157E+01 0.157E+01 0.157E+01 0.157E+01
 0.157E+01 0.157E+01 0.157E+01 0.157E+01 0.157E+01 0.157E+01
RDOM     16
 0.157E+01 0.157E+01 0.157E+01 0.157E+01 0.157E+01 0.157E+01 0.157E+01 0.157E+01
 0.157E+01 0.157E+01 0.157E+01 0.157E+01 0.157E+01 0.157E+01 0.157E+01 0.157E+01
LPOM     14
 0.750E+00 0.750E+00 0.750E+00 0.750E+00 0.750E+00 0.750E+00 0.750E+00 0.750E+00
 0.750E+00 0.750E+00 0.750E+00 0.750E+00 0.750E+00 0.750E+00
LPOM     16
 0.750E+00 0.750E+00 0.750E+00 0.750E+00 0.750E+00 0.750E+00 0.750E+00 0.750E+00
 0.750E+00 0.750E+00 0.750E+00 0.750E+00 0.750E+00 0.750E+00 0.750E+00 0.750E+00
ALG1     14
 0.650E+00 0.650E+00 0.650E+00 0.650E+00 0.650E+00 0.650E+00 0.650E+00 0.650E+00
 0.650E+00 0.650E+00 0.650E+00 0.650E+00 0.650E+00 0.650E+00
ALG1     16
 0.650E+00 0.650E+00 0.650E+00 0.650E+00 0.650E+00 0.650E+00 0.650E+00 0.650E+00
 0.650E+00 0.650E+00 0.650E+00 0.650E+00 0.650E+00 0.650E+00 0.650E+00 0.650E+00
DO       14
 0.108E+02 0.107E+02 0.107E+02 0.108E+02 0.108E+02 0.109E+02 0.109E+02 0.109E+02
 0.109E+02 0.110E+02 0.110E+02 0.110E+02 0.110E+02 0.110E+02
DO       16
 0.108E+02 0.107E+02 0.107E+02 0.108E+02 0.108E+02 0.109E+02 0.109E+02 0.109E+02
 0.109E+02 0.110E+02 0.110E+02 0.110E+02 0.110E+02 0.110E+02 0.110E+02 0.110E+02

```

The next output grouping consists of temperature/constituent concentrations output over time for the [dates](#) and [frequencies](#) specified in the control file. The first line includes:

1. Julian date [JDAY]
2. Gregorian date [GDAY]
3. water surface layer number [KTWB]
4. deviation of the water surface [Z] from the top of the surface layer [KT]
5. how many dates information has been written to the file

The next line contains the abbreviated constituent name and the number of active layers at the segment. This is also the number of values that have to be read in the following cards.

```

75.702 Mar 15, 1992 23 -0.1950 1
TEMP      14
 5.81      5.64      5.48      5.41      5.37      5.35      5.34      5.33
 5.32      5.32      5.32      5.32      5.32      5.32
TEMP      16

```

PROFILE PLOT

OUTPUT FILES

	6.07	5.89	5.67	5.52	5.41	5.34	5.30	5.29
	5.32	5.34	5.32	5.32	5.31	5.31	5.31	5.31
ISS	14							
	0.674E+00	0.850E+00	0.991E+00	0.116E+01	0.136E+01	0.148E+01	0.166E+01	0.191E+01
	0.208E+01	0.225E+01	0.239E+01	0.250E+01	0.255E+01	0.255E+01		
ISS	16							
	0.611E+00	0.771E+00	0.841E+00	0.873E+00	0.888E+00	0.893E+00	0.891E+00	0.870E+00
	0.877E+00	0.130E+01	0.217E+01	0.279E+01	0.296E+01	0.307E+01	0.307E+01	0.307E+01
PO4	14							
	0.157E-01	0.171E-01	0.182E-01	0.186E-01	0.188E-01	0.189E-01	0.191E-01	0.193E-01
	0.195E-01	0.196E-01	0.197E-01	0.198E-01	0.198E-01	0.198E-01		
PO4	16							
	0.155E-01	0.166E-01	0.177E-01	0.182E-01	0.185E-01	0.187E-01	0.189E-01	0.191E-01
	0.189E-01	0.181E-01	0.185E-01	0.193E-01	0.196E-01	0.199E-01	0.199E-01	0.199E-01
NH4	14							
	0.507E-01							
	0.507E-01	0.506E-01	0.506E-01	0.505E-01	0.503E-01	0.503E-01		
NH4	16							
	0.508E-01	0.508E-01	0.508E-01	0.508E-01	0.508E-01	0.508E-01	0.509E-01	0.509E-01
	0.509E-01	0.510E-01						
NO3	14							
	0.200E+00							
	0.200E+00	0.200E+00	0.200E+00	0.200E+00	0.200E+00	0.200E+00		
NO3	16							
	0.200E+00							
	0.200E+00							
LDOM	14							
	0.665E+00	0.666E+00						
	0.666E+00	0.666E+00	0.667E+00	0.667E+00	0.668E+00	0.668E+00		
LDOM	16							
	0.664E+00	0.665E+00						
	0.665E+00	0.664E+00						
RDOM	14							
	0.157E+01	0.157E+01	0.157E+01	0.157E+01	0.157E+01	0.158E+01	0.158E+01	0.158E+01
	0.158E+01	0.158E+01	0.158E+01	0.158E+01	0.158E+01	0.158E+01		
RDOM	16							
	0.157E+01							
	0.157E+01							
LPOM	14							
	0.641E+00	0.697E+00	0.717E+00	0.727E+00	0.732E+00	0.734E+00	0.739E+00	0.742E+00
	0.743E+00	0.744E+00	0.745E+00	0.746E+00	0.747E+00	0.747E+00		
LPOM	16							
	0.624E+00	0.683E+00	0.703E+00	0.711E+00	0.715E+00	0.718E+00	0.719E+00	0.721E+00
	0.728E+00	0.736E+00	0.742E+00	0.743E+00	0.743E+00	0.743E+00	0.743E+00	0.743E+00
ALG1	14							
	0.615E+00	0.636E+00	0.643E+00	0.646E+00	0.647E+00	0.648E+00	0.649E+00	0.650E+00
	0.650E+00	0.651E+00	0.652E+00	0.653E+00	0.655E+00	0.655E+00		
ALG1	16							
	0.607E+00	0.630E+00	0.637E+00	0.639E+00	0.640E+00	0.641E+00	0.641E+00	0.641E+00
	0.643E+00	0.645E+00	0.646E+00	0.646E+00	0.646E+00	0.646E+00	0.646E+00	0.646E+00
DO	14							
	0.110E+02	0.109E+02	0.108E+02	0.108E+02	0.108E+02	0.108E+02	0.108E+02	0.108E+02
	0.109E+02	0.109E+02	0.109E+02	0.109E+02	0.108E+02	0.108E+02		
DO	16							
	0.110E+02	0.109E+02	0.109E+02	0.108E+02	0.108E+02	0.108E+02	0.108E+02	0.108E+02
	0.108E+02	0.109E+02						

Vector Plot

As in the profile plot output, vector plot output was developed for a DISSPLA plotting program written using FORTRAN callable plotting subroutines. The information is sufficient to develop vector plots of velocities. Output consists initially of:

1. title cards
2. layer thicknesses [H]
3. branch upstream segment [US]
4. branch downstream segment [DS]
5. segment length [DLX]

Each title card takes up a separate line in the output. Items 2-5 are output on a single line. The user should refer to the code for the actual format of the output. The preceding information is time invariant and is used to set up the plotting grid. During simulations, the following information is output:

1. Julian date [JDAY]
2. Gregorian date [GDAY]
3. water surface layer [KTWB]
4. upstream segment number for each branch in a waterbody
5. water surface deviations at each segment for all branches in a waterbody
6. elevation for each layer at each segment for all branches in a waterbody
7. horizontal velocities for each layer at each segment for all branches in a waterbody
8. vertical velocities for each layer at each segment for all branches in a waterbody

Currently, the user must develop their own plotting program to use this feature, which will normally require “getting under the hood” of the model to customize model output. A future release of the model will include a plotting program that can be used to generate velocity vector plots.

Contour Plot

As in the profile and vector plot output, this output was originally included for developing DISSPLA contour plots of model output using FORTRAN callable subroutines. The information is sufficient to develop contour plots of temperatures and constituents. Output consists initially of:

1. title cards
2. number of branches [NBR]
3. grid dimensions [KMX] and [IMX]
4. branch upstream and downstream segments [US] and [DS]
5. segment length [DLX]
6. layer heights [H]
7. number of active constituents
8. active constituent names

Each title card takes up a separate line in the output and each of the remaining item number is output on a single line. The user should refer to the code for the actual format of the output. The preceding information is time invariant and is used to set up the plotting grid. During simulations, the following information is output:

1. Julian date [JDAY] and Gregorian date [GDAY]
3. water surface layer [KTWB]
3. tributary inflows [QTR]
4. tributary inflow temperatures [TTR]
5. tributary inflow concentrations for each active constituent [CTR]
6. current upstream segment [CUS]
7. branch inflow [QIN] and the sum of the branch inflow [QSUM]
8. interfacial area (width times height) [BHRKT1] for all active segments in the surface layer [KT]
9. interfacial area [BHR] for all remaining active computational cells
10. horizontal velocities [U]
11. flows [QC]
12. water surface deviations [Z]
13. temperatures
14. constituent concentrations

Currently, the user must develop their own plotting program to use this feature, which will normally require “getting under the hood” of the model to customize model output. A future release of the model will include a plotting program that can be used to generate velocity vector plots.

Kinetic Fluxes

The ability to compute kinetic fluxes is new in the latest version. Two types of output are available. The first is similar to snapshot output and is specified by setting the kinetic flux control variable [\[KFLC\]](#) to ASCII. The segments that are output are currently controlled by the snapshot segments in the control file that are specified for output. The user must then develop a method for plotting up the output in whatever format they decide upon.

The other option for output is a binary format specified as BINARY for the kinetic flux control variable [\[KFLC\]](#). The only information currently output using this option is the entire kinetic source/sink flux array. A future version will include a plotting program for plotting kinetic fluxes average over space and time.

KINETIC FLUXES

OUTPUT FILES

Burnsville Reservoir - March 15 through December 11, 1992
 Density placed inflow, point sink outflows
 Default hydraulic coefficients
 Default light absorption/extinction coefficients
 Default kinetic coefficients
 Temperature and water quality simulation
 Run 8
 Testing sensitivity to wind
 Wind sheltering set to 0.75
 Jim Stiles and Vince Marchese, USACE Huntington District
 Model run at 15:09:49 on 12/04/01

March 15, 1992						Julian Date = 75 days 16.86 hours							DO algal production - source, kg/day						
	2	3	4	5	6	7	8	9	10	11	12	13							
23						0.232E-02	0.164E-01	0.558	1.34	7.22	8.22								
24						0.296E-02	0.237E-01	0.375	0.980	4.52	4.99								
25						0.195E-02	0.297E-01	0.316	0.898	4.21	4.38								
26						0.509E-03	0.220E-01	0.267	0.821	3.82	3.85								
27							0.259E-01	0.218	0.702	1.01	1.00								
28							0.201E-01	0.159	0.489	0.567	0.543								
29								0.944E-01	0.270	0.258	0.247								
30								0.569E-01	0.160	0.144	0.138								
31								0.746E-01	0.965E-01	0.770E-01	0.744E-01								
32								0.652E-01	0.583E-01	0.449E-01	0.434E-01								
33								0.431E-01	0.318E-01	0.254E-01	0.246E-01								
34										0.113E-01	0.139E-01								

Withdrawal Outflow

Withdrawal outflow files contain information for plotting any release or withdrawal temperatures and/or constituent concentrations as a time series. The files can also be used to externally link upstream waterbodies to downstream waterbodies so that waterbasins can be broken up into multiple waterbodies. This is an important feature when runtimes for the entire waterbasin become excessive. With this option, calibration can start at the most upstream waterbody and proceed sequentially downstream.

Output consists of up to four separate files for each segment [\[IWDO\]](#) specified in the control file. The files include an outflow, outflow temperature, constituent concentrations, and derived constituent concentrations. The constituent concentration outflow file is only generated if constituent computations [\[CCC\]](#) are turned on. The derived constituent concentration outflow file is generated only if constituent computations [\[CCC\]](#) are turned on and one or more derived constituents [\[CDWBC\]](#) are turned on.

EXAMPLE

Flow file for segment 24

JDAY	QWD
75.702	12.42
75.801	12.35
75.901	12.28
76.000	12.21
76.103	12.14
76.203	12.07
76.300	12.00
76.403	11.57
76.500	11.07
76.602	10.59
76.701	10.10
76.804	9.58
76.904	9.09
77.000	8.58
77.106	8.08
77.205	7.59
77.300	7.09
77.406	7.08
77.500	7.14
77.600	7.20
77.703	7.27
77.805	7.33
77.902	7.39
78.000	7.46
78.102	7.52
78.203	7.59
78.300	7.65
78.406	9.44
78.500	11.50
78.601	13.49
78.703	15.55
78.803	17.60
78.900	19.60
79.000	21.69

Temperature file for segment 24

JDAY	T
75.702	5.54

WITHDRAWAL OUTFLOW

75.801	5.51
75.901	5.45
76.000	5.38
76.103	5.33
76.203	5.27
76.300	5.23
76.403	5.29
76.500	5.41
76.602	5.50
76.701	5.50
76.804	5.45
76.904	5.43
77.000	5.44
77.106	5.46
77.205	5.48
77.300	5.50
77.406	5.56
77.500	5.63
77.600	5.69
77.703	5.71
77.805	5.70
77.902	5.69
78.000	5.69

OUTPUT FILES

Concentration file for segment 24

JDAY	AGE	PO4	NH4	NO3	LDOM	RDOM	LPOM	ALG1	DO
75.706	.696	.201E-01	.509E-01	.200	.665	1.57	.708	.638	46.6
75.804	.793	.202E-01	.510E-01	.200	.663	1.57	.699	.634	46.0
75.902	.890	.202E-01	.511E-01	.200	.662	1.57	.693	.632	45.6
76.000	.987	.202E-01	.512E-01	.200	.660	1.57	.687	.630	45.2
76.102	1.09	.202E-01	.513E-01	.201	.659	1.57	.681	.628	44.8
76.201	1.18	.202E-01	.514E-01	.201	.657	1.57	.676	.626	44.5
76.300	1.29	.203E-01	.515E-01	.201	.656	1.57	.671	.624	44.1
76.402	1.39	.203E-01	.516E-01	.201	.655	1.57	.665	.623	43.8
76.500	1.48	.203E-01	.517E-01	.201	.653	1.57	.661	.622	43.5
76.604	1.59	.203E-01	.518E-01	.201	.652	1.57	.658	.622	43.2
76.703	1.69	.203E-01	.519E-01	.201	.651	1.57	.655	.621	43.0
76.806	1.79	.204E-01	.520E-01	.201	.649	1.57	.652	.621	42.8
76.902	1.89	.204E-01	.521E-01	.201	.648	1.57	.649	.619	42.5
77.000	1.99	.204E-01	.522E-01	.201	.647	1.57	.644	.618	42.1
77.102	2.08	.204E-01	.523E-01	.201	.645	1.57	.637	.616	41.7
77.201	2.18	.204E-01	.524E-01	.201	.644	1.57	.630	.613	41.3
77.300	2.28	.205E-01	.525E-01	.201	.642	1.57	.623	.610	40.9
77.400	2.38	.205E-01	.525E-01	.201	.641	1.57	.616	.608	40.5
77.500	2.48	.205E-01	.526E-01	.201	.639	1.57	.610	.607	40.1
77.606	2.59	.205E-01	.527E-01	.201	.638	1.57	.604	.605	39.7
77.702	2.68	.205E-01	.528E-01	.201	.637	1.57	.599	.604	39.3
77.804	2.78	.206E-01	.529E-01	.202	.635	1.57	.595	.602	39.0
77.902	2.88	.206E-01	.530E-01	.202	.634	1.57	.592	.601	38.8
78.000	2.98	.206E-01	.531E-01	.202	.632	1.57	.590	.600	38.6

Run-time Warnings

The model generates the following run-time warnings that can be useful when setting up the model.

1. *Water surface is above the top of layer 2 in segment 'x' at day 'y'*

This message is output to inform the user that the water surface elevation has gone above the top of the computational grid. This may be okay or it might indicate that additional layers need to be added to the grid so that the surface layer does not become inappropriately thick. This is a common message when first calibrating the water surface in a reservoir if either the inflows are overestimated or the outflows are underestimated. An application of the model to Lake Roosevelt did not include water pumped to another reservoir and the water surface ended up 70 m above the top of the grid.

2. *Computational warning at Julian day = 'x',' at segment 'y' timestep = 'z'
water surface deviation [Z] = 'x' m layer thickness = 'y' m*

This message indicates that the water surface elevation solution is starting to go unstable and is generally a result of velocities approaching supercritical values. What is happening is that from one timestep to the next, the water surface elevation has gone from residing in layer [KT] to layer [KT]+1, which causes a negative surface layer thickness (Figure C-4). The surface layer thickness, HKT1, is the layer thickness, H, minus the water surface deviation, z, from the top layer [KT]. As can be seen, this is negative when the solution begins to go unstable.

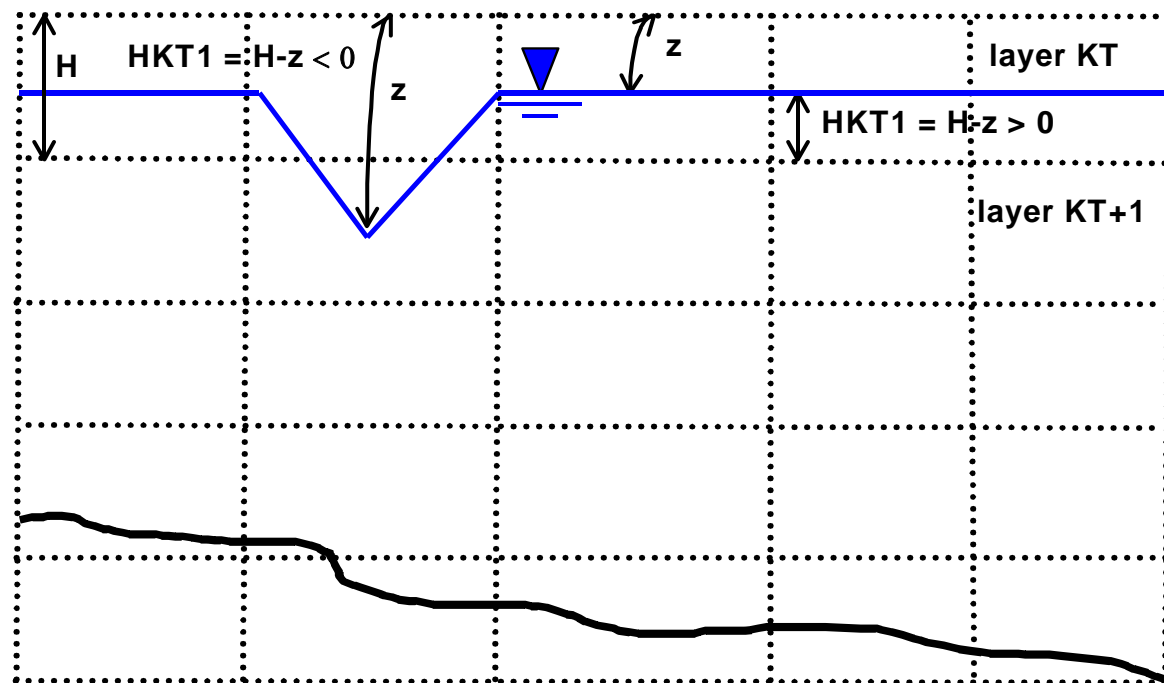


Figure C-4. Diagram illustrating unstable water surface elevation solution.

Normally, when the water surface elevation approaches the bottom of layer [KT], the model would subtract a layer thus allowing the water surface level to decline smoothly over time. However, if the

water surface elevation jumps below the bottom of layer [KT] in one timestep, the layer subtraction algorithm does not have a chance to adjust the water surface layer before solving for the velocities.

The model attempts to recover from the instability by decreasing the timestep by 90% and recomputing the water surface elevation. If the current timestep is greater than the minimum timestep [DLTMIN], then the following warning message is then generated.

3. *Unstable water surface elevation on day 'x',
negative surface layer thickness using minimum timestep at iteration 'y'*

If the current timestep is less than or equal to the minimum timestep [DLTMIN], then an error message is output and the run is stopped. However, all is not lost. Based on the Julian date in the warning messages, the user can reduce the maximum timestep [DLTMAX] and/or the fraction of the timestep [DLTF] just prior to the instability and then increase back to the original value(s) sometime later in the simulation. Oftentimes, this allows the model to get through the time period that was generating the instability. This may need to be done for several time periods during the simulation in order to get the model to run to completion, especially for river applications.

If the instability is occurring during high inflow periods, the user also has the option of spreading inflows out over a greater time period in order to reduce the maximum velocities. Care must be taken to ensure that the total inflows remain the same, especially if inflow interpolation [QINIC] is turned on. Likewise, velocities can also be reduced through adjustments to the bathymetry such as making cells wider. If inflows are placed according to density [PQINC] and/or [PQTRC], velocities can also be reduced by using the “distribute evenly from top to bottom” option. Still another option is to increase the minimum number of layers [NLMIN] for a segment to remain active. This has a similar action as distributing the inflow evenly from top to bottom in that it provides more layers for the inflow to be distributed over thus reducing velocities.

Problems in model setup can also generate these warning messages. For instance, if an external head boundary condition is inadvertently set way off from the starting water surface elevation (or vice versa), then large velocities can be generated that result in a water surface instability. Extremely small widths (<1 m) can also cause the same problems.

4. *Low water in segment 'x' water surface deviation = 'y' at day 'z'*

This warning message is to alert the user that water is drying up in a segment with only one active layer.

5. *Computational warning at Julian day = 'x'
spatial change = 'x' m³ temporal change = 'y' m³ volume error = 'z' m³*

This message is to let the user know that the volume error is more than 1000 m³. This should not normally happen unless the user has incorrectly modified the code or the water surface elevation solution has become unstable. The message is more informational and does not require the user to do anything as the volume error is arbitrarily set to 1000 m³.

Run-time Errors

The model generates the following run-time error messages.

1. Unstable water surface elevation on day 'x' negative surface layer thickness using minimum timestep at iteration 'y'

As discussed in the [RUN-TIME WARNINGS](#) section, this error message is generated by an unstable water surface elevation solution. Refer to that section on methods for eliminating the instability. Additional information is output to the error message file and includes the segment number, the water surface elevation at that segment, the bottom elevation of that segment, and the elevation difference for all segments in the offending branch.

2. Fatal error - Insufficient segments in branch 'x' Julian day = 'y' water surface layer = 'z'

Currently in the model, if the number of segments in a branch becomes less than two due to drying out and subsequent subtraction of upstream segments from the active computational grid, then the model issues this error message and terminates. The reason why is that there must be at least two active segments in a branch for many of the computations to proceed. This error is most common in reservoir simulations. Future plans include bypassing this limitation so that the model runs using only active branches. However, this will involve major coding changes and will take some time to implement.

If this occurs during water surface calibration due to insufficient inflows or excessive outflows, then adjust the flows so that either more water comes in or less water flows out. The user will have to decide the appropriate inflow/outflow to adjust. If this problem occurs with a correct water balance, then one option is to remove the branch from the computational grid and include the branch inflows as a tributary. The missing branch volume should then be evenly distributed throughout the active computational grid cells to ensure that the project volume is conserved.

Another workaround is to add additional depth to the bottom of the branch so that water levels can drop without segments being subtracted. Similarly, the number of active layers required to prevent segment subtraction [[NLMIN](#)] can be set to one if it is not already set to that value, which may prevent the branch from going dry.